THE CRYSTAL CHEMISTRY OF VESUVIANITE

by

© Lee Andrew Groat

A thesis
presented to the University of Manitoba
in partial fulfillment of the
requirements for the degree of
Ph.D.
in
Geological Sciences

Winnipeg, Manitoba, 1988

ISBN 0-315-48087-4

THE CRYSTAL CHEMISTRY OF VESUVIANITE

BY

LEE ANDREW GROAT

A thesis submitted to the Faculty of Graduate Studies of
the University of Manitoba in partial fulfillment of the requirements
of the degree of

DOCTOR OF PHILOSOPHY

I hereby declare that I am the sole author of this thesis. I authorize the University of Manitoba to lend this thesis to other institutions or individuals for the purpose of scholarly research.

L.A. Groat

I further authorize the University of Manitoba to reproduce this thesis by photocopying or by other means, in total or in part, at the request of other institutions or individuals for the purpose of scholarly research.

L.A. Groat

The University of Manitoba requires the signatures of all persons using or photocopying this thesis. Please sign below, and give address and date.

ABSTRACT

Vesuvianite (idocrase) is an accessory orthosilicate mineral found in skarns, rodingites, and altered alkali syenites. Previous studies have failed to determine the true symmetry, structure and formula of this mineral.

Careful investigation of the optical properties of 75 different vesuvianite specimens has shown that most are detectably biaxial ($2V$=0–62°). This indicates that the true symmetry is orthorhombic or lower. The only possible space groups (arrived at by precession photography and group theory calculations) are $P2/n$, $P2$, Pn, $P\bar{1}$, and $P1$. Attemps to refine the structure of a high-birefringence vesuvianite in space groups $P2/n$ and Pn were inconclusive.

A statistical study of microprobe analyses showed that normalization should be on the basis of 50 cations per formula unit. Six of the 75 vesuvianites were found to contain considerable amounts of boron. They also had more Mg, less Al and OH, and larger a cell dimensions than normal vesuvianites. IR spectra of these specimens are quite different than those of normal vesuvianites. Structure refinement of a boron-bearing vesuvianite showed B at the tetrahedral "T" site and at a position halfway between O(10) atoms in the channels, coordinated by one O(10) oxygen and by two new oxygens at the O(11) position. However, there are problems with this refinement, related to the occupancy of the new positions.

The channel configuration of the boron-bearing vesuvianite is polar, whereas there are two possible configurations for normal vesuvianite, both non-polar. An argument can be made that for these vesuvianites, growth on the {001} face leads to ordered arrangements $\parallel c$, whereas growth on {100} leads to disorder of channel configurations between adjacent channels. Such a model would account for the patterns of diffuse density (indicating short-range disorder) seen in some precession photographs.

Consideration of the chemistry of vesuvianite has indicated the general formula:

$$[Ca, Na, Ln, Pb, Th]_{19}[(Al, Fe^{3+})_x(Mg, Fe^{2+}, Mn)_y Ti_z^{4+}]_{13}Si_{18}O_{68.5}(OH, F)_{9.5}$$

with ideal values of x=10.0, y=2.75, z=0.25 atoms p.f.u.

DEDICATION

This thesis is dedicated to my grandmother, Mrs. Elizabeth Groat, who was always there when I needed encouragement.

ACKNOWLEDGEMENTS

I would like to thank Frank Hawthorne for suggesting and supervising this project, and for collecting the single-crystal IR spectra. Norman Halden helped with administration during Frank's leave. Bob Ferguson aided with interpretation of the precession photographs. Tony Secco (Department of Chemistry) answered some crystallographic questions and helped with ORTEP.

I would also like to acknowledge the efforts of Neil Ball, Wayne Blonski, and Ron Chapman, who helped with many aspects of the experimental work. The office staff (Anne Flynn, Sharon Kirsch, and Elizabeth Ross) deserve thanks for their administrative support, which often went beyond the call of duty. I would also like to thank Eva Zaleski, for lending a sympathetic ear when things were most frustrating.

A number of people outside of the University of Manitoba helped with aspects of this research. I would like to thank Scott Ercit for allowing me to use the JEOL microprobe at the National Museum, and both Scott and Judy for looking after me while in Ottawa. Joel Grice (National Museum) and Scott Ercit both provided scientific advice. George Rossman (Cal Tech) provided the single crystal IR facilities, and helped with interpreting the spectra. Jane Weitzel (Manitoba Government) and her co-workers helped with the AA spectroscopy and water analysis.

Support for the research was provided by NSERC operating grants to Frank Hawthorne. Personal financial support was provided by post-graduate scholarships from NSERC and the University of Manitoba.

Not least of all, I gratefully acknowledge the support of my wife, Anita.

CONTENTS

FIGURES

TABLES

Chapter 1

INTRODUCTION AND PREVIOUS STUDIES

1.1 Introduction

Vesuvianite (idocrase) is a rock-forming or accessory orthosilicate mineral found in skarns, rodingites, and altered alkali syenites. The general physical and optical properties of vesuvianite are listed in Table 1. The formula proposed by Rucklidge *et al.* (1975) is:

$$Ca_{19}Fe(Fe,Ti,Mn,Mg,Al)_8Al_4Si_{18}O_{70}(OH,F)_8$$

Vesuvianite is one of the least understood of all rock-forming minerals. The true symmetry remains unknown, the details of the atomic structure are unresolved, and there is no adequate general formula. These uncertainties are complicated by the diverse range of conditions under which vesuvianite forms in nature, with consequent variation in habit, chemistry and occurrence.

Proposed as a tetragonal mineral, vesuvianite should be optically uniaxial, but many biaxial samples have been described. Some researchers have attributed these anomalous optical properties to the presence of minor or trace elements. So far, however, no one has determined why some vesuvianites are biaxial, or what is their true symmetry.

The general structure of vesuvianite is similar to that of grossular garnet, although vesuvianite has additional atoms that lie along the four-fold axis. Some recent studies (Giuseppetti and Mazzi (1983), Allen (1983b, 1985), Fitzgerald *et al.* (1986b, 1987) have shown that cation ordering at these sites can reduce the symmetry to $P4/n$, a sub-group of the normal $P4/nnc$ space group. No one yet has attempted to refine the structure of vesuvianite in a non-tetragonal space group, as suggested by the optics.

These structural ambiguities, coupled with the wide range of possible substitutions, have made it difficult to determine an adequate general formula for vesuvianite. In addition, the chemical variations and limits of the species remain poorly characterized.

1.2 Optical Characteristics

The general optical character of vesuvianite is summarized in Table 1. Sections of vesuvianites from some localities show quite complex structures. Many authors have described complex sector zoning and various types of concentric zoning which can be related to the external crystal morphology. Aspects of this have been discussed by Arem (1970, 1973). An idealized case for sector zoning is shown in Figure 1. There are distinct optical differences between the sectors. They show different birefringences down [001], and $2V$s that range from 0–65°. However, nobody has recorded any corresponding compositional changes within these vesuvianites.

Other vesuvianites show complex zonal patterns and lamellae, again with very irregular birefringence from point to point.

None of these optical complexities have been related to any compositional, structural, or symmetry changes in the material, except for the obvious deviation from uniaxial behaviour. Many authors have related variations in refractive index of vesuvianite to variations in chemical composition. Such variations are (presumably) predicted by the Gladstone-Dale relationship. One other optical characteristic has been related to chemical composition. Oftedal (1964) found that boron-bearing vesuvianites with <0.5 wt.% B_2O_3 were optically negative, while those with >1.0 wt.% B_2O_3 were optically positive ("wiluites"). This was confirmed by Serdyuchenko *et al.* (1968) and Khotina (1968), although optically positive vesuvianites are known in which no appreciable boron has been recorded (Gädeke, 1938; Peters, 1963).

Table 1: General physical and optical properties of vesuvianite (Deer *et al.*, 1982).

Colour:	yellow, green, brown, rarely red or blue.
Cleavage:	{110} poor, {100} and {001} very poor.
Unit Cell:	a 15.4–15.6, $c \approx$11.8Å
Space Group:	$P4/nnc$
Z:	2
Optic sign:	negative
ϵ:	1.700–1.746
ω:	1.703–1.752
δ:	0.001–0.009
Dispersion:	strong
Colour (t.s.):	colourless to pale yellow, green, or brown.
Pleochroism:	weak; brownish yellow to yellowish brown.

Some vesuvianites with low birefringence may show brilliant blue or brown interference colours. Optically positive and biaxial varieties are also known.

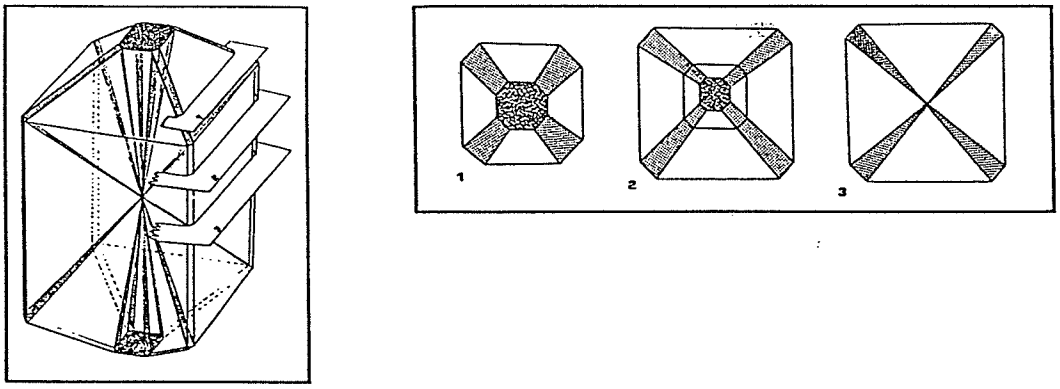

Figure 1: (a) A sector zoned vesuvianite crystal, from Arem (1973). (b) Sections through the crystal in (a).

1.3 The Symmetry of Vesuvianite

Warren and Modell (1931) solved the crystal structure of vesuvianite in the space group $P4/nnc$. This space group was assumed to be correct until Arem and Burnham (1969) found that vesuvianite from many localities show reflections that violate glide-plane extinction criteria for $P4/nnc$. They showed that violations of $P4/nnc$ symmetry could be classified into *strong* and *weak*, according to the number and strength of the glide-violating reflections. In addition, they suggested alternative space groups for some of the vesuvianites they examined (Table 2). Sapountzis and Katagas (1980) assigned the space group $P4/nnm$ to a vesuvianite from Greece. Giuseppetti and Mazzi (1983) were first to refine a vesuvianite in a space group lower than $P4/nnc$, that is $P4/n$. They also suggested that $P4nc$ is a possible space group. More recent refinements of vesuvianite in space groups $P4/n$ and $P\bar{4}$ have been reported by Allen (1983b, 1985) and Fitzgerald *et al.* (1986b, 1987).

Table 2: Space groups from Arem and Burnham (1969)

$P4/nnc$	$P4/nmm$—"strong"	$P4/nmm$—"weak"	$4/mmm$ $P-/---$*
Lake Jaco, Mexico	Black Lake, PQ	Monte Somma, Italy	Asbestos, PQ
Antamina, Peru	Coleraine, PQ	Telemark, Norway	Hindubagh, Pakistan
Crestmore, CA	Laurel, PQ	Franklin, NJ	San Benito Co., CA
Sanford, ME	Eden Mills, VT		
Franklin, NJ			
Ural Mts., USSR			
Wilui River, USSR			

*Possible space groups: $P\bar{4}2m$, $P\bar{4}m2$, $P4mm$, $P42$, and $P4/mmm$. A piezoelectric test showed that the Asbestos, PQ sample is noncentrosymmetric ($P4/mmm$ eliminated).

Previous authors have suggested the use of symmetries lower than tetragonal, as indicated by the optical characteristics of most vesuvianites. Allen (1985), in particular, stated that space groups $Pnn2$, $Pcc2$, $P2/n$ ($P2/c$), Pn (Pc), $P2$, $P\bar{1}$, and $P1$ are all possible. No one, however, has attempted to refine a vesuvianite structure in any of these space groups.

1.4 The Structure of Vesuvianite

1.4.1 Previous Studies *

The crystal structure of vesuvianite was first solved by Warren and Modell in 1931. They showed that it is closely related to that of grossular garnet, but has additional atoms which lie on the fourfold axes. The symmetry of their basic structure was $P4/nnc$, and it consisted of rods of the garnet structure separated by channels along Z. Warren and Modell (1931) suggested that there were two calciums along this channel, each coordinated by face-sharing square antiprisms of oxygen. Based on this model they proposed the following formula for vesuvianite:

$$4[Ca_{10}Al_4(Mg,Fe)_2Si_9O_{34}(OH)_4]$$

During the following 40 years, some modifications to this vesuvianite formula were suggested by various authors based on chemical data (see Table 6). These modifications suggested that although the basic features of the Warren-Modell model were correct, some of the more detailed aspects of the structure required further study.

Coda *et al.* (1970) refined the structure of a vesuvianite from Bric Camulá, Italy, in the space group $P4/nnc$. They confirmed the basic validity of the Warren-Modell model, but discovered an additional oxygen atom on the fourfold axis that runs down the centre of the prominent channels (see Figure 4). They suggested that this O(10) represented a hydroxyl group, and presented a single-crystal infrared absorption spectrum to support their hypothesis. These authors also focused their attention on the arrangements of Ca and Fe atoms down the fourfold axis. Their structural refinement showed that the channel Ca position, designated C, was only half occupied. This is in accord with the very short C–C distance of ≈ 2.8Å, suggesting that only one of this pair of sites can be occupied by Ca in any particular

* Projections of the vesuvianite structure are shown in Figures 2 and 3. These may be referred to during reading of the following text.

Table 3: Summary of previous structure refinements of vesuvianite.

Allowed		All		Space	Locality	Study
$R(\%)$	$R_w(\%)$	$R(\%)$	$R_w(\%)$	Group		
				†$P4/nnc$	Wilui River, USSR	Warren and Modell (1931)
7.9*				"	Bric Camulá, Italy	Coda *et al.* (1970)
3.9	5.0			"	Turnback Lake, NT	Rucklidge *et al.* (1975)
4.7	5.9			"	York River, ON	"
5.0	4.4			"	Wakefield, PQ	"
3.4				$P4/n$	Ala Piedmont, Italy	Giuseppetti and Mazzi (1983)
	4.5			$P4/nnc$	Ludwig, NV	Allen and Burnham (1983a)
				$P4/n$	Asbestos, PQ	Allen and Burnham (1983b)
				"	Eden Mills, VT	"
						Valley *et al.* 1985
8.6	7.0	10.3	9.6	$P4/nnc$	Asbestos, PQ	Allen (1985)
6.4	6.3	11.3	17.3	"	Georgetown, CA	"
4.8	4.0	5.7	25.5	"	Sanford, ME	"
5.6	5.8	6.5	7.3	"	Franklin, NJ	"
4.6	4.4	4.7	4.5	"	Luning, NV	"
14.0	9.0	15.9	9.8	"	Eden Mills, VT	"
6.0	3.2	6.4	3.4	$P4/n$	"	"
6.1*	3.3*	6.1*	3.3*	$P\bar{4}$	"	"
4.22	3.51			$P4/nnc$	Franklin, NJ	Fitzgerald *et al.* (1986a)
5.48	6.32			$P4/n$	Asbestos, PQ	Fitzgerald *et al.* (1986b)
3.04	3.71			$P4/nnc$	Nakatatsu Mine, Japan	Yoshiasa and Matsumoto (1986)
6.64	7.22			$P4/n$	San Benito Co., CA	Fitzgerald *et al.* (1987)

Allowed = only those reflections allowed by the space group were used.

*Isotropic temperature factors.

†Space group determined on crystals from Franklin, N.J., and Sanford, ME.

Table 4: Selected site occupancies from Giuseppetti and Mazzi (1983)

Site Population:	Ca	Al	Mg	Fe^{3+}	Fe^{2+}	Total Occupancy
CA	0.830					0.830
CB	0.170					0.170
AA, AB		1.000				1.000
ALFA		0.564	0.376	0.060		1.000
ALFB		0.180	0.145	0.045		1.000
BA				0.830		0.830
BB					0.170	0.170

instance; there is, however, local order associating Ca at C with a vacancy at the adjacent C site. They also identified another cation position down the fourfold axis, designated B, and again half occupied, this time by (Fe,Mg). The B–C distance is ≈ 1.4Å; this is too short for simultaneous occupancy of adjacent B and C positions, and again a situation of local order must prevail whereby occupancy of one C position must be accompanied by a vacancy at the adjacent B site. These modifications to the basic Warren and Modell structure resulted in a revised formula for vesuvianite (see Table 6).

Further work on the channel conformations in vesuvianite was done by Rucklidge *et al.* (1975). They confirmed the basic results of Coda *et al.* (1970) on three vesuvianites from Great Slave Lake, N.W.T., Bancroft, Ontario, and Wakefield, Quebec. They also illustrated the local conformation of the B and C sites down the fourfold axes, as shown in Figure 4.

Further $P4/nnc$ refinements of vesuvianite are given by Allen and Burnham (1983), Valley *et al.* (1985), Yoshiasa and Matsumoto (1986), and Fitzgerald *et al.* (1986a) (see Table 3). The latter refinement was done on a blue copper-bearing variety (cyprine) from Franklin, N.J., and showed that Cu occupies the B position, as would be expected.

Arem and Burham (1969) showed that vesuvianite from some localities show reflections that violate various of the glide-plane extinction criteria for the space group $P4/nnc$ (see Table 2). This problem was first addressed by Giuseppetti and Mazzi (1983) who refined the structure of a vesuvianite from Val d'Ala, Italy. This

vesuvianite showed strong $h0l$ and hhl reflections that violate the vertical n and c glides of the $P4/nnc$ space group. They also observed a few weak $hk0$ reflections, and thus reported that the horizontal mirror plane is only weakly violated. They also observed strong differences in intensity between hkl and khl reflections, indicating loss of the diagonal mirror planes in the Laue group. They refined the crystal structure in the space group $P4/n$, which resulted in the splitting of all the cation sites in the lower symmetry structure. In particular, the B and C sites split into pairs that show different site occupancies, as summarized in Table 4. They also suggested that $P4nc$ is a possible space group for vesuvianite, and that domains of ordered $P4/n$ and $P4nc$ structures can account for the glide-violating reflections in some vesuvianites.

Fitzgerald *et al.* (1986b, 1987) reported $P4/n$ refinements of vesuvianite from Asbestos, Quebec, and San Benito County, California. With the former sample they apparently confirmed the Giuseppetti and Mazzi model, but unfortunately do not give site occupancies, so the pattern of ordering associated with the symmetry lowering in the structure is not known. The San Benito County vesuvianite was enriched in Ti and REEs, but again the site occupancies are not explicitly given, so it is difficult to compare with the Giuseppetti and Mazzi model.

Allen (1985) reported refinements of six vesuvianites from Asbestos, Quebec; Georgetown, California; Sanford, Maine; Franklin, N.J.; Luning, Nevada; and Eden Mills, Vermont. Five of these were refined in space group $P4/nnc$. These essentially confirmed previous models and allowed assignment of site occupancies. Allen suggested that $P4/nnc$ structures may result from merohedral twinning of a lower-symmetry structure. Vesuvianite from Eden Mills was refined in the space groups $P4/nnc$, $P4/n$, and $P\bar{4}$. Allen concluded that this structure contained unequal values of oppositely-ordered domains, each of which had $P\bar{4}$ symmetry, but indicated that the $P4/n$–$P4nc$ domain model of Giuseppetti and Mazzi (1983) could also account for his observations.

All of this work is essentially summarized in Table 3.

Table 5: Atomic positions in vesuvianite (space group $P4/nnc$).

Site	Equi-point	Site Contents*	Bonded atoms*	Other studies	
				#1	#2
Si(1)	4d	Si	O(1)×4	Si(1)	Z(1)
Si(2)	16k	Si	O(2) O(3) O(4) O(7)	Si(2)	Z(2)
Si(3)	16K	Si	O(5) O(6) O(8) O(9)[b]	Si(3)	Z(3)
Ca(1)	4c	Ca	O(1)×4 O(2)×4	Ca(1)	X(1)
Ca(2)	16k	Ca	O(1) O(2) O(3) O(4) O(5)×2 O(6) O(8)	Ca(2)	X(2)
Ca(3)	16k	Ca	O(3) O(6)† O(7) O(7) O(7) O(8) O(10) OH	Ca(3)	X(3)
C	4e	0.5 Ca	O(6)×4 O(9)×4	Ca(4)	C
B	4e	0.5 Fe	O(6)×4 O(10)	M(3)	B
AlFe	16k	Al,Fe	O(1) O(2) O(3) O(4) O(5) OH	M(2)	Y
A	8f	Al	O4×2 O(8)×2 OH×2	M(1)	A
O(1)	16k	O	Si(1) Ca(1) Ca(2) AlFe	O(1)	O(1)
O(2)	16k	O	Si(2) Ca(1) Ca(2) AlFe	O(2)	O(2)
O(3)	16k	O	Si(2) Ca(2) Ca(3) AlFe	O(3)	O(3)
O(4)	16k	O	Si(2) Ca(2) AlFe A	O(4)	O(4)
O(5)	16k	O	Si(3) Ca(2)×2 AlFe	O(5)	O(5)
O(6)	16k	O	Si(3) Ca(2) Ca(3)×2† *C* or B	O(6)	O(6)
O(7)	16k	O	Si(2) Ca(3)×3	O(7)	O(7)
O(8)	16k	O	Si(3) Ca(2) Ca(3) A	O(8)	O(8)
O(9)	8h	O	Si(3)×2 C	O(9)	O(9)
O(10)	4e	O,OH	Ca(3)×4 B	O(10)	O(10)
OH	16k	OH	Ca(3) AlFe A	O(11)	O(11)

Origin at $\bar{1}$. The site notation used is that of Rucklidge *et al.*, (1976).

*Site contents and coordinations are for the Great Slave Lake crystal in Rucklidge *et al.* (1976).

#1 Giuseppetti and Mazzi (1983).

#2 Allen (1985).

[b]Bridging oxygen in Si_2O_7 group.

†Ca(3) is designated as nine-coordinated in some studies.

1.4.2 Description of the Structure

Based on the studies outlined in the previous section, Figures 2 and 3 show projections of the vesuvianite structure down [001] and [100].

The framework of octahedra and tetrahedra is topologically equivalent for all of the tetragonal space groups. Differences between structures in each of these space groups focus on the atomic arrangement down the fourfold axes.

The basic octahedral-tetrahedral framework of vesuvianite is well known. There are three nonequivalent Si sites in the $P4/nnc$ structure (see Table 5), each surrounded by four oxygens in a tetrahedral arrangement. The Si(1) and Si(2) tetrahedra link to no other tetrahedra, whereas the Si(3) tetrahedra share one corner to form an Si_2O_7 pyrosilicate group. There are two octahedrally- coordinated sites, A and AlFe, normally occupied by Al and (Al,Fe,Mg,Ti...) respectively. The AlFe site is a slightly distorted octahedron coordinated by five (symmetrically distinct) oxygens and one OH. One edge is shared with the A-site octahedron. Both sites link by corner sharing to the tetrahedra to form a heteropolyhedral framework.

There are three Ca sites that occupy interstices in this framework, Ca(1), Ca(2), and Ca(3); these are eight and/or (Ca(3)) nine coordinated. This forms a fairly tightly-bonded part of the vesuvianite structure.

There are two half-occupied cation sites down the channel; these are designated B and C. The C site is half occupied by Ca, as discussed above; it is coordinated by eight oxygens at the vertices of a square antiprism. The B site is half occupied by (Fe,Mg,Al...) and is coordinated by five oxygens arranged at the corners of a square pyramid. The O(10) oxygen also lies in the channel and the site is fully occupied. It is bonded to four Ca(3) cations and one B cation, forming a square pyramid, and is likely closely associated with a hydrogen; many previous authors have referred to it as an OH group. Chemical analyses and bond valence arguments show the presence of considerable additional H in the structure associated with the oxygen occupying the OH position; a hydrogen bond with O(7)(s) as the acceptor is indicated (see Figure 5). This constitutes the essential features of the normal $P4/nnc$ vesuvianite structure.

The $P4/n$ structure is characterized by a similar framework but with significant ordering on the B and C sites. The results of Giuseppetti and Mazzi are shown in Table 4. The reasons for such ordering are not clear.

1.4.3 Vesuvianite Structure Diagrams

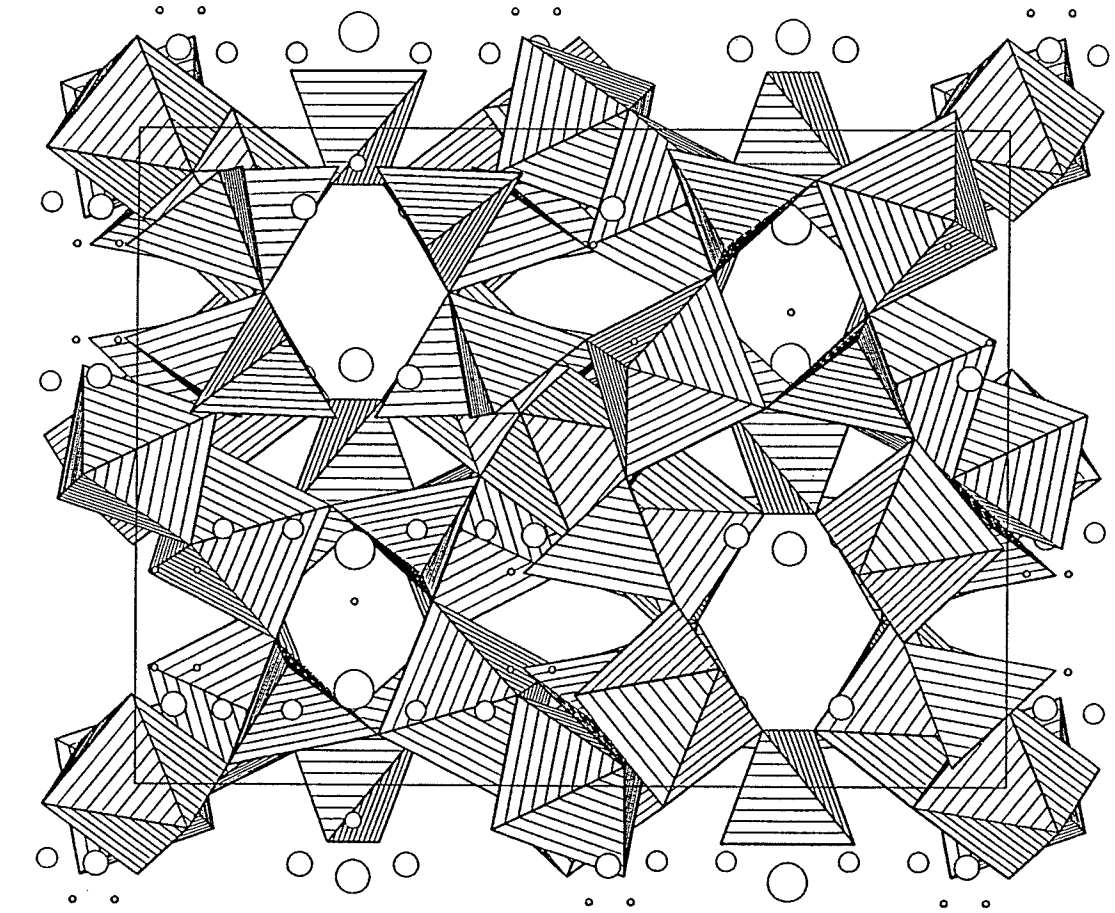

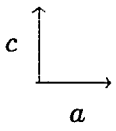

2Å

KEY

O(10)	Ca(3)
C	*B*
Ca(2)	H

Figure 2: A projection of the vesuvianite structure down [100]. The atomic positions are from Yoshiasa and Matsumoto (1986).

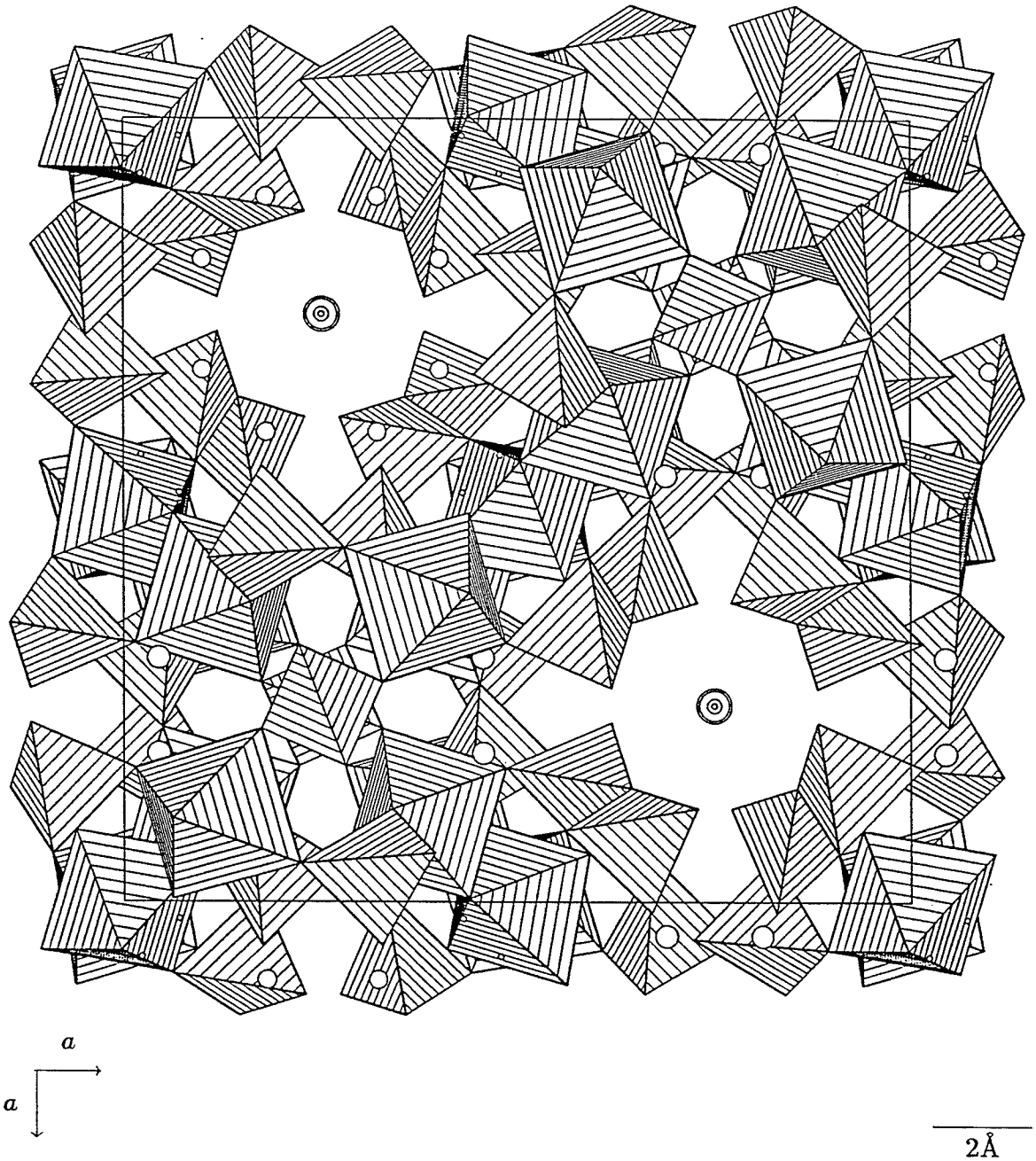

Figure 3: A projection of the vesuvianite structure down [001]. The atomic positions are from Yoshiasa and Matsumoto (1986).

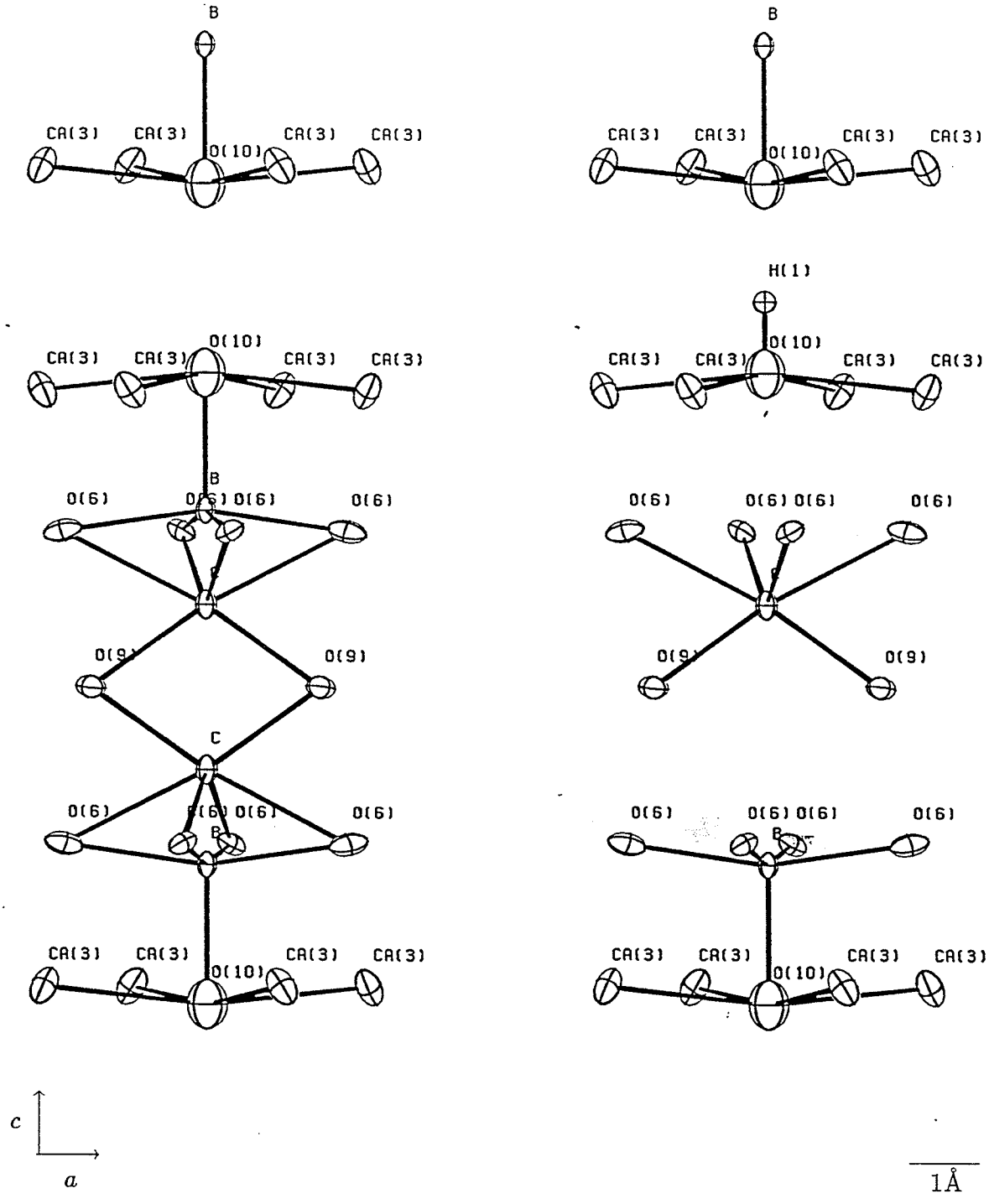

Figure 4: The atomic arrangement along the fourfold axes. (a) Coordination with each of the B and C positions occupied. (b) An arrangement of singly occupied B and C sites. The atomic positions are from Yoshiasa and Matsumoto (1986).

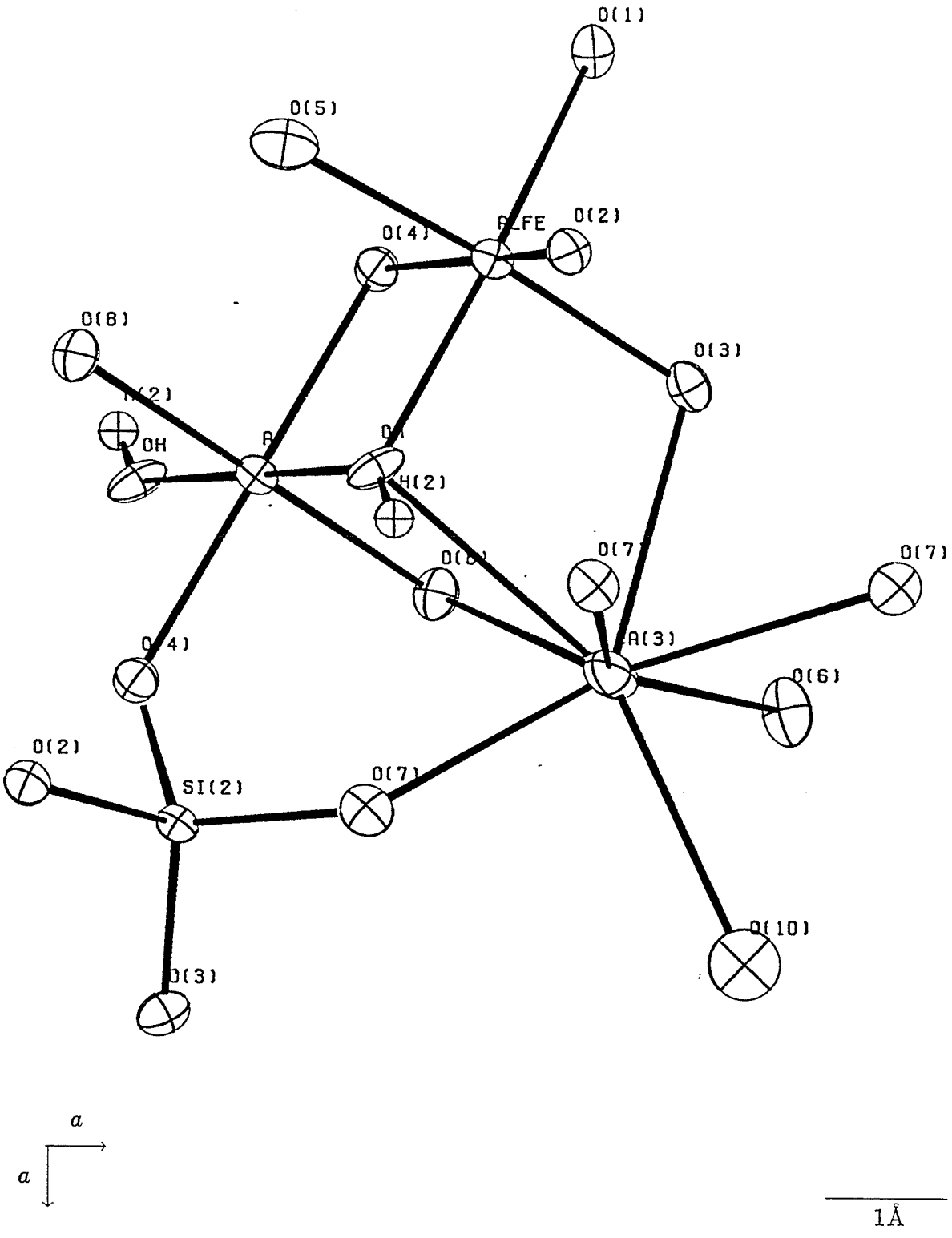

Figure 5: The atomic arrangement around OH. The atomic positions are from Yoshiasa and Matsumoto (1986).

1.5 Transmission Electron Microscopy

There has been a modicum of TEM work done on vesuvianite. Buseck and Iijima (1974) presented high-resolution images of a vesuvianite from Thetford Mines, Quebec. An electron diffraction pattern showed weak "forbidden" $hk0$ reflections that the authors thought might be due to antiphase domains. Allen (1985) reported attempts to image a domain structure but these were not successful. Veblen and Wiechmann (1988) examined a vesuvianite from Crestmore, California, and found a highly-variable domain structure. Electron- diffraction patterns appeared to be consistent with space group $P4/n$. X-ray analyses showed no detectable compositional variations associated with the different domains. Veblen and Wiechmann also found that the twinning was not strictly merohedral, indicating a true space group symmetry lower than $P4/n$. The authors suggest that the vesuvianite grew as $P4/nnc$, with disordered B and C sites, and that subsequent ordering lowered the symmetry and produced the domain structure.

Veblen and Wiechmann (1988) also examined a vesuvianite from Eden Mills, Vermont, and found no large-scale domains, only fine-scale modulations along X.

1.6 The Chemistry of Vesuvianite

The vesuvianite structure can accommodate a wide variety of ions in a number of different sites. This has contributed to the uncertainties associated with the structure.

1.6.1 Proposed General Formulae

On the basis of their crystal structure results, Warren and Modell (1931) proposed a general formula for vesuvianite (Table 6). Unfortunately, available chemical analyses showed more (Al, Mg, Fe) and less Ca than provided for by this formula. A year later, Machatschki (1932) proposed an empirical formula based on published chemical analyses of vesuvianite. Barth (1963) took a similar approach, and concluded that chemical data should be normalized on a total of 38 anions. A number of studies on the experimental stability of vesuvianite suggested a formula based on 76 anions (Ito and Arem, 1970). None of these formulae fit the crystal structure results of Warren and Modell (1931).

Coda *et al.* (1970) and Rucklidge *et al.* (1976) suggested new formulae based on their structural data (Table 6). Both have 19 X and a total of 13 Y cations, with 78 anions rather than the 76 of earlier studies. They differ only in the disposition of the 13 Y cations and in their approach to data normalization. Coda *et al.* (1970) recalculate their analyses on the basis of 19 Ca ions, while Rucklidge *et al.* (1976) normalize their data on 18 Si ions.

Deer *et al.* (1982) tried both methods, but saw no reason to alter their usual procedure of recalculating analyses on the total number of anions—in this case, on 78(O,OH,F). They also pointed out that the Y group cations are undivided, and that although the formula of Rucklidge *et al.* (1976) fits the samples studied by them, many other natural vesuvianites have less than 1.00 Fe cation p.f.u.. As a result, Deer *et al.* (1982) proposed two general formulae for the majority of natural vesuvianite specimens.

Table 6: Proposed general formulae for vesuvianite.

Formulae	Normal-ization	Study
$4[Ca_{10}Al_4(Mg,Fe)_2Si_9O_{34}OH_4]$		Warren and Modell (1931)*
$2[X_{19}Y_{13}Z_{18}(O,OH,F)_{76}]$ X = Ca (Na, K, Mn) Y = (Al, Fe^{3+}, Fe^{2+}, Mg, Ti, Zn, Mn) Z = Si		Machatschki (1930, 1932)
$4[X_{10-u}Y_{6+u}Z_9(O,OH,F)_{38}]$ $u \leq 1$ X = Ca (Na, K, Mn) Y = (Al, Fe^{3+}, Fe^{2+}, Mg, Ti, Zn, Mn) Z = Si	38(O,OH,F)	Barth (1963)
$2[Ca_{19}(Mg,Fe,Al,Ti,Mn)_5Al_8(O,OH)_{10}(SiO_4)_{10}(Si_2O_7)_4]$	19 Ca	Coda *et al.* (1970)*
$2[Ca_{19}Fe(Fe,Ti,Mn,Mg,Al)_8Al_4Si_{18}O_{70}(OH,F)_8]$	18 Si	Rucklidge *et al.* (1976)*
$2[Ca_{19}(Al,Mg,Fe,Mn,Ti)_{13}Si_{18}O_{70}(OH,F)_8]$ or $2[Ca_{19}(Al,Fe)_{10}(Mg,Fe)_2Si_{18}O_{70}(OH)_8]$	78(O,OH,F)	Deer *et al.* (1982)
$2[X_{18}[C_iB_j]A_4Y_8Z_{18}(O,OH,F)_{78}]$ $0 \leq i \leq 1$, $j = 2 - i$ X = Ca, Na, K, Fe^{2+}, Mn Y = Al, Mg, Fe^{2+}, Fe^{3+}, Ca, Ti, Cr, Mn, Cu, Zn Z = Si, Al B = Mg, Fe^{2+}, Fe^{3+}, Cu, Zn C = Ca, Na, Fe^{2+}, Mn	50 cations	Allen (1985)*
$2[Ca_{19}(Mn,Fe^{2+})(F,OH)_2(Mg,Fe^{2+},Mn,Al,Fe^{3+},Ti)_8-Al_4(OH,F,O)_8(SiO_4)_{10}(Si_2O_7)_4]$		Yoshiasa and Matsumoto (1986)*

*Based on structural data.

Hoisch (1985) studied the results of Coda *et al.* (1970) and Rucklidge *et al.* (1976) and decided that data normalization should be on the basis of 50 cation sites p.f.u.. Allen (1985) presented a new structural formula, and suggested that analyses should be recalculated on the basis of 50 cations and 78 anions p.f.u.. Charge balance is maintained by adjusting the O^{2-}/OH^{-} ratio.

No one to date has looked at how well these formulae and normalization schemes fit a large number of analyses of vesuvianite from a number of localities.

1.6.2 Major Element Chemistry *

Both Coda *et al.* (1970) and Rucklidge *et al.* (1976) suggested that all fourfold sites in vesuvianite are filled with Si and all occupied eightfold sites with Ca, for a total of 18 Si and 19 Ca ions p.f.u.. Ito and Arem (1970), however, proposed a substitution involving Al for Si in the Si(2) site, and many other studies have suggested that (based on chemical analyses) a small amount of Al→Si substitution is probable.

In previously published analyses, the Ca content is often less than 19 ions p.f.u., usually because of Na substitution (probably at the distorted Ca(3) site). It has also been suggested that a small amount of Fe^{2+} may also enter the Ca(2) site (Manning, 1975).

If normalized to 50 cations, analyses should show a total of 13 cations in the *A*, *B* and AlFe sites. Coda *et al.* (1970) and Rucklidge *et al.* (1976) both consider the symmetrical *A* site to be occupied only by Al. However, Manning and Tricker (1975) suggest that a small amount of Fe^{2+} can enter this site (see Section 1.7.1).

The solid solution in vesuvianite occurs mainly at the *B* and AlFe sites. The fivefold *B* sites are occupied by (Mg, Fe^{2+}, Fe^{3+}, Al) and the AlFe sites by (Al, Mg, Ti, Fe^{2+}, Fe^{3+}). These two sites are separated by a SiO_4 tetrahedron, and for this reason it is unlikely that coupled substitution occurs between the two sites (Hoisch, 1983).

Hoisch (1985) looked at 22 microprobe analyses of vesuvianite from the Big Maria Mountains in California, and identified eight independent chemical substitutions. Based on an observed one-for-one exchange of Mg for Ti, Hoisch (1985)

---

* Spectroscopic studies are discussed in more detail in Section 1.7.

suggested subdividing the AlFe site into at least two distinct sites. This is because the above exchange is possible only when the substitutions

$$H^+ + Al^{3+}_{AlFe} \rightleftharpoons Ti^{4+}_{AlFe}$$

and

$$2Al^{3+}_{AlFe} \rightleftharpoons Mg^{2+}_{AlFe} + Ti^{4+}_{AlFe}$$

operate at different AlFe sites. In addition, Hoisch (1985) presented a formula for a reference composition Mg-vesuvianite (with no Fe, Ti, or Na) in which one of the AlFe sites is filled with Mg, and the other seven with Al. In addition, the *B* sites are filled with Mg. Allen (1985) looked at the limits of solid solution in vesuvianite as well, and derived sixteen one-for-one substitutions, six coupled substitutions, and three involving vacancies. Allen (1985) also identified a formula for a reference composition vesuvianite similar to that of Hoisch (1985).

1.6.3 Minor Element Chemistry

A wide range of minor elements may be found in the vesuvianite structure. Many studies have suggested that the anomalous optical properties of some vesuvianites are due to the presence of minor or trace elements. The following are elements known to occur in vesuvianite in minor amounts.

Be: Numerous authors have reported minor amounts of beryllium in vesuvianite. Palache and Bauer (1930) found 9.2 wt.% BeO in a vesuvianite from Franklin, N.J., although a later spectroscopic examination of the same material (reported in Hurlbut, 1955) showed only 0.17 wt.% BeO. Silbermintz and Roschkowa (1933) examined fourteen samples from a number of localities and found Be (0.008–0.18 wt.% BeO) in only three of them. Meen (1939) reported 1.07 wt.% BeO in a sample from Great Slave Lake, and Hurlbut (1955) described a search for beryllian vesuvianite in which several hundred analyses gave a maximum of 1.5 wt.% BeO.

Beus (1957) suggested that Be replaces Si in vesuvianite, because of their similar ionic radii. Deer *et al.* (1962) thought that Be might substitute for Mg and Fe. Deer *et al.* (1982) noted that the unit cell volumes of beryllian vesuvianites are smaller than average, perhaps as a result of Be replacing Si in the tetrahedral sites.

Rucklidge *et al.* (1976) suggested that Be replaces Si in vesuvianite, or may occupy a vacant tetrahedral site; their crystal structure refinement of the sample analyzed by Meen (1939) showed that any Be would be in excess of the required number of cations. Allen (1985) discovered additional electron density in the structure of a vesuvianite from Luning, Nevada, and successfully refined Be in this (tetrahedral) site. An ion probe analysis, however, did not reveal any Be in the Luning vesuvianite.

B: Many analyses of vesuvianite report appreciable boron, although as with Be the structural role of B is unclear.

Jannasch (1884) found 2.81 wt.% B_2O_3 in optically-positive vesuvianite from the Wilui River in Siberia; a later analyses by Wherry and Chapin (1908) gave 4.10 wt.% B_2O_3 on material from the same locality. Oftedal (1964) studied boron-bearing vesuvianites from Norway and concluded that those with >1% B_2O_3 were optically positive ("wiluites") and those with less were optically negative. This was confirmed by Khotina (1968) and Serdyuchenko *et al.* (1968). However, other optically positive vesuvianites have been reported with no appreciable boron content.

Isetti and Penco (1961) placed B in the (OH,F) group, and Mel'nitskiy (1966) stated that B replaced Al in the structure. Serdyuchenko *et al.* (1968) found that there are few structural vacancies in the SiO_4 tetrahedra, and suggested that a BO_3 complex replaces OH_3 in brucite-like groupings.

F: Fluorine has been reported in a number of recent analyses. Hoisch (1985) found 3.48 wt.% F in a vesuvianite from the Big Maria Mountains in California, and Barth (1963) reports 2.45 wt.% F in a vesuvianite from Kristiansand, Norway. Fluorine undoubtedly replaces OH in the vesuvianite structure.

Na: Sodium has been reported in vesuvianites from a number of localities, but the most Na-rich specimens are from altered alkali syenites and related rocks. Quensel (1915) found 0.86 wt.% Na_2O in a vesuvianite from the nepheline-syenite at Almunge, Sweden, and Inoue and Miyashiro (1951) describe a sodium-rich sample (0.85 wt.% Na_2O) from a nepheline-syenite in Korea. In addition, Kononova (1961) found 0.87 wt.% Na_2O in a metamict sample from an alkaline pegmatite at Tuva, U.S.S.R..

Sodium probably substitutes for Ca in vesuvianite, probably at the distorted Ca(3) site.

K: Potassium is rarely present in vesuvianite. Serdyuchenko *et al.* (1968) found 0.19 wt.% K_2O in a vesuvianite from Uzun Tashty, U.S.S.R., and Bradshaw (1972) reported 0.52 wt.% K_2O in the unusual antimonian vesuvianite from Malaysia. Fitzgerald (1985) found that only one sample out of 53 analyzed for K_2O contained more than background (0.13 wt.% K_2O).

Like sodium, potassium is thought to substitute for Ca in the vesuvianite structure.

Ti: Titanium is often present in vesuvianite, sometimes in appreciable amounts. Vesuvianites with high rare-earth contents are often enriched in Ti, and Inoue and Miyashiro (1951) noted that samples from nepheline-syenites and related rocks frequently have higher than average Al and Ti contents. Murdoch and Ingram (1966) described a cerian vesuvianite from San Benito Co., California, that had 5.5 wt.% TiO_2. Fitzgerald (1985) analyzed a vesuvianite from the same locality and reported 6.69 wt.% TiO_2. Fitzgerald (1985) also noted that vesuvianites from the same locality may contain very different amounts of Ti—two samples from Lake Jaco, Mexico, for example, gave 0.48 and 3.41 wt.% TiO_2, and did not greatly differ in appearance.

Manning (1975) found that high-Ti vesuvianites are brown or yellow, and low-Ti vesuvianites are green. According to Deer *et al.* (1982), the pink colour seen in some Ti-rich vesuvianites in thin section is due to the presence of Ti^{3+}, and that in general an increase in the specific gravity and refractive indices of vesuvianite may be related to increasing amounts of Ti and Fe.

Ti is thought to occur in the general AlFe site in vesuvianite, although Manning (1976) suggested that minor amounts occupy the eight-coordinated *C* sites. Manning and Tricker (1975) suggest that it can also occupy the fivefold *B* site.

Cr: Trace amounts of chromium have been found in vesuvianites from a handful of localities, usually those associated with ultramafics. Fitzgerald (1985) describes a sample from Asbestos, Quebec, with 0.22 wt.% Cr_2O_3, and a vesuvianite from a serpentinite in Greece contained $\leq$0.69% Cr_2O_3 (Economou and Marcopoulos (1980)). In general, chromium-bearing vesuvianites are a vivid green colour, as Cr

is a strong chromophore in vesuvianite. Cr probably occurs at the general AlFe site in vesuvianite.

Mn: Arem (1970) found that almost all vesuvianites contain at least trace amounts of manganese. Glass *et al.* (1944) found 4.48% MnO in a vesuvianite from Iron Mountain, New Mexico, and Fitzgerald (1975) reports 3.34 wt.% MnO in a Swedish specimen. According to Fitzgerald (1985), Mn is a chromophore in vesuvianite, and small amounts often give rise to a purple colouration (but only if the Fe content is low).

Mn is thought to occur in the general AlFe site in vesuvianite, but some authors have suggested that it substitutes for Ca, probably in the distorted Ca(3) site.

Cu: Copper-bearing vesuvianites have been reported from the Telemark district, Norway; San Benito Co., California; and Franklin, N.J.. They are often green or blue ("cyprines"), and may have a fibrous habit. Neumann and Svinndal (1955) reported 0.73 wt.% CuO in a vesuvianite from Telemark, and Fitzgerald (1985) found 1.91 wt.% CuO in a cyprine from Franklin. Fitzgerald (1985) also discovered that some red and brown vesuvianites at Franklin contain as much Cu as the cyprines, and that the amount of Fe probably determines the colour. The crystal structure of a copper-bearing vesuvianite was refined by Fitzgerald *et al.* (1987); as expected, the Cu occurs at the B site.

Zn: Zinc is common in vesuvianites from Franklin, N.J.. Steiger (1922) and Lewis and Bauer (1922) report 1.42 and 1.70 wt.% ZnO in cyprines from Franklin, and Fitzgerald (1985) found 4.27 wt.% ZnO in a crystal from this deposit. Minor amounts of Zn have been reported in vesuvianites from some other localities as well. Zn probably occupies the general AlFe site in vesuvianite.

Y and the Rare Earths: A number of vesuvianites with appreciable rare earth contents have been reported. Orlov and Mart'yanov (1961) described specimens from the Yenisei Mountains with 4.31 wt.% RE_2O_3 (Ce, La, Nd). Fitzgerald *et al.* (1987) refined the structure of a cerian vesuvianite from San Benito Co., California (17.19 wt.% RE_2O_3) and found that the rare earths substitute for Ca at the Ca(3) site. These authors identified a coupled substitution of the rare-earths and Ti for Ca and Mg (at the AlFe site); note that this is unbalanced.

Metamict vesuvianites containing U, Th and rare-earth elements have also been reported, usually from alkali igneous rocks.

H_2O : There have been some reports linking high birefringence and large cell dimensions in vesuvianite with increased OH content (Deer *et al*, 1982). A number of studies have suggested that a "hydrovesuvianite" might exist, in which H_2O replaces a SiO_4 group, analogous to the hydrogarnets. Christie (1961, 1962) proposed that "californite" might be such a phase.

Fitzgerald (1985) analyzed four samples for H_2O using the Penfield method, and found that in all cases the amount recorded was much lower than expected by charge balance considerations. This may be because (according to Peters, 1961), most of the structurally-bound water is not lost until $\approx 1030°C$, nearly the melting point of vesuvianite.

Other Elements: Serdyuchenko *et al.* (1968) reported 0.33 wt.% Cl in a vesuvianite from Uzun Tashty, U.S.S.R.. Ito and Arem (1970) found that minor amounts of Co and Ni will substitute in synthetic vesuvianite. Dobson (1982) discovered up to 0.6 wt.% SnO_2 in vesuvianite from a skarn at Lost River, Alaska. Bradshaw (1972) reported a vesuvianite from Sarawak, Malaysia, with 15.73 wt.% Sb_2O_3 (replacing Ca). This sample also contained 0.28 wt.% Li_2O.

1.7 Spectroscopic Studies

1.7.1 Mössbauer Spectroscopy

Manning and Tricker (1975) used optical absorption and Mössbauer spectroscopy to determine site populations of Fe and Ti ions in a number of vesuvianites. They found that in green low-Ti samples, more than 90% of the total iron occurred as Fe^{3+} at the AlFe positions. In yellow-green vesuvianites with >1.0% TiO_2, most of the iron was present as Fe^{2+} at the *B* sites. These authors also found minor amounts of Fe^{2+}, Fe^{3+} and Ti^{4+} at the *C* sites. Ti was thought to occupy the AlFe sites with lesser amounts in eight and possibly five coordination.

Osborne and Burns (1978) noticed apparent peak asymmetry in some vesuvianite spectra. This led them to suggest that both Fe^{2+} and Fe^{3+} are found in the fivefold *B* site.

Other Mössbauer studies of vesuvianite include those of Tricker and Manning (1979) and Vaishnava *et al.* (1980). Tricker *et al.* (1981) found Fe^{2+} in the general AlFe site but also in the more symmetrical *A* site, which conflicts with X-ray structure refinement results (Allen, 1985).

Allen (1985) decided that the Fe^{3+} (VI) and Fe^{3+} (VIII) doublets seen in previous studies should be reassigned to Fe^{3+} (V) and Fe^{3+} (VI) respectively. He concluded that Fe^{3+} and Fe^{2+} may occupy both the *B* and AlFe sites, although Fe^{3+} shows a preference for the fivefold *B* site and Fe^{2+} favours the octahedral AlFe position. Small amounts of Fe^{2+} may also occupy the eight coordinated Ca or *C* positions.

1.7.2 Optical Absorption Spectroscopy

Manning (1968) described the optical absorption spectrum of a green vesuvianite from Eden Mills, Vermont. The principle absorptions were attributed to octahedrally bonded Fe^{3+}. However, the energies of sharp bands in this region were different from those seen in andradite and grossular (Manning 1967, 1969, 1972). This suggested that the octahedral sites in garnet and vesuvianite are dissimilar.

Manning (1975) examined the optical absorption spectra of three titanium-bearing vesuvianites. He found that their colour and pleochroism arise mainly from $Fe^{2+} \rightarrow Ti^{4+}$ and $O \rightarrow Fe$ charge-transfer processes. One polarized band was assigned to charge-transfer between Fe^{2+} and Ti^{4+} ions at adjacent C positions along the fourfold axes. Another absorption band was attributed to charge-transfer between Fe^{2+} and Ti^{4+} in adjacent AlFe and Ca(2) positions.

Manning (1976) suggested that the strongly-polarized bands present in absorption spectra of green vesuvianites are due to $Fe^{2+} \rightarrow Fe^{3+}$ charge-transfer between ions in adjacent antiprismatic C positions. This was refuted by Allen (1985) with the contention that a coordination number of eight for ferric iron is unreasonable based on the size ratio of Fe^{3+} to O^{2-}.

Osborne and Burns (1978) suggested that the colour and optical spectra of vesuvianite are dominated by *d–d* transitions involving Fe in five- and six-fold coordinations.

1.7.3 Infrared Spectroscopy

Coda *et al.* (1970) used single-crystal infrared absorption spectroscopy to confirm the presence of a hydrogen bond between O(10) atoms. Zabinski (1971) presented the OH-stretching regions of powder infrared spectra from five iron-bearing vesuvianites. Saksena (1961) and Morandi *et al.* (1979) also present powder infrared spectra of vesuvianites. To date no one has used single-crystal infrared spectroscopy to investigate the role of H in vesuvianites of different compositions.

1.8 Vesuvianite Paragenesis

Vesuvianite is found in a variety of rock types, including:

1. Skarns, calc-silicate hornfels, and calc-schists.
2. Rodingites associated with serpentinites.
3. Altered alkali syenites and related rocks.

It seems to be stable over a wide range of metamorphic temperatures. The compositional field of vesuvianite is closely related to that of grossular garnet, with which it is often associated. The controlling factor as to which of these two will actually crystallize may be the relative activities of H_2O and CO_2. Ito and Arem (1970) suggested that vesuvianite stability will tend to increase with increasing water and decrease as the CO_2 activity rises.

1.8.1 Skarns, Hornfels and Calc-Schists

Vesuvianite occurs most commonly in contact metamorphic skarns, such as those at Lake Jaco, Mexico; Crestmore, California; Sanford, Maine; and Franklin, N.J.. These rocks formed through the metasomatic alteration of impure limestones adjoining granitoid intrusions rich in volatile elements. This usually involves migration of Fe, Mg, Mn and Si into the country rock at a wide range of temperatures (500–800°C) and generally low pressures. In these deposits, vesuvianite is usually associated with diopside, wollastonite and grossular.

It is also found in calc-silicate hornfels, which are similar to calc-silicate skarns but form by isochemical recrystallization (and loss of volatiles) instead of metasomatism. These rocks are generally fine-grained and more homogeneous than the skarns. The vesuvianite-bearing rocks ejected from some volcanic pipes (such as Somma and Vesuvius, Italy) are calc-silicate hornfels.

Vesuvianite may also occur in calc-schists formed by regional metamorphism of calcareous-pelitic sedimentary rocks. Chatterjee (1962) describes a vesuvianite-epidote paragenesis resulting from greenschist facies regional metamorphism in the

Alps. Braitsch and Chatterjee (1964) and Trommsdorff (1968) describe similar occurrences.

1.8.2 Rodingites

Vesuvianite is commonly found in dense fine-grained rodingites associated with serpentinites. These are metasomatic rocks resulting from low temperature ($<$ 300°C) serpentinization of the adjacent ultramafic rock. They usually occur as dikes or sills enclosed in the serpentinite, and are made up of calc-silicate minerals such as vesuvianite, grossular, diopside, prehnite, zoisite and chlorite. These minerals often form fracture-filling veins within the rodingite. Examples of this paragenesis are Jeffrey Mine, Quebec; Georgetown, California; and Eden Mills, Vermont.

1.8.3 Altered Alkali Syenites

Altered alkali syenites and related rocks may also contain vesuvianite, resulting from the post-magmatic breakdown of melilite with decreasing temperature (Allen, 1985). The only vesuvianite-bearing localities of this type are Egan Chute, Ontario (a nepheline-gneiss complex); Fukushinzan, Korea; Seiland, Norway; Almunge, Sweden; Seward Peninsula, Alaska; Iron Hill, Colorado; and Tuva, U.S.S.R..

1.8.4 Composition vs. Paragenesis

Inoue and Miyashiro (1951) studied variations in the chemical composition of vesuvianite from the three modes of occurrence. They found that vesuvianites from nepheline-syenites are often enriched in Al and Ti. Allen (1985) found that vesuvianites from the high-temperature skarn, hornfels, and calc-schist deposits are usually optically uniaxial and show few reflections that violate the $P4/nnc$ space group ("high"-vesuvianites). Those from the lower-temperature rodingites or altered alkali rocks generally exhibit biaxial character and sector zoning, and many reflections that violate the $P4/nnc$ space group ("low"-vesuvianites). Allen (1985) believes that this is a result of ordering that takes place during crystal growth, rather than an ordering transformation on cooling.

1.9 The Present Status of Vesuvianite

It is apparent from the foregoing discussions that significant crystal chemical problems persist with respect to vesuvianite:

1. The current structure refinements are not compatible with the optical properties.
2. The general chemical formula seems to be rewritten with each structure refinement or chemical study.
3. The infrared spectra are highly unusual.
4. There seems to be a lack of information in HRTEM images of vesuvianite when compared to the optical, structural, chemical, and spectroscopic problems associated with this mineral.
4. The role of B in the structure is unknown.

Because of the uncertainties associated with work on vesuvianite, it seemed essential that any further study should try and address every aspect of its crystal chemistry and physical properties. Consequently I decided to examine a large number of vesuvianites from many localities, to characterize:

i) optical characteristics, including uniaxial/biaxial behaviour, 2V and optic sign.
ii) detailed chemistry, by microprobe and wet chemical techniques (for Be, Li, Fe^{2+}, H_2O and CO_2).
iii) diffraction characteristics on selected samples, including sector-zoned crystals.
iv) unit cell dimensions.
v) the crystal structures of non-tetragonal vesuvianites.
vi) polarized (and unpolarized) single-crystal infrared spectroscopy to examine the (possibly changing) role of H as a function of chemistry in the structure.

Chapter 2

EXPERIMENTAL METHODS

2.1 Sample Preparation

Each sample was observed under a binocular microscope, and the colour, size and morphology of the crystals were recorded (Appendix B). All large euhedral vesuvianite crystals were removed for sectioning, and accessory minerals were noted or set aside for identification by X-ray methods. The remaining material was crushed with a hammer or jaw crusher to a maximum size of 1–2 mm, and the fragments were separated manually for grinding. A magnet was used to remove any metal introduced at the crushing stage.

The separated material was ground by hand under methanol in an alumina mortar and pestle, then dried with a heat lamp. The powder was sieved through a 200 mesh nylon screen (allowing a maximum grain size of 0.74 μm) and the process was repeated several times. This usually resulted in 0.5–5.0 g of powder for use in wet-chemical analysis.

The large euhedral vesuvianite crystals were sectioned, usually perpendicular to Z, with a 0.36 mm thick diamond blade on a homemade saw. With practice, it was possible to cut sections about 1.2 mm in width. These were labelled and attached to frosted glass slides with Piccolyte, a reversible heat-setting adhesive. A Hillquist machine with a diamond lap was then used to grind the sections to a thickness of 0.5 mm for microprobe mounts, 0.25 mm for optical sections, and $<$100 μm for single-crystal IR samples.

The microprobe mounts were made from clear lucite disks (2.5 cm $\times$ 4.0 mm). Crystals and sections chosen for analysis were placed in the bottom of holes drilled in the disks; these were then filled with Petropoxy and the mounts were cured in an oven at $\approx$110°C for 12 hours. The surface of each mount was then ground with 600 grit SiC on a cast iron lap, and polished with 6 μm diamond paste followed by 0.05 μm alumina powder on silk laps. Mounts prepared in this way are transparent, and may be used for microscopy as well as electron microprobe analysis.

After grinding on a diamond lap, those sections chosen for single-crystal IR study were remounted on fresh slides with Crystalbond adhesive. Each section

was then hand-ground with 600 grit SiC and corundum paste on a glass surface. Depending on the expected H content, the final thickness was 10–90 μm. The completed section was soaked in xylene to release it from the glass slide.

A number of crystal fragments were selected from each sample for use with the spindle stage, precession cameras, and the single-crystal diffractometer. These were usually shaped with a razor blade until equant and 0.15-0.25 mm in diameter, and each crystal was then epoxied to the end of a glass fibre set in a brass pin. The crystals used for crystal structure analysis were taken from thin sections or microprobe mounts, shaped in a sphere grinder, and mounted in the same way.

2.2 Mineral Optics

A polarizing microscope was used to examine the sectioned crystals for optical zoning, optic sign and biaxiality. Tobi's method (Bloss, 1961) was used to determine $2V$ from the acute bisectrix figure in biaxial crystals. With this technique, a micrometer ocular is used to measure the intermelatope distance relative to the radius of the field of view R. If β is known (an average value of 1.715 was used in this study), the ratio $2D/2R$ allows $2V$ to be read from Figure 10–6 in Bloss (1961). Since the numerical aperture of the objective used was 0.85, it was possible to use this chart without modification. According to Bloss (1961), this method yields values of $2V$ with an error of one degree or less.

Kamb's method (Bloss, 1961) was used to determine $2V$ values greater than 58°, the angle at which the isogyres leave the field of view. With this technique, the angle of rotation of the stage necessary to move the isogyres to the edge of the field of view is recorded. If β is known (an average value of 1.715 was used) and the numerical aperture of the objective is 0.85, V may be read from Figure 9–20C in Bloss (1961).

In some cases, $2V$ was calculated with the program EXCALIBR (Bloss, 1981) from extinction measurements made with a Charles Supper Co. spindle stage, using a filtered light source ($\lambda = 590$ nm) and Cargille oil ($n = 1.720$) as an immersion medium.

2.3 Electron Microprobe Analysis

Approximately one-fifth of the analyses presented in this study are from the MAC-5 electron microprobe at the University of Manitoba, which is equipped with an energy-dispersion (ED) spectrometer. The bulk of the analyses were done with the JEOL 733 microprobe at the National Museum of Natural Sciences, which is equipped with four wavelength-dispersion (WD) spectrometers. All analyses are by the author, unless otherwise indicated.

2.3.1 Energy-Dispersion Spectrometry

Initial analyses were made with a Materials Analysis Company electron microprobe (model MAC-5) equipped with a Kevex Micro-X 7000 analytical spectrometer. The ED spectrometer uses a Si(Li) detector with a Be window and a 1024 multichannel analyzer. Resolution is 144.6 eV for Mn $K\alpha$ at 1000 Hz.

All ED analyses were done at an accelerating potential of 15 keV, chosen so as to minimize absorption, yet still provide good peak-to-background ratios of all lines analyzed (Ercit, 1986). The sample current was 10 nA, measured on fayalite. Under standard conditions of operation, the beam diameter was 1–2 μm.

In all cases, the multichannel analyzer was set for operation at 10 eV/channel, which allowed a detection range of 1–10 keV. Within this range, at least one α-line was potentially available for analysis for all elements from $Z = 11$ (Na) to $Z = 92$ (U). Sample spectra were collected for 200 live seconds (acquisition time less detector dead time).

The data were reduced using Kevex software based on the Magic V program (Colby, 1980) and modified by T.S. Ercit. Techniques for routine quantitative analysis of silicate minerals using this software were developed by T.S. Ercit and the author.

2.3.2 Wavelength-Dispersion Spectrometry

The majority of the analyses were done with a JEOL 733 electron microprobe equipped with one ED spectrometer and four automated WD spectrometers. The crystals used were lead stearate (STE), thallium acid phthalate (TAP), pentaerythritol (PET), and lithium fluoride (LiF), allowing for analysis of elements from $Z = 5$ (B) to $Z = 92$ (U).

All WD analyses were done with an accelerating potential of 15 keV and a sample current of 25 nA. Standards were collected to 0.25% precision or for 25 seconds, whichever was less. Sample collection was to 0.5% precision or for 50 seconds. The beam diameter was intentionally defocused to 20 μm, except for samples with fine banding, where a 10 μm beam was used. Backscattered-electron (BSE) imaging was routinely used to investigate compositional differences. For vesuvianite, which is made up of relatively light elements, it was possible to detect a difference of only 0.5 in average Z in the backscattered image. The ED spectrometer was used to preview spectra and to identify accessory phases.

The data were collected and reduced with the Task program by Tracor Northern, using conventional ZAF techniques. Rare-earth element data were corrected for line overlaps, using the methods of Roedder (1985).

2.3.3 Standards

The standards used were chosen primarily to minimize ZAF corrections, and are listed in Table 8. Spectral lines used in analysis are given in Table 7.

2.3.4 Precision of Microprobe Analyses

The program used to reduce EDS data (Magic V) gives estimates of the standard deviation in the weight percentages of elements analyzed. These are based solely on count statistics of the line analyzed (both standard and sample). The standard composition itself is assumed to be free of error, and other systematic errors are disregarded. As such, the estimated precision of analysis tends to be optimistic.

The program used to process WD analyses (Task) gives estimates of standard deviation in the k-ratio for each element. This value, expressed as a percentage, may also be used to calculate estimated standard deviations in the weight percentages of elements analyzed.

Table 7: X-ray spectral lines used in analysis.

Line	Elements
$K\alpha$	B, F, Na, Mg, Al, Si, S, Cl, K, Ca, Ti, Cr, Mn, Fe
$L\alpha$	Zn, La, Ce, Pr, Nd, Sm, Eu, Gd
$M\alpha$	Pb, Bi, Th

Table 8: Standards used in electron microprobe analyses.

Element	EDS standard	WDS standard
Si	pyrope	diopside
Al	pyrope	almandine
Ti	titanite	titanite
Mg	pyrope	almandine
Mn	spessartine	willemite
Fe	fayalite	almandine
Cr	-	synthetic nichromite
Cu	-	cuprite
Zn	-	willemite
Ca	titanite	gehlenite
Na	-	Na-amphibole
K	-	Na-amphibole
La	-	REE glass (S-254)
Ce	-	REE glass (S-254)
Pr	-	REE glass (S-254)
Sm	-	REE glass (S-254)
Nd	-	REE glass (S-254)
Eu	-	REE glass (S-254)
Gd	-	REE glass (S-254)
Pb	-	crocoite
Bi	-	bismutotantalite
Th	-	monazite
U	-	synthetic brannerite
B	-	elbaite
S	-	anhydrite
F	-	fluor-riebeckite
Cl	-	tugtupite

Table 9: Precision of microprobe analyses.

Analysis V1-1_M (EDS)

Oxide Formula	Oxide Percent	2σ*	Element	Ion Percent	2σ*	Detection Limit	Collection Time
SiO_2	36.42	–	Si^{4+}	17.02	0.11	0.02	†200
Al_2O_3	17.28	–	Al^{3+}	9.15	0.10	0.04	"
MgO	1.95	–	Mg^{2+}	1.18	0.05	0.07	"
FeO	3.87	–	Fe^{2+}	3.01	0.09	0.08	"
CaO	36.08	–	Ca^{2+}	25.79	0.19	0.02	"

Analysis V1-1 (WDS)

SiO_2	36.98	0.40	Si^{4+}	17.26	0.18	0.004	5
Al_2O_3	17.04	0.20	Al^{3+}	9.02	0.10	0.003	11
TiO_2	0.14	0.02	Ti^{4+}	0.08	0.02	0.03	50
MgO	1.98	0.04	Mg^{2+}	1.19	0.02	0.005	50
MnO	0.11	0.02	Mn^{2+}	0.09	0.02	0.05	50
FeO	3.64	0.12	Fe^{2+}	2.84	0.10	0.009	50
CaO	36.09	0.46	Ca^{2+}	25.78	0.34	0.003	14

*Calculated from the standard deviation on the k-ratio.
†Entire spectrum collected for 200 (live) seconds.

Table 9 is a comparison of an ED and a WD analysis on the same sample (V1). Standard deviations on major elements are lower for the ED analysis because of the 200 second collection time. Minor element standard deviations are lower for the WD analysis. Detection limits were estimated using the formula:

$$c = \frac{2(b^{\frac{1}{2}})}{i}$$

where c is the detection limit (in wt.%), b is the background counts per unit of concentration, and i is the peak counts per unit of concentration (Russ, 1972). The Task program (WDS) prints out peak and background counts. For the ED analysis, the counts had to be measured directly from the displayed spectrum. Because of this the EDS detection limits in Table 9 are presumably less accurate than those given for WDS.

WD analyses presented in this study (Appendices E.1 and E.2) are listed to two decimal places, because of low standard deviations on minor elements and because of low detection limits. ED analyses (Appendix D) are listed to only one decimal place because of high detection limits and poor precision on minor elements. In both cases, calculated ions and statistics are listed to two decimal places.

2.4 Chemical Methods

2.4.1 Atomic Absorption Spectroscopy

Be and Li analyses were done with a Varian AA-975 atomic absorption spectrophotometer at the W.M. Ward Laboratories (Government of Manitoba). The steps used for sample dissolution are listed in Appendix F. For each analysis, 5.0 ml of doubly-distilled water and 0.5 ml of a 20,000 ppm K buffer (to minimize ionization of Li in air-acetylene) were added to 5 ml of initial solution. Calibration standards were supplied by the lab, and internal standards were GSP-1 (30 ppm Li), SY-2 (31 ppm Be), and GH (45 ppm Li, 6 ppm Be). One vesuvianite sample (V4) was analyzed at regular intervals to provide a measure of experimental precision. The relative standard deviation on seven analyses of V4 was 11% for Li and 6% for Be. Detection limits were $\approx$5 ppm for Li and $\approx$2 ppm for Be (J. Weitzel, pers. comm.).

The spectrophotometer calculates elemental content (ppm) based on an initial sample weight of 0.2 g. A final value may be obtained by multiplying through by 0.2 g/initial weight (g).

2.4.2 Determination of Ferrous Iron

Ferrous iron determinations were done at the University of Manitoba using the modified "Pratt method" described by Donaldson (1982) and outlined in Appendix F. Nitrogen was bubbled through all solutions before use to minimize sample oxidation. Standards used were AN-G (2.24 wt.% FeO), SY-2 (3.62), PCC-1 (5.06–5.24), and MRG-1 (8.65). SY-2 and a vesuvianite sample (V4) were analyzed at regular intervals to provide a measure of experimental precision. The standard deviation of eight analyses of SY2 was 0.04 (1.10%); of eight analyses of V4, 1.46 relative percent.

2.4.3 H_2O and CO_2 Determinations

The H_2O and CO_2 determinations were done with a LECO 521 induction furnace. With this technique, $\approx$1.0 gm of dry, sieved powder was weighed into a ceramic

crucible, which was then heated to ≈1200°C by a RF induction coil for six minutes. A current of oxygen gas was passed over the sample and thence to a glass bulb containing anhydrous magnesium perchlorate, which selectively absorbs H_2O. A second bulb containing ascarite was used to trap CO_2. By weighing the bulbs between each analysis, the amount of H_2O and CO_2 present was determined; a sample calculation is presented in Appendix F. Before analyzing samples, a number of blanks were run to obtain a correction factor. Internal standards were SY-2 (0.43 wt.% H_2O, 0.46 wt.% CO_2), MRG-1 (0.98, 1.00), STM-1 (1.44, 0.02), BE-N (2.24, 0.74), and PCC-1 (4.70, 0.15). SY2 and PCC-1 were analyzed at regular intervals to provide a measure of experimental precision. The standard deviation on five analyses of SY-2 was 0.08 (16.77%); on five analyses of PCC-1, 0.01 (0.22%).

2.5 Single-Crystal Infrared Spectroscopy

The infrared spectra were collected by F.C. Hawthorne and G.R. Rossman at the Division of Geological Sciences, California Institute of Technology. A Nicolet 60SX FTIR (*F*ourier *T*ransform *I*nfra*R*ed) spectrometer fitted with a rotatable polarizer was used. A series of brass apertures (12–200 μm in diameter) was used to limit the area of the sample exposed to the beam, making this a true microprobe method.

The crystal fragments were examined with a polarizing light microscope, and points were selected for infrared examination on the basis of optical character. A crystal was then set on a brass plate such that the point of interest was over the aperture, the size of which was chosen to restrict examination to a homogeneous region. The orientation of the crystal was then adjusted in cross-polarized light until the optical axes were parallel and perpendicular to the polarizer axes in the spectrometer. Once in place, the section was attached to the brass plate by putting a drop of xylene at the crystal boundary (thereby keeping the section in place by surface tension) and allowing it to evaporate. The mounted crystal was then attached to a holder and placed in the spectrometer.

Spectra were obtained in both polarizations for both $a \cdot a$ and $a \cdot c$ sections; unpolarized spectra were also recorded. Spectral data were collected digitally and then transformed from transmission units to absorbance units.

2.6 Routine X-ray Diffraction Techniques

2.6.1 Gandolfi Photography

A 114.6 mm diameter Gandolfi camera (Charles Supper Co.) was used with Ni-filtered Cu radiation (40 keV, 40 nA) to obtain diffraction patterns of included phases and associated minerals. Patterns were measured with a Supper precision film reader; with this instrument, the 2θ angles of sharp patterns can be determined to about $\pm 0.06°2\theta$ (Ercit, 1986). These values were corrected for "film shrinkage" and intensities were estimated visually.

2.6.2 Unit Cell Refinement

All unit cell refinements were done with the Nicolet $R3m$ single-crystal diffractometer. The procedure is the same as that used in the initial stages of data collection for crystal structure analysis, and is described in Section 2.7.1.

2.6.3 Precession Photography

A Charles Supper Co. Model 8000 precession camera was used in this study. All precession photography used Mo$K\alpha$ radiation (40 keV, 40 mA), both Zr-filtered and unfiltered. Crystal-to-film distances, precession angles, screen radius and settings all varied depending on the photograph. High-speed Type 57 Polaroid film was used for orientation photographs; Kodak DEF-5 film was used for final photographs.

2.7 Crystal Structure Analysis

2.7.1 Data Collection

All intensity datasets were collected with a Nicolet $R3m$ single-crystal diffractometer at the University of Manitoba. Data collection with this instrument involves four preliminary stages:

1. Mounting and optical alignment of the crystal.
2. Orienting the crystal.
3. Automatic reflection indexing.
4. Least-squares refinement of the orientation matrix and unit cell parameters.

These steps are described below.

After shaping, each crystal was epoxied to the end of a glass rod set in a brass pin. This pin was placed in a goniometer head which was attached to the diffractometer and adjusted until the centre of mass of the crystal coincided with the centre of rotation of the goniometer assembly. This was done by using the optical alignment procedure, in which the crystal is rotated about ϕ at selected settings of χ, and vice-versa.

After optical alignment, a random orientation photograph of the crystal was taken. Horizontal and vertical spacings between up to 25 equivalent reflections was used as input to the orienting program, which refined 2θ, ω, and χ for each reflection while holding ϕ constant.

An indexing program uses the refined angles from the orienting routine to set up a list of up to 60 axial vectors and 59 inter-vector angles. Unless user-intervention is desired, the program automatically selects unrefined values for a, b, c, α, β and γ, and indexes the reflections.

After indexing, the unit cell parameters and orientation matrix were refined using a least-squares procedure. When the starting cell was not appropriate (i.e. a subcell or a pseudo-symmetric cell), a second program was used to transform the axes, and to re-refine the orientation matrix and unit cell parameters.

Intensity datasets were collected using 96 step $2\theta{:}\theta$ scans with scan ranges from 2.0–2.5° 2θ, adjusted automatically to larger values with higher 2θ. Scanning speeds were automatically varied from 4°/min. for weak diffractions to 29.3°/min. for intense diffraction maxima. Two standards were collected every 46 reflections to monitor changes in beam intensity or crystal orientation during data collection. All such changes were minimal. In each case, a hemisphere of data from 3–60° 2θ was collected. Background corrections were made during data collection.

After collecting the main dataset, an additional dataset, used in calculating an absorption correction, was collected on a subset of 11 strong diffraction maxima. These data were collected every 10° of 2θ while rotating each reflection 360° about its diffraction vector (ψ). Scan parameters were the same as those used in the main collection.

Before removing the crystal from the goniometer, up to 25 strong reflections with 2θ 20–40° were selected from the diffraction record and used as input to the orienting program. This resulted in more precise cell dimensions (Hamor *et al.*, 1987) than those obtained initially using a photograph ($2\theta_{\max} \approx 30°$).

2.7.2 Data Reduction

Data reduction was carried out with the SHELXTL package of programs. The datasets were first processed with XTAPE which rejects bad data (based on peak asymmetry, centroid location, and background balance), scales on the standard reflections, and calculates *Lp* corrections.

The program XEMP was used for empirical absorption correction (spherical absorption *and* shape correction). This program uses the psi-scan data to calculate a correction which is then applied to the main dataset after the method of North *et al.* (1968). Usually, a pseudo-ellipsoid is used as the shape model in the calculations. An average value for $\mu \cdot R$ is input, where R is the crystal radius and μ is the absorption coefficient. The lengths and orientations of the semi-axes of the ellipsoid are refined while $\langle \mu R \rangle$ is held constant. This approach works well, even with irregularly-shaped crystals, when the sample contains no strong X-ray absorbing elements (as is the case with vesuvianite).

2.7.3 Structure Refinement

Structure refinement was carried out with the SHELXTL program X, which uses scattering curves for neutral atoms from Cromer and Mann (1968) and anomalous dispersion coefficients from Cromer and Libermann (1970). X uses full-matrix least-squares methods in refinement, but uses a blocked-cascade procedure if the number of refined parameters exceeds 103, which was the case in all of the refinements done in this study. The residual indices used here are the following:

$$R = \frac{\sum[|F_o| - |F_c|]}{\sum |F_o|}$$

$$R_w = \frac{\sum\{[|F_o| - |F_c|]w^{\frac{1}{2}}\}}{\sum [|F_o|w^{\frac{1}{2}}]}$$

$$R_g = \frac{\sum\{w[|F_o| - |F_c|]^2\}}{\sum [w|F_o|^2]}$$

where :

$$w = \sigma^{-2}|F_o|$$

The index R_g is used for statistical tests (Chapter 3).

Chapter 3

EXPERIMENTAL RESULTS

3.1 Vesuvianite Samples

A total of 75 vesuvianites from ≈50 different localities was examined in this study. Most specimens were provided by the Royal Ontario Museum, although some were donated by individuals, and a few were purchased. Samples, localities, and sources are listed in Appendix A.

In most cases, there is only one sample per locality, although there are 13 from Jeffrey Mine (Quebec), and three each from Mt. St. Hilaire and Templeton Township (both in Quebec). Almost half of the specimens are from Canadian localities. The occurrence of one vesuvianite (V72) is unknown; in some cases (V49, V72) only the country of origin is specified. A few of the samples are from well-known localities (e.g. Jeffrey Mine, Quebec; Franklin, N.J.; and Wilui River, U.S.S.R.); others (V1, V2, V4, V51) have not been described in any previous studies.

A number of specimens obtained for this study were found to be minerals other than vesuvianite. This is not suprising; Hauy (1797) suggested the name idocrase (from the Greek *eidos* (appearance), and *krasis*, (a mixture)) because of its resemblance to other species. One sample with unusual morphology was found to be epidote; another, from Vesuvius, was identified as diopside (both were purchased).

Initially, the colour, habit, and size of each sample was recorded; these observations are in Appendix B.

3.2 Vesuvianite Optics

The preparation of thin sections and microprobe mounts was described in Section 2.1. A polarizing microscope was used to examine the sectioned crystals for optical zoning, sign, and biaxiality, using methods outlined in Section 2.2. The results are summarized in Appendix C.

Most of the vesuvianites were optically negative; all those with positive signs contained significant amounts of boron (Table 10). This confirms the observations of Oftedal (1964), Khotina (1968), and Serdyuchenko *et al.* (1968).

Table 10: Optic signs of boron-bearing vesuvianites.

Sample	B_2O_3 avg. wt.%	Sign
V61	1.44	?
V45	1.47	+
V38	1.77	+
V74	2.84	+
V30	2.90	+
V56	2.94	?

Biaxial figures were obtained for all oriented sections; no uniformly uniaxial vesuvianites were found, although this may be due to the thickness of the mounts ($\leq$500 μm). Optic axial angles ranged from 0–>60°, sometimes in the same section (Table 11). Since optics are very sensitive to slight changes in symmetry, this suggests that most vesuvianites are nontetragonal.

It is possible to divide vesuvianites into three general groups, based on the type of optical zoning seen in (001) sections:

1. "Normal" vesuvianites show uniform extinction and usually have small $2V$ angles. Most of the vesuvianites studied belong to this group.
2. The second group is made up of vesuvianites with "blocky" zoning, in which (001) sections are divided into irregularly shaped areas with variable birefringence and extinction angles. A high-birefringence rim and a rudimentary core

Table 11: Large $2V$ angles, as determined by various methods.

Sample	$2V$ (°)	Standard	$2V$ (°) meas.	lit.*
		Tobi's Method		
V12 (rim)	37	biotite	9	0–25
V16	39	aragonite	18	18
V12 (rim)	40	muscovite$_1$	45	30–47
V14	45	muscovite$_2$	46	"
		Kamb's Method		
V13 (rim)	60			
V13 (rim)	62			
		Spindle Stage		
V11$_3$	32.8(4)	barite$_1$	36.1(4)	37
V23$_r$	44.7(2)	barite$_2$	39.9(5)	"
V21	62.1(3)			

*literature values from Roberts *et al.*, (1972)

Table 12: Blocky- and sector-zoned vesuvianites.

Sample	Locality
Blocky-Zoning	
V5 (?)	Turnback Lake, NT
V11, V12, V16, V17 (?), V21 (?) V22 (?), V23	Jeffrey Mine, PQ
V32 (?)	Wakefield Twp., PQ
V41	Hindubagh, Pakistan
Sector-Zoning	
V8 (?)	Black Lake, PQ
V13	Jeffrey Mine, PQ
V45	Laguna del Jaco, Mexico
V71	Eden Mills, VT
V74	Wilui River, USSR

may be present. Vesuvianites with this type of zoning are usually prismatic with many high index faces. Most are found in rodingites associated with serpentinites (Table 12).

3. Sector-zoned vesuvianites were found from five localities (Table 12). Sections of these crystals show a low-birefringence core, a high- birefringence rim, and distinct (110) zones extending from the core to the corners of the section. An intermediate (101) zone may also be present. Sector-zoned vesuvianites are usually prismatic; common forms are {101} and {001}. They are generally found in rocks associated with serpentinites.

To further illustrate optical variations within the groups, we will now consider examples from each group.

3.2.1 Normal Vesuvianites

Part of a (001) section of a normal vesuvianite from Ariccia, Italy, is shown in Figure 6. A BSE image (Figure 7) shows that the optical zoning corresponds to differences in mean atomic number. A series of microprobe analyses across the section show variations in F, Mg, Al, Ti, Fe and lanthanide content (Figure 8). This boron-bearing vesuvianite ($\approx$1.77 wt.% B_2O_3) is biaxial positive, with a $2V$ angle of about 30°.

3.2.2 Blocky-Zoned Vesuvianites

Blocky-zoned vesuvianites from Jeffrey Mine, Quebec, are prismatic, with many high index faces; striations and intergrowths are common. A (001) section of one of these crystals (V23) is shown in Figure 9. A high-birefringence rim ($2V$=48°) surrounds a "blocky" intermediate zone with undulose extinction and variable birefringence ($2V$=16–21°). Relative to the intermediate zone, the rim is enriched in Fe and depleted in Al.

3.2.3 Sector-Zoned Vesuvianites

Sector-zoned vesuvianites from Wilui River, U.S.S.R., occur as doubly-terminated crystals; common forms are {101}, {001}, and {110} (Figure 10).

Part of a (001) section of one of these vesuvianites is shown in Figure 11. The core has a cross-hatched pattern suggesting twinning; both the rim and the

Figure 6: Part of a (001) section of a normal vesuvianite from Ariccia, Italy (V38) (transmitted, cross-polarized light, 16×).

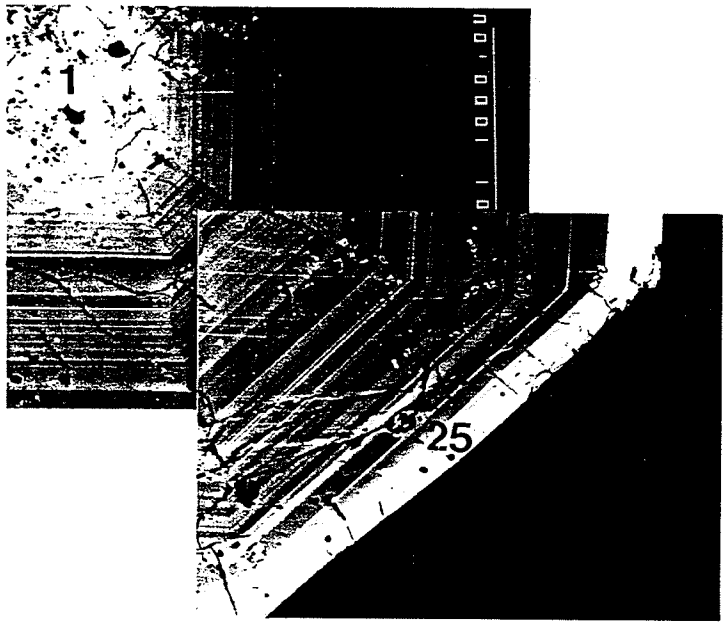

Figure 7: A BSE image of the section in Figure 6. The numbers correspond to microprobe analyses in Appendices E.1 and E.2, and to the points in Figure 8. Scale bar = 1 mm.

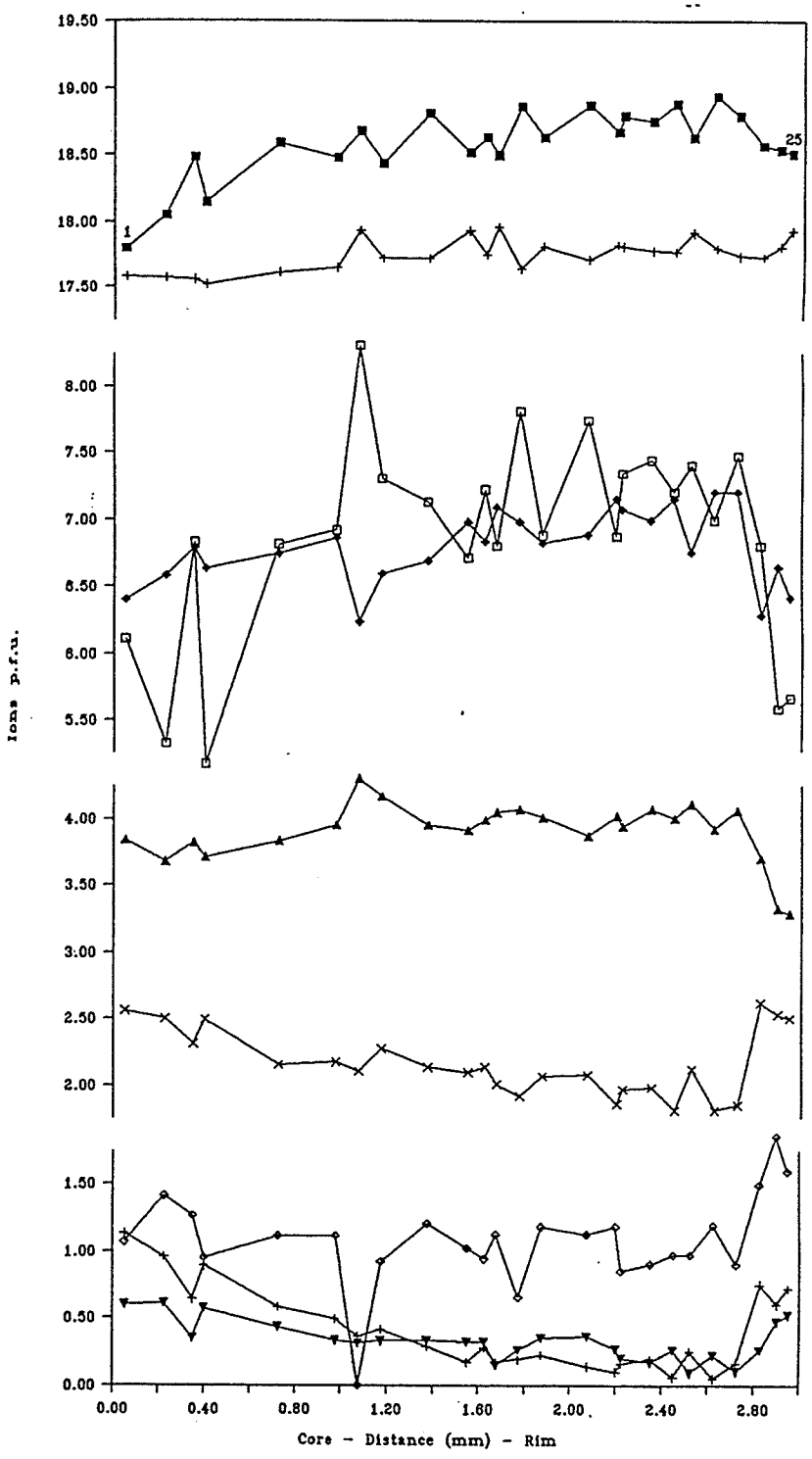

Figure 8: Variations in Ca (■), Si (+), Al (◆), calculated OH (□), Fe (▲), Mg (×), lanthanides (lower +), F (◇) and Ti (▼) across the section in Figure 6 (normal vesuvianite V38).

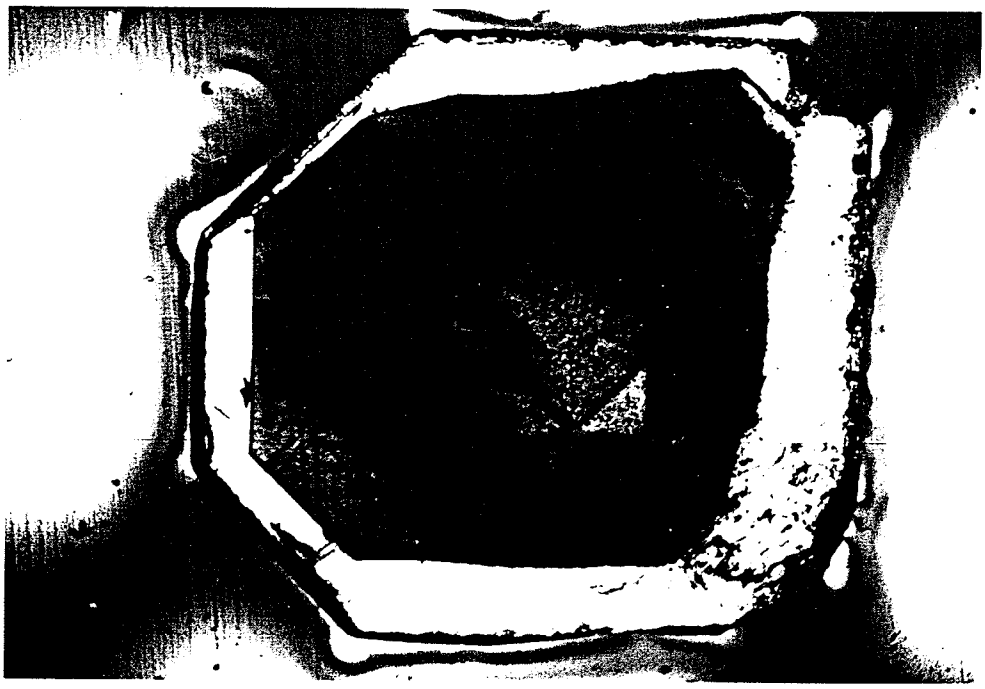

Figure 9: A (001) section of a blocky-zoned vesuvianite from Jeffrey Mine, Quebec (V23) (transmitted, cross-polarized light, 16×).

(110) zones show very fine optical striations. Also noteworthy are the birefringent grossular inclusions and the fractures following the (110)–(100) boundary.

This boron-bearing vesuvianite (≈2.84 wt.% B_2O_3) is biaxial positive, with a $2V$ angle that increases from 0–10° in the core to 10–25° in the rim. The optical zoning can be correlated to some extent with changes in composition. Figure 12 shows the results of a microprobe traverse across a section similar to that in Figure 11. There is no evidence of zoning with respect to boron content.

The sector-zoned vesuvianites from Jeffrey Mine are transparent, light brown in colour, and form singly-terminated prisms with {101} and {001} faces. A (001) section of one of these crystals is shown in Figure 13; note the low-birefringence core, the intermediate (101) zone, and the high-birefringence rim. In plane-polarized light, the core is colourless, and the outer zones are light brown. In cross-polarized light, the core appears uniaxial, with very low birefringence. The rim had a higher birefringence colour than the intermediate zone, indicating a greater difference between principal refractive indices. Figure 13 also shows light-coloured V-shaped

Figure 10: A sector-zoned vesuvianite crystal from Wilui River, U.S.S.R. (V74) (scale in mm).

Figure 11: Part of a (001) section of a crystal similar to that in Figure 10 (transmitted, cross-polarized light, 16×).

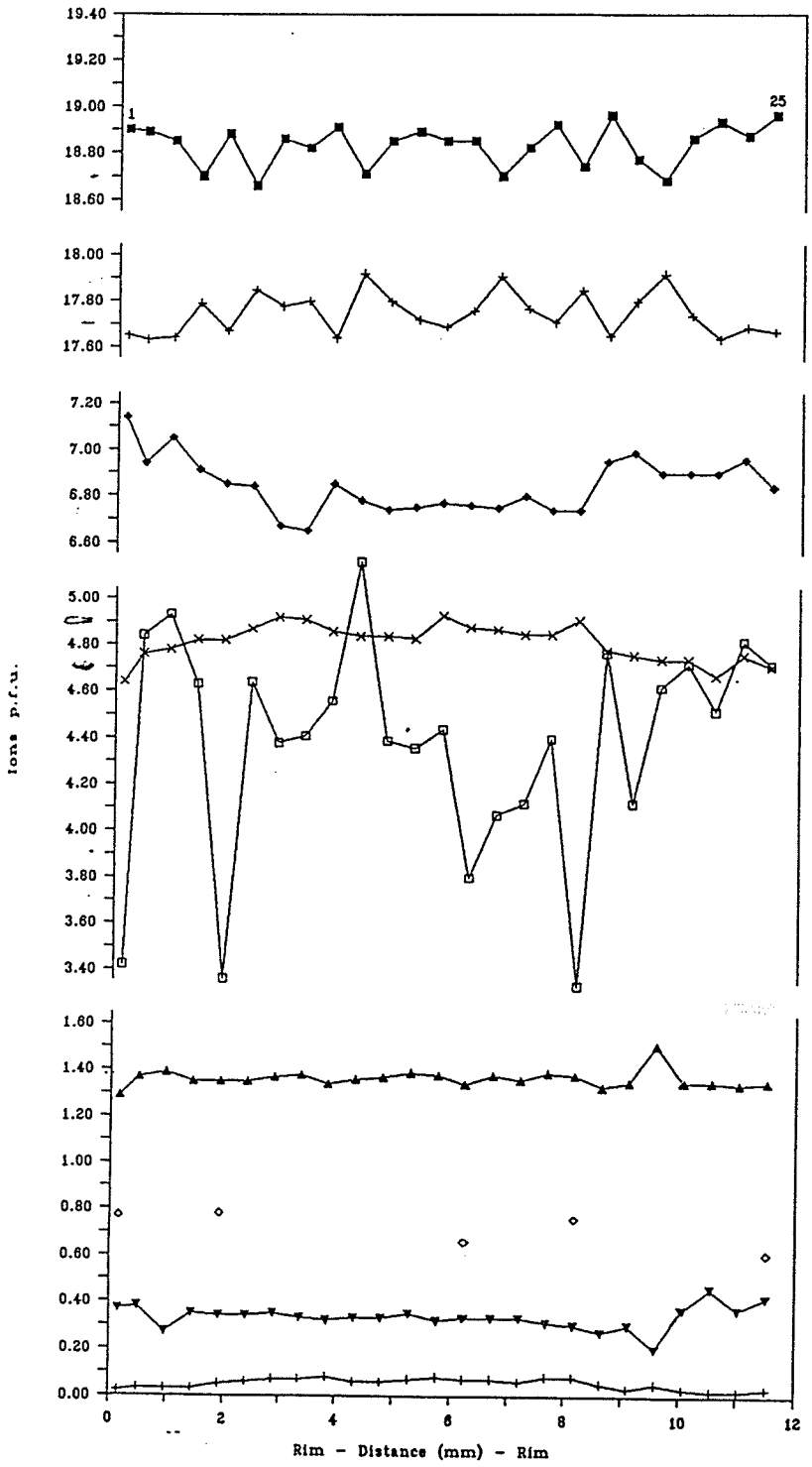

Figure 12: Variations in Ca (■), Si (+), Al (◆), calculated OH (□), Mg (×), Fe (▲), F (◇), Ti (▼) and lanthanides (lower +) across the section in Figure 10 (sector-zoned vesuvianite V74).

areas extending from the rim into the (101) zone. Another unusual feature is the low-birefringence (110) zones extending from the core to the corners of the section. These are also seen in the blocky-zoned section from Jeffrey Mine (Figure 9). These areas are very irregular in shape (note the "loops" in Figure 13) and are always surrounded by narrow extensions of the (101) zones.

All of the zones are optically positive. The core and rim of the section in Figure 13 gave perfectly centred figures, with optic axial angles of 0–10° for the core and 60–62° for the rim. The (101) zones showed off-centred figures, such that the acute bisectrix was tilted towards the core by ≈10°. Optic axial angles from this region are ≈36°, with strong dispersion (r≪v). In all of the zones, the optic axial plane is perpendicular to the edges of the section. Precession photographs (Section 3.8.1) confirm that *a* unit cell axes are parallel to the edges of the crystal.

All previous studies have reported that there is no compositional difference between the various zones. Figure 14 shows a backscattered electron image of a section similar to that in Figure 13. Note that there is a difference in mean atomic number between the zones. Variations in individual elements (from a microprobe traverse across the crystal) are shown in Figure 15. Note that the low-birefringence core is higher in Al and lower in Mg than the outer zones, suggesting an Al⇌Mg substitution. Compositional differences between the rim and the intermediate zone are less obvious.

Crystals fragments were removed from the rim, intermediate, and core zones of a section similar to that in Figure 13, and these were used for X-ray structure analysis. These crystals are referred to throughout the study as $V13_c$ (core), $V13_i$ (intermediate), and $V13_r$ (rim).

Eventually an entire V13 crystal was sectioned to investigate changes in zoning along the length of the crystal (Figure 16). Sections cut through the pyramid faces show large (101) zones and core regions. In sections taken below the {100}–{101} edge, the rim increases at the expense of the intermediate zone, and the core (which may change shape) eventually disappears. The narrow (110) zones may disappear as well, but the (101) extensions that surround them are seen in every section.

Figure 17 shows a (100) section of yet another V13 crystal. Note the irregular boundary between the (100) and (101) zones. BSE images show that this optical

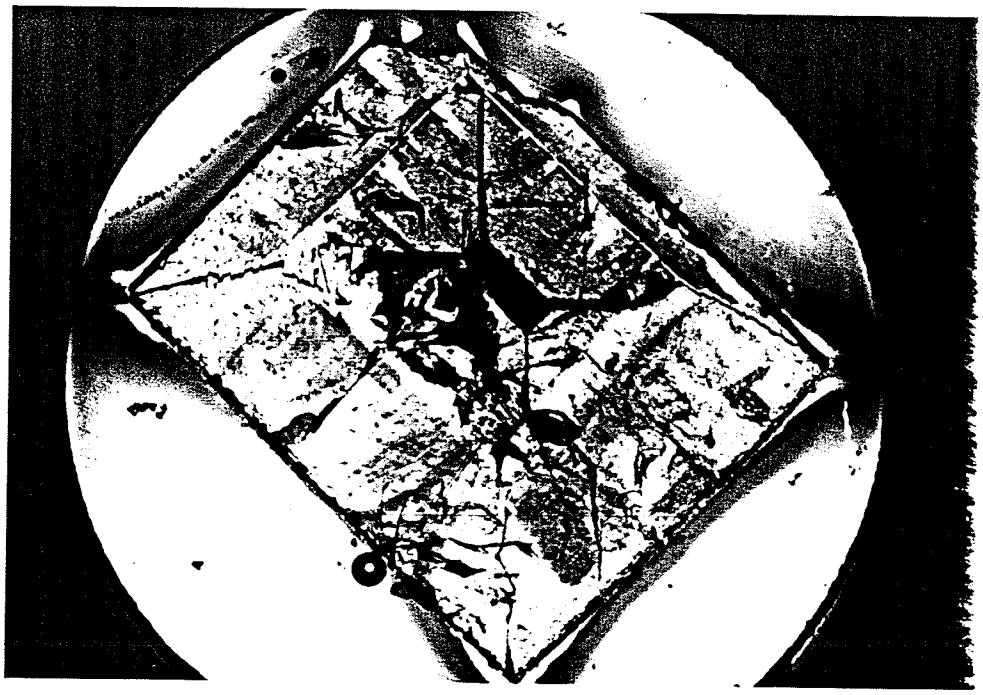

Figure 13: A (001) section of a sector-zoned vesuvianite from Jeffrey Mine, PQ (V13) (transmitted, cross-polarized light, 15×).

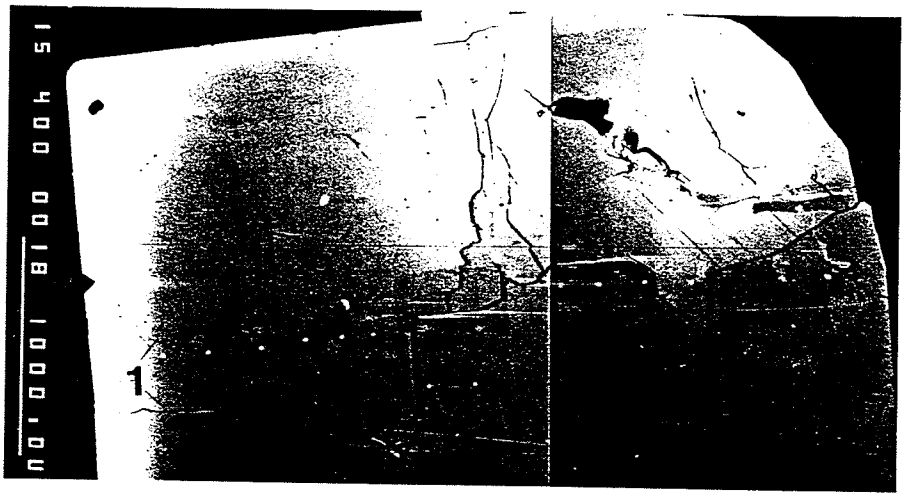

Figure 14: A BSE image of a section similar to that in Figure 13. The numbers correspond to microprobe analyses in Appendices E.1 and E.2, and to the points in Figure 15. Scale bar = 1 mm.

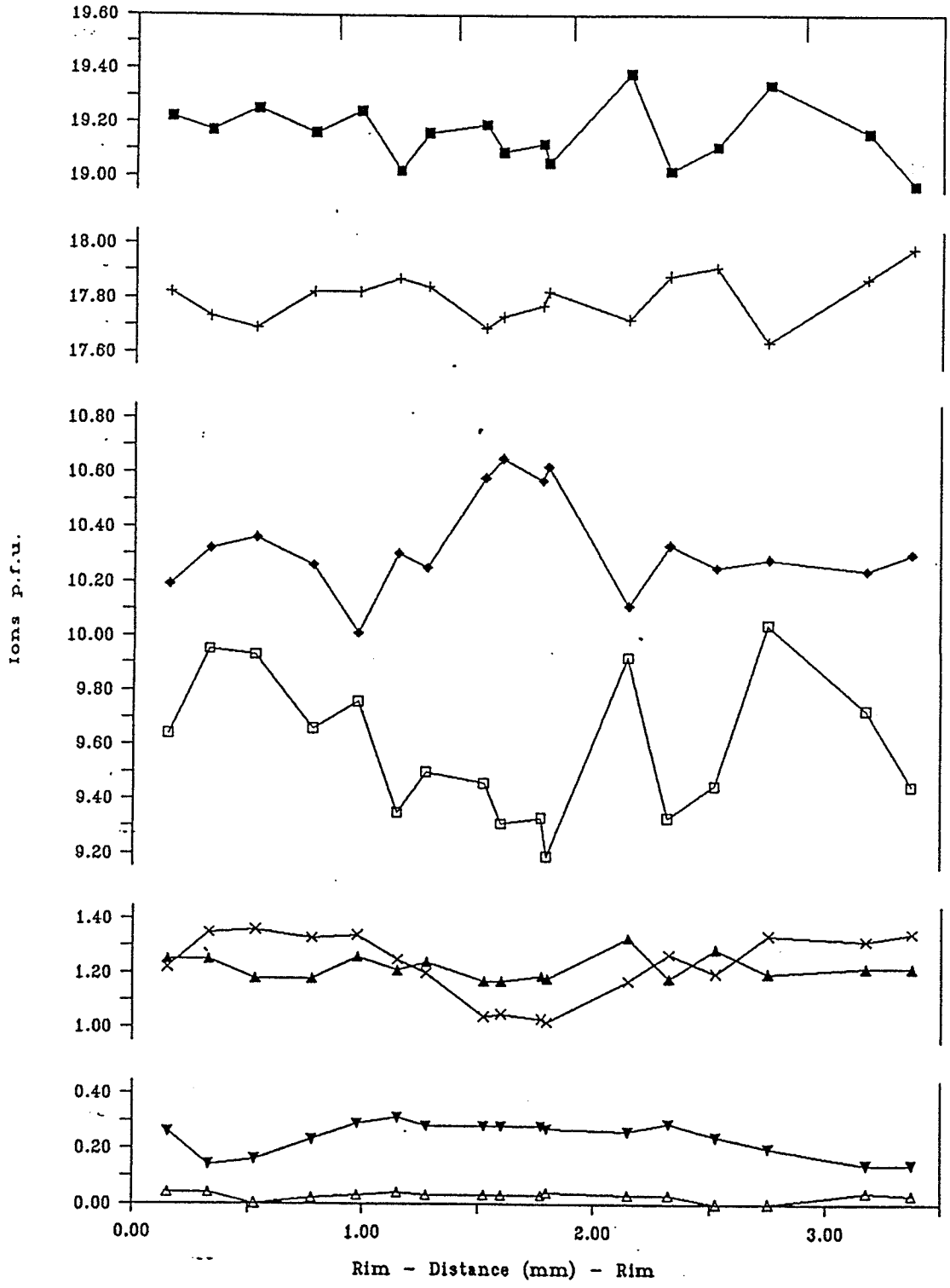

Figure 15: Variations in Ca (■), Si (+), Al (◆), calculated OH (□), Mg (×), Fe (▲), Ti (▼) and Mn (△) across the section in Figure 13 (sector-zoned vesuvianite V13).

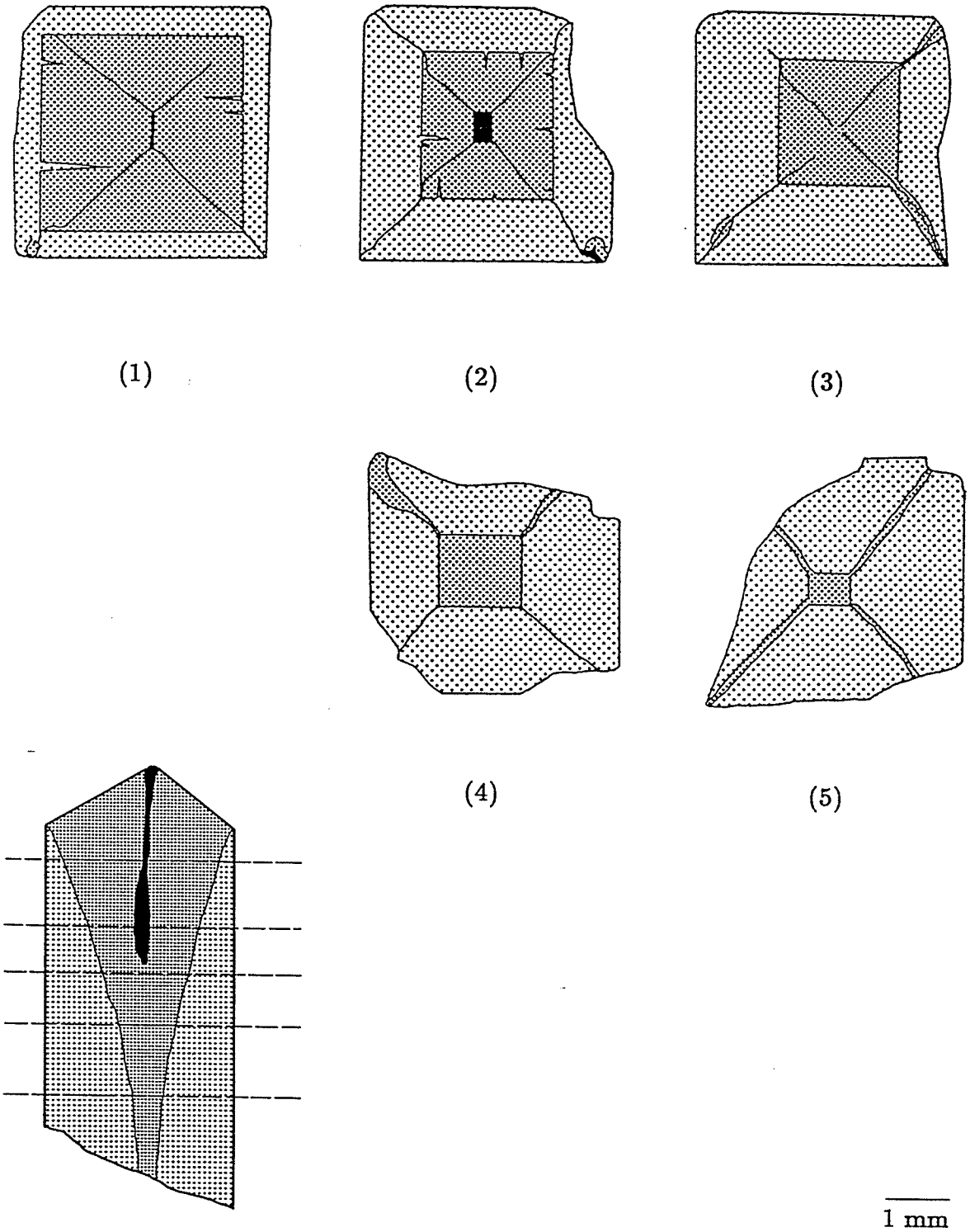

Figure 16: Serial (001) sections of a sector-zoned vesuvianite from Jeffrey Mine, Quebec (V13).

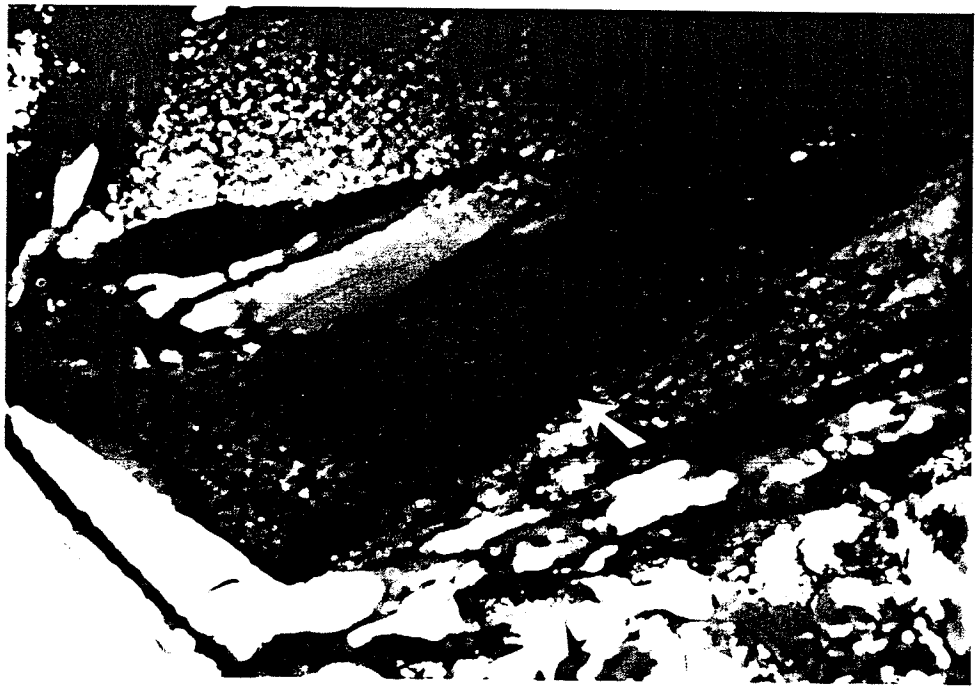

Figure 17: A (100) section of a sector-zoned vesuvianite from Jeffrey Mine, Quebec (V13). The arrow points to the boundary between the (100) and (101) zones. (transmitted, cross-polarized light, 16×).

zoning corresponds to differences in mean atomic number, but not enough analyses were done to identify variations in specific elements.

The sector-zoned vesuvianite from Mexico is similar to that from Wilui, and the Eden Mills sample is identical to the Jeffrey Mine crystals. The differences between these vesuvianites are presumably related to growth conditions, although all four occurrences are associated with serpentinites.

3.3 Electron Microprobe Analyses

In the first few years of this study, several hundred ED analyses were collected at the University of Manitoba, using the methods described in Section 2.3.1. With this technique, however, it was not possible to analyze for B or F, and high detection limits (Section 2.3.4) made it difficult to analyze trace elements. In addition, electron imaging with the MAC-5 microprobe was very limited.

In 1986, I had the opportunity to use the automated WDS microprobe at the National Museum of Natural Sciences (Ottawa). With this machine (a JEOL 733), it was possible to analyze B, F, and trace amounts of many other elements. It was also much easier to detect compositional zoning, and with online processing, many more analyses could be obtained in a given amount of time.

The original probe mounts used for ED analyses were prepared on lead laps, and despite careful cleaning, some of the spectra contained small Pb$M\alpha$ peaks. Many of these mounts were poorly polished, and most had very high topographic relief. Before using the WDS microprobe, new mounts were prepared using the methods outlined in Section 2.1; this prevented Pb contamination and led to much better polish and lower relief.

With the WDS microprobe, points for analysis were chosen from BSE images, and the elements present in a particular sample were identified from ED spectra. The Task program (Section 2.3.2) was set up to routinely analyze F, Na, Mg, Al, Si, S, Cl, K (later replaced by Cr), Ca, Ti, Mn, Fe and Zn, and to look for Ce. If cerium was detected, a second element list was used to analyze La, Ce, Pr, Nd, Sm, Eu and Gd. Other elements (Cu, Pb, Bi, Th) were added if seen in the ED spectra, and if Th was present, U was looked for as well. Boron analyses were done separately, because of a necessary (manual) change in voltage (15 to 5 keV), a change in slit width, and electronic re-alignment of the column.

A total of 462 WD analyses was obtained from 76 samples; these are listed in Appendix E.1. In addition, 111 ED analyses of 14 B- and F-free vesuvianites are

Table 13: Range of oxide weight percents for ED (left) and WD analyses*.

Oxide	$\bar{x}$	σ	Min.	Max.	$\bar{x}$	σ	Min.	Max.
SiO_2	36.8	0.4	35.8	37.5	36.5	0.7	33.24	38.10
Al_2O_3	17.6	1.1	14.8	19.2	15.9	2.2	10.27	19.20
TiO_2	–	–	–	0.7	–	–	–	5.06
MgO	2.8	0.7	1.3	4.3	3.0	1.4	0.84	6.69
MnO	–	–	–	0.5	–	–	–	3.80
FeO†	2.4	1.4	0.6	5.1	3.1	1.5	0.19	7.43
Cr_2O_3	–	–	–	0.5	–	–	–	0.63
CuO	–	–	–	–	–	–	–	1.55
ZnO	–	–	–	–	–	–	–	2.35
CaO	36.8	0.4	36.1	37.6	35.8	1.1	30.69	38.31
Na_2O	–	–	–	–	–	–	–	0.88
K_2O	–	–	–	–	–	–	–	0.04
La_2O_3	–	–	–	–	–	–	–	1.86
Ce_2O_3	–	–	–	–	–	–	–	3.09
Pr_2O_3	–	–	–	–	–	–	–	0.50
Nd_2O_3	–	–	–	–	–	–	–	0.62
Gd_2O_3	–	–	–	–	–	–	–	0.33
PbO	–	–	–	–	–	–	–	1.57‡
Bi_2O_3	–	–	–	–	–	–	–	2.49‡
ThO_2	–	–	–	–	–	–	–	1.50
B_2O_3	–	–	–	–	–	–	–	3.18
SO_3	–	–	–	0.5	–	–	–	1.00‡
F	–	–	–	–	–	–	–	3.15
Cl	–	–	–	0.2	–	–	–	1.18‡

*Analyses V67–1, –3, –4, –6, and V72–6, –7 not included (see text).

†All Fe as FeO.

‡Probably highest value ever reported for vesuvianite.

listed in Appendix D. These are included for comparison purposes; unless otherwise noted, the following discussions concern only the WD analyses.

The range of oxide contents (wt.%) for the WD analyses are listed in Table 13.*. Only five elements (Mg, Al, Si, Ca, Fe) are present in all the analyses, although the minimum value for FeO (0.19 wt.%) is very low. No Sm, Eu or U was found in any of the samples, even those with high RE or Th contents. Potassium was

* Analyses V67–1, –3, –4, –6, V72–6 and –7 are not included (Section 3.3.2)

dropped from the element list when several hundred analyses showed a maximum of only 0.04 wt.% K_2O. The maximum values for Cl and S, however, are probably the highest ever recorded for vesuvianite, and very high concentrations of F, Na and Fe were found in some samples. No previous studies have reported Bi or Pb in vesuvianite.

Table 13 also shows ranges of oxide contents from the ED analyses. As expected, the maximum values are lower than those found in the larger WD dataset, but mean values for the "essential" elements are generally higher.

The range and distribution of particular elements in vesuvianite will be discussed in more detail in Sections 3.3.2 and 3.3.3.

3.3.1 Data Normalization

As discussed in Section 1.6, a number of formulae and data normalization schemes have been proposed in previous studies. No one, however, has looked at how well these fit a large number of analyses of vesuvianites from many different localities.

Because of this, I decided to apply the various normalization schemes to the 462 WD analyses. All those containing boron (plus V72–6 and V72–7, both obviously non-stoichiometric) were set aside, because at this point the role of B in the structure was unknown. Unfortunately, not all of the samples were tested for B; some of the remaining 384 analyses may be from boron-bearing vesuvianites.

I began by normalizing on a total of 50 cations, as suggested by Hoisch (1985) and Allen (1985). This approach is consistent with both original and recent structure refinements, and makes no assumptions regarding the oxidation state of Fe, the degree of hydration, or the distribution of cations among the sites.

If normalized to 50 cations, analyses should show 18 Si, 19 Ca, and 13 other cations (mainly Al). Figure 18 shows a histogram of Si cations (p.f.u.) for the 384 B-free WD analyses. The observed mean (18.0(2)) is statistically identical to the ideal value of 18. The histogram itself is almost perfectly Gaussian. Both skew and kurtosis* are low (-0.09 and 0.30), indications of a statistically normal distribution.

---

* A distribution is "skewed" if it is not symmetrical; values are distibuted differently below the mean than above it. "Kurtosis" is a measure of the extent of the heaviness of the tails of a distribution. Both values are zero for a normally distributed population (SAS Institute

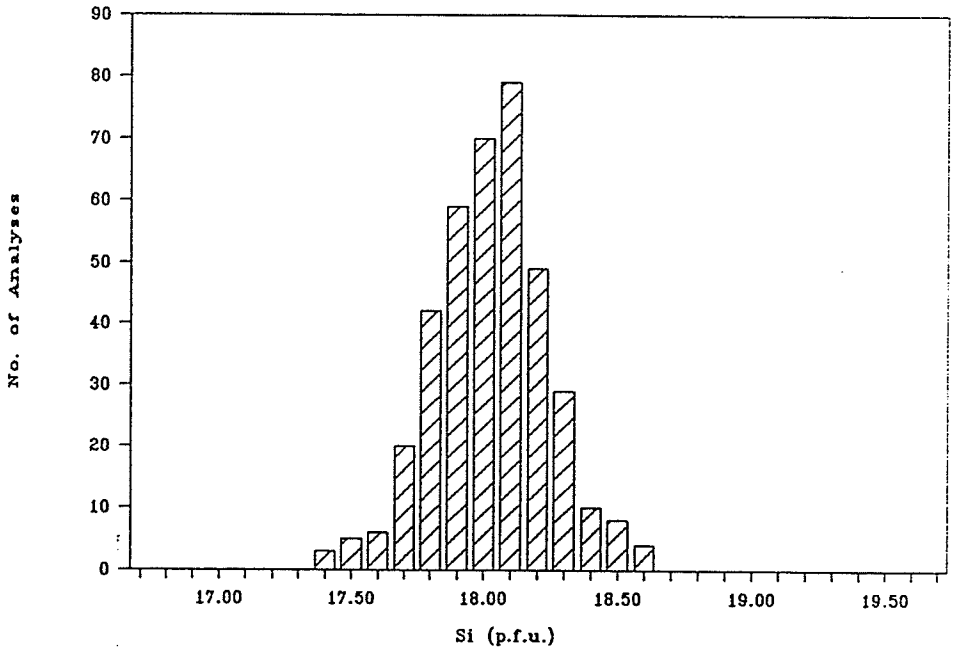

Figure 18: Histogram of Si abundance (p.f.u.); mean, skew and kurtosis (based on 380 WD analyses) are 18.0(2), -0.05 and 0.29 respectively.

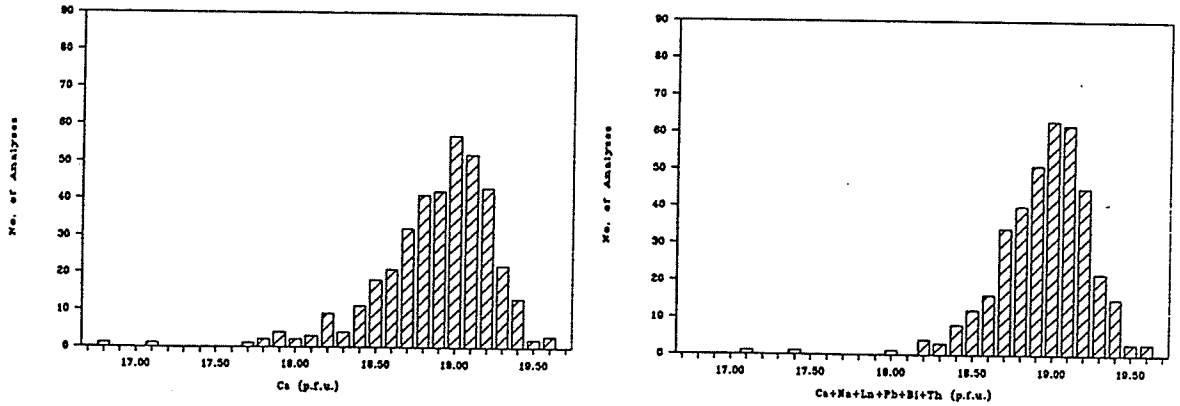

Figure 19: (a) Histogram of Ca abundance (p.f.u.); mean, skew and kurtosis (less analyses V67–1, –3, –4, V72-6 and –7) are 18.9(3), -0.80 and 0.85 respectively. (b) Histogram of Ca+Na+Ln+Pb+Bi+Th abundances (p.f.u.). Mean, skew and kurtosis (less outliers) are 19.0(3), -0.35 and 0.19 respectively.

Inc., 1982).

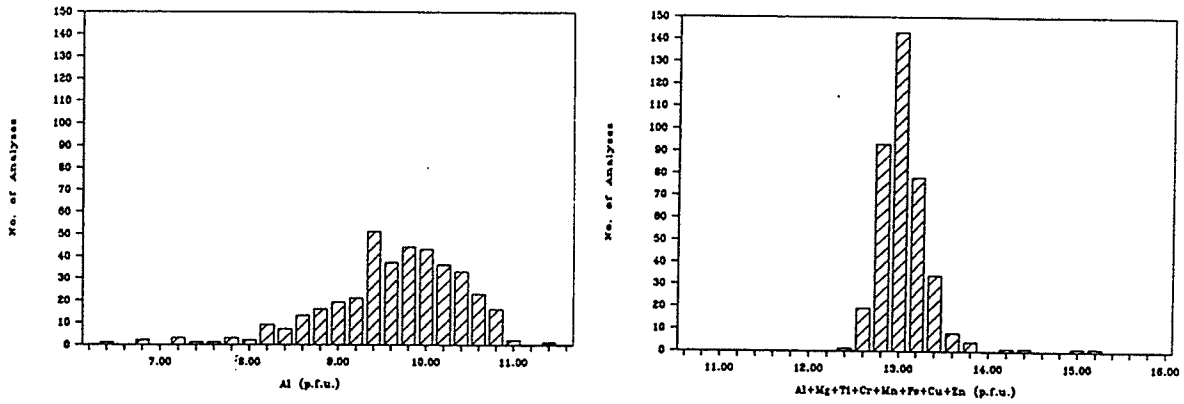

Figure 20: (a) Histogram of Al abundance (p.f.u.); mean, skew and kurtosis (less analyses V67–1, –3, –4, V72-6 and –7) are 9.6(8), -1.00 and 1.64 respectively. (b) Histogram of Al+Mg+Ti+Cr+Mn+Fe+Cu+Zn abundances (p.f.u.). Mean, skew and kurtosis (less outliers) are 13.02(22), 0.62 and 0.83 respectively.

This suggests that all of the fourfold sites are filled with Si, and that there is little or no Al→Si substitution.

A histogram of Ca abundance (p.f.u.) is shown in Figure 19(a). The observed mean is 18.9(4), which is statistically identical to the ideal value of 19, but the distribution is skewed towards lower values and the tails are heavy with datapoints (skewness and kurtosis are -1.37 and 4.01 respectively). This suggests that other elements are substituting for Ca at the eight/nine-coordinated sites. A histogram of Ca+Na+Ln+Pb+Bi+Th (p.f.u.) (Figure 19(b)) shows a more normal distribution, although several analyses still give grossly deficient Ca-site sums..* The observed

* These analyses (V67–3, –4, and –6) are of a fibrous vesuvianite from Franklin, N.J.. Other nonstoichiometric analyses are V67–1, 72–6 and V72–7 (mentioned previously).

mean (without the outlying analyses) is 19.0(3); skewness and kurtosis are -0.35 and 0.19 respectively.

A histogram of Al abundance (p.f.u.) is shown in Figure 20(a). The non-Gaussian character of the peak was expected, as a number of elements are known to substitute for Al in the vesuvianite structure. Figure 20(b) is a histogram of Al+Mg+Ti+Cr+Mn+Fe+Cu+Zn abundances (p.f.u.); the observed mean is 13.0(2), and skewness and kurtosis are 0.62 and 0.83 respectively. The outliers to the right of the curve are the same outlier analyses seen in the Ca histograms.

Table 14 lists mean cation abundances and oxide totals (wt.%) for analyses from a number of recent microprobe studies; all are normalized on a total of 50 cations (less B and S) and 78 anions. Fitzgerald's (1985) analyses deviate from the pattern established here; abundances for the Si, X- and Y-sites are 17.5, 18.6 and 13.9 respectively. All of the WD studies give mean oxide totals scattering about $\approx$99 wt.%, compared to the ED analyses, which give totals nearer 100 wt.%. The reasons for this are not yet clear.

From the above results, it seems as though normalization on 50 cations is justified, although it may be possible to use 18 Si (assuming no Al$\rightarrow$Si substitution). All of the analyses listed in this study were recalculated on the basis of 50 cations (less B and S) and 78 anions (with water calculated by charge balance). These are listed in Appendices D, E.1 and E.2.

3.3.2 Major Element Chemistry

The following cations were present in all of the analyses:

Mg: The Mg content of the vesuvianites ranges from 0.84–6.69 wt.% MgO (0.64–4.93 atoms p.f.u.). The most Mg-rich sample is from Wilui River, U.S.S.R., and a Mn- and Zn-rich cyprine from Franklin, N.J., has the lowest Mg content.

Mg occupies the B and AlFe sites in the vesuvianite structure. The AlFe site is coordinated by five oxygens and a hydroxyl ion.

These polyhedra are found at the ends of trimers of edge-sharing octahedra, with the A positions between them. Both Hoisch (1985) and Allen (1985) have suggested the following coupled substitution:

$$2Al^{3+} \rightleftharpoons Mg^{2+} + Ti^{4+}$$

Table 14: Mean cationic abundances and wt.% oxide totals for recent electron microprobe studies (based on 50 cation (less B and S), 78 anion normalization).

Data:	#1	#2	#3	#4	#5	#6	#7
$\overline{Si}$	18.0(2)	18.0(2)	17.8(1)	17.8(1)	17.5(1)	17.8(1)	18.01(8)
s	-0.09	-0.05	-0.10	-0.84	0.02	-0.48	0.41
k	0.30	0.29	0.27	-0.17	-0.07	-0.35	-0.44
$\overline{Ca}$	18.9(4)	18.9(3)	18.7(3)	19.1(1)	18.5(2)	18.9(2)	18.9(1)
s	-1.37	-0.80	-1.28	-0.63	-0.70	-1.74	-0.64
k	4.01	0.85	1.85	0.34	0.53	4.77	0.38
$\overline{Al}$	9.6(8)	9.6(8)	7.1(6)	10.0(6)	10.2(2)	10.00(7)	9.5(5)
s	-0.96	-1.00	1.77	-0.69	-1.01	-0.46	0.41
k	1.60	1.64	2.77	-0.32	1.55	-0.61	-1.51
$\overline{\Sigma X}$	18.9(3)	19.0(3)	18.9(2)	19.1(1)	18.6(2)	18.9(1)	19.02(9)
s	-1.28	-0.35	-0.38	-0.63	-0.16	-0.13	-0.13
k	5.44	0.19	0.76	0.34	-0.33	-0.16	-1.16
$\overline{\Sigma Y}$	13.0(3)	13.0(2)	13.3(2)	13.1(2)	13.9(2)	13.2(2)	12.97(7)
s	2.57	0.62	-0.31	1.18	-0.15	1.04	0.16
k	14.37	0.83	1.53	0.67	0.02	0.24	-0.99
$\overline{TOT}$	98.9(9)	99.0(9)	98.7(8)	99.8(5)	100.4(1.0)	98.8(4)	98.5(6)
s	-0.33	-0.35		-0.19	-1.63	-0.11	0.15
k	0.47	0.51		-0.08	4.96	-0.38	-1.27

#1 All WD analyses (except those containing B, V72–6 and V72–7) (384 analyses).
#2 As above, but without V67–1, –3, –4 and –6 (380).
#3 All WD analyses containing B (76).
#4 All ED analyses (111).
#5 WD analyses from Fitzgerald (1985) (without analysis of REE-vesuvianite) (52).
#6 WD analyses from Allen (1985) (without M4 and M14) (35).
#7 WD analyses from Hoisch (1985) (22).

s = skewness k = kurtosis TOT = wt.% oxide totals
ΣX = (Ca+Na+K+Ln+Pb+Bi+Th+U) ΣY = (Al+Ti+Mg+Mn+Fe+Cr+Cu+Zn)

in which Mg and Ti replace Al in neighbouring AlFe sites. Local charge balance is maintained by changing bond lengths. It is unlikely that this substitution can account for *all* divalent cations at the AlFe sites, as the amount of Ti in most analyses is low.

Al: The amount of Al in the vesuvianites ranges from 10.27–19.20 wt.% Al_2O_3 (6.23–11.03 atoms p.f.u.). A cyprine from Norway (V49) has the most Al, and a boron-bearing sample from Italy (V38) has the least.

Figure 21 is a histogram of Al abundance (p.f.u.). There is a bimodal distribution, with Al from analyses of boron-bearing vesuvianites clustered about 6.6 Al atoms p.f.u., and those from non-boron vesuvianites clustered around 9.8 atoms p.f.u..

Al occupies the A, B, and AlFe sites in the vesuvianite structure. A wide range of elements are known to substitute for Al at the AlFe and B sites. If the stoichiometric values of Si and the X-site cations are 18 and 19 (Section 3.3.1), then the sum of Al+Mg+Ti+Cr+Mn+Fe+Cu+Zn (Al and those cations which substitute for it) should be 13. Figure 22 shows a graph of Al versus those cations that substitute for Al in the vesuvianite structure. A least-squares fit of the line gives a slope of $-1.092(8)$ and a y-intercept of 13.9(2), which is somewhat higher than the ideal value of 13. The bimodal distribution seen in the histogram of Al abundance is also evident here. Most of the analyses with <8.00 Al atoms p.f.u. are of boron-bearing vesuvianites.

Mg is the major divalent cation replacing Al in the vesuvianite structure. Figure 23 is a graph of Al versus Mg (atoms p.f.u.). Most of the analyses above the arbitrary dividing line are of boron-bearing vesuvianites. These samples generally contain less OH than other vesuvianites (Section 3.4.3), which suggests that the substitution:

$$Al^{3+} \rightleftharpoons Mg^{2+} + H^{+}$$

is important in boron-bearing vesuvianites.

Si: All of the vesuvianites contain ≈18 Si atoms p.f.u., which suggests that there is no Al → Si, B → Si or H → Si ("hydrovesuvianite") substitution in the samples studied.

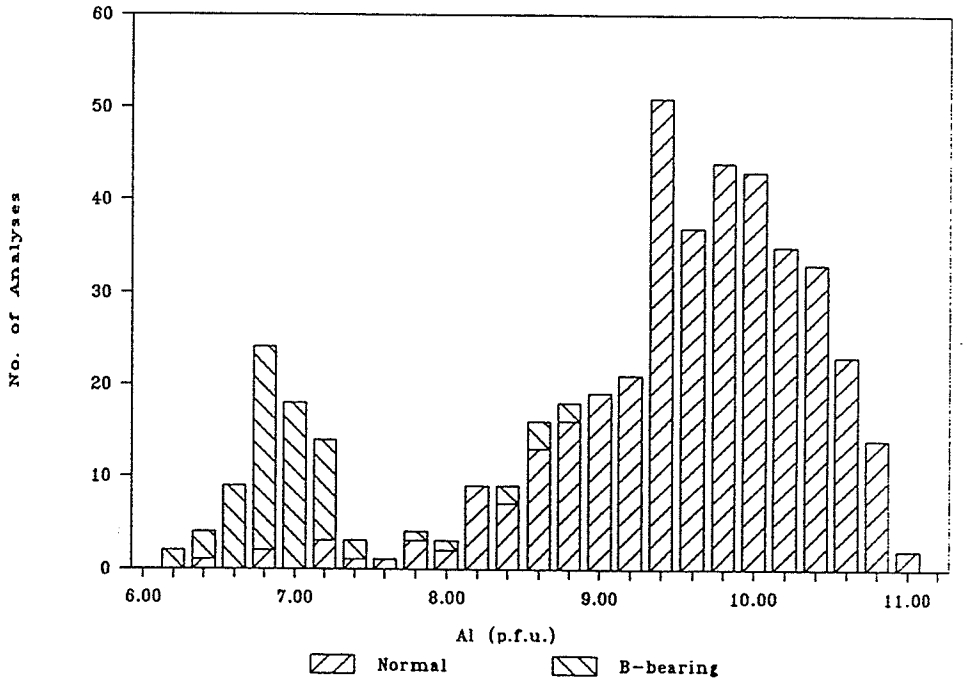

Figure 21: Histogram of Al abundance (p.f.u.; 456 WD analyses).

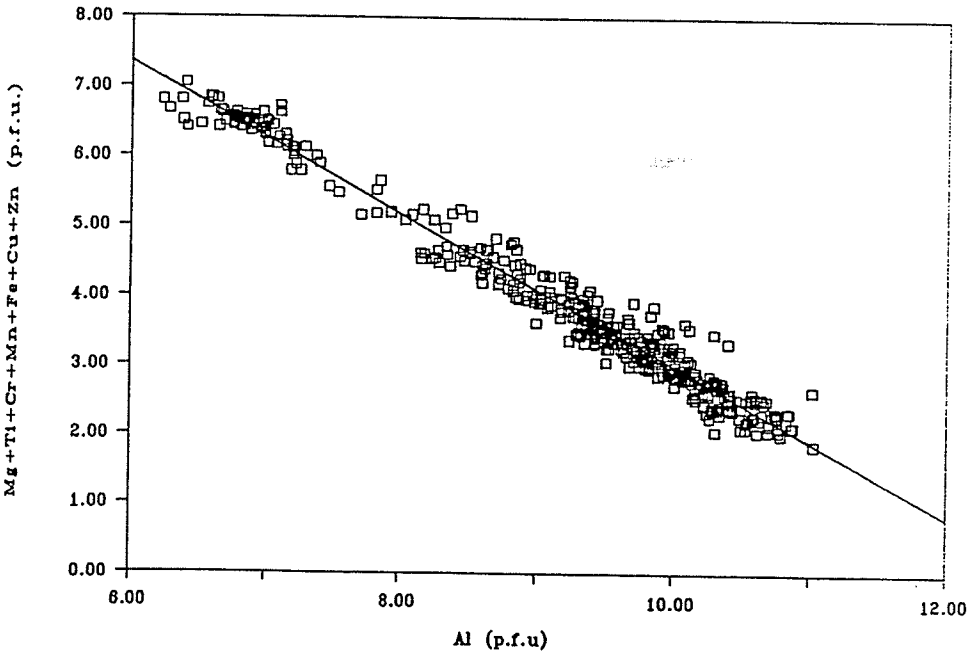

Figure 22: Al vs. Mg+Ti+Cr+Mn+Fe+Cu+Zn (atoms p.f.u.). A least-squares fit of the line gives a slope of -1.092(8) and a y-intercept of 13.9(2). Most of the analyses with <8.00 Al atoms p.f.u. are of boron-bearing vesuvianites.

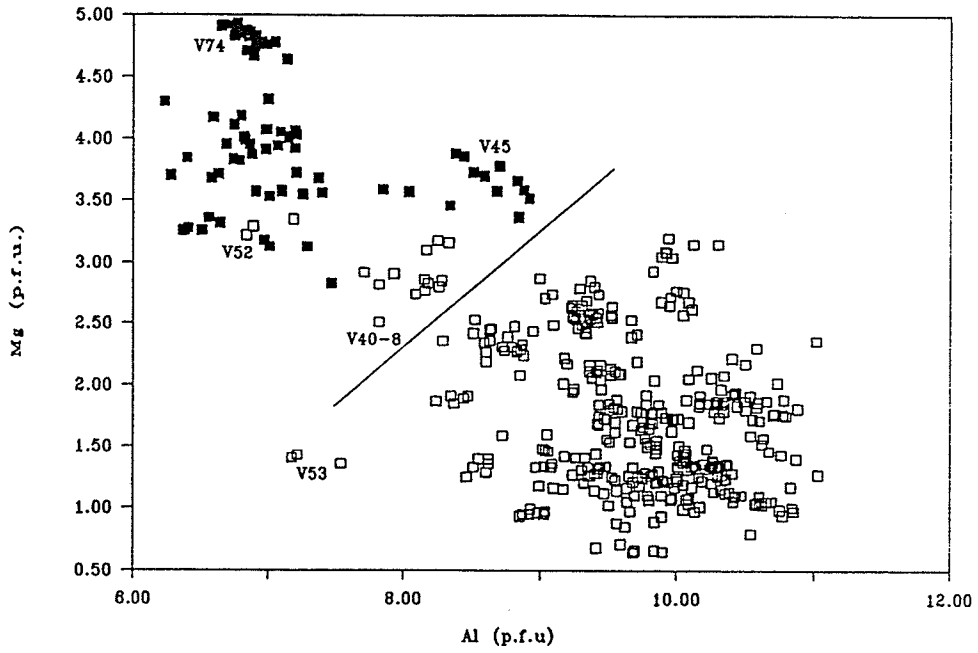

Figure 23: Al vs. Mg (atoms p.f.u.). The filled squares represent analyses of boron-bearing vesuvianites (including V46, which was not analyzed for B but is from the same locality as V45). Samples V52 and V53 are partially metamict. The only analysis above the line from a vesuvianite known to be B-free is V40–8.

The amount of Si often seems to vary inversely with the amount of Ca (see Figures 14 and 16), because of the closure effect of normalizing on 50 cations. Because Si+Ca account for $\leq$37 of these, a slight variation in one effects the other.

Ca: There are up to 19 Ca atoms in the formula unit. Na, K, lanthanide elements, Pb, Bi and Th replace Ca in the WD analyses, and are discussed in Section 3.3.3.

Fe: Iron, although not an essential element in vesuvianite, is present in all of the analyses, in amounts ranging from 0.19–7.43 wt.% FeO (0.08–3.26 atoms p.f.u.). The most Fe–rich sample is a partially metamict vesuvianite from Alaska (V53), and the specimen with the least Fe is a cyprine from Norway (V49). In general, vesuvianites from rodingites associated with serpentinites have the lowest Fe contents.

Fe occupies the AlFe and B sites in the vesuvianite structure, although minor amounts may occur at the A, C and Ca sites (see Section 1.7).

3.3.3 Minor Element Chemistry

The following elements were present in minor amounts:

B: Boron was found in six of the 49 samples analyzed for B. Few points were analyzed for B because of (1) time constraints, and (2) the points had to be analyzed manually. An average B_2O_3 value was added to other analyses from the same section (Appendices E.1 and E.2).

The highest amounts of boron ($\approx$3.18 wt.% B_2O_3) were found in samples from Templeton Township, Quebec (V30), and Tulare County, California (V56). The amount of boron in a particular sample may vary considerably. Most of the boron-bearing vesuvianites are optically positive, and two (V45, V74) are sector-zoned. Boron-bearing vesuvianites generally contain more Mg, less Al (and less OH) than those without boron. Four of the six samples also have high concentrations of lanthanide elements (although V56 has no rare earths). Boron does not appear to be replacing other elements, which suggests that it occupies a vacant site in the structure. One possibility is the "T" site at 0.05, 0.05, 1/4, which is coordinated by 2 O(7) and 2 OH positions in an approximately tetrahedral arrangement. If this is the case, the coupled substitution:

$$Al^{3+} + 2H^{+} \rightleftharpoons B^{3+} + Mg^{2+}$$

could account for the high Mg, low Al (and OH) contents of the boron-bearing vesuvianites.

A histogram of boron abundance (p.f.u.) is shown in Figure 24. There is a bimodal distribution; because so few analyses were obtained it is difficult to tell whether this is significant.

F: Most of the vesuvianites analyzed in this study contained minor amounts of F. A vesuvianite from Richardson Mountains, Y.T. (V33) contained up to 3.15 wt.% F (4.84 atoms p.f.u.). Both cyprines from Norway are F-rich; sample V49 had up to 2.82 wt.% F (4.32 atoms p.f.u.). Stoichiometric analyses of a leached, metamict vesuvianite (V72) indicate a maximum of 2.70 wt.% F (4.25 atoms p.f.u.). Four

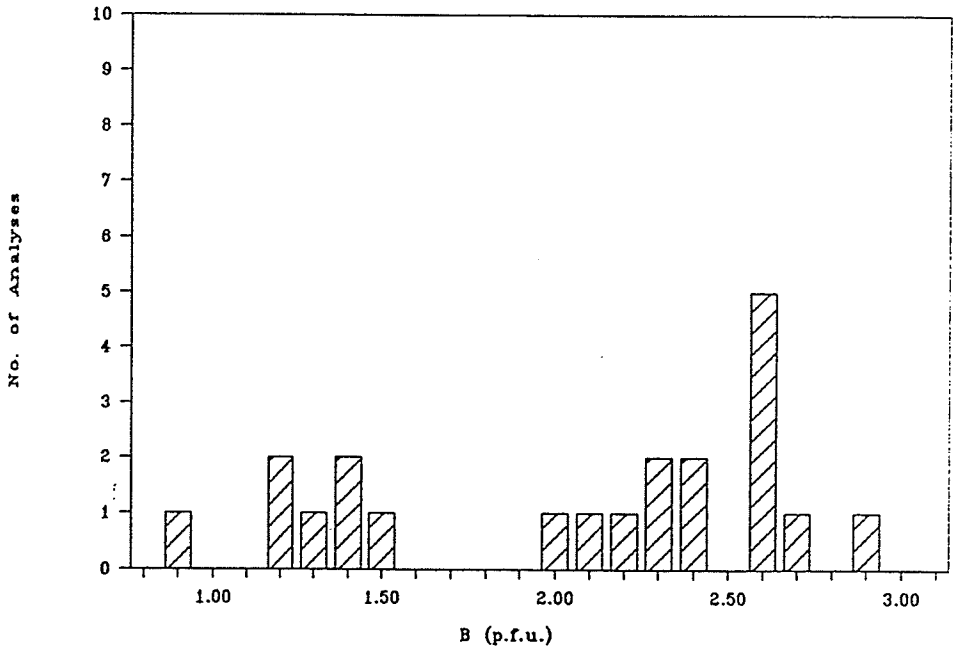

Figure 24: A histogram of B abundance (p.f.u.).

other vesuvianites (V5, V6, $V8_2$ and V70) gave analyses with more than 4.00 F atoms p.f.u..

Vesuvianites from altered alkali syenites and related rocks are generally described as being F-rich, but the material from York River, Ontario, had no fluorine. None of the vesuvianites from rodingites have more than trace amounts of F.

Fluorine replaces OH in the vesuvianite structure, probably at the OH site rather than the more tightly-bound O(10) position.

Na: The most Na-rich vesuvianites are found in altered alkali syenites and related rocks. A vesuvianite from the nepheline-gneiss complex near York River, Ontario (V7; described by Osborne, 1930) contained $\approx$0.88 wt.% Na_2O (0.85 atoms p.f.u.). A partially metamict sample from Alaska (V53), found in syenite boulders with nepheline and cancrinite (Himmelberg and Miller, 1980), gave 0.38–0.44 wt.% Na_2O. About half of the vesuvianites studied contain no Na; most of these are from rodingites associated with serpentinites.

Considering its ionic radius, Na probably replaces Ca in the Ca and *C* sites.

Charge balance is maintained through coupled substitutions such as the following:

$$Ca^{2+} + Mg^{2+} \rightleftharpoons Na^{+} + Fe^{3+}$$

$$Ca^{2+} + Al^{3+} \rightleftharpoons Na^{+} + Ti^{4+}$$

which involve either the B or AlFe sites.

S: Up to 1.00 wt.% SO_3 (0.37 atoms p.f.u.) was found in the boron-bearing vesuvianite from Laguna del Jaco, Mexico (V45). This is probably the most S reported in vesuvianite. The other sample from this locality (V46) showed a maximum of 0.63 wt.% SO_3 (0.23 atoms p.f.u.). A vesuvianite from Mt. St. Hilaire in Quebec (V25) contained 0.87 wt.% SO_3 (0.32 atoms p.f.u.). Many of the sulfur-bearing vesuvianites are rich in F, and some contain both S and Cl.

Cl: The F-rich vesuvianite from Long Lake Mine in Ontario (V6) also contains up to 1.18 wt.% Cl (0.56 atoms p.f.u.), and a vesuvianite from Amity, New York, gave a maximum of 0.37 wt.% Cl (0.31 atoms p.f.u.).

Almost all of the chlorine-bearing vesuvianites contain significant amounts of F, and a few have both S and Cl. Like F, Cl replaces OH in the vesuvianite structure, probably at the OH sites.

K: Only one vesuvianite (V67) out of several hundred analyzed for K_2O contained more than background (0.04 wt.% K_2O), possibly because the Ca sites are too small to accommodate this ion. Nonstoichiometric analyses of a leached vesuvianite (V72) show up to 0.35 wt.% K_2O. The lack of K in all other vesuvianites suggests that this is due to a minor admixed phase.

Ti: Titanium is a common accessary element in vesuvianite. A histogram of Ti abundance is shown in Figure 25. The highest TiO_2 analysis (5.06 wt.%, 1.90 atoms p.f.u.) is of a vesuvianite from Laguna del Jaco, Mexico (V46). Other analyses of this sample, however, show 0.26–1.33 wt.% TiO_2 (0.10–0.49 atoms p.f.u.).

In general, the highest-Ti vesuvianites are from altered alkali syenites and related rocks. The sample from York River, Ontario (V7) contained 4.39–4.67 wt. % TiO_2 (1.64–1.67 atoms p.f.u.). One of the partially metamict vesuvianites from Alaska (V53) had 2.80–3.09 wt.% TiO_2 (1.10–1.20 atoms p.f.u.). Both of these samples are enriched in Na. Figure 26 shows that there is a correlation between

Na and high Ti content. The "usual" Al $\rightleftharpoons$ Ti substitution is only effective up to $\approx$0.18 Na atoms, after which all Na is introduced by the coupled substitution:

$$Ca^{2+} + Al^{3+} \rightleftharpoons Na^{+} + Ti^{4+}$$

Other Ti-rich vesuvianites include three from Quebec (V28, V29, V31) with 2.61–2.93 wt.% TiO_2 (0.96–1.09 atoms p.f.u.). It is interesting to note that a boron-bearing vesuvianite (V30) from the same locality as V29 and V31 (Templeton Township) has only 0.15–1.55 wt.% TiO_2. There may be an inverse correlation between Ti and B in vesuvianite.

Seventeen of the 75 samples contained no detectable Ti. Most of these are from rodingites associated with serpentinites. The maximum amount of Ti found in a vesuvianite from Jeffrey Mine, Quebec, was 1.20 wt.% (0.44 atoms p.f.u.). All of the low-Ti samples from this locality are green, while all those with >0.10 wt.% TiO_2 are brown, confirming observations made by Manning (1975).

Ti is generally thought to occupy the AlFe site in vesuvianite, although Manning (1976) suggested that it may occupy the *C* site and Manning and Tricker (1975) suggest that it may also be found in the *B* site.

Cr: A dark green vesuvianite from Xanthi, Greece (V36) had the most Cr, with 0.34–0.63 wt.% Cr_2O_3 (0.13–0.24 atoms p.f.u.). This is the sample described by Frenzel *et al.* (1969); they reported a maximum of 0.48 wt.% Cr_2O_3. Other vesuvianites contained only minor amounts of Cr. A sample from El Dorado County in California (V59) gave 0.15 wt.% Cr_2O_3 (0.05 atoms p.f.u.), and a vesuvianite from Black Lake, Quebec (V9) had 0.09 wt.% Cr_2O_3 (0.03 atoms p.f.u.).

In general, the chromium-bearing vesuvianites are a vivid green colour, as Cr is a strong chromophore in vesuvianites. Chromium is probably found at the general AlFe site in the vesuvianite structure.

Mn: Although most of the vesuvianites contained minor amounts of Mn, very few had more than 0.5 wt.% MnO (Figure 27). Manganese in the bright red Bi-rich vesuvianite from Langban, Sweden (V50) ranged from 3.10–3.80 wt.% MnO (1.32–1.61 atoms p.f.u.). Both samples from Franklin, N.J., were rich in Mn; V66 had 1.68–1.97 wt.% MnO (0.71–0.85 atoms p.f.u.) and V67 gave 1.23–1.57 wt.% MnO (0.52–0.67 atoms p.f.u.). One of the cyprines from Norway (V49) contained 0.85

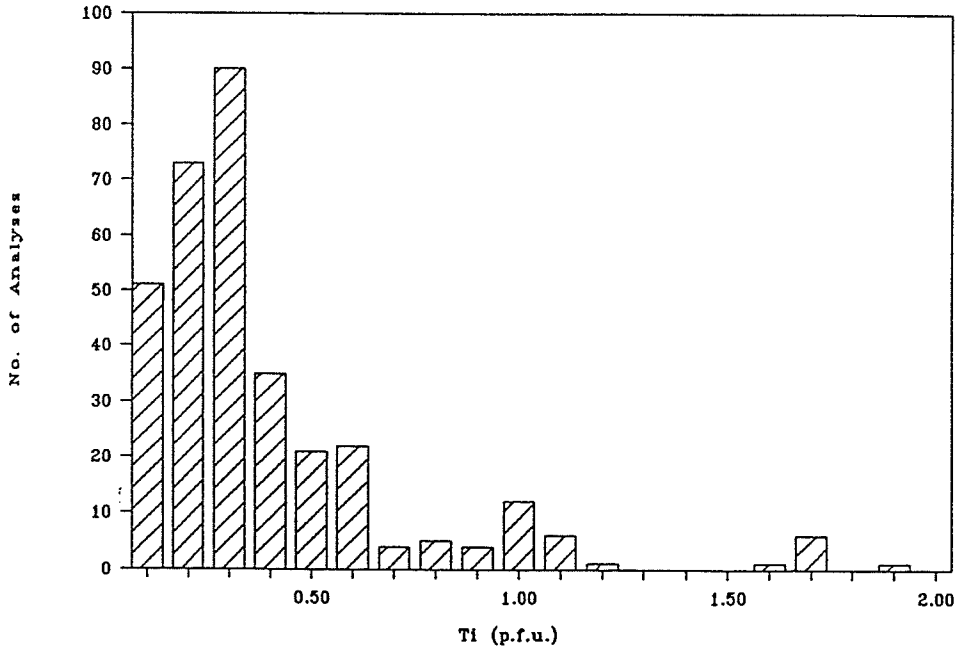

Figure 25: Histogram of Ti abundance (p.f.u.).

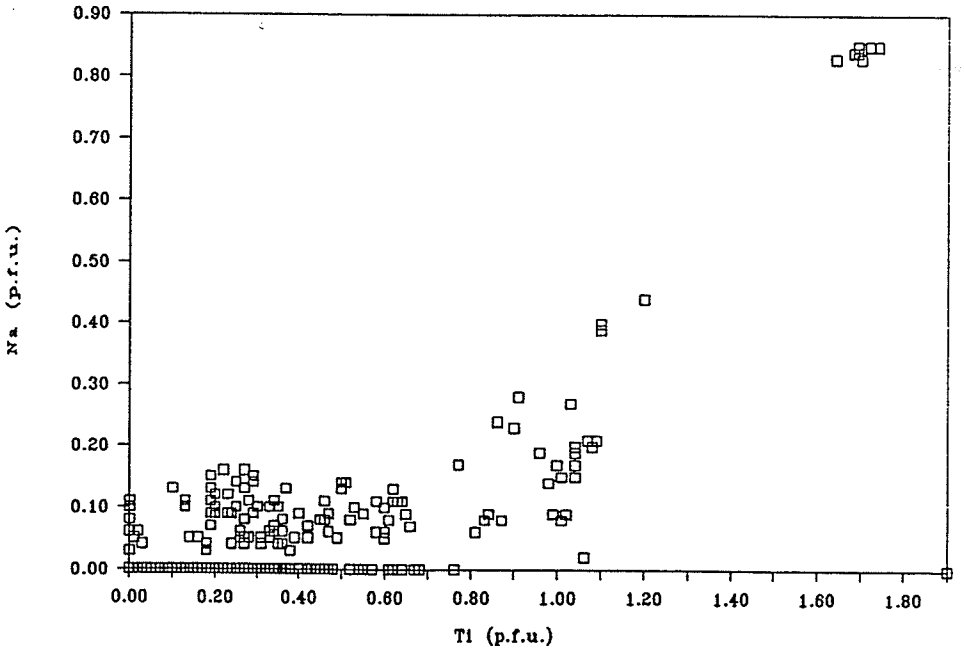

Figure 26: A graph of Ti vs. Na (atoms p.f.u.), showing the correlation between the two at high Ti values.

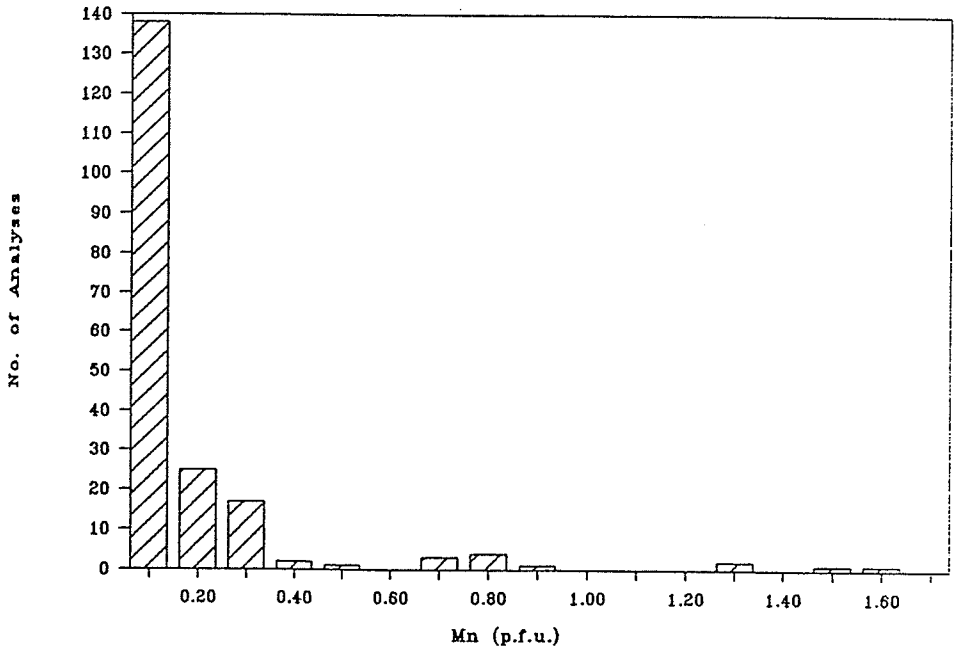

Figure 27: A histogram of Mn abundance (p.f.u.).

wt.% MnO (0.39 atoms p.f.u.), and the F- and Cl-rich vesuvianite from Long Lake Mine in Ontario (V6) had 0.75–0.80 wt.% MnO (0.33–0.34 atoms p.f.u.). The MnO content of the high-F vesuvianite from the Richardson Mountains (YT) ranged from 0.67–0.80 wt.% (0.28–0.33 atoms p.f.u.). Although Arem (1970) found that almost all vesuvianites contain trace amounts of Mn, no manganese was found in 15 of the 75 samples analyzed in this study. Mn is a chromophore in vesuvianite; a small amount in Fe-poor samples causes a pink or lilac colour. Some of the crystals from Jeffrey Mine, Quebec, have lilac-coloured (Mn-rich) pyramidal faces capping green (Fe-rich) prisms.

Manganese probably occupies the general AlFe site in the vesuvianite structure, although some authors have suggested that it substitutes for Ca, possibly at the distorted Ca(3) site.

Cu: Copper was found in vesuvianites from Franklin, N.J. (V66, V62) and Norway (V48, V49). Sample V67 contained 1.13–1.55 wt.% CuO (0.43–0.59 atoms p.f.u.), and V66 had 0.41–0.63 wt.% CuO (0.16–0.24 atoms p.f.u.). Copper in the

Norwegian samples ranged from 0.44–0.94 wt.% CuO (0.16–0.35 atoms p.f.u.).

All of these samples are "cyprines" (blue or green in colour) although Fitzgerald (1985) found that some red and brown vesuvianites at Franklin contain as much Cu as the cyprines, and that the amount of Fe probably determines the colour. The samples from Franklin also show a fibrous habit often reported for cyprines. The crystal structure of a copper-bearing vesuvianite was refined by Fitzgerald et. al. (1987); they found that Cu occupies the *B* site.

Zn: Both copper-bearing vesuvianites from Franklin, N.J., also contain Zn, in amounts ranging from 1.43–2.35 wt.% ZnO (0.53–0.87 atoms p.f.u.). The Pb-rich material (V67) contains slightly more Cu and less Zn than the other sample. Only trace amounts of Zn were found in any other vesuvianites.

Zinc probably occupies the general AlFe site in vesuvianite, although it may enter the pyramidal *B* position as well. It is interesting to note that samples V66 and V67 contain 0.99–1.04 and 1.03–1.13 Cu+Zn cations respectively, enough to completely fill the *B* site.

Lanthanide Elements: Lanthanides were found in a number of vesuvianites, usually with Ce>La>Nd>Pr>Gd. No Sm or Eu was found in any of these samples. Only four vesuvianites had >0.45 wt.% Ln_2O_3. The highest amounts ($\approx$6.00 wt.% Ln_2O_3, or $\approx$1.15 atoms p.f.u.) were found in the B-rich samples from Templeton Township, Quebec (V30) and Ariccia, Italy (V38). Figure 28 shows that the Ln content of the Ariccia vesuvianite is highest in the core and rim (compare with Figures X and Y). The other boron-bearing vesuvianites contain only minor amounts of these elements.

One of the partially metamict vesuvianites from Alaska (V53) showed 3.17–3.86 wt.% Ln_2O_3 (0.56–0.72 atoms p.f.u.), and the F-rich material from Long Lake Mine in Ontario (V6) had up to 1.39 wt.% Ln_2O_3 (0.26 atoms p.f.u.). All of these samples show varying amounts of F and Ti, and most lanthanide-bearing vesuvianites also contain appreciable amounts of iron.

The lanthanides replace Ca in the vesuvianite structure, probably at the Ca(3) site (Fitzgerald *et al.*, 1987).

Pb: Stoichiometric analyses of the unusual Cu-rich vesuvianite from Franklin, N.J. (V67) show 0.31–1.57 wt.% PbO (0.04–0.21 atoms p.f.u.). No Pb was found, how-

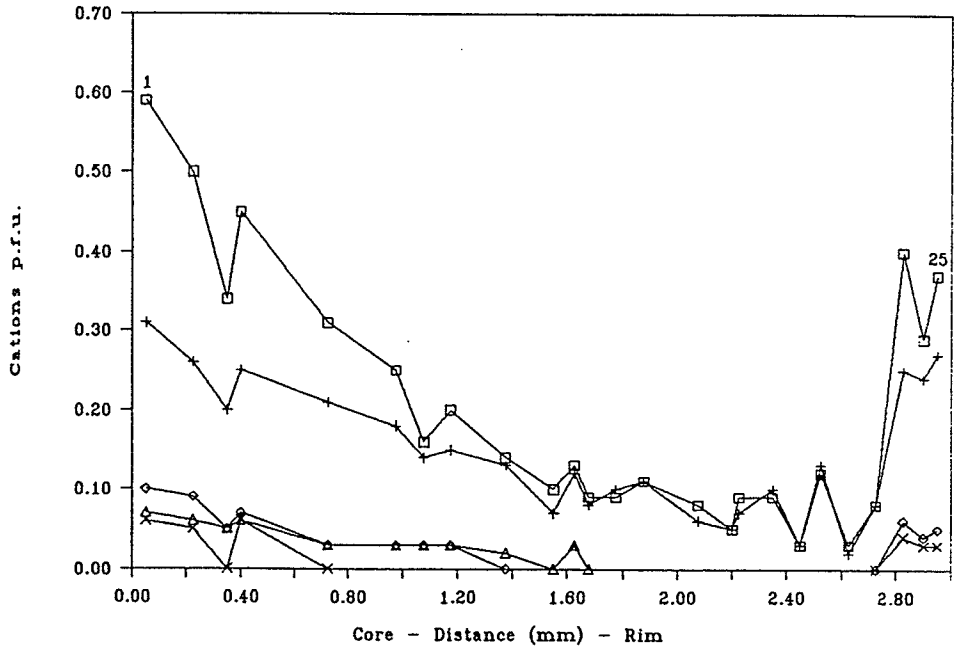

Figure 28: Variations in Ce (□), La (+), Nd (◇), Pr (×) and Gd (△) across a (001) section of sample V38 (Ariccia, Italy). The points are the same as those in Figures 7 and 8.

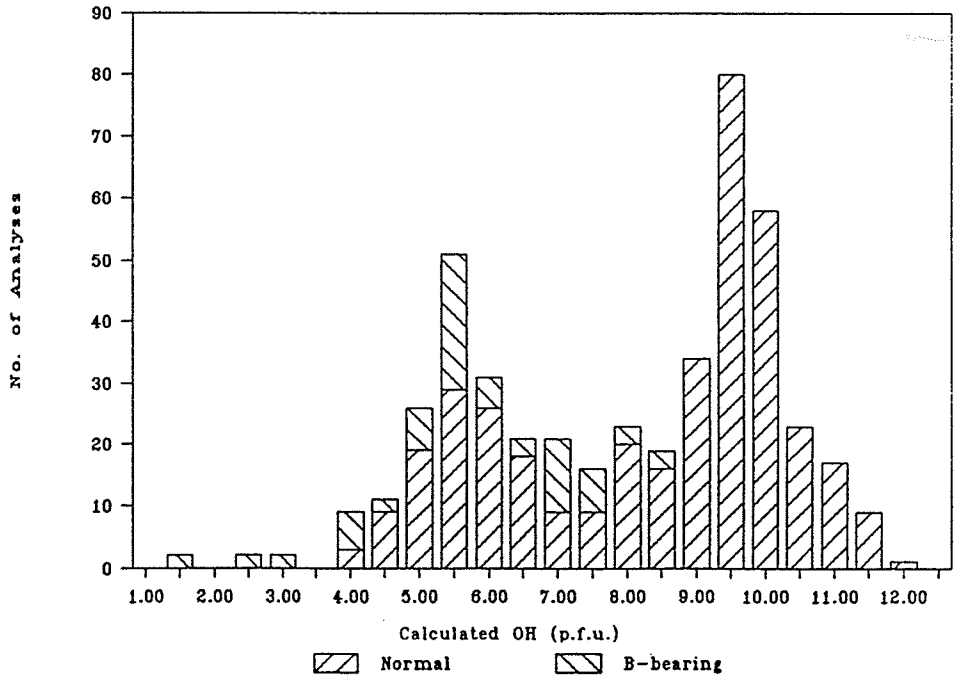

Figure 29: A histogram of OH abundance (atoms p.f.u.).

ever, in the other sample from this locality (V66). This is the first study to report Pb in vesuvianite; it replaces Ca in the vesuvianite structure.

Bi: Up to 2.49 wt.% Bi_2O_3 (0.32 atoms p.f.u.) was found in the Mn-rich vesuvianite from Langban, Sweden (V50); no previous studies have reported Bi in vesuvianite. The Bi replaces Ca in the vesuvianite structure, possibly at the Ca(3) site.

Th: The partially metamict, Fe- and Ln-rich vesuvianite from Alaska (V53) was found to contain 1.43–1.50 wt.% ThO_2 (0.17–0.18 atoms p.f.u.). Thorium replaces Ca in the vesuvianite structure. No U was found in this sample.

H_2O : Water was calculated by charge balance, assuming 78 anions p.f.u. and ferrous iron. Figure 29 is a histogram of OH abundance. There is a bimodal distribution, with OH from analyses of boron-bearing vesuvianites clustered around 5.5 (atoms p.f.u.), and the others centred about 9.5 OH atoms p.f.u.

Mean OH content of the 76 boron-bearing analyses was 5.8(1.5) atoms p.f.u.; for the 380 non-boron analyses it was 8.4(2.0). This is considerably lower than 9.5, presumably because the dataset contains analyses of some boron-bearing vesuvianites that were not identified as such.

The role of OH in the vesuvianite structure will be discussed in more detail in Section 3.8.

3.4 Chemical Analyses

3.4.1 Li and Be Analyses (AAS)

A number of previous studies have reported minor amounts of Li and/or Be in vesuvianites (Section 1.6.3). As described in Section 2.4.1, atomic absorption spectroscopy was used to analyze for these elements.

A total of 39 analyses (for both elements) was done on 30 different samples from a number of localities. The results are listed in Appendix F. One vesuvianite (V4) was periodically analyzed throughout the run as a measure of experimental precision. The relative standard deviation on seven analyses was 11% for Li and 6% for Be. Internal standards for the Li analyses were GSP-1 (30 ppm) and GH (45 ppm); measured values were 46 and 30 ppm respectively, suggesting that the samples were switched. Fresh solutions were made and the analyses were repeated in absorbance mode. This time the Li contents were identical for both solutions, indicating that the problem was due to analytical precision. Internal standards for the Be analyses were GH (6 ppm) and SY2 (23 ppm); the measured values were 4 ppm and 23 ppm respectively.

The results show a maximum of 0.04 wt.% Li_2O and 0.15 wt.% BeO in the vesuvianites examined. *Thus Li and Be are present in vesuvianites only in very minor amounts.*

3.4.2 Ferrous Iron Determinations

A total of 39 ferrous iron determinations was done on 25 different samples, using the methods described in Section 2.4.2. A number of internal standards were used, and in each case, the measured amount of Fe^{2+} was almost identical to the accepted value (Appendix F). One vesuvianite sample (V4) and one standard (SY2) were reanalyzed eight times; in both cases the (average) relative standard deviation was $\approx$1%.

The amount of Fe^{3+} in each sample was obtained by subtracting the measured Fe^{2+} value from the average amount of Fe present in the microprobe analysis. The

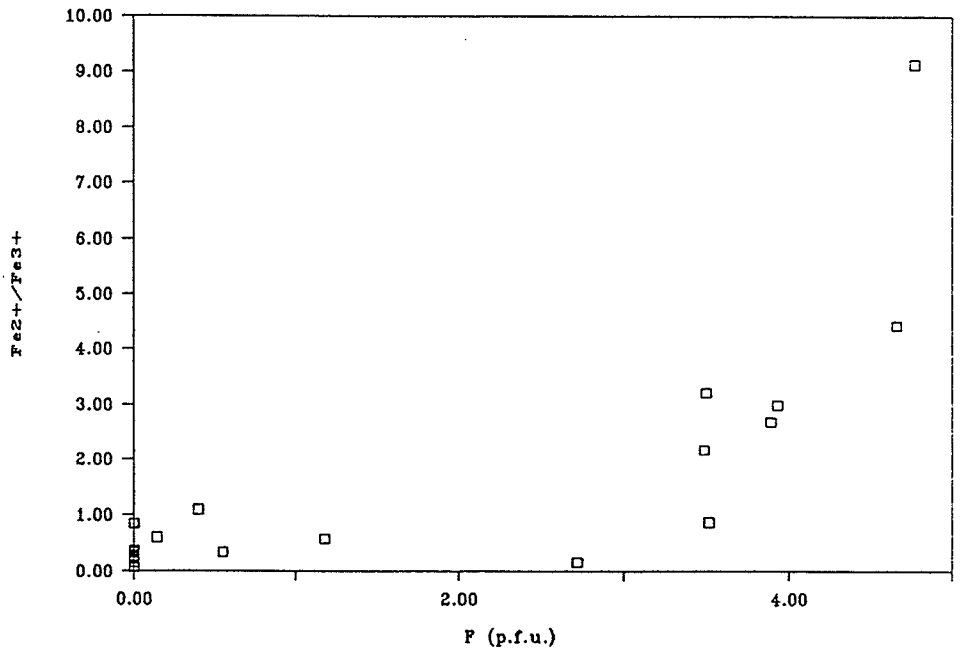

Figure 30: A graph of F (fluorine) content (p.f.u.) vs. Fe^{2+}/Fe^{3+}.

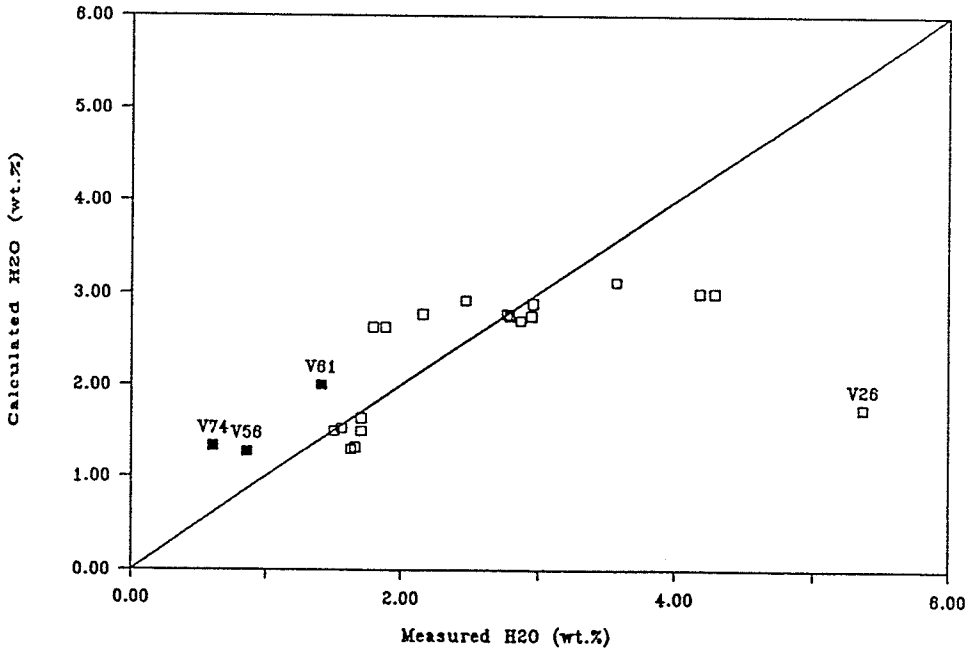

Figure 31: Measured H_2O vs. calculated H_2O (both wt.%). The filled squares represent analyses of B-bearing vesuvianites. All Fe was assumed to be ferrous, unless the Fe^{2+}/Fe^{3+} was known.

Fe^{2+}/Fe^{3+} ratio was then used to calculate the amounts of ferrous and ferric iron present in each analysis. These are included in the ED and WD analyses given in Appendices D, E.1 and E.2. Details of the calculations are presented in Appendix F.

Only 7 of the 25 samples had more ferrous than ferric iron ($Fe^{2+}/Fe^{3+} > 1.00$). The F- and Mn-rich vesuvianite from the Richardson Mountains, YT (V33), has the highest Fe^{2+}/Fe^{3+} ratio (9.14). Most of the iron in the low-Fe vesuvianites from rodingites associated with serpentinites is ferric; the Fe^{2+}/Fe^{3+} ratio is generally <0.50.

There are many possible substitutions involving Fe in the vesuvianite structure. However, there are no *simple* substitutional trends involving Fe^{2+} and/or Fe^{3+}, apart from the relationship between F and the Fe^{2+}/Fe^{3+} ratio (Figure 30). The role of Fe in the vesuvianite structure will be considered in more detail in Section 3.8.

3.4.3 H_2O and CO_2 Determinations

Water and CO_2 analyses were done using the methods described in Section 2.4.3. Because of the amount of material required ($\approx$1 gm) only 22 analyses were done on 18 different samples. The results are summarized in Appendix F.

Two standard samples (SY2 and PCC–1) were analyzed at regular intervals to provide a measure of experimental precision. Five analyses of PCC–1 gave average values of 4.64(1) wt.% H_2O and 0.17 wt.% CO_2; these compare well with the accepted values of 4.70 wt.% H_2O and 0.15 wt.% CO_2. For SY2 the averages of five determinations were 0.48(8) wt.% H_2O and 0.55(1) wt.% CO_2 (the accepted values are 0.43 wt.% H_2O and 0.46 wt.% CO_2). A number of other standards were analyzed as well; these are listed in Appendix F.

The amount of H_2O in the vesuvianites ranges from 0.61–5.37 wt.%. Figure 31 shows the relationship between measured H_2O content and the amount calculated from averaged microprobe analyses. In most cases, the results are comparable. The highest measured H_2O content (5.37 wt.%) belongs to a fibrous vesuvianite from Mt. St. Hilaire, Quebec (V26). The calculated H_2O content is much lower (2.10 wt.%), which suggests that the sample was not completely free of adsorbed water, despite heating at 110° for 12 hours.

The trend shown in Figure 31 is curvilinear. This suggests that water calculations are only good for samples with up to 3.00 wt.% H_2O. Additional water may enter the structure as molecular H_2O and as such could not be predicted by simple charge balance calculations.

Figure 31 also shows that the B-bearing vesuvianites have low H_2O contents. Samples V56 and V74 (both with $\approx$2.90 wt.% B_2O_3) have the lowest H_2O contents (0.61 and 0.86 wt.%). This is approximately 2 OH atoms per formula unit. Sample V61, with less B ($\approx$1.44 wt.% B_2O_3) has more water (1.41 wt.% H_2O, or $\approx$4 OH atoms p.f.u.). The role of water in the vesuvianite structure will be considered in more detail in Chapter 4.

Only minor amounts of CO_2 were found in the vesuvianites analyzed. One of the boron-bearing samples (V56) had 0.50 wt.% CO_2, and three more vesuvianites (V44, V60 and V61) had >0.30 wt.% CO_2. The role of CO_2 in the vesuvianite structure is unclear; possibly these small amounts result from carbonate inclusions in the separates analyzed.

3.5 Vesuvianite Cell Dimensions

All of the cell dimensions given in this study were recorded with a Nicolet $R3m$ single-crystal diffractometer, using the orienting routine discussed in Section 2.3.1. Wherever possible, 25 reflections were used as input; both constrained (tetragonal) and unconstrained cells were output, with the latter transformed such that a_2 was aways greater than a_1. One crystal (V4) was remounted and reoriented five times, as a measure of experimental precision (Table 15). The standard deviations obtained by averaging these results were similar to those calculated by the orienting program, which uses a least-squares algorithm.

The diffractometer uses a random orientation photograph to record reflections for orienting; these reflections are limited to $2\theta_{max} \approx 30°$. For those crystals selected for crystal structure data collection, an additional 25 reflections with 2θ 20–40° were chosen from the diffraction record and used for reorienting; this should result in more precise cell dimensions (Hamor *et al.*, 1987). The values obtained for both methods are listed in Table 16. The "high-angle" cells are larger than those resulting from low-angle reflections, but the standard deviations are comparable.

A total of 86 sets of cell dimensions were recorded from 71 different specimens; these are listed in Appendices F.1 and F.2. In most cases, the crystals used were from the bulk sample, and were not taken from microprobe mounts or thin sections. Three of the vesuvianites were found to be microcrystalline aggregates (V3, V57, and V58) and one was completely metamict (V72). The minimum cell volume belongs to a copper-bearing vesuvianite from Norway ($V49_2$); the largest cell was recorded from a partially metamict sample from Alaska (V53). The a_1 and a_2 dimensions for unconstrained cells are plotted in Figure 32. It is obvious that the a dimension varies a great deal in vesuvianite; however, most samples with $a > 15.62$Å either contain boron (filled squares) or are partially metamict (V52, V53). Evidently boron has a major effect on the cell dimensions of vesuvianite. Two of the samples with $a > 15.62$Å contain no boron and are non-metamict (V6 and $V21_p$); there is no apparent compositional reason for this.

Table 15: Constrained cell dimensions for sample V4.

Sample	a (Å)	c (Å)	V (Å^3)
V4	15.557(1)	11.791(1)	2853.7(5)
$V4_{R2}$	15.561(1)	11.787(2)	2854.0(6)
$V4_{R3}$	15.556(1)	11.790(2)	2853.0(6)
$V4_{R4}$	15.550(1)	11.785(1)	2849.5(4)
$V4_{R5}$	15.554(1)	11.786(1)	2851.3(5)
AVG	15.555(4)	11.788(3)	2852(2)

Table 16: Constrained cell dimensions, using low- and high-angle reflections.

Sample	a (Å)	c (Å)	V (Å^3)
	Low-Angle Reflections		
$V13_c$	15.522(1)	11.802(2)	2843.3(7)
$V13_i$	15.521(1)	11.813(1)	2845.7(6)
$V13_r$	15.538(3)	11.819(3)	2853(1)
$V74_c$	15.750(1)	11.704(2)	2903.4(6)
	High-Angle Reflections		
$V13_c$	15.5236(8)	11.807(2)	2845.2(6)
$V13_i$	15.538(1)	11.821(3)	2853.9(7)
$V13_r$	15.552(2)	11.824(4)	2860(1)
$V74_c$	15.7474(9)	11.709(3)	2903.5(7)

The smallest a dimensions are from the copper-bearing sample from Norway. Ito and Arem (1970) found that synthetic and natural copper-bearing vesuvianites all have small cell volumes. The a cell length for copper-bearing vesuvianites in this study ranges from 15.490–15.541Å, and seems relatively insensitive to variation in Cu content.

Note that many of the points in Figure 32 lie above the $a_1 = a_2$ line, indicating relatively major differences in the a cell dimensions for the unconstrained cell. This

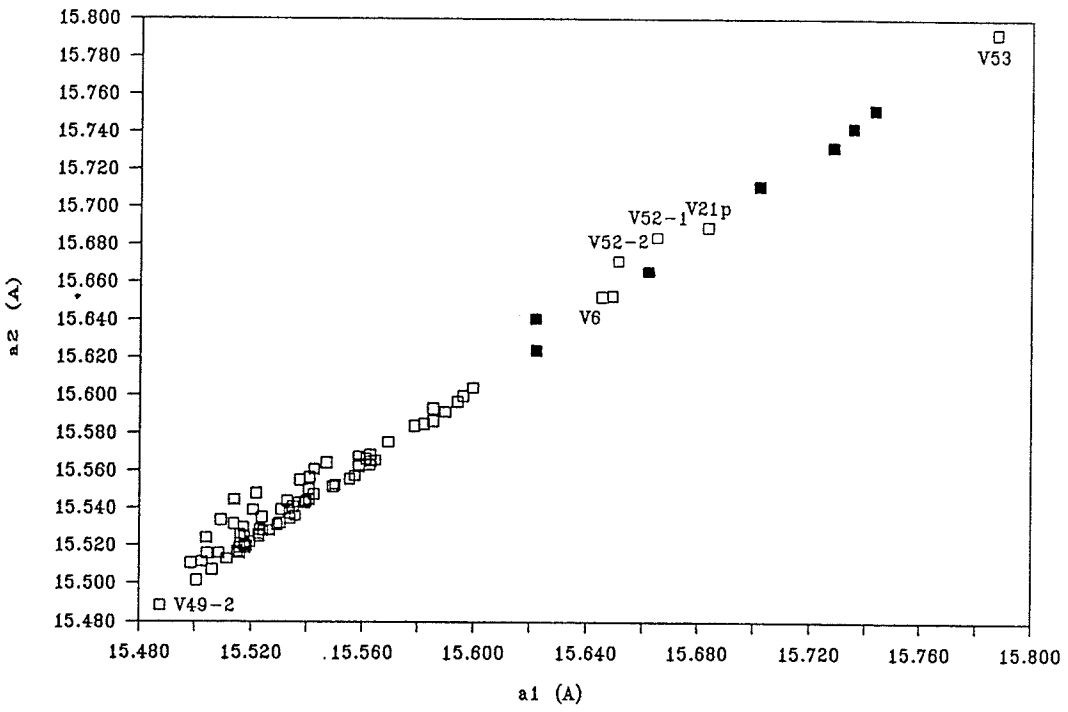

Figure 32: Vesuvianite cell dimensions; a_1 vs. a_2 (unconstrained cell). The filled squares are boron-bearing vesuvianites; they are (left to right) V45 (top), V46, V61, V38, V30, V56, and $V74_c$. Sample V46 was not analyzed for B but is from the same locality as V45. Samples V45 (V46)–$V74_c$ contain, on average, 1.47, 1.44, 1.77, 2.90, 2.94, and 2.84 wt.% B_2O_3 respectively. Samples V52 and V53 are partially metamict, and samples V6 and $V21_p$ contain no B. The edge of a point on this graph and most succeeding cell dimension plots is equivalent to two standard deviations.

point will be considered later in the discussion.

In the next diagram (Figure 33), a is plotted against c (constrained cells). Note that the boron-bearing vesuvianites have much larger a dimensions than other vesuvianites, but only slightly smaller c dimensions. Most of the remaining points define a general trend whereby a and c increase sympathetically. Part of this diagram is shown enlarged in Figure 34. Samples from Jeffrey Mine, Quebec, are shown as filled squares; vesuvianites known to be from similar environments (rodingites associated with serpentinites) are represented by dotted squares. These samples seem to define a distinct group within this diagram. As vesuvianites from these localities are known to be Al-rich and Mg-poor, a was plotted against Mg/(Al+Mg) (averaged NMNS analyses) for all of the samples (Figure 35). There is an obvious inverse relationship between a cell dimensions and Al content, and a direct relationship between a and Mg. The relationship between a and Mg/(Al+Mg) is not suprising, as the ionic radii of Al and Mg (octahedral coordination) differ by 0.18Å (Shannon, 1976). A second graph showed that there is no relationship between c and Mg/(Al+Mg). Other elements (Ti, Fe, etc.) were plotted against a, c and V, but no correlations were seen.

Ito and Arem (1970) found that a synthetic Mg-vesuvianite had a larger cell than most natural samples, and reasoned that this was indirectly because most natural samples contain F or are partially dehydroxylated. Numano *et al.* (1978) attributed the large cell dimensions of some Japanese vesuvianites to high water contents. Graphs of a, c and V against F and F+Cl+OH^-(calc.) showed no such relationship in the samples of this study.

As mentioned earlier, a number of samples gave very different a_1 and a_2 values for the unconstrained cell (see Table 17), although all interaxial angles were within 3σ of 90°. In one case ($V13_r$, high-angle reflections), $a_2 - a_1 = 0.044$Å; this is about 15 times the combined standard deviation. This difference in a cell edges was first described by Allen (1985) for a crystal from Eden Mills, Vermont.

It is obvious that for some vesuvianites, there is a metric difference in a_1 and a_2; these samples cannot be tetragonal. Figure 36 is a graph of a_1 vs. a_2 for samples from Jeffrey Mine, Quebec. Note that although most samples plot on a line defined by $a_1 = a_2$, many lie above the line. This departure from tetragonal symmetry

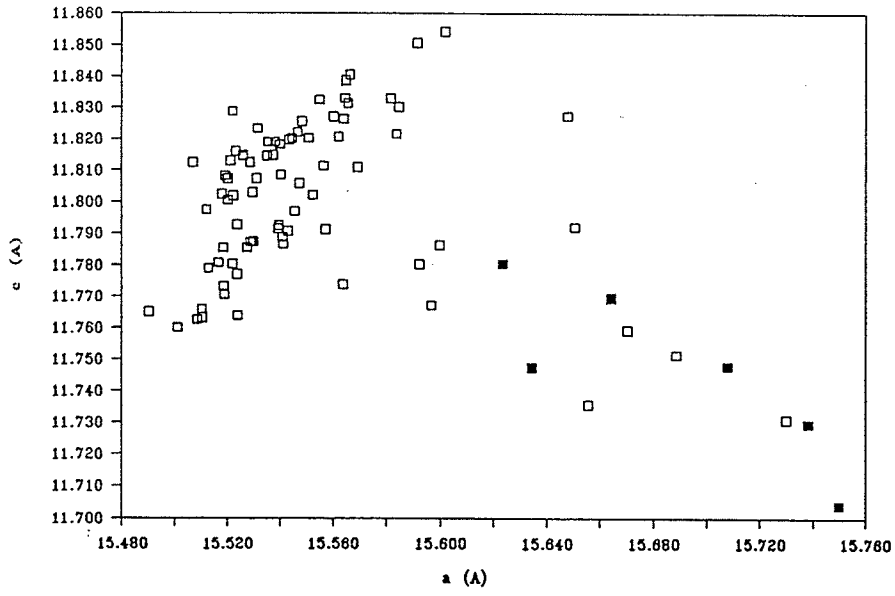

Figure 33: Vesuvianite cell dimensions; a vs. c (constrained cell). Symbols are the same as in Figure 32, except that the order of the boron-bearing samples is (left to right) V46, V45, V61, V38, V56, and $V74_c$. Sample V53 has not been plotted.

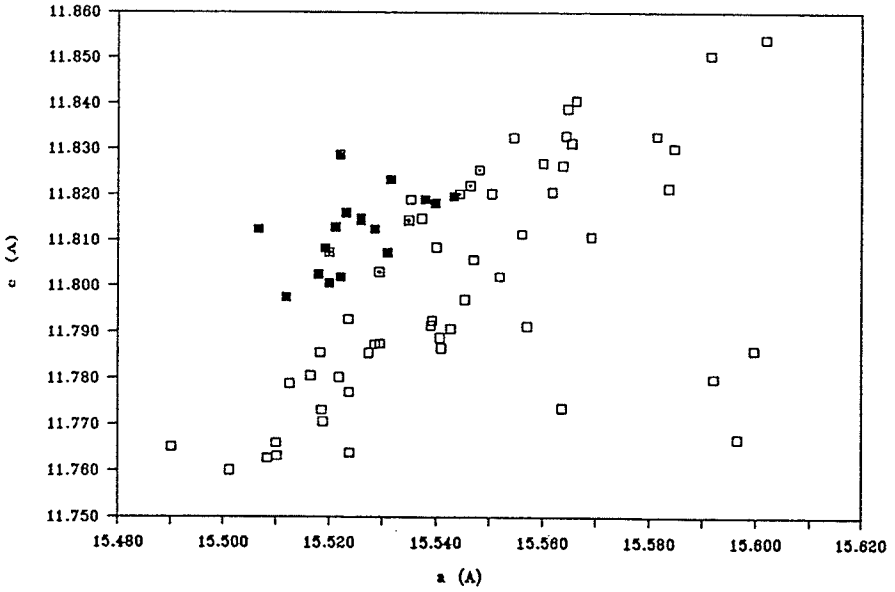

Figure 34: An enlargement of Figure 33. Samples from Jeffrey Mine, Quebec, are represented by filled squares ($V21_p$ is not shown). Other vesuvianites from similar environments are shown as dotted squares (see text). In this graph the edge of a point is approximately equal to one standard deviation.

Table 17: Maximum values of $(a_2 - a_1)$.

Sample	$a_2 - a_1$ (Å)
$V23_r$	0.020
$V52_2$	0.021
V20	0.024
$V13_r$	0.026
V21	0.031
$V13_r$ (HA)	0.044

Table 18: Selected $2V$ angles and associated values of $(a_2 - a_1)$.

Sample	$2V(°)$	$a_2 - a_1$ (Å)
$V11_3$	32.8(4)	0.018
$V23_r$	44.7(2)	0.020
V21	62.1(3)	0.031

can be correlated with the optic axial angle $(2V)$ as measured with the spindle stage (Table 18). In general, those vesuvianites with a large $2V$ also show a large difference between a_1 and a_2 in the unconstrained cell.

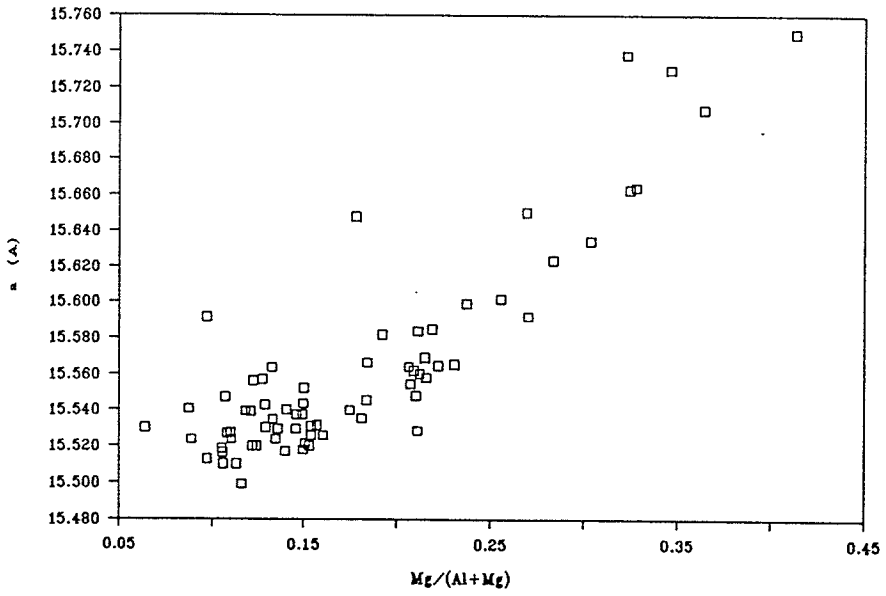

Figure 35: A graph of Mg/(Al+Mg) vs. a (averaged WD analyses).

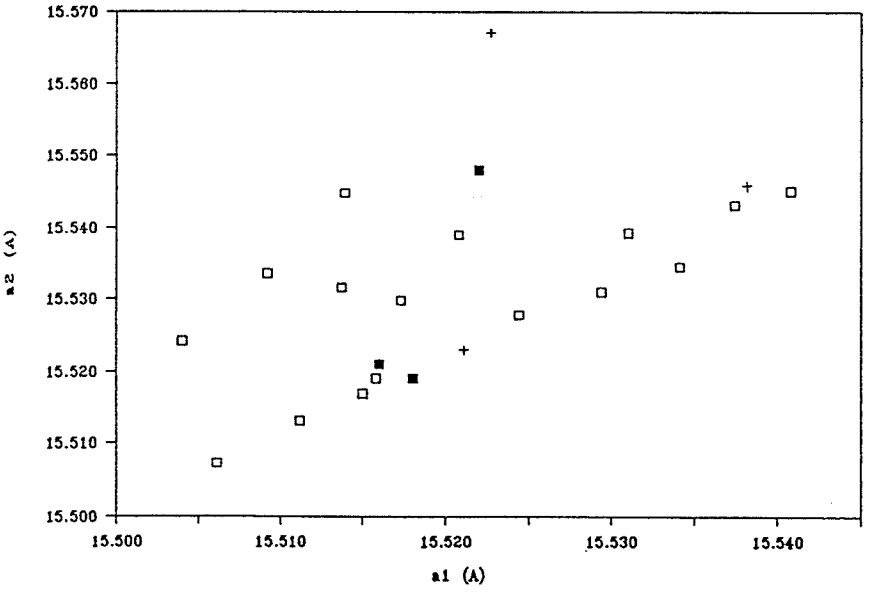

Figure 36: A graph of a_1 vs. a_2 (unconstrained cells) for all of the Jeffrey Mine samples (except $V21_p$). The filled squares are (top to bottom) $V13_r$, $V13_c$, and $V13_i$. The crosses represent "high-angle" cells for the same crystals, except that the order (top to bottom) is $V13_r$, $V13_i$, and $V13_c$. The edge of a point is approximately equal to one standard deviation.

3.6 Single-Crystal Infrared Spectroscopy

Single-crystal infrared spectra were collected from six different samples using the methods outlined in Section 2.5. The initial spectra suffered from interference effects, resulting in a periodic modulation imposed on the real spectrum (Figure 37). This was due to internal reflection of the transmitted beam, and was overcome by coating the crystal surfaces with a thin film of mineral oil.

Approximately 50 spectra, both polarized and unpolarized, were collected from six different vesuvianite samples, selected on the basis of optical zoning and chemistry. The following are qualitative comparisons. Significant structural interpretation requires integration with the structural and chemical results, and will be dealt with in Chapter 4.

V13 Jeffrey Mine, Quebec: Figure 38 shows unpolarized spectra from the (001) and (101) zones in the (100) orientation (propagation vector ||[100]); the spectra are offset vertically for clarity. Small differences in the two zones are apparent, particularly below $\approx$3600 cm^{-1}, indicating that the birefringence differences do correlate with small differences in hydrogen-bonding. There are two fairly sharp bands at 3672 and 3637 cm^{-1}, and there is a suggestion of a third band at $\approx$3650 cm^{-1}. Sharp bands such as these are fairly typical of OH groups involved in fairly weak hydrogen-bonding. Below 3600 cm^{-1} is a very irregular and intense envelope consisting of at least 5 very broad bands. The band widths are much greater than normally encountered in hydroxyl-stretching spectra, and the band energies (going down to $\approx$3000 cm^{-1}) are also lower than normal.

Figure 39 shows polarized spectra from the (001) sector in (100) orientation. The basic features are similar to the unpolarized spectrum, with the addition that there is a very strong orientation dependence of the absorption intensity; the more intense spectrum occurs when the electric vector is ||[001]. Comparison of polarized spectra (E ||[001]) for the (001) and (101) sectors, as shown in Figure 40, indicates slightly more OH in the (101) zone than in the (001) zone.

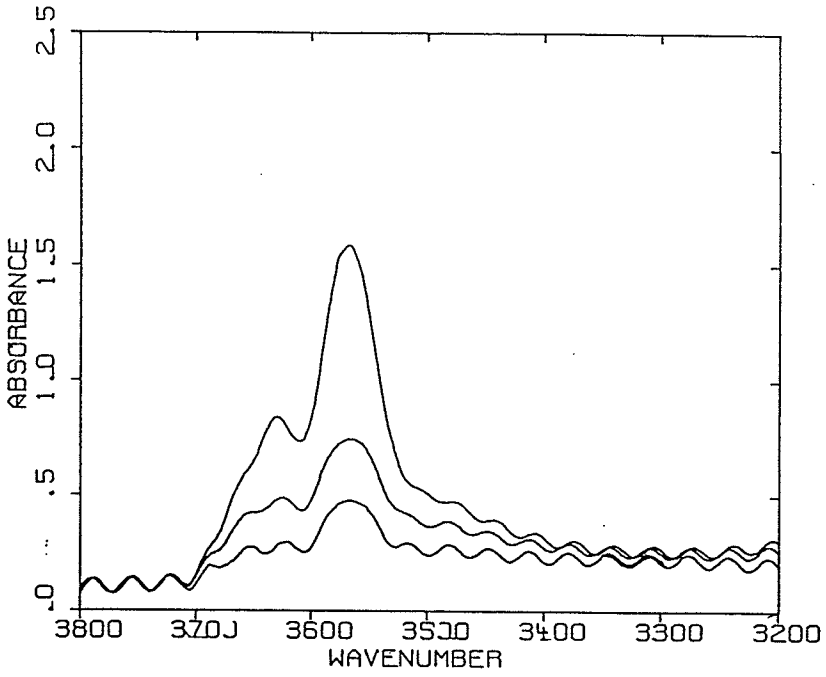

Figure 37: IR spectra from sample V74, showing modulations due to interference effects.

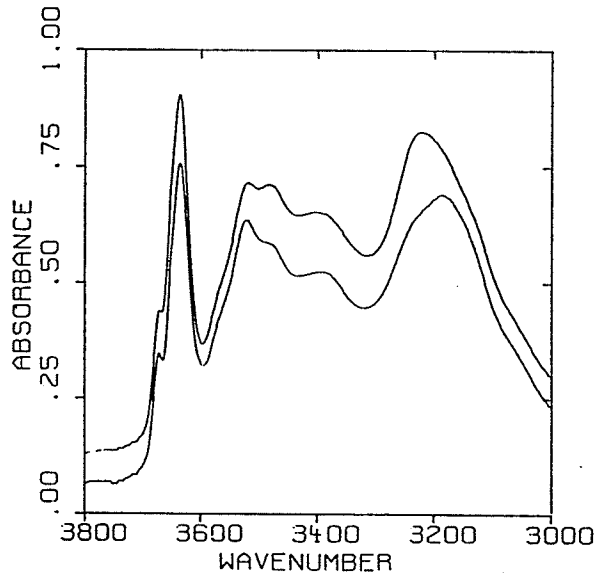

Figure 38: Unpolarized IR spectra from the (001) (top) and (101) zones of sample V13 ((100) section).

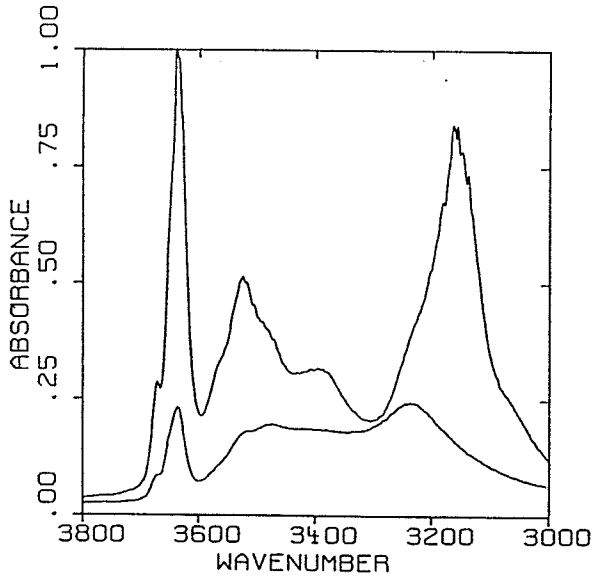

Figure 39: Polarized IR spectra from the (001) sector in (100) orientation (sample V13).

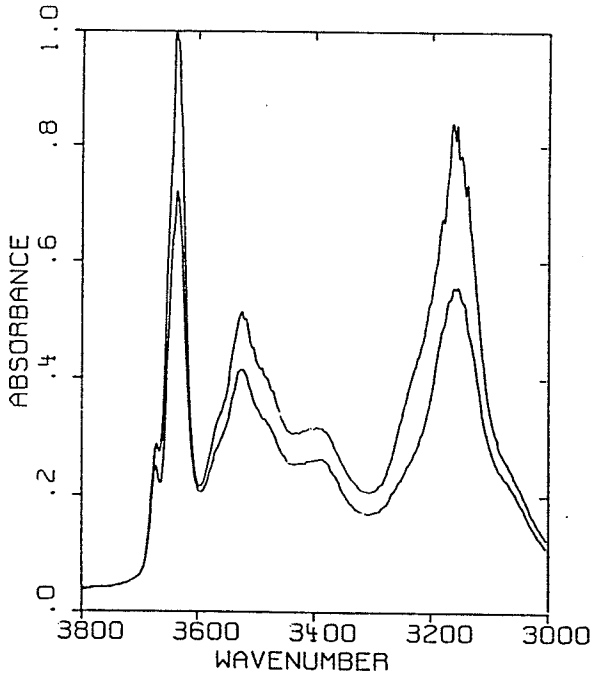

Figure 40: Polarized IR spectra (E||[001]) for the (101) (top) and (001) zones of sample V13.

Figure 41 shows polarized spectra from the (001) sector in (001) orientation (propagation vector ||[001]). This has very low birefringence and $2V$ (0–10°), and in agreement with this, there is very little difference between the spectra with E||[100] and E||[010].

V28 Jeffrey Mine, Quebec: This crystal has a blocky-zoned core and a high-birefringence rim zone. No spectral differences were seen between the different blocky zones of the core. Figure 42 shows an unpolarized spectrum from the blocky core in (001) orientation. The general features are similar to V13 from the same location, with a sharp doublet above 3600 cm^{-1} and a broad irregular envelope below 3600 cm^{-1}. However, the shape of the low energy envelope differs in detail between the two samples.

Polarized spectra of the birefingent rim ((001) orientation) are shown in Figure 43 (where the spectra are vertically offset for clarity). At high energies, the spectra are identical, but the lower energy envelopes differ significantly, showing that the deviation from tetragonal character apparent in the optics also finds expression in the infrared spectra. Obviously the genesis of these peculiar peaks is very pertinent to the non-tetragonal nature of the vesuvianite structure.

V30 Templeton Township, Quebec: Polarized spectra in (100) orientation are shown in Figure 44; there is a strong dependence of intensity on orientation, with maximum absorption occurring when E||[001]. The spectra are similar to those of the Ariccia vesuvianite (V38), with a major peak at 3570 cm^{-1} and minor peaks at 3630 cm^{-1} and 3490 cm^{-1}. However, the relative intensities of the three peaks differ, the higher energy peak being relatively more intense in V30. In addition, there is a prominent high-energy shoulder at $\approx$3665 cm^{-1} in this vesuvianite.

V38 Ariccia, Italy: Figure 45 shows polarized spectra of the (low) birefringent rim in (001) orientation; note the slight polarization dependence of intensity only at the maximum absorption. There is a major peak at 3570 cm^{-1} that shows some evidence of fine-structure, together with a prominent higher-energy shoulder at $\approx$3630 cm^{-1}. At lower energies, there is a prominent symmetrical peak at 3480 cm^{-1}, and at lower energies the absorption tails away, but is still significant at 3000 cm^{-1}.

In (001) section the Ariccia vesuvianite shows several narrow zones surrounding

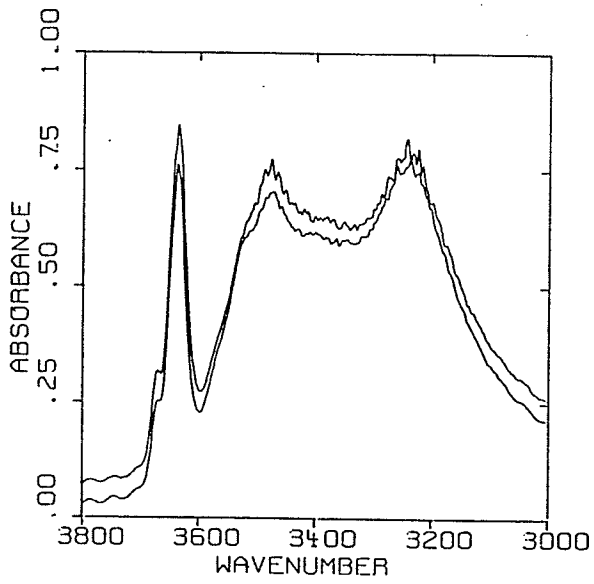

Figure 41: Polarized IR spectra from the (001) zone of sample V13 ((001) orientation; propagation vector ||[001]).

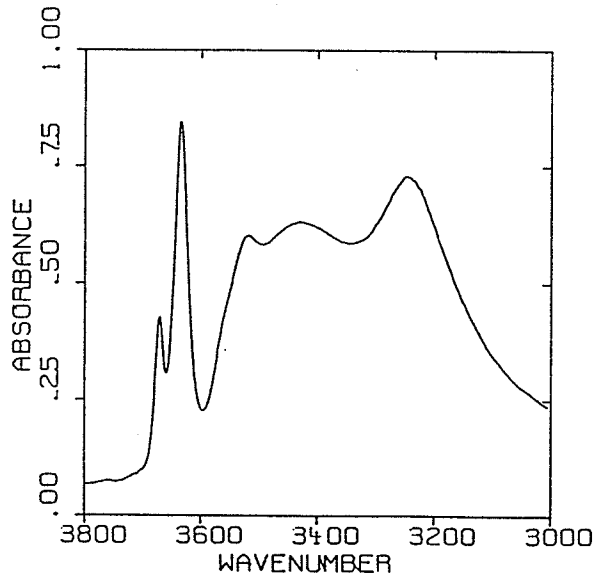

Figure 42: Unpolarized IR spectrum from the blocky-zoned core of sample V28 ((001) section).

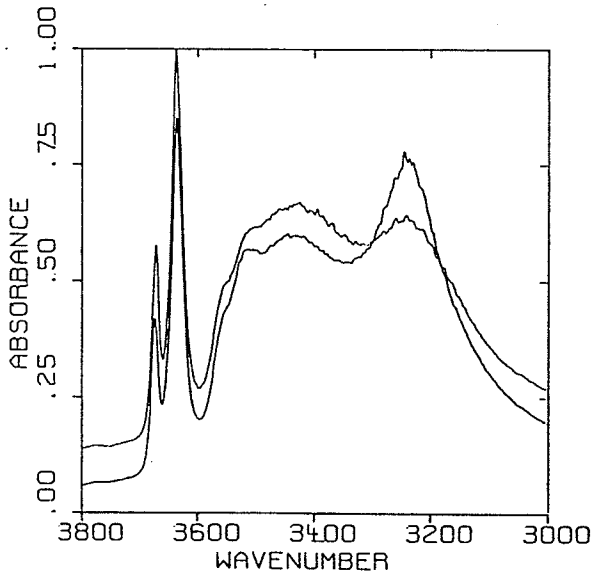

Figure 43: Polarized IR spectra of the birefringent rim of V28 ((001) orientation). The spectra are vertically offset for clarity.

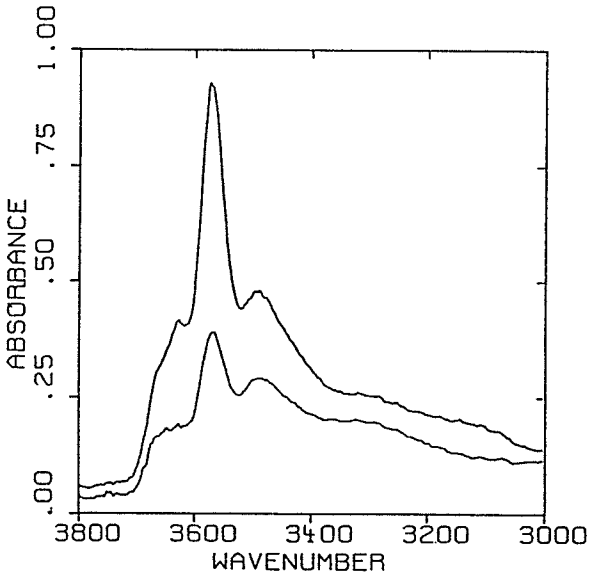

Figure 44: Polarized IR spectra in (100) orientation; sample V30.

a substantial core (see Figure 6). Figure 46 shows unpolarized spectra from these zones, starting at the rim (lowest spectrum) and ending at the core (highest spectrum). Moving inwards, there is a gradual increase in intensity. As the thickness of the section is uniform, this indicates a zoning of the H content (assuming no radial change in the transition probability), with an increase of ≈50 from rim to core. In addition, the relative intensities of the three principal peak changes, indicating some change in the hydrogen-bond conformations in the various zones.

V45 Laguna del Jaco, Mexico: Because of sample preparation problems and limited material, only a (100) sample could be prepared. The polarized spectra are shown in Figure 47, in which the intense spectrum has E||[001]. The spectra are radically different from those from the Jeffrey samples. At ≈3658 cm^{-1}, there is a broad band with a suggestion of a shoulder at ≈3681 cm^{-1}. Below these is the most intense band at 3570 cm^{-1}; but with E ||[001], the band seems to have a fine-structure with (at least) 3 components. There is a third broad band at ≈3475 cm^{-1}. The less-intense spectrum then tails away at lower energies, but the more-intense spectrum shows a very broad band at 3170 cm^{-1}. Note the prominent transmission window in the range 3400-3250 cm^{-1} in the intense spectrum, and contrast this with the intense absorption right across the energy range in the Jeffrey samples.

V74 Wilui River, U.S.S.R.: The Wilui vesuvianites show complex optical zoning, and the IR spectra show significant differences between these zones. Figure 48 ((a) and (b)) shows polarized spectra for different zones in the (100) orientation; intense spectra are for E||[001]. The energies of the bands are identical in the different spectra, but there is a significant difference in the relative intensities. There is a prominent band at 3570 cm^{-1} with significant fine-structure (cf. V30 and V38), and prominent weaker bands at 3490 and 3630 cm^{-1}, the latter having a prominent shoulder at ≈3660 cm^{-1}. In addition, there is a broad weak band in the lower energy region at ≈3150 cm^{-1}.

Figure 49 shows polarized (E||[001]) spectra for all the major zones. The bands are as described above (see Figures 48a, b), but the relative intensity of the spectra change, indicating a zoning of H; however, no obvious pattern emerges from this. However, what is prominent in these spectra is the lack of a broad absorption in the low-energy region, as observed in the Jeffrey vesuvianite spectra (samples V13

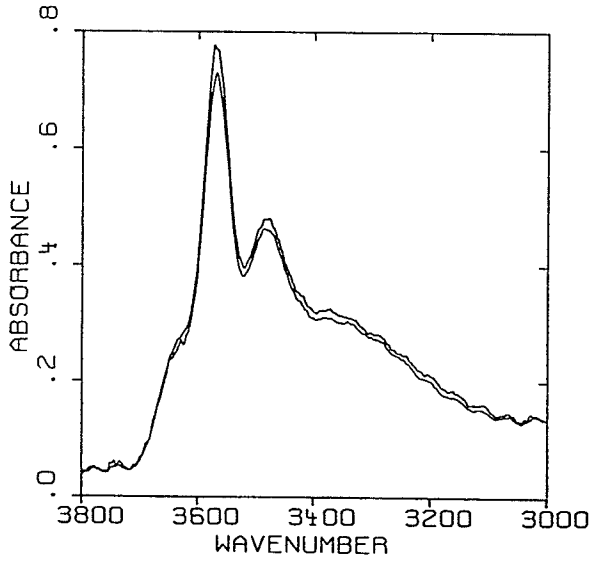

Figure 45: Polarized IR spectra of the low birefringence rim zone of sample V38 ((001) orientation).

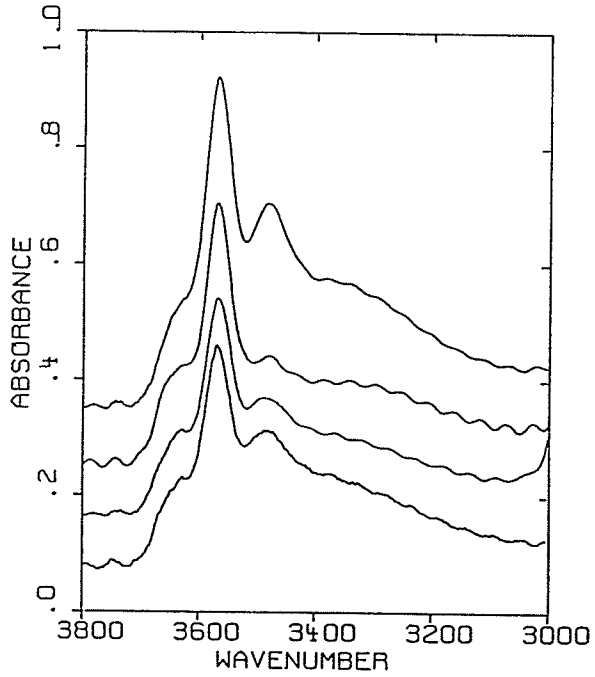

Figure 46: Unpolarized IR spectra from the core (top) to the rim of sample V38 ((001) section).

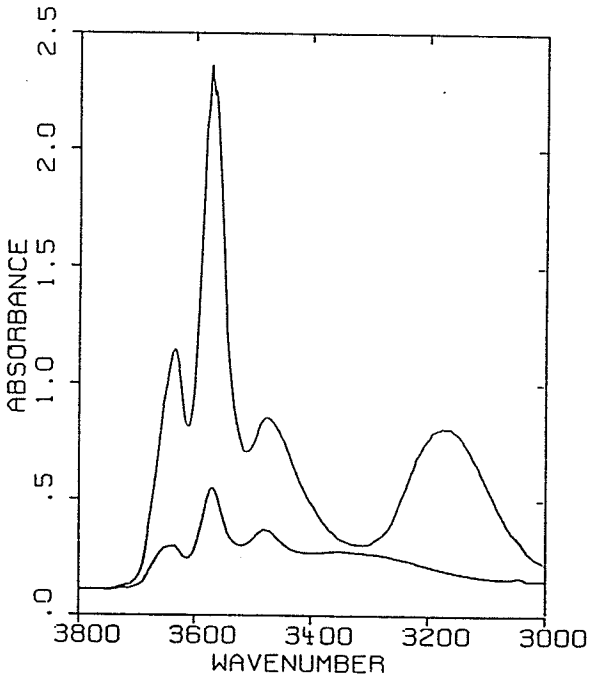

Figure 47: Polarized IR spectra, sample V45 ((100) section).

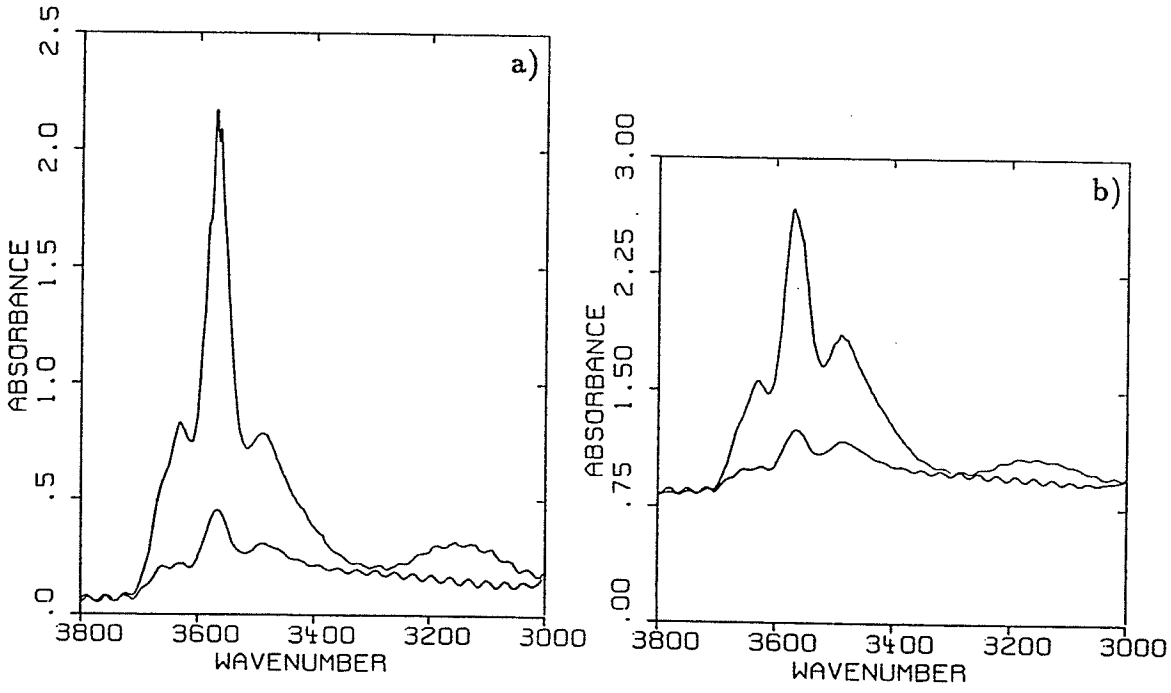

Figure 48: a) and b) Polarized IR spectra for different zones in (100) orientation (sample V74).

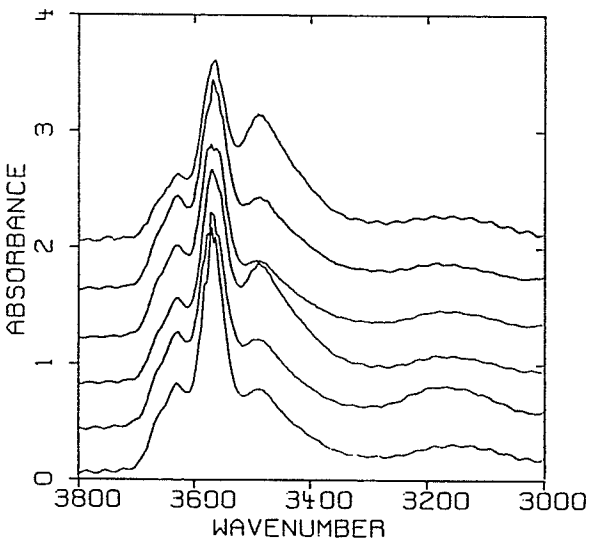

Figure 49: Polarized (E||[001]) IR spectra for all the major zones in sample V74. and V28).

3.7 Space Group Symmetry of Vesuvianite

Many different space groups have been suggested for vesuvianite; these were discussed in Section 1.3. Use of the correct space group is a fundamental assumption in crystal structure analysis; an incorrect choice will necessarily lead to some incorrect stereochemical conclusions. For this reason, a number of methods were used to determine the space groups of those crystals selected for crystal structure refinement.

3.7.1 Precession Photography

Four crystals ($V74_c$, $V13_c$, $V13_1$ and $V13_r$) were selected for intensity data collection. The Wilui vesuvianite was choosen because microprobe analysis indicated significant B and the wet-chemical analyses and IR spectroscopy showed it to have a low hydrogen content. The Jeffrey sample was chosen because of the spectacular optical zoning and variable $2V$; crystals were removed from the core, intermediate zone, and rim of a (001) section similar to that in Figure 13; these were designated $V13_c$, $V13_1$ and $V13_r$ respectively.

All four crystals were shaped in a sphere grinder to minimize differential absorption. Up to 14 precession photographs were taken of each crystal; some of these are shown in Appendix H. Many of the photographs showed reflections that violate $P4/nnc$ symmetry. There are two types of violating reflections to consider; those that violate translational symmetry elements, and reflections that violate point symmetry elements. Reflections of the first type can be divided into three classes (Table 19), depending on which extinction conditions of space group $P4/nnc$ they violate.

In some cases, Renninger (double diffraction) reflections were observed violating certain translational symmetry elements (Figure 50). Two full sets of precession photographs were taken (using different precession angles) in order to identify these diffractions.

Reflections that violate point symmetry elements are most apparent in $hk0$ or upper level photographs. If the fourfold axis is violated, reflections related by

Table 19: $P4/nnc$ extinction conditions.

Symbol	Glide Plane	Violating Conditions
a'	n glide $\perp c$	$hk0$, $h+k$ odd
b'	n glide $\perp a$	$h0l$, $h+l$ odd
		$0kl$, $k+l$ odd
c'	c glide $\perp$[110]	hhl, l odd

a rotation angle of 90° will have nonequivalent intensities (as judged by eye). Because $P4/nnc$ belongs to the Laue group $P4mm$, violations of glide-plane extinction criteria can also be accompanied by intensity equivalence violations across the corresponding mirror plane. We will now discuss the results of the precession photographs for each crystal in detail.

V74c: No violating reflections are seen in any of the $V74_c$ photographs. The allowed reflections are sharp and of uniform shape, and no streaking is seen. All reflections related by mirror planes or by a 90° rotation about the fourfold axis are of equal intensity.

V13c: Figure 50(a) shows the $h0l$ zero-level photograph for $V13_c$. The allowed reflections are not as sharp as those in the equivalent $V74_c$ photograph, and there are many b'–type violating reflections (Table 20). Some of those are quite strong (especially 104), but most are relatively weak and show streaking in the a^* direction. This streaking (indicating short-range disorder) is especially noticeable around the stronger allowed reflections such as 004 and 008, and along the $h03$ and $h06$ rows. Also seen in this photograph is a sharp Renninger reflection (702) that is not seen in an equivalent photograph taken at a different precession angle (Figure 50b). All allowed and violating reflections related by the horizontal mirror plane (n glide $\perp c$) were judged to be of equal intensity. The $h1l$ photograph (Appendix H) shows much less streaking, and the violating reflections along the c^* axis (014 and 016) are poorly defined.

The $hk0$ photograph shows faint streaking $\parallel \bar{1}10$, especially around 440 and 880. All reflections related by a 90° rotation about the fourfold axis appeared of equal intensity, but this was not the case for reflections related by vertical mirror planes. Weak, high hk reflections such as 11 7 0 (≡7 11 0) show the greatest differences in

(a)

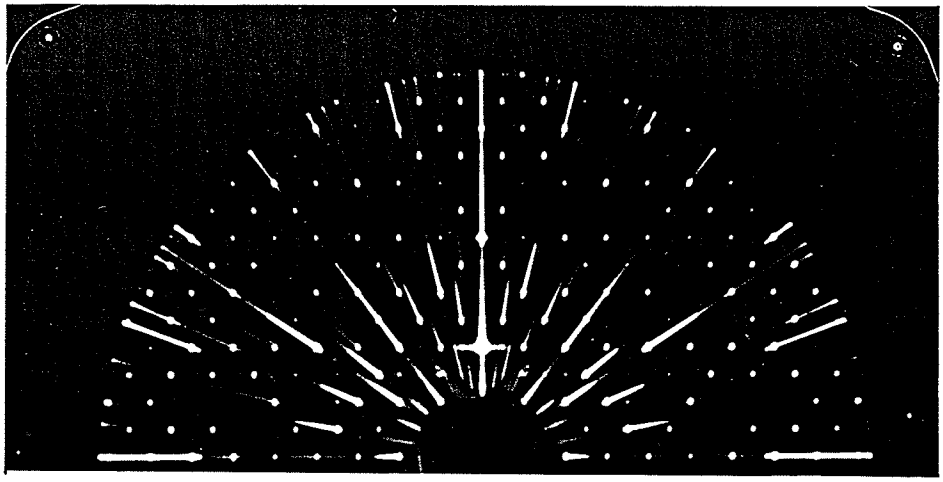

(b)

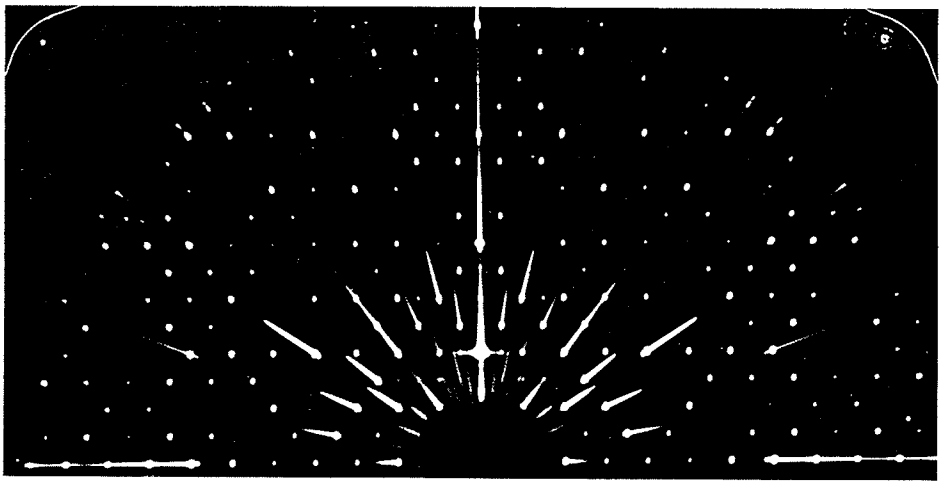

Figure 50: (a) *h0l* photograph of $V13_c$. Note the Renninger reflection (702) not seen in (b). (b) *h0l* photograph taken at a different precession angle. Note that the Renninger reflection is absent.

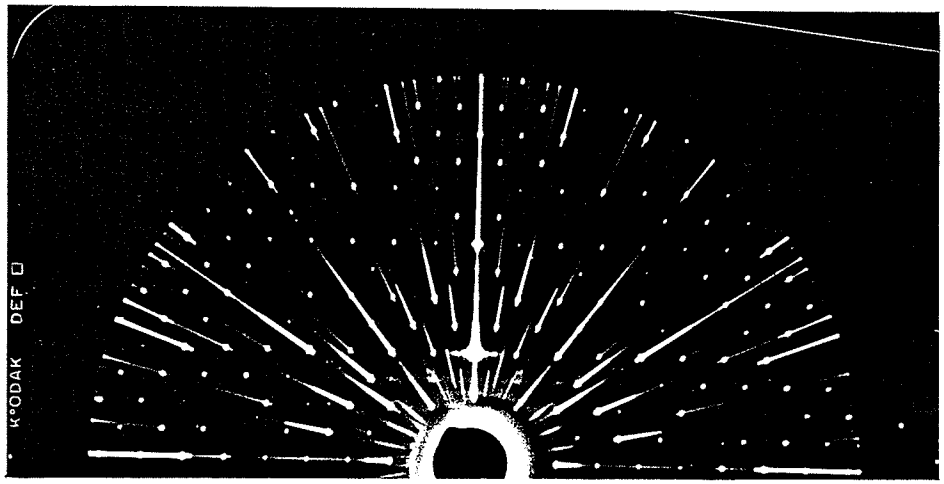

Figure 51: $h0l$ photograph of $V13_i$.

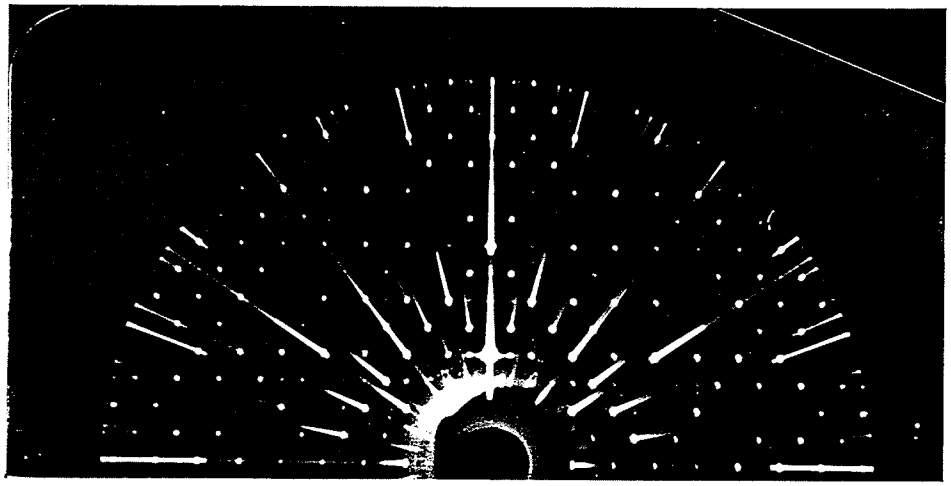

Figure 52: $h0l$ photograph of $V13_r$.

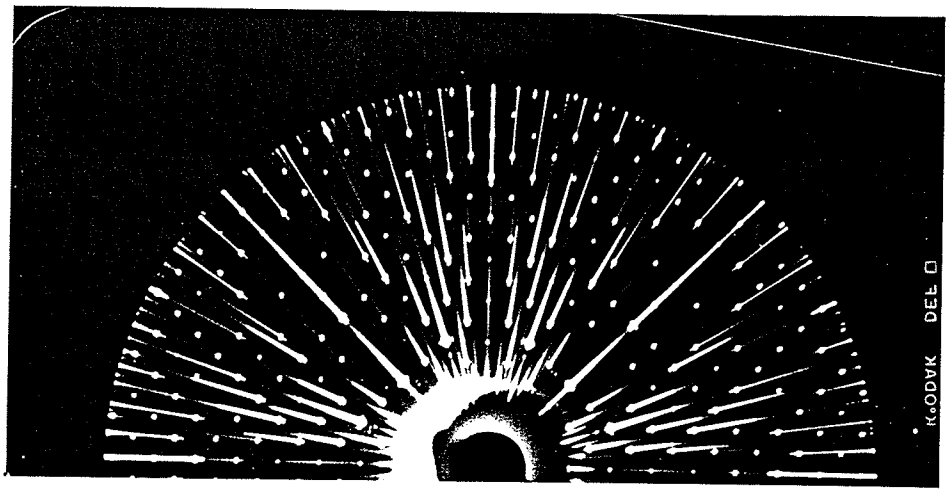

Figure 53: $hk0$ photograph of $V13_r$.

intensity. A number of c'–type violating reflections are seen in the $hk1$ upper level photograph. Once again, all reflections related by a 90° rotation about the fourfold axis are equivalent. More c'–type violating reflections are seen in the $hk3$ upper level photograph.

V13i: Precession photographs of this crystal show many of the features seen in the $V13_c$ photographs. The violating reflections are less intense, presumably because the crystal itself is smaller. The $h0l$ photographs (Figure 51) show the same streaking seen in the equivalent $V13_c$ photographs. Once again, 104 is the strongest violating reflection, and the 702 Renninger reflection is seen in the $\overline{\mu} = 25°$ photograph. No violations of the horizontal mirror plane are seen. Reflection 014 is present in the $h1l$ upper level photograph, but is more indistinct than for $V13_c$.

In the $hk0$ photographs, the same non-equivalency of reflections across the vertical mirror planes is apparent. A few very faint c'–type reflections are seen in the upper level hk photographs.

V13r: Many violating reflections are seen in the $h0l$ photographs of this crystal (Figure 52 and Table 20). Compared to those in previous photographs, violating

h	k	l	F	σF	$F/\sigma F$	a'	b'	c'	h	k	l	F	σF	$F/\sigma F$	a'	b'	c'
0	1	4	26.86	5.43	4.95		x		6	6	1	*	*	*			x
0	1	6	*	*	*		x		7	7	1	*	*	*			x
1	0	4	33.42	5.42	6.17		x		8	0	3	*	*	*		x	
1	0	6	*	*	*		x		8	8	1	*	*	*			x
1	0	12	40.34	9.94	4.06		x		9	9	1	*	*	*			x
2	0	3	19.98	4.96	4.03		x		10	0	3	27.68	8.11	3.41		x	
3	0	6	50.66	6.27	8.08		x		10	10	1	*	*	*			x
4	4	1	*	*	*			x	11	11	1	*	*	*			x
5	0	2	*	*	*		x		15	15	1	*	*	*			x
5	0	6	28.10	6.44	4.36		x										
1	0	1	*	*	*		x		2	0	5	*	*	*		x	
1	0	4	*	*	*		x		5	0	2	*	*	*		x	
1	0	6	*	*	*		x		6	6	1	*	*	*			x
2	0	3	*	*	*			x									
0	1	4	77.90	5.29	14.73		x		5	0	2	*	*	*		x	
0	1	6	36.42	5.35	6.81		x		5	0	6	27.68	5.79	4.78		x	
0	1	8	*	*	*		x		5	0	8	25.94	6.90	3.76		x	
0	1	12	50.02	8.97	5.58		x		6	6	3	36.90	5.28	6.99			x
0	1	14	*	*	*		x		6	6	1	*	*	*			x
1	0	4	95.87	5.35	17.92		x		8	0	3	31.81	6.08	5.23		x	
1	0	6	36.77	5.49	6.70		x		8	8	1	27.99	6.92	4.04			x
1	0	8	*	*	*		x		9	0	10	*	*	*		x	
1	0	12	53.57	9.25	5.79		x		9	0	12	*	*	*		x	
2	0	3	31.84	4.88	6.52		x		10	0	3	78.35	8.06	9.72		x	
3	0	4	18.80	4.54	4.14		x		10	0	7	45.45	8.41	5.40		x	
3	0	6	*	*	*		x		10	10	1	*	*	*			x
3	0	8	*	*	*		x		11	0	2	62.17	7.94	7.83		x	
3	0	12	*	*	*		x		11	11	1	*	*	*			x
4	4	1	*	*	*			x	12	12	1	*	*	*			x

*$F/\sigma F < 3.00$

Table 20: Unique (positive quadrant) violating reflections from precession photographs (top to bottom, V13c, V13i and $V13_r$; F and σF are from the intensity datasets).

reflections are sharp, and there is much less streaking. The 702 Renninger reflection is present in the $\overline{\mu} = 25°$ photograph. Violating reflections present in the $h1l$ photograph are 014, 016, 018, 0 1 12, and 0 1 14. No streaking is seen, and the reflections themselves are sharp.

The $hk0$ photograph (Figure 53) shows the same non-equivalency across the vertical mirrors seen previously. All reflections related by a 90° rotation about the fourfold axis are equivalent, as judged by eye. The $hk1$ photograph shows a number of c'–type violating reflections. Nothing unusual is seen in 3rd and 4th level photographs in this orientation.

Diffraction evidence from the precession photographs allows us to make some conclusions about the space groups of the four crystals. Photographs of the Wilui crystal show no reflections violating $P4/nnc$ extinction conditions, so this was the only space group used in the structure work. All photographs of the Jeffrey crystals show many b'–type and c'–type violating reflections. No a'–type violating reflections are seen in any of the photographs. For these reasons, the maximum space group for the V13 crystals is $P4/n$. There is no evidence to suggest loss of the fourfold axis, even though optical investigation shows that these crystals cannot be tetragonal.

3.7.2 Diffraction Evidence from X-ray Intensity Data Collections

Additional diffraction evidence was obtained from the X-ray intensity data collections (Section 3.9.5). The program X in SHELX automatically flags violating reflections, and treats them as unobserved in subsequent stages of the refinements. Appendix I lists these reflections (with $F/\sigma F > 3.00$) for all four of the crystals. The histograms in Figure 54 show the number and distribution of unique (positive octant) violating reflections with $F/\sigma F > 4.00$ in the V13 datasets. These are listed in Table 21.

The diffraction evidence from the X-ray intensity data collections corresponds to that in the precession photographs. The V74$_c$ collection shows only one violating reflection with $F/\sigma F > 4.00$ (111). The V13 datasets show many b'– and c'–type violating reflections; one of these (104 in V13$_r$) has a $F/\sigma F$ value of 17.92. Very few a'–type violating reflections are seen.

Some of the stronger violating reflections were examined with psi scans to determine whether or not they were due to double diffraction. The psi scans are

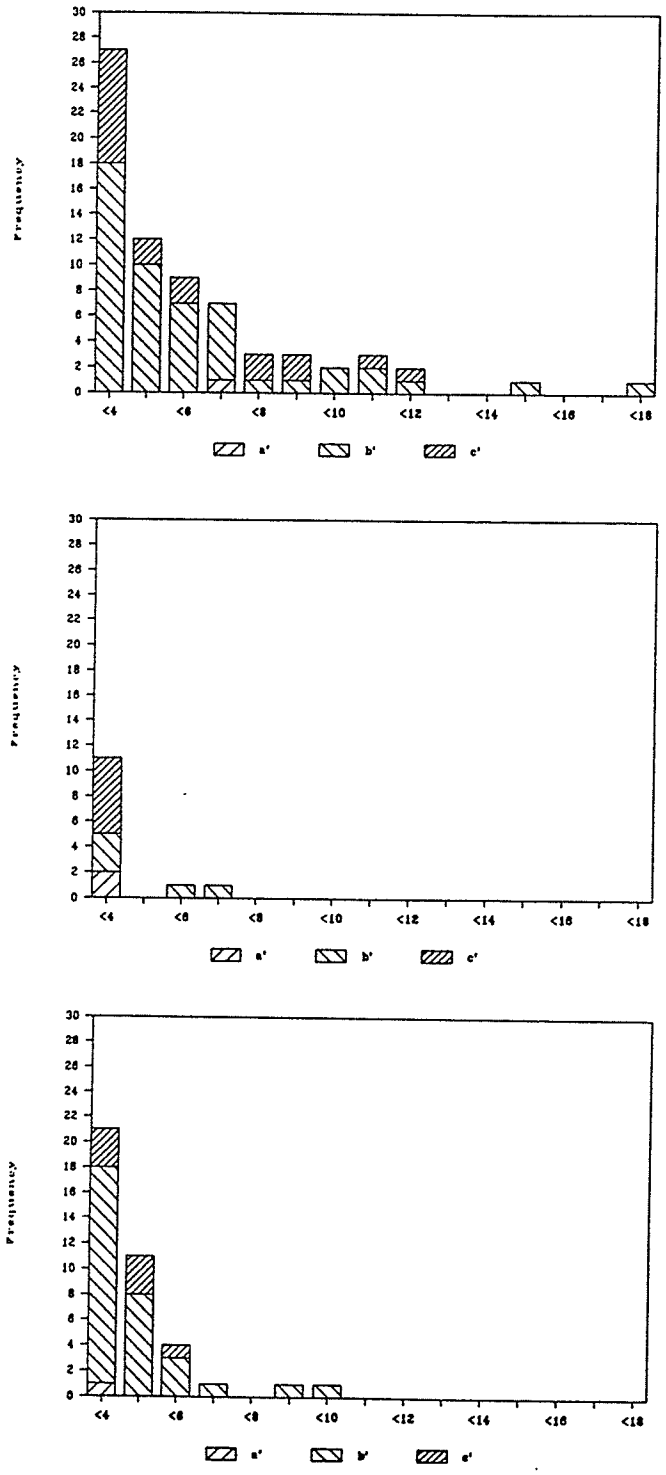

Figure 54: Histograms of unique (positive h, k and l) violating reflections from the X-ray intensity data collections for $V13_c$, $V13_i$ and $V13_r$. $V74_c$ showed only one violating reflection with $F/\sigma F > 4.00$ (111).

h	k	l	F	σF	$F/\sigma F$	a'	b'	c'	h	k	l	F	σF	$F/\sigma F$	a'	b'	c'
0	1	4	26.86	5.43	4.95		x		1	0	12	40.34	9.94	4.06		x	
0	1	14	42.99	10.30	4.17		x		1	1	11	42.93	8.53	5.03			x
0	6	3	26.20	5.77	4.54		x		2	0	3	19.98	4.96	4.03		x	
0	8	3	27.09	6.54	4.14		x		2	2	3	23.02	5.28	4.36			x
0	10	3	47.60	8.73	5.45		x		3	0	6	50.66	6.27	8.08		x	
0	10	11	40.38	10.03	4.03		x		5	0	6	28.10	6.44	4.36		x	
0	11	8	47.30	9.32	5.08		x		7	7	3	40.44	8.44	4.79			x
0	14	11	70.29	12.34	5.70		x		7	7	7	43.73	9.67	4.52			x
1	0	4	33.42	5.421	6.17		x		19	0	2	130.29	13.34	9.77		x	
0	7	6	35.55	6.28	5.66		x		7	0	10	57.92	8.29	6.99		x	
0	0	3	22.12	4.54	4.87		x	x	1	0	12	53.57	9.25	5.79		x	
0	0	7	26.48	5.68	4.66		x	x	1	1	1	19.34	2.53	7.64			x
0	0	11	109.75	9.59	11.44		x	x	2	0	3	31.84	4.88	6.52		x	
0	1	4	77.90	5.29	14.73		x		2	2	3	51.32	5.05	10.16			x
0	1	6	36.42	5.35	6.81		x		3	0	4	18.80	4.54	4.14		x	
0	1	12	50.02	8.97	5.58		x		3	3	3	42.57	5.20	8.19			x
0	2	3	33.35	5.03	6.63		x		4	0	3	54.91	5.10	10.77		x	
0	4	3	54.38	5.29	10.28		x		4	0	7	37.13	6.31	5.88		x	
0	4	5	24.49	5.23	4.68		x		5	0	6	27.68	5.79	4.78		x	
0	4	7	29.86	6.21	4.81		x		5	4	0	32.10	4.62	6.95		x	
0	4	11	38.37	8.32	4.61		x		6	0	3	36.90	5.28	6.99		x	
0	5	6	27.56	5.97	4.62		x		6	6	3	35.29	6.38	5.53			x
0	6	3	29.62	5.48	5.41		x		7	7	3	54.41	7.73	7.04			x
0	8	3	30.11	6.03	4.99		x		7	7	7	83.43	9.41	8.87			x
0	9	10	34.93	8.50	4.11		x		8	0	3	31.81	6.08	5.23		x	
0	10	3	78.53	8.30	9.46		x		8	8	1	27.99	6.92	4.04			x
0	10	7	59.95	8.84	6.78		x		10	0	3	78.35	8.06	9.72		x	
0	11	2	70.86	8.16	8.68		x		10	0	7	45.45	8.41	5.40		x	
0	11	6	47.91	8.71	5.50		x		11	0	2	62.17	7.94	7.83		x	
1	0	4	95.87	5.35	17.92		x		11	11	3	49.19	9.63	5.11			x
1	0	6	36.77	5.49	6.70		x		14	0	11	48.18	11.42	4.22		x	

Table 21: Unique violating reflections ($F/\sigma F > 4.00$) from X-ray intensity datasets (top to bottom, V13c, V13i and $V13_r$).

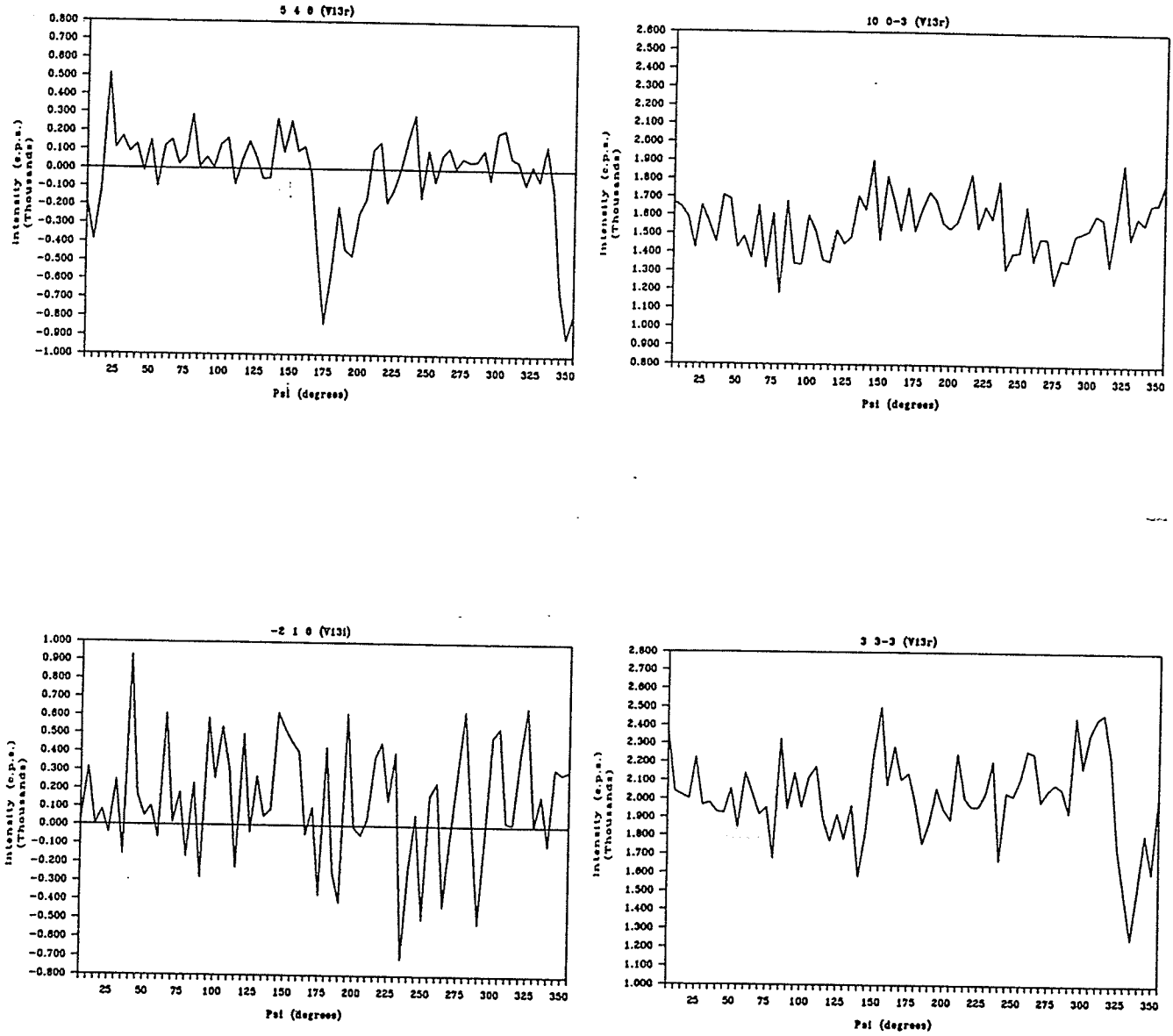

Figure 55: Psi scans of reflections violating $P4/nnc$ extinction criteria. Both -210 ($V13_i$) and 540 ($V13_r$), seen as strong violating reflections in the intensity datasets, are Renninger reflections. The psi scans for 3 3-3 ($V13_r$; a'–type reflection) and 10 0-3 ($V13_i$; b'–type) show that these violating reflections are real.

Table 22: Intensities (cps$\times 10^{-3}$) for 346 and equivalent reflections ($P4/nnc$).

h k l	$V74_c$	$V13_c$	$V13_i$	$V13_r$
$\bar{4}$ 3 $\bar{6}$	215(3)	499(4)	235(3)	290(3)
$\bar{4}$ 3 6	217(3)	496(4)	223(3)	293(3)
$\bar{3}$ 4 $\bar{6}$	214(3)	490(4)	228(3)	263(3)
$\bar{3}$ 4 6	219(3)	495(4)	233(3)	257(3)
3 4 $\bar{6}$	211(3)	484(4)	225(3)	298(3)
3 4 6	215(3)	476(4)	228(3)	299(3)
4 3 $\bar{6}$	216(3)	482(4)	227(3)	260(3)
4 3 6	213(3)	484(4)	223(3)	264(3)

shown in Figure 55; note that scans of the a'–type reflections show irregular peaks superimposed on a zero background. This suggests that these are Renninger reflections. The scans of the other diffractions, however, show peaks superimposed on a background of 1800–2100 cps, which indicates that these are real.

Allen (1985) reported that a crystal from Eden Mills showed unequal intensity distribution for the 346 set of equivalent reflections, indicating $P4/m$ Laue symmetry. Table 22 lists intensities (with background correction) for the 346 set of reflections in each dataset. Note that reflections related by a mirror plane $\perp c$, or by a 90° rotation about the fourfold axis, are statistically identical. Those reflections in the $V13_r$ column related by vertical mirror planes are non-equivalent, indicating $P4/m$ Laue symmetry.

3.7.3 Possible Space Groups for Vesuvianite

In the previous two Sections, the diffraction evidence for space group selection was discussed. As is common for diffraction evidence, often one cannot make a unique choice for a space group, as the extinctions are not totally definitive.

The basic vesuvianite structure has space group $P4/nnc$; structural modifications of this can only occur in space groups that are subgroups (or supergroups) of this basic structure. There are no 3-dimensional supergroups of $P4/nnc$ and thus an additional constraint on the symmetry of vesuvianite is that it must assume a symmetry that is a subgroup of $P4/nnc$. This may be easily derived using

techniques of elementary group theory.

The space group $P4/nnc$ is of rank 16. Any subgroup (except itself; every group is a subgroup of itself) must have a rank that is a factor of 16, i.e. 1, 2, 4 or 8. Using the basic axioms of group theory, we can systematically delete each symmetry element in turn to derive all subgroups of rank 8. Iteration of this procedure gives us the lower rank space groups.

An example of this is shown in Figure 56. We begin by removing the $2'$ operation from the multiplication table for space group $P4/nnc$. First we delete the column and row headed $2'$; inspection of the table shows that $2'$ operations remain in the table. We remove these by systematically serially deleting all rows and columns containing the $2'$ operation. This is not a unique series of steps, as different combinations of deleted rows and columns give rise to different space groups, but by working through each possible alternative, all the possible space groups are derived. Repeating this procedure for all symmetry elements and for all possible combination of symmetry elements gives us the space group tree seen in Figure 57, which lists the only possible space groups for derivatives of the $P4/nnc$ vesuvianite structure.

We can go farther by continuing these arguments with some conclusions based on the optical measurements. Most of our vesuvianites are detectably biaxial. Formally, this precludes a tetragonal structure (however, it must be realized that optics is extremely sensitive to very small changes in symmetry, and such deviations might not always be apparent in the diffraction data). Biaxial vesuvianites can be orthorhombic, monoclinic or triclinic.

The group reduction techniques used above show that any orthorhombic vesuvianites must have (orthogonal) axes at 45° to the ideal tetragonal axes (orthorhombic space groups use the diagonal $2'$ and $2''$ axes). We know the orientation of the ideal tetragonal axes from the morphology of the crystal and its correspondence with the tetragonal axes of the ideal $P4/nnc$ structure. An orthorhombic derivative would therefore have its crystallographic axes at 45° to the ideal tetragonal axes, that is corresponding to a tetragonal orientation of [110] and $[1\bar{1}0]$. As orthorhombic symmetry constrains the optic axes to correspond with the crystallographic axes, the optic axial plane thus has to correspond to a principal plane in the orthorhom-

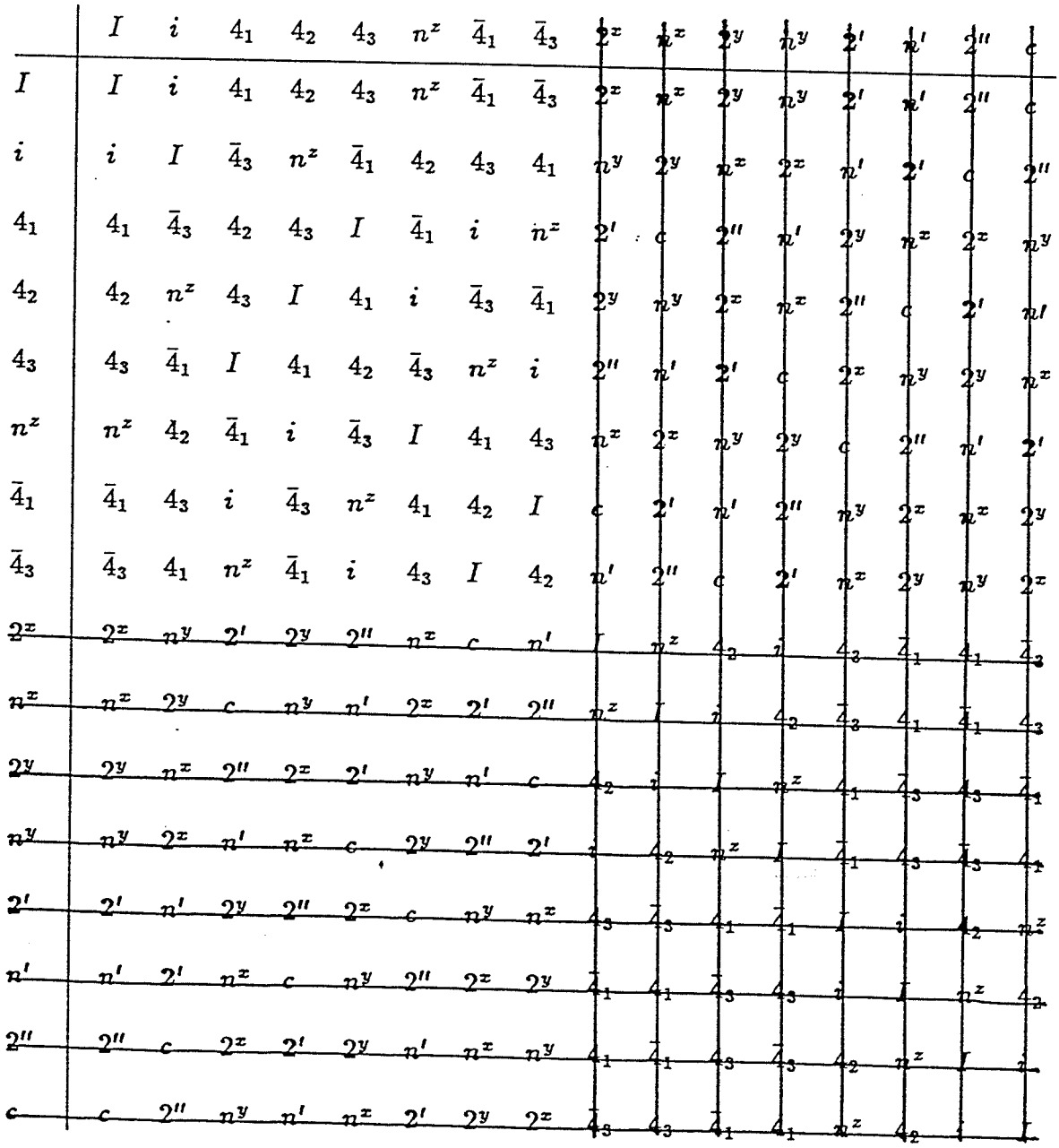

Figure 56: Multiplication table for $P4/nnc$. If all of the columns and rows containing $2'$ (bold) are deleted, only the symmetry operators for $P4/n$ remain.

bic system. In Section 3.2, I showed that the optic axial plane for the V13 crystal is always parallel to (100) and/or (010) of the ideal tetragonal morphology. This is at 45° to the orientation required for orthorhombic symmetry. *The derivative*

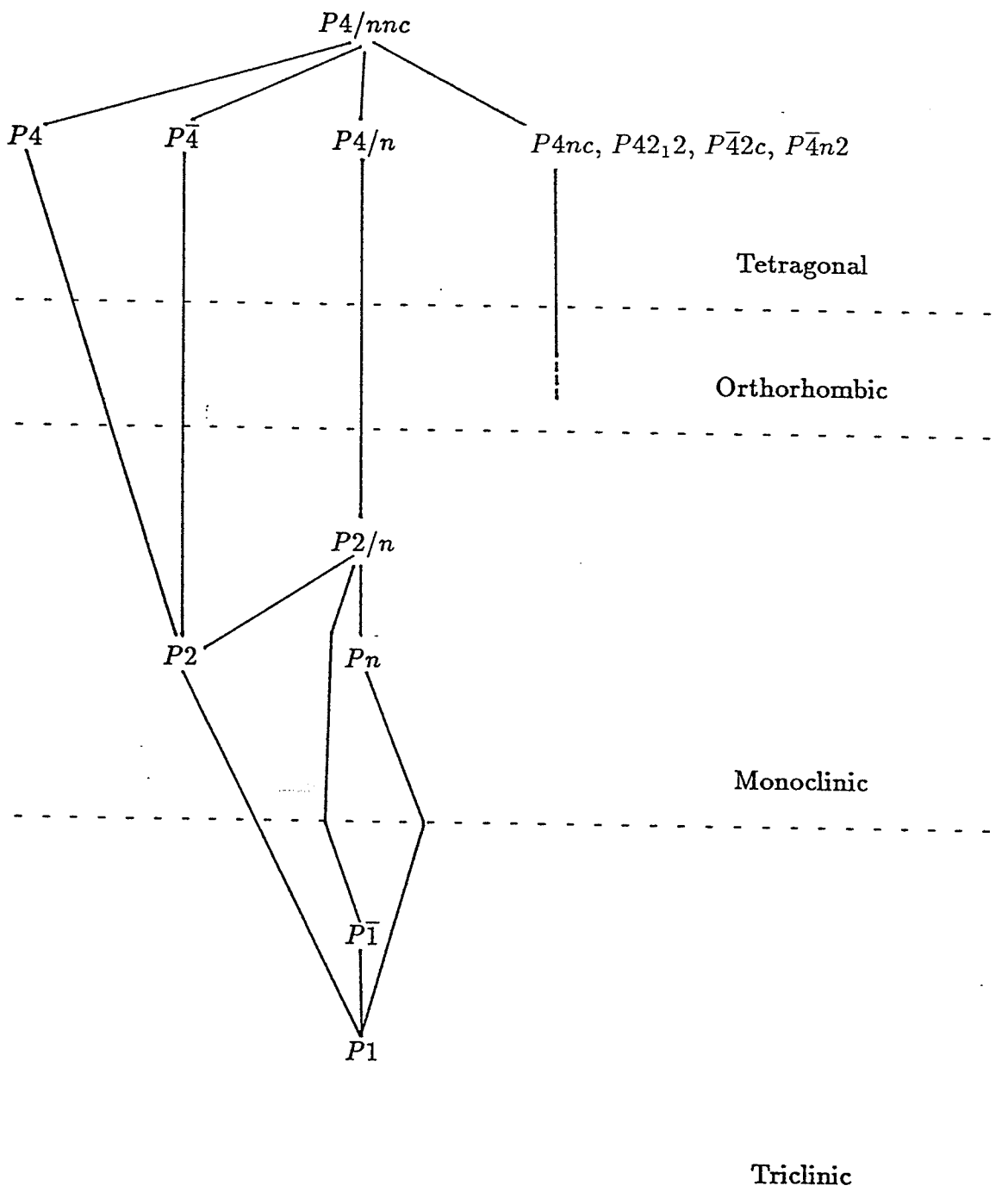

Figure 57: Space group tree for vesuvianite. No orthorhombic space groups are included, because optical investigations show that the optic axial plane is parallel to (100) and/or (010) of the ideal tetragonal morphology, and this is at 45° to the orientation required for orthorhombic symmetry.

vesuvianite structures therefore cannot be orthorhombic; they must be monoclinic or triclinic. A similar argument forbids the occurrence of the monoclinic subgroups $P2/c$ and Pc. The space groups remaining to us are $P2/n$, $P2$, Pn, $P\bar{1}$, and $P1$.

3.8 Crystal Structure Analysis

All intensity datasets were collected using the methods outlined in Section 2.7.1. In each case, a hemisphere of data from 3–60° 2θ was collected. Miscellaneous information concerning the data collections and reductions are listed in Table 23.

Structure refinement was carried out with the SHELXTL program X, using techniques discussed in Section 2.7.3. Table 24 outlines the general steps followed in most of the refinements.

3.8.1 V74c Wilui River, U.S.S.R.

This particular vesuvianite was selected for structure refinement because microprobe analyses indicated significant B and the wet-chemical analysis and infrared spectroscopy showed it to have a low hydrogen content. $2V$ is in the range of 0–10°, and no violating reflections were seen in the precession photographs. Only one violating reflection with $F/\sigma F > 4.00$ (111) was present in the X-ray intensity dataset. Consequently, the space group $P4/nnc$ was adopted. The input model used was taken from Yoshiasa and Matsumoto (1986), modified for known differences in composition.

Full-matrix least-squares refinement of all variables for an isotropic vibration model resulted in convergence at an R index of 10.4%. At this stage, there were a number of discrepancies between the model and the data:

1. The temperature factor for O(10) was extremely large (U=0.19), indicating much less scattering than was formally assigned. Having decided that this was due to partial occupancy of the site, I fixed the temperature factor at a value typical for oxygen atoms in the vesuvianite structure (U=0.015), and let the occupancy refine.
2. Difference-Fourier maps showed the presence of significant unassigned intensity at or near two special positions in the structure. These were:

$$i)\ \ 1/4\ 1/4\ 1/4\ \ (2a)$$

Table 23: Miscellaneous information for data collections and refinements.

	$V74_c$	$V13_c$	$V13_i$	$V13_r$
a_1^*	15.746(2)	15.521(3)	15.538(1)	15.523(3)
a_2^*	15.751(3)	15.523(2)	15.547(3)	15.567(2)
c	11.708(2)	11.807(2)	11.822(2)	11.825(2)
α	89.97(2)	90.01(1)	89.98(2)	90.01(1)
β	90.00(1)	89.99(1)	89.98(1)90.01(2)	
γ	90.00(1)	89.99(1)	89.98(1)	90.03(1)
Crystal size (mm)	0.22	0.28	0.15	0.20
Rad/Mono	Mo/Gr	Mo/Gr	Mo/Gr	Mo/Gr
Data Collected	18417	18021	18037	18028
$R_{azimuthal}(\%)$	1.22	1.07	0.90	0.93

Table 24: General crystal-structure refinement sequence.

1. The refinements began with positional parameters modified from Yoshiasa and Matsumoto (1986). Initially, the isotropic temperature factors were fixed, but the scale factor and positional parameters were refined (for $V13_c$, there were 48 parameters at this stage; the final R value was 11.0%).
2. The isotropic temperature factors were refined (69 parameters; R=7.5%).
3. An extinction correction was applied, and x and y for O(9) were combined as a single variable (69; 7.0).
4. Anisotropic temperature factors used for all atoms except Ca(3), C, B, O(6) and O(10) (140; 6.8).
5. Ca(3) and O(6) were set anisotropic (150; 3.9).
6. The channel atoms (B, C and O(10) were set anisotropic (153; 3.6).
7. The occupancy of the AlFe site was refined for Al/Mg and Fe (3.6).
8. The occupancy of the B site was refined for Al/Mg and Fe (3.5).

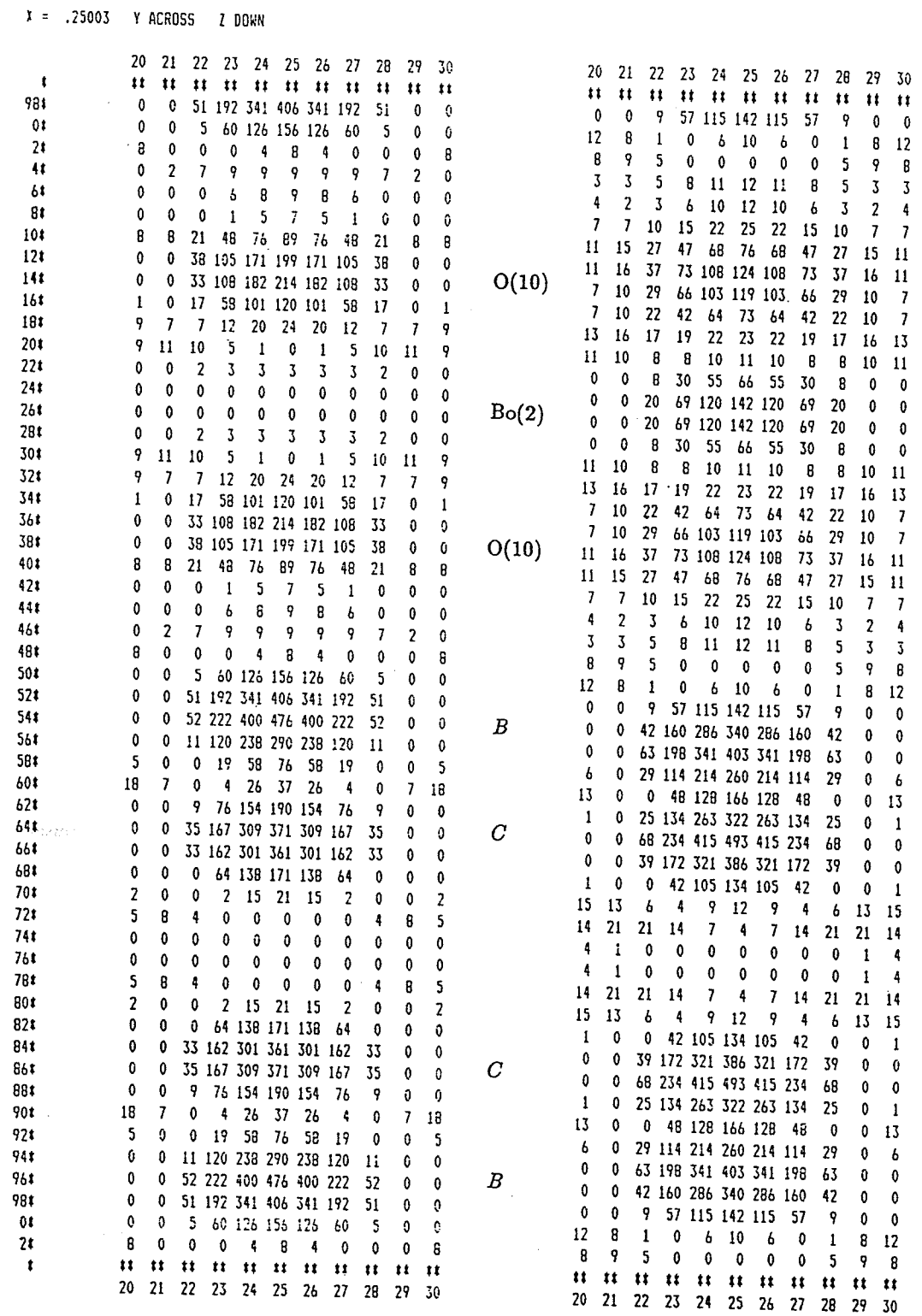

Figure 58: Difference-Fourier maps for $V13_c$ (normal vesuvianite—left) and $V74_c$ (boron vesuvianite—right) with channel cations removed.

$V74_c$ (analysis V74–15)

$$\underbrace{(Ca_{18.70}Ce_{0.04}La_{0.03})_{18.77}}_{37.6+}\underbrace{(Al_{6.75}Mg_{4.87}Fe^{3+}_{0.87}Fe^{2+}_{0.51}Ti_{0.33})_{13.33}}_{34.9+}\underbrace{Si_{17.91}}_{71.6+}\underbrace{B_{2.37}}_{7.1+}\underbrace{(O_{73.26}OH_{4.74})_{78.00}}_{151.3-}$$

$V13_c$ (average of 4 analyses)

$$\underbrace{Ca_{19.11}}_{38.2+}\underbrace{(Al_{10.61}Mg_{1.04}Fe^{3+}_{0.64}Fe^{2+}_{0.53}Ti_{0.28}Mn_{0.03})_{13.13}}_{38.1+}\underbrace{Si_{17.75}}_{71.0+}\underbrace{(O_{69.31}OH_{8.68})_{77.99}}_{147.3-}$$

Figure 59: Chemical formula of $V74_c$ compared to that of $V13_c$.

ii) 0.05 0.05 1/4 (8*h*)

Figure 58 shows difference-Fourier maps for $V13_c$ (normal vesuvianite) and $V74_c$, with the channel cations left out. The unassigned intensity at the 2*a* position in $V74_c$ is not seen in the normal vesuvianite. However, the O(10) position has only half the density seen in $V13_c$, and it is more spread out. The *B* and *C* positions are similar for both structures.

An oxygen atom was assigned to each of the new positions as a general scattering species. Isotropic temperature factors were fixed at U=0.015 and the occupancies were considered as variables in the following cycles of refinement.

Full-matrix least-squares refinement of this model converged to an *R* index of 6.5%. When the temperature factors of the heteropolyhedral framework atoms were set anisotropic, this fell to 5.11%. The O(7) oxygen was extremely anisotropic and was split into two half atoms, which refined to a stable arrangement with an $O(7)_a$–$O(7)_b$ distance of ≈0.5Å and an *R* index of 5.1%. At this point, more unassigned intensity was seen at the general position:

iii) 0.18 0.23 0.30 (16*k*)

An oxygen was assigned to this site, with a fixed isotropic temperature factor and variable occupancy. Refinement of this model converged to an *R* index of 4.4%. Bond lengths and angles were calculated in order to aid in the interpretation of this density for the final refinement steps.

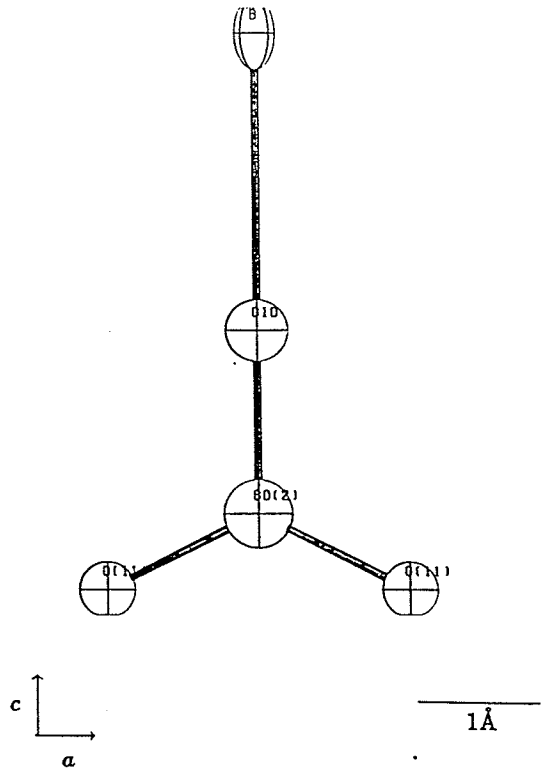

Figure 60: ORTEP diagram of the local stereochemistry around the Bo(1) position.

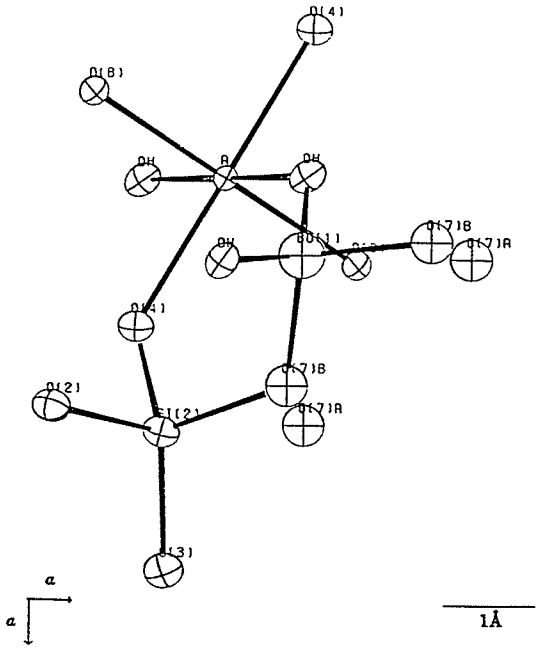

Figure 61: ORTEP diagram of the local stereochemistry around the Bo(2) and O(11) positions.

At this point, it was necessary to consider information from other experimental techniques in order to interpret the stereochemistry of this vesuvianite. Chemical analyses showed that the Wilui River vesuvianite contains significant B and greatly reduced H, suggesting a B⇌H dependence of some sort. In Figure 59, the chemistry of this vesuvianite is compared to that of a "normal" vesuvianite ($V13_c$). The differences are summarized below:

1. There are larger amounts of small divalent cations replacing Al in the Wilui vesuvianite. Comparison of the total formal charges of the small divalent and trivalent cations shows a sum of 36+ for normal vesuvianite and 33+ for the Wilui material.
2. Normally, there are ≈9 hydrogen atoms p.f.u. in the vesuvianite structure. Wet-chemical analyses of the Wilui vesuvianite show it to have almost exactly 2 H atoms per formula unit.
3. In most vesuvianites, the O(10) position is fully occupied by O for a total charge of 4−. In the Wilui material, this site is only half-occupied, for a charge of 2−.

The local stereochemistry of the three new positions is shown in Figures 60 and 61. The "T" site ($8h$) is coordinated by four oxygens in an approximately tetrahedral arrangement, with a mean bond length of 1.54Å. Position $2a$ is coordinated by three oxygens in a triangular arrangement with a mean bond length of 1.34Å. Both of these sites can accomodate B. The last position ($16k$) is 2.23–2.70Å away from three Ca(3) cations. As Ca(3) is completely occupied, the atom at the $16k$ position must be an anion, and thus the atom at the $2a$ position must be a cation. Consequently, B was inserted at the $8h$ and $2a$ positions, subsequently labelled Bo(1) and Bo(2). Least-squares refinement of this model (which included anisotropic temperature factors for all atoms except $O(7)_a$ and $O(7)_b$, O(10), and the three new atom positions) converged to an R index of 4.4% and R_w of 2.9%. Final atomic parameters and temperature factors are listed in Appendix J. Selected interatomic distances and bond-valence calculations (from the parameters of Brown, 1981) are listed in Tables 25 and 26.

The charge consequences of this model are discussed in more detail in the next chapter. A total of 5 boron atoms have been added to the formula unit, resulting in

Table 25: Selected interatomic distances for $V74_c$.

Si(1)-O(1)	1.634(2)	x4	C-O(6)	2.320(2)	x4
	---		C-O(9)	2.625(2)	x4
⟨Si(1)-O⟩	1.634			---	
	========			2.473	
				========	
Si(2)-O(2)	1.628(2)				
Si(2)-O(3)	1.623(2)		B-O(6)	2.065(2)	x4
Si(2)-O(4)	1.663(2)		B-O(10)	2.219(8)	x4
Si(2)-O(7)b	1.657(4)			---	
	---			2.096	
⟨Si(2)-O⟩	1.643			========	
	========				
			AlFe-O(1)	1.969(2)	
Si(3)-O(5)	1.624(2)		AlFe-O(2)	1.934(2)	
Si(3)-O(6)	1.612(2)		AlFe-O(3)	2.072(2)	
Si(3)-O(8)	1.631(2)		AlFe-O(4)	2.054(2)	
Si(3)-O(9)	1.666(1)		AlFe-O(5)	2.055(2)	
	---		AlFe-OH	1.999(2)	
⟨Si(3)-O⟩	1.633			---	
	========		⟨AlFe-O⟩	2.014	
				========	
Ca(1)-O(1)	2.337(2)	x4			
Ca(1)-O(2)	2.497(2)	x4	A-O(4)	1.941(2)	x2
	---		A-O(8)	1.904(2)	x2
	2.417		A-OH	1.945(2)	x2
	========			---	
			⟨A-O⟩	1.930	
Ca(2)-O(1)	2.488(2)			========	
Ca(2)-O(2)	2.404(2)				
Ca(2)-O(3)	2.388(2)		Bo(1)-O(7)b	1.530(10)	x2
Ca(2)-O(4)	2.476(2)		Bo(1)-OH	1.450(6)	x2
Ca(2)-O(5)	2.337(2)			---	
Ca(2)-O(5)	2.424(2)		⟨Bo(1)-O⟩	1.490	
Ca(2)-O(6)	3.069(2)			========	
Ca(2)-O(8)	2.357(2)				
	---		Bo(2)-O(10)	1.367(8)	x2
⟨Ca(2)-O⟩	2.493		Bo(2)-O(11)	1.290(14)	x2
	========			---	
				1.329	
Ca(3)-O(3)	2.381(2)			========	
Ca(3)-O(6)	2.405(2)				
Ca(3)-O(6)	2.791(2)		B-C	1.014(3)	
Ca(3)-O(7)a	2.440(4)				
Ca(3)-O(7)b	2.487(4)		C-C	2.509(4)	
Ca(3)-O(7)a	2.597(4)				
Ca(3)-O(8)	2.498(2)				
Ca(3)-O(10)	2.617(1)				
Ca(3)-OH	2.564(2)				

⟨Ca(3)-O⟩	2.531				
	========				

Table 26: Empirical bond-valence* table for $V74_c$.

	Si(1)	Si(2)	Si(3)	Ca(1)	Ca(2)	Ca(3)	C^*	B^*	AlFe	A	Σ
O(1)	$0.966^{\times 4}_{\downarrow}$			$0.355^{\times 4}_{\downarrow}$	0.240				0.447		1.988
O(2)		0.979		$0.237^{\times 4}_{\downarrow}$	0.288				0.479		1.983
O(3)		0.997			0.300	0.303			0.355		1.955
O(4)		0.896			0.244				0.370	$0.463^{\times 4}_{\downarrow}$	1.973
O(5)			1.005		0.274 0.335				0.369		1.983
O(6)			1.021		0.078	0.289 0.128	$0.173^{\times 4}_{\downarrow}$	0.408/2			1.893
$O(7)_a$		0.873				0.176 0.181 0.263					1.493
$O(7)_b$		0.924				0.184 0.073 0.233					1.414
O(8)			0.979		0.319	0.234				$0.505^{\times 2}_{\downarrow}$	2.037
O(9)			$0.889^{\times 2}_{\rightarrow}$				$0.090^{\times 4 \times 2}_{\downarrow \rightarrow}$				1.958
O(10)						$0.182^{\times 4}_{\rightarrow}$		0.275/2			0.866
OH						0.204			0.415	$0.456^{\times 2}_{\downarrow}$	1.075
Σ	3.864	3.771	3.894	2.288	2.078	1.895	1.052	2.732	2.435	2.848	

	Bo(1)	Σ
$O(7)_b$	$0.560^{\times 2}_{\downarrow}$	1.974
OH	$0.724^{\times 2}_{\downarrow}$	1.799
Σ	2.568	

a charge increase of 15+. If $O(7)_a$ was fully occupied Bo(1) would be coordinated by two OH and two O(7) atoms in an approximately tetrahedral arrangement (Figure 60). In normal vesuvianite, each OH hydrogen bonds to O(7). In boron vesuvianite, the hydrogens are absent, replaced by a central B which provides (more than) the necessary charge to satisfy the bond-valence requirements of O(7) and OH. A total

of 8 H are lost from the normal vesuvianite formula unit in this way. One extra oxygen (p.f.u.) is added at the 1/8 occupied O(11) position, which is vacant in normal vesuvianite. The overall result is that the current model has four excess charges relative to normal vesuvianite.

There are a number of problems with the current model:

1. Both the Bo(1) and Bo(2) sites are fully occupied, for a total of 5 boron atoms per formula unit. This is double the amount of boron in the microprobe analyses.
2. There is no explanation for the apparent disorder at the O(7) site.
3. The Bo(2) position is coordinated by O(10) and O(11) oxygens. However, the O(11) site is only 1/8 occupied, for a total of 1 O(11) oxygen p.f.u., half the amount needed.

In an attempt to resolve these problems, the isotropic temperature factors for the boron positions were fixed at U=0.006, and those for O(10) and O(11) were fixed at U=0.015 (a typical value for framework oxygens). Occupancies of the boron sites were halved, and the occupancies of all four sites (Bo(1), Bo(2), O(10) and O(11)) were refined. In each case, the values obtained were similar to the occupancies in previous refinements.

The Bo(1) position was then split into two half-occupied positions separated by ≈0.5Å. A refinement of this arrangement was unsuccessful.

It is obvious that there are some inconsistencies in the details of the current model with respect to the three new sites. The rest of the structure, however, is similar to that of other vesuvianites. Refinement of the occupancy of the B site for Fe and Mg/Al showed a total of 0.40 Fe atoms p.f.u. (mean bond length=2.096Å). This is similar to the value obtained for Fe^{2+} in the wet-chemical analyses. The smaller AlFe site (mean bond length=2.014Å) contained 0.84 Fe atoms p.f.u., which is almost identical to the wet-chemical value of 0.87 Fe^{3+} atoms per formula unit. If Al is assumed to fill the A site exclusively, Mg is the dominant cation in the AlFe site, and the amounts of Mg and Fe in the B site are approximately equal.

3.8.2 V13 Jeffrey Mine, Quebec

This vesuvianite was selected for crystal structure refinement because of the spec-

tacular sector zoning and variable $2V$. A (001) section of a V13 crystal is shown in Figure 13; there is a low birefringence core ($2V \approx 0$–$10°$), a patchy intermediate zone ($2V \approx 36°$) and a high birefringence rim ($2V = 60$–$62°$).

Crystals removed from the intermediate zone, core and rim showed increasing numbers of b'– and c'–type violating reflections in precession photographs and in the intensity data sets. Some reflections related by vertical mirror planes had non-equivalent intensities. This evidence suggests a Laue symmetry no higher than $4/m$.

Initial refinements of all three crystals were carried out in the space group $P4/nnc$. The input model was taken from Yoshiasa and Matsumoto (1986), and was modified for known differences in composition. Full-matrix least-square refinements for anisotropic vibration models resulted in convergence at R indices for $V13_c$, $V13_i$ and $V13_r$ of 3.5, 4.3, and 5.5% respectively (Table 27; atomic parameters and temperature factors are listed in Appendix J). Thus the R indices correlate with the increase in $2V$ from core to rim. Difference-Fourier maps for $V13_c$ showed additional unassigned intensity at the following positions:

1/4 1/4 0.22

0.03 0.06 0.17

corresponding to H atoms bonded to O(10) (H(1)) and O(11) (H(2)). Both were included in subsequent refinements (with fixed occupancies and temperature factors) but only H(1) refined to a stable position (0.85Å away from O(10)), and the R value was unchanged.

In all three refinements the Ca(3) atom was the most anisotropic ($U_{eq} \approx 0.167$). U for O(10) increased from 0.104 in the core refinement to 0.151 in the intermediate zone and 0.164 in the rim. O(6) and B also had relatively high temperature factors.

Occupancies of the AlFe and B sites were refined for Fe and Mg/Al, resulting in 0.18, 0.14 and 0.22 Fe atoms p.f.u. at the B sites, and 0.94, 1.10 and 1.11 Fe atoms p.f.u. at the AlFe sites for $V13_c$, $V13_i$ and $V13_r$ respectively. The mean B–O bond length was shorter in $V13_r$ (2.055Å) than in the other two crystals ($\approx$2.063Å).

The wet chemical analyses showed 0.56 Fe^{2+} atoms p.f.u., which suggests that in the Jeffrey vesuvianite, ferrous iron occupies the B and AlFe sites. Mg is probably found in both these sites, and Al is the dominant cation at the AlFe site.

Refinement	R(%)	Rw(%)	Rg(%)	Unique Reflections
V13c P4/nnc*	7.0	6.0	5.9	2085
	3.5	2.5	2.8	
P4/n	7.7	6.3	6.0	4008
	4.3	3.0	3.2	
P-4	6.0	4.9	4.8	7429
	3.4 @	2.7	2.8	
P4	12.2 @	10.9	11.8	7416
P4/nnc#	7.6	6.3	6.0	7416
	4.2	3.1	3.3	
P4/n#	7.6	6.3	6.0	7416
	4.2	3.1	3.3	
V13i P4/nnc	7.2	5.9	5.4	2070
	4.3	3.0	3.0	
V13r P4/nnc	5.5	4.3	3.9	2094
	8.2	7.1	6.1	
P4/n	8.4	6.7	6.0	4030
	6.0	4.3	4.1	
P2/n	8.0	6.3	5.7	7580
	5.4 @	3.9	3.7	
Pn	6.2	4.9	4.5	7758
	4.2 @	3.2	3.0	

*Isotropic model (top) and anisotropic model (bottom)
#Refined using P4 Fo file (no violating reflections)
@Did not converge

Table 27: R values obtained for V13 crystal structure refinements. compared to that of $V13_c$ (average of four analyses).

$V13_c$ was also refined in space group $P4/nnc$ using an input dataset (from the $P4$ refinement) that includes reflections that violate $P4/nnc$ extinction criteria. The resulting R value (anisotropic model) was 4.2%.

$V13_c$ and $V13_r$ were also refined in space froup $P4/n$ as suggested by the diffraction evidence. As shown in Table 27, there was no significant improvement in the R indices. The value for $V13_c$ (4.3%) was almost identical to that obtained using $P4/nnc$ and the $P4$ dataset.

$V13_c$ was also refined in space groups $P\bar{4}$ and $P4$. Neither refinement converged satisfactorily. Temperature factors were either unrealistically high or low, and the refinements failed to converge. This is a result of high correlations between atoms that are equivalent in $P4/nnc$.

Since the optical data suggest that the high-birefringence rim zone is the most non-tetragonal, $V13_r$ was refined in $P2/n$ and Pn space groups. The $P2/n$ refinement (anisotropic model) converged to an R value of 5.4%, almost identical to that of $P4/nnc$. Temperature factors, however, varied considerably for $P4/nnc$-equivalent atoms.

The Pn refinement (isotropic model) converged to an R index of 6.2%, lower than that of the other refinements. The anisotropic model, with $\approx$1200 parameters, failed to converge, even after $\approx$50 cycles. Once again, the high degree of correlation between pseudo-equivalent atoms resulted in unrealistic temperature factors, and in some cases, non-positive definite atoms.

Although the optical and IR studies indicate nontetragonal symmetry, it was not possible to determine the true space group using X-ray crystallography. There was little difference between the results obtained using monoclinic or tetragonal space groups. Thus the deviation from tetragonal symmetry must be very slight.

Chapter 4

DISCUSSION AND CONCLUSIONS

4.1 Channel Configurations in Vesuvianite

Much effort has gone into the study of channels in the vesuvianite structure (Chapter 1). The string of sites down the channel is shown diagramatically in Figure 62. Previous authors have shown that adjacent C sites and adjacent C and B sites cannot be simultaneously occupied because of unrealistic cation-cation approaches. This seems to be the reason for half occupancy of both the B and C sites in the channel. However, no one seems to have examined the longer-range consequences of such stereochemical restrictions on channel configurations.

4.1.1 Normal Vesuvianite

The column labelled "normal"in Figure 62 begins with an atom at the first B position. This requires the adjacent C position to be vacant, with B bonding to the O(10) atom below. O(10) bonds to four Ca(3)'s, each with a bond-valence of 0.5 v.u.; it also bonds to the B cation with a bond-valence of 0.5 v.u.. This gives a valence sum of 1.5 v.u. and leaves O(10) needing an additional 0.5 v.u. to completely satisfy its local bond-valence requirements. Many previous workers have assigned O(10) as a hydroxyl, and the obvious way for O(10) to receive this additional 0.5 v.u. is from a hydrogen atom. In some of my structures, I have also observed a small peak between the O(10)s that can also be assigned to a H atom.

Consider next the bond-valence requirements around this H. It provides 0.5 v.u. to the overlying O(10), and consequently must provide 0.5 v.u. to an underlying O(10). It is thus a *symmetrical hydrogen bond.* Consider now the bond-valence requirements of the lower O(10). This is bonded to four Ca(3)s and one H, supplying a bond-valence of 1.5 v.u.. It must therefore bond to an underlying B site cation to satisfy its requirement for electrons. As this B site is occupied, the underlying C site must be empty. This provides us with a configuration that is labelled "1" in Figure 62.

Let us continue this procedure. The next C site can be filled; its bond valence requirements are satisfied by four O(6) and four O(9) oxygens that lie off

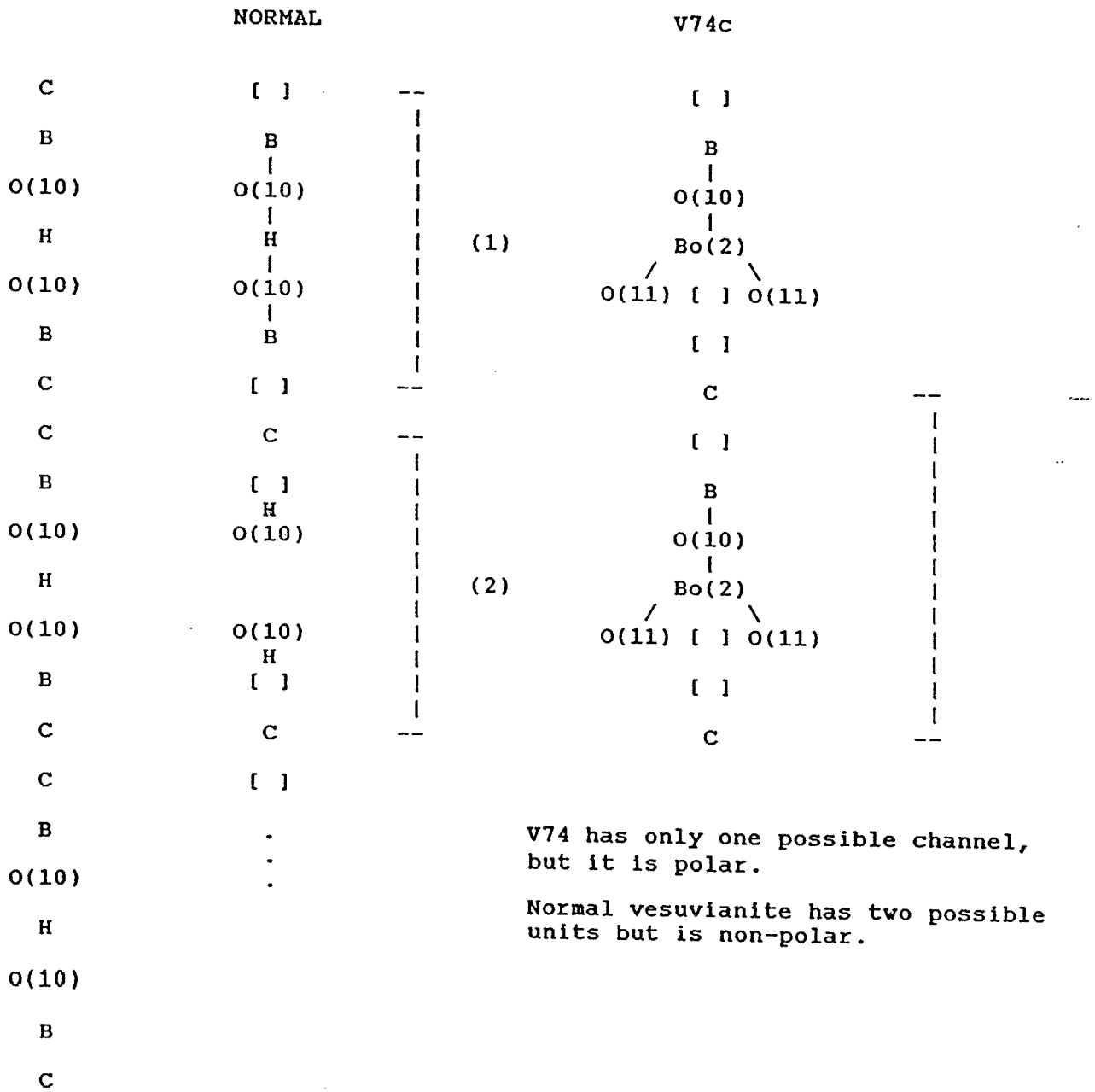

Figure 62: Channel configurations for normal and boron vesuvianites.

the channel. The adjacent B site below is empty, but as O(10) is fully occupied, both the subsequent O(10) sites are occupied by oxygen. Now let us examine the bond-valence requirements of these O(10)s. Each is bonded to 4 Ca(3) cations that provide it with a total of 1.0 v.u.; as there are no neighbouring cations, this must be provided by 2 H atoms. These cannot occupy the space between the two O(10)s, as there is no room. Instead, they must point outwards towards the adjacent B positions (the upper one of which we have already shown to be empty). The H atom bonded to the lower O(10) points downwards towards the adjacent B position which consequently must be unoccupied; this allows the adjacent C position to be occupied, and forces the subsequent C position to be vacant. This second configuration is labelled "2" in Figure 62.

It is very important to note the different H bonding arrangements in these two different configurations as these have important consequences on the stoichiometry of the mineral.

In a perfectly ordered crystal with half-occupied B and C sites, configurations 1 and 2 will alternate down a single channel (however, at the moment we see no mechanism that would connect configurations in adjacent channels in an ordered fashion). It is possible, in fact easy, to disorder these configurations up and down the channel by omitting a C cation from the second type of configuration. However, extensive amounts of this will produce nonstoichiometry in the mineral, so presumably it does not occur to any great extent. Note also that neither configurations are polar.

4.1.2 Boron Vesuvianite (V74c)

Let us start at the top of the column labelled $V74_c$ in Figure 62, and let us start in exactly the same way as we did before, putting a B atom at the first B position and a vacancy in the adjacent C position. The B atom bonds to the adjacent O(10), *but* this O(10) is bonded to a boron. Note that the B–O(10) bond lengthens to accommodate the much stronger Bo(2)–O(10) bond. The next O(10) down the channel must be unoccupied. *Note that the full occupancy of the Bo(2) position thus accounts for the half occupancy of the O(10) position in the Wilui vesuvianite.* Ignoring positional disorder and some stoichiometry problems, the O(11) atoms complete the trigonal coordination around Bo(2). This unit provides a basic configurational unit

for Wilui vesuvianite. The next B site down must be unoccupied because it has no O(10) with which to bond and satisfy its bond-strength requirements. To maintain stoichiometry the adjacent C sites must be occupied, the following C site must be vacant, and we start again with our basic unit repeating down the channel. Hence the Wilui vesuvianite only has one configurational unit down the channel rather than two. However, unlike normal vesuvianite, this unit is polar. A perfectly ordered (stoichiometric) channel is polar, but there seems to be no reason for adjacent channels to show the same polarity.

4.2 Channel Configurations as a Control of Space Group

In normal vesuvianite, there are two channel configurations as deduced above. As all structure refinements and systematic examinations of chemistry show, the B and C sites are half-occupied. *Hence, the two channel configurations must occur in equal amounts.*

Let us first consider a single channel. If the configurations do not alternate along the channel, additional vacancies are introduced at the B and C positions. As the latter would cause significant departures from the observed stoichiometry (*i.e.* less than half-filled B and C sites), we can conclude that the two configurations *must* alternate along the channel (i.e. parallel to Z). Such an ordered arrangement along the channel direction is also suggested by the fact that the precession photographs of all crystals do *not* show diffuse intensity parallel to $c^*(=Z)$, the channel direction. $hk0$ and $h0l$ precession photographs of all three zones of the Jeffrey crystal show diffuse intensity parallel to the principal axes. Such diffuse intensity is indicative of short-range order/disorder in the direction of the streaking. In turn, this suggests that adjacent channel configurations are disordered, that is they do not obey the $P4/nnc$ space group operations that ideally relate them.

Adjacent channels are separated by $\approx$8Å, and it seems difficult to suggest interactions between channels over this type of distance. However, the channels are the most variable part of the structure, and consequently it is here that we must look for the reasons for the space group complexities in vesuvianite.

Jeffrey vesuvianite shows three sectors, corresponding to growth out to the {001}, {101} and {100} forms (core, intermediate and rim zones respectively). The complexities of the Jeffrey crystals documented in the section on optics suggests that these sectors are the result of growth zoning; similar textures are observed in other high symmetry minerals such as beryl and milarite. Thus we will consider what can occur as a vesuvianite crystal grows with these forms as its external growth faces.

Let us consider first the (001) zone. This is bounded by the {001} face that cuts orthogonally across all the channels of the growing crystal. At nucleation, the {001} face will start to form *identical* channels parallel to c, as conditions will be uniform across the minute proto-crystal face. Continued growth of alternating 1 and 2 configurations (forced by the observed stoichiometry) will produce ordered channels *that obey $P4/nnc$ symmetry.*

Consider next the (100) zone. This is bounded by the {100} face that is *parallel* to the channels in the growing crystal. Thus on a {100} growing face of a crystal, the whole length of a channel is exposed at any one time. Atoms at the B and C sites will nucleate essentially at random along the channel, and ordered 1– and 2–type configurations will grow away from the initial nucleating sites. There are now 2 possibilities for growing ordered configurations that impinge upon each other:

1. they may be related by the translational symmetry of the crystal, whereupon they merge to form a single ordered array.
2. they are not related by translational symmetry of the crystal, wherupon they form two domains related by an anti-phase boundary.

If the process is entirely random, then we may expect equal amounts of both types of chains with continued growth. We know that the number of anti-phase boundaries must be fairly low or the stoichiometry of mineral would be significantly altered. There is no discernable diffuse intensity (streaking) parallel to the Z-axis (i.e. parallel to the channel), indicating little short-range disorder along Z. The stoichiometry constraint of half-occupied B and C sites suggests that there are few (fairly large) anti-phase configurations along any one channel in the (100) sector of the crystal.

As the growing surface of the (100) sector advances along [100], the nucleation and growth process outlined above occurs along each new channel length that forms. As nucleation in each adjacent channel along [100] is essentially random, the local ideal symmetry relationships between channels are in many cases violated, resulting in short-range disorder. Within a single unit cell, there are two chains related by n– and c–glides. If these glide-symmetries were broken by long-range order, we would see sharp glide-violating relections in the diffraction patterns. However, the glide violating intensities tend to be diffuse, with additional streaking parallel to $[100]^*$. This is indicative of short-range disorder between adjacent-channels. However,

within the diffuse intensity are sharper diffractions violating the glide symmetry conditions. These are indicative of a longer range order in the symmetry-violating structural array. These two types of diffraction phenomena are characteristic of an anti-phase relationship in which the domain size spans the range of the transition from diffraction incoherence to diffraction coherence; this dimension is of the order of 200Å for Mo$K\alpha$ X-rays. Thus the long-range symmetry is lowered in the (100) zone of normal vesuvianite.

The (101) zone is bounded by the {101} face, structurally intermediate between the {001} and the {100} faces. Consequently one would expect a growth mechanism intermediate between those suggested for the (001) and (100) sectors, with intermediate-type diffraction and optical evidence for non-ideal space group symmetry. As outlined in previous sections, this indeed is the case. In Jeffrey vesuvianite, the (101) sector shows an intermediate $2V$ value (36°) and streaking with much more diffuse and weak glide-violating reflections.

Let us now summarize the arguments and evidence that pertain to the space group symmetry and sector zoning of Jeffrey vesuvianite:

1. The heteropolyhedral framework of the 'idealized' vesuvianite structure has $P4/nnc$ space group symmetry. Group theory arguments used to derive the possible sub-group symmetries for derivative arrangements show that only a limited number of space groups are possible.
2. Optical measurements show that the orientation of the optic axial plane (OAP) is parallel to the 'ideal' tetragonal axes. Group theory arguments show that the principal axes of the possible orthorhombic space groups must be at 45° to the "ideal" tetragonal axes. In the orthorhombic system, the OAP is constrained to be parallel to two principal axes. These three observations are not mutually consistent, and thus *vesuvianite cannot have orthorhombic symmetry.*
3. None of the vesuvianites were optically uniaxial; all were biaxial, indicating orthorhombic, monoclinic and triclinic as possible symmetries. Point (2) precludes orthorhombic symmetry, and thus *vesuvianites must be monoclinic or triclinic.* However, in some cases, the measured $2V$ angle was small ($< 5°$), indicating that the deviation from uniaxial character (compatible with tetragonal symmetry) is very small. In addition, optics are extremely sensitive to sym-

metry, much more so than X-ray diffraction, and hence the lower symmetry character need not necessarily be apparent in the diffraction record.

4. Optical observations in cross-polarized light on (100) and (001) sections showed the presence of sector zoning, in which the different sectors had different birefringence and optic axial angles. The sectors could be correlated with the external forms of the crystal (specifically {001}, {101} and {100}), such that each face subtended a sector that narrowed towards the centre point of the crystal. This is indicative of growth zoning.

5. Both precession photographs and complete single-crystal intensity data collections show the presence of glide-violating reflections when compared with the extinction criteria for space group symmetry $P4/nnc$. Vertical n– and c–glides are violated but the horizontal n–glide seems intact. *In terms of the glide-violating reflection criteria, tetragonal space groups are still possible.*

6. Precession photographs indicated the presence of streaking (diffuse intensity) along some reciprocal lattice rows parallel to a^* but not along rows parallel to c^*. The glide-violating reflections were embedded in this streaking, and became less diffuse in the order (001)>(101)>(100). *Such diffuse intensity is indicative of short-range order.*

7. There are two possible chain configurations, and an argument can be made that growth on the {001} face will lead to configurations ordered along the c–axis, whereas growth on 100 will lead to disorder of chain configurations between adjacent channels in the [100] and [010] directions. Such a model would account for the patterns of diffuse intensity recorded in the precession photographs from each of the three sectors.

8. Crystal structure refinements of fragments from the three different sectors led to gradually increasing R indices in the sequence (001)<(101)<(100). All attempts (and there were many) at refinement in monoclinic space groups were unsuccessful; either the refinements would not converge properly, or the statistics of the refinement were not improved over the higher symmetry ($P4/n$) refinement. These results also suggest that there is a contribution to the diffractions in the (100) crystal (and to a lesser extent the (101) crystal) that is not being adequately modeled. The local disorder proposed for these sectors

suggests that this intensity contribution is diffuse scattering that cannot be modeled by the normal Bragg diffraction (long-range) scattering model used here. Thus *the higher R indices obtained for the (100) and (101) sector crystals may be due to increased diffuse scattering due to the increased short-range disorder in these crystals.*

In terms of the evidence so far gathered, this is as specific a model as is possible. This proposal may be easily tested by imaging the structure through the glide-violating reflections in a very high resolution transmission electron microscope.

4.3 Channel Conformation and Space Group of Boron Vesuvianite

As outlined previously, there is only one channel configuration in boron-bearing vesuvianite (see Figure 62), and hence it cannot disorder with an alternate configuration as was the case for normal vesuvianite. However, this arrangement is polar, and hence it can occur in two different orientations. Attempting to incorporate adjacent arrangements of different polarity in a single channel leads to a very unlikely stereochemistry at the boundary, suggesting that this does not occur. This is in line with the lack of diffuse intensity parallel to the c–axis in precession photographs of this type of vesuvianite.

Conversely, neighbouring channels may be of differing polarity without causing any local stereochemical problems at all. However, the difference between adjacent channels in an anti-phase arrangement is extremely slight in terms of scattering power, and consequently there is very little (i.e. no observable) diffuse intensity (or glide-violating reflections) parallel to [100] or [010]. *Hence boron-vesuvianite may be satisfactory refined in space group* $P4/nnc$.

4.4 The Chemical Formula of "Normal" Vesuvianite

4.4.1 Cation Contents

A chemical analysis gives the *relative* porportions of different elements in a mineral, and is usually expressed as wt.%'s of oxides. The reduction of a chemical analysis to the unit formula of a mineral (expressed as atoms per formula unit, or p.f.u.) is a non-trivial problem. One needs some basis on which to normalize the ratios that one derives by chemical analysis. As discussed in previous sections, several different schemes have been proposed, and these were investigated in detail.

In a mineral containing hydroxyl or molecular H_2O, one cannot normalize to a specific number of anions without either

1. having an analysis for hydrogen (expressed as H_2O), or
2. assuming a fixed (and known) amount of H (as hydroxyl) in the structure.

Although (2) has often been assumed, the (OH) content is often variable. The ideal case is (1), but usually an analysis for H is not available or (in micro-samples) impossible to get.

In these circumstances, it is preferable to normalize to a fixed number of cations if possible. Crystal structure work suggested that the unit cell contains 50 cations (Hoisch, 1985; Allen, 1985; this study), and this was taken as a provisional approach. The 50 cations are constituted as follows:

1. 18 tetrahedrally coordinated cations (primarily Si).
2. 19 [8]–coordinated cations (primarily Ca).
3. 13 [6]– and [5]–coordinated cations (primarily Al, Mg, Fe).

Although the total number of cations is constrained by the normalization procedure (to a sum of 50), the individual cations are not. Consequently the distribution of all cations in all analyses should be crystal-chemically compatible with the known structural characteristics of vesuvianite as outlined in points (1)–(3) above.

The <Si–O> distances in vesuvianite range from 1.628–1.642Å, typical of the range found for silicate garnets when the tetrahedral site is occupied by Si only. For

the (large number of) analyses done here, the Si content distribution is symmetrically Gaussian, showing that there is insignificant substitution of other cations (i.e. Al) for Si at the tetrahedral sites in vesuvianite. Note also that the observed mean value of the Si content is 18.0(2), exactly equal to the number of tetrahedral sites available in the vesuvianite structure.

We cannot make the same size argument for the [8]–fold sites, as these more weakly-bonded coordination polyhedra always show strong inductive effects from the rest of the structure that perturb the bond lengths. However, simple ionic radii arguments suggest that those sites can potentially be occupied by alkaline earth, alkali and REE cations. The distribution of the Ca content is negatively skewed, suggesting substitution of additional cations at these sites. In addition, the mean value of 18.9(4) is slightly less than the ideal value of 19, supporting this contention. Including probable substituents at these sites (Na, Ln, Pb, Bi, Th) results in a symmetric Gaussian distribution and a mean value of 19.0(3), exactly equal to the number of available sites.

The [5]– and [6]–coordinate sites contain the medium sized divalent, trivalent and tetravalent cations, with Al as the dominant species. The Al distribtion shows a strong negative skew and mean value of $\approx$9.8. Incorporating the other substituents into the sums gives an almost symmetrical Gaussian (a slight positive skew is observed) with a mean value of 13.0(2), again exactly equal to the number of available sites.

The fact that the distributions of the three different groupings of cations are symmetric Gaussians indicates that partition of the cations into these three groups is correct. Similarly, the fact that the *individual* means for the sums were all exactly equal to the number of available sites for each group *substantiates the normalization of the vesuvianite formula on the basis of 50 cations (exclusive of boron).*

4.4.2 Anion Contents

We have seen above that there are 50 cations in the unit formula of vesuvianite. If we knew the valence state of all the elements and the OH content, then the anion content would be fixed by the electroneutrality principle. However, we do not and so we have to resort to other means.

The refined crystal structures show the presence of 68 anions that may definitely

be identified as O^{2-} on the basis of bond-valence considerations. Another 8 anions may similarly be identified as OH^-. This leaves (from the structure refinement results) another 2 anions, designated as O(10) in the refined structures. This has been interpreted as both O^{2-} and OH^-, and as half-occupied by both O^{2-} and OH^-, giving total OH^- contents of the unit formula as 8, 10 and 9 respectively. Thus the area of uncertainty involves the exact identity of the O(10) anion.

At the beginning of this chapter, the possible channel configurations were considered; these were illustrated in Figure 62. As O(10) is a component of these configurations and because the stoichiometry of vesuvianite constrains these configurations to occur in equal amounts, then the sum of the channel configurations gives the total (sum) identity of the O(10) anion. In the type 1 configuration, there are two O(10) oxygens and one associated hydrogen; in the type 2 configuration, there are two O(10) oxygens and two associated hydrogens. Summing these values and normalizing to the equipoint rank of the O(10) position gives $O_2^{2-}H_{1.5}^+$, or $O_{0.5}^{2-}OH_{1.5}^-$. Thus we can write the anion part of the vesuvianite formula as $O_{68.5}(OH)_{9.5}$, and the full formula becomes

$$[Ca,\ldots]_{19}[Al,Mg,Fe^{2+},Fe^{3+},Ti^{4+}\ldots]_{13}[Si]_{18}O_{68.5}(OH)_{9.5}$$

First of all, what direct evidence do we have for the derived (OH) content? First let us consider the calculated (OH) content. There is an initial problem in using this data, because as we will see later, the (OH) content of vesuvianite is sensitive to its B (boron) content. Boron is not easy to analyze (or even detect), and not all the samples were examined for boron. Consequently, even if we remove the known boron-vesuvianites from these data, we cannot know if the remaining low (OH) vesuvianites contain boron or not. Inspection of all data for (OH) (Figure 29) shows a bimodal distribution. The upper population has a fairly symmetric Gaussian distribution with a mean value of $\approx$9.5 (OH) p.f.u.. This supports the above formula.

4.4.3 Cation Oxidation States and Substitutions

The principal substitutions that concern the charge-balance within the vesuvianite cell occur at the [5]– and [6]–coordinated sites; at the [8]–coordinate sites, Ca dominates the chemistry, with only minor Na^+ and Ln^{3+}; this leaves the small divalent,

trivalent and tetravalent cations. Taking a mean Ti^{4+} content of 0.25 atoms p.f.u., electroneutrality gives the following "formula":

$$[(Al, Fe^{3+})_{10.00}(Mg, Fe^{2+}, Mn)_{2.75}Ti^{4+}_{0.25}]_{13}$$

The distribution of Al, a negatively skewed Gaussian with a mean value of $\approx$9.8 atoms p.f.u., is compatible with the above formula.

The above discussion ignores the presence of fluorine. This is present usually in small quantities (often zero), but can reach substantial amounts in some vesuvianites, up to 5 atoms p.f.u.. Here, F obviously substitutes for OH, accounting for some of the low values of H in non-boron bearing vesuvianites. Thus F must be incorporated into the vesuvianite formula as a solid solution substituent for OH.

From the above considerations, we may write the general formula of vesuvianite as:

$$[Ca, Na, Ln, Pb, Th]_{19}[(Al, Fe^{3+})_x(Mg, Fe^{2+}, Mn)_y Ti^{4+}_z]_{13}Si_{18}O_{68.5}(OH, F)_{9.5}$$

with ideal values of x=10.0, y=2.75, z=0.25 atoms p.f.u.

4.5 The Substitution of Boron in Vesuvianite

This study has recognized the incorporation of B into vesuvianite as a more common occurrence than hitherto was recognized. This is of particular interest as the substitution has drastic effects on the general chemistry and spectroscopy of vesuvianite. First we will consider the crystal structure results.

4.5.1 Structure Refinements and Boron Substitution

There are some significant problems associated with the structure refinement of Wilvi vesuvianite; the following points are pertinent:

1. *the site-occupancy refinements for Bo(1) and Bo(2) show these sites to be fully occupied by B.*
2. Bo(1) is coordinated by four anions in a tetrahedral arrangement, but there is some positional disorder perturbing the situation. The site is ostensibly surrounded by two OH and two O(7) atoms. However, the O(7) shows strong positional disorder, and can only be satisfactorily modeled as a 'split' position, with ≈0.5Å separating the $O(7)_a$ and $O(7)_b$ half-atoms. Tetrahedral coordination of Bo(1) occurs only for occupancy of $O(7)_b$. When $O(7)_a$ is occupied, the distance is far too long ($\approx 2A$) to be considered as a B–O bond, and there is not a reasonable coordination for Bo(1), either in terms of geometrical criteria or in terms of local bond-valence requirements. *Thus the local coordination around Bo(1) is compatible only with half-occupancy of the site.*
3. Bo(2) is coordinated to O(10) and to O(11). The latter is in a general position, but the site occupancy refinement shows that the site is only 1/8 occupied. There are 8 symmetrically equivalent O(11) sites adjoining Bo(2), but all of them cannot be occupied, both from the low partial occupancy of this site, and also because the resulting interatomic separations would be unreasonable. Stereochemical expectations are satisfied by filling 2 of the 8 possible positions, whereupon Bo(2) has a planar triangular coordination. However, the O(11) occupancy is exactly half what it must be for such a triangular coordination.

Thus the local coordination around Bo(2) is compatible only with half-occupancy of the site.

4.5.2 Analytical Aspects of Boron Substitution

Again there are some significant results that pertain to the boron problem:

1. The electron microprobe results for B in Wilui vesuvianite indicate exactly 1/2 of the B suggested by the site-occupancy refinement results.
2. The H_2O analysis for $V74_c$ indicates exactly 1/2 the H suggested by the charge-balance calculations from the electron-microprobe and wet-chemical analyses.

Let us first consider the overall charge-balance in the structure of boron-free and boron-bearing vesuvianite. Parts of the structure are essentially identical in both types of vesuvianite in that the charge associated with them does not change. In this category are the [8]–coordinated (Ca) sites, the [4]–coordinated Si sites and the O(1)–O(9) oxygen sites. Of greater interest are the [5]– and [6]–coordinated (Al,Mg...) sites, O(10) and O(11), the H sites and the boron sites. Table 28 summarizes the charge-balance differences at these (groups of) sites in each type of vesuvianite, with the charge due to hydrogen being denoted by X and Y for boron-bearing vesuvianites. Electroneutrality requires that the sum(s) of the charges in the boron-bearing vesuvianite be the same as the sum of the charges in the boron-free vesuvianite.

It is apparent from Table 28 that this criterion cannot hold for positive values of X. Hence *Wilvi vesuvianite cannot have fully occupied boron sites.* However, the criterion does hold for Y=5, that is for 5 hydrogen atoms in the formula unit. This compares with 2 H p.f.u. derived from the chemical analysis for $V74_c$, and 4 H p.f.u. derived by charge-balance criteria. Hence this argument suggests half-occupancy of the boron sites.

We may summarize the above arguments as follows:

1. The site-occupancy refinements indicate 5 B^{3+} atoms p.f.u.
2. The local sterochemistry suggests 2 1/2 B^{3+} atoms p.f.u.
3. The electroneutrality criterion indicates that 5 B^{3+} atoms p.f.u. is not possible.
4. The electron microprobe results indicate 2.5 B^{3+} atoms p.f.u.

Table 28: Charge-balance in boron-bearing and boron-free vesuvianites.

	$V13_c$	$V74_c^*$	$V74_c$†
Ca_{19}	≡	≡	≡
Si_{18}	≡	≡	≡
O_{68}	≡	≡	≡
B^{3+}	–	15^+	7.5^+
Σ(Al, Mg...)	37^+	34^+	34^+
H	9.5^+	X	Y
O(10)	4^-	2^-	2^-
O(11)	–	2^-	2^-
Σ	42.5^+	45^++X	37.5^++Y

*$V74_c$ with boron from structure refinement.

†$V74_c$ with boron from electron microprobe analyses.

5. The analyzed H content is about half what it should be for 2.5 B^{3+} atoms p.f.u. but is not compatible with 5 B^{3+} atoms p.f.u.

The weight of the evidence suggests that Wilui vesuvianite contains 2.5 B^{3+} atoms p.f.u., and the structure results show the B^{3+} to occur in both tetrahedral and triangular coordinations. The chemical substitution may be written as:

$$B^{3+} + Mg^{2+} \rightleftharpoons 2H^+ + Al^{3+}$$

but the structural aspects are much more complex than this, as outlined above.

Notwithstanding the problems still extant with the model for boron-bearing vesuvianite, certain aspects of vesuvianite chemistry are now clear:

1. Chemical analyses of boron-bearing vesuvianites generally show <8.00 Al atoms per formula unit, and more than 2.5 Mg atoms p.f.u. (Figure 23). It is apparent that the wide range of $Al^{3+} \rightleftharpoons Mg^{2+}$ and $O^{2-} \rightleftharpoons OH^-$ substitutions are due to the occurrence of B^{3+} in the structure. The compositional range of boron-free vesuvianite is thus much more constrained than was previously thought.
2. Boron-bearing vesuvianites contain much less OH than those without boron. Figure 29 shows that normal vesuvianites have, on average, 9.5 OH atoms p.f.u. (as calculated for charge balance), compared with ≈ 5.5 OH atoms p.f.u. for boron-bearing vesuvianites.

3. Boron-bearing vesuvianites are optically positive, whereas normal vesuvianites are optically negative.
4. Boron-bearing vesuvianites have longer a cell dimensions and slightly shorter c axes than boron-free vesuvianites. Samples with $a > 15.62$Å are generally boron-bearing or partially metamict.

4.6 Infrared Spectroscopy of Vesuvianites

The polarized single-crystal infrared spectra of vesuvianite show great variability. Several other workers have investigated this problem, but they were unable to interpret the results; thus little published work has appeared. The samples used in this study were selected on the basis of optical variability and the suitability of the material for sample preparation (i.e. large, well-developed crystals). The reasons for problems encountered by previous workers became apparent upon detailed analysis and structure refinement of (some of) the vesuvianites. The presence of boron had previously gone unrecognized, and as the substitution of B into vesuvianite in part involves the substitution B $\rightleftharpoons$ H, it has a marked effect on the infrared spectrum in the principal OH stretching region. Interpretation of the spectra is still not straightforward, but some reasonable assignments may be made.

We begin by considering what happens when B^{3+} substitutes into vesuvianite. The Bo(2) site is occupied and O(10) no longer has an accompanying H atom; thus there should be a peak in boron-free vesuvianites that is absent in boron-bearing vesuvianites. Furthermore, this peak should have two specific characteristics:

1. As the O–H bond is $\|[001]$, there will be a strong absorption when $E\|[001]$ and no absorption when $E\perp[001]$. As seen in Figure 39, the peak at $\approx$3150 cm^{-1} has this polarization dependence, but seems too intense, given the relative amount of H in this configuration in the structure. This suggests that the transition probabilities of the crystallographically distinct H-bonds in the structure are radically different.
2. The configuration O(10)–H–O(10) in boron-free vesuvianites is very unusual, as it infers a symmetrical hydrogen bond. Two models have been proposed for this, as seen in Figure 62. A symmetrical H-bond will have a potential well with a single minimum at the centre; alternatively, there is a double-potential well with a low barrier between the minima. The latter appears to be the more common case, and is compatible with the spectra shown here. In particular, if the hydrogen between the adjacent O(10) atoms shows such static (or even

dynamic) disorder with a very low energy barrier between the two positions, the transition probability (for absorption) will be much higher than is the case for a "normal" hydrogen bond, accounting for its greatly enhanced intensity in the non-B vesuvianite spectra. Further experiments are planned to test this idea by taking low-temperature IR spectra of sample V13 to see if the relative intensity of the peak at 3150cm^{-1} is positively correlated with temperature (as our argument would suggest).

Next let us consider the high energy peaks near 3600cm^{-1} ($\pm$100cm^{-1}). It is apparent from Figures 39, 41, 43 and 44 that the peaks at $\approx$3670 and $\approx$3640 cm^{-1} have the same relative intensity in different polarizations for the same sample. This indicates that these two peaks are due to OH bonds with identical spatial configurations. The fine-structures are due to different *local* configurations. There is additional hyperfine structure (see Figure 40, on the major peak at 3640 cm^{-1}) that we will ignore for the moment. This doublet is present in all spectra, but its intensity relative to the rest of the spectrum is much less in the boron-bearing vesuvianites than in those without B, and the resolution is poorer.

Prominent in the spectra of the boron-bearing vesuvianites is the peak at $\approx$3570 cm^{-1}, the intensity of which shows considerable polarization dependence, with maximum absorption when E$\|$[001]. Careful examination of the spectra of the boron-free vesuvianites shows a slight shoulder at $\approx$3570 cm^{-1} that could be the same peak but with much less relative intensity.

Similarly, the peak at $\approx$3475 cm^{-1} is present in both boron-bearing and boron-free vesuvianites. Conversely, there are three prominent peaks at $\approx$3530, 3380 and 3230 cm^{-1} that are present in boron-free vesuvianites but not in boron-bearing vesuvianites. This results in seven prominent peaks in the spectra of normal vesuvianites.

Let us first consider the OH–O(7) configuration. Each OH is coordinated to one cation at each of the Ca(3), A and AlFe sites. Variation in the species of the cations (here called M) at these sites will cause changes in the strength of the M–OH bond and changes in the associated H–O(7) hydrogen bonds. Consequently there will be different populations of hydrogen bonds with different strengths, giving rise to different bands in the infrared. There is possible variation at the Ca(3), A

Table 29: The possible local combinations of cations that can bond to a single OH.

Cations	Importance
$Al^{3+} - Al^{3+}$	**
$Al^{3+} - Mg^{2+}$	**
$Al^{3+} - Fe^{3+}$	*
$Al^{3+} - Ti^{4+}$	
$Mg^{2+} - Fe^{3+}$	*
$Mg^{2+} - Ti^{4+}$	
$Mg^{2+} - Mg^{2+}$	**
$Fe^{3+} - Ti^{4+}$	

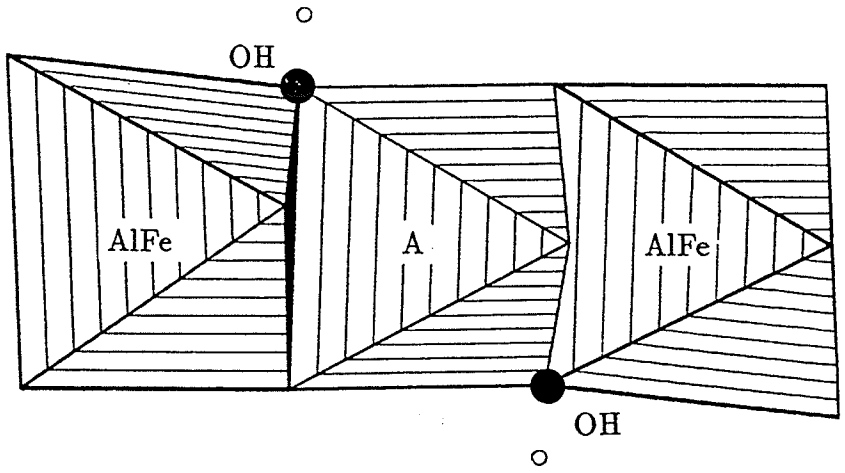

Figure 63: Diagram of the A and AlFe octahedra with their associated OH anions.

and AlFe sites; however, all of the Ca sites are effectively filled with Ca (including Ca(3)). From the extensive discussions on chemistry given previously it is apparent that AlFe (and perhaps A) are occupied by Al, Mg, Fe^{3+} and Ti^{4+} in decreasing order of importance. The possible local combinations of cations that can bond to a single OH are listed in Table 29. In terms of the known chemistry of vesuvianite, the most important of these are marked by asterisks; the small amount of Ti^{4+} normally present in vesuvianites indicates that local arrangements involving Ti^{4+} are less common, and thus will not be observed in the spectra.

The situation is not as straightforward as this, because the A and AlFe octahedra form a trimer (Figure 63). Any cation at the AlFe site coordinates one OH

Table 30: Tentative assignments of principal OH stretching bands.

Label	Energy	Configuration
A	See text	See text
B	3570 cm^{-1}	$Mg^{2+} - Mg^{2+}$
C	3530 cm^{-1}	$Mg^{2+} - Al^{3+}$
D	3480 cm^{-1}	$Mg^{2+} - Fe^{3+}$
E	3390 cm^{-1}	$Al^{3+} - Al^{3+}$
F	3220 cm^{-1}	$Al^{3+} - Fe^{3+}$
G	See text	See text

anion, whereas a cation at the A site coordinates two OH anions. Thus the long-range ordering of cations over the AlFe and A also affects the relative intensities of the OH stretching bands.

With this background, we can now consider the assignment of bands in the vesuvianite spectra. There are two important points:

1. The general configuration of the OH–O(7) bond(s) indicate that the corresponding absorption band(s) should appear in all polarizations in all principal orientations, but that E||[001] should be stronger than the other polarizations.
2. The arguments given above indicate that there should be five significant peaks due to local ordering around OH.

From detailed infrared spectroscopy of amphiboles (Hawthorne, 1983), it is well-known that coordination to cations of progressively higher mass *and* higher charge shifts the principal OH stretching band to lower energies. Consequently we can make the tentative assignments listed in Table 30. The relative intensities of the peaks correspond reasonably well with these assignments and the known chemical compositions of the various samples. However, a quantitative comparison cannot be made at the moment, as the degree of ordering over the AlFe and A sites is not known for individual samples. More crystal structure work is needed to test this model at a fully quantitative level.

Peak A (the doublet at $\approx$3640 cm^{-1}) has been left unassigned in Table 30. The characteristic aspects of this peak are the strong polarization dependence of the

intensity (again E||[001]) and the fairly high energy (indicative of a weak hydrogen bond). We saw earlier that in boron-free vesuvianite, there are two distinct channel arrangements that involve the following configurations around O(10):

1. □ –B–O(10)···H···O(10)–B–□
2. □ –H–O(10)–□ –O(10)–H–□

Configuration (1) gives rise to the peak G. In configuration (2), the bond-valence to O(10) is approximately equal to unity, exclusive of the hydrogen atom associated with O(10). This indicates that any hydrogen-bonding will be weak, and thus the principal stretching band will be of high energy; this suggests that band A can be assigned to this configuration. Furthermore, this band is very sharp, another feature indicative of weak hydrogen-bonding. If we examine the local environment around O(10) in configuration (2), we see that there is no anion along the channel that is close enough to hydrogen bond to O(10), and consequently the hydrogen bonding must be to an anion off the channel axis, suggesting that the hydrogen in this arrangement is slightly positionally disordered off the axis to attain the necessary configuration. This would account for the polarization dependence of the A band, which has a strong intensity when E||[001] and a much weaker intensity when E⊥[001]. However, the reason for the occurrence of a doublet is not clear; perhaps this is due to occupancy of the Ca(3) site by a another cation (Na?) in addition to Ca.

4.7 General Summary

We can summarize the principal conclusions (and remaining questions) as follows:

1. The general chemical formula of vesuvianite can be written thus:

$$X_{19}Y_{13}Z_{18}T_{0-5}O_{68}(OH,O)_{10}$$

$$\text{where } X = Ca,\ Na,\ Ln,\ Pb^{2+},\ Sb^{3+}$$

$$Y = Al,\ Mg,\ Fe^{3+},\ Fe^{2+},\ Ti^{4+},\ Mn,\ Cu,\ Zn$$

$$Z = Si$$

$$T = B$$

   Important aspects of this work are the discovery of B as a significant component in some vesuvianites, and its effect on the rest of the chemistry via the substitution:

$$B^{3+} + Mg^{2+} \rightleftharpoons 2H^{+} + Al^{3+}$$

   Also, the details of the possible channel configurations have been identified, and their effect on the OH content is now understood. Similarly, the site-occupancy restrictions indicated by the above definitions for X, Y and Z have been established as generally applicable for vesuvianites from all environments.

2. All vesuvianites show optical evidence of biaxial symmetry, although optic axial angles show great variation. Group theory may be used to determine the possible space group symmetries of vesuvianite. Measurements of the orientation of the optic axial plane preclude orthorhombic symmetry, and thus the space groups $P2/n$, Pn, $P2$, $P\bar{1}$ and $P1$ are possible. However, efforts to refine biaxial vesuvianite in non-tetragonal space groups produced no significant improvement in the refined models. The next step is to examine these crystals by HRTEM to look for possible low-symmetry domain structures.

3. Details of the substitution of B into the structure are now known, although details of the substitution at the atomic level are not completely clear. Boron

occurs in both tetrahedral and triangular coordination, and its incorporation into the structure is associated with significant local disorder.

4. The wide variations seen in infrared spectra of vesuvianite are shown to be due to seven (principal) OH–stretching bands that can be assigned to the hydrogen-bond configurations within the structure. Substitution of B by the $B^{3+} + Mg^{2+} \rightleftharpoons 2H^{+} + Al^{3+}$ substitution drastically effects the infrared spectrum because of the *selective* replacement of specific H configurations. It is the substitution of B (previously unrecognized) that results in the wide variation in appearance of the vesuvianite spectra.

Although significant advances in the crystal chemistry of vesuvianite have resulted from this study, the following research is necessary:

1. Further structure refinements on the known boron-bearing vesuvianites to try and completely elucidate the substitution mechanism.
2. HRTEM work to examine the strongly non-tetragonal vesuvianites for short-range domain structures, as the crystal structure has shown that the non-tetragonal aspects of the structure are not long-range.

REFERENCES

References

Allen, F.M. (1985): Structural and chemical variation in vesuvianite. Ph.D. thesis, Harvard University, Cambridge.

Allen, F.M. and Burnham, C.W. (1983a): Structure refinement of an iron-poor vesuvianite. EOS **64**, 353.

Allen, F.M. and Burnham, C.W. (1983b): Cation ordering in low-symmetry vesuvuanites. Geological Society of America Program with Abstracts **15**, 613.

Arem, J.E. (1970): Crystal chemistry and structure of idocrase. Ph.D. thesis, Harvard University, Cambridge.

Arem, J.E. (1973): Idocrase (vesuvianite)–a 250-year puzzle. Mineralogical Record **4**, 164–174.

Arem, J.E. and Burnham, C.W. (1969): Structural variations in idocrase. American Mineralogist **54**, 1546–1550.

Barth, T.F.W. (1963): Contributions to the mineralogy of Norway. No. 22. Vesuvianite from Kristiansand; other occurrences in Norway; the general formula of vesuvianite. Norsk Geologisk Tidsskrift **43**, 457–472.

Beus, A.A. (1957): [On beryllium idocrase]. Trans. Min. Mus. Acad. Sci., USSR **8**, 25–28.

Bloss, F.D. (1961): An introduction to the methods of optical crystallography. Holt, Rinehalt and Winston, New York.

Bloss, F.D. (1981): The spindle stage: principles and practice. Cambridge University Press, New York.

Bradshaw, N. (1972): An antimonian idocrase from Bau mining district, Sarawak, Malaysia. Mineralogical Magazine **38**, 894–896.

Brown, I.D. (1981): The bond-valence method: an empirical approach to chemical structure and bonding. In Structural and Bonding in Crystals, Vol. 2. Academic Press, New York.

Buseck, P.R. and Iijima, S. (1974): High resolution electron microscopy of silicates. American Mineralogist **59**, 1–21.

Christie, O.H.J. (1961): On subsolidus relations of silicates. I. The lower breakdown temperature of the akermanite-gehlenite mixed crystal series at moderate water pressure. Norsk Geologisk Tidsskrift **41**, 255–269.

Christie, O.H.J. (1962): On subsolidus relations of silicates. Norsk Geologisk Tidsskrift **42**, 1–29.

Coda, A., Della Giusta, A., Isetti, G. and Mazzi, F. (1970): On the crystal structure of vesuvianite. Atti della R. accademia delle scienze di Torino **105**, 63–84.

Chatterjee, N.D. (1962): Vesuvianite-epidote paragenesis as a product of greenschist facies of regional metamorphism in the western Alps. Beitr. Min. Petr. **8**, 432–439.

Cromer, D.T. and Liberman, D. (1970): Relativistic calculation of anomalous scattering factors for X-rays. Journal of Chemical Physics **53**, 1891–1898.

Cromer, D.T. and Mann, J. (1968): X-ray scattering factors computed from numerical Hartree-Fock wave functions. Acta Crystallographica **A24**, 321–324.

Deer, W.A., Howie, R.A. and Zussman, J. (1962): Rock-Forming Minerals. Longmans, Green and Co. Ltd., London.

Deer, W.A., Howie, R.A. and Zussman, J. (1982): Rock-Forming Minerals. Vol. 1A. Orthosilicates. (2nd ed.). Longmans, Green and Co. Ltd., London.

Dobson, D.C. (1982): Geology and alteration at the Lost River Sn-W-F deposit, Alaska. Economic Geology **77**, 1033–1052.

Donaldson, E.M. (1982): Methods for the Analysis of Ores, Rocks and Related Materials. Energy Mines and Resources (Canada) Monograph **881**.

Economou, M. and Marcopoulos, T. (1980): Vesuviane in den Magnetiterzen der Serpentinite von Vermion, Griechenland. Chemie der Erde **39**, 140–145.

Fitzgerald, S. (1985): Crystal chemistry and structure of vesuvianite. Ph. D. thesis, University of Delaware, Newark.

Fitzgerald, S., Rheingold, A. L., Leavens, P. B. (1986a): Crystal structure of a Cu-bearing vesuvianite. American Mineralogist **71**, 1011–1014.

Fitzgerald, S., Rheingold, A.L., Leavens, P.B. (1986b): Crystal structure of a non-$P4/nnc$ vesuvianite from Asbestos, Quebec. American Mineralogist **71**, 1483–1488.

Fitzgerald, S., Leavens, P.B., Rheingold, A.L. and Nelen, J.A. (1987): Crystal structure of a REE-bearing vesuvianite from San Benito County, California. American Mineralogist **72**, 625–628.

Gädeke, R. (1938): Die gesetzmassingen Zusammenhänge und Anomalien in der Vesuviangruppe und einigen anderen Kalksilikaten. Chemie der Erde **11**, 592–636.

Giuseppetti, G. and Mazzi, F. (1983): The crystal structure of a vesuvianite with $P4/n$ symmetry. Tschermaks Mineralogische und Petrographische Mitteilungen. **31**, 277–288.

Himmelberg, G.R. and Miller, T.P. (1980): Uranium and thorium-rich vesuvianite from the Seward Peninsula, Alaska. American Mineralogist **65**, 1020–1025.

Hoisch, T.D. (1985): The solid solution chemistry of vesuvianite. Contributions to Mineralogy and Petrology **89**, 205–214.

Hurlbut, C.S., Jr. (1955): Beryllian idocrase from Franklin, New Jersey. American Mineralogist **40**, 118–120.

Inoue, T. and Miyashiro, A. (1951): Occurrence of vesuvianite in nepheline-syenitic rocks of the Fukushinzan district, Korea; with general consideration of the relation between the composition and occurrence of vesuvianite. Journal of the Geological Society of Japan **57**, 51–57.

Isetti, G. and Penco, A.M. (1961): Ricerche sulla vesuvianite di Bric Camulà (Gruppo di Voltri). Ann. Mus. Civ. St. Natur. Genova **72**, 220–233.

Ito, J. and Arem, J.E. (1970): Idocrase: synthesis, phase relations and crystal chemistry. American Mineralogist **55**, 880–912.

Khotina, M.I. (1968): [The chemical composition of the vesuvianite with zonal and sectorial structure from the Norilsk district.] Zapiski Vsesoiuznogo Mineralogicheskogo Obshchestva, 312–630 (in Russian).

Kononova, V.A. (1961): On a metamict variety of vesuvianite from an alkaline pegmatite in southwest Tuva. Doklady Akademii Nauk USSR, Earth Science Section **130**, 129–132.

Lewis, J.V. and Bauer, L.H. (1922): Cyprine and associated minerals from the zinc mine at Franklin, New Jersey. American Mineralogist **67**, 846–847.

Machatschki, F. (1930): Die Summenformel des Vesuvians und seine Beziehungen zum Granat. Centralblatt für Mineralogie **7**, 284–293.

Machatschki, F. (1932): Zur Formel des Vesuvian. Zeitschrift für Kristallographie **81**, 148–152.

Manning, P.G. (1968): Optical absorption spectra of octahedrally bonded Fe^{3+} in vesuvianite. Canadian Journal of Earth Science **5**, 89–92.

Manning, P.G. (1975): Charge-transfer processes and the origin of colour and pleochroism of some Ti-rich vesuvianites. Canadian Mineralogist **13**, 110–116.

Manning, P.G. (1976): Ferrous-ferric interaction on adjacent face-sharing antiprismatic sites in vesuvianites: evidence for ferric ion in eight coordination. Canadian Mineralogist **14**, 216–220.

Manning, P.G. and Tricker, M.J. (1975): Optical-absorption and Mössbauer spectral studies of iron and titanium site-populations in vesuvianites. Canadian Mineralogist **13**, 259–265.

Meen, V.B. (1939): Vesuvianite from Great Slave Lake region, Canada. University of Toronto Studies, Geological Series. **42**, 69–74.

Mel'nitskiy, V.V. (1966): [The isomorphism of boron in prehnite, vesuvianite, and other silicates and its importance for prospecting.] Geol. Rud. Mestorozhd. **4**, 95–100 (in Russian).

Morandi, N., Minguzzi, V. and Nannetti, M.C. (1979): Spettri IR comportamento termico e prodotti di riscaldamento di vesuviane e granati variamente idrati. Mineralogica et Petrograhica Acta **23**, 151–173.

Neumann, H. and Svinndal, S. (1955): The cyprine-thulite deposit at Ovstebo near Kleppan in Sauland, Telemark. Norsk Geologisk Tidsskrift **34**, 139–156.

North, A.C.T., Phillips, D.C. and Mathews, F.S. (1968): A semi-empirical method of absorption correction. Acta Crystallographica **A24**, 351–359.

Numano, K., Kusachi, I., Henmi, C. and Henmi, K. (1978): Lattice constants of idocrase from Kushiro, Hiroshima Prefecture. Bull. Sch. Educ., Okayama Univ. **49**, 49–60.

Oftedal, I. (1964): Contributions to the mineralogy of Norway No. 29. Vesuvianite as a host mineral for boron. Norsk Geologisk Tidsskrift. **44**, 377–383.

Orlov, Yu.L. and Mart'yanov, N.N. (1961): [Vesuvianite, containing rare-earth elements, from the Yenisei Mountain Range]. Trudy Mineralogicheskogo muzeia Akademii Nauk SSSR **11**, 187 (in Russian).

Osborne, F.F. (1930): The nepheline-gneiss complex near Egan Chute, Dungannon Township, and its bearing on the origin of the nepheline syenite. American Journal of Science **20**, 33–60.

Osborne, M. and Burns, R.G. (1978): Crystal chemistry, optical properties and Mössbauer spectroscopy of vesuvianite. Significance of five-coordinated iron sites. Geological Association Canada, Abstracts with Programs 1978 Joint Annual Meeting, 466.

Palache, C. and Bauer, L.H. (1930): On the occurrence of beryllium in the zinc deposits of Franklin, New Jersey. American Mineralogist **15**, 29–33.

Peters, T. (1963): Mineralogie und Petrographie des Totalpserpentins bei Davos. Schweiz Min. Petr. Mitt. **43**, 529–685.

Quensel, P. (1915): Vesuvian und Hastingsit aus dem Nephelinsyenit von Almunge. Centralblatt für Mineralogie, 201–208.

Roeder, (1985): Electron microprobe analysis of minerals for rare earth elements: use of calculated peak-overlap corrections. Canadian Mineralogist **23(2)**, 263–271.

Rucklidge, J.C., Kocman, V., Whitlow, S.H. and Gabe, E.J. (1975): The crystal structures of three Canadian vesuvianites. Canadian Mineralogist, **13**, 15–21.

Saksena, B.D. (1961): Infra-red absorption studies of some silicate structures. Transcript of the Faraday Society, 242–255.

Sapountzis, E.S. and Katagas, C. (1980): Idocrase (vesuvianite) from the Kozani area (North Greece). Neues Jahrbuch für Mineralogie, Monatshefte **10**, 461–468.

Serdyuchenko, D.P., Gubaydulin, F.G., Pavlov, V.A. and Sundakova, I. Ya. (1968): Idocrases from skarns in central Asia and their chemical composition. Doklady Akademii Nauk USSR, Earth Science Section **180**, 135–137.

Silbermintz, B.A. and Roschkowa, E.W. (1933): Zur Frage des Vorkommens von Beryllium in Vesuvianen. Centralblatt für Mineralogie, Abstract A, 249–253.

Tricker, M.J. and Manning, P.G. (1979): Can electron exchange processes in vesuvianite be detected by Mössbauer spectroscopy? Journ. de Phys. Colloq. **C2**, 477–479.

Tricker, M.J., Vaishnava, P.P. and Manning, P.G. (1981): ^{57}Fe Mössbauer spectroscopic studies of electron-hopping processes in vesuvianites. Journal of Inorganic and Nuclear Chemistry. **43**, 1169–1174.

Trommsdorff, V. (1968): Mineralreaktionen mit Wollastonit und Vesuvian in einem Kalksilikatfels der alpinen Disthenzone (Claro, Tessin). Schweizerische Mineralogische und Petrographische Mitteilungen **48**, 655–666.

Vaishnava, P.P., Tricker, M.J. and Manning, P.G. (1980): Observation of electron-hopping in vesuvianite by Mössbauer spectroscopy. Physica Status Solidi (a) **62**, K89–K93.

Valley, J.W., Peacor, D.R., Bowman, J.R., Essene, E.J. and Allard, M. J. (1985): Crystal chemistry of Mg-vesuvianite and implications of phase equilibria in the

system calcia-magnesia-alumina-silica-water-carbon dioxide. Journal of Metamorphic Geology **3**, 137–153.

Veblen, D.R. and Wiechmann, M.J. (1988): Domain structure in low-symmetry vesuvianite. V. M. Goldschmidt Conference Program with Abstracts, 80.

Warren, B.E. and Modell, D.I., (1931): The structure of vesuvianite $Ca_{10}Al_4(Mg, Fe)_2Si_9O_{34}(OH)_4$. Zeitschrift für Kristallographie **78**, 422–432.

Wherry, E.T. and Chapin, W.H. (1908): Boric acid in vesuvianite. Journal of the American Chemistry Society **30**, 1684–1687.

Yoshiasa, A. and Matsumoto, T. (1986): The crystal structure of vesuvianite from Nakatatsu mine: reinvestigation of the cation site-population and of the hydroxyl groups. Mineralogical Journal **13**, 1–12.

Zabiński, W. (1971): The hydroxyl-stretching region of the vesuvianite infra-red spectrum. Mineralogia Polonica **2**, 45–48.

Appendix A
VESUVIANITE SAMPLES

VESUVIANITE SAMPLES

Sample	Country	Locality	Source
V1	Australia	Bowling Alley Point, Nundle, NSW	Royal Ontario Museum (M14160)
V2	Canada	Silent Lake Mine, Raft River, BC	S.G. Baker Collection
V3	"	Frye's Island, Charlotte Co., NB	Royal Ontario Museum (M5460)
V4	"	Marne Claims, NT	P. Lhotka
V5	"	Turnback Lake, NT	Royal Ontario Museum (M19485)
V6	"	Long Lake Mine, Olden Twp., ON	" " " (M33459)
V7	"	York River, Dungannon Twp., ON	" " " (M24961)
V8	"	Black Lake, Megantic Co., PQ	" " " (M8509)
V9	"	" " "	" " " (M11064)
V10	"	Coleraine Twp., Megantic Co., PQ	" " " (M38244)
V11	"	Jeffrey Mine, Richmond Co., PQ	" " " (M25566)
V12	"	" " "	" " " (M29851)
V13	"	" " "	" " " (M33894)
V14	"	" " "	" " " (M36316)
V15	"	" " "	" " " (M36318)
V16	"	" " "	" " " (M38075)
V17	"	" " "	Dr. R. Martin
V18	"	" " "	purchased
V19	"	" " "	" " "
V20	"	" " "	" " "
V21	"	" " "	? ? ?
V22	"	" " "	" " "
V23	"	" " "	" " "
V24	"	Laurel, PQ	Royal Ontario Museum (M27846)
V25	"	Mount St. Hilaire, PQ	" " " (M26554)
V26	"	" " "	" " " (M26555)
V27	"	" " "	" " " (M31812)
V28	"	Quebec	" " " (M7816)
V29	"	Templeton Twp., Ottawa Co., PQ	" " " (E2207)
V30	"	" " "	" " " (M5440)
V31	"	" " "	" " " (M7827)
V32	"	Wakefield Twp., Ottawa Co., PQ	" " " (E2206)
V33	"	Richardson Mountains, YT	Dr. P. Černý
V34	"	" " "	? ? ?
V35	Czechoslovakia	Hazlov, near Cheb	Royal Ontario Museum (M23448)
V36	Greece	Xanthi	Dr. G. Frenzel

VESUVIANITE SAMPLES

Sample	Country	Locality	Source
V37	Italy	Ala Piedmont	Royal Ontario Museum (M5442)
V38	"	Ariccia, Rome	" " " (M19263)
V39	"	Bellecombe, Aosta	purchased
V40	"	Monte Somma	Royal Ontario Museum (E1541)
V41	Pakistan	Hindubagh, Baluchistan	" " " (M21515)
V42	Japan	Chichibu Mine, Saitama Pref.	" " " (M26108)
V43	Kenya	Magadi	" " " (M32914)
V44	Mexico	Cerro Los Muerlos, Chihuahua	" " " (M19001)
V45	"	Laguna del Jaco, Chihuahua	purchased
V46	"	" " "	Royal Ontario Museum (M31745)
V47	Morocco	Othuren	" " " (M29144)
V48	Norway	Stromsheia, Setesdal	" " " (M19128)
V49	"	? ? ?	" " " (E1610)
V50	Sweden	Langban	" " " (M14567)
V51	Taiwan	Feng Tien Mine	purchased
V52	United States	Brooks Mountains, AK	" " "
V53	"	Seward Peninsula, AK	Dr. G. Rossman
V54	"	Magnet Cove, AR	Royal Ontario Museum (M16539)
V55	"	Big Sandy Draw, Mahave Co., AZ	" " " (M28255)
V56	"	Bill Waley Mine, Tulare Co., CA	purchased
V57	"	Butte Co., CA	Royal Ontario Museum (M5459)
V58	"	" " "	" " " (M13839)
V59	"	El Dorado Co., CA	" " " (M29149)
V60	"	Plumas Co., CA	" " " (M28840)
V61	"	Tulare Co., CA	purchased
V62	"	Italian Mountains, CO	Royal Ontario Museum (M16538)
V63	"	Sanford, York Co., ME	" " " (M5453)
V64	"	" " "	B. Dutrow
V65	"	Woodstock, ME	Royal Ontario Museum (M5443)
V66	"	Franklin, Sussex Co., NJ	" " " (M15193)

VESUVIANITE SAMPLES

Sample	Country	Locality	Source
V67	"	" " "	purchased
V68	"	Ludwig, NV	Royal Ontario Museum (M28637)
V69	"	Amity, Orange Co., NY	" " " (M5461)
V70	"	Olmstedville, Essex Co., NY	" " " (M21483)
V71	"	Mt. Belvidere, Eden Mills, VT	" " " (M31358)
V72	"	? ? ?	Dr. B. Chakomakous
V73	USSR	Lupikko, Fennoscandia	Royal Ontario Museum (M23644)
V74	"	Wilui River, Yakutskaya ASSR	purchased
V75	?	? ? ?	Royal Ontario Museum (M22188)

Appendix B
VESUVIANITE SAMPLE DESCRIPTIONS

ABBREVIATIONS USED IN APPENDIX B

(e): identified with EDS
(g): identified with Gandolfi camera
(w): identified with WDS
(x): identified with XRD

Crystal dimensions are in order from smallest to largest. In some cases a dimension is labelled as being associated with a particular axis. Forms are listed in order of decreasing area. Forms of approximately equal area are not separated by commas.

VESUVIANITE SAMPLE DESCRIPTIONS

Sample	Colour	Habit	Size
V1	yellow-green	massive, with irregular crystal faces	$\leq$1 mm
V2	yellow-brown	irregular prisms, striated $\parallel Z$	up to 6 mm $\times$ 7 mm
V3	light green	microcrystalline aggregate	
V4	dark green	prismatic crystal, coarsely striated $\parallel Z$	3 cm $\times$ 4 cm $\times$ 5 cm (Z)
V5	dark brown	prismatic crystal	7 mm $\times$ 9 mm $\times$ 2 cm (Z)
V6	dark brown to black	prismatic crystal, striated $\parallel Z$	4 mm $\times$ 4 mm
V7	dark brown	massive	up to 7 mm $\times$ 7 mm
V8	dark green	striated prismatic crystals	up to 8 mm wide
V9	light to dark green, purple	granular aggregate with some irregular crystals	$\leq$1 mm
V10	light green	striated prismatic crystals	1 mm $\times$ 4 mm
V11	light green		3 mm $\times$ 3.5 mm $\times$ 7 mm (Z)
V12	light green	prismatic crystals, striated $\parallel Z$	2.5 mm $\times$ 5 mm (Z)
V13	dark brown	prismatic crystals, finely striated $\parallel Z$	up to 5 mm $\times$ 5 mm $\times$ 1.3 cm (Z)
V14	light green	massive	
V15	light purple	massive	
V16	light green	irregular crystals, striated $\parallel Z$	2.5 mm $\times$ 6 mm

VESUVIANITE SAMPLE DESCRIPTIONS

Sample	Forms	Inclusions	Associated Minerals
V1			quartz
V2	{001}, {100} (indistinct)		
V3		clinochlore^{w}	clinochlore^{xg}
V4			
V5	{100}, {110}, {001} + others		galena^{g}
V6	{100}, {110}	diopside^{w}, pyrite^{g}	
V7	{100}, {110} (indistinct)		
V8	{100}, {001}, {110}		crystals are rimmed with garnet
V9			andradite^{w}, chromite^{c}, grossular^{g} (?)
V10	many forms	apatite^{c}	almandine^{w}, chrysotile^{g}, diopside^{w}
V11			
V12	many forms		
V13	{100}, {101}, {001}, sometimes {110}		lizardite^{g}
V14			
V15			
V16			grossular^{g}

VESUVIANITE SAMPLE DESCRIPTIONS

Sample	Colour	Habit	Size
V17	light green	massive, or in radiating aggregates	0.5 mm × 5 mm (Z)
V18	light green	prismatic crystals	up to 0.5 mm × 2 mm (Z)
V19	brown	radiating aggregates of prismatic crystals, finely striated $\parallel Z$	up to 0.5 mm × 3 mm (Z)
V20	brown	radiating aggregates of prismatic crystals, finely striated $\parallel Z$	up to 0.5 mm × 3 mm (Z)
V21	light green to pink (along edges)	massive	
V22	light yellow-green	massive with poorly developed crystals (often finely striated)	up to 1 cm in length
V23	light green	striated prismatic crystals	5 mm × 5 mm × 2.5 cm (Z)
V24	yellow	massive	
V25	yellow	poorly developed prismatic crystals	up to 5 mm × 1 cm
V26	yellow-green	radiating aggregates of acicular crystals	up to 0.2 mm × 4 mm (Z)
V27	yellow-brown	columnar crystals	1 mm × 8 mm (Z)
V28	brown	fractured prismatic crystals	up to 1.8 cm × 2.6 cm (Z)
V29	brown	prismatic crystals	up to 1 cm × 2.5 cm (Z)
V30	black	massive with subconchoidal fracture	6 mm × 6 mm
V31	brown	prismatic crystals	6 mm × 7 mm × 1.2 cm (Z)
V32	dark brown	coarsely striated prismatic crystals	up to 1 cm wide

VESUVIANITE SAMPLE DESCRIPTIONS

Sample	Forms	Inclusions	Associated Minerals
V17			
V18	many forms		
V19			
V20			
V21	some poorly developed forms		
V22	many complex forms		
V23	{100}, {110} + many others		
V24			
V25			
V26			apatite[c], apophyllite[x], pectolite[w]
V27			
V28	{100}, {001}, sometimes {110} and {101}	quartz[c]	
V29	{100}, {001}, {110}, {101}	quartz	
V30	{100}, {110}	cuspidine[w] (?)	quartz
V31	{100}, {001}, {110}, {101}	quartz	
V32	{100}, {001}		

VESUVIANITE SAMPLE DESCRIPTIONS

Sample	Colour	Habit	Size
V33	light brown to green	massive	4 mm × 5 mm
V34	light to dark green	radiating aggregates of acicular crystals	up to 0.5 mm × 1 cm (Z)
V35	dark brown	massive	$\leq$8 mm
V36	dark green	prismatic crystals	2 cm × 2 cm × 1.5 cm (Z)
V37	pale green	prismatic crystals	4 mm × 4 mm × 1.1 cm (Z)
V38	dark brown-green	prismatic crystals (often finely striated)	$\leq$7 mm (X)
V39	dark brown	prismatic crystals, finely striated $\parallel Z$	3 mm × 3 mm × 4 mm (Z)
V40	brown	prismatic crystals	$\leq$3.5 mm (X)
V41	light green	granular aggregate	$\leq$5 mm across
V42	brown	massive	
V43	yellow	granular aggregate	$\leq$8 mm across
V44	yellow	massive	
V45	yellow	prismatic crystals	$\leq$1.3 cm (X) × 1.2 cm (Z)
V46	yellow	massive with some irregular crystals	
V47	light brown	massive	
V48	dark green to light blue	massive, with some coarsely striated crystal faces	
V49	light blue	massive	
V50	red	granular aggregate	up to $\leq$1 mm across
V51	light green	prismatic crystals, finely striated $\parallel Z$	2 mm × 2 mm × 1 cm (Z)
V52	dark green	granular aggregate	

VESUVIANITE SAMPLE DESCRIPTIONS

Sample	Forms	Inclusions	Associated Minerals
V33			orthoclase
V34		calcite^{c}, fluorite^{c}	fluorite^{g}, orthoclase, phlogopite^{g}
V35			quartz
V36	{101}, {001}, {112}	calcite^{c}	
V37	{100}, {101}, small {001}		
V38	{100} {101} {110} {001}		
V39	{100}, {001}, {110} + others		
V40	{100} {110} {001} {101}	grossular^{c}, phlogopite^{c}	
V41			
V42			
V43			
V44			
V45	{001}, {110}, {100}, {101}		
V46		garnet^{w}	chrysotile^{g}
V47			
V48			
V49			
V50			hausmannite^{wg}
V51	Many prism faces; large {001}, small {101} and {111}		
V52			

VESUVIANITE SAMPLE DESCRIPTIONS

Sample	Colour	Habit	Size
V53	dark brown	massive	
V54	light yellow-brown	massive	
V55	light brown	radiating aggregates of prismatic crystals, striated $\parallel Z$	5 mm × 3 cm (Z)
V56	black	massive with some poorly developed crystal faces	faces up to 5 mm across
V57	light green	prismatic crystals	1 cm × 1 cm × 7 mm
V58	light green	microcrystalline aggregate	
V59	green	prismatic crystals	3 cm × 3 cm × 1.5 mm (Z)
V60	yellow	massive	
V61	yellow-brown	massive	$\leq$5 mm × 7 mm
V62	light yellow-brown	massive	
V63	dark brown	prismatic crystals	6 mm × 6 mm × 1 cm (Z)
V64	light yellow-brown	massive aggregate of acicular crystals, finely striated $\parallel Z$	
V65	brown	prismatic crystals, coarsely striated $\parallel Z$	2 cm (Z)
V66	dark green to light blue	acicular crystals	microscopic
V67	dark to light blue	acicular crystals	$\leq$ 0.1 mm × 1 mm
V68	light green	massive	
V69	brown	prismatic crystals	$\leq$3 mm
V70	dark brown	massive	

VESUVIANITE SAMPLE DESCRIPTIONS

Sample	Forms	Inclusions	Associated Minerals
V53			orthoclase^{w}, quartz
V54		perovskite^{w}	
V55			quartz
V56			calcite^{g}, diopside^{g}, loellingite^{g}, pyrrhotite^{g}
V57	{101}, {001}, {112}	calcite^{cw}, cuspidine^{w}, diopside^{c}, monticellite^{w}, wollastonite^{c}	
V58		grossular^{g}	
V59	{101}, {001}, {112}	clinochlore^{w}	quartz
V60		diopside^{w}, grossular^{c}	
V61			grossular^{g}
V62		diopside^{w}	clinochlore^{g}, diopside^{g}
V63			
V64			quartz
V65			
V66			andradite^{w}
V67			calcite^{c}, grossular^{g}, hedenbergite^{g}, willemite^{c}
V68		diopside^{w}	diopside^{g}
V69			quartz
V70			diopside (?)

VESUVIANITE SAMPLE DESCRIPTIONS

Sample	Colour	Habit	Size
V71	light green	prismatic crystals	6 mm × 6 mm × 2.5 cm (Z)
V72	black	massive with conchoidal fracture	
V73	light brown	massive with some prismatic crystals	1.2 mm × 2 mm
V74	dark green	prismatic crystals, often faintly striated $\parallel X$; step features seen on {100} and {110}	11 mm × 11 mm × 16 mm to 2.2 cm × 2.2 cm × 4.2 cm (Z)
V75	light green	microcrystalline aggregate	

Sample	Forms	Inclusions	Associated Minerals
V71	{100}, {001}, {110}	andradite^{w}, diopside^{w}	
V72		apatite^{c}, calcite^{c}, diopside^{c}, zircon^{c}	
V73	{100}, {001}, {110}	phlogopite^{c}	
V74	{100}, {110}, {101}, {001}; on some smaller crystals the order is {100}, {001}, {101}, {110}	grossular^{c}	chrysotile^{x}, grossular^{g}
V75			

Appendix C

VESUVIANITE OPTICAL DESCRIPTIONS

ABBREVIATIONS USED IN APPENDIX C

(k): $2V$ determined using Kamb's method
(s): $2V$ determined using spindle stage

Colours are those seen in plane polarized light (sections $\leq$500 μm thick). Multiple entries under colour refer to different sections; remarks that apply to only one section are labelled (i.e. (1)). All $2V$s were determined using Tobi's method unless otherwise indicated.

VESUVIANITE OPTICAL DESCRIPTIONS

Sample	Colour	Sign	$2V$ (°)	Remarks
V1	light brown			
V2	colourless to light yellow	–	13, 13, 17, 19	faint banding near rim heavily fractured
V3	light brown to green			microcrystalline
V4	yellow-brown	–	12, 16, 21, 11, 24	variable $2V$s heavily fractured
V5	light brown	– –	7 (core) 8, 16, 19 (rim)	blocky-zoned (?) faint banding near rim undulose extinction
V6	light brown	–	8, 13, 18, 21 (rim)	diopside, pyrite, quartz inclusions
V7	dark brown	–	6, 6, 8	wide banding near rim many regular fractures quartz inclusions
V8	colourless light brown	– –	large $2V$ (rim) 6, 8, 9	probably sector-zoned some banding seen
V9	colourless to green purple			microcrystalline; grains $\leq$0.2 mm in diameter microcrystalline; grains $\leq$0.06 mm in diameter
V10	colourless to light yellow			
V11	colourless	– – –	$\leq$9 (core) 24 (core near rim) 29–31 (rim) 32.8(4)^s ($V11_3$)	blocky-zoned undulose extinction
V12	colourless	– – –	30–33 (core) 10, 12, 19 ((101)) 37, 40 (rim)	blocky-zoned dispersion r$\ll$v (core), r<v ((101) and rim)

VESUVIANITE OPTICAL DESCRIPTIONS

Sample	Colour	Sign	$2V$ (°)	Remarks
V13	colourless to pale yellow	– – –	0–10 (rim) 36, 36 ((101)) 60–62[k] (rim)	sector-zoned core appears uniaxial wide, complex (101) zone narrow (110) zone dispersion r≪v ((101)), r<v (core and rim)
V14	colourless colourless	– – – –	18, 18 (core) 43, 43, 43 (rim) 19-21 (core) 41, 45 (rim)	some fine banding undulose extinction dispersion r≪v (core), r<v (rim)
V15	colourless to light yellow			
V16	colourless	–	0–>60	blocky-zoning undulose extinction variable $2V$s
V17	colourless			blocky-zoned (?)
V18	colourless to light yellow			
V19	colourless to light yellow			blocky-zoned
V20	yellow			
V21	colourless with pink edges		large $2V$ 62.1(3)[s]	blocky-zoned (?)
V22	yellow			blocky-zoned (?)
V23	colourless colourless	– – – – – –	13 (core) 15–20 ((101)) large $2V$ (rim) 21 (core) 16–21 ((101)) 48 (rim) 62.1(3)[s] $V23_r$	blocky-zoned rudimentary core (1) dispersion r≪v ((101)) (2)

VESUVIANITE OPTICAL DESCRIPTIONS

Sample	Colour	Sign	$2V$ (°)	Remarks
V24	yellow			
V25	colourless to light yellow			
V26	colourless to yellow			very fibrous
V27	pleochroic yellow to pink	–	45	
V28	medium brown	–	14, 14, 14	unusual fracture pattern quartz inclusions
V29	medium brown	–	4, 7, 10, 12, 13	quartz inclusions
V30	medium brown	+	large $2V$	fine banding near edge
V31	light brown light brown	– –	10, 11, 11, 11 0–17	wide banding near edge undulose extinction unusual fracture pattern quartz inclusions
V32	light brown light brown	– – –	9, 11, 23 0–10 (core) 14 (rim)	blocky-zoned (?) wide banding near rim undulose extinction dispersion r<v (rim) (2)
V33	colourless	–	11, 13, 14, 21	fine banding around rim
V34	yellow-brown	–		heavily fractured
V35	light brown medium brown medium brown	– – –	9, 10, 11, 13 0–7 7, 10	
V36	light green	–	large $2V$	
V37	colourless to light yellow			
V38	yellow to brown	+	large $2V$	fine banding
V39	light brown	–	large $2V$	undulose extinction
V40	light to medium brown	– –	9 (core) 15, 16 (rim)	fine banding

VESUVIANITE OPTICAL DESCRIPTIONS

Sample	Colour	Sign	$2V$ (°)	Remarks
V41	colourless to light green	–	large $2V$	blocky-zoned
V42	pleochroic pink to green			
V43	colourless light green			
V44	colourless	–	18	some fine banding
V45	colourless to light yellow	+	large $2V$	sector-zoned fine banding near edge
V46	colourless		large $2V$	fine banding near edge
V47	light brown	–	13–16	
V48				
V49	light blue	–	0–5	
V50	red			
V51				
V52				
V53				
V54	colourless to light brown	–	large $2V$	
V55	medium brown	–	0–5	some wide banding
V56	dark brown			
V57	colourless to light brown	–	16	
V58	colourless to light green			microcrystalline
V59	colourless to light green			some banding near edge
V60	light brown			
V61	medium brown			
V62	pleochroic colourless to light yellow		large $2V$	

VESUVIANITE OPTICAL DESCRIPTIONS

Sample	Colour	Sign	$2V$ (°)	Remarks
V63	light brown	–		
V64	yellow-brown	–	0–10	heavily fractured
V65	yellow-brown		0 (?)	
V66	blue			fibrous
V67	dark blue			fibrous
V68	colourless			
V69	light brown			
V70	light brown			
V71	pale green			sector-zoned fine banding near edge many grossular inclusions
V72	light brown			many inclusions
V73	brown	–	0–5	
V74	dark green	+ +	0–10 (core) 10–25 ((110) and rim)	sector-zoned fine banding grossular inclusions
V75	light green			microcrystalline

Appendix D

EDS ANALYSES OF VESUVIANITE (UM)

ABBREVIATIONS USED IN APPENDIX D

ΣX : (Ca+Na+K+REE+Pb+Bi+Th+U)
ΣY : (Al+Ti+Mg+Mn+Fe+Cr+Cu+Zn)
ΣZ : (Si)

Fe_2O_3 values are derived from total Fe (by EDS) and bulk Fe^{2+} (by wet chemistry). The analyses are normalized to 50-cations (less B, S) and 78 anions per formula unit.

QUANTITATIVE EDS RESULTS (UM)

	$V1\text{-}1_M$	$V1\text{-}2_M$	$V1\text{-}3_M$	$V1\text{-}4_M$	$V1\text{-}5_M$	$V1\text{-}6_M$	$V1\text{-}7_M$	$V1\text{-}8_M$	$V1\text{-}9_M$	$V1\text{-}10_M$
SiO_2	36.4	36.3	36.3	36.4	36.5	37.1	37.1	36.7	36.9	36.5
Al_2O_3	17.3	17.3	17.2	17.2	17.0	17.2	17.1	17.1	17.0	17.1
TiO_2	–	–	–	–	–	–	–	–	–	–
MgO	2.0	1.5	1.7	1.7	2.1	2.3	2.4	2.4	2.4	2.4
MnO	–	0.1	–	–	–	–	–	–	–	–
FeO	3.9	4.2	4.2	4.3	3.8	3.5	3.5	3.4	3.6	3.6
Fe_2O_3	–	–	–	–	–	–	–	–	–	–
Cr_2O_3	–	–	–	–	–	–	–	–	–	–
CaO	36.1	36.2	36.2	36.5	36.4	36.6	36.6	36.6	36.6	36.4
SO_3	–	–	–	–	–	0.2	–	0.1	0.2	–
Cl	–	–	–	–	–	0.1	–	0.1	0.1	0.2
H_2O^*	3.1	3.1	3.1	3.2	3.2	3.0	3.1	3.1	3.0	3.2
	98.8	98.7	98.7	99.3	99.0	100.0	99.8	99.5	99.8	99.4
O≡Cl	–	–	–	–	–	0.0	–	0.0	0.0	0.0
TOTAL	98.8	98.7	98.7	99.3	99.0	100.0	99.8	99.5	99.8	99.4
Si^{4+}	17.89	17.92	17.90	17.86	17.92	18.02	18.01	17.90	17.96	17.85
Al^{3+}	10.02	10.06	10.00	9.95	9.84	9.85	9.79	9.83	9.75	9.86
Ti^{4+}	–	–	–	–	–	–	–	–	–	–
Mg^{2+}	1.47	1.10	1.25	1.24	1.54	1.67	1.74	1.75	1.74	1.75
Mn^{2+}	–	0.04	–	–	–	–	–	–	–	–
Fe^{2+}	1.60	1.73	1.73	1.76	1.56	1.42	1.42	1.39	1.47	1.47
Fe^{3+}	–	–	–	–	–	–	–	–	–	–
Cr^{3+}	–	–	–	–	–	–	–	–	–	–
Ca^{2+}	19.01	19.14	19.12	19.19	19.15	19.05	19.04	19.13	19.08	19.07
S^{6+}	–	–	–	–	–	0.07	–	0.04	0.07	–
Cl^-	–	–	–	–	–	0.08	–	0.08	0.08	0.17
OH^{-*}	10.19	10.11	10.21	10.34	10.33	9.60	10.19	10.06	9.81	10.28
O	67.81	67.89	67.79	67.66	67.67	68.32	67.81	67.86	68.10	67.55
				Statistics						
ΣX	19.01	19.14	19.12	19.19	19.15	19.05	19.04	19.13	19.08	19.07
ΣY	13.10	12.94	12.98	12.95	12.93	12.93	12.94	12.97	12.96	13.08
ΣZ	17.89	17.92	17.90	17.86	17.92	18.02	18.01	17.90	17.96	17.85

*Calculated for charge balance.

QUANTITATIVE EDS RESULTS (UM)

	V1-11$_M$	V1-12$_M$	V1-13$_M$	V1-14$_M$	V1-15$_M$	V1-16$_M$	V1-17$_M$	V1-18$_M$	V1-19$_M$	V1-20$_M$
SiO_2	36.6	36.5	36.6	36.5	36.6	36.8	36.8	36.8	36.7	36.7
Al_2O_3	17.2	17.4	17.6	17.4	17.4	17.3	17.4	17.5	17.1	17.3
TiO_2	0.2	0.3	–	0.3	0.2	–	–	–	–	–
MgO	1.4	1.3	1.6	1.5	1.5	2.1	2.4	1.9	2.1	1.9
MnO	0.2	–	–	0.1	–	–	–	–	–	–
FeO	4.4	4.3	4.3	4.2	4.2	3.9	3.6	4.2	3.7	3.7
Fe_2O_3	–	–	–	–	–	–	–	–	–	–
Cr_2O_3	–	–	–	–	–	–	–	–	–	–
CaO	36.1	36.1	36.1	36.2	36.1	36.5	36.7	36.5	36.3	36.4
SO_3	–	–	–	–	–	–	–	–	–	–
Cl	–	–	–	–	–	–	–	–	–	–
H_2O^*	3.0	2.9	3.0	3.0	3.0	3.2	3.2	3.1	3.1	3.1
	99.1	98.8	99.2	99.2	99.0	99.8	100.1	100.0	99.0	99.1
O≡Cl	–	–	–	–	–	–	–	–	–	–
TOTAL	99.1	98.8	99.2	99.2	99.0	99.8	100.1	100.0	99.0	99.1
Si^{4+}	18.01	17.99	17.94	17.92	18.00	17.92	17.83	17.89	18.00	17.99
Al^{3+}	9.97	10.11	10.17	10.07	10.08	9.93	9.93	10.02	9.88	9.99
Ti^{4+}	0.07	0.11	–	0.11	0.07	–	–	–	–	–
Mg^{2+}	1.03	0.96	1.17	1.10	1.10	1.52	1.73	1.38	1.54	1.39
Mn^{2+}	0.08	–	–	0.04	–	–	–	–	–	–
Fe^{2+}	1.81	1.77	1.76	1.72	1.73	1.59	1.46	1.71	1.52	1.52
Fe^{3+}	–	–	–	–	–	–	–	–	–	–
Cr^{3+}	–	–	–	–	–	–	–	–	–	–
Ca^{2+}	19.03	19.06	18.96	19.04	19.02	19.04	19.05	19.01	19.07	19.11
S^{6+}	–	–	–	–	–	–	–	–	–	–
Cl^-	–	–	–	–	–	–	–	–	–	–
OH^{-*}	9.87	9.69	9.95	9.88	9.78	10.24	10.41	10.21	10.13	10.03
O	68.13	68.31	68.05	68.12	68.22	67.76	67.59	67.79	67.87	67.97
					Statistics					
ΣX	19.03	19.06	18.96	19.04	19.02	19.04	19.05	19.01	19.07	19.11
ΣY	12.97	12.94	13.10	13.04	12.98	13.04	13.12	13.10	12.93	12.90
ΣZ	18.01	18.00	17.94	17.92	18.00	17.92	17.83	17.89	18.00	17.99

*Calculated for charge balance.

QUANTITATIVE EDS RESULTS (UM)

	$V3\text{-}1_M$	$V3\text{-}2_M$	$V3\text{-}3_M$	$V3\text{-}4_M$	$V3\text{-}5_M$	$V3\text{-}6_M$	$V3\text{-}7_M$	$V3\text{-}8_M$	$V3\text{-}9_M$	$V3\text{-}10_M$
SiO_2	36.9	36.8	36.7	36.9	36.7	37.1	36.6	36.9	36.7	36.9
Al_2O_3	16.6	16.8	16.2	17.0	16.5	16.7	16.6	16.4	17.1	16.3
TiO_2	–	–	–	–	–	–	–	–	–	–
MgO	4.0	4.0	4.0	3.8	4.0	3.8	4.0	4.2	4.1	4.0
MnO	–	–	–	–	–	–	–	–	–	–
FeO	0.2	0.2	0.2	0.1	0.2	0.2	0.2	0.2	0.2	0.3
Fe_2O_3	1.8	1.6	2.0	1.3	1.9	2.1	2.2	1.9	1.6	2.3
Cr_2O_3	–	–	–	–	–	–	–	–	–	–
CaO	37.1	37.3	37.2	37.2	37.0	37.1	36.9	37.2	37.0	37.1
SO_3	–	0.2	–	0.5	0.5	0.3	–	0.2	0.2	–
Cl	–	–	–	–	–	0.1	–	0.1	–	–
H_2O^*	3.2	3.1	3.3	2.8	2.9	2.9	3.2	3.1	3.1	3.2
	99.8	100.0	99.6	99.6	99.7	100.3	99.7	100.2	100.0	100.1
O≡Cl	–	–	–	–	–	0.0	–	0.0	–	–
TOTAL	99.8	100.0	99.6	99.6	99.7	100.3	99.7	100.2	100.0	100.1
Si^{4+}	17.79	17.71	17.77	17.82	17.76	17.85	17.68	17.75	17.65	17.77
Al^{3+}	9.43	9.53	9.24	9.68	9.41	9.47	9.45	9.30	9.69	9.25
Ti^{4+}	–	–	–	–	–	–	–	–	–	–
Mg^{2+}	2.88	2.87	2.89	2.74	2.88	2.72	2.88	3.01	2.94	2.87
Mn^{2+}	–	–	–	–	–	–	–	–	–	–
Fe^{2+}	0.08	0.08	0.08	0.04	0.08	0.08	0.08	0.08	0.08	0.12
Fe^{3+}	0.65	0.58	0.73	0.47	0.69	0.76	0.80	0.69	0.58	0.83
Cr^{3+}	–	–	–	–	–	–	–	–	–	–
Ca^{2+}	19.17	19.23	19.29	19.25	19.18	19.12	19.10	19.17	19.06	19.15
S^{6+}	–	0.07	–	0.18	0.18	0.11	–	0.07	0.07	–
Cl^-	–	–	–	–	–	0.08	–	0.08	–	–
OH^{-*}	10.33	10.04	10.50	9.12	9.30	19.35	10.38	10.00	10.00	10.37
O	67.67	67.96	67.50	68.88	68.70	68.57	67.62	67.92	68.00	67.63
					Statistics					
ΣX	19.17	19.23	19.29	19.25	19.18	19.12	19.10	19.17	19.06	19.15
ΣY	13.04	13.06	12.94	12.93	13.06	13.03	13.22	13.08	13.29	13.08
ΣZ	17.79	17.71	17.77	17.82	17.76	17.85	17.68	17.75	17.65	17.77

*Calculated for charge balance.

QUANTITATIVE EDS RESULTS (UM)

	V10-1_M	V10-2_M	V10-3_M	V10-4_M	V10-5_M	V12-1_M	V12-2_M	V12-3_M	V12-4_M	V12-5_M
SiO_2	37.0	36.9	36.7	36.5	36.7	37.4	37.0	37.3	37.0	37.1
Al_2O_3	18.2	17.9	18.3	17.5	17.9	18.9	18.6	18.6	18.7	18.8
TiO_2	–	–	–	0.1	–	–	–	–	–	–
MgO	2.2	2.3	2.1	2.3	2.2	2.8	2.4	2.4	2.6	2.5
MnO	0.4	0.4	0.5	0.3	0.5	–	–	0.2	0.2	–
FeO	2.2	2.3	2.2	2.4	2.6	1.0	1.2	1.4	1.3	0.9
Fe_2O_3	–	–	–	–	–	–	–	–	–	–
Cr_2O_3	–	–	–	–	–	–	–	–	–	–
CaO	36.6	36.6	36.6	36.4	36.6	37.0	37.1	37.2	37.1	37.2
SO_3	–	–	–	–	–	–	–	–	–	–
Cl	–	–	–	–	–	–	–	–	–	–
H_2O^*	3.0	3.1	3.0	3.0	3.1	3.0	3.0	3.0	3.1	2.9
	99.6	99.5	99.4	98.5	99.6	100.1	99.3	100.1	100.0	99.4
O≡Cl	–	–	–	–	–	–	–	–	–	–
TOTAL	99.6	99.5	99.4	98.5	99.6	100.1	99.3	100.1	100.0	99.4
Si^{4+}	17.94	17.93	17.84	17.91	17.84	17.92	17.92	17.93	17.80	17.91
Al^{3+}	10.40	10.25	10.48	10.12	10.25	10.68	10.62	10.54	10.60	10.69
Ti^{4+}	–	–	–	0.04	–	–	–	–	–	–
Mg^{2+}	1.59	1.67	1.52	1.68	1.59	2.00	1.73	1.72	1.86	1.80
Mn^{2+}	0.16	0.16	0.21	0.12	0.21	–	–	0.08	0.08	–
Fe^{2+}	0.89	0.93	0.89	0.98	1.06	0.40	0.49	0.56	0.52	0.36
Fe^{3+}	–	–	–	–	–	–	–	–	–	–
Cr^{3+}	–	–	–	–	–	–	–	–	–	–
Ca^{2+}	19.01	19.05	19.06	19.14	19.06	19.00	19.25	19.16	19.12	19.24
S^{6+}	–	–	–	–	–	–	–	–	–	–
Cl^-	–	–	–	–	–	–	–	–	–	–
OH^{-*}	9.72	9.89	9.84	9.98	10.08	9.48	9.55	9.59	9.79	9.49
O	68.28	68.11	68.16	68.02	67.92	68.52	68.45	68.41	68.21	68.51
				Statistics						
ΣX	19.01	19.05	19.06	19.14	19.06	19.00	19.25	19.16	19.12	19.24
ΣY	13.05	13.02	13.10	12.95	13.10	13.08	12.83	12.91	13.08	12.85
ΣZ	17.94	17.93	17.84	17.91	17.84	17.92	17.92	17.93	17.80	17.91

*Calculated for charge balance.

QUANTITATIVE EDS RESULTS (UM)

	$V12\text{-}6_M$	$V12\text{-}7_M$	$V12\text{-}8_M$	$V12\text{-}9_M$	$V12\text{-}10_M$	$V12\text{-}11_M$	$V12\text{-}12_M$	$V12\text{-}13_M$	$V12\text{-}14_M$	$V12\text{-}15_M$
SiO_2	37.1	37.2	37.2	37.2	37.1	37.0	37.3	37.2	37.5	37.4
Al_2O_3	19.2	19.0	18.8	18.7	18.6	19.1	18.9	19.1	19.1	18.6
TiO_2	–	–	–	–	–	–	–	–	–	–
MgO	2.5	2.6	2.6	2.6	2.5	2.4	2.5	2.6	2.7	2.7
MnO	–	–	–	–	0.1	–	–	–	–	–
FeO	0.9	0.9	1.1	1.2	1.1	1.1	0.9	1.0	0.8	1.0
Fe_2O_3	–	–	–	–	–	–	–	–	–	–
Cr_2O_3	–	–	–	–	–	–	–	–	–	–
CaO	37.0	37.1	37.1	37.3	37.2	37.1	37.3	37.2	37.3	37.4
SO_3	–	–	–	–	–	–	–	–	–	–
Cl	–	–	–	–	–	–	–	–	–	–
H_2O^*	2.9	2.9	3.0	3.0	3.0	3.0	2.9	3.0	3.0	3.0
	99.6	99.7	99.8	100.0	99.6	99.7	99.8	100.1	100.4	100.1
$O \equiv Cl$	–	–	–	–	–	–	–	–	–	–
TOTAL	99.6	99.7	99.8	100.0	99.6	99.7	99.8	100.1	100.4	100.1
Si^{4+}	17.86	17.89	17.90	17.87	17.90	17.83	17.93	17.84	17.91	17.94
Al^{3+}	10.89	10.77	10.66	10.59	10.58	10.85	10.71	10.79	10.75	10.51
Ti^{4+}	–	–	–	–	–	–	–	–	–	–
Mg^{2+}	1.79	1.86	1.87	1.86	1.80	1.72	1.79	1.86	1.92	1.93
Mn^{2+}	–	–	–	–	0.04	–	–	–	–	–
Fe^{2+}	0.36	0.36	0.44	0.48	0.44	0.44	0.36	0.40	0.32	0.40
Fe^{3+}	–	–	–	–	–	–	–	–	–	–
Cr^{3+}	–	–	–	–	–	–	–	–	–	–
Ca^{2+}	19.09	19.12	19.13	19.20	19.23	19.15	19.21	19.11	19.09	19.22
S^{6+}	–	–	–	–	–	–	–	–	–	–
Cl^-	–	–	–	–	–	–	–	–	–	–
OH^{-*}	9.38	9.45	9.54	9.67	9.61	9.49	9.43	9.53	9.42	9.61
O	68.62	68.55	68.46	68.33	68.39	68.51	68.57	68.47	68.58	68.39
					Statistics					
ΣX	19.09	19.12	19.13	19.20	19.23	19.15	19.21	19.11	19.09	19.22
ΣY	13.05	12.99	12.97	12.93	12.87	13.02	12.86	13.05	13.00	12.84
ΣZ	17.86	17.89	17.90	17.87	17.90	17.83	17.93	17.84	17.91	17.94

*Calculated for charge balance.

QUANTITATIVE EDS RESULTS (UM)

	$V14\text{-}1_M$	$V14\text{-}2_M$	$V14\text{-}3_M$	$V14\text{-}4_M$	$V14\text{-}5_M$	$V14\text{-}6_M$	$V14\text{-}7_M$	$V14\text{-}8_M$	$V14\text{-}9_M$	$V14\text{-}10_M$
SiO_2	37.4	37.3	37.3	37.1	37.2	37.0	37.3	37.4	37.2	37.2
Al_2O_3	18.5	18.6	18.5	18.8	18.5	19.0	18.6	18.4	18.4	19.1
TiO_2	–	–	–	–	–	–	–	–	–	–
MgO	2.8	2.6	2.8	2.8	2.7	2.6	2.6	2.7	2.6	2.5
MnO	–	–	–	–	–	–	–	–	–	–
FeO	0.2	0.2	0.2	0.2	0.2	0.2	0.2	0.3	0.3	0.2
Fe_2O_3	1.2	1.1	1.1	0.8	1.2	0.9	1.2	1.3	1.3	0.8
Cr_2O_3	–	–	–	–	–	–	–	–	–	–
CaO	37.3	37.0	37.2	37.5	37.3	37.5	37.2	37.2	37.1	37.1
SO_3	–	–	–	–	–	–	–	–	–	–
Cl	–	–	–	–	–	–	–	–	–	–
H_2O^*	2.9	2.8	2.9	3.0	2.9	3.0	2.9	2.9	2.9	2.8
	100.3	99.6	100.0	100.2	100.0	100.2	100.0	100.2	99.8	99.7
$O \equiv Cl$	–	–	–	–	–	–	–	–	–	–
TOTAL	100.3	99.6	100.0	100.2	100.0	100.2	100.0	100.2	99.8	99.7
Si^{4+}	17.91	17.98	17.91	17.77	17.87	17.74	17.93	17.95	17.93	17.89
Al^{3+}	10.44	10.57	10.47	10.61	10.48	10.74	10.54	10.41	10.45	10.83
Ti^{4+}	–	–	–	–	–	–	–	–	–	–
Mg^{2+}	2.00	1.87	2.00	2.00	1.93	1.86	1.86	1.93	1.87	1.79
Mn^{2+}	–	–	–	–	–	–	–	–	–	–
Fe^{2+}	0.08	0.08	0.08	0.08	0.08	0.08	0.08	0.12	0.12	0.08
Fe^{3+}	0.43	0.40	0.40	0.29	0.43	0.32	0.43	0.47	0.47	0.29
Cr^{3+}	–	–	–	–	–	–	–	–	–	–
Ca^{2+}	19.14	19.11	19.14	19.25	19.20	19.26	19.16	19.13	19.16	19.12
S^{6+}	–	–	–	–	–	–	–	–	–	–
Cl^-	–	–	–	–	–	–	–	–	–	–
OH^{-*}	9.31	9.08	9.31	9.56	9.34	9.46	9.17	9.23	9.22	9.10
O	68.69	68.92	68.69	68.44	68.66	68.54	68.83	68.77	68.78	68.90
				Statistics						
ΣX	19.14	19.11	19.14	19.25	19.20	19.26	19.16	19.13	19.16	19.12
ΣY	12.95	12.91	12.95	12.98	12.93	13.00	12.91	12.92	12.91	12.99
ΣZ	17.91	17.98	17.91	17.77	17.87	17.74	17.93	17.95	17.93	17.89

*Calculated for charge balance.

QUANTITATIVE EDS RESULTS (UM)

	$V14\text{-}11_M$	$V14\text{-}12_M$	$V14\text{-}13_M$	$V16\text{-}1_M$	$V16\text{-}2_M$	$V16\text{-}3_M$	$V16\text{-}4_M$	$V16\text{-}5_M$	$V41\text{-}1_M$	$V41\text{-}2_M$
SiO_2	37.2	37.3	37.2	36.6	36.6	36.7	36.8	36.4	36.6	36.5
Al_2O_3	19.1	18.8	18.7	17.4	17.3	17.6	17.3	17.4	15.4	15.0
TiO_2	–	–	–	–	–	–	–	–	–	–
MgO	2.6	2.8	2.6	2.2	2.2	2.2	2.2	2.4	2.9	3.1
MnO	–	–	–	0.4	0.3	0.3	0.3	0.3	–	–
FeO	0.2	0.1	0.2	2.9	2.6	2.7	2.7	2.7	4.3	4.8
Fe_2O_3	0.9	0.7	0.9	–	–	–	–	–	–	–
Cr_2O_3	–	–	–	–	–	–	–	–	–	–
CaO	37.4	37.2	37.2	37.0	36.7	37.0	37.0	36.6	36.6	37.0
SO_3	–	–	–	–	–	–	–	–	–	–
Cl	–	–	–	–	–	–	–	–	–	–
H_2O^*	2.9	2.9	2.9	3.2	3.1	3.2	3.1	3.2	3.4	3.6
	100.3	99.8	99.7	99.7	98.8	99.7	99.4	99.0	99.2	100.0
$O \equiv Cl$	–	–	–	–	–	–	–	–	–	–
TOTAL	100.3	99.8	99.7	99.7	98.8	99.7	99.4	99.0	99.2	100.0
Si^{4+}	17.80	17.92	17.92	17.80	17.94	17.84	17.93	17.81	17.96	17.81
Al^{3+}	10.77	10.64	10.61	9.97	9.99	10.08	9.93	10.03	8.91	8.63
Ti^{4+}	–	–	–	–	–	–	–	–	–	–
Mg^{2+}	1.85	2.00	1.87	1.60	1.61	1.59	1.60	1.75	2.12	2.26
Mn^{2+}	–	–	–	0.16	0.12	0.12	0.12	0.12	–	–
Fe^{2+}	0.08	0.04	0.08	1.18	1.07	1.10	1.10	1.10	1.76	1.96
Fe^{3+}	0.32	0.25	0.33	–	–	–	–	–	–	–
Cr^{3+}	–	–	–	–	–	–	–	–	–	–
Ca^{2+}	19.17	19.14	19.20	19.28	19.27	19.27	19.31	19.18	19.24	19.35
S^{6+}	–	–	–	–	–	–	–	–	–	–
Cl^-	–	–	–	–	–	–	–	–	–	–
OH^{-*}	9.31	9.27	9.23	10.42	10.13	10.25	10.21	10.36	11.17	11.75
O	68.69	68.73	68.77	67.58	67.87	67.75	67.79	67.64	66.83	66.25
				Statistics						
ΣX	19.17	19.14	19.20	19.28	19.27	19.27	19.31	19.18	19.24	19.35
ΣY	13.03	12.94	12.88	12.92	12.79	12.89	12.76	13.01	12.80	12.84
ΣZ	17.80	17.92	17.92	17.80	17.94	17.84	17.93	17.81	17.96	17.81

*Calculated for charge balance.

QUANTITATIVE EDS RESULTS (UM)

	$V41\text{-}3_M$	$V41\text{-}4_M$	$V41\text{-}5_M$	$V54\text{-}1_M$	$V54\text{-}2_M$	$V54\text{-}3_M$	$V54\text{-}4_M$	$V54\text{-}5_M$	$V58\text{-}1_M$	$V58\text{-}2_M$
SiO_2	36.7	36.7	36.6	36.4	36.0	36.5	36.4	36.1	37.0	37.1
Al_2O_3	15.6	14.8	15.1	16.2	16.5	16.4	16.2	16.4	18.7	18.9
TiO_2	–	–	–	0.4	0.4	0.6	0.7	0.5	–	–
MgO	3.1	3.1	3.0	3.0	3.1	3.1	3.4	3.1	2.8	2.8
MnO	–	–	–	–	–	–	–	–	–	–
FeO	4.5	5.1	4.7	4.3	3.8	4.1	4.1	3.8	0.1	0.1
Fe_2O_3	–	–	–	–	–	–	–	–	1.1	1.1
Cr_2O_3	–	–	–	–	–	–	–	–	–	–
CaO	36.9	36.6	36.7	36.8	36.4	36.3	36.5	36.4	37.1	36.9
SO_3	–	–	–	–	–	–	–	–	–	–
Cl	–	–	–	–	–	–	–	–	–	–
H_2O^*	3.5	3.5	3.5	3.5	3.4	3.4	3.5	3.4	2.9	2.9
	100.3	99.8	99.6	100.6	99.6	100.4	100.8	99.7	99.7	99.8
$O\equiv Cl$	–	–	–	–	–	–	–	–	–	–
TOTAL	100.3	99.8	99.6	100.6	99.6	100.4	100.8	99.7	99.7	99.8
Si^{4+}	17.81	17.95	17.92	17.62	17.55	17.68	17.56	17.59	17.81	17.84
Al^{3+}	8.92	8.53	8.71	9.24	9.48	9.36	9.21	9.42	10.61	10.71
Ti^{4+}	–	–	–	0.15	0.15	0.22	0.25	0.18	–	–
Mg^{2+}	2.24	2.26	2.19	2.16	2.25	2.24	2.45	2.25	2.01	2.01
Mn^{2+}	–	–	–	–	–	–	–	–	–	–
Fe^{2+}	1.83	2.09	1.92	1.74	1.55	1.66	1.65	1.55	0.04	0.04
Fe^{3+}	–	–	–	–	–	–	–	–	0.40	0.40
Cr^{3+}	–	–	–	–	–	–	–	–	–	–
Ca^{2+}	19.19	19.18	19.25	19.09	19.02	18.84	18.87	19.00	19.13	19.01
S^{6+}	–	–	–	–	–	–	–	–	–	–
Cl^-	–	–	–	–	–	–	–	–	–	–
OH^{-*}	11.45	11.58	11.45	11.23	11.12	10.84	11.15	11.03	9.37	9.22
O	66.55	66.42	66.55	66.77	66.88	67.16	66.85	66.97	68.63	68.78
				Statistics						
ΣX	19.19	19.18	19.25	19.09	19.02	18.84	18.87	19.00	19.13	19.01
ΣY	13.00	12.87	12.83	13.29	13.43	13.48	13.57	13.41	13.06	13.15
ΣZ	17.81	17.95	17.92	17.62	17.55	17.68	17.56	17.59	17.81	17.84

*Calculated for charge balance.

QUANTITATIVE EDS RESULTS (UM)

	$V58\text{-}3_M$	$V58\text{-}4_M$	$V58\text{-}5_M$	$V59\text{-}1_M$	$V59\text{-}2_M$	$V59\text{-}3_M$	$V59\text{-}4_M$	$V59\text{-}5_M$	$V60\text{-}1_M$	$V60\text{-}2_M$
SiO_2	37.5	36.9	37.0	36.7	36.4	36.3	36.7	36.5	35.8	36.2
Al_2O_3	19.2	18.3	18.5	18.2	18.1	17.7	18.1	18.0	16.6	16.8
TiO_2	–	–	–	–	–	–	–	–	–	–
MgO	2.7	2.8	2.9	3.7	3.7	3.8	3.7	3.5	3.7	3.7
MnO	–	–	–	–	–	–	–	–	–	–
FeO	0.0	0.1	0.1	0.1	0.2	0.2	0.1	0.1	0.6	0.6
Fe_2O_3	0.7	1.7	0.9	0.9	1.2	1.5	0.9	0.9	3.1	3.1
Cr_2O_3	–	–	–	0.3	0.1	0.3	0.2	0.5	–	–
CaO	37.2	37.0	36.8	36.9	37.1	36.8	37.0	36.9	36.2	36.5
SO_3	–	–	–	–	–	0.2	–	–	–	0.3
Cl	–	–	–	–	–	–	–	–	–	–
H_2O^*	2.8	2.9	2.9	3.1	3.2	3.1	3.2	3.1	3.2	3.0
	100.1	99.7	99.1	99.9	100.0	99.9	99.9	99.5	99.2	100.2
$O\equiv Cl$	–	–	–	–	–	–	–	–	–	–
TOTAL	100.1	99.7	99.1	99.9	100.0	99.9	99.9	99.5	99.2	100.2
Si^{4+}	17.94	17.80	17.91	17.61	17.48	17.49	17.63	17.61	17.46	17.50
Al^{3+}	10.82	10.40	10.55	10.29	10.24	10.05	10.25	10.24	9.54	9.57
Ti^{4+}	–	–	–	–	–	–	–	–	–	–
Mg^{2+}	1.93	2.01	2.09	2.65	2.65	2.73	2.65	2.52	2.69	2.67
Mn^{2+}	–	–	–	–	–	–	–	–	–	–
Fe^{2+}	0.00	0.04	0.04	0.04	0.08	0.08	0.04	0.04	0.24	0.24
Fe^{3+}	0.25	0.62	0.33	0.32	0.43	0.54	0.33	0.33	1.14	1.13
Cr^{3+}	–	–	–	0.11	0.04	0.11	0.08	0.19	–	–
Ca^{2+}	19.06	19.12	19.08	18.97	19.08	18.99	19.04	19.08	18.92	18.90
S^{6+}	–	–	–	–	–	0.07	–	–	–	0.11
Cl^-	–	–	–	–	–	–	–	–	–	–
OH^{-*}	9.05	9.38	9.31	10.05	10.34	9.88	10.10	10.02	10.39	9.66
O	68.95	68.62	68.69	67.95	67.66	68.12	67.90	67.98	67.61	68.34
					Statistics					
ΣX	19.06	19.12	19.08	18.97	19.08	18.99	19.04	19.08	18.92	18.90
ΣY	13.00	13.08	13.01	13.42	13.44	13.52	13.33	13.31	13.62	13.60
ΣZ	17.94	17.80	17.91	17.61	17.48	17.49	17.63	17:61	17.46	17.50

*Calculated for charge balance.

QUANTITATIVE EDS RESULTS (UM)

	$V60\text{-}3_M$	$V60\text{-}4_M$	$V60\text{-}5_M$	$V68\text{-}1_M$	$V68\text{-}2_M$	$V68\text{-}3_M$	$V68\text{-}4_M$	$V68\text{-}5_M$	$V71\text{-}1_M$	$V71\text{-}2_M$
SiO_2	36.2	36.2	36.2	36.7	37.1	37.2	37.1	37.0	36.8	36.5
Al_2O_3	16.9	16.6	16.7	18.2	18.1	18.2	18.0	17.9	15.7	15.6
TiO_2	0.2	0.3	0.2	–	–	–	–	–	–	–
MgO	3.7	3.6	3.6	3.9	4.0	3.8	4.3	3.7	3.0	3.0
MnO	–	–	–	–	–	–	–	–	–	0.1
FeO	0.6	0.7	0.6	1.0	1.1	1.2	0.9	1.8	4.5	4.6
Fe_2O_3	3.2	3.3	3.2	–	–	–	–	–	–	–
Cr_2O_3	–	–	–	–	–	–	–	–	0.2	0.2
CaO	36.2	36.2	36.2	36.7	36.9	37.2	37.1	37.0	36.8	36.9
SO_3	0.2	0.2	0.2	–	–	0.2	–	–	–	–
Cl	–	–	–	–	–	–	–	–	–	–
H_2O^*	3.0	3.0	3.0	3.3	3.3	3.2	3.4	3.3	3.5	3.6
	100.2	100.1	99.9	99.8	100.5	101.0	100.8	100.7	100.5	100.5
$O \equiv Cl$	–	–	–	–	–	–	–	–	–	–
TOTAL	100.2	100.1	99.9	99.8	100.5	101.0	100.8	100.7	100.5	100.5
Si^{4+}	17.49	17.54	17.56	17.62	17.69	17.68	17.63	17.66	17.84	17.72
Al^{3+}	9.62	9.48	9.55	10.30	10.17	10.20	10.08	10.07	8.97	8.93
Ti^{4+}	0.07	0.11	0.07	–	–	–	–	–	–	–
Mg^{2+}	2.67	2.60	2.60	2.79	2.84	2.69	3.05	2.63	2.17	2.17
Mn^{2+}	–	–	–	–	–	–	–	–	–	0.04
Fe^{2+}	0.24	0.28	0.24	0.40	0.44	0.48	0.36	0.72	1.82	1.87
Fe^{3+}	1.16	1.20	1.17	–	–	–	–	–	–	–
Cr^{3+}	–	–	–	–	–	–	–	–	0.08	0.08
Ca^{2+}	18.74	18.79	18.81	18.88	18.85	18.95	18.89	18.92	19.12	19.19
S^{6+}	0.07	0.07	0.07	–	–	0.07	–	–	–	–
Cl^-	–	–	–	–	–	–	–	–	–	–
OH^{-*}	9.65	9.59	9.59	10.45	10.44	10.01	10.66	10.61	11.27	11.55
O	68.35	68.41	68.41	67.55	67.56	67.99	67.34	67.39	66.73	66.45
				Statistics						
ΣX	18.74	18.79	18.81	18.88	18.85	18.95	18.89	18.92	19.12	19.19
ΣY	13.77	13.67	13.63	13.50	13.46	13.37	13.48	13.42	13.04	13.09
ΣZ	17.49	17.54	17.56	17.62	17.69	17.68	17.63	17.66	17.84	17.72

*Calculated for charge balance.

QUANTITATIVE EDS RESULTS (UM)

	$V71\text{-}3_M$	$V71\text{-}4_M$	$V71\text{-}5_M$	$V75\text{-}1_M$	$V75\text{-}2_M$	$V75\text{-}3_M$	$V75\text{-}4_M$	$V75\text{-}5_M$	$V75\text{-}6_M$	$V75\text{-}7_M$
SiO_2	36.6	36.7	36.9	36.7	37.5	37.2	37.4	37.2	36.4	36.6
Al_2O_3	15.5	15.2	15.4	18.6	18.7	18.7	18.7	18.7	17.4	18.1
TiO_2	–	–	–	–	–	–	–	–	0.2	–
MgO	3.0	2.8	3.0	3.1	2.9	3.2	3.2	3.4	3.1	3.3
MnO	–	–	–	–	–	–	–	–	–	–
FeO	4.4	4.7	4.6	0.1	0.2	0.1	0.2	0.2	0.4	0.2
Fe_2O_3	–	–	–	0.7	1.0	0.6	0.8	0.8	1.9	1.1
Cr_2O_3	0.1	0.2	–	–	–	–	–	–	0.5	–
CaO	36.8	36.7	37.0	37.2	36.9	37.4	37.6	37.3	36.8	37.0
SO_3	–	–	–	–	–	–	–	–	–	–
Cl	–	–	–	–	–	–	–	–	–	–
H_2O^*	3.5	3.4	3.5	3.0	2.9	3.0	3.1	3.1	3.0	3.1
	99.9	99.7	100.4	99.4	100.1	100.2	101.0	100.7	99.7	99.4
$O \equiv Cl$	–	–	–	–	–	–	–	–	–	–
TOTAL	99.9	99.7	100.4	99.4	100.1	100.2	101.0	100.7	99.7	99.4
Si^{4+}	17.85	17.96	17.91	17.69	17.97	17.78	17.76	17.71	17.62	17.68
Al^{3+}	8.91	8.76	8.81	10.57	10.56	10.53	10.47	10.49	9.93	10.31
Ti^{4+}	–	–	–	–	–	–	–	–	0.07	–
Mg^{2+}	2.18	2.04	2.17	2.23	2.07	2.28	2.27	2.41	2.24	2.38
Mn^{2+}	–	–	–	–	–	–	–	–	–	–
Fe^{2+}	1.79	1.92	1.87	0.04	0.08	0.04	0.08	0.08	0.16	0.08
Fe^{3+}	–	–	–	0.25	0.36	0.22	0.29	0.29	0.69	0.40
Cr^{3+}	0.04	0.08	–	–	–	–	–	–	0.19	–
Ca^{2+}	19.23	19.24	19.24	19.22	18.95	19.15	19.14	19.02	19.09	19.15
S^{6+}	–	–	–	–	–	–	–	–	–	–
Cl^-	–	–	–	–	–	–	–	–	–	–
OH^{-*}	11.36	11.25	11.37	9.79	9.13	9.69	9.72	9.81	9.79	9.93
O	66.64	66.75	66.63	68.21	68.87	68.31	68.28	68.19	68.21	68.07
				Statistics						
ΣX	19.23	19.24	19.24	19.22	18.95	19.15	19.14	19.02	19.09	19.15
ΣY	12.92	12.80	12.85	13.09	13.08	13.07	13.10	13.27	13.29	13.17
ΣZ	17.85	17.96	17.91	17.69	17.97	17.78	17.76	17.71	17.62	17.68

*Calculated for charge balance.

QUANTITATIVE EDS RESULTS (UM)

	$V75\text{-}8_M$
SiO_2	37.2
Al_2O_3	18.7
TiO_2	–
MgO	3.5
MnO	–
FeO	0.1
Fe_2O_3	0.7
Cr_2O_3	–
CaO	37.2
SO_3	–
Cl	–
H_2O^*	3.1
	100.5
$O \equiv Cl$	–
TOTAL	100.5
Si^{4+}	17.73
Al^{3+}	10.50
Ti^{4+}	–
Mg^{2+}	2.49
Mn^{2+}	–
Fe^{2+}	0.04
Fe^{3+}	0.25
Cr^{3+}	–
Ca^{2+}	18.99
S^{6+}	–
Cl^-	–
OH^{-*}	9.79
O	68.21
ΣX	18.99
ΣY	13.28
ΣZ	17.73

*Calculated for charge balance.

Appendix E.1

WDS ANALYSES OF VESUVIANITE (NMNS)

Oxide Percents

ABBREVIATIONS USED IN APPENDIX E.1

(c): centre of grain
(r): rim of grain
(i): intermediate between core and rim
(d): dark in BSE image
(l): light in BSE image

Subscripted numbers refer to different grains. Fe_2O_3 values are derived from total Fe (by WDS) and bulk Fe^{2+} (by wet chemistry).

QUANTITATIVE WDS RESULTS (NMNS)

Oxide Percents

	V1-1_1	V1-2_2	V1-3_2	V1-4_2	V1-5_3	V1-6_4	V1-7_4	V2-1_c	V2-2_r	V3-1
SiO_2	36.98	36.61	36.98	36.69	37.12	37.15	37.04	37.09	37.07	37.33
Al_2O_3	17.04	16.31	17.14	16.50	16.41	16.39	16.63	17.48	16.83	16.42
TiO_2	0.14	0.17	0.28	0.11	0.18	0.16	0.13	0.54	0.71	0.00
MgO	1.98	2.36	1.27	2.32	2.33	2.40	2.39	1.48	1.72	3.87
MnO	0.11	0.00	0.19	0.00	0.00	0.08	0.06	0.36	0.35	0.06
FeO	3.64	4.12	4.25	3.99	4.01	3.85	3.87	3.18	3.49	0.21
Fe_2O_3	–	–	–	–	–	–	–	0.81	0.89	1.58
Cr_2O_3	–	–	–	–	–	–	–	–	–	0.00
CuO	–	–	–	–	–	–	–	–	–	–
ZnO	0.00	0.00	0.00	0.00	0.00	0.00	0.00	0.00	0.00	0.00
CaO	36.09	36.01	36.56	36.18	36.65	36.35	37.05	35.46	35.54	36.46
Na_2O	0.00	0.00	0.00	0.00	0.00	0.00	0.00	0.13	0.06	0.00
K_2O	0.00	0.00	0.00	0.00	0.00	0.00	0.00	0.00	0.00	–
La_2O_3	–	–	–	–	–	–	–	–	–	–
Ce_2O_3	0.00	0.00	0.00	0.00	0.00	0.00	0.00	–	–	0.00
Pr_2O_3	–	–	–	–	–	–	–	–	–	–
Nd_2O_3	–	–	–	–	–	–	–	–	–	–
Sm_2O_3	–	–	–	–	–	–	–	–	–	–
Eu_2O_3	–	–	–	–	–	–	–	–	–	–
Gd_2O_3	–	–	–	–	–	–	–	–	–	–
PbO	–	–	–	–	–	–	–	–	–	–
Bi_2O_3	–	–	–	–	–	–	–	–	–	–
ThO_2	–	–	–	–	–	–	–	–	–	–
UO_2	–	–	–	–	–	–	–	–	–	–
B_2O_3	–	–	–	–	–	–	–	0.00	–	–
SO_3	0.00	0.00	0.00	0.00	0.00	0.00	0.00	0.00	0.11	0.19
F	0.00	0.00	0.00	0.00	0.00	0.00	0.00	3.04	2.99	0.00
Cl	0.00	0.00	0.05	0.00	0.00	0.00	0.00	0.00	0.00	0.07
H_2O^*	2.98	3.15	2.96	3.15	3.17	3.12	3.27	1.32	1.32	2.86
	98.96	98.73	99.68	98.94	99.87	99.50	100.44	100.89	101.08	99.06
O≡F	–	–	–	–	–	–	–	1.28	1.26	–
O≡Cl	–	–	0.01	–	–	–	–	–	–	0.02
TOTAL	98.96	98.73	99.67	98.94	99.87	99.50	100.44	99.61	99.82	99.04

*Calculated for charge balance.

V2 includes 0.02 Li_2O, 0.11 BeO.

QUANTITATIVE WDS RESULTS (NMNS)

Oxide Percents

	V3-2	V3-3	V3-4	V3-5	V4-1_r	V4-2_r	V4-3_r	V4-4	V4-5	V4-6
SiO_2	36.84	37.02	37.05	36.98	35.97	35.96	36.19	36.17	35.97	35.77
Al_2O_3	16.38	16.21	15.89	16.44	14.52	14.26	14.50	14.61	14.55	14.33
TiO_2	0.00	0.00	0.00	0.00	1.46	1.66	1.37	1.20	1.21	1.61
MgO	3.89	3.90	4.00	3.77	1.72	1.67	1.88	1.82	1.87	1.77
MnO	0.07	0.00	0.00	0.00	0.32	0.36	0.36	0.32	0.33	0.33
FeO	0.20	0.20	0.24	0.19	2.72	2.91	2.70	2.72	2.73	2.78
Fe_2O_3	1.52	1.47	1.78	1.41	3.49	3.73	3.47	3.49	3.51	3.57
Cr_2O_3	0.00	0.00	0.00	0.00	–	–	–	–	–	–
CuO	–	–	–	–	–	–	–	–	–	–
ZnO	0.00	0.00	0.00	0.00	0.00	0.00	0.00	0.00	0.00	0.00
CaO	37.91	36.17	38.00	36.86	34.86	34.49	34.98	35.05	34.81	34.61
Na_2O	0.00	0.00	0.00	0.00	0.09	0.11	0.08	0.08	0.08	0.08
K_2O	–	–	–	–	0.00	0.00	0.00	0.00	0.00	0.00
La_2O_3	–	–	–	–	0.00	0.10	0.00	0.00	0.00	0.13
Ce_2O_3	0.00	0.00	0.00	0.00	0.09	0.17	0.00	0.00	0.00	0.27
Pr_2O_3	–	–	–	–	0.00	0.00	0.00	0.00	0.00	0.00
Nd_2O_3	–	–	–	–	0.00	0.00	0.00	0.00	0.00	0.16
Sm_2O_3	–	–	–	–	0.00	0.00	0.00	0.00	0.00	0.00
Eu_2O_3	–	–	–	–	0.00	0.00	0.00	0.00	0.00	0.00
Gd_2O_3	–	–	–	–	0.00	0.00	0.00	0.00	0.00	0.00
PbO	–	–	–	–	–	–	–	–	–	–
Bi_2O_3	–	–	–	–	–	–	–	–	–	–
ThO_2	–	–	–	–	–	–	–	–	–	–
UO_2	–	–	–	–	–	–	–	–	–	–
B_2O_3	–	0.00	–	–	–	–	–	–	0.00	–
SO_3	0.25	0.35	0.12	0.25	0.00	0.00	0.00	0.00	0.00	0.00
F	0.00	0.00	0.00	0.00	2.00	2.35	2.16	2.13	1.98	2.31
Cl	0.00	0.00	0.00	0.00	0.24	0.21	0.18	0.17	0.20	0.21
H_2O*	3.17	2.75	3.26	2.92	1.64	1.43	1.62	1.65	1.71	1.48
	100.23	98.07	100.34	98.82	99.11	99.41	99.49	99.42	98.95	99.41
O≡F	–	–	–	–	0.84	0.99	0.91	0.90	0.83	0.97
O≡Cl	–	–	–	–	0.05	0.05	0.04	0.04	0.05	0.05
TOTAL	100.23	98.07	100.34	98.82	98.22	98.37	98.54	98.48	98.07	98.39

*Calculated for charge balance.

V4 includes 0.03 Li_2O, 0.02 BeO.

QUANTITATIVE WDS RESULTS (NMNS)

Oxide Percents

	V4-7	V4-8	V4-9	V5-1	V5-2	V5-3	V5-4	V5-5	V5-6	V5-7
SiO_2	36.37	36.35	36.22	36.31	36.78	36.53	36.45	36.38	36.49	36.70
Al_2O_3	15.33	15.52	15.44	16.81	16.78	17.14	16.96	16.95	16.80	16.94
TiO_2	1.34	1.36	1.34	0.91	0.96	0.65	0.73	0.72	0.75	0.84
MgO	1.59	1.54	1.56	1.71	1.69	1.59	1.63	1.65	1.63	1.63
MnO	0.31	0.31	0.33	0.35	0.38	0.31	0.33	0.32	0.32	0.37
FeO	2.41	2.39	2.43	2.93	2.87	2.95	2.90	3.00	2.94	2.99
Fe_2O_3	3.09	3.07	3.12	1.20	1.18	1.21	1.19	1.23	1.21	1.23
Cr_2O_3	–	–	–	–	–	–	–	–	–	–
CuO	–	–	–	–	–	–	–	–	–	–
ZnO	0.00	0.00	0.00	0.00	0.11	0.00	0.00	0.00	0.00	0.00
CaO	35.26	34.43	34.84	35.33	35.29	35.27	34.91	35.21	35.00	35.19
Na_2O	0.13	0.14	0.14	0.07	0.06	0.04	0.04	0.00	0.05	0.05
K_2O	0.00	0.00	0.00	0.00	0.00	0.00	0.00	0.00	0.00	0.00
La_2O_3	0.00	0.00	0.00	–	–	–	–	–	–	–
Ce_2O_3	0.08	0.00	0.00	0.00	0.00	0.00	0.00	0.00	0.00	0.00
Pr_2O_3	0.00	0.00	0.00	–	–	–	–	–	–	–
Nd_2O_3	0.00	0.00	0.00	–	–	–	–	–	–	–
Sm_2O_3	0.00	0.00	0.00	–	–	–	–	–	–	–
Eu_2O_3	0.00	0.00	0.00	–	–	–	–	–	–	–
Gd_2O_3	0.00	0.00	0.00	–	–	–	–	–	–	–
PbO	–	–	–	–	–	–	–	–	–	–
Bi_2O_3	–	–	–	–	–	–	–	–	–	–
ThO_2	–	–	–	–	–	–	–	–	–	–
UO_2	–	–	–	–	–	–	–	–	–	–
B_2O_3	–	–	–	–	–	–	–	–	–	0.00
SO_3	0.00	0.00	0.00	0.09	0.00	0.00	0.00	0.00	0.00	0.00
F	2.44	2.21	2.39	2.71	2.49	2.38	2.42	2.57	2.46	2.50
Cl	0.19	0.15	0.18	0.09	0.09	0.09	0.08	0.06	0.08	0.09
H_2O^*	1.44	1.40	1.41	1.41	1.50	1.57	1.49	1.49	1.49	1.48
	99.97	98.87	99.41	99.92	100.18	99.73	99.14	99.57	99.23	100.01
O≡F	1.03	0.93	1.01	1.14	1.05	1.00	1.02	1.08	1.04	1.05
O≡Cl	0.04	0.03	0.04	0.02	0.02	0.02	0.02	0.01	0.02	0.02
TOTAL	98.90	97.91	98.36	98.76	99.11	98.71	98.10	98.48	98.17	98.94

*Calculated for charge balance.

V4 includes 0.03 Li_2O, 0.02 BeO.

QUANTITATIVE WDS RESULTS (NMNS)

Oxide Percents

	V5-8	V6-1	V6-2	V6-3	V6-4	V6-5	V6-6	V7-1	V7-2	V7-3
SiO_2	36.56	36.24	34.85	36.05	36.02	36.10	36.23	36.91	36.76	36.48
Al_2O_3	16.59	16.11	15.16	15.99	16.12	16.06	16.00	15.19	15.15	15.33
TiO_2	0.82	0.82	1.97	1.26	0.83	0.86	1.12	4.49	4.67	4.49
MgO	1.68	2.78	2.55	2.63	2.78	2.84	2.74	1.28	1.26	1.28
MnO	0.36	0.78	0.77	0.75	0.77	0.79	0.80	0.00	0.00	0.00
FeO	3.11	1.70	2.47	1.77	1.78	1.81	1.93	3.14	3.19	3.14
Fe_2O_3	1.28	–	–	–	–	–	–	–	–	–
Cr_2O_3	–	–	–	–	–	–	–	–	–	–
CuO	–	–	–	–	–	–	–	–	–	–
ZnO	0.00	0.00	0.00	0.00	0.00	0.00	0.00	0.00	0.00	0.00
CaO	34.86	34.13	32.65	34.93	34.48	34.51	34.90	33.55	34.09	33.50
Na_2O	0.04	0.00	0.17	0.00	0.00	0.00	0.00	0.87	0.88	0.88
K_2O	0.00	0.00	0.00	0.00	0.00	0.00	0.00	0.00	0.00	0.00
La_2O_3	–	0.29	0.37	0.32	0.27	0.29	0.20	–	–	–
Ce_2O_3	0.00	0.64	1.02	0.77	0.65	0.60	0.39	0.00	0.00	0.00
Pr_2O_3	–	0.00	0.00	0.00	0.00	0.00	0.00	–	–	–
Nd_2O_3	–	0.00	0.00	0.00	0.00	0.00	0.00	–	–	–
Sm_2O_3	–	0.00	0.00	0.00	0.00	0.00	0.00	–	–	–
Eu_2O_3	–	0.00	0.00	0.00	0.00	0.00	0.00	–	–	–
Gd_2O_3	–	0.00	0.00	0.00	0.00	0.00	0.00	–	–	–
PbO	–	–	–	–	–	–	–	–	–	–
Bi_2O_3	–	–	–	–	–	–	–	–	–	–
ThO_2	–	–	–	–	–	–	–	–	–	–
UO_2	–	–	–	–	–	–	–	–	–	–
B_2O_3	–	–	0.00	0.00	–	–	–	–	0.00	–
SO_3	0.00	0.00	0.27	0.21	0.00	0.00	0.00	0.00	0.00	0.00
F	2.30	2.65	2.20	2.32	2.53	2.43	2.51	0.00	0.00	0.00
Cl	0.06	0.71	1.18	0.77	0.75	0.71	0.73	0.00	0.00	0.00
H_2O^*	1.56	1.23	1.09	1.33	1.38	1.45	1.43	2.34	2.45	2.40
	99.22	98.09	96.72	99.09	98.37	98.45	98.97	97.77	98.45	97.50
$O \equiv F$	0.97	1.12	0.93	0.98	1.07	1.02	1.06	–	–	–
$O \equiv Cl$	0.01	0.16	0.27	0.17	0.17	0.16	0.16	–	–	–
TOTAL	98.24	96.81	95.52	97.94	97.13	97.27	97.75	97.77	98.45	97.50

*Calculated for charge balance.

QUANTITATIVE WDS RESULTS (NMNS)

Oxide Percents

	V7-4	V7-5	V7-6	V7-7	V8-1_{1c}	V8-2_{1r}	V8-3_{2d}	V8-4_{2l}	V9-1_1	V9-2_1
SiO_2	36.48	36.71	36.50	36.92	36.69	37.38	37.72	36.50	37.26	36.71
Al_2O_3	15.21	15.39	15.25	15.17	16.67	16.59	18.44	16.90	18.94	18.45
TiO_2	4.54	4.39	4.49	4.61	0.00	0.00	1.28	1.06	0.00	0.13
MgO	1.33	1.31	1.29	1.28	2.49	2.48	1.10	2.01	2.82	3.17
MnO	0.00	0.00	0.00	0.00	0.18	0.16	0.06	0.40	0.08	0.09
FeO	3.19	3.13	3.05	3.11	4.14	4.02	3.01	4.38	0.47	0.49
Fe_2O_3	–	–	–	–	–	–	–	–	–	–
Cr_2O_3	–	–	–	–	–	–	–	–	0.07	0.03
CuO	–	–	–	–	–	–	–	–	–	–
ZnO	0.00	0.00	0.00	0.00	0.00	0.00	0.00	0.00	0.00	0.00
CaO	33.82	33.57	33.64	33.86	36.42	36.12	35.77	34.23	37.06	36.39
Na_2O	0.86	0.86	0.87	0.88	0.00	0.00	0.10	0.05	0.00	0.00
K_2O	0.00	0.00	0.00	0.00	0.00	0.00	0.00	0.00	0.00	0.00
La_2O_3	–	–	–	–	–	–	–	–	–	–
Ce_2O_3	0.00	0.00	0.00	0.00	–	–	–	–	–	–
Pr_2O_3	–	–	–	–	–	–	–	–	–	–
Nd_2O_3	–	–	–	–	–	–	–	–	–	–
Sm_2O_3	–	–	–	–	–	–	–	–	–	–
Eu_2O_3	–	–	–	–	–	–	–	–	–	–
Gd_2O_3	–	–	–	–	–	–	–	–	–	–
PbO	–	–	–	–	–	–	–	–	–	–
Bi_2O_3	–	–	–	–	–	–	–	–	–	–
ThO_2	–	–	–	–	–	–	–	–	–	–
UO_2	–	–	–	–	–	–	–	–	–	–
B_2O_3	–	–	–	–	0.00	–	0.00	–	–	0.00
SO_3	0.00	0.12	0.00	0.00	0.00	0.00	0.00	0.00	0.00	0.00
F	0.00	0.00	0.00	0.00	0.00	0.00	1.81	2.65	0.00	0.00
Cl	0.00	0.00	0.00	0.00	0.00	0.00	0.00	0.07	0.00	0.00
H_2O^*	2.45	2.30	2.40	2.38	3.30	3.13	1.63	1.53	2.94	2.96
	97.88	97.78	97.49	98.21	99.89	99.88	100.92	99.79	99.64	98.42
O≡F	–	–	–	–	–	–	0.76	1.12	–	–
O≡Cl	–	–	–	–	–	–	–	0.02	–	–
TOTAL	97.88	97.78	97.49	98.21	99.89	99.88	100.16	98.65	99.64	98.42

*Calculated for charge balance.

QUANTITATIVE WDS RESULTS (NMNS)

Oxide Percents

	V9-3$_2$	V10-1	V10-2	V10-3	V11-1	V11-2	V11-3	V11-4	V11-5	V11-6
SiO_2	37.01	36.92	37.30	36.75	37.33	37.21	37.40	37.37	37.35	36.99
Al_2O_3	18.97	17.88	17.33	16.97	18.73	18.77	18.54	18.33	18.39	18.59
TiO_2	0.33	0.00	0.00	0.00	0.00	0.00	0.00	0.00	0.00	0.00
MgO	1.62	2.04	2.24	2.08	2.44	2.42	2.36	2.49	2.37	2.43
MnO	0.20	0.60	0.29	0.29	0.13	0.15	0.28	0.15	0.21	0.15
FeO	1.95	2.20	2.79	3.51	0.59	0.72	1.07	0.90	0.98	0.79
Fe_2O_3	–	–	–	–	–	–	–	–	–	–
Cr_2O_3	0.09	–	–	–	–	–	–	–	–	–
CuO	–	–	–	–	–	–	–	–	–	–
ZnO	0.00	0.00	0.00	0.00	0.00	0.00	0.00	0.00	0.00	0.00
CaO	36.70	37.06	36.24	36.33	36.91	36.46	36.59	35.92	36.60	36.38
Na_2O	0.00	0.00	0.00	0.00	0.00	0.00	0.00	0.00	0.00	0.00
K_2O	0.00	0.00	0.00	0.00	0.00	0.00	0.00	0.00	0.00	0.00
La_2O_3	–	–	–	–	–	–	–	–	–	–
Ce_2O_3	–	0.00	0.00	0.00	0.00	0.00	0.00	0.00	0.00	0.00
Pr_2O_3	–	–	–	–	–	–	–	–	–	–
Nd_2O_3	–	–	–	–	–	–	–	–	–	–
Sm_2O_3	–	–	–	–	–	–	–	–	–	–
Eu_2O_3	–	–	–	–	–	–	–	–	–	–
Gd_2O_3	–	–	–	–	–	–	–	–	–	–
PbO	–	–	–	–	–	–	–	–	–	–
Bi_2O_3	–	–	–	–	–	–	–	–	–	–
ThO_2	–	–	–	–	–	–	–	–	–	–
UO_2	–	–	–	–	–	–	–	–	–	–
B_2O_3	–	–	–	–	–	–	–	–	0.00	–
SO_3	0.00	0.00	0.00	0.00	0.00	0.00	0.00	0.00	0.00	0.00
F	0.00	0.00	0.00	0.00	0.00	0.00	0.00	0.00	0.00	0.00
Cl	0.00	0.00	0.00	0.00	0.00	0.00	0.00	0.00	0.00	0.00
H_2O*	2.80	3.08	2.96	3.10	2.82	2.78	2.82	2.69	2.81	2.80
	99.67	99.78	99.15	99.03	98.95	98.51	99.06	97.85	98.71	98.13
O≡F	–	–	–	–	–	–	–	–	–	–
O≡Cl	–	–	–	–	–	–	–	–	–	–
TOTAL	99.67	99.78	99.15	99.03	98.95	98.51	99.06	97.85	98.71	98.13

*Calculated for charge balance.

QUANTITATIVE WDS RESULTS (NMNS)

Oxide Percents

	V11-7	V11-8	V12-1	V12-2	V12-3	V13-1_1	V13-2_1	V13-3_1	V13-4_1	V13-5_1
SiO_2	37.20	37.38	37.38	37.39	37.40	36.69	36.81	36.86	36.35	37.03
Al_2O_3	18.93	18.25	18.63	18.55	18.78	16.91	17.44	17.60	17.29	17.04
TiO_2	0.00	0.00	0.05	0.07	0.00	0.43	0.92	0.72	0.99	0.52
MgO	2.49	2.18	2.59	2.62	2.60	2.27	2.02	1.96	1.86	2.17
MnO	0.08	0.26	0.07	0.00	0.08	0.09	0.10	0.00	0.08	0.06
FeO	0.68	1.19	0.91	0.90	0.99	1.45	1.17	1.28	1.28	1.42
Fe_2O_3	–	–	–	–	–	1.94	1.57	1.72	1.72	1.91
Cr_2O_3	–	–	–	–	–	–	–	–	–	–
CuO	–	–	–	–	–	–	–	–	–	–
ZnO	0.00	0.00	0.00	0.00	0.00	0.00	0.00	0.00	0.00	0.00
CaO	36.12	36.09	37.01	37.55	36.94	36.38	36.22	37.14	36.13	36.70
Na_2O	0.00	0.00	0.00	0.00	0.00	0.00	0.00	0.00	0.00	0.00
K_2O	0.00	0.00	0.00	0.00	0.00	0.00	0.00	0.00	0.00	0.00
La_2O_3	–	–	–	–	–	–	–	–	–	–
Ce_2O_3	0.00	0.00	0.00	0.00	0.00	0.00	0.00	0.00	0.00	0.00
Pr_2O_3	–	–	–	–	–	–	–	–	–	–
Nd_2O_3	–	–	–	–	–	–	–	–	–	–
Sm_2O_3	–	–	–	–	–	–	–	–	–	–
Eu_2O_3	–	–	–	–	–	–	–	–	–	–
Gd_2O_3	–	–	–	–	–	–	–	–	–	–
PbO	–	–	–	–	–	–	–	–	–	–
Bi_2O_3	–	–	–	–	–	–	–	–	–	–
ThO_2	–	–	–	–	–	–	–	–	–	–
UO_2	–	–	–	–	–	–	–	–	–	–
B_2O_3	–	–	–	–	–	–	–	–	–	–
SO_3	0.00	0.00	0.00	0.00	0.00	0.00	0.00	0.00	0.00	0.00
F	0.00	0.00	0.00	0.00	0.00	0.00	0.00	0.00	0.00	0.00
Cl	0.00	0.00	0.00	0.00	0.00	0.00	0.00	0.00	0.00	0.00
H_2O*	2.72	2.70	2.90	2.99	2.91	2.83	2.64	2.81	2.65	2.80
	98.22	98.05	99.54	100.07	99.70	98.99	98.89	100.09	98.35	99.65
O≡F	–	–	–	–	–	–	–	–	–	–
O≡Cl	–	–	–	–	–	–	–	–	–	–
TOTAL	98.22	98.05	99.54	100.07	99.70	98.99	98.89	100.09	98.35	99.65

*Calculated for charge balance.

QUANTITATIVE WDS RESULTS (NMNS)

Oxide Percents

	V13-6_1	V13-7_1	V13-8_1	V13-9_1	V13-10_1	V13-11_1	V13-12_1	V13-13_1	V13-14_1	V13-15_1
SiO_2	37.12	36.72	36.61	36.74	36.62	37.09	36.59	36.84	36.77	36.66
Al_2O_3	17.00	17.04	17.43	17.68	17.98	17.66	17.89	17.73	17.72	18.01
TiO_2	0.32	0.43	0.84	0.60	0.40	0.71	0.61	0.51	0.82	0.55
MgO	2.31	2.27	1.89	1.86	1.83	1.99	1.69	1.83	1.72	1.58
MnO	0.06	0.06	0.08	0.00	0.09	0.00	0.10	0.08	0.09	0.06
FeO	1.43	1.50	1.36	1.35	1.35	1.21	1.36	1.36	1.36	1.45
Fe_2O_3	1.92	2.01	1.83	1.81	1.81	1.63	1.83	1.83	1.82	1.95
Cr_2O_3	–	–	–	–	–	–	–	–	–	–
CuO	–	–	–	–	–	–	–	–	–	–
ZnO	0.00	0.00	0.00	0.00	0.00	0.00	0.00	0.00	0.00	0.00
CaO	35.97	37.15	36.20	36.94	36.70	37.03	35.98	36.96	36.76	36.82
Na_2O	0.00	0.00	0.00	0.00	0.00	0.00	0.00	0.00	0.00	0.00
K_2O	0.00	0.00	0.00	0.00	0.00	0.00	0.00	0.00	0.00	0.00
La_2O_3	–	–	–	–	–	–	–	–	–	–
Ce_2O_3	0.00	0.00	0.00	0.00	0.00	0.00	0.00	0.00	0.00	0.00
Pr_2O_3	–	–	–	–	–	–	–	–	–	–
Nd_2O_3	–	–	–	–	–	–	–	–	–	–
Sm_2O_3	–	–	–	–	–	–	–	–	–	–
Eu_2O_3	–	–	–	–	–	–	–	–	–	–
Gd_2O_3	–	–	–	–	–	–	–	–	–	–
PbO	–	–	–	–	–	–	–	–	–	–
Bi_2O_3	–	–	–	–	–	–	–	–	–	–
ThO_2	–	–	–	–	–	–	–	–	–	–
UO_2	–	–	–	–	–	–	–	–	–	–
B_2O_3	–	–	–	–	–	–	–	–	–	–
SO_3	0.00	0.00	0.00	0.00	0.00	0.00	0.00	0.00	0.00	0.00
F	0.00	0.00	0.00	0.00	0.00	0.00	0.00	0.00	0.00	0.00
Cl	0.00	0.00	0.00	0.00	0.00	0.00	0.07	0.00	0.00	0.00
H_2O^*	2.72	2.97	2.67	2.79	2.80	2.76	2.60	2.80	2.72	2.75
	98.85	100.15	98.91	99.77	99.58	100.08	98.72	99.94	99.78	99.83
O≡F	–	–	–	–	–	–	–	–	–	–
O≡Cl	–	–	–	–	–	–	0.02	–	–	–
TOTAL	98.85	100.15	98.91	99.77	99.58	100.08	98.70	99.94	99.78	99.83

*Calculated for charge balance.

QUANTITATIVE WDS RESULTS (NMNS)

Oxide Percents

	$V13\text{-}16_1$	$V13\text{-}17_1$	$V13\text{-}18_1$	$V13\text{-}19_1$	$V13\text{-}20_1$	$V13\text{-}21_1$	$V13\text{-}22_1$	$V13\text{-}23_1$	$V13\text{-}24_1$	$V13\text{-}25_1$
SiO_2	36.33	36.37	36.72	36.72	36.65	36.16	36.68	36.49	36.61	36.44
Al_2O_3	18.04	17.69	17.85	17.66	18.16	18.75	18.84	18.77	18.09	18.27
TiO_2	0.66	0.60	0.61	0.37	0.63	0.44	0.35	0.38	0.37	0.31
MgO	1.49	1.86	1.84	1.87	1.45	1.37	1.36	1.33	1.55	1.48
MnO	0.07	0.08	0.06	0.00	0.00	0.00	0.06	0.07	0.12	0.00
FeO	1.39	1.35	1.29	1.41	1.39	1.29	1.34	1.30	1.41	1.48
Fe_2O_3	1.86	1.81	1.73	1.88	1.87	1.74	1.80	1.74	1.88	1.99
Cr_2O_3	–	–	–	–	–	–	–	–	–	–
CuO	–	–	–	–	–	–	–	–	–	–
ZnO	0.00	0.00	0.00	0.00	0.00	0.00	0.00	0.00	0.00	0.00
CaO	36.47	35.95	36.66	36.34	36.91	36.27	36.95	36.05	36.81	35.89
Na_2O	0.00	0.00	0.00	0.00	0.00	0.00	0.00	0.00	0.00	0.00
K_2O	0.00	0.00	0.00	0.00	0.00	0.00	0.00	0.00	0.00	0.00
La_2O_3	–	–	–	–	–	–	–	–	–	–
Ce_2O_3	0.00	0.00	0.00	0.00	0.00	0.00	0.00	0.00	0.00	0.00
Pr_2O_3	–	–	–	–	–	–	–	–	–	–
Nd_2O_3	–	–	–	–	–	–	–	–	–	–
Sm_2O_3	–	–	–	–	–	–	–	–	–	–
Eu_2O_3	–	–	–	–	–	–	–	–	–	–
Gd_2O_3	–	–	–	–	–	–	–	–	–	–
PbO	–	–	–	–	–	–	–	–	–	–
Bi_2O_3	–	–	–	–	–	–	–	–	–	–
ThO_2	–	–	–	–	–	–	–	–	–	–
UO_2	–	–	–	–	–	–	–	–	–	–
B_2O_3	–	–	–	–	–	–	–	–	–	–
SO_3	0.00	0.00	0.00	0.00	0.00	0.00	0.00	0.00	0.00	0.00
F	0.00	0.00	0.16	0.00	0.00	0.00	0.00	0.00	0.00	0.00
Cl	0.05	0.00	0.00	0.00	0.07	0.00	0.07	0.00	0.00	0.00
H_2O^*	2.68	2.68	2.67	2.72	2.69	2.66	2.73	2.58	2.77	2.61
	99.03	98.39	99.59	98.97	99.83	98.68	100.11	98.71	99.61	98.47
O≡F	–	–	0.07	–	–	–	–	–	–	–
O≡Cl	0.01	–	–	–	0.02	–	–	–	–	–
TOTAL	99.02	98.39	99.52	98.97	99.81	98.68	100.11	98.71	99.61	98.47

*Calculated for charge balance.

QUANTITATIVE WDS RESULTS (NMNS)

Oxide Percents

	V13-26$_1$	V13-27$_1$	V13-28$_1$	V13-29$_1$	V13-30$_{2c}$	V13-31$_{2c}$	V13-32$_{2c}$	V13-33$_{2c}$	V13-34$_{2c}$	V13-35$_{2i}$
SiO_2	36.14	36.69	36.46	36.33	36.23	36.06	36.07	36.36	36.43	36.45
Al_2O_3	18.72	18.11	18.26	18.35	18.39	18.21	18.38	18.39	18.50	18.00
TiO_2	0.32	0.28	0.25	0.78	0.77	0.76	0.76	0.73	0.76	0.77
MgO	1.29	1.51	1.52	1.43	1.43	1.40	1.44	1.40	1.41	1.69
MnO	0.06	0.10	0.09	0.00	0.08	0.08	0.08	0.09	0.06	0.08
FeO	1.33	1.45	1.44	1.32	1.30	1.31	1.29	1.30	1.29	1.36
Fe_2O_3	1.78	1.94	1.93	1.78	1.74	1.76	1.74	1.74	1.73	1.83
Cr_2O_3	–	–	–	–	–	–	–	–	–	–
CuO	–	–	–	–	–	–	–	–	–	–
ZnO	0.00	0.00	0.00	0.00	0.00	0.00	0.00	0.00	0.00	0.00
CaO	36.96	36.45	37.00	36.14	36.68	36.23	36.25	36.27	36.92	36.57
Na_2O	0.00	0.00	0.00	0.00	0.00	0.00	0.00	0.00	0.00	0.00
K_2O	0.00	0.00	0.00	0.00	0.00	0.00	0.00	0.00	0.00	0.00
La_2O_3	–	–	–	–	–	–	–	–	–	–
Ce_2O_3	0.00	0.00	0.00	0.00	0.00	0.00	0.00	0.00	0.00	0.00
Pr_2O_3	–	–	–	–	–	–	–	–	–	–
Nd_2O_3	–	–	–	–	–	–	–	–	–	–
Sm_2O_3	–	–	–	–	–	–	–	–	–	–
Eu_2O_3	–	–	–	–	–	–	–	–	–	–
Gd_2O_3	–	–	–	–	–	–	–	–	–	–
PbO	–	–	–	–	–	–	–	–	–	–
Bi_2O_3	–	–	–	–	–	–	–	–	–	–
ThO_2	–	–	–	–	–	–	–	–	–	–
UO_2	–	–	–	–	–	–	–	–	–	–
B_2O_3	–	–	–	–	0.00	–	–	–	–	–
SO_3	0.00	0.00	0.00	0.00	0.00	0.00	0.00	0.00	0.00	0.00
F	0.00	0.00	0.00	0.00	0.00	0.00	0.00	0.00	0.00	0.00
Cl	0.00	0.00	0.00	0.00	0.00	0.00	0.04	0.00	0.00	0.00
H_2O*	2.79	2.70	2.83	2.59	2.71	2.64	2.64	2.62	2.72	2.73
	99.39	99.23	99.78	98.72	99.33	98.45	98.69	98.90	99.82	99.48
O≡F	–	–	–	–	–	–	–	–	–	–
O≡Cl	–	–	–	–	–	–	0.01	–	–	–
TOTAL	99.39	99.23	99.78	98.72	99.33	98.45	98.68	98.90	99.82	99.48

*Calculated for charge balance.

QUANTITATIVE WDS RESULTS (NMNS)

Oxide Percents

	V13-36$_{2i}$	V13-37$_{2i}$	V13-38$_{2i}$	V13-39$_{2r}$	V13-40$_{2r}$	V13-41$_{2r}$	V13-42$_{2r}$	V13-33$_{2i}$	V13-44$_{2i}$	V13-45$_{2i}$
SiO_2	36.50	36.45	36.54	36.50	36.51	36.39	36.50	36.44	36.22	36.45
Al_2O_3	17.79	17.82	17.42	17.83	18.14	17.98	17.71	17.81	17.54	17.87
TiO_2	0.77	0.84	0.80	0.62	0.45	0.37	0.71	0.82	0.72	0.79
MgO	1.64	1.71	1.84	1.83	1.88	1.86	1.68	1.55	1.61	1.74
MnO	0.08	0.09	0.07	0.06	0.00	0.09	0.09	0.07	0.07	0.07
FeO	1.38	1.34	1.41	1.31	1.32	1.39	1.38	1.44	1.47	1.30
Fe_2O_3	1.85	1.80	1.88	1.76	1.77	1.87	1.85	1.93	1.97	1.74
Cr_2O_3	–	–	–	–	–	–	–	–	–	–
CuO	–	–	–	–	–	–	–	–	–	–
ZnO	0.00	0.00	0.00	0.00	0.00	0.00	0.00	0.00	0.00	0.00
CaO	36.58	36.22	36.82	36.64	37.07	36.72	36.74	36.51	36.97	36.20
Na_2O	0.00	0.00	0.00	0.00	0.00	0.00	0.00	0.00	0.00	0.00
K_2O	0.00	0.00	0.00	0.00	0.00	0.00	0.00	0.00	0.00	0.00
La_2O_3	–	–	–	–	–	–	–	–	–	–
Ce_2O_3	0.00	0.00	0.00	0.00	0.00	0.00	0.00	0.00	0.00	0.00
Pr_2O_3	–	–	–	–	–	–	–	–	–	–
Nd_2O_3	–	–	–	–	–	–	–	–	–	–
Sm_2O_3	–	–	–	–	–	–	–	–	–	–
Eu_2O_3	–	–	–	–	–	–	–	–	–	–
Gd_2O_3	–	–	–	–	–	–	–	–	–	–
PbO	–	–	–	–	–	–	–	–	–	–
Bi_2O_3	–	–	–	–	–	–	–	–	–	–
ThO_2	–	–	–	–	–	–	–	–	–	–
UO_2	–	–	–	–	–	–	–	–	–	–
B_2O_3	–	–	–	–	0.00	–	–	–	–	–
SO_3	0.00	0.00	0.00	0.00	0.00	0.00	0.00	0.00	0.00	0.00
F	0.00	0.00	0.00	0.00	0.00	0.00	0.00	0.00	0.00	0.00
Cl	0.00	0.00	0.00	0.00	0.00	0.00	0.00	0.06	0.00	0.00
H_2O*	2.71	2.66	2.79	2.77	2.87	2.85	2.75	2.67	2.82	2.66
	99.30	98.93	99.57	99.32	100.01	99.52	99.41	99.29	99.39	98.82
O≡F	–	–	–	–	–	–	–	–	–	–
O≡Cl	–	–	–	–	–	–	–	0.01	–	–
TOTAL	99.30	98.93	99.57	99.32	100.01	99.52	99.41	99.28	99.39	98.82

*Calculated for charge balance.

QUANTITATIVE WDS RESULTS (NMNS)

Oxide Percents

	V13-46$_{2i}$	V13-47$_{2i}$	V13-48$_{2r}$	V13-49$_{2r}$	V13-50$_{2r}$	V13-51$_{2}$	V13-52$_{2}$	V13-53$_{2}$	V13-54$_{3c}$	V13-55$_{3i}$
SiO_2	36.74	35.95	36.70	36.65	36.62	36.46	36.58	35.97	36.33	36.69
Al_2O_3	17.84	17.77	17.85	17.81	17.70	17.49	18.11	18.38	17.95	17.63
TiO_2	0.65	0.54	0.38	0.39	0.71	0.95	0.40	0.66	0.54	0.37
MgO	1.65	1.83	1.82	1.85	1.68	1.80	1.86	1.43	1.53	1.85
MnO	0.00	0.00	0.10	0.07	0.08	0.00	0.08	0.07	0.09	0.07
FeO	1.43	1.32	1.36	1.35	1.46	1.38	1.31	1.29	1.43	1.46
Fe_2O_3	1.92	1.78	1.82	1.81	1.96	1.85	1.76	1.74	1.92	1.96
Cr_2O_3	–	–	–	–	–	–	–	–	–	–
CuO	–	–	–	–	–	–	–	–	–	–
ZnO	0.00	0.00	0.00	0.00	0.00	0.00	0.00	0.00	0.00	0.00
CaO	36.59	36.78	36.72	36.09	36.59	36.60	36.81	36.04	36.65	36.84
Na_2O	0.00	0.00	0.00	0.00	0.00	0.00	0.00	0.00	0.00	0.00
K_2O	0.00	0.00	0.00	0.00	0.00	0.00	0.00	0.00	0.00	0.00
La_2O_3	–	–	–	–	–	–	–	–	–	–
Ce_2O_3	0.00	0.00	0.00	0.00	0.00	0.00	0.00	0.00	0.00	0.00
Pr_2O_3	–	–	–	–	–	–	–	–	–	–
Nd_2O_3	–	–	–	–	–	–	–	–	–	–
Sm_2O_3	–	–	–	–	–	–	–	–	–	–
Eu_2O_3	–	–	–	–	–	–	–	–	–	–
Gd_2O_3	–	–	–	–	–	–	–	–	–	–
PbO	–	–	–	–	–	–	–	–	–	–
Bi_2O_3	–	–	–	–	–	–	–	–	–	–
ThO_2	–	–	–	–	–	–	–	–	–	–
UO_2	–	–	–	–	–	–	–	–	–	–
B_2O_3	–	–	–	–	–	–	–	–	–	–
SO_3	0.00	0.00	0.00	0.00	0.00	0.00	0.00	0.00	0.00	0.00
F	0.00	0.00	0.00	0.00	0.00	0.00	0.00	0.00	0.00	0.00
Cl	0.00	0.00	0.00	0.00	0.00	0.00	0.00	0.00	0.00	0.00
H_2O*	2.69	2.86	2.79	2.68	2.72	2.72	2.83	2.64	2.75	2.83
	99.51	98.83	99.54	98.70	99.52	99.25	99.74	98.22	99.19	99.70
O≡F	–	–	–	–	–	–	–	–	–	–
O≡Cl	–	–	–	–	–	–	–	–	–	–
TOTAL	99.51	98.83	99.54	98.70	99.52	99.25	99.74	98.22	99.19	99.70

*Calculated for charge balance.

QUANTITATIVE WDS RESULTS (NMNS)

Oxide Percents

	V14-1_c	V14-2_r	V15-1	V15-2	V15-3	V16-1	V16-2	V16-3	V17-1	V17-2
SiO_2	36.98	37.21	38.07	37.40	37.58	37.04	36.99	37.28	36.83	37.11
Al_2O_3	17.96	18.01	18.02	18.08	18.08	16.90	16.98	17.00	17.39	17.28
TiO_2	0.00	0.00	0.00	0.00	0.00	0.11	0.12	0.07	0.00	0.00
MgO	2.57	2.46	2.48	2.58	2.73	2.33	2.26	2.31	2.38	2.35
MnO	0.10	0.12	0.16	0.17	0.11	0.31	0.46	0.43	0.00	0.05
FeO	0.19	0.22	0.97	0.89	0.91	2.73	2.72	2.57	0.72	0.74
Fe_2O_3	1.06	1.24	–	–	–	–	–	–	2.26	2.34
Cr_2O_3	–	–	–	–	–	–	–	–	–	–
CuO	–	–	–	–	–	–	–	–	–	–
ZnO	0.00	0.00	0.00	0.00	0.00	0.00	0.00	0.00	0.00	0.00
CaO	37.04	36.65	36.81	36.95	36.81	36.44	36.38	35.98	36.58	36.06
Na_2O	0.00	0.00	0.00	0.00	0.00	0.00	0.00	0.00	0.00	0.00
K_2O	0.00	0.00	0.00	0.00	0.00	0.00	0.00	0.00	0.00	0.00
La_2O_3	–	–	–	–	–	–	–	–	–	–
Ce_2O_3	0.00	0.00	0.00	0.00	0.00	0.00	0.00	0.00	0.00	0.00
Pr_2O_3	–	–	–	–	–	–	–	–	–	–
Nd_2O_3	–	–	–	–	–	–	–	–	–	–
Sm_2O_3	–	–	–	–	–	–	–	–	–	–
Eu_2O_3	–	–	–	–	–	–	–	–	–	–
Gd_2O_3	–	–	–	–	–	–	–	–	–	–
PbO	–	–	–	–	–	–	–	–	–	–
Bi_2O_3	–	–	–	–	–	–	–	–	–	–
ThO_2	–	–	–	–	–	–	–	–	–	–
UO_2	–	–	–	–	–	–	–	–	–	–
B_2O_3	0.00	–	–	–	–	–	0.00	–	0.00	–
SO_3	0.00	0.00	0.00	0.00	0.00	0.00	0.00	0.00	0.00	0.00
F	0.00	0.00	0.00	0.00	0.00	0.00	0.00	0.00	0.00	0.00
Cl	0.00	0.00	0.00	0.00	0.00	0.00	0.00	0.00	0.00	0.00
H_2O*	2.86	2.75	2.76	2.89	2.87	3.03	3.03	2.91	2.82	2.69
	98.76	98.66	99.27	98.96	99.09	98.89	98.94	98.55	98.98	98.62
O≡F	–	–	–	–	–	–	–	–	–	–
O≡Cl	–	–	–	–	–	–	–	–	–	–
TOTAL	98.76	98.66	99.27	98.96	99.09	98.89	98.94	98.55	98.98	98.62

*Calculated for charge balance.

QUANTITATIVE WDS RESULTS (NMNS)

Oxide Percents

	V17-3	V17-4	V17-5	V17-6	V17-7	V17-8	V17-9	V17-10	$V18\text{-}1_1$	$V18\text{-}2_1$
SiO_2	36.88	36.79	37.06	36.48	36.77	36.94	37.18	37.31	37.53	38.10
Al_2O_3	17.27	17.37	17.11	17.00	17.11	17.07	17.08	17.13	18.52	18.45
TiO_2	0.00	0.00	0.04	0.05	0.00	0.00	0.00	0.00	0.00	0.00
MgO	2.39	2.32	2.45	2.51	2.43	2.34	2.44	2.37	2.56	2.70
MnO	0.00	0.00	0.00	0.00	0.00	0.06	0.00	0.00	0.09	0.06
FeO	0.72	0.71	0.75	0.74	0.77	0.73	0.75	0.77	1.20	1.04
Fe_2O_3	2.27	2.23	2.38	2.35	2.43	2.30	2.37	2.42	–	–
Cr_2O_3	–	–	–	–	–	–	–	–	–	–
CuO	–	–	–	–	–	–	–	–	–	–
ZnO	0.00	0.00	0.00	0.00	0.00	0.00	0.00	0.00	0.00	0.00
CaO	36.72	35.93	36.61	36.20	36.35	35.45	36.57	35.70	37.58	36.96
Na_2O	0.00	0.00	0.00	0.00	0.00	0.00	0.00	0.00	0.00	0.00
K_2O	0.00	0.00	0.00	0.00	0.00	0.00	0.00	0.00	0.00	0.00
La_2O_3	–	–	–	–	–	–	–	–	–	–
Ce_2O_3	0.00	0.00	0.00	0.00	0.00	0.00	0.00	0.00	0.00	0.00
Pr_2O_3	–	–	–	–	–	–	–	–	–	–
Nd_2O_3	–	–	–	–	–	–	–	–	–	–
Sm_2O_3	–	–	–	–	–	–	–	–	–	–
Eu_2O_3	–	–	–	–	–	–	–	–	–	–
Gd_2O_3	–	–	–	–	–	–	–	–	–	–
PbO	–	–	–	–	–	–	–	–	–	–
Bi_2O_3	–	–	–	–	–	–	–	–	–	–
ThO_2	–	–	–	–	–	–	–	–	–	–
UO_2	–	–	–	–	–	–	–	–	–	–
B_2O_3	–	–	–	–	–	–	–	–	–	–
SO_3	0.00	0.00	0.00	0.00	0.00	0.00	0.00	0.00	0.00	0.00
F	0.00	0.00	0.00	0.00	0.00	0.00	0.00	0.00	0.00	0.00
Cl	0.00	0.00	0.00	0.00	0.00	0.00	0.00	0.00	0.00	0.00
H_2O^*	2.84	2.69	2.81	2.82	2.80	2.59	2.78	2.60	3.02	2.84
	99.09	98.04	99.21	98.15	98.66	97.48	99.17	98.30	100.50	100.15
O≡F	–	–	–	–	–	–	–	–	–	–
O≡Cl	–	–	–	–	–	–	–	–	–	–
TOTAL	99.09	98.64	99.21	98.15	98.66	97.48	99.17	98.30	100.50	100.15

*Calculated for charge balance.

QUANTITATIVE WDS RESULTS (NMNS)

Oxide Percents

	$V18\text{-}3_1$	$V18\text{-}4_{2r}$	$V18\text{-}5_{2c}$	V19-1	V19-2	V19-3	V19-4	V19-5	V19-6	V20-1
SiO_2	37.60	37.72	37.32	37.00	36.90	36.92	36.93	37.48	37.31	36.86
Al_2O_3	18.52	18.26	18.50	16.89	16.95	16.82	16.73	16.99	17.11	16.44
TiO_2	0.00	0.00	0.00	0.89	0.46	0.38	0.38	0.47	0.68	1.20
MgO	2.72	2.67	2.60	2.44	2.47	2.61	2.58	2.52	2.35	2.53
MnO	0.00	0.00	0.13	0.08	0.16	0.16	0.13	0.18	0.18	0.15
FeO	1.30	1.15	1.17	2.65	2.53	2.63	2.50	2.46	2.47	2.58
Fe_2O_3	–	–	–	–	–	–	–	–	–	–
Cr_2O_3	–	–	–	0.00	0.00	0.00	0.00	0.00	0.00	–
CuO	–	–	–	–	–	–	–	–	–	–
ZnO	0.00	0.00	0.00	0.00	0.00	0.00	0.00	0.00	0.00	0.00
CaO	37.41	36.70	37.07	36.16	37.05	35.56	37.99	35.95	37.78	36.93
Na_2O	0.00	0.00	0.00	0.00	0.00	0.00	0.00	0.00	0.00	0.00
K_2O	0.00	0.00	0.00	–	–	–	–	–	–	0.00
La_2O_3	–	–	–	–	–	–	–	–	–	–
Ce_2O_3	0.00	0.00	0.00	0.00	0.00	0.00	0.00	0.00	0.00	0.00
Pr_2O_3	–	–	–	–	–	–	–	–	–	–
Nd_2O_3	–	–	–	–	–	–	–	–	–	–
Sm_2O_3	–	–	–	–	–	–	–	–	–	–
Eu_2O_3	–	–	–	–	–	–	–	–	–	–
Gd_2O_3	–	–	–	–	–	–	–	–	–	–
PbO	–	–	–	–	–	–	–	–	–	–
Bi_2O_3	–	–	–	–	–	–	–	–	–	–
ThO_2	–	–	–	–	–	–	–	–	–	–
UO_2	–	–	–	–	–	–	–	–	–	–
B_2O_3	–	–	–	–	–	–	–	–	–	–
SO_3	0.00	0.00	0.00	0.00	0.00	0.00	0.00	0.00	0.00	0.00
F	0.00	0.00	0.00	0.00	0.00	0.00	0.00	0.00	0.00	0.00
Cl	0.00	0.00	0.00	0.00	0.00	0.00	0.00	0.00	0.00	0.00
H_2O^*	3.03	2.84	2.97	2.89	3.11	2.89	3.29	2.84	3.13	3.03
	100.58	99.34	99.76	99.00	99.63	97.97	100.53	98.89	101.01	99.72
O≡F	–	–	–	–	–	–	–	–	–	–
O≡Cl	–	–	–	–	–	–	–	–	–	–
TOTAL	100.58	99.34	99.76	99.00	99.63	97.97	100.53	98.89	101.01	99.72

*Calculated for charge balance.

QUANTITATIVE WDS RESULTS (NMNS)

Oxide Percents

	V20-2	V20-3	V21-1_1	V21-2_1	V21-3_{2r}	V21-4_{2r}	V21-5_{2r}	V21-6_{2c}	V21-7_{2c}	V21-8_{2c}
SiO_2	37.05	36.66	37.05	37.11	37.71	37.08	36.93	37.07	37.43	37.29
Al_2O_3	16.68	16.62	18.05	17.87	17.81	18.47	18.63	17.75	18.70	18.44
TiO_2	1.10	1.20	0.00	0.00	0.00	0.00	0.00	0.00	0.00	0.00
MgO	2.46	2.51	2.95	2.38	2.83	2.65	2.57	2.63	2.40	2.50
MnO	0.15	0.15	0.18	0.28	0.21	0.12	0.12	0.00	0.09	0.22
FeO	2.64	2.61	0.37	0.47	0.42	0.31	0.31	1.49	0.52	0.50
Fe_2O_3	–	–	–	–	–	–	–	–	–	–
Cr_2O_3	–	–	0.00	0.00	0.00	0.00	0.00	0.00	0.00	0.00
CuO	–	–	–	–	–	–	–	–	–	–
ZnO	0.00	0.00	0.00	0.00	0.00	0.00	0.00	0.00	0.00	0.00
CaO	36.28	36.80	35.58	37.18	36.31	37.48	36.14	37.02	36.02	37.47
Na_2O	0.00	0.00	0.00	0.00	0.00	0.00	0.00	0.00	0.00	0.00
K_2O	0.00	0.00	–	–	–	–	–	–	–	–
La_2O_3	–	–	–	–	–	–	–	–	–	–
Ce_2O_3	0.00	0.00	0.00	0.00	0.00	0.00	0.00	0.00	0.00	0.00
Pr_2O_3	–	–	–	–	–	–	–	–	–	–
Nd_2O_3	–	–	–	–	–	–	–	–	–	–
Sm_2O_3	–	–	–	–	–	–	–	–	–	–
Eu_2O_3	–	–	–	–	–	–	–	–	–	–
Gd_2O_3	–	–	–	–	–	–	–	–	–	–
PbO	–	–	–	–	–	–	–	–	–	–
Bi_2O_3	–	–	–	–	–	–	–	–	–	–
ThO_2	–	–	–	–	–	–	–	–	–	–
UO_2	–	–	–	–	–	–	–	–	–	–
B_2O_3	–	–	–	–	–	–	–	–	0.00	–
SO_3	0.00	0.00	0.00	0.00	0.00	0.00	0.00	0.00	0.00	0.00
F	0.00	0.00	0.00	0.00	0.00	0.00	0.00	0.00	0.00	0.00
Cl	0.00	0.00	0.00	0.00	0.00	0.00	0.00	0.00	0.00	0.00
H_2O^*	2.89	3.03	2.71	2.87	2.73	2.97	2.73	3.01	2.63	2.94
	99.25	99.58	96.89	98.16	98.02	99.08	97.43	98.97	97.79	99.36
O≡F	–	–	–	–	–	–	–	–	–	–
O≡Cl	–	–	–	–	–	–	–	–	–	–
TOTAL	99.25	99.58	96.89	98.16	98.02	99.08	97.43	98.97	97.79	99.36

*Calculated for charge balance.

QUANTITATIVE WDS RESULTS (NMNS)

Oxide Percents

	V21-9_{2c}	V21-10_{2c}	V22-1	V22-2	V22-3	V23-1_r	V23-2_i	V23-3_i	V23-4_i	V23-5_i
SiO_2	36.99	37.24	37.11	36.87	37.04	37.68	37.64	37.67	37.28	37.53
Al_2O_3	18.18	18.12	16.56	16.71	16.52	17.79	18.09	18.05	17.99	17.87
TiO_2	0.00	0.07	0.96	1.01	0.98	0.00	0.00	0.00	0.00	0.00
MgO	2.06	2.55	2.89	2.60	2.85	2.57	2.60	2.56	2.54	2.55
MnO	0.30	0.00	0.00	0.07	0.00	0.15	0.15	0.16	0.18	0.22
FeO	0.93	1.21	0.31	0.35	0.30	0.35	0.23	0.25	0.27	0.28
Fe_2O_3	–	–	2.16	2.47	2.10	1.38	0.90	0.96	1.05	1.09
Cr_2O_3	0.00	0.00	–	–	–	–	–	–	–	–
CuO	–	–	–	–	–	–	–	–	–	–
ZnO	0.00	0.00	0.00	0.00	0.00	0.00	0.00	0.00	0.00	0.00
CaO	35.82	37.24	36.09	36.95	36.30	36.51	37.11	36.80	37.02	36.73
Na_2O	0.00	0.00	0.00	0.00	0.00	0.00	0.00	0.00	0.00	0.00
K_2O	–	–	0.00	0.00	0.00	0.00	0.00	0.00	0.00	0.00
La_2O_3	–	–	–	–	–	–	–	–	–	–
Ce_2O_3	0.00	0.00	0.00	0.00	0.00	0.00	0.00	0.00	0.00	0.00
Pr_2O_3	–	–	–	–	–	–	–	–	–	–
Nd_2O_3	–	–	–	–	–	–	–	–	–	–
Sm_2O_3	–	–	–	–	–	–	–	–	–	–
Eu_2O_3	–	–	–	–	–	–	–	–	–	–
Gd_2O_3	–	–	–	–	–	–	–	–	–	–
PbO	–	–	–	–	–	–	–	–	–	–
Bi_2O_3	–	–	–	–	–	–	–	–	–	–
ThO_2	–	–	–	–	–	–	–	–	–	–
UO_2	–	–	–	–	–	–	–	–	–	–
B_2O_3	–	–	–	–	–	0.00	–	–	–	–
SO_3	0.00	0.00	0.00	0.00	0.00	0.00	0.00	0.00	0.00	0.00
F	0.00	0.00	0.00	0.00	0.00	0.00	0.00	0.00	0.00	0.00
Cl	0.00	0.00	0.00	0.00	0.00	0.00	0.00	0.00	0.00	0.00
H_2O*	2.64	2.97	2.65	2.78	2.68	2.71	2.81	2.75	2.84	2.76
	96.92	99.40	98.73	99.81	98.77	99.14	99.53	99.20	99.17	99.03
O≡F	–	–	–	–	–	–	–	–	–	–
O≡Cl	–	–	–	–	–	–	–	–	–	–
TOTAL	96.92	99.40	98.73	99.81	98.77	99.14	99.53	99.20	99.17	99.03

*Calculated for charge balance.

QUANTITATIVE WDS RESULTS (NMNS)

Oxide Percents

	V23-6_i	V23-7_i	V23-8_r	V24-1	V24-2	V24-3	V25-1_1	V25-2_1	V25-3_2	V26-1
SiO_2	37.57	37.75	37.33	37.34	36.80	37.15	36.91	37.03	37.04	36.03
Al_2O_3	18.03	18.10	17.78	16.28	16.17	16.30	16.12	16.24	17.05	16.13
TiO_2	0.00	0.00	0.00	2.38	2.27	2.22	2.09	1.84	0.88	0.72
MgO	2.57	2.55	2.56	3.41	3.45	3.45	3.63	3.33	3.35	2.10
MnO	0.22	0.20	0.18	0.00	0.00	0.00	0.11	0.12	0.06	0.00
FeO	0.27	0.25	0.38	0.63	0.65	0.64	1.11	1.39	1.23	0.52
Fe_2O_3	1.06	0.97	1.49	0.34	0.35	0.34	–	–	–	3.94
Cr_2O_3	–	–	–	–	–	–	–	–	–	–
CuO	–	–	–	–	–	–	–	–	–	–
ZnO	0.00	0.00	0.00	0.00	0.00	0.00	0.00	0.00	0.00	0.00
CaO	37.29	36.60	36.76	36.42	35.92	36.47	36.40	36.06	36.90	35.18
Na_2O	0.00	0.00	0.00	0.08	0.09	0.06	0.00	0.00	0.00	0.17
K_2O	0.00	0.00	0.00	0.00	0.00	0.00	0.00	0.00	0.00	0.00
La_2O_3	–	–	–	–	–	–	–	0.00	0.00	–
Ce_2O_3	0.00	0.00	0.00	0.00	0.00	0.00	0.00	0.00	0.09	0.00
Pr_2O_3	–	–	–	–	–	–	–	0.00	0.00	–
Nd_2O_3	–	–	–	–	–	–	–	0.00	0.00	–
Sm_2O_3	–	–	–	–	–	–	–	0.00	0.00	–
Eu_2O_3	–	–	–	–	–	–	–	0.00	0.00	–
Gd_2O_3	–	–	–	–	–	–	–	0.00	0.00	–
PbO	–	–	–	–	–	–	–	–	–	–
Bi_2O_3	–	–	–	–	–	–	–	–	–	–
ThO_2	–	–	–	–	–	–	–	–	–	–
UO_2	–	–	–	–	–	–	–	–	–	–
B_2O_3	–	–	–	–	–	–	–	–	–	0.00
SO_3	0.00	0.00	0.00	0.19	0.27	0.18	0.41	0.82	0.87	0.48
F	0.00	0.00	0.00	2.10	2.33	2.38	0.75	0.70	0.86	1.55
Cl	0.00	0.00	0.00	0.11	0.12	0.13	0.00	0.00	0.00	0.00
H_2O^*	2.86	2.70	2.81	1.58	1.42	1.50	2.26	1.92	2.05	1.54
	99.87	99.12	99.29	100.85	99.84	100.82	99.80	99.45	100.38	98.36
O≡F	–	–	–	0.88	0.98	1.00	0.32	0.29	0.36	0.65
O≡Cl	–	–	–	0.02	0.03	0.03	–	–	–	–
TOTAL	99.87	99.12	99.29	99.95	98.83	99.79	99.48	99.16	100.02	97.71

*Calculated for charge balance.

V26 includes 0.02 Li_2O, 0.03 BeO.

QUANTITATIVE WDS RESULTS (NMNS)

Oxide Percents

	V26-2	V26-3	V26-4	V26-5	V27-1	V27-2	V27-3	V27-4	V28-1	V28-2
SiO_2	36.30	36.02	35.33	35.90	36.14	36.28	36.23	36.33	36.82	36.63
Al_2O_3	16.28	17.44	15.93	17.36	16.13	16.11	16.29	16.10	16.24	16.06
TiO_2	0.58	0.27	0.89	0.65	0.07	0.06	0.00	0.04	2.65	2.82
MgO	2.19	2.48	2.25	2.56	2.94	2.84	2.90	2.86	1.80	1.75
MnO	0.07	0.08	0.00	0.00	0.24	0.27	0.30	0.28	0.00	0.00
FeO	0.47	0.29	0.49	0.24	3.23	3.23	3.18	3.24	2.46	2.58
Fe_2O_3	3.59	2.21	3.77	1.81	–	–	–	–	–	–
Cr_2O_3	–	–	–	–	–	–	–	–	0.00	0.00
CuO	–	–	–	–	–	–	–	–	–	–
ZnO	0.00	0.00	0.00	0.00	0.00	0.00	0.00	0.00	0.00	0.00
CaO	35.30	35.93	35.45	36.62	36.36	35.75	36.51	35.49	35.92	37.02
Na_2O	0.17	0.14	0.11	0.09	0.04	0.06	0.06	0.05	0.15	0.16
K_2O	0.00	0.00	0.00	0.00	0.00	0.00	0.00	0.00	–	–
La_2O_3	–	–	–	–	–	–	–	–	–	–
Ce_2O_3	0.00	0.00	0.00	0.00	0.00	0.00	0.00	0.00	0.00	0.00
Pr_2O_3	–	–	–	–	–	–	–	–	–	–
Nd_2O_3	–	–	–	–	–	–	–	–	–	–
Sm_2O_3	–	–	–	–	–	–	–	–	–	–
Eu_2O_3	–	–	–	–	–	–	–	–	–	–
Gd_2O_3	–	–	–	–	–	–	–	–	–	–
PbO	–	–	–	–	–	–	–	–	–	–
Bi_2O_3	–	–	–	–	–	–	–	–	–	–
ThO_2	–	–	–	–	–	–	–	–	–	–
UO_2	–	–	–	–	–	–	–	–	–	–
B_2O_3	–	–	–	–	–	–	0.00	–	–	–
SO_3	0.43	0.34	0.00	0.00	0.00	0.26	0.00	0.27	0.20	0.21
F	1.54	1.58	2.05	1.91	1.90	1.92	1.92	1.61	1.36	1.38
Cl	0.00	0.00	0.00	0.00	0.00	0.00	0.00	0.00	0.23	0.24
H_2O^*	1.61	1.87	1.75	2.00	2.46	2.13	2.48	2.23	1.74	1.93
	98.53	98.65	98.01	99.14	99.51	98.92	99.87	98.50	99.56	100.77
O≡F	0.65	0.67	0.86	0.80	0.80	0.81	0.81	0.68	0.57	0.58
O≡Cl	–	–	–	–	–	–	–	–	0.05	0.05
TOTAL	97.88	97.98	97.15	98.34	98.71	98.11	99.06	97.82	98.94	100.14

*Calculated for charge balance.

V26 includes 0.02 Li_2O, 0.03 BeO.

QUANTITATIVE WDS RESULTS (NMNS)

Oxide Percents

	V28-3	V28-4	V28-5	V29-1	V29-2	V29-3	V29-4	V29-5	$V30\text{-}1_{rl}$	$V30\text{-}2_{rl}$
SiO_2	36.60	36.86	37.10	37.15	36.76	37.01	37.01	37.30	33.25	34.23
Al_2O_3	16.16	16.18	16.10	16.15	16.09	16.46	16.07	16.26	10.36	10.63
TiO_2	2.80	2.74	2.85	2.78	2.93	2.67	2.90	2.87	1.12	1.24
MgO	1.81	1.73	1.73	1.80	1.71	1.79	1.64	1.65	4.19	4.21
MnO	0.00	0.00	0.00	0.00	0.00	0.00	0.06	0.00	0.30	0.27
FeO	2.63	2.55	2.83	2.63	2.67	2.56	2.74	2.79	6.22	5.97
Fe_2O_3	–	–	–	–	–	–	–	–	–	–
Cr_2O_3	0.00	0.00	0.00	0.00	0.00	0.00	0.00	0.00	0.00	0.00
CuO	–	–	–	–	–	–	–	–	–	–
ZnO	0.00	0.00	0.00	0.00	0.00	0.00	0.00	0.00	0.00	0.00
CaO	35.34	36.41	35.18	34.41	35.56	34.18	35.72	34.09	30.69	32.82
Na_2O	0.18	0.16	0.02	0.20	0.22	0.18	0.22	0.21	0.00	0.00
K_2O	–	–	–	–	–	–	–	–	–	–
La_2O_3	–	–	–	–	–	–	–	–	1.86	1.68
Ce_2O_3	0.00	0.00	0.00	0.00	0.00	0.00	0.00	0.00	3.09	2.61
Pr_2O_3	–	–	–	–	–	–	–	–	0.28	0.28
Nd_2O_3	–	–	–	–	–	–	–	–	0.57	0.38
Sm_2O_3	–	–	–	–	–	–	–	–	0.00	0.00
Eu_2O_3	–	–	–	–	–	–	–	–	0.00	0.00
Gd_2O_3	–	–	–	–	–	–	–	–	0.16	0.22
PbO	–	–	–	–	–	–	–	–	–	–
Bi_2O_3	–	–	–	–	–	–	–	–	–	–
ThO_2	–	–	–	–	–	–	–	–	–	–
UO_2	–	–	–	–	–	–	–	–	–	–
B_2O_3	0.00	–	–	–	–	–	–	–	3.17	†
SO_3	0.23	0.17	0.00	0.20	0.24	0.17	0.23	0.20	0.00	0.00
F	1.17	1.40	1.20	1.31	1.16	1.41	1.15	1.45	0.85	0.77
Cl	0.17	0.22	0.17	0.14	0.18	0.18	0.20	0.16	0.00	0.00
H_2O*	1.77	1.81	1.72	1.51	1.78	1.44	1.78	1.34	0.38	0.84
	98.86	100.23	98.91	98.27	99.30	98.05	99.73	98.33	96.49	99.04
O≡F	0.49	0.59	0.51	0.55	0.49	0.59	0.48	0.61	0.36	0.32
O≡Cl	0.04	0.05	0.04	0.03	0.04	0.04	0.05	0.04	–	–
TOTAL	98.33	99.59	98.36	97.69	98.77	97.42	99.20	97.68	96.13	98.72

*Calculated for charge balance. †Average value of 2.90 B_2O_3 used in calculations.

QUANTITATIVE WDS RESULTS (NMNS)

Oxide Percents

	V30-3_r	V30-4_{rd}	V30-5_d	V30-6	V30-7_c	V30-8	V30-9_{rl}	V31-1_c	V31-2_i	V31-3_r
SiO_2	34.47	35.50	34.90	35.35	36.11	35.87	33.75	36.67	36.67	36.93
Al_2O_3	11.91	11.80	11.36	12.16	11.58	11.73	10.30	16.54	16.42	16.46
TiO_2	1.55	1.23	1.07	0.15	0.65	0.38	1.06	2.77	2.80	2.61
MgO	4.04	4.70	4.64	5.37	5.63	5.73	4.16	1.42	1.55	1.70
MnO	0.25	0.23	0.27	0.27	0.19	0.22	0.29	0.00	0.00	0.00
FeO	5.25	4.95	5.74	4.40	4.58	4.62	6.15	2.74	2.82	2.54
Fe_2O_3	–	–	–	–	–	–	–	–	–	–
Cr_2O_3	0.00	0.00	0.00	0.00	0.00	0.00	0.00	–	–	–
CuO	–	–	–	–	–	–	–	–	–	–
ZnO	0.00	0.00	0.00	0.00	0.00	0.00	0.00	0.00	0.00	0.00
CaO	32.49	34.46	32.39	34.65	34.79	33.47	32.22	35.40	35.50	35.84
Na_2O	0.00	0.00	0.00	0.00	0.00	0.05	0.05	0.28	0.21	0.20
K_2O	–	–	–	–	–	–	–	0.00	0.00	0.00
La_2O_3	1.43	0.73	1.13	0.82	0.63	0.43	1.83	–	–	–
Ce_2O_3	1.58	0.80	1.17	0.76	0.57	0.33	3.08	–	–	–
Pr_2O_3	0.00	0.00	0.50	0.00	0.00	0.00	0.34	–	–	–
Nd_2O_3	0.00	0.00	0.00	0.00	0.18	0.00	0.62	–	–	–
Sm_2O_3	0.00	0.00	0.00	0.00	0.00	0.00	0.00	–	–	–
Eu_2O_3	0.00	0.00	0.00	0.00	0.00	0.00	0.00	–	–	–
Gd_2O_3	0.00	0.00	0.15	0.00	0.00	0.00	0.27	–	–	–
PbO	–	–	–	–	–	–	–	–	–	–
Bi_2O_3	–	–	–	–	–	–	–	–	–	–
ThO_2	–	–	–	–	–	–	–	–	–	–
UO_2	–	–	–	–	–	–	–	–	–	–
B_2O_3	†	2.55	†	†	2.99	†	†	0.00	–	–
SO_3	0.00	0.00	0.00	0.00	0.28	0.00	0.00	0.00	0.22	0.19
F	0.94	0.59	0.73	0.70	0.64	0.61	0.94	1.47	1.64	1.55
Cl	0.00	0.00	0.00	0.00	0.00	0.00	0.00	0.13	0.15	0.18
H_2O*	0.50	1.30	0.79	1.24	0.95	1.11	0.78	1.79	1.57	1.66
	97.32	98.84	97.74	98.77	99.77	97.45	98.75	99.21	99.54	99.86
O≡F	0.40	0.25	0.31	0.29	0.27	0.26	0.40	0.62	0.69	0.65
O≡Cl	–	–	–	–	–	–	–	0.03	0.03	0.04
TOTAL	96.92	98.59	97.43	98.48	99.50	97.19	98.35	98.56	98.82	99.17

*Calculated for charge balance. †Average value of 2.90 B_2O_3 used in calculations.

QUANTITATIVE WDS RESULTS (NMNS)

Oxide Percents

	V32-1	V32-2	V32-3	V32-4	V32-5	V33-1_c	V33-2_r	V34-1	V34-2	V34-3
SiO_2	37.15	37.31	37.05	37.24	37.01	37.61	37.47	36.91	36.10	36.64
Al_2O_3	16.89	16.81	16.43	16.63	16.75	17.40	17.26	15.52	15.27	16.00
TiO_2	0.67	0.77	0.75	0.77	0.67	0.64	0.69	0.97	0.89	0.90
MgO	2.05	2.09	2.10	2.07	2.11	1.71	1.80	1.80	1.96	1.78
MnO	0.00	0.00	0.00	0.00	0.00	0.67	0.80	0.40	0.41	0.36
FeO	3.18	3.41	3.46	3.36	3.31	3.16	3.16	4.78	4.70	4.10
Fe_2O_3	–	–	–	–	–	0.37	0.37	–	–	–
Cr_2O_3	0.00	0.00	0.00	0.00	0.00	–	–	–	–	–
CuO	–	–	–	–	–	–	–	–	–	–
ZnO	0.00	0.00	0.00	0.00	0.00	0.00	0.00	0.00	0.00	0.00
CaO	35.49	34.03	35.94	33.98	36.08	35.21	35.64	35.13	34.96	35.91
Na_2O	0.15	0.14	0.12	0.15	0.15	0.09	0.11	0.08	0.06	0.10
K_2O	–	–	–	–	–	0.00	0.00	0.00	0.00	0.00
La_2O_3	0.00	0.00	0.00	0.00	0.00	–	–	–	–	–
Ce_2O_3	0.10	0.12	0.17	0.11	0.08	–	–	0.00	0.00	0.00
Pr_2O_3	0.00	0.00	0.00	0.00	0.00	–	–	–	–	–
Nd_2O_3	0.00	0.00	0.00	0.00	0.00	–	–	–	–	–
Sm_2O_3	0.00	0.00	0.00	0.00	0.00	–	–	–	–	–
Eu_2O_3	0.00	0.00	0.00	0.00	0.00	–	–	–	–	–
Gd_2O_3	0.00	0.00	0.00	0.00	0.00	–	–	–	–	–
PbO	–	–	–	–	–	–	–	–	–	–
Bi_2O_3	–	–	–	–	–	–	–	–	–	–
ThO_2	–	–	–	–	–	–	–	–	–	–
UO_2	–	–	–	–	–	–	–	–	–	–
B_2O_3	–	–	–	–	–	0.00	–	–	0.00	–
SO_3	0.14	0.16	0.00	0.20	0.16	0.00	0.00	0.00	0.00	0.00
F	1.78	1.71	1.73	1.85	1.90	3.05	3.15	2.26	2.05	1.99
Cl	0.14	0.18	0.21	0.15	0.15	0.00	0.00	0.23	0.18	0.22
H_2O^*	1.85	1.60	2.06	1.51	1.94	1.26	1.35	1.78	1.99	2.01
	99.59	98.33	100.03	98.02	100.30	101.17	101.81	99.86	98.57	100.01
O≡F	0.75	0.72	0.73	0.78	0.80	1.28	1.33	0.95	0.86	0.84
O≡Cl	0.03	0.04	0.05	0.03	0.03	–	–	0.05	0.04	0.05
TOTAL	98.81	97.57	99.25	97.21	99.47	99.89	100.48	98.86	97.67	99.12

*Calculated for charge balance.

V33 includes 0.15 BeO.

QUANTITATIVE WDS RESULTS (NMNS)

Oxide Percents

	V34-4	V34-5	V35-1$_c$	V35-2$_r$	V36-1	V36-2	V36-3	V36-4	V36-5	V37-1
SiO_2	36.02	36.49	36.63	36.69	36.46	36.84	36.76	36.55	36.67	36.89
Al_2O_3	15.25	15.65	16.28	16.40	15.96	16.04	16.17	15.98	15.93	16.01
TiO_2	0.88	0.81	1.78	1.75	0.14	0.13	0.11	0.14	0.15	0.14
MgO	1.94	1.91	1.38	1.14	3.80	3.49	3.49	3.55	3.78	2.78
MnO	0.37	0.40	0.00	0.00	0.00	0.00	0.00	0.00	0.00	0.11
FeO	4.87	4.55	4.18	4.20	0.42	0.37	0.37	0.40	0.43	3.88
Fe_2O_3	–	–	–	–	3.29	2.89	2.89	3.11	3.34	–
Cr_2O_3	–	–	–	–	0.34	0.62	0.51	0.63	0.41	–
CuO	–	–	–	–	–	–	–	–	–	–
ZnO	0.00	0.00	0.00	0.00	0.00	0.00	0.00	0.00	0.00	0.00
CaO	34.62	35.20	35.59	35.27	36.71	35.58	36.37	35.25	36.86	36.88
Na_2O	0.06	0.10	0.07	0.09	0.00	0.00	0.00	0.00	0.00	0.00
K_2O	0.00	0.00	0.00	0.00	–	–	–	–	–	0.00
La_2O_3	–	–	–	–	–	–	–	–	–	–
Ce_2O_3	0.00	0.00	0.00	0.00	0.00	0.00	0.00	0.00	0.00	0.00
Pr_2O_3	–	–	–	–	–	–	–	–	–	–
Nd_2O_3	–	–	–	–	–	–	–	–	–	–
Sm_2O_3	–	–	–	–	–	–	–	–	–	–
Eu_2O_3	–	–	–	–	–	–	–	–	–	–
Gd_2O_3	–	–	–	–	–	–	–	–	–	–
PbO	–	–	–	–	–	–	–	–	–	–
Bi_2O_3	–	–	–	–	–	–	–	–	–	–
ThO_2	–	–	–	–	–	–	–	–	–	–
UO_2	–	–	–	–	–	–	–	–	–	–
B_2O_3	–	–	0.00	–	–	–	0.00	–	–	–
SO_3	0.00	0.00	0.00	0.00	0.13	0.00	0.00	0.00	0.00	0.00
F	2.19	2.16	2.32	2.14	0.00	0.00	0.00	0.00	0.00	0.00
Cl	0.15	0.11	0.00	0.00	0.00	0.00	0.00	0.00	0.00	0.00
H_2O*	1.89	1.95	1.61	1.60	3.09	2.84	3.00	2.84	3.17	3.35
	98.24	99.33	99.85	99.27	100.34	98.80	99.67	98.45	100.74	100.04
O≡F	0.92	0.91	0.98	0.90	–	–	–	–	–	–
O≡Cl	0.03	0.02	–	–	–	–	–	–	–	–
TOTAL	97.29	98.40	98.87	98.37	100.34	98.80	99.67	98.45	100.74	100.04

*Calculated for charge balance.

V35 includes 0.04 Li_2O.

QUANTITATIVE WDS RESULTS (NMNS)

Oxide Percents

	V37-2	V37-3	V38-1_{cl}	V38-2_{cl}	V38-3_{cd}	V38-4_{cl}	V38-5_{il}	V38-6_{il}	V38-7_{id}	V38-8_{il}
SiO_2	37.30	36.73	33.24	33.56	34.46	33.70	34.53	34.71	35.56	34.75
Al_2O_3	16.40	16.21	10.27	10.67	11.30	10.82	11.21	11.44	10.49	10.97
TiO_2	0.13	0.17	1.50	1.55	0.91	1.45	1.13	0.87	0.82	0.87
MgO	2.85	2.89	4.87	4.72	5.03	4.79	5.04	5.21	5.72	5.48
MnO	0.08	0.07	0.11	0.11	0.12	0.12	0.15	0.19	0.22	0.16
FeO	3.24	3.28	5.79	5.70	5.43	5.74	5.05	5.10	4.97	5.33
Fe_2O_3	–	–	–	–	–	–	–	–	–	–
Cr_2O_3	–	–	–	–	–	–	–	–	–	–
CuO	–	–	–	–	–	–	–	–	–	–
ZnO	0.00	0.00	0.00	0.00	0.00	0.00	0.00	0.00	0.00	0.00
CaO	36.67	36.38	31.41	32.19	33.85	32.59	34.03	33.91	34.59	33.75
Na_2O	0.00	0.00	0.05	0.00	0.00	0.00	0.00	0.00	0.00	0.00
K_2O	0.00	0.00	0.00	0.00	0.00	0.00	0.00	0.00	0.00	0.00
La_2O_3	–	–	1.58	1.33	1.09	1.29	1.13	0.95	0.76	0.80
Ce_2O_3	0.00	0.00	3.05	2.62	1.82	2.36	1.66	1.35	0.88	1.08
Pr_2O_3	–	–	0.38	0.34	0.26	0.30	0.15	0.14	0.14	0.14
Nd_2O_3	–	–	0.56	0.48	0.28	0.42	0.20	0.16	0.16	0.18
Sm_2O_3	–	–	0.00	0.00	0.00	0.00	0.00	0.00	0.00	0.00
Eu_2O_3	–	–	0.00	0.00	0.00	0.00	0.00	0.00	0.00	0.00
Gd_2O_3	–	–	0.33	0.27	0.00	0.32	0.00	0.00	0.00	0.00
PbO	–	–	–	–	–	–	–	–	–	–
Bi_2O_3	–	–	–	–	–	–	–	–	–	–
ThO_2	–	–	–	–	–	–	–	–	–	–
UO_2	–	–	–	–	–	–	–	–	–	–
B_2O_3	–	–	1.55	†	†	2.30	†	†	†	†
SO_3	0.00	0.00	0.31	0.24	0.00	0.00	0.00	0.00	0.00	0.00
F	0.00	0.00	0.64	0.85	0.78	0.58	0.69	0.69	0.00	0.57
Cl	0.00	0.00	0.00	0.00	0.00	0.00	0.00	0.00	0.00	0.00
H_2O*	3.19	3.22	1.74	1.53	2.01	1.49	2.00	2.04	2.47	2.15
	99.86	98.95	97.38	97.94	99.11	98.27	98.74	98.53	98.55	98.00
O≡F	–	–	0.27	0.36	0.33	0.24	0.29	0.29	–	0.24
O≡Cl	–	–	–	–	–	–	–	–	–	–
TOTAL	99.86	98.95	97.11	97.58	98.78	98.03	98.45	98.24	98.55	97.76

*Calculated for charge balance. †Average value of 1.77 B_2O_3 used in calculations.

QUANTITATIVE WDS RESULTS (NMNS)

Oxide Percents

	V38-9$_{id}$	V38-10$_{id}$	V38-11$_{il}$	V38-12$_{id}$	V38-13$_{id}$	V38-14$_{il}$	V38-15$_{id}$	V38-16$_{id}$	V38-17$_{il}$	V38-18$_{il}$
SiO_2	35.35	35.55	35.32	35.85	35.33	35.28	35.56	35.68	35.81	35.51
Al_2O_3	11.33	11.75	11.53	12.01	11.86	11.46	11.73	12.15	12.06	11.84
TiO_2	0.87	0.84	0.84	0.40	0.68	0.92	0.95	0.71	0.54	0.45
MgO	5.29	5.20	5.32	5.42	5.47	5.33	5.21	5.40	5.31	5.45
MnO	0.18	0.18	0.19	0.17	0.22	0.16	0.17	0.19	0.16	0.22
FeO	5.09	4.95	5.07	4.78	4.58	4.88	4.96	4.42	4.72	4.70
Fe_2O_3	–	–	–	–	–	–	–	–	–	–
Cr_2O_3	–	–	–	–	–	–	–	–	–	–
CuO	–	–	–	–	–	–	–	–	–	–
ZnO	0.00	0.00	0.00	0.00	0.00	0.00	0.00	0.00	0.00	0.00
CaO	35.03	34.29	34.61	34.47	35.24	34.45	35.37	34.89	35.26	34.96
Na_2O	0.00	0.00	0.00	0.00	0.00	0.04	0.04	0.05	0.00	0.00
K_2O	0.00	0.00	0.00	0.00	0.00	0.00	0.00	0.00	0.00	0.00
La_2O_3	0.70	0.39	0.64	0.42	0.52	0.58	0.33	0.25	0.36	0.53
Ce_2O_3	0.77	0.56	0.70	0.51	0.48	0.59	0.44	0.28	0.52	0.47
Pr_2O_3	0.13	0.00	0.15	0.00	0.00	0.00	0.00	0.00	0.00	0.00
Nd_2O_3	0.00	0.00	0.00	0.00	0.00	0.00	0.00	0.00	0.00	0.00
Sm_2O_3	0.00	0.00	0.00	0.00	0.00	0.00	0.00	0.00	0.00	0.00
Eu_2O_3	0.00	0.00	0.00	0.00	0.00	0.00	0.00	0.00	0.00	0.00
Gd_2O_3	0.00	0.00	0.00	0.00	0.00	0.00	0.00	0.00	0.00	0.00
PbO	–	–	–	–	–	–	–	–	–	–
Bi_2O_3	–	–	–	–	–	–	–	–	–	–
ThO_2	–	–	–	–	–	–	–	–	–	–
UO_2	–	–	–	–	–	–	–	–	–	–
B_2O_3	†	†	†	†	†	†	1.46	†	†	†
SO_3	0.00	0.00	0.00	0.00	0.00	0.00	0.12	0.00	0.00	0.00
F	0.76	0.64	0.59	0.71	0.41	0.74	0.71	0.75	0.54	0.57
Cl	0.00	0.00	0.00	0.00	0.00	0.00	0.00	0.00	0.00	0.00
H_2O*	2.13	2.00	2.15	2.03	2.34	2.04	2.33	2.06	2.21	2.23
	99.40	98.12	98.89	98.55	98.90	98.24	99.38	98.61	99.26	98.70
O≡F	0.32	0.27	0.25	0.30	0.17	0.31	0.30	0.32	0.23	0.24
O≡Cl	–	–	–	–	–	–	–	–	–	–
TOTAL	99.08	97.85	98.64	98.25	98.73	97.93	99.08	98.29	99.03	98.46

*Calculated for charge balance. †Average value of 1.77 B_2O_3 used in calculations.

QUANTITATIVE WDS RESULTS (NMNS)

Oxide Percents

	$V38\text{-}19_{id}$	$V38\text{-}20_{il}$	$V38\text{-}21_{id}$	$V38\text{-}22_{id}$	$V38\text{-}23_{rl}$	$V38\text{-}24_{rl}$	$V38\text{-}25_{rl}$	V39-1	V39-2	V39-3
SiO_2	35.76	35.65	35.99	35.40	34.54	34.22	35.00	36.35	36.05	36.43
Al_2O_3	12.20	11.40	12.35	12.19	10.39	10.83	10.62	14.31	14.34	14.33
TiO_2	0.70	0.25	0.60	0.27	0.67	1.19	1.36	1.65	1.47	1.64
MgO	5.40	5.48	5.31	5.44	4.84	4.28	4.30	2.54	2.51	2.56
MnO	0.19	0.31	0.19	0.27	0.24	0.25	0.28	0.15	0.12	0.12
FeO	4.34	5.03	4.35	4.39	6.08	5.79	5.82	1.00	1.00	0.96
Fe_2O_3	–	–	–	–	–	–	–	4.19	4.21	4.05
Cr_2O_3	–	–	–	–	–	–	–	0.00	0.00	0.00
CuO	–	–	–	–	–	–	–	–	–	–
ZnO	0.00	0.00	0.00	0.00	0.00	0.00	0.00	0.00	0.00	0.00
CaO	35.46	34.60	35.74	34.99	33.77	33.24	33.71	35.07	36.41	34.91
Na_2O	0.00	0.00	0.00	0.00	0.00	0.00	0.00	0.00	0.00	0.00
K_2O	0.00	0.00	0.00	0.00	0.00	0.00	0.00	–	–	–
La_2O_3	0.14	0.68	0.10	0.43	1.30	1.24	1.44	–	–	–
Ce_2O_3	0.19	0.64	0.15	0.41	2.11	1.50	1.97	0.00	0.00	0.00
Pr_2O_3	0.00	0.00	0.00	0.00	0.00	0.00	0.00	–	–	–
Nd_2O_3	0.00	0.00	0.00	0.00	0.35	0.24	0.28	–	–	–
Sm_2O_3	0.00	0.00	0.00	0.00	0.00	0.00	0.00	–	–	–
Eu_2O_3	0.00	0.00	0.00	0.00	0.00	0.00	0.00	–	–	–
Gd_2O_3	0.00	0.00	0.00	0.00	0.22	0.16	0.20	–	–	–
PbO	–	–	–	–	–	–	–	–	–	–
Bi_2O_3	–	–	–	–	–	–	–	–	–	–
ThO_2	–	–	–	–	–	–	–	–	–	–
UO_2	–	–	–	–	–	–	–	–	–	–
B_2O_3	†	†	†	†	†	†	†	–	–	0.00
SO_3	0.00	0.00	0.00	0.00	0.00	0.00	0.00	0.00	0.00	0.00
F	0.62	0.61	0.76	0.57	0.92	1.13	0.98	0.00	0.00	0.00
Cl	0.00	0.00	0.00	0.00	0.00	0.00	0.00	0.00	0.00	0.00
H_2O^*	2.17	2.21	2.12	2.23	1.99	1.61	1.66	2.51	2.80	2.46
	98.94	98.63	99.43	98.36	99.19	97.45	99.38	97.77	98.91	97.46
O≡F	0.26	0.26	0.32	0.24	0.39	0.48	0.41	–	–	–
O≡Cl	–	–	–	–	–	–	–	–	–	–
TOTAL	98.68	98.37	99.11	98.12	98.80	96.97	98.97	97.77	98.91	97.46

*Calculated for charge balance. †Average value of 1.77 B_2O_3 used in calculations.

QUANTITATIVE WDS RESULTS (NMNS)

Oxide Percents

	V39-4	V39-5	V40-1_{cd}	V40-2_{id}	V40-3_{id}	V40-4_{id}	V40-5_{id}	V40-6_{id}	V40-7_{id}	V40-8_{il}
SiO_2	36.28	36.65	36.35	36.92	36.51	36.36	36.52	36.70	36.50	36.12
Al_2O_3	14.14	14.19	17.00	16.44	16.87	17.69	15.94	16.08	14.75	13.40
TiO_2	1.79	1.63	1.00	1.51	1.14	0.73	1.42	0.52	0.70	0.74
MgO	2.54	2.57	2.79	2.98	3.01	2.84	2.64	3.00	3.46	3.40
MnO	0.12	0.11	0.32	0.29	0.30	0.27	0.28	0.32	0.29	0.24
FeO	0.98	1.02	2.89	2.74	2.89	2.92	3.99	4.47	5.46	6.35
Fe_2O_3	4.13	4.26	–	–	–	–	–	–	–	–
Cr_2O_3	0.00	0.00	–	–	–	–	–	–	–	–
CuO	–	–	–	–	–	–	–	–	–	–
ZnO	0.00	0.00	0.00	0.00	0.00	0.00	0.00	0.00	0.00	0.00
CaO	36.46	35.02	34.99	35.48	35.29	35.90	35.08	35.83	35.02	34.97
Na_2O	0.00	0.00	0.14	0.10	0.07	0.08	0.11	0.07	0.05	0.00
K_2O	–	–	0.00	0.00	0.00	0.00	0.00	0.00	0.00	0.00
La_2O_3	–	–	0.00	0.00	0.00	0.00	0.00	0.00	0.00	0.48
Ce_2O_3	0.00	0.00	0.19	0.00	0.00	0.00	0.00	0.00	0.00	0.74
Pr_2O_3	–	–	0.00	0.00	0.00	0.00	0.00	0.00	0.00	0.00
Nd_2O_3	–	–	0.00	0.00	0.00	0.00	0.00	0.00	0.00	0.10
Sm_2O_3	–	–	0.00	0.00	0.00	0.00	0.00	0.00	0.00	0.00
Eu_2O_3	–	–	0.00	0.00	0.00	0.00	0.00	0.00	0.00	0.00
Gd_2O_3	–	–	0.00	0.00	0.00	0.00	0.00	0.00	0.00	0.00
PbO	–	–	–	–	–	–	–	–	–	–
Bi_2O_3	–	–	–	–	–	–	–	–	–	–
ThO_2	–	–	–	–	–	–	–	–	–	–
UO_2	–	–	–	–	–	–	–	–	–	–
B_2O_3	–	–	–	–	–	–	–	–	0.00	–
SO_3	0.00	0.00	0.00	0.00	0.00	0.00	0.00	0.00	0.00	0.00
F	0.00	0.00	1.11	1.42	1.21	1.37	0.37	1.66	1.48	1.56
Cl	0.00	0.00	0.07	0.07	0.05	0.07	0.00	0.08	0.00	0.08
H_2O*	2.74	2.46	2.45	2.25	2.44	2.51	2.37	2.55	2.73	2.76
	99.18	97.91	99.31	100.21	99.77	100.74	99.72	101.29	100.44	100.95
O≡F	–	–	0.47	0.60	0.51	0.58	0.58	0.70	0.62	0.66
O≡Cl	–	–	0.02	0.02	0.01	0.02	–	0.02	–	0.02
TOTAL	99.18	97.91	98.82	99.59	99.25	100.14	99.14	100.57	99.82	100.27

*Calculated for charge balance.

QUANTITATIVE WDS RESULTS (NMNS)

Oxide Percents

	V40-9$_{rd}$	V41-1	V41-2	V41-3	V41-4	V41-5	V42-1	V42-2	V42-3	V42-4
SiO_2	36.61	37.11	36.69	37.36	36.92	36.85	36.91	36.60	37.34	36.85
Al_2O_3	15.35	15.12	14.37	14.98	14.92	14.57	14.22	13.99	14.13	14.17
TiO_2	0.48	0.08	0.09	0.07	0.11	0.07	0.36	0.37	0.37	0.38
MgO	2.85	3.14	3.23	3.14	3.00	3.04	3.81	3.88	3.86	3.80
MnO	0.32	0.07	0.09	0.09	0.06	0.00	0.00	0.00	0.00	0.00
FeO	5.60	4.34	5.00	4.37	4.75	4.87	3.93	3.92	3.99	3.98
Fe_2O_3	–	–	–	–	–	–	–	–	–	–
Cr_2O_3	–	0.00	0.00	0.00	0.00	0.00	–	–	–	–
CuO	–	–	–	–	–	–	–	–	–	–
ZnO	0.00	0.00	0.00	0.00	0.00	0.00	0.00	0.00	0.00	0.00
CaO	35.38	34.63	36.75	35.27	36.55	34.68	35.96	36.10	35.85	36.84
Na_2O	0.03	0.00	0.00	0.00	0.00	0.00	0.00	0.00	0.00	0.00
K_2O	0.00	–	–	–	–	–	0.00	0.00	0.00	0.00
La_2O_3	0.00	–	–	–	–	–	–	–	–	–
Ce_2O_3	0.00	0.00	0.00	0.00	0.00	0.00	–	–	–	–
Pr_2O_3	0.00	–	–	–	–	–	–	–	–	–
Nd_2O_3	0.00	–	–	–	–	–	–	–	–	–
Sm_2O_3	0.00	–	–	–	–	–	–	–	–	–
Eu_2O_3	0.00	–	–	–	–	–	–	–	–	–
Gd_2O_3	0.00	–	–	–	–	–	–	–	–	–
PbO	–	–	–	–	–	–	–	–	–	–
Bi_2O_3	–	–	–	–	–	–	–	–	–	–
ThO_2	–	–	–	–	–	–	–	–	–	–
UO_2	–	–	–	–	–	–	–	–	–	–
B_2O_3	–	–	–	0.00	–	–	0.00	–	–	–
SO_3	0.00	0.00	0.00	0.00	0.00	0.00	0.00	0.00	0.00	0.00
F	1.63	0.00	0.00	0.00	0.00	0.00	0.90	0.85	0.90	0.85
Cl	0.06	0.00	0.00	0.00	0.00	0.00	0.00	0.00	0.00	0.00
H_2O*	2.59	3.05	3.59	3.14	3.44	3.12	2.94	3.04	2.89	3.14
	100.90	97.54	99.81	98.42	99.75	97.20	99.04	98.76	99.33	100.01
O≡F	0.69	–	–	–	–	–	0.38	0.36	0.38	0.36
O≡Cl	0.01	–	–	–	–	–	–	–	–	–
TOTAL	100.20	97.54	99.81	98.42	99.75	97.20	98.66	98.40	98.95	99.65

*Calculated for charge balance.

QUANTITATIVE WDS RESULTS (NMNS)

Oxide Percents

	V42-5	V43-1	V43-2	V43-3	V43-4	V44-1	V44-2	V44-3	V44-4	$V45\text{-}1_r$
SiO_2	36.82	36.50	36.30	36.07	36.23	36.90	37.25	37.19	37.05	36.60
Al_2O_3	14.28	15.07	14.78	14.86	14.92	17.54	17.61	17.45	17.93	14.96
TiO_2	0.41	0.31	0.31	0.38	0.40	0.00	0.00	0.00	0.00	0.44
MgO	3.88	3.25	3.32	3.34	3.35	4.46	4.33	4.26	4.33	5.19
MnO	0.00	0.00	0.00	0.00	0.00	0.00	0.00	0.00	0.00	0.00
FeO	4.00	0.38	0.39	0.39	0.39	0.75	0.92	1.04	0.75	1.85
Fe_2O_3	–	5.04	5.21	5.15	5.17	–	–	–	–	–
Cr_2O_3	–	–	–	–	–	0.00	0.00	0.00	0.00	0.00
CuO	–	–	–	–	–	–	–	–	–	–
ZnO	0.00	0.00	0.00	0.00	0.00	0.00	0.00	0.00	0.00	0.00
CaO	35.92	35.44	36.58	35.76	36.03	36.51	34.85	36.44	34.82	37.15
Na_2O	0.00	0.00	0.00	0.00	0.00	0.00	0.00	0.00	0.00	0.00
K_2O	0.00	0.00	0.00	0.00	0.00	–	–	–	–	–
La_2O_3	–	–	0.00	–	–	–	–	–	–	0.00
Ce_2O_3	–	–	0.00	–	–	0.00	0.00	0.00	0.00	0.00
Pr_2O_3	–	–	0.00	–	–	–	–	–	–	0.00
Nd_2O_3	–	–	0.00	–	–	–	–	–	–	0.00
Sm_2O_3	–	–	0.00	–	–	–	–	–	–	0.00
Eu_2O_3	–	–	0.00	–	–	–	–	–	–	0.00
Gd_2O_3	–	–	0.00	–	–	–	–	–	–	0.00
PbO	–	–	–	–	–	–	–	–	–	–
Bi_2O_3	–	–	–	–	–	–	–	–	–	–
ThO_2	–	–	–	–	–	–	–	–	–	–
UO_2	–	–	–	–	–	–	–	–	–	–
B_2O_3	–	0.00	–	–	–	–	–	–	–	†
SO_3	0.00	0.00	0.00	0.00	0.00	0.31	0.28	0.45	0.25	0.18
F	0.77	0.00	0.00	0.00	0.00	0.44	0.64	0.61	0.48	0.73
Cl	0.00	0.00	0.00	0.00	0.00	0.00	0.00	0.00	0.00	0.00
H_2O^*	3.03	2.78	3.03	2.91	2.94	2.88	2.45	2.64	2.55	2.08
	99.11	98.77	99.92	98.86	99.43	99.79	98.33	100.08	98.16	100.65
O≡F	0.32	–	–	–	–	0.19	0.27	0.26	0.20	0.31
O≡Cl	–	–	–	–	–	–	–	–	–	–
TOTAL	98.79	98.77	99.92	98.86	99.43	99.60	98.06	99.82	97.96	100.34

*Calculated for charge balance. †Average value of 1.47 B_2O_3 used in calculations.

QUANTITATIVE WDS RESULTS (NMNS)

Oxide Percents

	V45-2_r	V45-3_r	V45-4_r	V45-5_r	V45-6_c	V45-7_c	V45-8_c	V46-1	V46-2	V46-3
SiO_2	36.59	36.57	36.50	36.46	35.91	36.32	36.06	36.32	37.26	36.69
Al_2O_3	15.24	15.02	15.00	15.21	14.53	13.94	14.42	12.67	15.41	14.43
TiO_2	0.45	0.49	0.44	0.45	1.24	1.74	0.99	5.06	0.88	0.26
MgO	5.00	5.12	5.15	4.96	5.25	4.89	5.28	3.79	4.81	4.74
MnO	0.07	0.00	0.00	0.00	0.07	0.06	0.07	0.06	0.07	0.10
FeO	2.24	2.02	2.16	2.02	2.18	2.09	2.18	0.68	0.46	0.97
Fe_2O_3	–	–	–	–	–	–	–	1.36	0.92	1.93
Cr_2O_3	0.00	0.00	0.00	0.00	0.00	0.00	0.00	0.00	0.00	0.00
CuO	–	–	–	–	–	–	–	–	–	–
ZnO	0.00	0.00	0.00	0.00	0.00	0.00	0.00	0.00	0.00	0.00
CaO	34.92	36.35	34.96	36.68	35.20	36.27	35.33	34.96	34.89	35.92
Na_2O	0.00	0.00	0.05	0.00	0.00	0.00	0.00	0.00	0.00	0.00
K_2O	–	–	–	–	–	–	–	–	–	–
La_2O_3	0.00	0.11	0.11	0.11	0.00	0.15	0.00	0.09	–	0.16
Ce_2O_3	0.14	0.24	0.18	0.17	0.13	0.30	0.13	0.25	0.00	0.33
Pr_2O_3	0.00	0.00	0.00	0.00	0.00	0.00	0.00	0.00	–	0.00
Nd_2O_3	0.00	0.00	0.00	0.00	0.00	0.00	0.00	0.17	–	0.00
Sm_2O_3	0.00	0.00	0.00	0.00	0.00	0.00	0.00	0.00	–	0.00
Eu_2O_3	0.00	0.00	0.00	0.00	0.00	0.00	0.00	0.00	–	0.00
Gd_2O_3	0.00	0.00	0.00	0.00	0.00	0.00	0.00	0.00	–	0.00
PbO	–	–	–	–	–	–	–	–	–	–
Bi_2O_3	–	–	–	–	–	–	–	–	–	–
ThO_2	–	–	–	–	–	–	–	–	–	–
UO_2	–	–	–	–	–	–	–	–	–	–
B_2O_3	1.62	1.07	†	†	1.71	1.46	†	–	–	–
SO_3	0.16	0.22	0.25	0.25	0.16	1.00	0.15	0.18	0.57	0.63
F	0.85	0.72	0.74	0.78	0.68	0.84	0.43	0.75	0.76	0.81
Cl	0.00	0.00	0.00	0.00	0.00	0.00	0.00	0.22	0.07	0.00
H_2O*	1.54	2.23	1.71	1.91	1.65	1.18	2.00	1.80	2.13	2.46
	98.82	100.16	98.72	100.48	98.72	100.23	98.51	98.37	98.23	99.43
O≡F	0.36	0.30	0.31	0.33	0.29	0.35	0.18	0.32	0.32	0.34
O≡Cl	–	–	–	–	–	–	–	0.05	0.02	–
TOTAL	98.46	99.86	98.41	100.15	98.43	99.88	98.33	98.00	97.89	99.09

*Calculated for charge balance. †Average value of 1.47 B_2O_3 used in calculations.

QUANTITATIVE WDS RESULTS (NMNS)

Oxide Percents

	V46-4	V46-5	V47-1	V47-2	V47-3	V48-1	V48-2	V48-3	V48-4	V49-1
SiO_2	37.35	37.01	36.82	36.59	36.83	36.66	36.61	37.05	36.75	36.97
Al_2O_3	15.19	15.55	16.75	16.22	16.73	17.34	17.24	17.86	16.96	18.54
TiO_2	1.33	1.00	1.57	2.23	1.63	0.53	0.68	0.53	0.77	0.00
MgO	4.58	4.97	1.51	1.52	1.59	1.96	1.89	1.91	2.05	2.00
MnO	0.10	0.09	0.09	0.00	0.07	0.22	0.30	0.21	0.08	0.95
FeO	0.48	0.42	3.83	3.81	3.71	1.57	1.73	1.41	2.07	1.10
Fe_2O_3	0.94	0.84	–	–	–	–	–	–	–	–
Cr_2O_3	0.00	0.00	–	–	–	–	–	–	–	–
CuO	–	–	–	–	–	0.94	0.88	0.86	0.81	0.44
ZnO	0.00	0.00	0.00	0.00	0.00	0.00	0.00	0.00	0.00	0.00
CaO	34.41	36.02	35.91	35.37	36.23	36.63	35.90	36.39	35.92	35.90
Na_2O	0.05	0.00	0.06	0.08	0.06	0.09	0.10	0.10	0.09	0.06
K_2O	–	–	0.00	0.00	0.00	0.00	0.00	0.00	0.00	0.00
La_2O_3	–	–	–	0.00	–	–	–	–	–	–
Ce_2O_3	0.00	0.00	0.00	0.17	0.00	0.00	0.00	0.00	0.00	0.00
Pr_2O_3	–	–	–	0.00	–	–	–	–	–	–
Nd_2O_3	–	–	–	0.00	–	–	–	–	–	–
Sm_2O_3	–	–	–	0.00	–	–	–	–	–	–
Eu_2O_3	–	–	–	0.00	–	–	–	–	–	–
Gd_2O_3	–	–	–	0.00	–	–	–	–	–	–
PbO	–	–	–	–	–	–	–	–	–	–
Bi_2O_3	–	–	–	–	–	–	–	–	–	–
ThO_2	–	–	–	–	–	–	–	–	–	–
UO_2	–	–	–	–	–	–	–	–	–	–
B_2O_3	–	–	–	–	–	–	–	–	–	–
SO_3	0.54	0.21	0.00	0.12	0.00	0.00	0.00	0.00	0.00	0.00
F	0.72	0.76	2.21	1.90	1.98	2.64	2.61	2.43	2.58	2.51
Cl	0.07	0.00	0.00	0.00	0.00	0.00	0.00	0.00	0.00	0.00
H_2O^*	2.00	2.65	1.72	1.64	1.88	1.73	1.62	1.71	1.65	1.67
	97.76	99.52	100.47	99.65	100.71	100.31	99.56	100.46	99.73	100.14
O≡F	0.30	0.32	0.93	0.80	0.83	1.11	1.10	1.02	1.09	1.06
O≡Cl	0.02	–	–	–	–	–	–	–	–	–
TOTAL	97.44	99.20	99.54	98.85	99.88	99.20	98.46	99.44	98.64	99.08

*Calculated for charge balance.

QUANTITATIVE WDS RESULTS (NMNS)

Oxide Percents

	V49-2	V49-3	V49-4	V49-5	V50-1	V50-2	V50-3	V50-4	V51-1	V51-2
SiO_2	36.75	37.00	37.04	37.29	35.49	35.84	35.56	35.98	37.49	37.24
Al_2O_3	18.62	18.67	19.00	19.20	13.86	13.80	14.09	13.84	17.92	17.62
TiO_2	0.00	0.00	0.00	0.00	0.00	0.00	0.00	0.00	0.09	0.16
MgO	2.17	1.96	1.94	1.75	4.22	3.70	4.22	4.15	1.87	2.10
MnO	0.68	0.90	0.74	0.61	3.11	3.51	3.10	3.80	0.12	0.10
FeO	0.41	0.76	0.54	0.19	1.26	2.29	1.18	1.27	2.91	2.99
Fe_2O_3	–	–	–	–	–	–	–	–	–	–
Cr_2O_3	–	–	–	–	–	–	–	–	–	–
CuO	0.56	0.54	0.51	0.69	0.13	0.00	0.00	0.00	–	–
ZnO	0.00	0.00	0.00	0.00	0.00	0.00	0.00	0.00	0.00	0.00
CaO	37.23	35.78	36.52	36.02	34.08	35.35	34.57	34.53	36.31	37.10
Na_2O	0.03	0.08	0.06	0.12	0.00	0.00	0.00	0.00	0.00	0.00
K_2O	0.00	0.00	0.00	0.00	0.00	0.00	0.00	0.00	0.00	0.00
La_2O_3	–	–	–	–	–	–	–	–	–	–
Ce_2O_3	0.00	0.00	0.00	0.00	0.00	0.00	0.00	0.00	0.00	0.00
Pr_2O_3	–	–	–	–	–	–	–	–	–	–
Nd_2O_3	–	–	–	–	–	–	–	–	–	–
Sm_2O_3	–	–	–	–	–	–	–	–	–	–
Eu_2O_3	–	–	–	–	–	–	–	–	–	–
Gd_2O_3	–	–	–	–	–	–	–	–	–	–
PbO	–	–	–	–	–	–	–	–	–	–
Bi_2O_3	–	–	–	–	2.49	0.66	2.14	0.48	–	–
ThO_2	–	–	–	–	–	–	–	–	–	–
UO_2	–	–	–	–	–	–	–	–	–	–
B_2O_3	–	–	–	–	–	–	–	–	–	–
SO_3	0.00	0.00	0.00	0.00	0.00	0.00	0.00	0.00	0.00	0.00
F	2.82	2.68	2.62	2.60	1.62	1.43	1.49	1.25	0.00	0.00
Cl	0.00	0.00	0.00	0.00	0.63	0.18	0.66	0.16	0.00	0.00
H_2O^*	1.69	1.52	1.61	1.45	2.52	2.95	2.63	2.89	2.85	3.08
	100.97	99.90	100.58	99.91	99.40	99.71	99.64	98.35	99.56	100.39
O≡F	1.19	1.13	1.10	1.09	0.68	0.60	0.63	0.53	–	–
O≡Cl	–	–	–	–	0.14	0.04	0.15	0.04	–	–
TOTAL	99.78	98.77	99.48	98.82	98.58	99.07	98.86	97.78	99.56	100.39

*Calculated for charge balance.

QUANTITATIVE WDS RESULTS (NMNS)

Oxide Percents

	V51-3	V52-1	V52-2	V52-3	V52-4	V53-1	V53-2	V53-3	V54-1	V54-2
SiO_2	37.10	35.41	35.65	35.72	35.68	34.25	34.08	34.90	36.35	36.27
Al_2O_3	17.87	10.83	11.69	12.32	11.58	11.70	11.69	12.37	15.48	15.36
TiO_2	0.10	1.43	0.66	0.58	1.14	2.81	2.80	3.09	0.72	0.51
MgO	1.89	4.39	4.41	4.54	4.31	1.82	1.83	1.76	3.33	3.14
MnO	0.10	0.26	0.24	0.24	0.29	0.17	0.20	0.17	0.00	0.00
FeO	3.08	6.95	6.68	5.92	6.50	7.38	7.43	6.60	4.10	4.52
Fe_2O_3	–	–	–	–	–	–	–	–	–	–
Cr_2O_3	–	–	–	–	–	–	–	–	0.00	0.00
CuO	–	–	–	–	–	–	–	–	–	–
ZnO	0.00	0.00	0.00	0.00	0.00	0.00	0.00	0.00	0.00	0.00
CaO	36.87	35.86	35.20	35.83	35.00	32.08	31.60	32.06	35.83	36.34
Na_2O	0.00	0.00	0.00	0.00	0.00	0.39	0.39	0.44	0.00	0.00
K_2O	0.00	0.00	0.00	0.00	0.00	0.00	0.00	0.00	–	–
La_2O_3	–	–	–	–	–	1.01	1.03	0.70	–	–
Ce_2O_3	0.00	0.00	0.00	0.00	0.00	1.83	1.81	1.46	0.00	0.00
Pr_2O_3	–	–	–	–	–	0.26	0.24	0.21	–	–
Nd_2O_3	–	–	–	–	–	0.45	0.34	0.39	–	–
Sm_2O_3	–	–	–	–	–	0.00	0.00	0.00	–	–
Eu_2O_3	–	–	–	–	–	0.00	0.00	0.00	–	–
Gd_2O_3	–	–	–	–	–	0.31	0.20	0.21	–	–
PbO	–	–	–	–	–	–	–	–	–	–
Bi_2O_3	–	–	–	–	–	–	–	–	–	–
ThO_2	–	–	–	–	–	1.43	1.50	†	–	–
UO_2	–	–	–	–	–	–	0.00	–	–	–
B_2O_3	–	–	–	–	–	–	–	–	–	–
SO_3	0.00	0.00	0.00	0.00	0.00	0.17	0.16	0.16	0.00	0.00
F	0.00	1.50	1.83	1.99	1.66	2.15	1.83	1.77	0.00	0.00
Cl	0.00	0.13	0.14	0.17	0.18	0.06	0.05	0.00	0.00	0.00
H_2O^*	3.03	3.24	2.98	2.95	2.92	1.81	1.92	1.81	3.32	3.45
	100.04	99.99	99.48	100.27	99.26	100.08	99.10	99.60	99.13	99.59
O≡F	–	0.63	0.77	0.84	0.70	0.91	0.77	0.75	–	–
O≡Cl	–	0.03	0.03	0.04	0.04	0.01	0.01	–	–	–
TOTAL	100.04	99.33	98.68	99.39	98.52	99.16	98.32	98.85	99.13	99.59

*Calculated for charge balance. †Average value of 1.47 ThO_2 used in calculations.

QUANTITATIVE WDS RESULTS (NMNS)

Oxide Percents

	V54-3	V54-4	V54-5	V55-1_c	V55-2_r	V56-1_l	V56-2_l	V56-3_d	V56-4_d	V57-1
SiO_2	35.80	36.46	35.73	36.71	36.49	34.57	34.77	35.01	35.25	36.87
Al_2O_3	15.97	15.36	14.95	16.44	16.31	11.63	11.85	12.13	12.18	16.62
TiO_2	0.59	0.56	0.62	1.01	1.54	0.54	0.47	0.43	0.41	0.29
MgO	3.06	3.06	3.24	1.30	1.19	4.20	4.18	4.84	4.84	3.51
MnO	0.00	0.00	0.00	0.22	0.22	0.22	0.22	0.13	0.13	0.00
FeO	3.78	4.39	4.60	4.55	4.63	3.85	3.83	3.67	3.60	2.29
Fe_2O_3	–	–	–	–	–	3.94	3.92	3.76	3.69	–
Cr_2O_3	0.00	0.00	0.00	–	–	–	–	–	–	0.00
CuO	–	–	–	–	–	–	–	–	–	–
ZnO	0.00	0.00	0.00	0.00	0.00	0.00	0.00	0.00	0.00	0.00
CaO	37.11	36.08	36.85	34.94	35.14	34.53	35.36	35.31	35.50	36.37
Na_2O	0.00	0.00	0.00	0.03	0.11	0.00	0.04	0.00	0.00	0.00
K_2O	–	–	–	0.00	0.00	0.00	0.00	0.00	0.00	–
La_2O_3	–	–	0.21	–	–	–	–	–	–	–
Ce_2O_3	0.00	0.00	0.20	0.00	0.00	–	–	–	–	0.00
Pr_2O_3	–	–	0.00	–	–	–	–	–	–	–
Nd_2O_3	–	–	0.00	–	–	–	–	–	–	–
Sm_2O_3	–	–	0.00	–	–	–	–	–	–	–
Eu_2O_3	–	–	0.00	–	–	–	–	–	–	–
Gd_2O_3	–	–	0.00	–	–	–	–	–	–	–
PbO	–	–	–	–	–	–	–	–	–	–
Bi_2O_3	–	–	–	–	–	–	–	–	–	–
ThO_2	–	–	–	–	–	–	–	–	–	–
UO_2	–	–	–	–	–	–	–	–	–	–
B_2O_3	0.00	–	–	0.00	–	2.66	2.82	3.18	3.09	–
SO_3	0.00	0.00	0.00	0.00	0.00	0.00	0.00	0.00	0.00	0.00
F	0.00	0.00	0.39	2.10	1.85	0.47	0.55	0.00	0.00	0.42
Cl	0.00	0.00	0.00	0.07	0.00	0.00	0.00	0.00	0.00	0.00
H_2O*	3.53	3.33	3.45	1.69	1.87	1.23	1.22	1.28	1.34	3.00
	99.84	99.24	100.23	99.06	99.35	97.85	99.23	99.74	100.03	99.38
O≡F	–	–	0.16	0.88	0.78	0.20	0.23	–	–	0.18
O≡Cl	–	–	–	0.02	–	–	–	–	–	–
TOTAL	99.84	99.24	100.07	98.16	98.57	97.65	99.00	99.74	100.03	99.20

*Calculated for charge balance.

QUANTITATIVE WDS RESULTS (NMNS)

Oxide Percents

	V57-2	V57-3	V57-4	V57-5	V57-6	V57-7	V57-8	V58-1	V58-2	V58-3
SiO_2	36.54	35.87	36.49	36.63	36.61	36.19	36.16	37.10	36.49	36.71
Al_2O_3	16.51	15.15	16.17	16.30	16.34	16.52	16.49	17.75	17.87	18.02
TiO_2	0.60	0.74	0.80	0.70	0.86	0.70	0.75	0.00	0.00	0.00
MgO	3.59	3.37	3.49	3.56	3.68	3.62	3.40	2.93	3.01	2.86
MnO	0.00	0.00	0.00	0.00	0.00	0.00	0.00	0.00	0.00	0.00
FeO	2.15	4.85	2.73	2.23	2.15	2.14	2.93	0.06	0.05	0.05
Fe_2O_3	–	–	–	–	–	–	–	1.10	0.96	0.87
Cr_2O_3	0.00	0.00	0.00	0.07	0.00	0.00	0.00	0.00	0.00	0.00
CuO	–	–	–	–	–	–	–	–	–	–
ZnO	0.00	0.00	0.00	0.00	0.00	0.00	0.00	0.00	0.00	0.00
CaO	37.64	35.43	38.31	36.35	37.86	36.23	37.73	37.17	35.91	37.14
Na_2O	0.00	0.00	0.00	0.00	0.00	0.00	0.00	0.00	0.00	0.00
K_2O	–	–	–	–	–	–	–	–	–	–
La_2O_3	–	–	–	–	–	–	–	–	–	–
Ce_2O_3	0.00	0.00	0.00	0.00	0.00	0.00	0.00	0.00	0.00	0.00
Pr_2O_3	–	–	–	–	–	–	–	–	–	–
Nd_2O_3	–	–	–	–	–	–	–	–	–	–
Sm_2O_3	–	–	–	–	–	–	–	–	–	–
Eu_2O_3	–	–	–	–	–	–	–	–	–	–
Gd_2O_3	–	–	–	–	–	–	–	–	–	–
PbO	–	–	–	–	–	–	–	–	–	–
Bi_2O_3	–	–	–	–	–	–	–	–	–	–
ThO_2	–	–	–	–	–	–	–	–	–	–
UO_2	–	–	–	–	–	–	–	–	–	–
B_2O_3	–	–	0.00	–	–	–	–	–	0.00	–
SO_3	0.00	0.00	0.00	0.00	0.00	0.00	0.00	0.00	0.00	0.00
F	0.41	0.00	0.00	0.54	0.39	0.44	0.50	0.00	0.00	0.00
Cl	0.00	0.00	0.00	0.00	0.00	0.00	0.00	0.00	0.00	0.00
H_2O^*	3.25	3.41	3.60	2.93	3.28	3.02	3.32	2.93	2.80	2.96
	100.68	98.82	101.59	99.32	101.17	98.87	101.28	99.04	97.09	98.61
O≡F	0.17	–	–	0.23	0.16	0.19	0.21	–	–	–
O≡Cl	–	–	–	–	–	–	–	–	–	–
TOTAL	100.51	98.82	101.59	99.09	101.01	98.68	101.07	99.04	97.09	98.61

*Calculated for charge balance.

QUANTITATIVE WDS RESULTS (NMNS)

Oxide Percents

	V59-1	V59-2	V59-3	V59-4	V59-5	V60-1	V60-2	V60-3	V60-4	V60-5
SiO_2	36.85	36.88	36.85	37.14	36.80	37.21	37.22	36.88	36.78	37.02
Al_2O_3	17.80	17.62	17.53	17.57	17.68	16.80	16.12	16.31	16.36	16.35
TiO_2	0.00	0.00	0.00	0.00	0.00	0.12	0.33	0.29	0.17	0.19
MgO	3.65	3.82	3.76	3.79	3.72	3.29	3.53	3.53	3.51	3.49
MnO	0.00	0.00	0.00	0.00	0.00	0.00	0.00	0.00	0.06	0.00
FeO	0.15	0.17	0.15	0.19	0.17	0.58	0.67	0.64	0.64	0.62
Fe_2O_3	0.93	0.96	0.94	1.13	1.07	2.79	3.26	3.09	3.16	3.00
Cr_2O_3	0.15	0.07	0.00	0.14	0.00	–	–	–	–	–
CuO	–	–	–	–	–	–	–	–	–	–
ZnO	0.00	0.00	0.00	0.00	0.00	0.00	0.00	0.00	0.00	0.00
CaO	36.89	36.41	37.75	36.74	37.87	35.29	35.54	35.43	35.95	35.90
Na_2O	0.00	0.00	0.00	0.00	0.00	0.00	0.00	0.00	0.00	0.00
K_2O	–	–	–	–	–	0.00	0.00	0.00	0.00	0.00
La_2O_3	–	–	–	–	–	–	–	–	–	–
Ce_2O_3	0.00	0.00	0.00	0.00	0.00	0.00	0.00	0.00	0.00	0.00
Pr_2O_3	–	–	–	–	–	–	–	–	–	–
Nd_2O_3	–	–	–	–	–	–	–	–	–	–
Sm_2O_3	–	–	–	–	–	–	–	–	–	–
Eu_2O_3	–	–	–	–	–	–	–	–	–	–
Gd_2O_3	–	–	–	–	–	–	–	–	–	–
PbO	–	–	–	–	–	–	–	–	–	–
Bi_2O_3	–	–	–	–	–	–	–	–	–	–
ThO_2	–	–	–	–	–	–	–	–	–	–
UO_2	–	–	–	–	–	–	–	–	–	–
B_2O_3	–	–	0.00	–	–	–	–	0.00	–	–
SO_3	0.00	0.00	0.00	0.00	0.00	0.13	0.17	0.14	0.15	0.00
F	0.00	0.00	0.00	0.00	0.00	0.00	0.00	0.00	0.00	0.00
Cl	0.00	0.00	0.00	0.00	0.00	0.05	0.00	0.00	0.00	0.00
H_2O*	3.10	3.05	3.28	3.08	3.30	2.63	2.70	2.75	2.86	2.90
	99.52	98.98	100.26	99.78	100.61	98.89	99.54	99.06	99.64	99.47
O≡F	–	–	–	–	–	–	–	–	–	–
O≡Cl	–	–	–	–	–	0.01	–	–	–	–
TOTAL	99.52	98.98	100.26	99.78	100.61	98.88	99.54	99.06	99.64	99.47

*Calculated for charge balance.

QUANTITATIVE WDS RESULTS (NMNS)

Oxide Percents

	V61-1	V61-2	V61-3	V61-4	V61-5	V62-1_c	V62-2	V62-3	V62-4	V62-5_{id}
SiO_2	35.72	35.59	35.82	36.22	35.89	36.93	36.71	36.89	36.98	36.85
Al_2O_3	12.20	12.65	13.30	12.54	12.51	16.17	16.09	16.21	16.17	16.80
TiO_2	0.54	0.63	0.46	0.58	0.61	0.65	0.64	0.63	0.87	0.59
MgO	4.98	4.81	4.81	4.84	4.94	3.64	3.65	3.69	3.61	3.47
MnO	0.08	0.09	0.10	0.11	0.10	0.00	0.06	0.07	0.06	0.06
FeO	1.28	1.24	1.10	1.20	1.23	2.47	2.56	2.49	2.33	2.11
Fe_2O_3	4.29	4.14	3.68	4.01	4.10	–	–	–	–	–
Cr_2O_3	0.00	0.00	0.00	0.00	0.00	–	–	–	–	–
CuO	–	–	–	–	–	–	–	–	–	–
ZnO	0.00	0.00	0.00	0.00	0.00	0.00	0.00	0.00	0.00	0.00
CaO	34.88	35.85	34.63	36.37	34.91	35.82	36.19	35.61	36.05	35.78
Na_2O	0.00	0.00	0.00	0.00	0.00	0.00	0.00	0.00	0.00	0.00
K_2O	–	–	–	–	–	0.00	0.00	0.00	0.00	0.00
La_2O_3	–	–	–	–	–	–	–	–	–	–
Ce_2O_3	0.00	0.00	0.00	0.00	0.00	0.00	0.00	0.00	0.00	0.00
Pr_2O_3	–	–	–	–	–	–	–	–	–	–
Nd_2O_3	–	–	–	–	–	–	–	–	–	–
Sm_2O_3	–	–	–	–	–	–	–	–	–	–
Eu_2O_3	–	–	–	–	–	–	–	–	–	–
Gd_2O_3	–	–	–	–	–	–	–	–	–	–
PbO	–	–	–	–	–	–	–	–	–	–
Bi_2O_3	–	–	–	–	–	–	–	–	–	–
ThO_2	–	–	–	–	–	–	–	–	–	–
UO_2	–	–	–	–	–	–	–	–	–	–
B_2O_3	†	1.44	†	†	†	–	–	–	–	–
SO_3	0.00	0.00	0.00	0.00	0.00	0.22	0.18	0.22	0.17	0.18
F	0.38	0.44	0.00	0.43	0.51	0.66	0.74	0.77	0.81	0.88
Cl	0.00	0.07	0.08	0.08	0.08	0.07	0.07	0.06	0.09	0.06
H_2O*	1.97	2.06	2.03	2.08	1.85	2.63	2.74	2.58	2.58	2.49
	97.76	99.02	97.45	99.90	99.17	99.27	99.63	99.21	99.72	99.27
O≡F	0.16	0.19	–	0.18	0.21	0.28	0.31	0.32	0.34	0.37
O≡Cl	–	0.02	0.02	0.02	0.02	0.02	0.02	0.01	0.02	0.01
TOTAL	97.60	98.81	97.43	99.70	97.94	98.97	99.30	98.88	99.36	98.89

*Calculated for charge balance. †Average value of 1.44 B_2O_3 used in calculations.

QUANTITATIVE WDS RESULTS (NMNS)

Oxide Percents

	V62-6_{id}	V62-7_{il}	V62-8_{il}	V62-9	V62-10	V62-11	V62-12_r	V63-1	V63-2	V63-3
SiO_2	36.82	37.24	36.97	37.12	37.25	36.89	37.09	36.30	36.63	36.90
Al_2O_3	16.49	16.25	16.27	16.58	16.45	16.30	16.48	16.96	16.76	16.88
TiO_2	0.54	0.88	0.90	0.41	0.61	0.48	0.48	0.51	0.36	0.50
MgO	3.58	3.40	3.35	3.54	3.46	3.54	3.53	1.45	1.61	1.66
MnO	0.00	0.07	0.10	0.07	0.00	0.07	0.06	0.62	0.53	0.53
FeO	2.41	2.23	2.40	2.32	2.39	2.36	2.38	2.99	3.17	2.97
Fe_2O_3	–	–	–	–	–	–	–	1.03	1.10	1.03
Cr_2O_3	–	–	–	–	–	–	–	0.00	0.00	0.00
CuO	–	–	–	–	–	–	–	–	–	–
ZnO	0.00	0.00	0.00	0.00	0.00	0.00	0.00	0.00	0.00	0.00
CaO	36.46	35.96	36.11	35.79	36.05	35.53	36.43	34.83	35.79	34.47
Na_2O	0.00	0.00	0.00	0.00	0.00	0.00	0.00	0.15	0.10	0.11
K_2O	0.00	0.00	0.00	0.00	0.00	0.00	0.00	–	–	–
La_2O_3	–	–	–	–	–	–	–	–	–	–
Ce_2O_3	0.00	0.00	0.00	0.00	0.00	0.00	0.00	0.00	0.00	0.00
Pr_2O_3	–	–	–	–	–	–	–	–	–	–
Nd_2O_3	–	–	–	–	–	–	–	–	–	–
Sm_2O_3	–	–	–	–	–	–	–	–	–	–
Eu_2O_3	–	–	–	–	–	–	–	–	–	–
Gd_2O_3	–	–	–	–	–	–	–	–	–	–
PbO	–	–	–	–	–	–	–	–	–	–
Bi_2O_3	–	–	–	–	–	–	–	–	–	–
ThO_2	–	–	–	–	–	–	–	–	–	–
UO_2	–	–	–	–	–	–	–	–	–	–
B_2O_3	–	0.00	–	–	–	–	–	–	–	–
SO_3	0.18	0.20	0.15	0.26	0.25	0.28	0.35	0.00	0.00	0.00
F	0.76	0.76	0.66	0.60	0.73	0.56	0.63	2.15	2.48	2.06
Cl	0.06	0.06	0.09	0.07	0.07	0.05	0.05	0.00	0.00	0.00
H_2O^*	2.74	2.48	2.63	2.60	2.53	2.58	2.64	1.74	1.75	1.65
	100.03	99.52	99.63	99.36	99.80	98.65	100.12	98.74	100.32	98.77
O≡F	0.32	0.32	0.28	0.25	0.31	0.24	0.27	0.91	1.08	0.87
O≡Cl	0.01	0.01	0.02	0.02	0.02	0.01	0.01	–	–	–
TOTAL	99.70	99.19	99.33	99.09	99.47	98.40	99.84	97.83	99.24	97.90

*Calculated for charge balance.

QUANTITATIVE WDS RESULTS (NMNS)

Oxide Percents

	V63-4	V63-5	V63-6	V63-7	V64-1	V64-2	V64-3	V64-4	V64-5	V65-1
SiO_2	36.36	36.30	36.26	36.45	36.63	36.23	36.54	36.87	37.27	37.10
Al_2O_3	16.97	16.59	16.83	17.08	16.03	16.21	16.54	17.01	17.27	17.38
TiO_2	0.50	0.52	0.61	0.34	1.08	1.25	0.93	0.74	0.00	1.67
MgO	1.49	1.73	1.50	1.60	1.80	1.56	1.63	1.47	1.67	1.37
MnO	0.52	0.58	0.62	0.49	0.72	0.72	0.57	0.42	0.47	0.06
FeO	2.96	2.97	3.05	2.99	4.43	4.28	4.38	3.55	3.79	2.98
Fe_2O_3	1.03	1.03	1.06	1.03	–	–	–	–	–	–
Cr_2O_3	0.00	0.00	0.00	0.00	0.00	0.00	0.00	0.00	0.00	0.00
CuO	–	–	–	–	–	–	–	–	–	–
ZnO	0.00	0.00	0.00	0.00	0.00	0.00	0.00	0.00	0.00	0.00
CaO	35.61	34.83	35.83	34.56	35.05	36.04	34.74	36.39	35.25	34.53
Na_2O	0.14	0.10	0.13	0.11	0.09	0.12	0.10	0.14	0.10	0.13
K_2O	–	–	–	–	–	–	–	–	–	–
La_2O_3	–	–	–	–	–	–	–	–	–	–
Ce_2O_3	0.00	0.00	0.00	0.00	0.00	0.00	0.00	0.00	0.00	0.00
Pr_2O_3	–	–	–	–	–	–	–	–	–	–
Nd_2O_3	–	–	–	–	–	–	–	–	–	–
Sm_2O_3	–	–	–	–	–	–	–	–	–	–
Eu_2O_3	–	–	–	–	–	–	–	–	–	–
Gd_2O_3	–	–	–	–	–	–	–	–	–	–
PbO	–	–	–	–	–	–	–	–	–	–
Bi_2O_3	–	–	–	–	–	–	–	–	–	–
ThO_2	–	–	–	–	–	–	–	–	–	–
UO_2	–	–	–	–	–	–	–	–	–	–
B_2O_3	0.00	–	–	–	–	–	0.00	–	–	–
SO_3	0.00	0.00	0.00	0.00	0.00	0.00	0.00	0.00	0.00	0.00
F	2.16	2.28	2.18	2.31	2.43	2.24	2.21	2.28	2.38	1.62
Cl	0.00	0.00	0.00	0.00	0.07	0.12	0.00	0.00	0.08	0.00
H_2O^*	1.86	1.70	1.91	1.61	1.77	2.00	1.81	1.90	1.72	1.60
	99.60	98.63	99.98	98.57	100.10	100.77	99.45	100.77	100.00	98.44
O≡F	0.91	0.96	0.92	0.97	1.02	0.94	0.93	0.96	1.00	0.68
O≡Cl	–	–	–	–	0.02	0.03	–	–	0.02	–
TOTAL	98.69	97.67	99.06	97.61	99.06	99.80	98.52	99.81	98.98	97.76

*Calculated for charge balance.

QUANTITATIVE WDS RESULTS (NMNS)

Oxide Percents

	V65-2	V65-3	V65-4	V65-5	V65-6	V66-1	V66-2	V66-3	V66-4	V66-5
SiO_2	37.13	37.44	36.83	37.14	37.20	35.91	35.64	35.57	35.99	36.06
Al_2O_3	17.29	16.84	17.28	17.14	17.34	16.35	15.96	15.87	16.10	16.83
TiO_2	1.70	1.72	1.68	1.66	1.62	0.05	0.00	0.05	0.06	0.00
MgO	1.47	1.73	1.45	1.38	1.35	0.88	0.93	0.91	0.84	0.87
MnO	0.06	0.07	0.07	0.07	0.07	1.83	1.97	1.97	1.77	1.68
FeO	2.82	3.05	2.78	2.91	3.02	2.19	2.29	2.40	2.30	1.53
Fe_2O_3	–	–	–	–	–	–	–	–	–	–
Cr_2O_3	0.00	0.00	0.00	0.00	0.00	0.00	0.00	0.00	0.00	0.00
CuO	–	–	–	–	–	0.46	0.44	0.46	0.41	0.63
ZnO	0.00	0.00	0.00	0.00	0.00	2.20	2.32	2.35	2.29	2.16
CaO	36.10	34.55	35.42	34.29	35.51	35.02	34.16	35.44	33.94	35.66
Na_2O	0.12	0.11	0.11	0.11	0.11	0.00	0.00	0.00	0.00	0.00
K_2O	–	–	–	–	–	–	–	–	–	–
La_2O_3	–	–	–	–	–	–	–	–	–	–
Ce_2O_3	0.00	0.00	0.00	0.00	0.00	0.00	0.00	0.00	0.00	0.00
Pr_2O_3	–	–	–	–	–	–	–	–	–	–
Nd_2O_3	–	–	–	–	–	–	–	–	–	–
Sm_2O_3	–	–	–	–	–	–	–	–	–	–
Eu_2O_3	–	–	–	–	–	–	–	–	–	–
Gd_2O_3	–	–	–	–	–	–	–	–	–	–
PbO	–	–	–	–	–	–	–	–	–	–
Bi_2O_3	–	–	–	–	–	–	–	–	–	–
ThO_2	–	–	–	–	–	–	–	–	–	–
UO_2	–	–	–	–	–	–	–	–	–	–
B_2O_3	–	–	–	–	–	–	–	0.00	–	–
SO_3	0.00	0.00	0.00	0.12	0.00	0.00	0.00	0.00	0.00	0.00
F	1.55	1.54	1.57	1.56	1.62	1.28	1.34	1.34	1.27	1.23
Cl	0.00	0.00	0.00	0.00	0.00	0.00	0.00	0.00	0.00	0.00
H_2O*	1.91	1.67	1.80	1.48	1.76	2.42	2.32	2.57	2.21	2.45
	100.14	98.72	98.99	97.86	99.60	98.59	97.37	98.93	97.18	99.10
O≡F	0.65	0.65	0.66	0.66	0.68	0.54	0.56	0.56	0.53	0.52
O≡Cl	–	–	–	–	–	–	–	–	–	–
TOTAL	99.49	98.07	98.33	97.20	98.92	98.05	96.81	98.37	96.65	98.58

*Calculated for charge balance.

QUANTITATIVE WDS RESULTS (NMNS)

Oxide Percents

	V66-6	V67-1	V67-2	V67-3	V67-4	V67-5	V67-6	V67-7	V68-1	V68-2
SiO_2	36.12	34.93	36.09	35.37	35.14	35.55	35.21	35.95	36.94	36.63
Al_2O_3	16.48	19.34	16.63	17.35	18.34	17.52	18.12	17.10	17.43	17.52
TiO_2	0.04	0.00	0.05	0.00	0.00	0.00	0.00	0.00	0.00	0.00
MgO	0.88	1.07	1.19	3.89	3.47	1.71	2.67	1.30	4.27	3.84
MnO	1.92	1.27	1.23	1.59	1.42	1.56	1.44	1.53	0.00	0.00
FeO	1.91	0.94	1.41	0.66	0.27	0.81	0.38	0.93	1.12	1.23
Fe_2O_3	–	–	–	–	–	–	–	–	–	–
Cr_2O_3	0.00	–	–	–	–	–	–	–	–	–
CuO	0.43	1.49	1.55	0.67	0.32	1.13	0.66	1.34	–	–
ZnO	2.27	1.53	1.47	1.87	1.73	1.62	1.65	1.43	0.00	0.00
CaO	34.14	34.24	35.06	31.26	31.84	33.67	32.98	34.56	36.03	36.62
Na_2O	0.00	0.00	0.00	0.00	0.00	0.00	0.00	0.00	0.00	0.00
K_2O	–	0.00	0.00	0.04	0.03	0.00	0.00	0.00	0.00	0.00
La_2O_3	–	–	–	–	–	–	–	–	–	–
Ce_2O_3	0.00	0.00	0.00	0.00	0.00	0.00	0.00	0.00	0.00	0.00
Pr_2O_3	–	–	–	–	–	–	–	–	–	–
Nd_2O_3	–	–	–	–	–	–	–	–	–	–
Sm_2O_3	–	–	–	–	–	–	–	–	–	–
Eu_2O_3	–	–	–	–	–	–	–	–	–	–
Gd_2O_3	–	–	–	–	–	–	–	–	–	–
PbO	–	0.86	0.31	2.01	2.06	1.57	2.03	1.06	–	–
Bi_2O_3	–	–	–	–	–	–	–	–	–	–
ThO_2	–	–	–	–	–	–	–	–	–	–
UO_2	–	–	–	–	–	–	–	–	–	–
B_2O_3	–	–	–	–	–	–	–	–	–	0.00
SO_3	0.00	0.00	0.00	0.00	0.00	0.00	0.00	0.00	0.18	0.27
F	1.26	1.57	1.81	1.15	1.33	1.03	1.37	1.52	0.00	0.00
Cl	0.00	0.00	0.00	0.00	0.00	0.00	0.00	0.00	0.00	0.00
H_2O^*	2.22	2.22	2.10	2.50	2.32	2.43	2.33	2.19	3.08	3.08
	97.67	99.45	98.90	98.35	98.27	98.60	98.84	98.91	99.05	99.19
O≡F	0.53	0.66	0.76	0.48	0.56	0.43	0.58	0.64	–	–
O≡Cl	–	–	–	–	–	–	–	–	–	–
TOTAL	97.14	98.79	98.14	97.87	97.71	98.17	98.26	98.27	99.05	99.19

*Calculated for charge balance.

V67 includes 0.06 BeO.

QUANTITATIVE WDS RESULTS (NMNS)

Oxide Percents

	V68-3	V68-4	V68-5	V69-1	V69-2	V69-3	V70-1_{1c}	V70-2_{1r}	V70-3_2	V71-1
SiO_2	36.75	37.31	37.26	36.88	36.54	36.84	36.82	37.20	36.43	36.61
Al_2O_3	17.36	17.46	17.30	16.33	16.59	16.19	15.52	15.42	15.51	15.27
TiO_2	0.00	0.00	0.00	2.76	2.68	2.75	2.45	2.33	2.40	0.05
MgO	4.28	4.21	4.07	1.76	1.71	1.93	1.82	1.81	1.83	3.10
MnO	0.00	0.00	0.00	0.00	0.08	0.00	0.09	0.07	0.07	0.12
FeO	1.13	1.12	1.05	2.74	2.73	2.77	3.28	3.22	3.22	4.45
Fe_2O_3	–	–	–	–	–	–	1.22	1.24	1.19	–
Cr_2O_3	–	–	–	–	–	–	–	–	–	–
CuO	–	–	–	–	–	–	–	–	–	–
ZnO	0.00	0.00	0.00	0.00	0.00	0.00	0.00	0.00	0.00	0.00
CaO	36.04	35.60	36.50	36.28	35.61	36.32	34.81	34.86	34.70	36.20
Na_2O	0.00	0.00	0.00	0.09	0.09	0.08	0.29	0.25	0.24	0.00
K_2O	0.00	0.00	0.00	0.00	0.00	0.00	0.00	0.00	0.00	0.00
La_2O_3	–	–	–	–	–	–	–	–	–	–
Ce_2O_3	0.00	0.00	0.00	0.00	0.00	0.00	0.00	0.00	0.00	0.00
Pr_2O_3	–	–	–	–	–	–	–	–	–	–
Nd_2O_3	–	–	–	–	–	–	–	–	–	–
Sm_2O_3	–	–	–	–	–	–	–	–	–	–
Eu_2O_3	–	–	–	–	–	–	–	–	–	–
Gd_2O_3	–	–	–	–	–	–	–	–	–	–
PbO	–	–	–	–	–	–	–	–	–	–
Bi_2O_3	–	–	–	–	–	–	–	–	–	–
ThO_2	–	–	–	–	–	–	–	–	–	–
UO_2	–	–	–	–	–	–	–	–	–	–
B_2O_3	–	–	–	–	–	–	0.00	–	–	–
SO_3	0.13	0.00	0.63	0.14	0.00	0.22	0.00	0.00	0.00	0.00
F	0.00	0.00	0.00	1.76	1.67	1.91	2.38	2.33	2.83	0.00
Cl	0.00	0.00	0.00	0.34	0.30	0.37	0.07	0.07	0.08	0.00
H_2O*	3.15	3.06	2.76	1.60	1.68	1.52	1.47	1.42	1.25	3.42
	98.84	98.76	99.57	100.68	99.68	100.89	100.22	100.23	99.75	99.22
O≡F	–	–	–	0.74	0.70	0.80	1.00	0.98	1.19	–
O≡Cl	–	–	–	0.08	0.07	0.08	0.02	0.02	0.02	–
TOTAL	98.84	98.76	99.57	99.86	98.91	100.01	99.20	99.23	98.54	99.22

*Calculated for charge balance.

QUANTITATIVE WDS RESULTS (NMNS)

Oxide Percents

	V71-2	V71-3	V71-4	V71-5	V72-1	V72-2	V72-3	V72-4	V72-5	V72-6
SiO_2	37.06	36.71	37.11	37.22	36.48	36.87	36.49	36.57	36.69	36.98
Al_2O_3	15.12	15.20	15.27	15.02	15.19	14.87	15.76	15.40	15.78	18.43
TiO_2	0.04	0.00	0.05	0.00	1.25	1.21	0.84	1.01	0.88	0.80
MgO	3.12	3.15	3.12	3.23	2.12	2.14	1.91	2.00	1.90	1.69
MnO	0.13	0.13	0.10	0.11	0.56	0.52	0.33	0.32	0.29	0.27
FeO	4.65	4.27	4.25	4.70	4.74	4.99	4.42	4.60	4.45	4.04
Fe_2O_3	–	–	–	–	–	–	–	–	–	–
Cr_2O_3	–	–	–	–	0.00	0.00	0.00	0.00	0.00	0.00
CuO	–	–	–	–	–	–	–	–	–	–
ZnO	0.00	0.00	0.00	0.00	0.00	0.00	0.00	0.00	0.00	0.00
CaO	35.80	36.26	35.89	36.67	33.53	34.85	33.75	35.47	35.10	27.70
Na_2O	0.00	0.00	0.00	0.00	0.06	0.00	0.00	0.00	0.05	0.06
K_2O	0.00	0.00	0.00	0.00	–	–	–	–	–	–
La_2O_3	–	–	–	–	–	–	–	–	–	–
Ce_2O_3	0.00	0.00	0.00	0.00	0.00	0.00	0.00	0.00	0.00	0.00
Pr_2O_3	–	–	–	–	–	–	–	–	–	–
Nd_2O_3	–	–	–	–	–	–	–	–	–	–
Sm_2O_3	–	–	–	–	–	–	–	–	–	–
Eu_2O_3	–	–	–	–	–	–	–	–	–	–
Gd_2O_3	–	–	–	–	–	–	–	–	–	–
PbO	–	–	–	–	–	–	–	–	–	–
Bi_2O_3	–	–	–	–	–	–	–	–	–	–
ThO_2	–	–	–	–	0.00	0.00	0.00	0.00	0.00	0.00
UO_2	–	–	–	–	0.00	0.00	0.00	0.00	0.00	0.00
B_2O_3	0.00	–	–	–	–	–	–	–	–	–
SO_3	0.00	0.00	0.00	0.00	0.12	0.00	0.00	0.00	0.00	0.00
F	0.00	0.00	0.00	0.00	2.55	2.23	2.56	2.65	2.70	1.56
Cl	0.00	0.00	0.00	0.00	0.08	0.15	0.20	0.27	0.22	0.13
H_2O^*	3.32	3.41	3.27	3.49	1.42	1.82	1.39	1.65	1.56	0.65
	99.24	99.13	99.06	100.44	98.10	99.64	97.65	99.94	99.62	91.92
O≡F	–	–	–	–	1.07	0.94	1.08	1.12	1.14	0.66
O≡Cl	–	–	–	–	0.02	0.03	0.05	0.06	0.05	0.03
TOTAL	99.24	99.13	99.06	100.44	97.01	98.67	96.52	98.76	98.43	91.23

*Calculated for charge balance.

QUANTITATIVE WDS RESULTS (NMNS)

Oxide Percents

	V72-7	V73-1	V73-2	V73-3	V74-1$_r$	V74-2	V74-3	V74-4	V74-5	V74-6
SiO_2	46.03	36.29	36.33	35.84	35.69	35.52	35.52	35.95	35.99	36.26
Al_2O_3	19.57	13.33	13.24	13.51	12.25	11.87	12.05	11.85	11.84	11.79
TiO_2	1.23	0.00	0.00	0.00	0.99	1.02	0.71	0.95	0.93	0.93
MgO	1.70	3.80	3.96	3.92	6.29	6.43	6.45	6.54	6.59	6.64
MnO	0.34	0.19	0.17	0.20	0.00	0.00	0.00	0.06	0.06	0.07
FeO	5.45	5.48	5.24	5.31	1.16	1.22	1.24	1.22	1.22	1.22
Fe_2O_3	–	–	–	–	2.18	2.29	2.34	2.29	2.30	2.29
Cr_2O_3	0.00	–	–	–	–	–	–	–	–	–
CuO	–	–	–	–	–	–	–	–	–	–
ZnO	0.00	0.00	0.00	0.00	0.00	0.00	0.00	0.00	0.00	0.00
CaO	3.96	35.47	36.24	35.62	35.67	35.52	35.42	35.27	35.89	35.39
Na_2O	0.59	0.00	0.00	0.00	0.00	0.00	0.00	0.00	0.00	0.00
K_2O	0.35	0.00	0.00	0.00	0.00	0.00	0.00	0.00	0.00	0.00
La_2O_3	–	–	–	–	0.00	0.08	0.00	0.00	0.11	0.11
Ce_2O_3	0.09	0.00	0.00	0.00	0.12	0.11	0.16	0.19	0.16	0.20
Pr_2O_3	–	–	–	–	0.00	0.00	0.00	0.00	0.00	0.00
Nd_2O_3	–	–	–	–	0.00	0.00	0.00	0.00	0.00	0.00
Sm_2O_3	–	–	–	–	0.00	0.00	0.00	0.00	0.00	0.00
Eu_2O_3	–	–	–	–	0.00	0.00	0.00	0.00	0.00	0.00
Gd_2O_3	–	–	–	–	0.00	0.00	0.00	0.00	0.00	0.00
PbO	–	–	–	–	–	–	–	–	–	–
Bi_2O_3	–	–	–	–	–	–	–	–	–	–
ThO_2	0.00	–	–	–	–	–	–	–	–	–
UO_2	0.00	–	–	–	–	–	–	–	–	–
B_2O_3	–	–	–	–	3.05	†	†	†	3.02	†
SO_3	0.00	0.00	0.00	0.00	0.00	0.00	0.00	0.00	0.18	0.00
F	0.00	2.13	2.04	1.92	0.49	0.00	0.00	0.00	0.50	0.00
Cl	0.00	0.16	0.21	0.19	0.00	0.00	0.00	0.00	0.00	0.00
H_2O*	-3.32	2.57	2.74	2.76	1.04	1.46	1.49	1.40	1.03	1.41
	75.99	99.43	100.17	99.27	98.93	98.36	98.22	98.56	99.82	99.15
O≡F	–	0.90	0.86	0.81	0.21	–	–	–	0.21	–
O≡Cl	–	0.04	0.05	0.04	–	–	–	–	–	–
TOTAL	75.99	98.49	99.26	98.42	98.72	98.36	98.22	98.56	99.61	99.15

*Calculated for charge balance. †Average value of 2.84 B_2O_3 used in calculations.

V74 includes 0.03 BeO.

QUANTITATIVE WDS RESULTS (NMNS)

Oxide Percents

	V74-7	V74-8	V74-9	V74-10	V74-11	V74-12	V74-13	V74-14	V74-15	V74-16
SiO_2	36.00	36.01	35.84	36.46	36.28	35.92	35.82	36.01	36.36	35.82
Al_2O_3	11.45	11.42	11.82	11.71	11.66	11.61	11.63	11.63	11.63	11.63
TiO_2	0.93	0.90	0.87	0.89	0.90	0.93	0.85	0.89	0.88	0.88
MgO	6.68	6.67	6.62	6.60	6.62	6.57	6.69	6.63	6.63	6.56
MnO	0.00	0.08	0.00	0.00	0.00	0.00	0.00	0.00	0.00	0.00
FeO	1.23	1.24	1.21	1.23	1.24	1.25	1.24	1.21	1.24	1.22
Fe_2O_3	2.31	2.34	2.27	2.31	2.33	2.35	2.34	2.27	2.34	2.29
Cr_2O_3	–	–	–	–	–	–	–	–	–	–
CuO	–	–	–	–	–	–	–	–	–	–
ZnO	0.00	0.00	0.00	0.00	0.00	0.00	0.00	0.00	0.00	0.00
CaO	35.63	35.54	35.87	35.53	35.86	35.74	35.62	35.67	35.45	35.41
Na_2O	0.00	0.00	0.00	0.00	0.00	0.00	0.00	0.00	0.00	0.00
K_2O	0.00	0.00	0.00	0.00	0.00	0.00	0.00	0.00	0.00	0.00
La_2O_3	0.11	0.11	0.18	0.13	0.11	0.12	0.14	0.16	0.14	0.13
Ce_2O_3	0.26	0.27	0.27	0.25	0.25	0.26	0.25	0.24	0.24	0.23
Pr_2O_3	0.00	0.00	0.00	0.00	0.00	0.00	0.00	0.00	0.00	0.00
Nd_2O_3	0.00	0.00	0.00	0.00	0.00	0.00	0.00	0.00	0.00	0.00
Sm_2O_3	0.00	0.00	0.00	0.00	0.00	0.00	0.00	0.00	0.00	0.00
Eu_2O_3	0.00	0.00	0.00	0.00	0.00	0.00	0.00	0.00	0.00	0.00
Gd_2O_3	0.00	0.00	0.00	0.00	0.00	0.00	0.00	0.00	0.00	0.00
PbO	–	–	–	–	–	–	–	–	–	–
Bi_2O_3	–	–	–	–	–	–	–	–	–	–
ThO_2	–	–	–	–	–	–	–	–	–	–
UO_2	–	–	–	–	–	–	–	–	–	–
B_2O_3	†	†	†	2.40	†	†	†	†	2.79	†
SO_3	0.23	0.21	0.21	0.24	0.21	0.25	0.26	0.19	0.30	0.30
F	0.00	0.00	0.00	0.00	0.00	0.00	0.00	0.42	0.00	0.00
Cl	0.00	0.00	0.05	0.00	0.00	0.00	0.00	0.00	0.00	0.00
H_2O^*	1.33	1.34	1.39	1.58	1.34	1.33	1.35	1.16	1.24	1.24
	99.00	98.97	99.44	99.33	99.64	99.17	99.03	99.32	99.24	98.55
O≡F	–	–	–	–	–	–	–	0.18	–	–
O≡Cl	–	–	0.01	–	–	–	–	–	–	–
TOTAL	99.00	98.97	99.43	99.33	99.64	99.17	99.03	99.14	99.24	98.55

*Calculated for charge balance. †Average value of 2.84 B_2O_3 used in calculations.

V74 includes 0.03 BeO.

QUANTITATIVE WDS RESULTS (NMNS)

Oxide Percents

	V74-17	V74-18	V74-19	V74-20	V74-21	V74-22	V74-23	V74-24	$V74\text{-}25_r$	V75-1
SiO_2	36.14	36.17	35.88	36.11	36.42	35.86	35.78	35.92	35.94	35.46
Al_2O_3	11.67	11.59	11.99	12.03	11.90	11.84	11.87	11.98	11.81	18.97
TiO_2	0.84	0.82	0.74	0.80	0.55	1.00	1.25	0.99	1.13	0.05
MgO	6.64	6.67	6.52	6.48	6.46	6.43	6.36	6.48	6.42	3.21
MnO	0.00	0.00	0.00	0.00	0.00	0.00	0.09	0.00	0.06	0.00
FeO	1.26	1.24	1.20	1.21	1.36	1.22	1.21	1.21	1.22	0.17
Fe_2O_3	2.37	2.33	2.26	2.28	2.56	2.29	2.28	2.26	2.29	0.51
Cr_2O_3	–	–	–	–	–	–	–	–	–	–
CuO	–	–	–	–	–	–	–	–	–	–
ZnO	0.00	0.00	0.00	0.00	0.00	0.00	0.00	0.00	0.00	0.00
CaO	36.03	35.43	35.98	35.54	35.43	35.58	35.84	35.75	35.99	35.76
Na_2O	0.00	0.00	0.00	0.00	0.00	0.00	0.00	0.00	0.00	0.00
K_2O	0.00	0.00	0.00	0.00	0.00	0.00	0.00	0.00	0.00	0.00
La_2O_3	0.14	0.12	0.09	0.00	0.10	0.00	0.00	0.00	0.00	–
Ce_2O_3	0.28	0.31	0.17	0.18	0.19	0.19	0.13	0.11	0.14	0.00
Pr_2O_3	0.00	0.00	0.00	0.00	0.00	0.00	0.00	0.00	0.00	–
Nd_2O_3	0.00	0.00	0.00	0.00	0.00	0.00	0.00	0.00	0.00	–
Sm_2O_3	0.00	0.00	0.00	0.00	0.00	0.00	0.00	0.00	0.00	–
Eu_2O_3	0.00	0.00	0.00	0.00	0.00	0.00	0.00	0.00	0.00	–
Gd_2O_3	0.00	0.00	0.00	0.00	0.00	0.00	0.00	0.00	0.00	–
PbO	–	–	–	–	–	–	–	–	–	–
Bi_2O_3	–	–	–	–	–	–	–	–	–	–
ThO_2	–	–	–	–	–	–	–	–	–	–
UO_2	–	–	–	–	–	–	–	–	–	–
B_2O_3	†	†	†	3.06	†	†	†	†	2.66	–
SO_3	0.30	0.29	0.14	0.00	0.00	0.00	0.12	0.00	0.00	0.00
F	0.00	0.49	0.00	0.00	0.00	0.00	0.00	0.00	0.39	0.00
Cl	0.00	0.00	0.00	0.00	0.00	0.00	0.00	0.00	0.00	0.00
H_2O^*	1.34	1.01	1.45	1.25	1.41	1.43	1.38	1.47	1.44	2.99
	99.85	99.32	99.26	98.94	99.22	98.68	99.15	99.01	99.49	97.12
O≡F	–	0.21	–	–	–	–	–	–	0.16	–
O≡Cl	–	–	–	–	–	–	–	–	–	–
TOTAL	99.85	99.11	99.26	98.94	99.22	98.68	99.15	99.01	99.33	97.12

*Calculated for charge balance. †Average value of 2.84 B_2O_3 used in calculations.

V74 includes 0.03 BeO.

QUANTITATIVE WDS RESULTS (NMNS)

Oxide Percents

	V75-2	V75-3
SiO_2	35.80	36.57
Al_2O_3	17.54	17.46
TiO_2	0.00	0.00
MgO	3.69	3.53
MnO	0.06	0.00
FeO	0.21	0.17
Fe_2O_3	0.63	0.56
Cr_2O_3	–	–
CuO	–	–
ZnO	0.00	0.00
CaO	37.15	36.74
Na_2O	0.00	0.00
K_2O	0.00	0.00
La_2O_3	–	–
Ce_2O_3	0.00	0.00
Pr_2O_3	–	–
Nd_2O_3	–	–
Sm_2O_3	–	–
Eu_2O_3	–	–
Gd_2O_3	–	–
PbO	–	–
Bi_2O_3	–	–
ThO_2	–	–
UO_2	–	–
B_2O_3	0.00	–
SO_3	0.00	0.00
F	0.00	0.00
Cl	0.00	0.00
H_2O^*	3.30	3.07
	98.38	98.10
$O \equiv F$	–	–
$O \equiv Cl$	–	–
TOTAL	98.38	98.10

*Calculated for charge balance.

Appendix E.2

WDS ANALYSES OF VESUVIANITE (NMNS)

Ions p.f.u. (50-Cation Normalization)

ABBREVIATIONS USED IN APPENDIX E.2

(c): centre of grain
(r): rim of grain
(i): intermediate between core and rim
(d): dark in BSE image
(l): light in BSE image

ΣX : (Ca+Na+K+REE+Pb+Bi+Th+U)
ΣY : (Al+Ti+Mg+Mn+Fe+Cr+Cu+Zn)
ΣZ : (Si)

Subscripted numbers refer to different grains. The analyses are normalized to 50-cations (less B, S) and 78 anions per formula unit.

QUANTITATIVE WDS RESULTS (NMNS)

Ions p.f.u. (50-Cation Normalization)

	V1-1_1	V1-2_2	V1-3_2	V1-4_2	V1-5_3	V1-6_4	V1-7_4	V2-1_c	V2-2_r	V3-1
Si^{4+}	18.14	18.03	18.10	18.02	18.07	18.14	17.93	18.16	18.16	18.13
Al^{3+}	9.85	9.47	9.89	9.55	9.42	9.48	9.49	10.09	9.72	9.40
Ti^{4+}	0.05	0.06	0.10	0.04	0.07	0.06	0.05	0.20	0.26	0.00
Mg^{2+}	1.45	1.73	0.93	1.70	1.69	1.75	1.72	1.08	1.26	2.80
Mn^{2+}	0.05	0.00	0.08	0.00	0.00	0.03	0.02	0.15	0.15	0.02
Fe^{2+}	1.49	1.70	1.74	1.64	1.63	1.57	1.57	1.30	1.43	0.09
Fe^{3+}	–	–	–	–	–	–	–	0.30	0.33	0.58
Cr^{3+}	–	–	–	–	–	–	–	–	–	0.00
Cu^{2+}	–	–	–	–	–	–	–	–	–	–
Zn^{2+}	0.00	0.00	0.00	0.00	0.00	0.00	0.00	0.00	0.00	0.00
Ca^{2+}	18.97	19.00	19.17	19.04	19.12	19.02	19.22	18.60	18.65	18.98
Na^{+}	0.00	0.00	0.00	0.00	0.00	0.00	0.00	0.12	0.06	0.00
K^{+}	0.00	0.00	0.00	0.00	0.00	0.00	0.00	0.00	0.00	–
La^{3+}	–	–	–	–	–	–	–	–	–	–
Ce^{3+}	0.00	0.00	0.00	0.00	0.00	0.00	0.00	–	–	0.00
Pr^{3+}	–	–	–	–	–	–	–	–	–	–
Nd^{3+}	–	–	–	–	–	–	–	–	–	–
Sm^{3+}	–	–	–	–	–	–	–	–	–	–
Eu^{3+}	–	–	–	–	–	–	–	–	–	–
Gd^{3+}	–	–	–	–	–	–	–	–	–	–
Pb^{2+}	–	–	–	–	–	–	–	–	–	–
Bi^{3+}	–	–	–	–	–	–	–	–	–	–
Th^{4+}	–	–	–	–	–	–	–	–	–	–
U^{4+}	–	–	–	–	–	–	–	–	–	–
B^{3+}	–	–	–	–	–	–	–	0.00	–	–
S^{6+}	0.00	0.00	0.00	0.00	0.00	0.00	0.00	0.00	0.04	0.07
F^{-}	0.00	0.00	0.00	0.00	0.00	0.00	0.00	4.71	4.63	0.00
Cl^{-}	0.00	0.00	0.04	0.00	0.00	0.00	0.00	0.00	0.00	0.06
OH^{-}*	9.76	10.34	9.67	10.32	10.30	10.17	10.56	4.32	4.30	9.28
O	68.24	67.66	68.28	67.68	67.70	67.83	67.44	68.98	69.06	68.66
					Statistics					
ΣX	18.97	19.00	19.17	19.04	19.12	19.02	19.22	18.72	18.71	18.98
ΣY	12.89	12.96	12.73	12.93	12.81	12.84	12.85	13.12	13.14	12.89
ΣZ	18.14	18.03	18.10	18.02	18.07	18.14	17.93	18.16	18.16	18.13

*Calculated for charge balance.

V2 includes 0.01 Li, 0.04 Be.

QUANTITATIVE WDS RESULTS (NMNS)

Ions p.f.u. (50-Cation Normalization)

	V3-2	V3-3	V3-4	V3-5	V4-1$_r$	V4-2$_r$	V4-3$_r$	V4-4	V4-5	V4-6
Si^{4+}	17.72	18.15	17.81	18.01	18.08	18.10	18.11	18.11	18.08	18.02
Al^{3+}	9.29	9.37	9.00	9.43	8.60	8.46	8.55	8.62	8.62	8.51
Ti^{4+}	0.00	0.00	0.00	0.00	0.55	0.63	0.52	0.45	0.46	0.61
Mg^{2+}	2.79	2.85	2.87	2.74	1.29	1.25	1.40	1.36	1.40	1.33
Mn^{2+}	0.03	0.00	0.00	0.00	0.14	0.15	0.15	0.14	0.14	0.14
Fe^{2+}	0.08	0.08	0.10	0.08	1.14	1.23	1.13	1.14	1.15	1.17
Fe^{3+}	0.55	0.54	0.64	0.52	1.32	1.41	1.31	1.31	1.33	1.35
Cr^{3+}	0.00	0.00	0.00	0.00	–	–	–	–	–	–
Cu^{2+}	–	–	–	–	–	–	–	–	–	–
Zn^{2+}	0.00	0.00	0.00	0.00	0.00	0.00	0.00	0.00	0.00	0.00
Ca^{2+}	19.54	19.00	19.57	19.23	18.77	18.60	18.75	18.80	18.75	18.68
Na^{+}	0.00	0.00	0.00	0.00	0.09	0.11	0.08	0.08	0.08	0.08
K^{+}	–	–	–	–	0.00	0.00	0.00	0.00	0.00	0.00
La^{3+}	–	–	–	–	0.00	0.02	0.00	0.00	0.00	0.02
Ce^{3+}	0.00	0.00	0.00	0.00	0.02	0.03	0.00	0.00	0.00	0.05
Pr^{3+}	–	–	–	–	0.00	0.00	0.00	0.00	0.00	0.00
Nd^{3+}	–	–	–	–	0.00	0.00	0.00	0.00	0.00	0.03
Sm^{3+}	–	–	–	–	0.00	0.00	0.00	0.00	0.00	0.00
Eu^{3+}	–	–	–	–	0.00	0.00	0.00	0.00	0.00	0.00
Gd^{3+}	–	–	–	–	0.00	0.00	0.00	0.00	0.00	0.00
Pb^{2+}	–	–	–	–	–	–	–	–	–	–
Bi^{3+}	–	–	–	–	–	–	–	–	–	–
Th^{4+}	–	–	–	–	–	–	–	–	–	–
U^{4+}	–	–	–	–	–	–	–	–	–	–
B^{3+}	–	0.00	–	–	–	–	–	–	0.00	–
S^{6+}	0.09	0.13	0.04	0.09	0.00	0.00	0.00	0.00	0.00	0.00
F^{-}	0.00	0.00	0.00	0.00	3.18	3.74	3.42	3.37	3.15	3.68
Cl^{-}	0.00	0.00	0.00	0.00	0.20	0.18	0.15	0.14	0.17	0.18
OH^{-*}	10.18	9.01	10.47	9.49	5.50	4.80	5.40	5.51	5.74	4.99
O	67.82	68.99	67.53	68.51	69.11	69.28	69.03	68.97	68.94	69.15
					Statistics					
ΣX	19.54	19.00	19.57	19.23	18.88	18.76	18.83	18.88	18.83	18.86
ΣY	12.74	12.84	12.62	12.76	13.04	13.13	13.06	13.02	13.09	13.11
ΣZ	17.72	18.15	17.81	18.01	18.08	18.10	18.11	18.11	18.08	18.02

*Calculated for charge balance.

V4 includes 0.01 Li, 0.01 Be.

QUANTITATIVE WDS RESULTS (NMNS)

Ions p.f.u. (50-Cation Normalization)

	V4-7	V4-8	V4-9	V5-1	V5-2	V5-3	V5-4	V5-5	V5-6	V5-7
Si^{4+}	18.10	18.23	18.11	17.98	18.13	18.07	18.13	18.05	18.15	18.12
Al^{3+}	8.99	9.17	9.10	9.81	9.75	9.99	9.94	9.91	9.85	9.86
Ti^{4+}	0.50	0.51	0.50	0.34	0.36	0.24	0.27	0.27	0.28	0.31
Mg^{2+}	1.18	1.15	1.16	1.26	1.24	1.17	1.21	1.22	1.21	1.20
Mn^{2+}	0.13	0.13	0.14	0.15	0.16	0.13	0.14	0.13	0.13	0.15
Fe^{2+}	1.00	1.00	1.02	1.21	1.18	1.22	1.21	1.24	1.22	1.23
Fe^{3+}	1.16	1.16	1.17	0.45	0.44	0.45	0.45	0.46	0.45	0.46
Cr^{3+}	–	–	–	–	–	–	–	–	–	–
Cu^{2+}	–	–	–	–	–	–	–	–	–	–
Zn^{2+}	0.00	0.00	0.00	0.00	0.04	0.00	0.00	0.00	0.00	0.00
Ca^{2+}	18.80	18.50	18.66	18.74	18.64	18.69	18.61	18.71	18.65	18.62
Na^{+}	0.13	0.14	0.14	0.07	0.06	0.04	0.04	0.00	0.05	0.05
K^{+}	0.00	0.00	0.00	0.00	0.00	0.00	0.00	0.00	0.00	0.00
La^{3+}	0.00	0.00	0.00	–	–	–	–	–	–	–
Ce^{3+}	0.01	0.00	0.00	0.00	0.00	0.00	0.00	0.00	0.00	0.00
Pr^{3+}	0.00	0.00	0.00	–	–	–	–	–	–	–
Nd^{3+}	0.00	0.00	0.00	–	–	–	–	–	–	–
Sm^{3+}	0.00	0.00	0.00	–	–	–	–	–	–	–
Eu^{3+}	0.00	0.00	0.00	–	–	–	–	–	–	–
Gd^{3+}	0.00	0.00	0.00	–	–	–	–	–	–	–
Pb^{2+}	–	–	–	–	–	–	–	–	–	–
Bi^{3+}	–	–	–	–	–	–	–	–	–	–
Th^{4+}	–	–	–	–	–	–	–	–	–	–
U^{4+}	–	–	–	–	–	–	–	–	–	–
B^{3+}	–	–	–	–	–	–	–	–	–	0.00
S^{6+}	0.00	0.00	0.00	0.03	0.00	0.00	0.00	0.00	0.00	0.00
F^{-}	3.84	3.51	3.78	4.24	3.88	3.72	3.81	4.03	3.87	3.90
Cl^{-}	0.16	0.13	0.15	0.08	0.08	0.08	0.07	0.05	0.07	0.08
OH^{-*}	4.76	4.68	4.71	4.66	4.93	5.18	4.96	4.92	4.95	4.89
O	69.24	69.68	69.36	69.02	69.11	69.02	69.17	69.00	69.11	69.13
					Statistics					
ΣX	18.94	18.64	18.80	18.81	18.70	18.73	18.65	18.71	18.70	18.66
ΣY	12.96	13.13	13.09	13.21	13.17	13.21	13.22	13.24	13.15	13.22
ΣZ	18.10	18.23	18.11	17.98	18.13	18.07	18.13	18.05	18.15	18.12

*Calculated for charge balance.

V4 includes 0.01 Li, 0.01 Be.

QUANTITATIVE WDS RESULTS (NMNS)

Ions p.f.u. (50-Cation Normalization)

	V5-8	V6-1	V6-2	V6-3	V6-4	V6-5	V6-6	V7-1	V7-2	V7-3
Si^{4+}	18.18	18.31	18.05	18.08	18.15	18.16	18.13	18.39	18.22	18.23
Al^{3+}	9.72	9.59	9.25	9.45	9.58	9.52	9.44	8.92	8.85	9.03
Ti^{4+}	0.31	0.31	0.77	0.48	0.31	0.33	0.42	1.68	1.74	1.69
Mg^{2+}	1.25	2.09	1.97	1.97	2.09	2.13	2.04	0.95	0.93	0.95
Mn^{2+}	0.15	0.33	0.34	0.32	0.33	0.34	0.34	0.00	0.00	0.00
Fe^{2+}	1.29	0.72	1.07	0.74	0.75	0.76	0.81	1.31	1.32	1.31
Fe^{3+}	0.48	–	–	–	–	–	–	–	–	–
Cr^{3+}	–	–	–	–	–	–	–	–	–	–
Cu^{2+}	–	–	–	–	–	–	–	–	–	–
Zn^{2+}	0.00	0.00	0.00	0.00	0.00	0.00	0.00	0.00	0.00	0.00
Ca^{2+}	18.58	18.47	18.12	18.77	18.62	18.60	18.71	17.91	18.10	17.94
Na^{+}	0.04	0.00	0.17	0.00	0.00	0.00	0.00	0.84	0.85	0.85
K^{+}	0.00	0.00	0.00	0.00	0.00	0.00	0.00	0.00	0.00	0.00
La^{3+}	–	0.05	0.07	0.06	0.05	0.05	0.04	–	–	–
Ce^{3+}	0.00	0.12	0.19	0.14	0.12	0.11	0.07	0.00	0.00	0.00
Pr^{3+}	–	0.00	0.00	0.00	0.00	0.00	0.00	–	–	–
Nd^{3+}	–	0.00	0.00	0.00	0.00	0.00	0.00	–	–	–
Sm^{3+}	–	0.00	0.00	0.00	0.00	0.00	0.00	–	–	–
Eu^{3+}	–	0.00	0.00	0.00	0.00	0.00	0.00	–	–	–
Gd^{3+}	–	0.00	0.00	0.00	0.00	0.00	0.00	–	–	–
Pb^{2+}	–	–	–	–	–	–	–	–	–	–
Bi^{3+}	–	–	–	–	–	–	–	–	–	–
Th^{4+}	–	–	–	–	–	–	–	–	–	–
U^{4+}	–	–	–	–	–	–	–	–	–	–
B^{3+}	–	–	0.00	0.00	–	–	–	–	0.00	–
S^{6+}	0.00	0.00	0.10	0.08	0.00	0.00	0.00	0.00	0.00	0.00
F^{-}	3.62	4.23	3.60	3.68	4.03	3.87	3.97	0.00	0.00	0.00
Cl^{-}	0.05	0.61	1.04	0.65	0.64	0.61	0.62	0.00	0.00	0.00
OH^{-*}	5.19	4.16	3.75	4.43	4.65	4.87	4.76	7.78	8.09	7.99
O	69.14	69.00	69.61	69.23	68.68	68.66	68.65	70.22	69.91	70.01
					Statistics					
ΣX	18.61	18.64	18.55	18.97	18.79	18.76	18.82	18.75	18.94	18.79
ΣY	13.20	13.05	13.40	12.95	13.06	13.08	13.05	12.86	12.84	12.98
ΣZ	18.18	18.31	18.05	18.08	18.15	18.16	18.13	18.39	18.22	18.23

*Calculated for charge balance.

QUANTITATIVE WDS RESULTS (NMNS)

Ions p.f.u. (50-Cation Normalization)

	V7-4	V7-5	V7-6	V7-7	V8-1_{1c}	V8-2_{1r}	V8-3_{2d}	V8-4_{2l}	V9-1_1	V9-2_1
Si^{4+}	18.17	18.29	18.24	18.32	17.87	18.18	18.29	18.07	17.91	17.86
Al^{3+}	8.93	9.04	8.98	8.87	9.57	9.51	10.54	9.86	10.73	10.58
Ti^{4+}	1.70	1.64	1.69	1.72	0.00	0.00	0.47	0.39	0.00	0.05
Mg^{2+}	0.99	0.97	0.96	0.95	1.81	1.80	0.79	1.48	2.02	2.30
Mn^{2+}	0.00	0.00	0.00	0.00	0.07	0.07	0.02	0.17	0.03	0.04
Fe^{2+}	1.33	1.30	1.27	1.29	1.69	1.63	1.22	1.81	0.19	0.20
Fe^{3+}	–	–	–	–	–	–	–	–	–	–
Cr^{3+}	–	–	–	–	–	–	–	–	0.03	0.01
Cu^{2+}	–	–	–	–	–	–	–	–	–	–
Zn^{2+}	0.00	0.00	0.00	0.00	0.00	0.00	0.00	0.00	0.00	0.00
Ca^{2+}	18.05	17.92	18.01	18.00	19.00	18.82	18.58	18.16	19.09	18.97
Na^{+}	0.83	0.83	0.84	0.85	0.00	0.00	0.09	0.05	0.00	0.00
K^{+}	0.00	0.00	0.00	0.00	0.00	0.00	0.00	0.00	0.00	0.00
La^{3+}	–	–	–	–	–	–	–	–	–	–
Ce^{3+}	0.00	0.00	0.00	0.00	–	–	–	–	–	–
Pr^{3+}	–	–	–	–	–	–	–	–	–	–
Nd^{3+}	–	–	–	–	–	–	–	–	–	–
Sm^{3+}	–	–	–	–	–	–	–	–	–	–
Eu^{3+}	–	–	–	–	–	–	–	–	–	–
Gd^{3+}	–	–	–	–	–	–	–	–	–	–
Pb^{2+}	–	–	–	–	–	–	–	–	–	–
Bi^{3+}	–	–	–	–	–	–	–	–	–	–
Th^{4+}	–	–	–	–	–	–	–	–	–	–
U^{4+}	–	–	–	–	–	–	–	–	–	–
B^{3+}	–	–	–	–	0.00	–	0.00	–	–	0.00
S^{6+}	0.00	0.04	0.00	0.00	0.00	0.00	0.00	0.00	0.00	0.00
F^{-}	0.00	0.00	0.00	0.00	0.00	0.00	2.77	4.15	0.00	0.00
Cl^{-}	0.00	0.00	0.00	0.00	0.00	0.00	0.00	0.06	0.00	0.00
OH^{-}*	8.16	7.66	8.01	7.89	10.70	10.14	5.28	5.05	9.42	9.60
O	69.84	70.34	69.99	70.11	67.30	67.86	69.94	68.75	68.58	68.40
					Statistics					
ΣX	18.88	18.75	18.85	18.85	19.00	18.82	18.67	18.21	19.09	18.97
ΣY	12.95	12.96	12.90	12.83	13.13	13.01	13.04	13.72	13.00	13.17
ΣZ	18.17	18.29	18.24	18.32	17.87	18.18	18.29	18.07	17.91	17.86

*Calculated for charge balance.

QUANTITATIVE WDS RESULTS (NMNS)

Ions p.f.u. (50-Cation Normalization)

	V9-3_2	V10-1	V10-2	V10-3	V11-1	V11-2	V11-3	V11-4	V11-5	V11-6
Si^{4+}	17.93	17.91	18.20	18.02	18.09	18.11	18.14	18.31	18.17	18.08
Al^{3+}	10.83	10.22	9.97	9.81	10.70	10.77	10.60	10.58	10.55	10.71
Ti^{4+}	0.12	0.00	0.00	0.00	0.00	0.00	0.00	0.00	0.00	0.00
Mg^{2+}	1.17	1.48	1.63	1.52	1.76	1.76	1.71	1.82	1.72	1.77
Mn^{2+}	0.08	0.25	0.12	0.12	0.05	0.06	0.12	0.06	0.09	0.06
Fe^{2+}	0.79	0.89	1.14	1.44	0.24	0.29	0.43	0.37	0.40	0.32
Fe^{3+}	–	–	–	–	–	–	–	–	–	–
Cr^{3+}	0.09	–	–	–	–	–	–	–	–	–
Cu^{2+}	–	–	–	–	–	–	–	–	–	–
Zn^{2+}	0.00	0.00	0.00	0.00	0.00	0.00	0.00	0.00	0.00	0.00
Ca^{2+}	19.05	19.26	18.95	19.09	19.16	19.01	19.01	18.86	19.08	19.05
Na^{+}	0.00	0.00	0.00	0.00	0.00	0.00	0.00	0.00	0.00	0.00
K^{+}	0.00	0.00	0.00	0.00	0.00	0.00	0.00	0.00	0.00	0.00
La^{3+}	–	–	–	–	–	–	–	–	–	–
Ce^{3+}	–	0.00	0.00	0.00	0.00	0.00	0.00	0.00	0.00	0.00
Pr^{3+}	–	–	–	–	–	–	–	–	–	–
Nd^{3+}	–	–	–	–	–	–	–	–	–	–
Sm^{3+}	–	–	–	–	–	–	–	–	–	–
Eu^{3+}	–	–	–	–	–	–	–	–	–	–
Gd^{3+}	–	–	–	–	–	–	–	–	–	–
Pb^{2+}	–	–	–	–	–	–	–	–	–	–
Bi^{3+}	–	–	–	–	–	–	–	–	–	–
Th^{4+}	–	–	–	–	–	–	–	–	–	–
U^{4+}	–	–	–	–	–	–	–	–	–	–
B^{3+}	–	–	–	–	–	–	–	–	0.00	–
S^{6+}	0.00	0.00	0.00	0.00	0.00	0.00	0.00	0.00	0.00	0.00
F^{-}	0.00	0.00	0.00	0.00	0.00	0.00	0.00	0.00	0.00	0.00
Cl^{-}	0.00	0.00	0.00	0.00	0.00	0.00	0.00	0.00	0.00	0.00
OH^{-}*	9.04	9.97	9.63	10.15	9.13	9.01	9.13	8.80	9.11	9.13
O	68.96	68.03	68.37	67.85	68.87	68.99	68.87	69.20	68.89	68.87
					Statistics					
ΣX	19.05	19.26	18.95	19.09	19.16	19.01	19.01	18.86	19.08	19.05
ΣY	13.02	12.83	12.85	12.89	12.75	12.88	12.85	12.83	12.75	12.87
ΣZ	17.93	17.91	18.20	18.02	18.09	18.11	18.14	18.31	18.17	18.08

*Calculated for charge balance.

QUANTITATIVE WDS RESULTS (NMNS)
Ions p.f.u. (50-Cation Normalization)

	V11-7	V11-8	V12-1	V12-2	V12-3	V13-1_1	V13-2_1	V13-3_1	V13-4_1	V13-5_1
Si^{4+}	18.14	18.32	18.02	17.94	18.00	17.98	18.02	17.85	17.93	18.02
Al^{3+}	10.88	10.54	10.59	10.49	10.65	9.76	10.06	10.05	10.05	9.77
Ti^{4+}	0.00	0.00	0.02	0.03	0.00	0.16	0.34	0.26	0.37	0.19
Mg^{2+}	1.81	1.59	1.86	1.87	1.87	1.66	1.47	1.42	1.37	1.57
Mn^{2+}	0.03	0.11	0.03	0.00	0.03	0.04	0.04	0.00	0.03	0.02
Fe^{2+}	0.28	0.49	0.37	0.36	0.40	0.59	0.48	0.52	0.53	0.58
Fe^{3+}	–	–	–	–	–	0.72	0.58	0.63	0.64	0.70
Cr^{3+}	–	–	–	–	–	–	–	–	–	–
Cu^{2+}	–	–	–	–	–	–	–	–	–	–
Zn^{2+}	0.00	0.00	0.00	0.00	0.00	0.00	0.00	0.00	0.00	0.00
Ca^{2+}	18.87	18.95	19.12	19.31	19.05	19.10	19.00	19.27	19.09	19.14
Na^{+}	0.00	0.00	0.00	0.00	0.00	0.00	0.00	0.00	0.00	0.00
K^{+}	0.00	0.00	0.00	0.00	0.00	0.00	0.00	0.00	0.00	0.00
La^{3+}	–	–	–	–	–	–	–	–	–	–
Ce^{3+}	0.00	0.00	0.00	0.00	0.00	0.00	0.00	0.00	0.00	0.00
Pr^{3+}	–	–	–	–	–	–	–	–	–	–
Nd^{3+}	–	–	–	–	–	–	–	–	–	–
Sm^{3+}	–	–	–	–	–	–	–	–	–	–
Eu^{3+}	–	–	–	–	–	–	–	–	–	–
Gd^{3+}	–	–	–	–	–	–	–	–	–	–
Pb^{2+}	–	–	–	–	–	–	–	–	–	–
Bi^{3+}	–	–	–	–	–	–	–	–	–	–
Th^{4+}	–	–	–	–	–	–	–	–	–	–
U^{4+}	–	–	–	–	–	–	–	–	–	–
B^{3+}	–	–	–	–	–	–	–	–	–	–
S^{6+}	0.00	0.00	0.00	0.00	0.00	0.00	0.00	0.00	0.00	0.00
F^{-}	0.00	0.00	0.00	0.00	0.00	0.00	0.00	0.00	0.00	0.00
Cl^{-}	0.00	0.00	0.00	0.00	0.00	0.00	0.00	0.00	0.00	0.00
OH^{-}*	8.85	8.82	9.34	9.57	9.35	9.25	8.63	9.09	8.73	9.10
O	69.15	69.18	68.66	68.43	68.65	68.75	69.37	68.91	69.27	68.90
					Statistics					
ΣX	18.87	18.95	19.12	19.31	19.05	19.10	19.00	19.27	19.09	19.14
ΣY	13.00	12.73	12.86	12.75	12.95	12.92	12.98	12.73	12.91	12.84
ΣZ	18.14	18.32	18.02	17.94	18.00	17.98	18.02	17.85	17.93	18.02

*Calculated for charge balance.

QUANTITATIVE WDS RESULTS (NMNS)

Ions p.f.u. (50-Cation Normalization)

	V13-6$_1$	V13-7$_1$	V13-8$_1$	V13-9$_1$	V13-10$_1$	V13-11$_1$	V13-12$_1$	V13-13$_1$	V13-14$_1$	V13-15$_1$
Si^{4+}	18.18	17.80	17.95	17.86	17.82	17.95	17.97	17.88	17.88	17.82
Al^{3+}	9.81	9.74	10.07	10.13	10.31	10.07	10.36	10.14	10.16	10.32
Ti^{4+}	0.12	0.16	0.31	0.22	0.15	0.26	0.23	0.19	0.30	0.20
Mg^{2+}	1.69	1.64	1.38	1.35	1.33	1.44	1.24	1.32	1.25	1.15
Mn^{2+}	0.02	0.02	0.03	0.00	0.04	0.00	0.04	0.03	0.04	0.02
Fe^{2+}	0.59	0.61	0.56	0.55	0.55	0.49	0.56	0.55	0.55	0.59
Fe^{3+}	0.71	0.73	0.68	0.66	0.66	0.59	0.68	0.67	0.67	0.71
Cr^{3+}	–	–	–	–	–	–	–	–	–	–
Cu^{2+}	–	–	–	–	–	–	–	–	–	–
Zn^{2+}	0.00	0.00	0.00	0.00	0.00	0.00	0.00	0.00	0.00	0.00
Ca^{2+}	18.88	19.30	19.02	19.24	19.14	19.20	18.93	19.22	19.16	19.18
Na^{+}	0.00	0.00	0.00	0.00	0.00	0.00	0.00	0.00	0.00	0.00
K^{+}	0.00	0.00	0.00	0.00	0.00	0.00	0.00	0.00	0.00	0.00
La^{3+}	–	–	–	–	–	–	–	–	–	–
Ce^{3+}	0.00	0.00	0.00	0.00	0.00	0.00	0.00	0.00	0.00	0.00
Pr^{3+}	–	–	–	–	–	–	–	–	–	–
Nd^{3+}	–	–	–	–	–	–	–	–	–	–
Sm^{3+}	–	–	–	–	–	–	–	–	–	–
Eu^{3+}	–	–	–	–	–	–	–	–	–	–
Gd^{3+}	–	–	–	–	–	–	–	–	–	–
Pb^{2+}	–	–	–	–	–	–	–	–	–	–
Bi^{3+}	–	–	–	–	–	–	–	–	–	–
Th^{4+}	–	–	–	–	–	–	–	–	–	–
U^{4+}	–	–	–	–	–	–	–	–	–	–
B^{3+}	–	–	–	–	–	–	–	–	–	–
S^{6+}	0.00	0.00	0.00	0.00	0.00	0.00	0.00	0.00	0.00	0.00
F^{-}	0.00	0.00	0.00	0.00	0.00	0.00	0.00	0.00	0.00	0.00
Cl^{-}	0.00	0.00	0.00	0.00	0.00	0.00	0.06	0.00	0.00	0.00
OH^{-*}	8.88	9.61	8.73	9.06	9.08	8.92	8.52	9.06	8.81	8.92
O	69.12	68.39	69.27	68.94	68.92	69.08	69.42	68.94	69.19	69.08
					Statistics					
ΣX	18.88	19.30	19.02	19.24	19.14	19.20	18.93	19.22	19.16	19.18
ΣY	12.94	12.90	13.03	12.90	13.04	12.85	13.10	12.90	12.96	13.00
ΣZ	18.18	17.80	17.95	17.86	17.82	17.95	17.97	17.88	17.88	17.82

*Calculated for charge balance.

QUANTITATIVE WDS RESULTS (NMNS)

Ions p.f.u. (50-Cation Normalization)

	V13-16$_1$	V13-17$_1$	V13-18$_1$	V13-19$_1$	V13-20$_1$	V13-21$_1$	V13-22$_1$	V13-23$_1$	V13-24$_1$	V13-25$_1$
Si^{4+}	17.81	17.91	17.88	17.98	17.83	17.75	17.76	17.89	17.83	17.93
Al^{3+}	10.42	10.27	10.25	10.19	10.41	10.85	10.75	10.85	10.38	10.60
Ti^{4+}	0.24	0.22	0.22	0.14	0.23	0.16	0.13	0.14	0.14	0.11
Mg^{2+}	1.09	1.37	1.34	1.36	1.05	1.00	0.98	0.97	1.13	1.09
Mn^{2+}	0.03	0.03	0.02	0.00	0.00	0.00	0.02	0.03	0.05	0.00
Fe^{2+}	0.57	0.56	0.53	0.58	0.57	0.53	0.54	0.53	0.57	0.61
Fe^{3+}	0.69	0.67	0.63	0.69	0.68	0.64	0.66	0.64	0.69	0.74
Cr^{3+}	–	–	–	–	–	–	–	–	–	–
Cu^{2+}	–	–	–	–	–	–	–	–	–	–
Zn^{2+}	0.00	0.00	0.00	0.00	0.00	0.00	0.00	0.00	0.00	0.00
Ca^{2+}	19.15	18.97	19.13	19.06	19.23	19.07	19.16	18.94	19.21	18.92
Na^{+}	0.00	0.00	0.00	0.00	0.00	0.00	0.00	0.00	0.00	0.00
K^{+}	0.00	0.00	0.00	0.00	0.00	0.00	0.00	0.00	0.00	0.00
La^{3+}	–	–	–	–	–	–	–	–	–	–
Ce^{3+}	0.00	0.00	0.00	0.00	0.00	0.00	0.00	0.00	0.00	0.00
Pr^{3+}	–	–	–	–	–	–	–	–	–	–
Nd^{3+}	–	–	–	–	–	–	–	–	–	–
Sm^{3+}	–	–	–	–	–	–	–	–	–	–
Eu^{3+}	–	–	–	–	–	–	–	–	–	–
Gd^{3+}	–	–	–	–	–	–	–	–	–	–
Pb^{2+}	–	–	–	–	–	–	–	–	–	–
Bi^{3+}	–	–	–	–	–	–	–	–	–	–
Th^{4+}	–	–	–	–	–	–	–	–	–	–
U^{4+}	–	–	–	–	–	–	–	–	–	–
B^{3+}	–	–	–	–	–	–	–	–	–	–
S^{6+}	0.00	0.00	0.00	0.00	0.00	0.00	0.00	0.00	0.00	0.00
F^{-}	0.00	0.00	0.25	0.00	0.00	0.00	0.00	0.00	0.00	0.00
Cl^{-}	0.04	0.00	0.00	0.00	0.06	0.00	0.06	0.00	0.00	0.00
OH^{-*}	8.75	8.79	8.66	8.89	8.74	8.70	8.83	8.44	8.99	8.57
O	69.21	69.21	69.09	69.11	69.20	69.30	69.17	69.56	69.01	69.43
					Statistics					
ΣX	19.15	18.97	19.13	19.06	19.23	19.07	19.16	18.94	19.21	18.92
ΣY	13.04	13.12	12.99	12.96	12.94	13.18	13.08	13.17	12.96	13.15
ΣZ	17.81	17.91	17.88	17.98	17.83	17.75	17.76	17.89	17.83	17.93

*Calculated for charge balance.

QUANTITATIVE WDS RESULTS (NMNS)

Ions p.f.u. (50-Cation Normalization)

	$V13\text{-}26_1$	$V13\text{-}27_1$	$V13\text{-}28_1$	$V13\text{-}29_1$	$V13\text{-}30_{2c}$	$V13\text{-}31_{2c}$	$V13\text{-}32_{2c}$	$V13\text{-}33_{2c}$	$V13\text{-}34_{2c}$	$V13\text{-}35_{2i}$
Si^{4+}	17.63	17.93	17.73	17.84	17.69	17.77	17.73	17.82	17.70	17.78
Al^{3+}	10.77	10.43	10.47	10.62	10.59	10.57	10.65	10.62	10.60	10.35
Ti^{4+}	0.12	0.10	0.09	0.29	0.28	0.28	0.28	0.27	0.28	0.28
Mg^{2+}	0.94	1.10	1.10	1.05	1.04	1.03	1.05	1.02	1.02	1.23
Mn^{2+}	0.02	0.04	0.04	0.00	0.03	0.03	0.03	0.04	0.02	0.03
Fe^{2+}	0.54	0.59	0.59	0.54	0.53	0.54	0.53	0.53	0.52	0.55
Fe^{3+}	0.65	0.71	0.71	0.66	0.64	0.65	0.64	0.64	0.63	0.67
Cr^{3+}	–	–	–	–	–	–	–	–	–	–
Cu^{2+}	–	–	–	–	–	–	–	–	–	–
Zn^{2+}	0.00	0.00	0.00	0.00	0.00	0.00	0.00	0.00	0.00	0.00
Ca^{2+}	19.32	19.09	19.28	19.01	19.19	19.12	19.09	19.05	19.22	19.11
Na^{+}	0.00	0.00	0.00	0.00	0.00	0.00	0.00	0.00	0.00	0.00
K^{+}	0.00	0.00	0.00	0.00	0.00	0.00	0.00	0.00	0.00	0.00
La^{3+}	–	–	–	–	–	–	–	–	–	–
Ce^{3+}	0.00	0.00	0.00	0.00	0.00	0.00	0.00	0.00	0.00	0.00
Pr^{3+}	–	–	–	–	–	–	–	–	–	–
Nd^{3+}	–	–	–	–	–	–	–	–	–	–
Sm^{3+}	–	–	–	–	–	–	–	–	–	–
Eu^{3+}	–	–	–	–	–	–	–	–	–	–
Gd^{3+}	–	–	–	–	–	–	–	–	–	–
Pb^{2+}	–	–	–	–	–	–	–	–	–	–
Bi^{3+}	–	–	–	–	–	–	–	–	–	–
Th^{4+}	–	–	–	–	–	–	–	–	–	–
U^{4+}	–	–	–	–	–	–	–	–	–	–
B^{3+}	–	–	–	–	0.00	–	–	–	–	–
S^{6+}	0.00	0.00	0.00	0.00	0.00	0.00	0.00	0.00	0.00	0.00
F^{-}	0.00	0.00	0.00	0.00	0.00	0.00	0.00	0.00	0.00	0.00
Cl^{-}	0.00	0.00	0.00	0.00	0.00	0.00	0.03	0.00	0.00	0.00
OH^{-}*	9.08	8.79	9.18	8.48	8.82	8.68	8.67	8.55	8.81	8.87
O	68.92	69.21	68.82	68.52	69.18	69.32	69.30	69.45	69.19	69.13
					Statistics					
ΣX	19.32	19.09	19.28	19.01	19.19	19.12	19.09	19.05	19.22	19.11
ΣY	13.05	12.98	12.99	13.15	13.12	13.11	13.18	13.13	13.08	13.11
ΣZ	17.63	17.93	17.73	17.84	17.69	17.77	17.73	17.82	17.70	17.78

*Calculated for charge balance.

QUANTITATIVE WDS RESULTS (NMNS)

Ions p.f.u. (50-Cation Normalization)

	V13-36$_{2i}$	V13-37$_{2i}$	V13-38$_{2i}$	V13-39$_{2r}$	V13-40$_{2r}$	V13-41$_{2r}$	V13-42$_{2r}$	V13-33$_{2i}$	V13-44$_{2i}$	V13-45$_{2i}$
Si^{4+}	17.84	17.87	17.82	17.82	17.69	17.73	17.82	17.83	17.72	17.88
Al^{3+}	10.25	10.30	10.01	10.26	10.36	10.32	10.19	10.27	10.11	10.33
Ti^{4+}	0.28	0.31	0.29	0.23	0.16	0.14	0.26	0.30	0.26	0.29
Mg^{2+}	1.19	1.25	1.34	1.33	1.36	1.35	1.22	1.13	1.17	1.27
Mn^{2+}	0.03	0.04	0.03	0.02	0.00	0.04	0.04	0.03	0.03	0.03
Fe^{2+}	0.56	0.55	0.58	0.53	0.53	0.57	0.56	0.59	0.60	0.53
Fe^{3+}	0.68	0.66	0.69	0.65	0.65	0.69	0.68	0.71	0.73	0.64
Cr^{3+}	–	–	–	–	–	–	–	–	–	–
Cu^{2+}	–	–	–	–	–	–	–	–	–	–
Zn^{2+}	0.00	0.00	0.00	0.00	0.00	0.00	0.00	0.00	0.00	0.00
Ca^{2+}	19.16	19.02	19.24	19.16	19.25	19.17	19.22	19.14	19.38	19.02
Na^{+}	0.00	0.00	0.00	0.00	0.00	0.00	0.00	0.00	0.00	0.00
K^{+}	0.00	0.00	0.00	0.00	0.00	0.00	0.00	0.00	0.00	0.00
La^{3+}	–	–	–	–	–	–	–	–	–	–
Ce^{3+}	0.00	0.00	0.00	0.00	0.00	0.00	0.00	0.00	0.00	0.00
Pr^{3+}	–	–	–	–	–	–	–	–	–	–
Nd^{3+}	–	–	–	–	–	–	–	–	–	–
Sm^{3+}	–	–	–	–	–	–	–	–	–	–
Eu^{3+}	–	–	–	–	–	–	–	–	–	–
Gd^{3+}	–	–	–	–	–	–	–	–	–	–
Pb^{2+}	–	–	–	–	–	–	–	–	–	–
Bi^{3+}	–	–	–	–	–	–	–	–	–	–
Th^{4+}	–	–	–	–	–	–	–	–	–	–
U^{4+}	–	–	–	–	–	–	–	–	–	–
B^{3+}	–	–	–	–	0.00	–	–	–	–	–
S^{6+}	0.00	0.00	0.00	0.00	0.00	0.00	0.00	0.00	0.00	0.00
F^{-}	0.00	0.00	0.00	0.00	0.00	0.00	0.00	0.00	0.00	0.00
Cl^{-}	0.00	0.00	0.00	0.00	0.00	0.00	0.00	0.05	0.00	0.00
OH^{-}*	8.83	8.68	9.07	9.01	9.28	9.26	8.96	8.71	9.20	8.69
O	69.17	69.32	68.93	68.99	68.72	68.74	69.04	69.24	68.80	69.31
					Statistics					
ΣX	19.16	19.02	19.24	19.16	19.25	19.17	19.22	19.14	19.38	19.02
ΣY	13.00	13.11	12.94	13.02	13.06	13.10	12.96	13.03	12.90	13.10
ΣZ	17.84	17.87	17.82	17.82	17.69	17.73	17.82	17.83	17.72	17.88

*Calculated for charge balance.

QUANTITATIVE WDS RESULTS (NMNS)

Ions p.f.u. (50-Cation Normalization)

	V13-46$_{2i}$	V13-47$_{2i}$	V13-48$_{2r}$	V13-49$_{2r}$	V13-50$_{2r}$	V13-51$_{2}$	V13-52$_{2}$	V13-53$_{2}$	V13-54$_{3c}$	V13-55$_{3i}$
Si^{4+}	17.91	17.64	17.87	17.98	17.87	17.83	17.77	17.75	17.78	17.86
Al^{3+}	10.25	10.28	10.25	10.30	10.18	10.08	10.37	10.69	10.35	10.11
Ti^{4+}	0.24	0.20	0.14	0.14	0.26	0.35	0.15	0.24	0.20	0.14
Mg^{2+}	1.20	1.34	1.32	1.35	1.22	1.31	1.35	1.05	1.12	1.34
Mn^{2+}	0.00	0.00	0.04	0.03	0.03	0.00	0.03	0.03	0.04	0.03
Fe^{2+}	0.58	0.54	0.55	0.55	0.60	0.56	0.53	0.53	0.59	0.59
Fe^{3+}	0.70	0.66	0.67	0.67	0.72	0.68	0.64	0.65	0.71	0.72
Cr^{3+}	–	–	–	–	–	–	–	–	–	–
Cu^{2+}	–	–	–	–	–	–	–	–	–	–
Zn^{2+}	0.00	0.00	0.00	0.00	0.00	0.00	0.00	0.00	0.00	0.00
Ca^{2+}	19.11	19.34	19.16	18.97	19.13	19.18	19.16	19.06	19.22	19.21
Na^{+}	0.00	0.00	0.00	0.00	0.00	0.00	0.00	0.00	0.00	0.00
K^{+}	0.00	0.00	0.00	0.00	0.00	0.00	0.00	0.00	0.00	0.00
La^{3+}	–	–	–	–	–	–	–	–	–	–
Ce^{3+}	0.00	0.00	0.00	0.00	0.00	0.00	0.00	0.00	0.00	0.00
Pr^{3+}	–	–	–	–	–	–	–	–	–	–
Nd^{3+}	–	–	–	–	–	–	–	–	–	–
Sm^{3+}	–	–	–	–	–	–	–	–	–	–
Eu^{3+}	–	–	–	–	–	–	–	–	–	–
Gd^{3+}	–	–	–	–	–	–	–	–	–	–
Pb^{2+}	–	–	–	–	–	–	–	–	–	–
Bi^{3+}	–	–	–	–	–	–	–	–	–	–
Th^{4+}	–	–	–	–	–	–	–	–	–	–
U^{4+}	–	–	–	–	–	–	–	–	–	–
B^{3+}	–	–	–	–	–	–	–	–	–	–
S^{6+}	0.00	0.00	0.00	0.00	0.00	0.00	0.00	0.00	0.00	0.00
F^{-}	0.00	0.00	0.00	0.00	0.00	0.00	0.00	0.00	0.00	0.00
Cl^{-}	0.00	0.00	0.00	0.00	0.00	0.00	0.00	0.00	0.00	0.00
OH^{-*}	8.75	9.38	9.07	8.78	8.85	8.88	9.16	8.67	8.98	9.18
O	69.25	68.62	68.93	69.22	69.15	69.12	68.84	69.33	69.02	68.82
					Statistics					
ΣX	19.11	19.34	19.16	18.97	19.13	19.18	19.16	19.06	19.22	19.21
ΣY	12.98	13.02	12.97	13.05	13.00	12.99	13.07	13.20	13.00	12.93
ΣZ	17.91	17.64	17.87	17.98	17.87	17.83	17.77	17.75	17.78	17.86

*Calculated for charge balance.

QUANTITATIVE WDS RESULTS (NMNS)

Ions p.f.u. (50-Cation Normalization)

	V14-1_c	V14-2_r	V15-1	V15-2	V15-3	V16-1	V16-2	V16-3	V17-1	V17-2
Si^{4+}	18.00	18.14	18.41	18.15	18.20	18.14	18.11	18.30	17.99	18.18
Al^{3+}	10.30	10.35	10.27	10.34	10.32	9.75	9.80	9.83	10.01	9.98
Ti^{4+}	0.00	0.00	0.00	0.00	0.00	0.04	0.04	0.03	0.00	0.00
Mg^{2+}	1.87	1.79	1.79	1.87	1.97	1.70	1065	1.69	1.73	1.72
Mn^{2+}	0.04	0.05	0.07	0.07	0.05	0.13	0.19	0.18	0.00	0.02
Fe^{2+}	0.08	0.09	0.39	0.36	0.37	1.12	1.11	1.05	0.29	0.30
Fe^{3+}	0.39	0.45	–	–	–	–	–	–	0.83	0.86
Cr^{3+}	–	–	–	–	–	–	–	–	–	–
Cu^{2+}	–	–	–	–	–	–	–	–	–	–
Zn^{2+}	0.00	0.00	0.00	0.00	0.00	0.00	0.00	0.00	0.00	0.00
Ca^{2+}	19.32	19.14	19.07	19.21	19.10	19.12	19.09	18.92	19.14	18.93
Na^{+}	0.00	0.00	0.00	0.00	0.00	0.00	0.00	0.00	0.00	0.00
K^{+}	0.00	0.00	0.00	0.00	0.00	0.00	0.00	0.00	0.00	0.00
La^{3+}	–	–	–	–	–	–	–	–	–	–
Ce^{3+}	0.00	0.00	0.00	0.00	0.00	0.00	0.00	0.00	0.00	0.00
Pr^{3+}	–	–	–	–	–	–	–	–	–	–
Nd^{3+}	–	–	–	–	–	–	–	–	–	–
Sm^{3+}	–	–	–	–	–	–	–	–	–	–
Eu^{3+}	–	–	–	–	–	–	–	–	–	–
Gd^{3+}	–	–	–	–	–	–	–	–	–	–
Pb^{2+}	–	–	–	–	–	–	–	–	–	–
Bi^{3+}	–	–	–	–	–	–	–	–	–	–
Th^{4+}	–	–	–	–	–	–	–	–	–	–
U^{4+}	–	–	–	–	–	–	–	–	–	–
B^{3+}	0.00	–	–	–	–	–	0.00	–	0.00	–
S^{6+}	0.00	0.00	0.00	0.00	0.00	0.00	0.00	0.00	0.00	0.00
F^{-}	0.00	0.00	0.00	0.00	0.00	0.00	0.00	0.00	0.00	0.00
Cl^{-}	0.00	0.00	0.00	0.00	0.00	0.00	0.00	0.00	0.00	0.00
OH^{-*}	9.30	8.93	8.91	9.36	9.29	9.89	9.88	9.52	9.18	8.79
O	68.70	69.07	69.09	68.64	68.71	68.11	68.12	68.48	68.82	69.21
					Statistics					
ΣX	19.32	19.14	19.07	19.21	19.10	19.12	19.09	18.92	19.14	18.93
ΣY	12.68	12.73	12.52	12.64	12.70	12.74	12.80	12.78	12.86	12.88
ΣZ	18.00	18.14	18.41	18.15	18.20	18.14	18.11	18.30	18.00	18.18

*Calculated for charge balance.

QUANTITATIVE WDS RESULTS (NMNS)

Ions p.f.u. (50-Cation Normalization)

	V17-3	V17-4	V17-5	V17-6	V17-7	V17-8	V17-9	V17-10	V18-1_1	V18-2_1
Si^{4+}	18.00	18.13	18.07	17.98	18.03	18.30	18.13	18.33	17.95	18.25
Al^{3+}	9.93	10.09	9.83	9.87	9.89	9.97	9.82	9.92	10.44	10.42
Ti^{4+}	0.00	0.00	0.01	0.02	0.00	0.00	0.00	0.00	0.00	0.00
Mg^{2+}	1.74	1.70	1.78	1.84	1.78	1.73	1.77	1.74	1.83	1.93
Mn^{2+}	0.00	0.00	0.00	0.00	0.00	0.03	0.00	0.00	0.04	0.02
Fe^{2+}	0.29	0.29	0.31	0.30	0.32	0.30	0.31	0.32	0.48	0.42
Fe^{3+}	0.83	0.83	0.87	0.87	0.90	0.86	0.87	0.89	–	–
Cr^{3+}	–	–	–	–	–	–	–	–	–	–
Cu^{2+}	–	–	–	–	–	–	–	–	–	–
Zn^{2+}	0.00	0.00	0.00	0.00	0.00	0.00	0.00	0.00	0.00	0.00
Ca^{2+}	19.20	18.97	19.12	19.11	19.10	18.82	19.11	18.80	19.26	18.97
Na^{+}	0.00	0.00	0.00	0.00	0.00	0.00	0.00	0.00	0.00	0.00
K^{+}	0.00	0.00	0.00	0.00	0.00	0.00	0.00	0.00	0.00	0.00
La^{3+}	–	–	–	–	–	–	–	–	–	–
Ce^{3+}	0.00	0.00	0.00	0.00	0.00	0.00	0.00	0.00	0.00	0.00
Pr^{3+}	–	–	–	–	–	–	–	–	–	–
Nd^{3+}	–	–	–	–	–	–	–	–	–	–
Sm^{3+}	–	–	–	–	–	–	–	–	–	–
Eu^{3+}	–	–	–	–	–	–	–	–	–	–
Gd^{3+}	–	–	–	–	–	–	–	–	–	–
Pb^{2+}	–	–	–	–	–	–	–	–	–	–
Bi^{3+}	–	–	–	–	–	–	–	–	–	–
Th^{4+}	–	–	–	–	–	–	–	–	–	–
U^{4+}	–	–	–	–	–	–	–	–	–	–
B^{3+}	–	–	–	–	–	–	–	–	–	–
S^{6+}	0.00	0.00	0.00	0.00	0.00	0.00	0.00	0.00	0.00	0.00
F^{-}	0.00	0.00	0.00	0.00	0.00	0.00	0.00	0.00	0.00	0.00
Cl^{-}	0.00	0.00	0.00	0.00	0.00	0.00	0.00	0.00	0.00	0.00
OH^{-*}	9.24	8.84	9.13	9.27	9.16	8.57	9.06	8.52	9.65	9.09
O	68.76	69.16	68.87	68.73	68.84	69.43	68.94	69.48	68.35	68.91
					Statistics					
ΣX	19.20	18.97	19.12	19.11	19.10	18.82	19.11	18.80	19.26	18.97
ΣY	12.80	12.91	12.81	12.91	12.88	12.88	12.76	12.87	12.79	12.78
ΣZ	18.00	18.13	18.07	17.98	18.03	18.30	18.13	18.33	17.95	18.25

*Calculated for charge balance.

QUANTITATIVE WDS RESULTS (NMNS)

Ions p.f.u. (50-Cation Normalization)

	V18-3_1	V18-4_{2r}	V18-5_{2c}	V19-1	V19-2	V19-3	V19-4	V19-5	V19-6	V20-1
Si^{4+}	17.96	18.22	17.98	18.09	17.94	18.21	17.81	18.31	17.91	17.93
Al^{3+}	10.43	10.40	10.50	9.74	9.71	9.78	9.51	9.78	9.68	9.43
Ti^{4+}	0.00	0.00	0.00	0.33	0.17	0.14	0.14	0.17	0.25	0.44
Mg^{2+}	1.94	1.92	1.87	1.78	1.79	1.92	1.85	1.84	1.68	1.84
Mn^{2+}	0.00	0.00	0.05	0.03	0.07	0.07	0.05	0.07	0.07	0.06
Fe^{2+}	0.52	0.46	0.47	1.08	1.03	1.09	1.01	1.01	0.99	1.05
Fe^{3+}	–	–	–	–	–	–	–	–	–	–
Cr^{3+}	–	–	–	0.00	0.00	0.00	0.00	0.00	0.00	–
Cu^{2+}	–	–	–	–	–	–	–	–	–	–
Zn^{2+}	0.00	0.00	0.00	0.00	0.00	0.00	0.00	0.00	0.00	0.00
Ca^{2+}	19.15	18.99	19.13	18.95	19.30	18.80	19.63	18.82	19.43	19.25
Na^{+}	0.00	0.00	0.00	0.00	0.00	0.00	0.00	0.00	0.00	0.00
K^{+}	0.00	0.00	0.00	–	–	–	–	–	–	0.00
La^{3+}	–	–	–	–	–	–	–	–	–	–
Ce^{3+}	0.00	0.00	0.00	0.00	0.00	0.00	0.00	0.00	0.00	0.00
Pr^{3+}	–	–	–	–	–	–	–	–	–	–
Nd^{3+}	–	–	–	–	–	–	–	–	–	–
Sm^{3+}	–	–	–	–	–	–	–	–	–	–
Eu^{3+}	–	–	–	–	–	–	–	–	–	–
Gd^{3+}	–	–	–	–	–	–	–	–	–	–
Pb^{2+}	–	–	–	–	–	–	–	–	–	–
Bi^{3+}	–	–	–	–	–	–	–	–	–	–
Th^{4+}	–	–	–	–	–	–	–	–	–	–
U^{4+}	–	–	–	–	–	–	–	–	–	–
B^{3+}	–	–	–	–	–	–	–	–	–	–
S^{6+}	0.00	0.00	0.00	0.00	0.00	0.00	0.00	0.00	0.00	0.00
F^{-}	0.00	0.00	0.00	0.00	0.00	0.00	0.00	0.00	0.00	0.00
Cl^{-}	0.00	0.00	0.00	0.00	0.00	0.00	0.00	0.00	0.00	0.00
OH^{-*}	9.64	9.16	9.55	9.42	10.08	9.51	10.60	9.25	10.02	9.83
O	68.36	68.84	68.45	68.58	67.92	68.49	67.40	68.75	67.98	68.17
					Statistics					
ΣX	19.15	18.99	19.13	18.95	19.30	18.80	19.63	18.82	19.43	19.25
ΣY	12.89	12.78	12.89	12.96	12.76	12.99	12.56	12.87	12.66	12.82
ΣZ	17.96	18.22	17.98	18.09	17.94	18.21	17.81	18.31	17.91	17.93

*Calculated for charge balance.

QUANTITATIVE WDS RESULTS (NMNS)

Ions p.f.u. (50-Cation Normalization)

	V20-2	V20-3	V21-1_1	V21-2_1	V21-3_{2r}	V21-4_{2r}	V21-5_{2r}	V21-6_{2c}	V21-7_{2c}	V21-8_{2c}
Si^{4+}	18.09	17.86	18.29	18.16	18.42	17.95	18.14	18.03	18.32	18.01
Al^{3+}	9.60	9.54	10.50	10.31	10.25	10.53	10.78	10.17	10.79	10.50
Ti^{4+}	0.40	0.44	0.00	0.00	0.00	0.00	0.00	0.00	0.00	0.00
Mg^{2+}	1.79	1.82	2.17	1.74	2.06	1.91	1.88	1.91	1.75	1.80
Mn^{2+}	0.06	0.06	0.08	0.12	0.09	0.05	0.05	0.00	0.04	0.09
Fe^{2+}	1.08	1.06	0.15	0.19	0.17	0.13	0.13	0.61	0.21	0.20
Fe^{3+}	–	–	–	–	–	–	–	–	–	–
Cr^{3+}	–	–	0.00	0.00	0.00	0.00	0.00	0.00	0.00	0.00
Cu^{2+}	–	–	–	–	–	–	–	–	–	–
Zn^{2+}	0.00	0.00	0.00	0.00	0.00	0.00	0.00	0.00	0.00	0.00
Ca^{2+}	18.98	19.21	18.82	19.49	19.00	19.43	19.02	19.29	18.89	19.39
Na^{+}	0.00	0.00	0.00	0.00	0.00	0.00	0.00	0.00	0.00	0.00
K^{+}	0.00	0.00	–	–	–	–	–	–	–	–
La^{3+}	–	–	–	–	–	–	–	–	–	–
Ce^{3+}	0.00	0.00	0.00	0.00	0.00	0.00	0.00	0.00	0.00	0.00
Pr^{3+}	–	–	–	–	–	–	–	–	–	–
Nd^{3+}	–	–	–	–	–	–	–	–	–	–
Sm^{3+}	–	–	–	–	–	–	–	–	–	–
Eu^{3+}	–	–	–	–	–	–	–	–	–	–
Gd^{3+}	–	–	–	–	–	–	–	–	–	–
Pb^{2+}	–	–	–	–	–	–	–	–	–	–
Bi^{3+}	–	–	–	–	–	–	–	–	–	–
Th^{4+}	–	–	–	–	–	–	–	–	–	–
U^{4+}	–	–	–	–	–	–	–	–	–	–
B^{3+}	–	–	–	–	–	–	–	–	0.00	–
S^{6+}	0.00	0.00	0.00	0.00	0.00	0.00	0.00	0.00	0.00	0.00
F^{-}	0.00	0.00	0.00	0.00	0.00	0.00	0.00	0.00	0.00	0.00
Cl^{-}	0.00	0.00	0.00	0.00	0.00	0.00	0.00	0.00	0.00	0.00
OH^{-*}	9.42	9.86	8.93	9.38	8.90	9.58	8.94	9.78	8.57	9.47
O	68.58	68.14	69.07	68.62	69.10	68.42	69.06	68.22	69.43	68.53
					Statistics					
ΣX	18.98	19.21	18.82	19.49	19.00	19.43	19.02	19.29	18.89	19.39
ΣY	12.93	12.93	12.90	12.35	12.57	12.62	12.84	12.69	12.79	12.59
ΣZ	18.09	17.86	18.29	18.16	18.42	17.95	18.14	18.03	18.32	18.01

*Calculated for charge balance.

QUANTITATIVE WDS RESULTS (NMNS)

Ions p.f.u. (50-Cation Normalization)

	V21-9_{2c}	V21-10_{2c}	V22-1	V22-2	V22-3	V23-1_r	V23-2_i	V23-3_i	V23-4_i	V23-5_i
Si^{4+}	18.33	18.01	18.15	17.90	18.12	18.28	18.17	18.24	18.08	18.22
Al^{3+}	10.62	10.33	9.55	9.56	9.52	10.17	10.29	10.30	10.28	10.23
Ti^{4+}	0.00	0.03	0.35	0.37	0.36	0.00	0.00	0.00	0.00	0.00
Mg^{2+}	1.52	1.84	2.11	1.88	2.08	1.86	1.87	1.85	1.84	1.85
Mn^{2+}	0.13	0.00	0.00	0.03	0.00	0.06	0.06	0.07	0.07	0.09
Fe^{2+}	0.39	0.49	0.13	0.14	0.12	0.14	0.09	0.10	0.11	0.11
Fe^{3+}	–	–	0.80	0.90	0.77	0.50	0.33	0.35	0.38	0.40
Cr^{3+}	0.00	0.00	–	–	–	–	–	–	–	–
Cu^{2+}	–	–	–	–	–	–	–	–	–	–
Zn^{2+}	0.00	0.00	0.00	0.00	0.00	0.00	0.00	0.00	0.00	0.00
Ca^{2+}	19.02	19.30	18.92	19.22	19.02	18.98	19.19	19.09	19.24	19.11
Na^{+}	0.00	0.00	0.00	0.00	0.00	0.00	0.00	0.00	0.00	0.00
K^{+}	–	–	0.00	0.00	0.00	0.00	0.00	0.00	0.00	0.00
La^{3+}	–	–	–	–	–	–	–	–	–	–
Ce^{3+}	0.00	0.00	0.00	0.00	0.00	0.00	0.00	0.00	0.00	0.00
Pr^{3+}	–	–	–	–	–	–	–	–	–	–
Nd^{3+}	–	–	–	–	–	–	–	–	–	–
Sm^{3+}	–	–	–	–	–	–	–	–	–	–
Eu^{3+}	–	–	–	–	–	–	–	–	–	–
Gd^{3+}	–	–	–	–	–	–	–	–	–	–
Pb^{2+}	–	–	–	–	–	–	–	–	–	–
Bi^{3+}	–	–	–	–	–	–	–	–	–	–
Th^{4+}	–	–	–	–	–	–	–	–	–	–
U^{4+}	–	–	–	–	–	–	–	–	–	–
B^{3+}	–	–	–	–	–	0.00	–	–	–	–
S^{6+}	0.00	0.00	0.00	0.00	0.00	0.00	0.00	0.00	0.00	0.00
F^{-}	0.00	0.00	0.00	0.00	0.00	0.00	0.00	0.00	0.00	0.00
Cl^{-}	0.00	0.00	0.00	0.00	0.00	0.00	0.00	0.00	0.00	0.00
OH^{-}*	8.72	9.59	8.64	9.00	8.75	8.76	9.05	8.87	9.18	8.94
O	69.28	68.41	69.36	69.00	69.25	69.24	68.95	69.13	68.82	69.06
					Statistics					
ΣX	19.02	19.30	18.92	19.22	19.02	18.98	19.19	19.09	19.24	19.11
ΣY	12.65	12.68	12.93	12.88	12.86	12.74	12.64	12.67	12.69	12.67
ΣZ	18.33	18.01	18.15	17.90	18.12	18.28	18.17	18.24	18.08	18.22

*Calculated for charge balance.

QUANTITATIVE WDS RESULTS (NMNS)

Ions p.f.u. (50-Cation Normalization)

	V23-6_i	V23-7_i	V23-8_r	V24-1	V24-2	V24-3	V25-1_1	V25-2_1	V25-3_2	V26-1
Si^{4+}	18.10	18.29	18.11	18.06	18.01	18.01	17.93	18.08	17.90	17.99
Al^{3+}	10.23	10.33	10.16	9.28	9.33	9.31	9.23	9.34	9.71	9.49
Ti^{4+}	0.00	0.00	0.00	0.87	0.84	0.81	0.76	0.68	0.32	0.27
Mg^{2+}	1.85	1.84	1.85	2.46	2.52	2.49	2.63	2.42	2.41	1.56
Mn^{2+}	0.09	0.08	0.07	0.00	0.00	0.00	0.05	0.05	0.02	0.00
Fe^{2+}	0.11	0.10	0.15	0.25	0.27	0.26	0.45	0.57	0.50	0.22
Fe^{3+}	0.38	0.35	0.54	0.12	0.13	0.12	–	–	–	1.48
Cr^{3+}	–	–	–	–	–	–	–	–	–	–
Cu^{2+}	–	–	–	–	–	–	–	–	–	–
Zn^{2+}	0.00	0.00	0.00	0.00	0.00	0.00	0.00	0.00	0.00	0.00
Ca^{2+}	19.24	19.00	19.10	18.88	18.83	18.94	18.95	18.86	19.11	18.82
Na^{+}	0.00	0.00	0.00	0.08	0.09	0.06	0.00	0.00	0.00	0.16
K^{+}	0.00	0.00	0.00	0.00	0.00	0.00	0.00	0.00	0.00	0.00
La^{3+}	–	–	–	–	–	–	–	0.00	0.00	–
Ce^{3+}	0.00	0.00	0.00	0.00	0.00	0.00	0.00	0.00	0.02	0.00
Pr^{3+}	–	–	–	–	–	–	–	0.00	0.00	–
Nd^{3+}	–	–	–	–	–	–	–	0.00	0.00	–
Sm^{3+}	–	–	–	–	–	–	–	0.00	0.00	–
Eu^{3+}	–	–	–	–	–	–	–	0.00	0.00	–
Gd^{3+}	–	–	–	–	–	–	–	0.00	0.00	–
Pb^{2+}	–	–	–	–	–	–	–	–	–	–
Bi^{3+}	–	–	–	–	–	–	–	–	–	–
Th^{4+}	–	–	–	–	–	–	–	–	–	–
U^{4+}	–	–	–	–	–	–	–	–	–	–
B^{3+}	–	–	–	–	–	–	–	–	–	0.00
S^{6+}	0.00	0.00	0.00	0.07	0.10	0.07	0.15	0.30	0.32	0.18
F^{-}	0.00	0.00	0.00	3.21	3.61	3.65	1.15	1.08	1.31	2.45
Cl^{-}	0.00	0.00	0.00	0.09	0.10	0.11	0.00	0.00	0.00	0.00
OH^{-*}	9.19	8.74	9.08	5.10	4.64	4.84	7.33	6.27	6.61	5.14
O	68.81	69.26	68.92	69.60	69.65	69.40	69.52	70.65	70.07	70.41
					Statistics					
ΣX	19.24	19.00	19.10	18.95	18.92	19.00	18.95	18.86	19.13	18.99
ΣY	12.66	12.71	12.79	12.99	13.07	13.00	13.12	13.06	12.97	13.02
ΣZ	18.10	18.29	18.11	18.06	18.01	18.01	17.93	18.08	17.90	17.99

*Calculated for charge balance.

V26 includes 0.01 Li, 0.01 Be.

QUANTITATIVE WDS RESULTS (NMNS)

Ions p.f.u. (50-Cation Normalization)

	V26-2	V26-3	V26-4	V26-5	V27-1	V27-2	V27-3	V27-4	V28-1	V28-2
Si^{4+}	18.06	17.79	17.74	17.66	17.80	17.98	17.78	18.04	18.14	17.88
Al^{3+}	9.55	10.15	9.43	10.07	9.36	9.41	9.42	9.42	9.43	9.24
Ti^{4+}	0.22	0.10	0.34	0.24	0.03	0.02	0.00	0.01	0.98	1.04
Mg^{2+}	1.62	1.83	1.68	1.88	2.16	2.10	2.12	2.12	1.32	1.27
Mn^{2+}	0.03	0.03	0.00	0.00	0.10	0.11	0.12	0.12	0.00	0.00
Fe^{2+}	0.20	0.12	0.21	0.10	1.33	1.34	1.30	1.35	1.01	1.05
Fe^{3+}	1.34	0.82	1.42	0.67	–	–	–	–	–	–
Cr^{3+}	–	–	–	–	–	–	–	–	0.00	0.00
Cu^{2+}	–	–	–	–	–	–	–	–	–	–
Zn^{2+}	0.00	0.00	0.00	0.00	0.00	0.00	0.00	0.00	0.00	0.00
Ca^{2+}	18.82	19.02	19.07	19.30	19.19	18.98	19.19	18.89	18.96	19.36
Na^{+}	0.16	0.13	0.11	0.09	0.04	0.06	0.06	0.05	0.14	0.15
K^{+}	0.00	0.00	0.00	0.00	0.00	0.00	0.00	0.00	–	–
La^{3+}	–	–	–	–	–	–	–	–	–	–
Ce^{3+}	0.00	0.00	0.00	0.00	0.00	0.00	0.00	0.00	0.00	0.00
Pr^{3+}	–	–	–	–	–	–	–	–	–	–
Nd^{3+}	–	–	–	–	–	–	–	–	–	–
Sm^{3+}	–	–	–	–	–	–	–	–	–	–
Eu^{3+}	–	–	–	–	–	–	–	–	–	–
Gd^{3+}	–	–	–	–	–	–	–	–	–	–
Pb^{2+}	–	–	–	–	–	–	–	–	–	–
Bi^{3+}	–	–	–	–	–	–	–	–	–	–
Th^{4+}	–	–	–	–	–	–	–	–	–	–
U^{4+}	–	–	–	–	–	–	–	–	–	–
B^{3+}	–	–	–	–	–	–	0.00	–	–	–
S^{6+}	0.16	0.13	0.00	0.00	0.00	0.10	0.00	0.10	0.07	0.08
F^{-}	2.42	2.47	3.26	2.97	2.96	3.01	2.98	2.53	2.12	2.13
Cl^{-}	0.00	0.00	0.00	0.00	0.00	0.00	0.00	0.00	0.19	0.20
OH^{-}*	5.33	6.15	5.85	6.58	8.07	7.06	8.10	7.37	5.71	6.29
O	70.25	69.38	68.90	68.45	66.97	67.93	66.92	68.10	69.98	69.38
					Statistics					
ΣX	18.98	19.15	19.18	19.39	19.22	19.04	19.25	18.93	19.11	19.51
ΣY	12.96	13.06	13.08	12.95	12.98	12.98	12.97	13.02	12.75	12.61
ΣZ	18.06	17.79	17.74	17.66	17.80	17.98	17.78	18.04	18.14	17.88

*Calculated for charge balance.

V26 includes 0.01 Li, 0.01 Be.

QUANTITATIVE WDS RESULTS (NMNS)

Ions p.f.u. (50-Cation Normalization)

	V28-3	V28-4	V28-5	V29-1	V29-2	V29-3	V29-4	V29-5	V30-1_{rl}	V30-2_{rl}
Si^{4+}	18.14	18.06	18.39	18.50	18.16	18.47	18.21	18.59	17.86	17.78
Al^{3+}	9.44	9.35	9.40	9.48	9.37	9.68	9.32	9.55	6.56	6.51
Ti^{4+}	1.04	1.01	1.06	1.04	1.09	1.00	1.07	1.08	0.45	0.48
Mg^{2+}	1.34	1.26	1.28	1.34	1.26	1.33	1.20	1.23	3.36	3.26
Mn^{2+}	0.00	0.00	0.00	0.00	0.00	0.00	0.03	0.00	0.14	0.12
Fe^{2+}	1.09	1.05	1.17	1.10	1.10	1.07	1.13	1.16	2.79	2.59
Fe^{3+}	–	–	–	–	–	–	–	–	–	–
Cr^{3+}	0.00	0.00	0.00	0.00	0.00	0.00	0.00	0.00	0.00	0.00
Cu^{2+}	–	–	–	–	–	–	–	–	–	–
Zn^{2+}	0.00	0.00	0.00	0.00	0.00	0.00	0.00	0.00	0.00	0.00
Ca^{2+}	18.77	19.12	18.68	18.36	18.82	18.27	18.83	18.20	17.67	18.27
Na^{+}	0.17	0.15	0.02	0.19	0.21	0.17	0.21	0.20	0.00	0.00
K^{+}	–	–	–	–	–	–	–	–	–	–
La^{3+}	–	–	–	–	–	–	–	–	0.37	0.32
Ce^{3+}	0.00	0.00	0.00	0.00	0.00	0.00	0.00	0.00	0.61	0.50
Pr^{3+}	–	–	–	–	–	–	–	–	0.05	0.05
Nd^{3+}	–	–	–	–	–	–	–	–	0.10	0.07
Sm^{3+}	–	–	–	–	–	–	–	–	0.00	0.00
Eu^{3+}	–	–	–	–	–	–	–	–	0.00	0.00
Gd^{3+}	–	–	–	–	–	–	–	–	0.03	0.04
Pb^{2+}	–	–	–	–	–	–	–	–	–	–
Bi^{3+}	–	–	–	–	–	–	–	–	–	–
Th^{4+}	–	–	–	–	–	–	–	–	–	–
U^{4+}	–	–	–	–	–	–	–	–	–	–
B^{3+}	0.00	–	–	–	–	–	–	–	2.94	†2.60
S^{6+}	0.09	0.06	0.00	0.07	0.09	0.06	0.08	0.07	0.00	0.00
F^{-}	1.83	2.17	1.88	2.06	1.81	2.23	1.79	2.28	1.44	1.27
Cl^{-}	0.14	0.18	0.14	0.12	0.15	0.15	0.17	0.14	0.00	0.00
OH^{-*}	5.87	5.93	5.70	5.01	5.86	4.79	5.86	4.46	1.37	2.91
O	70.16	69.72	70.28	70.81	70.18	70.83	70.19	71.12	75.18	73.83
					Statistics					
ΣX	18.94	19.27	18.70	18.55	19.03	18.45	19.04	18.40	18.84	19.25
ΣY	12.91	12.66	12.92	12.95	12.82	13.08	12.75	13.01	13.30	12.96
ΣZ	18.14	18.06	18.39	18.50	18.16	18.47	18.21	18.59	17.87	17.78

*Calculated for charge balance. †Average value of 2.90 B_2O_3 used in calculations.

QUANTITATIVE WDS RESULTS (NMNS)

Ions p.f.u. (50-Cation Normalization)

	V30-3_r	V30-4_{rd}	V30-5_d	V30-6	V30-7_c	V30-8	V30-9_{rl}	V31-1_c	V31-2_i	V31-3_r
Si^{4+}	17.91	17.90	18.02	17.78	17.98	18.15	17.74	18.13	18.11	18.15
Al^{3+}	7.29	7.01	6.91	7.21	6.80	7.00	6.38	9.64	9.56	9.53
Ti^{4+}	0.61	0.47	0.42	0.06	0.24	0.14	0.42	1.03	1.04	0.96
Mg^{2+}	3.13	3.53	3.57	4.03	4.18	4.32	3.26	1.05	1.14	1.25
Mn^{2+}	0.11	0.10	0.12	0.12	0.08	0.09	0.13	0.00	0.00	0.00
Fe^{2+}	2.28	2.09	2.48	1.85	1.91	1.96	2.70	1.13	1.16	1.04
Fe^{3+}	–	–	–	–	–	–	–	–	–	–
Cr^{3+}	0.00	0.00	0.00	0.00	0.00	0.00	0.00	–	–	–
Cu^{2+}	–	–	–	–	–	–	–	–	–	–
Zn^{2+}	0.00	0.00	0.00	0.00	0.00	0.00	0.00	0.00	0.00	0.00
Ca^{2+}	18.09	18.62	17.92	18.67	18.56	18.15	18.14	18.75	18.78	18.87
Na^{+}	0.00	0.00	0.00	0.00	0.00	0.05	0.05	0.27	0.20	0.19
K^{+}	–	–	–	–	–	–	–	0.00	0.00	0.00
La^{3+}	0.27	0.14	0.22	0.15	0.12	0.08	0.35	–	–	–
Ce^{3+}	0.30	0.15	0.22	0.14	0.10	0.06	0.59	–	–	–
Pr^{3+}	0.00	0.00	0.09	0.00	0.00	0.00	0.07	–	–	–
Nd^{3+}	0.00	0.00	0.00	0.00	0.03	0.00	0.12	–	–	–
Sm^{3+}	0.00	0.00	0.00	0.00	0.00	0.00	0.00	–	–	–
Eu^{3+}	0.00	0.00	0.00	0.00	0.00	0.00	0.00	–	–	–
Gd^{3+}	0.00	0.00	0.03	0.00	0.00	0.00	0.05	–	–	–
Pb^{2+}	–	–	–	–	–	–	–	–	–	–
Bi^{3+}	–	–	–	–	–	–	–	–	–	–
Th^{4+}	–	–	–	–	–	–	–	–	–	–
U^{4+}	–	–	–	–	–	–	–	–	–	–
B^{3+}	†2.60	2.22	†2.59	†2.52	2.57	†2.53	†2.63	0.00	–	–
S^{6+}	0.00	0.00	0.00	0.00	0.10	0.00	0.00	0.00	0.08	0.07
F^{-}	1.54	0.94	1.19	1.11	1.01	0.98	1.56	2.30	2.56	2.41
Cl^{-}	0.00	0.00	0.00	0.00	0.00	0.00	0.00	0.11	0.13	0.15
OH^{-}*	1.74	4.37	2.71	4.16	3.16	3.75	2.73	5.90	5.17	5.45
O	74.71	72.69	74.10	72.72	73.83	73.28	73.71	69.69	70.15	69.99
					Statistics					
ΣX	18.66	18.90	18.48	18.96	18.81	18.34	19.38	19.02	18.99	19.06
ΣY	13.43	13.20	13.50	13.26	13.21	13.51	12.89	12.85	12.90	12.79
ΣZ	17.91	17.90	18.02	17.78	17.98	18.15	17.74	18.13	18.11	18.15

*Calculated for charge balance. †Average value of 2.90 B_2O_3 used in calculations.

QUANTITATIVE WDS RESULTS (NMNS)

Ions p.f.u. (50-Cation Normalization)

	V32-1	V32-2	V32-3	V32-4	V32-5	V33-1_c	V33-2_r	V34-1	V34-2	V34-3
Si^{4+}	18.28	18.57	18.20	18.61	18.12	18.34	18.19	18.32	18.13	18.10
Al^{3+}	9.79	9.86	9.51	9.79	9.66	10.00	9.87	9.08	9.04	9.31
Ti^{4+}	0.25	0.29	0.28	0.29	0.25	0.23	0.25	0.36	0.34	0.33
Mg^{2+}	1.50	1.55	1.54	1.54	1.54	1.24	1.30	1.33	1.47	1.31
Mn^{2+}	0.00	0.00	0.00	0.00	0.00	0.28	0.33	0.17	0.17	0.15
Fe^{2+}	1.31	1.42	1.42	1.40	1.35	1.29	1.28	1.98	1.97	1.69
Fe^{3+}	–	–	–	–	–	0.14	0.14	–	–	–
Cr^{3+}	0.00	0.00	0.00	0.00	0.00	–	–	–	–	–
Cu^{2+}	–	–	–	–	–	–	–	–	–	–
Zn^{2+}	0.00	0.00	0.00	0.00	0.00	0.00	0.00	0.00	0.00	0.00
Ca^{2+}	18.71	18.15	18.91	18.19	18.92	18.40	18.53	18.68	18.82	19.00
Na^{+}	0.14	0.14	0.11	0.15	0.14	0.09	0.10	0.08	0.06	0.10
K^{+}	–	–	–	–	–	0.00	0.00	0.00	0.00	0.00
La^{3+}	0.00	0.00	0.00	0.00	0.00	–	–	–	–	–
Ce^{3+}	0.02	0.02	0.03	0.02	0.01	–	–	0.00	0.00	0.00
Pr^{3+}	0.00	0.00	0.00	0.00	0.00	–	–	–	–	–
Nd^{3+}	0.00	0.00	0.00	0.00	0.00	–	–	–	–	–
Sm^{3+}	0.00	0.00	0.00	0.00	0.00	–	–	–	–	–
Eu^{3+}	0.00	0.00	0.00	0.00	0.00	–	–	–	–	–
Gd^{3+}	0.00	0.00	0.00	0.00	0.00	–	–	–	–	–
Pb^{2+}	–	–	–	–	–	–	–	–	–	–
Bi^{3+}	–	–	–	–	–	–	–	–	–	–
Th^{4+}	–	–	–	–	–	–	–	–	–	–
U^{4+}	–	–	–	–	–	–	–	–	–	–
B^{3+}	–	–	–	–	–	0.00	–	–	0.00	–
S^{6+}	0.05	0.06	0.00	0.08	0.06	0.00	0.00	0.00	0.00	0.00
F^{-}	2.77	2.69	2.69	2.92	2.94	4.70	4.84	3.55	3.26	3.11
Cl^{-}	0.12	0.15	0.17	0.13	0.12	0.00	0.00	0.19	0.15	0.18
OH^{-}*	6.08	5.33	6.76	5.03	6.32	4.10	4.38	5.90	6.67	6.63
O	69.03	69.83	68.37	69.92	68.61	69.20	68.78	68.36	67.92	68.08
					Statistics					
ΣX	18.87	18.31	19.06	18.36	19.08	18.48	18.64	18.76	18.87	19.10
ΣY	12.85	13.12	12.75	13.03	12.80	13.18	13.17	12.92	12.99	12.80
ΣZ	18.28	18.57	18.20	18.61	18.12	18.34	18.19	18.32	18.13	18.10

*Calculated for charge balance.

V33 includes 0.05 Be.

QUANTITATIVE WDS RESULTS (NMNS)

Ions p.f.u. (50-Cation Normalization)

	V34-4	V34-5	V35-1_c	V35-2_r	V36-1	V36-2	V36-3	V36-4	V36-5	V37-1
Si^{4+}	18.17	18.16	18.14	18.25	17.62	18.03	17.85	17.97	17.65	17.93
Al^{3+}	9.06	9.18	9.50	9.62	9.09	9.25	9.25	9.26	9.04	9.17
Ti^{4+}	0.33	0.30	0.66	0.65	0.05	0.05	0.04	0.05	0.05	0.05
Mg^{2+}	1.46	1.42	1.02	0.85	2.74	2.55	2.53	2.60	2.71	2.01
Mn^{2+}	0.16	0.17	0.00	0.00	0.00	0.00	0.00	0.00	0.00	0.05
Fe^{2+}	2.05	1.89	1.73	1.75	0.17	0.15	0.15	0.16	0.17	1.58
Fe^{3+}	–	–	–	–	1.20	1.06	1.06	1.15	1.21	–
Cr^{3+}	–	–	–	–	0.13	0.24	0.20	0.24	0.16	–
Cu^{2+}	–	–	–	–	–	–	–	–	–	–
Zn^{2+}	0.00	0.00	0.00	0.00	0.00	0.00	0.00	0.00	0.00	0.00
Ca^{2+}	18.71	18.77	18.88	18.80	19.01	18.66	18.92	18.56	19.01	19.21
Na^{+}	0.06	0.10	0.07	0.09	0.00	0.00	0.00	0.00	0.00	0.00
K^{+}	0.00	0.00	0.00	0.00	–	–	–	–	–	0.00
La^{3+}	-	–	–	–	–	–	–	–	–	–
Ce^{3+}	0.00	0.00	0.00	0.00	0.00	0.00	0.00	0.00	0.00	0.00
Pr^{3+}	–	–	–	–	–	–	–	–	–	–
Nd^{3+}	–	–	–	–	–	–	–	–	–	–
Sm^{3+}	–	–	–	–	–	–	–	–	–	–
Eu^{3+}	–	–	–	–	–	–	–	–	–	–
Gd^{3+}	–	–	–	–	–	–	–	–	–	–
Pb^{2+}	–	–	–	–	–	–	–	–	–	–
Bi^{3+}	–	–	–	–	–	–	–	–	–	–
Th^{4+}	–	–	–	–	–	–	–	–	–	–
U^{4+}	–	–	–	–	–	–	–	–	–	–
B^{3+}	–	–	0.00	–	–	–	0.00	–	–	–
S^{6+}	0.00	0.00	0.00	0.00	0.05	0.00	0.00	0.00	0.00	0.00
F^{-}	3.49	3.40	3.63	3.37	0.00	0.00	0.00	0.00	0.00	0.00
Cl^{-}	0.13	0.09	0.00	0.00	0.00	0.00	0.00	0.00	0.00	0.00
OH^{-*}	6.37	6.49	5.33	5.29	9.96	9.28	9.71	9.31	10.19	10.86
O	68.00	68.02	69.03	69.34	68.04	68.72	68.29	68.69	67.81	67.14
					Statistics					
ΣX	18.77	18.87	18.95	18.89	19.01	18.66	18.92	18.56	19.01	19.21
ΣY	13.07	12.97	12.91	12.86	13.37	13.30	13.23	13.47	13.34	12.86
ΣZ	18.17	18.16	18.14	18.25	17.62	18.03	17.85	17.97	17.65	17.93

*Calculated for charge balance.

V35 includes 0.02 Li.

QUANTITATIVE WDS RESULTS (NMNS)

Ions p.f.u. (50-Cation Normalization)

	V37-2	V37-3	V38-1_{cl}	V38-2_{cl}	V38-3_{cd}	V38-4_{cl}	V38-5_{il}	V38-6_{il}	V38-7_{id}	V38-8_{il}
Si^{4+}	18.10	18.00	17.58	17.57	17.56	17.51	17.61	17.65	17.93	17.72
Al^{3+}	9.38	9.36	6.40	6.58	6.79	6.63	6.74	6.86	6.23	6.59
Ti^{4+}	0.05	0.06	0.60	0.61	0.35	0.57	0.43	0.33	0.31	0.33
Mg^{2+}	2.06	2.11	3.84	3.68	3.82	3.71	3.83	3.95	4.30	4.17
Mn^{2+}	0.03	0.03	0.05	0.05	0.05	0.05	0.06	0.08	0.09	0.07
Fe^{2+}	1.31	1.34	2.56	2.50	2.31	2.49	2.15	2.17	2.10	2.27
Fe^{3+}	–	–	–	–	–	–	–	–	–	–
Cr^{3+}	–	–	–	–	–	–	–	–	–	–
Cu^{2+}	–	–	–	–	–	–	–	–	–	–
Zn^{2+}	0.00	0.00	0.00	0.00	0.00	0.00	0.00	0.00	0.00	0.00
Ca^{2+}	19.06	19.10	17.79	18.05	18.48	18.15	18.59	18.48	18.68	18.44
Na^{+}	0.00	0.00	0.05	0.00	0.00	0.00	0.00	0.00	0.00	0.00
K^{+}	0.00	0.00	0.00	0.00	0.00	0.00	0.00	0.00	0.00	0.00
La^{3+}	–	–	0.31	0.26	0.20	0.25	0.21	0.18	0.14	0.15
Ce^{3+}	0.00	0.00	0.59	0.50	0.34	0.45	0.31	0.25	0.16	0.20
Pr^{3+}	–	–	0.07	0.06	0.05	0.06	0.03	0.03	0.03	0.03
Nd^{3+}	–	–	0.11	0.09	0.05	0.08	0.04	0.03	0.03	0.03
Sm^{3+}	–	–	0.00	0.00	0.00	0.00	0.00	0.00	0.00	0.00
Eu^{3+}	–	–	0.00	0.00	0.00	0.00	0.00	0.00	0.00	0.00
Gd^{3+}	–	–	0.06	0.05	0.00	0.06	0.00	0.00	0.00	0.00
Pb^{2+}	–	–	–	–	–	–	–	–	–	–
Bi^{3+}	–	–	–	–	–	–	–	–	–	–
Th^{4+}	–	–	–	–	–	–	–	–	–	–
U^{4+}	–	–	–	–	–	–	–	–	–	–
B^{3+}	–	–	1.41	†1.60	†1.56	2.06	†1.56	†1.55	†1.54	†1.56
S^{6+}	0.00	0.00	0.12	0.09	0.00	0.00	0.00	0.00	0.00	0.00
F^{-}	0.00	0.00	1.07	1.41	1.26	0.95	1.11	1.11	0.00	0.92
Cl^{-}	0.00	0.00	0.00	0.00	0.00	0.00	0.00	0.00	0.00	0.00
OH^{-}*	10.33	10.52	6.12	5.33	6.83	5.18	6.81	6.92	8.31	7.30
O	67.67	67.48	70.81	71.26	69.91	71.86	70.07	69.97	69.69	69.78
					Statistics					
ΣX	19.06	19.10	18.98	19.01	19.12	19.04	19.19	18.96	19.04	18.85
ΣY	12.84	12.90	13.44	13.40	13.32	13.45	13.21	13.39	13.03	13.43
ΣZ	18.10	18.00	17.58	17.57	17.56	17.51	17.61	17.65	17.93	17.72

*Calculated for charge balance. †Average value of 1.77 B_2O_3 used in calculations.

QUANTITATIVE WDS RESULTS (NMNS)

Ions p.f.u. (50-Cation Normalization)

	V38-9$_{id}$	V38-10$_{id}$	V38-11$_{il}$	V38-12$_{id}$	V38-13$_{id}$	V38-14$_{il}$	V38-15$_{id}$	V38-16$_{id}$	V38-17$_{il}$	V38-18$_{il}$
Si^{4+}	17.72	17.93	17.75	17.96	17.64	17.81	17.71	17.82	17.81	17.78
Al^{3+}	6.69	6.98	6.83	7.09	6.98	6.82	6.88	7.15	7.07	6.99
Ti^{4+}	0.33	0.32	0.32	0.15	0.26	0.35	0.36	0.27	0.20	0.17
Mg^{2+}	3.95	3.91	3.99	4.05	4.07	4.01	3.87	4.02	3.94	4.07
Mn^{2+}	0.08	0.08	0.08	0.07	0.09	0.07	0.07	0.08	0.07	0.09
Fe^{2+}	2.13	2.09	2.13	2.00	1.91	2.06	2.07	1.85	1.96	1.97
Fe^{3+}	–	–	–	–	–	–	–	–	–	–
Cr^{3+}	–	–	–	–	–	–	–	–	–	–
Cu^{2+}	–	–	–	–	–	–	–	–	–	–
Zn^{2+}	0.00	0.00	0.00	0.00	0.00	0.00	0.00	0.00	0.00	0.00
Ca^{2+}	18.81	18.52	18.63	18.50	18.86	18.63	18.87	18.67	18.79	18.75
Na^{+}	0.00	0.00	0.00	0.00	0.00	0.04	0.04	0.05	0.00	0.00
K^{+}	0.00	0.00	0.00	0.00	0.00	0.00	0.00	0.00	0.00	0.00
La^{3+}	0.13	0.07	0.12	0.08	0.10	0.11	0.06	0.05	0.07	0.10
Ce^{3+}	0.14	0.10	0.13	0.09	0.09	0.11	0.08	0.05	0.09	0.09
Pr^{3+}	0.02	0.00	0.03	0.00	0.00	0.00	0.00	0.00	0.00	0.00
Nd^{3+}	0.00	0.00	0.00	0.00	0.00	0.00	0.00	0.00	0.00	0.00
Sm^{3+}	0.00	0.00	0.00	0.00	0.00	0.00	0.00	0.00	0.00	0.00
Eu^{3+}	0.00	0.00	0.00	0.00	0.00	0.00	0.00	0.00	0.00	0.00
Gd^{3+}	0.00	0.00	0.00	0.00	0.00	0.00	0.00	0.00	0.00	0.00
Pb^{2+}	–	–	–	–	–	–	–	–	–	–
Bi^{3+}	–	–	–	–	–	–	–	–	–	–
Th^{4+}	–	–	–	–	–	–	–	–	–	–
U^{4+}	–	–	–	–	–	–	–	–	–	–
B^{3+}	†1.53	†1.54	†1.54	†1.53	†1.53	†1.54	1.25	†1.53	†1.52	†1.53
S^{6+}	0.00	0.00	0.00	0.00	0.00	0.00	0.04	0.00	0.00	0.00
F^{-}	1.20	1.02	0.94	1.12	0.65	1.18	1.12	1.18	0.85	0.90
Cl^{-}	0.00	0.00	0.00	0.00	0.00	0.00	0.00	0.00	0.00	0.00
OH^{-}*	7.13	6.71	7.22	6.80	7.81	6.88	7.74	6.87	7.34	7.44
O	69.67	70.27	69.84	70.08	69.54	69.93	69.14	69.95	69.81	69.65
					Statistics					
ΣX	19.10	18.70	18.91	18.67	19.04	18.89	19.05	18.82	18.95	18.94
ΣY	13.18	13.37	13.34	13.37	13.32	13.30	13.24	13.36	13.24	13.28
ΣZ	17.72	17.93	17.75	17.96	17.64	17.81	17.71	17.82	17.81	17.78

*Calculated for charge balance. †Average value of 1.77 B_2O_3 used in calculations.

QUANTITATIVE WDS RESULTS (NMNS)

Ions p.f.u. (50-Cation Normalization)

	$V38\text{-}19_{id}$	$V38\text{-}20_{il}$	$V38\text{-}21_{id}$	$V38\text{-}22_{id}$	$V38\text{-}23_{rl}$	$V38\text{-}24_{rl}$	$V38\text{-}25_{rl}$	V39-1	V39-2	V39-3
Si^{4+}	17.77	17.92	17.80	17.74	17.73	17.81	17.93	18.19	17.86	18.27
Al^{3+}	7.15	6.75	7.20	7.20	6.28	6.64	6.41	8.44	8.37	8.47
Ti^{4+}	0.26	0.09	0.22	0.10	0.26	0.47	0.52	0.62	0.55	0.62
Mg^{2+}	4.00	4.11	3.92	4.06	3.70	3.32	3.28	1.89	1.85	1.91
Mn^{2+}	0.08	0.13	0.08	0.11	0.10	0.11	0.12	0.06	0.05	0.05
Fe^{2+}	1.80	2.11	1.80	1.84	2.61	2.52	2.49	0.42	0.41	0.40
Fe^{3+}	–	–	–	–	–	–	–	1.58	1.57	1.53
Cr^{3+}	–	–	–	–	–	–	–	0.00	0.00	0.00
Cu^{2+}	–	–	–	–	–	–	–	–	–	–
Zn^{2+}	0.00	0.00	0.00	0.00	0.00	0.00	0.00	0.00	0.00	0.00
Ca^{2+}	18.88	18.63	18.94	18.79	18.57	18.53	18.50	18.80	19.33	18.75
Na^{+}	0.00	0.00	0.00	0.00	0.00	0.00	0.00	0.00	0.00	0.00
K^{+}	0.00	0.00	0.00	0.00	0.00	0.00	0.00	–	–	–
La^{3+}	0.03	0.13	0.02	0.08	0.25	0.24	0.27	–	–	–
Ce^{3+}	0.03	0.12	0.03	0.08	0.40	0.29	0.37	0.00	0.00	0.00
Pr^{3+}	0.00	0.00	0.00	0.00	0.00	0.00	0.00	–	–	–
Nd^{3+}	0.00	0.00	0.00	0.00	0.06	0.04	0.05	–	–	–
Sm^{3+}	0.00	0.00	0.00	0.00	0.00	0.00	0.00	–	–	–
Eu^{3+}	0.00	0.00	0.00	0.00	0.00	0.00	0.00	–	–	–
Gd^{3+}	0.00	0.00	0.00	0.00	0.04	0.03	0.03	–	–	–
Pb^{2+}	–	–	–	–	–	–	–	–	–	–
Bi^{3+}	–	–	–	–	–	–	–	–	–	–
Th^{4+}	–	–	–	–	–	–	–	–	–	–
U^{4+}	–	–	–	–	–	–	–	–	–	–
B^{3+}	†1.52	†1.54	†1.51	†1.53	†1.57	†1.59	†1.57	–	–	0.00
S^{6+}	0.00	0.00	0.00	0.00	0.00	0.00	0.00	0.00	0.00	0.00
F^{-}	0.97	0.97	1.19	0.90	1.49	1.86	1.59	0.00	0.00	0.00
Cl^{-}	0.00	0.00	0.00	0.00	0.00	0.00	0.00	0.00	0.00	0.00
OH^{-}*	7.20	7.40	6.99	7.47	6.80	5.58	5.67	8.37	9.24	8.24
O	69.82	69.63	69.82	69.63	69.70	70.56	70.75	69.63	68.76	69.76
					Statistics					
ΣX	18.94	18.88	18.98	18.94	19.31	19.12	19.22	18.80	19.33	18.75
ΣY	13.29	13.20	13.22	13.32	12.96	13.06	12.84	13.01	12.81	12.98
ΣZ	17.77	17.92	17.80	17.74	17.73	17.81	17.93	18.19	17.86	18.27

*Calculated for charge balance. †Average value of 1.77 B_2O_3 used in calculations.

QUANTITATIVE WDS RESULTS (NMNS)

Ions p.f.u. (50-Cation Normalization)

	V39-4	V39-5	V40-1_{cd}	V40-2_{id}	V40-3_{id}	V40-4_{id}	V40-5_{id}	V40-6_{id}	V40-7_{id}	V40-8_{il}
Si^{4+}	17.93	18.31	17.85	17.99	17.84	17.60	17.96	17.81	17.89	17.88
Al^{3+}	8.24	8.35	9.84	9.44	9.71	10.09	9.24	9.20	8.52	7.82
Ti^{4+}	0.67	0.61	0.37	0.55	0.42	0.27	0.53	0.19	0.26	0.28
Mg^{2+}	1.87	1.91	2.04	2.16	2.19	2.05	1.94	2.17	2.53	2.51
Mn^{2+}	0.05	0.05	0.13	0.12	0.12	0.11	0.12	0.13	0.12	0.10
Fe^{2+}	0.41	0.43	1.19	1.12	1.18	1.18	1.64	1.81	2.24	2.63
Fe^{3+}	1.54	1.60	–	–	–	–	–	–	–	–
Cr^{3+}	0.00	0.00	–	–	–	–	–	–	–	–
Cu^{2+}	–	–	–	–	–	–	–	–	–	–
Zn^{2+}	0.00	0.00	0.00	0.00	0.00	0.00	0.00	0.00	0.00	0.00
Ca^{2+}	19.31	18.74	18.41	18.52	18.47	18.62	18.48	18.63	18.39	18.55
Na^{+}	0.00	0.00	0.13	0.09	0.07	0.08	0.10	0.07	0.05	0.00
K^{+}	–	–	0.00	0.00	0.00	0.00	0.00	0.00	0.00	0.00
La^{3+}	–	–	0.00	0.00	0.00	0.00	0.00	0.00	0.00	0.09
Ce^{3+}	0.00	0.00	0.03	0.00	0.00	0.00	0.00	0.00	0.00	0.13
Pr^{3+}	–	–	0.00	0.00	0.00	0.00	0.00	0.00	0.00	0.00
Nd^{3+}	–	–	0.00	0.00	0.00	0.00	0.00	0.00	0.00	0.02
Sm^{3+}	–	–	0.00	0.00	0.00	0.00	0.00	0.00	0.00	0.00
Eu^{3+}	–	–	0.00	0.00	0.00	0.00	0.00	0.00	0.00	0.00
Gd^{3+}	–	–	0.00	0.00	0.00	0.00	0.00	0.00	0.00	0.00
Pb^{2+}	–	–	–	–	–	–	–	–	–	–
Bi^{3+}	–	–	–	–	–	–	–	–	–	–
Th^{4+}	–	–	–	–	–	–	–	–	–	–
U^{4+}	–	–	–	–	–	–	–	–	–	–
B^{3+}	–	–	–	–	–	–	–	–	0.00	–
S^{6+}	0.00	0.00	0.00	0.00	0.00	0.00	0.00	0.00	0.00	0.00
F^{-}	0.00	0.00	1.72	2.19	1.87	2.10	2.13	2.55	2.29	2.44
Cl^{-}	0.00	0.00	0.06	0.06	0.04	0.06	0.00	0.07	0.00	0.07
OH^{-*}	9.04	8.21	8.04	7.32	7.94	8.09	7.77	8.26	8.93	9.12
O	68.96	69.79	68.18	68.43	68.15	67.75	68.10	67.12	66.77	66.37
					Statistics					
ΣX	19.31	18.74	18.58	18.62	18.54	18.70	18.59	18.69	18.44	18.79
ΣY	12.76	12.95	13.57	13.39	13.62	13.70	13.45	13.50	13.67	13.33
ΣZ	17.93	18.31	17.85	17.99	17.84	17.60	17.96	17.81	17.89	17.88

*Calculated for charge balance.

QUANTITATIVE WDS RESULTS (NMNS)
Ions p.f.u. (50-Cation Normalization)

	$V40\text{-}9_{rd}$	V41-1	V41-2	V41-3	V41-4	V41-5	V42-1	V42-2	V42-3	V42-4
Si^{4+}	17.91	18.47	17.96	18.45	18.06	18.46	18.19	18.10	18.34	18.01
Al^{3+}	8.85	8.87	8.29	8.72	8.60	8.60	8.26	8.15	8.18	8.16
Ti^{4+}	0.18	0.03	0.03	0.03	0.04	0.03	0.13	0.14	0.14	0.14
Mg^{2+}	2.08	2.33	2.36	2.31	2.19	2.27	2.80	2.86	2.83	2.77
Mn^{2+}	0.13	0.03	0.04	0.04	0.02	0.00	0.00	0.00	0.00	0.00
Fe^{2+}	2.29	1.81	2.05	1.80	1.94	2.04	1.62	1.62	1.64	1.63
Fe^{3+}	–	–	–	–	–	–	–	–	–	–
Cr^{3+}	–	0.00	0.00	0.00	0.00	0.00	–	–	–	–
Cu^{2+}	–	–	–	–	–	–	–	–	–	–
Zn^{2+}	0.00	0.00	0.00	0.00	0.00	0.00	0.00	0.00	0.00	0.00
Ca^{2+}	18.54	18.47	19.27	18.66	19.15	18.61	18.99	19.13	18.87	19.29
Na^{+}	0.03	0.00	0.00	0.00	0.00	0.00	0.00	0.00	0.00	0.00
K^{+}	0.00	–	–	–	–	–	0.00	0.00	0.00	0.00
La^{3+}	0.00	–	–	–	–	–	–	–	–	–
Ce^{3+}	0.00	0.00	0.00	0.00	0.00	0.00	–	–	–	–
Pr^{3+}	0.00	–	–	–	–	–	–	–	–	–
Nd^{3+}	0.00	–	–	–	–	–	–	–	–	–
Sm^{3+}	0.00	–	–	–	–	–	–	–	–	–
Eu^{3+}	0.00	–	–	–	–	–	–	–	–	–
Gd^{3+}	0.00	–	–	–	–	–	–	–	–	–
Pb^{2+}	–	–	–	–	–	–	–	–	–	–
Bi^{3+}	–	–	–	–	–	–	–	–	–	–
Th^{4+}	–	–	–	–	–	–	–	–	–	–
U^{4+}	–	–	–	–	–	–	–	–	–	–
B^{3+}	–	–	–	0.00	–	–	0.00	–	–	–
S^{6+}	0.00	0.00	0.00	0.00	0.00	0.00	0.00	0.00	0.00	0.00
F^{-}	2.52	0.00	0.00	0.00	0.00	0.00	1.40	1.33	1.40	1.31
Cl^{-}	0.05	0.00	0.00	0.00	0.00	0.00	0.00	0.00	0.00	0.00
OH^{-}*	8.45	10.13	11.72	10.34	11.21	10.44	9.68	10.04	9.46	10.22
O	66.98	67.87	66.28	67.66	66.79	67.56	66.91	66.63	67.14	66.46
					Statistics					
ΣX	18.57	18.47	19.27	18.66	19.15	18.61	18.99	19.13	18.87	19.29
ΣY	13.52	13.06	12.77	12.90	12.79	12.94	12.81	12.77	12.78	12.70
ΣZ	17.91	18.47	17.96	18.45	18.06	18.46	18.19	18.10	18.34	18.01

*Calculated for charge balance.

QUANTITATIVE WDS RESULTS (NMNS)

Ions p.f.u. (50-Cation Normalization)

	V42-5	V43-1	V43-2	V43-3	V43-4	V44-1	V44-2	V44-3	V44-4	V45-1$_r$
Si^{4+}	18.13	17.99	17.74	17.79	17.77	17.75	18.16	17.88	18.06	17.66
Al^{3+}	8.28	8.76	8.51	8.64	8.63	9.94	10.12	9.89	10.30	8.51
Ti^{4+}	0.15	0.11	0.11	0.14	0.15	0.00	0.00	0.00	0.00	0.16
Mg^{2+}	2.85	2.39	2.42	2.46	2.45	3.20	3.15	3.05	3.15	3.73
Mn^{2+}	0.00	0.00	0.00	0.00	0.00	0.00	0.00	0.00	0.00	0.00
Fe^{2+}	1.65	0.16	0.16	0.16	0.16	0.30	0.38	0.42	0.31	0.75
Fe^{3+}	–	1.87	1.92	1.91	1.91	–	–	–	–	–
Cr^{3+}	–	–	–	–	–	0.00	0.00	0.00	0.00	0.00
Cu^{2+}	–	–	–	–	–	–	–	–	–	–
Zn^{2+}	0.00	0.00	0.00	0.00	0.00	0.00	0.00	0.00	0.00	0.00
Ca^{2+}	18.94	18.72	19.15	18.90	18.94	18.81	18.20	18.77	18.19	19.20
Na^{+}	0.00	0.00	0.00	0.00	0.00	0.00	0.00	0.00	0.00	0.00
K^{+}	0.00	0.00	0.00	0.00	0.00	–	–	–	–	–
La^{3+}	–	–	0.00	–	–	–	–	–	–	0.00
Ce^{3+}	–	–	0.00	–	–	0.00	0.00	0.00	0.00	0.00
Pr^{3+}	–	–	0.00	–	–	–	–	–	–	0.00
Nd^{3+}	–	–	0.00	–	–	–	–	–	–	0.00
Sm^{3+}	–	–	0.00	–	–	–	–	–	–	0.00
Eu^{3+}	–	–	0.00	–	–	–	–	–	–	0.00
Gd^{3+}	–	–	0.00	–	–	–	–	–	–	0.00
Pb^{2+}	–	–	–	–	–	–	–	–	–	–
Bi^{3+}	–	–	–	–	–	–	–	–	–	–
Th^{4+}	–	–	–	–	–	–	–	–	–	–
U^{4+}	–	–	–	–	–	–	–	–	–	–
B^{3+}	–	0.00	–	–	–	–	–	–	–	†1.22
S^{6+}	0.00	0.00	0.00	0.00	0.00	0.11	0.10	0.16	0.09	0.07
F^{-}	1.20	0.00	0.00	0.00	0.00	0.67	0.99	0.93	0.74	1.11
Cl^{-}	0.00	0.00	0.00	0.00	0.00	0.00	0.00	0.00	0.00	0.00
OH^{-*}	9.96	9.16	9.88	9.58	9.63	9.23	7.97	8.46	8.29	6.69
O	66.84	68.84	68.12	68.42	68.37	68.10	69.05	68.61	68.97	70.20
					Statistics					
ΣX	18.94	18.72	19.15	18.90	18.94	18.81	18.20	18.77	18.19	19.20
ΣY	12.93	13.29	13.11	13.31	13.29	13.44	13.64	13.35	13.75	13.14
ΣZ	18.13	17.99	17.74	17.79	17.77	17.75	18.16	17.88	18.06	17.66

*Calculated for charge balance. †Average value of 1.47 B_2O_3 used in calculations.

QUANTITATIVE WDS RESULTS (NMNS)

Ions p.f.u. (50-Cation Normalization)

	V45-2_r	V45-3_r	V45-4_r	V45-5_r	V45-6_c	V45-7_c	V45-8_c	V46-1	V46-2	V46-3
Si^{4+}	17.98	17.75	17.95	17.66	17.70	17.77	17.77	18.16	18.31	17.99
Al^{3+}	8.83	8.59	8.70	8.68	8.44	8.04	8.38	7.47	8.92	8.34
Ti^{4+}	0.17	0.18	0.16	0.16	0.46	0.64	0.37	1.90	0.33	0.10
Mg^{2+}	3.66	3.70	3.78	3.58	3.86	3.57	3.88	2.83	3.52	3.46
Mn^{2+}	0.03	0.00	0.00	0.00	0.03	0.02	0.03	0.03	0.03	0.04
Fe^{2+}	0.92	0.82	0.89	0.82	0.90	0.86	0.90	0.28	0.19	0.40
Fe^{3+}	–	–	–	–	–	–	–	0.51	0.34	0.71
Cr^{3+}	0.00	0.00	0.00	0.00	0.00	0.00	0.00	0.00	0.00	0.00
Cu^{2+}	–	–	–	–	–	–	–	–	–	–
Zn^{2+}	0.00	0.00	0.00	0.00	0.00	0.00	0.00	0.00	0.00	0.00
Ca^{2+}	18.39	18.90	18.42	19.04	18.59	19.02	18.66	18.73	18.37	18.87
Na^{+}	0.00	0.00	0.05	0.00	0.00	0.00	0.00	0.00	0.00	0.00
K^{+}	–	–	–	–	–	–	–	–	–	–
La^{3+}	0.00	0.02	0.02	0.02	0.00	0.03	0.00	0.02	–	0.03
Ce^{3+}	0.03	0.04	0.03	0.03	0.02	0.05	0.02	0.05	0.00	0.06
Pr^{3+}	0.00	0.00	0.00	0.00	0.00	0.00	0.00	0.00	–	0.00
Nd^{3+}	0.00	0.00	0.00	0.00	0.00	0.00	0.00	0.03	–	0.00
Sm^{3+}	0.00	0.00	0.00	0.00	0.00	0.00	0.00	0.00	–	0.00
Eu^{3+}	0.00	0.00	0.00	0.00	0.00	0.00	0.00	0.00	–	0.00
Gd^{3+}	0.00	0.00	0.00	0.00	0.00	0.00	0.00	0.00	–	0.00
Pb^{2+}	–	–	–	–	–	–	–	–	–	–
Bi^{3+}	–	–	–	–	–	–	–	–	–	–
Th^{4+}	–	–	–	–	–	–	–	–	–	–
U^{4+}	–	–	–	–	–	–	–	–	–	–
B^{3+}	1.37	0.90	†1.25	†1.23	1.45	1.23	†1.25	–	–	–
S^{6+}	0.06	0.08	0.09	0.09	0.06	0.37	0.06	0.07	0.21	0.23
F^{-}	1.32	1.10	1.15	1.20	1.06	1.30	0.67	1.19	1.18	1.26
Cl^{-}	0.00	0.00	0.00	0.00	0.00	0.00	0.00	0.19	0.06	0.00
OH^{-}*	5.05	7.22	5.62	6.19	5.44	3.85	6.57	6.02	6.98	8.04
O	71.62	69.67	71.23	70.62	71.50	72.85	70.76	70.61	69.78	68.70
					Statistics					
ΣX	18.41	18.96	18.52	19.09	18.61	19.10	18.68	18.82	18.37	18.96
ΣY	13.61	13.29	13.53	13.25	13.69	13.13	13.55	13.02	13.33	13.05
ΣZ	17.98	17.75	17.95	17.66	17.70	17.77	17.77	18.16	18.31	17.99

*Calculated for charge balance. †Average value of 1.47 B_2O_3 used in calculations.

QUANTITATIVE WDS RESULTS (NMNS)

Ions p.f.u. (50-Cation Normalization)

	V46-4	V46-5	V47-1	V47-2	V47-3	V48-1	V48-2	V48-3	V48-4	V49-1
Si^{4+}	18.45	17.94	18.07	18.12	18.01	17.96	18.07	18.07	18.11	18.04
Al^{3+}	8.84	8.88	9.69	9.47	9.64	10.01	10.03	10.26	9.85	10.67
Ti^{4+}	0.49	0.36	0.58	0.83	0.60	0.20	0.25	0.19	0.29	0.00
Mg^{2+}	3.37	3.59	1.10	1.12	1.16	1.43	1.39	1.39	1.51	1.46
Mn^{2+}	0.04	0.04	0.04	0.00	0.03	0.09	0.13	0.09	0.03	0.39
Fe^{2+}	0.20	0.17	1.57	1.58	1.52	0.64	0.71	0.58	0.85	0.45
Fe^{3+}	0.35	0.31	–	–	–	–	–	–	–	–
Cr^{3+}	0.00	0.00	–	–	–	–	–	–	–	–
Cu^{2+}	–	–	–	–	–	0.35	0.33	0.32	0.30	0.16
Zn^{2+}	0.00	0.00	0.00	0.00	0.00	0.00	0.00	0.00	0.00	0.00
Ca^{2+}	18.21	18.71	18.89	18.77	18.98	19.23	18.99	19.01	18.97	18.77
Na^{+}	0.05	0.00	0.06	0.08	0.06	0.09	0.10	0.09	0.09	0.06
K^{+}	–	–	0.00	0.00	0.00	0.00	0.00	0.00	0.00	0.00
La^{3+}	–	–	–	0.00	–	–	–	–	–	–
Ce^{3+}	0.00	0.00	0.00	0.03	0.00	0.00	0.00	0.00	0.00	0.00
Pr^{3+}	–	–	–	0.00	–	–	–	–	–	–
Nd^{3+}	–	–	–	0.00	–	–	–	–	–	–
Sm^{3+}	–	–	–	0.00	–	–	–	–	–	–
Eu^{3+}	–	–	–	0.00	–	–	–	–	–	–
Gd^{3+}	–	–	–	0.00	–	–	–	–	–	–
Pb^{2+}	–	–	–	–	–	–	–	–	–	–
Bi^{3+}	–	–	–	–	–	–	–	–	–	–
Th^{4+}	–	–	–	–	–	–	–	–	–	–
U^{4+}	–	–	–	–	–	–	–	–	–	–
B^{3+}	–	–	–	–	–	–	–	–	–	–
S^{6+}	0.20	0.08	0.00	0.04	0.00	0.00	0.00	0.00	0.00	0.00
F^{-}	1.12	1.17	3.43	2.98	3.06	4.09	4.07	3.75	4.02	3.87
Cl^{-}	0.06	0.00	0.00	0.00	0.00	0.00	0.00	0.00	0.00	0.00
OH^{-}*	6.59	8.58	5.63	5.43	6.13	5.67	5.34	5.56	5.42	5.43
O	70.22	68.26	68.94	69.60	68.81	68.24	68.59	68.69	68.56	68.70
					Statistics					
ΣX	18.26	18.71	18.94	18.88	19.04	19.31	19.08	19.11	19.05	18.83
ΣY	13.30	13.35	12.98	13.00	12.95	12.73	12.84	12.83	12.83	13.12
ΣZ	18.45	17.94	18.07	18.12	18.01	17.96	18.07	18.07	18.11	18.04

*Calculated for charge balance.

QUANTITATIVE WDS RESULTS (NMNS)

Ions p.f.u. (50-Cation Normalization)

	V49-2	V49-3	V49-4	V49-5	V50-1	V50-2	V50-3	V50-4	V51-1	V51-2
Si^{4+}	17.80	18.10	17.97	18.18	17.91	17.82	17.84	18.01	18.22	17.97
Al^{3+}	10.63	10.76	10.87	11.03	8.25	8.09	8.33	8.17	10.26	10.02
Ti^{4+}	0.00	0.00	0.00	0.00	0.00	0.00	0.00	0.00	0.03	0.06
Mg^{2+}	1.57	1.43	1.40	1.27	3.18	2.74	3.16	3.10	1.35	1.51
Mn^{2+}	0.28	0.37	0.30	0.25	1.33	1.48	1.32	1.61	0.05	0.04
Fe^{2+}	0.17	0.31	0.22	0.08	0.53	0.95	0.50	0.53	1.18	1.21
Fe^{3+}	–	–	–	–	–	–	–	–	–	–
Cr^{3+}	–	–	–	–	–	–	–	–	–	–
Cu^{2+}	0.20	0.20	0.19	0.25	0.05	0.00	0.00	0.00	–	–
Zn^{2+}	0.00	0.00	0.00	0.00	0.00	0.00	0.00	0.00	0.00	0.00
Ca^{2+}	19.32	18.75	18.99	18.82	18.43	18.83	18.58	18.52	18.90	19.19
Na^{+}	0.03	0.08	0.06	0.11	0.00	0.00	0.00	0.00	0.00	0.00
K^{+}	0.00	0.00	0.00	0.00	0.00	0.00	0.00	0.00	0.00	0.00
La^{3+}	–	–	–	–	–	–	–	–	–	–
Ce^{3+}	0.00	0.00	0.00	0.00	0.00	0.00	0.00	0.00	0.00	0.00
Pr^{3+}	–	–	–	–	–	–	–	–	–	–
Nd^{3+}	–	–	–	–	–	–	–	–	–	–
Sm^{3+}	–	–	–	–	–	–	–	–	–	–
Eu^{3+}	–	–	–	–	–	–	–	–	–	–
Gd^{3+}	–	–	–	–	–	–	–	–	–	–
Pb^{2+}	–	–	–	–	–	–	–	–	–	–
Bi^{3+}	–	–	–	–	0.32	0.08	0.28	0.06	–	–
Th^{4+}	–	–	–	–	–	–	–	–	–	–
U^{4+}	–	–	–	–	–	–	–	–	–	–
B^{3+}	–	–	–	–	–	–	–	–	–	–
S^{6+}	0.00	0.00	0.00	0.00	0.00	0.00	0.00	0.00	0.00	0.00
F^{-}	4.32	4.15	4.02	4.01	2.59	2.25	2.36	1.98	0.00	0.00
Cl^{-}	0.00	0.00	0.00	0.00	0.54	0.15	0.56	0.14	0.00	0.00
OH^{-}*	5.47	4.97	5.22	4.71	8.48	9.79	8.79	9.64	9.24	9.91
O	68.20	68.88	68.76	69.28	66.40	65.81	66.29	66.25	68.76	68.09
					Statistics					
ΣX	19.35	18.83	19.04	18.93	18.75	18.92	18.86	18.58	18.90	19.19
ΣY	12.85	13.08	12.99	12.89	13.04	13.26	13.30	13.41	12.88	12.84
ΣZ	17.80	18.10	17.97	18.18	17.91	17.82	17.84	18.01	18.22	17.97

*Calculated for charge balance.

QUANTITATIVE WDS RESULTS (NMNS)

Ions p.f.u. (50-Cation Normalization)

	V51-3	V52-1	V52-2	V52-3	V52-4	V53-1	V53-2	V53-3	V54-1	V54-2
Si^{4+}	17.97	17.66	17.82	17.69	17.88	17.83	17.87	18.04	17.83	17.75
Al^{3+}	10.20	6.37	6.89	7.19	6.84	7.18	7.23	7.54	8.95	8.86
Ti^{4+}	0.04	0.54	0.25	0.22	0.43	1.10	1.10	1.20	0.27	0.19
Mg^{2+}	1.36	3.26	3.29	3.35	3.22	1.41	1.43	1.36	2.44	2.29
Mn^{2+}	0.04	0.11	0.10	0.10	0.12	0.07	0.09	0.07	0.00	0.00
Fe^{2+}	1.25	2.90	2.79	2.45	2.72	3.21	3.26	2.85	1.68	1.85
Fe^{3+}	–	–	–	–	–	–	–	–	–	–
Cr^{3+}	–	–	–	–	–	–	–	–	0.00	0.00
Cu^{2+}	–	–	–	–	–	–	–	–	–	–
Zn^{2+}	0.00	0.00	0.00	0.00	0.00	0.00	0.00	0.00	0.00	0.00
Ca^{2+}	19.14	19.16	18.86	19.01	18.79	17.90	17.75	17.76	18.83	19.06
Na^{+}	0.00	0.00	0.00	0.00	0.00	0.39	0.40	0.44	0.00	0.00
K^{+}	0.00	0.00	0.00	0.00	0.00	0.00	0.00	0.00	–	–
La^{3+}	–	–	–	–	–	0.19	0.20	0.13	–	–
Ce^{3+}	0.00	0.00	0.00	0.00	0.00	0.35	0.35	0.28	0.00	0.00
Pr^{3+}	–	–	–	–	–	0.05	0.05	0.04	–	–
Nd^{3+}	–	–	–	–	–	0.08	0.06	0.07	–	–
Sm^{3+}	–	–	–	–	–	0.00	0.00	0.00	–	–
Eu^{3+}	–	–	–	–	–	0.00	0.00	0.00	–	–
Gd^{3+}	–	–	–	–	–	0.05	0.03	0.04	–	–
Pb^{2+}	–	–	–	–	–	–	–	–	–	–
Bi^{3+}	–	–	–	–	–	–	–	–	–	–
Th^{4+}	–	–	–	–	–	0.17	0.18	†0.18	–	–
U^{4+}	–	–	–	–	–	–	0.00	–	–	–
B^{3+}	–	–	–	–	–	–	–	–	–	–
S^{6+}	0.00	0.00	0.00	0.00	0.00	0.07	0.06	0.06	0.00	0.00
F^{-}	0.00	2.37	2.89	3.12	2.63	3.54	3.04	2.89	0.00	0.00
Cl^{-}	0.00	0.11	0.12	0.14	0.15	0.05	0.04	0.00	0.00	0.00
OH^{-}*	9.78	10.76	9.95	9.75	9.77	6.29	6.71	6.24	10.85	11.26
O	68.22	64.76	65.03	64.99	65.45	68.12	68.21	68.87	67.15	66.74
					Statistics					
ΣX	19.14	19.16	18.86	19.01	18.79	19.19	19.02	18.93	18.83	19.06
ΣY	12.89	13.18	13.32	13.30	13.33	12.98	13.11	13.02	13.34	13.19
ΣZ	17.97	17.66	17.82	17.69	17.88	17.83	17.87	18.04	17.83	17.75

*Calculated for charge balance. †Average value of 1.47 ThO_2 used in calculations.

QUANTITATIVE WDS RESULTS (NMNS)

Ions p.f.u. (50-Cation Normalization)

	V54-3	V54-4	V54-5	V55-1_c	V55-2_r	V56-1_l	V56-2_l	V56-3_d	V56-4_d	V57-1
Si^{4+}	17.46	17.89	17.49	18.31	18.14	17.58	17.45	17.39	17.44	17.93
Al^{3+}	9.18	8.88	8.63	9.66	9.56	6.97	7.01	7.10	7.10	9.53
Ti^{4+}	0.22	0.21	0.23	0.38	0.58	0.21	0.18	0.16	0.15	0.11
Mg^{2+}	2.22	2.24	2.36	0.97	0.88	3.18	3.13	3.58	3.57	2.55
Mn^{2+}	0.00	0.00	0.00	0.09	0.09	0.09	0.09	0.05	0.05	0.00
Fe^{2+}	1.54	1.80	1.88	1.90	1.93	1.64	1.61	1.52	1.49	0.93
Fe^{3+}	–	–	–	–	–	1.51	1.48	1.41	1.37	–
Cr^{3+}	0.00	0.00	0.00	–	–	–	–	–	–	0.00
Cu^{2+}	–	–	–	–	–	–	–	–	–	–
Zn^{2+}	0.00	0.00	0.00	0.00	0.00	0.00	0.00	0.00	0.00	0.00
Ca^{2+}	19.39	18.97	19.33	18.67	18.72	18.82	19.01	18.79	18.82	18.95
Na^{+}	0.00	0.00	0.00	0.03	0.11	0.00	0.04	0.00	0.00	0.00
K^{+}	–	–	–	0.00	0.00	0.00	0.00	0.00	0.00	–
La^{3+}	–	–	0.04	–	–	–	–	–	–	–
Ce^{3+}	0.00	0.00	0.04	0.00	0.00	–	–	–	–	0.00
Pr^{3+}	–	–	0.00	–	–	–	–	–	–	–
Nd^{3+}	–	–	0.00	–	–	–	–	–	–	–
Sm^{3+}	–	–	0.00	–	–	–	–	–	–	–
Eu^{3+}	–	–	0.00	–	–	–	–	–	–	–
Gd^{3+}	–	–	0.00	–	–	–	–	–	–	–
Pb^{2+}	–	–	–	–	–	–	–	–	–	–
Bi^{3+}	–	–	–	–	–	–	–	–	–	–
Th^{4+}	–	–	–	–	–	–	–	–	–	–
U^{4+}	–	–	–	–	–	–	–	–	–	–
B^{3+}	0.00	–	–	0.00	–	2.34	2.44	2.73	2.64	–
S^{6+}	0.00	0.00	0.00	0.00	0.00	0.00	0.00	0.00	0.00	0.00
F^{-}	0.00	0.00	0.60	3.31	2.91	0.76	0.87	0.00	0.00	0.65
Cl^{-}	0.00	0.00	0.00	0.06	0.00	0.00	0.00	0.00	0.00	0.00
OH^{-*}	11.48	10.91	11.25	5.63	6.20	4.18	4.09	4.23	4.42	9.75
O	66.52	67.09	66.14	69.00	68.89	73.06	73.04	73.77	73.58	67.61
					Statistics					
ΣX	19.39	18.97	19.40	18.70	18.82	18.82	19.05	18.79	18.82	18.95
ΣY	13.15	13.14	13.11	13.00	13.03	13.60	13.50	13.82	13.74	13.12
ΣZ	17.46	17.89	17.49	18.31	18.14	17.58	17.45	17.39	17.44	17.93

*Calculated for charge balance.

QUANTITATIVE WDS RESULTS (NMNS)

Ions p.f.u. (50-Cation Normalization)

	V57-2	V57-3	V57-4	V57-5	V57-6	V57-7	V57-8	V58-1	V58-2	V58-3
Si^{4+}	17.58	17.70	17.43	17.86	17.54	17.71	17.37	17.99	18.02	17.87
Al^{3+}	9.36	8.81	9.10	9.37	9.23	9.53	9.33	10.15	10.40	10.34
Ti^{4+}	0.22	0.27	0.29	0.26	0.31	0.26	0.27	0.00	0.00	0.00
Mg^{2+}	2.57	2.48	2.49	2.59	2.63	2.64	2.43	2.12	2.22	2.08
Mn^{2+}	0.00	0.00	0.00	0.00	0.00	0.00	0.00	0.00	0.00	0.00
Fe^{2+}	0.87	2.00	1.09	0.91	0.86	0.88	1.18	0.02	0.02	0.02
Fe^{3+}	–	–	–	–	–	–	–	0.40	0.36	0.32
Cr^{3+}	0.00	0.00	0.00	0.03	0.00	0.00	0.00	0.00	0.00	0.00
Cu^{2+}	–	–	–	–	–	–	–	–	–	–
Zn^{2+}	0.00	0.00	0.00	0.00	0.00	0.00	0.00	0.00	0.00	0.00
Ca^{2+}	19.40	18.73	19.61	18.99	19.43	18.99	19.42	19.32	18.99	19.37
Na^{+}	0.00	0.00	0.00	0.00	0.00	0.00	0.00	0.00	0.00	0.00
K^{+}	–	–	–	–	–	–	–	–	–	–
La^{3+}	–	–	–	–	–	–	–	–	–	–
Ce^{3+}	0.00	0.00	0.00	0.00	0.00	0.00	0.00	0.00	0.00	0.00
Pr^{3+}	–	–	–	–	–	–	–	–	–	–
Nd^{3+}	–	–	–	–	–	–	–	–	–	–
Sm^{3+}	–	–	–	–	–	–	–	–	–	–
Eu^{3+}	–	–	–	–	–	–	–	–	–	–
Gd^{3+}	–	–	–	–	–	–	–	–	–	–
Pb^{2+}	–	–	–	–	–	–	–	–	–	–
Bi^{3+}	–	–	–	–	–	–	–	–	–	–
Th^{4+}	–	–	–	–	–	–	–	–	–	–
U^{4+}	–	–	–	–	–	–	–	–	–	–
B^{3+}	–	–	0.00	–	–	–	–	–	0.00	–
S^{6+}	0.00	0.00	0.00	0.00	0.00	0.00	0.00	0.00	0.00	0.00
F^{-}	0.62	0.00	0.00	0.83	0.59	0.68	0.76	0.00	0.00	0.00
Cl^{-}	0.00	0.00	0.00	0.00	0.00	0.00	0.00	0.00	0.00	0.00
OH^{-*}	10.42	11.24	11.47	9.54	10.48	9.86	10.63	9.47	9.22	9.60
O	66.95	66.76	66.53	67.63	66.92	67.45	66.61	68.53	68.78	68.40
					Statistics					
ΣX	19.40	18.73	19.61	18.99	19.43	18.99	19.42	19.32	18.99	19.37
ΣY	13.02	13.57	12.96	13.15	13.03	13.30	13.21	12.69	12.99	12.76
ΣZ	17.58	17.70	17.43	17.86	17.54	17.71	17.37	17.99	18.02	17.87

*Calculated for charge balance.

QUANTITATIVE WDS RESULTS (NMNS)

Ions p.f.u. (50-Cation Normalization)

	V59-1	V59-2	V59-3	V59-4	V59-5	V60-1	V60-2	V60-3	V60-4	V60-5
Si^{4+}	17.76	17.86	17.65	17.86	17.57	18.17	18.10	18.01	17.87	17.99
Al^{3+}	10.11	10.05	9.90	9.96	9.95	9.67	9.24	9.39	9.37	9.37
Ti^{4+}	0.00	0.00	0.00	0.00	0.00	0.04	0.12	0.11	0.06	0.07
Mg^{2+}	2.62	2.76	2.68	2.72	2.65	2.39	2.56	2.57	2.54	2.53
Mn^{2+}	0.00	0.00	0.00	0.00	0.00	0.00	0.00	0.00	0.02	0.00
Fe^{2+}	0.06	0.07	0.06	0.08	0.07	0.24	0.27	0.26	0.26	0.25
Fe^{3+}	0.34	0.35	0.34	0.41	0.38	1.03	1.19	1.14	1.16	1.10
Cr^{3+}	0.06	0.03	0.00	0.05	0.00	–	–	–	–	–
Cu^{2+}	–	–	–	–	–	–	–	–	–	–
Zn^{2+}	0.00	0.00	0.00	0.00	0.00	0.00	0.00	0.00	0.00	0.00
Ca^{2+}	19.05	18.89	19.37	18.93	19.38	18.46	18.52	18.53	18.72	18.69
Na^{+}	0.00	0.00	0.00	0.00	0.00	0.00	0.00	0.00	0.00	0.00
K^{+}	–	–	–	–	–	0.00	0.00	0.00	0.00	0.00
La^{3+}	–	–	–	–	–	–	–	–	–	–
Ce^{3+}	0.00	0.00	0.00	0.00	0.00	0.00	0.00	0.00	0.00	0.00
Pr^{3+}	–	–	–	–	–	–	–	–	–	–
Nd^{3+}	–	–	–	–	–	–	–	–	–	–
Sm^{3+}	–	–	–	–	–	–	–	–	–	–
Eu^{3+}	–	–	–	–	–	–	–	–	–	–
Gd^{3+}	–	–	–	–	–	–	–	–	–	–
Pb^{2+}	–	–	–	–	–	–	–	–	–	–
Bi^{3+}	–	–	–	–	–	–	–	–	–	–
Th^{4+}	–	–	–	–	–	–	–	–	–	–
U^{4+}	–	–	–	–	–	–	–	–	–	–
B^{3+}	–	–	0.00	–	–	–	–	0.00	–	–
S^{6+}	0.00	0.00	0.00	0.00	0.00	0.05	0.06	0.05	0.05	0.00
F^{-}	0.00	0.00	0.00	0.00	0.00	0.00	0.00	0.00	0.00	0.00
Cl^{-}	0.00	0.00	0.00	0.00	0.00	0.04	0.00	0.00	0.00	0.00
OH^{-}*	9.97	9.86	10.47	9.86	10.52	8.55	8.76	8.94	9.28	9.41
O	68.03	68.14	67.53	68.14	67.48	69.40	69.24	69.06	68.72	68.59
					Statistics					
ΣX	19.05	18.89	19.37	18.93	19.38	18.46	18.52	18.53	18.72	18.69
ΣY	13.19	13.25	12.98	13.21	13.05	13.37	13.38	13.46	13.41	13.32
ΣZ	17.76	17.86	17.65	17.86	17.57	18.17	18.10	18.01	17.87	17.99

*Calculated for charge balance.

QUANTITATIVE WDS RESULTS (NMNS)

Ions p.f.u. (50-Cation Normalization)

	V61-1	V61-2	V61-3	V61-4	V61-5	V62-1_c	V62-2	V62-3	V62-4	V62-5_{id}
Si^{4+}	17.92	17.66	17.93	17.80	17.93	18.04	17.90	18.04	18.00	17.99
Al^{3+}	7.21	7.40	7.85	7.26	7.37	9.31	9.24	9.34	9.28	9.67
Ti^{4+}	0.20	0.24	0.17	0.21	0.23	0.24	0.23	0.23	0.32	0.22
Mg^{2+}	3.72	3.56	3.59	3.55	3.68	2.65	2.65	2.69	2.62	2.53
Mn^{2+}	0.03	0.04	0.04	0.05	0.04	0.00	0.02	0.03	0.02	0.02
Fe^{2+}	0.54	0.51	0.46	0.49	0.51	1.01	1.04	1.02	0.95	0.86
Fe^{3+}	1.62	1.55	1.39	1.48	1.54	–	–	–	–	–
Cr^{3+}	0.00	0.00	0.00	0.00	0.00	–	–	–	–	–
Cu^{2+}	–	–	–	–	–	–	–	–	–	–
Zn^{2+}	0.00	0.00	0.00	0.00	0.00	0.00	0.00	0.00	0.00	0.00
Ca^{2+}	18.75	19.06	18.57	19.15	18.69	18.75	18.90	18.65	18.80	18.72
Na^{+}	0.00	0.00	0.00	0.00	0.00	0.00	0.00	0.00	0.00	0.00
K^{+}	–	–	–	–	–	0.00	0.00	0.00	0.00	0.00
La^{3+}	–	–	–	–	–	–	–	–	–	–
Ce^{3+}	0.00	0.00	0.00	0.00	0.00	0.00	0.00	0.00	0.00	0.00
Pr^{3+}	–	–	–	–	–	–	–	–	–	–
Nd^{3+}	–	–	–	–	–	–	–	–	–	–
Sm^{3+}	–	–	–	–	–	–	–	–	–	–
Eu^{3+}	–	–	–	–	–	–	–	–	–	–
Gd^{3+}	–	–	–	–	–	–	–	–	–	–
Pb^{2+}	–	–	–	–	–	–	–	–	–	–
Bi^{3+}	–	–	–	–	–	–	–	–	–	–
Th^{4+}	–	–	–	–	–	–	–	–	–	–
U^{4+}	–	–	–	–	–	–	–	–	–	–
B^{3+}	†1.25	1.23	†1.24	†1.22	†1.24	–	–	–	–	–
S^{6+}	0.00	0.00	0.00	0.00	0.00	0.08	0.07	0.08	0.06	0.07
F^{-}	0.60	0.69	0.00	0.67	0.81	1.02	1.14	1.19	1.25	1.36
Cl^{-}	0.00	0.06	0.07	0.07	0.07	0.06	0.06	0.05	0.07	0.05
OH^{-}*	6.58	6.83	6.76	6.82	6.16	8.57	8.90	8.40	8.38	8.12
O	70.82	70.42	71.17	70.44	70.96	68.35	67.90	68.36	68.30	68.47
					Statistics					
ΣX	18.75	19.06	18.57	19.15	18.69	18.75	18.90	18.65	18.80	18.72
ΣY	13.33	13.28	13.50	13.05	13.38	13.21	13.20	13.31	13.19	13.29
ΣZ	17.92	17.66	17.93	17.80	17.93	18.04	17.90	18.04	18.00	17.99

*Calculated for charge balance. †Average value of 1.44 B_2O_3 used in calculations.

QUANTITATIVE WDS RESULTS (NMNS)

Ions p.f.u. (50-Cation Normalization)

	$V62\text{-}6_{id}$	$V62\text{-}7_{il}$	$V62\text{-}8_{il}$	V62-9	V62-10	V62-11	$V62\text{-}12_{r}$	V63-1	V63-2	V63-3
Si^{4+}	17.86	18.15	18.02	18.09	18.10	18.11	17.97	18.11	18.04	18.36
Al^{3+}	9.43	9.34	9.34	9.52	9.42	9.43	9.41	9.97	9.73	9.90
Ti^{4+}	0.20	0.32	0.33	0.15	0.22	0.18	0.17	0.19	0.13	0.19
Mg^{2+}	2.59	2.47	2.43	2.57	2.51	2.59	2.55	1.08	1.18	1.23
Mn^{2+}	0.00	0.03	0.04	0.03	0.00	0.03	0.02	0.26	0.22	0.22
Fe^{2+}	0.98	0.91	0.98	0.95	0.97	0.97	0.96	1.25	1.31	1.24
Fe^{3+}	–	–	–	–	–	–	–	0.39	0.41	0.39
Cr^{3+}	–	–	–	–	–	–	–	0.00	0.00	0.00
Cu^{2+}	–	–	–	–	–	–	–	–	–	–
Zn^{2+}	0.00	0.00	0.00	0.00	0.00	0.00	0.00	0.00	0.00	0.00
Ca^{2+}	18.95	18.78	18.85	18.69	18.77	18.69	18.91	18.61	18.89	18.37
Na^{+}	0.00	0.00	0.00	0.00	0.00	0.00	0.00	0.15	0.10	0.11
K^{+}	0.00	0.00	0.00	0.00	0.00	0.00	0.00	–	–	–
La^{3+}	–	–	–	–	–	–	–	–	–	–
Ce^{3+}	0.00	0.00	0.00	0.00	0.00	0.00	0.00	0.00	0.00	0.00
Pr^{3+}	–	–	–	–	–	–	–	–	–	–
Nd^{3+}	–	–	–	–	–	–	–	–	–	–
Sm^{3+}	–	–	–	–	–	–	–	–	–	–
Eu^{3+}	–	–	–	–	–	–	–	–	–	–
Gd^{3+}	–	–	–	–	–	–	–	–	–	–
Pb^{2+}	–	–	–	–	–	–	–	–	–	–
Bi^{3+}	–	–	–	–	–	–	–	–	–	–
Th^{4+}	–	–	–	–	–	–	–	–	–	–
U^{4+}	–	–	–	–	–	–	–	–	–	–
B^{3+}	–	0.00	–	–	–	–	–	–	–	–
S^{6+}	0.07	0.07	0.05	0.10	0.09	0.10	0.13	0.00	0.00	0.00
F^{-}	1.17	1.17	1.02	0.92	1.12	0.87	0.97	3.39	3.86	3.24
Cl^{-}	0.05	0.05	0.07	0.06	0.06	0.04	0.04	0.00	0.00	0.00
OH^{-}*	8.85	8.05	8.54	8.44	8.20	8.46	8.54	5.80	5.75	5.49
O	67.93	68.72	68.37	68.58	68.62	68.63	68.46	68.81	68.39	69.27
					Statistics					
ΣX	18.95	18.78	18.85	18.69	18.77	18.69	18.91	18.76	18.98	18.48
ΣY	13.19	13.07	13.13	13.22	13.12	13.20	13.12	13.14	12.98	13.16
ΣZ	17.86	18.15	18.02	18.09	18.10	18.11	17.97	18.11	18.04	18.36

*Calculated for charge balance.

QUANTITATIVE WDS RESULTS (NMNS)

Ions p.f.u. (50-Cation Normalization)

	V63-4	V63-5	V63-6	V63-7	V64-1	V64-2	V64-3	V64-4	V64-5	V65-1
Si^{4+}	17.99	18.13	17.90	18.20	18.12	17.82	18.14	18.03	18.33	18.43
Al^{3+}	9.89	9.77	9.79	10.05	9.35	9.40	9.68	9.80	10.01	10.17
Ti^{4+}	0.19	0.20	0.23	0.13	0.40	0.46	0.35	0.27	0.00	0.62
Mg^{2+}	1.10	1.29	1.10	1.19	1.33	1.14	1.21	1.07	1.22	1.01
Mn^{2+}	0.22	0.25	0.26	0.21	0.30	0.30	0.24	0.17	0.20	0.03
Fe^{2+}	1.22	1.24	1.26	1.25	1.83	1.76	1.82	1.45	1.56	1.24
Fe^{3+}	0.38	0.39	0.39	0.39	–	–	–	–	–	–
Cr^{3+}	0.00	0.00	0.00	0.00	0.00	0.00	0.00	0.00	0.00	0.00
Cu^{2+}	–	–	–	–	–	–	–	–	–	–
Zn^{2+}	0.00	0.00	0.00	0.00	0.00	0.00	0.00	0.00	0.00	0.00
Ca^{2+}	18.87	18.64	18.95	18.49	18.58	19.00	18.48	19.07	18.58	18.37
Na^{+}	0.13	0.10	0.12	0.11	0.09	0.11	0.10	0.13	0.10	0.13
K^{+}	–	–	–	–	–	–	–	–	–	–
La^{3+}	–	–	–	–	–	–	–	–	–	–
Ce^{3+}	0.00	0.00	0.00	0.00	0.00	0.00	0.00	0.00	0.00	0.00
Pr^{3+}	–	–	–	–	–	–	–	–	–	–
Nd^{3+}	–	–	–	–	–	–	–	–	–	–
Sm^{3+}	–	–	–	–	–	–	–	–	–	–
Eu^{3+}	–	–	–	–	–	–	–	–	–	–
Gd^{3+}	–	–	–	–	–	–	–	–	–	–
Pb^{2+}	–	–	–	–	–	–	–	–	–	–
Bi^{3+}	–	–	–	–	–	–	–	–	–	–
Th^{4+}	–	–	–	–	–	–	–	–	–	–
U^{4+}	–	–	–	–	–	–	–	–	–	–
B^{3+}	0.00	–	–	–	–	–	0.00	–	–	–
S^{6+}	0.00	0.00	0.00	0.00	0.00	0.00	0.00	0.00	0.00	0.00
F^{-}	3.38	3.60	3.40	3.65	3.80	3.49	3.47	3.53	3.70	2.54
Cl^{-}	0.00	0.00	0.00	0.00	0.06	0.10	0.00	0.00	0.07	0.00
OH^{-*}	6.13	5.68	6.29	5.37	5.83	6.56	5.98	6.20	5.65	5.31
O	68.49	68.72	68.30	68.98	68.31	67.85	68.55	68.27	68.58	70.15
					Statistics					
ΣX	19.01	18.74	19.07	18.59	18.67	19.11	18.57	19.20	18.67	18.50
ΣY	13.00	13.13	13.03	13.21	13.21	13.07	13.29	12.77	12.99	13.07
ΣZ	17.99	18.13	17.90	18.20	18.12	17.82	18.14	18.03	18.33	18.43

*Calculated for charge balance.

QUANTITATIVE WDS RESULTS (NMNS)

Ions p.f.u. (50-Cation Normalization)

	V65-2	V65-3	V65-4	V65-5	V65-6	V66-1	V66-2	V66-3	V66-4	V66-5
Si^{4+}	18.15	18.53	18.20	18.55	18.29	18.06	18.17	17.89	18.35	18.00
Al^{3+}	9.96	9.83	10.07	10.09	10.05	9.69	9.59	9.41	9.68	9.90
Ti^{4+}	0.62	0.64	0.62	0.62	0.60	0.02	0.00	0.02	0.02	0.00
Mg^{2+}	1.07	1.28	1.07	1.03	0.99	0.66	0.71	0.68	0.64	0.65
Mn^{2+}	0.02	0.03	0.03	0.03	0.03	0.78	0.85	0.84	0.76	0.71
Fe^{2+}	1.15	1.26	1.15	1.22	1.24	0.92	0.98	1.01	0.98	0.64
Fe^{3+}	–	–	–	–	–	–	–	–	–	–
Cr^{3+}	0.00	0.00	0.00	0.00	0.00	0.00	0.00	0.00	0.00	0.00
Cu^{2+}	–	–	–	–	–	0.17	0.17	0.17	0.16	0.24
Zn^{2+}	0.00	0.00	0.00	0.00	0.00	0.82	0.87	0.87	0.86	0.80
Ca^{2+}	18.90	18.33	18.76	18.35	18.70	18.87	18.66	19.10	18.54	19.07
Na^{+}	0.11	0.11	0.11	0.11	0.10	0.00	0.00	0.00	0.00	0.00
K^{+}	–	–	–	–	–	–	–	–	–	–
La^{3+}	–	–	–	–	–	–	–	–	–	–
Ce^{3+}	0.00	0.00	0.00	0.00	0.00	0.00	0.00	0.00	0.00	0.00
Pr^{3+}	–	–	–	–	–	–	–	–	–	–
Nd^{3+}	–	–	–	–	–	–	–	–	–	–
Sm^{3+}	–	–	–	–	–	–	–	–	–	–
Eu^{3+}	–	–	–	–	–	–	–	–	–	–
Gd^{3+}	–	–	–	–	–	–	–	–	–	–
Pb^{2+}	–	–	–	–	–	–	–	–	–	–
Bi^{3+}	–	–	–	–	–	–	–	–	–	–
Th^{4+}	–	–	–	–	–	–	–	–	–	–
U^{4+}	–	–	–	–	–	–	–	–	–	–
B^{3+}	–	–	–	–	–	–	–	0.00	–	–
S^{6+}	0.00	0.00	0.00	0.04	0.00	0.00	0.00	0.00	0.00	0.00
F^{-}	2.40	2.41	2.45	2.46	2.52	2.04	2.16	2.13	2.05	1.94
Cl^{-}	0.00	0.00	0.00	0.00	0.00	0.00	0.00	0.00	0.00	0.00
OH^{-}*	6.21	5.52	5.93	4.93	5.77	8.11	7.91	8.64	7.52	8.16
O	69.39	70.07	69.61	70.61	69.71	67.85	67.93	67.23	68.43	67.90
					Statistics					
ΣX	19.02	18.43	18.86	18.46	18.81	18.87	18.66	19.10	18.54	19.07
ΣY	12.83	13.03	12.94	12.99	12.91	13.06	13.17	13.09	13.10	12.93
ΣZ	18.15	18.53	18.20	18.55	18.29	18.06	18.17	17.81	18.35	18.00

*Calculated for charge balance.

QUANTITATIVE WDS RESULTS (NMNS)

Ions p.f.u. (50-Cation Normalization)

	V66-6	V67-1	V67-2	V67-3	V67-4	V67-5	V67-6	V67-7	V68-1	V68-2
Si^{4+}	18.30	17.40	18.11	17.78	17.64	17.90	17.66	18.07	17.86	17.74
Al^{3+}	9.84	11.36	9.84	10.28	10.85	10.40	10.71	10.13	9.93	10.00
Ti^{4+}	0.02	0.00	0.02	0.00	0.00	0.00	0.00	0.00	0.00	0.00
Mg^{2+}	0.66	0.79	0.89	2.91	2.60	1.28	2.00	0.97	3.08	2.77
Mn^{2+}	0.82	0.54	0.52	0.68	0.60	0.67	0.61	0.65	0.00	0.00
Fe^{2+}	0.81	0.39	0.59	0.28	0.11	0.34	0.16	0.39	0.45	0.50
Fe^{3+}	–	–	–	–	–	–	–	–	–	–
Cr^{3+}	0.00	–	–	–	–	–	–	–	–	–
Cu^{2+}	0.16	0.56	0.59	0.25	0.12	0.43	0.25	0.51	–	–
Zn^{2+}	0.85	0.56	0.54	0.69	0.64	0.60	0.61	0.53	0.00	0.00
Ca^{2+}	18.53	18.28	18.85	16.83	17.13	18.17	17.72	18.61	18.67	19.00
Na^{+}	0.00	0.00	0.00	0.00	0.00	0.00	0.00	0.00	0.00	0.00
K^{+}	–	0.00	0.00	0.03	0.02	0.00	0.00	0.00	0.00	0.00
La^{3+}	–	–	–	–	–	–	–	–	–	–
Ce^{3+}	0.00	0.00	0.00	0.00	0.00	0.00	0.00	0.00	0.00	0.00
Pr^{3+}	–	–	–	–	–	–	–	–	–	–
Nd^{3+}	–	–	–	–	–	–	–	–	–	–
Sm^{3+}	–	–	–	–	–	–	–	–	–	–
Eu^{3+}	–	–	–	–	–	–	–	–	–	–
Gd^{3+}	–	–	–	–	–	–	–	–	–	–
Pb^{2+}	–	0.12	0.04	0.27	0.28	0.21	0.27	0.14	–	–
Bi^{3+}	–	–	–	–	–	–	–	–	–	–
Th^{4+}	–	–	–	–	–	–	–	–	–	–
U^{4+}	–	–	–	–	–	–	–	–	–	–
B^{3+}	–	–	–	–	–	–	–	–	–	0.00
S^{6+}	0.00	0.00	0.00	0.00	0.00	0.00	0.00	0.00	0.07	0.10
F^{-}	2.02	2.47	2.87	1.83	2.11	1.64	2.17	2.42	0.00	0.00
Cl^{-}	0.00	0.00	0.00	0.00	0.00	0.00	0.00	0.00	0.00	0.00
OH^{-}*	7.51	7.36	7.03	8.37	7.77	8.16	7.79	7.33	9.95	9.94
O	68.47	68.16	68.10	67.80	68.12	68.20	68.03	68.26	68.05	68.06
					Statistics					
ΣX	18.53	18.39	18.89	17.13	17.43	18.38	18.00	18.75	18.67	19.00
ΣY	13.17	14.21	12.99	15.09	14.93	13.72	14.34	13.18	13.47	13.26
ΣZ	18.30	17.40	18.11	17.78	17.64	17.90	17.66	18.07	17.86	17.74

*Calculated for charge balance.

V67 includes 0.02 Be.

QUANTITATIVE WDS RESULTS (NMNS)

Ions p.f.u. (50-Cation Normalization)

	V68-3	V68-4	V68-5	V69-1	V69-2	V69-3	V70-1_{1c}	V70-2_{1r}	V70-3_2	V71-1
Si^{4+}	17.81	18.07	17.97	18.05	18.03	18.01	18.18	18.35	18.12	17.97
Al^{3+}	9.92	9.97	9.83	9.42	9.65	9.33	9.03	8.97	9.09	8.83
Ti^{4+}	0.00	0.00	0.00	1.02	0.99	1.01	0.91	0.86	0.90	0.02
Mg^{2+}	3.09	3.04	2.93	1.28	1.26	1.41	1.34	1.33	1.36	2.27
Mn^{2+}	0.00	0.00	0.00	0.00	0.03	0.00	0.04	0.03	0.03	0.05
Fe^{2+}	0.46	0.45	0.42	1.12	1.13	1.13	1.35	1.33	1.34	1.83
Fe^{3+}	–	–	–	–	–	–	0.45	0.46	0.45	–
Cr^{3+}	–	–	–	–	–	–	–	–	–	–
Cu^{2+}	–	–	–	–	–	–	–	–	–	–
Zn^{2+}	0.00	0.00	0.00	0.00	0.00	0.00	0.00	0.00	0.00	0.00
Ca^{2+}	18.72	18.47	18.86	19.02	18.83	19.03	18.42	18.43	18.49	19.04
Na^{+}	0.00	0.00	0.00	0.09	0.09	0.08	0.28	0.24	0.23	0.00
K^{+}	0.00	0.00	0.00	0.00	0.00	0.00	0.00	0.00	0.00	0.00
La^{3+}	–	–	–	–	–	–	–	–	–	–
Ce^{3+}	0.00	0.00	0.00	0.00	0.00	0.00	0.00	0.00	0.00	0.00
Pr^{3+}	–	–	–	–	–	–	–	–	–	–
Nd^{3+}	–	–	–	–	–	–	–	–	–	–
Sm^{3+}	–	–	–	–	–	–	–	–	–	–
Eu^{3+}	–	–	–	–	–	–	–	–	–	–
Gd^{3+}	–	–	–	–	–	–	–	–	–	–
Pb^{2+}	–	–	–	–	–	–	–	–	–	–
Bi^{3+}	–	–	–	–	–	–	–	–	–	–
Th^{4+}	–	–	–	–	–	–	–	–	–	–
U^{4+}	–	–	–	–	–	–	–	–	–	–
B^{3+}	–	–	–	–	–	–	0.00	–	–	–
S^{6+}	0.05	0.00	0.23	0.05	0.00	0.08	0.00	0.00	0.00	0.00
F^{-}	0.00	0.00	0.00	2.72	2.61	2.95	3.72	3.64	4.45	0.00
Cl^{-}	0.00	0.00	0.00	0.28	0.25	0.31	0.06	0.06	0.07	0.00
OH^{-*}	10.17	9.90	8.87	5.22	5.54	4.95	4.84	4.68	4.15	11.19
O	67.83	68.10	69.13	69.77	69.61	69.79	69.39	69.62	69.34	66.81
					Statistics					
ΣX	18.72	18.47	18.86	19.11	18.91	19.10	18.69	18.67	18.72	19.04
ΣY	13.47	13.46	13.17	12.84	13.06	12.88	13.13	12.98	13.16	12.99
ΣZ	17.81	18.07	17.97	18.05	18.03	18.01	18.18	18.35	18.12	17.97

*Calculated for charge balance.

QUANTITATIVE WDS RESULTS (NMNS)

Ions p.f.u. (50-Cation Normalization)

	V71-2	V71-3	V71-4	V71-5	V72-1	V72-2	V72-3	V72-4	V72-5	V72-6
Si^{4+}	18.18	18.02	18.21	18.06	18.43	18.35	18.49	18.18	18.26	19.49
Al^{3+}	8.74	8.79	8.83	8.59	9.05	8.72	9.41	9.02	9.26	11.45
Ti^{4+}	0.01	0.00	0.02	0.00	0.47	0.45	0.32	0.38	0.33	0.32
Mg^{2+}	2.28	2.31	2.28	2.34	1.60	1.59	1.44	1.48	1.41	1.33
Mn^{2+}	0.05	0.05	0.04	0.05	0.24	0.22	0.14	0.13	0.12	0.12
Fe^{2+}	1.91	1.75	1.74	1.91	2.00	2.08	1.87	1.91	1.85	1.60
Fe^{3+}	–	–	–	–	–	–	–	–	–	–
Cr^{3+}	–	–	–	–	0.00	0.00	0.00	0.00	0.00	0.00
Cu^{2+}	–	–	–	–	–	–	–	–	–	–
Zn^{2+}	0.00	0.00	0.00	0.00	0.00	0.00	0.00	0.00	0.00	0.00
Ca^{2+}	18.82	19.07	18.87	19.06	18.15	18.59	18.32	18.89	18.72	15.64
Na^{+}	0.00	0.00	0.00	0.00	0.06	0.00	0.00	0.00	0.05	0.06
K^{+}	0.00	0.00	0.00	0.00	–	–	–	–	–	–
La^{3+}	–	–	–	–	–	–	–	–	–	–
Ce^{3+}	0.00	0.00	0.00	0.00	0.00	0.00	0.00	0.00	0.00	0.00
Pr^{3+}	–	–	–	–	–	–	–	–	–	–
Nd^{3+}	–	–	–	–	–	–	–	–	–	–
Sm^{3+}	–	–	–	–	–	–	–	–	–	–
Eu^{3+}	–	–	–	–	–	–	–	–	–	–
Gd^{3+}	–	–	–	–	–	–	–	–	–	–
Pb^{2+}	–	–	–	–	–	–	–	–	–	–
Bi^{3+}	–	–	–	–	–	–	–	–	–	–
Th^{4+}	–	–	–	–	0.00	0.00	0.00	0.00	0.00	0.00
U^{4+}	–	–	–	–	0.00	0.00	0.00	0.00	0.00	0.00
B^{3+}	0.00	–	–	–	–	–	–	–	–	–
S^{6+}	0.00	0.00	0.00	0.00	0.05	0.00	0.00	0.00	0.00	0.00
F^{-}	0.00	0.00	0.00	0.00	4.07	3.51	4.10	4.17	4.25	2.60
Cl^{-}	0.00	0.00	0.00	0.00	0.07	0.13	0.17	0.23	0.19	0.12
OH^{-*}	10.87	11.16	10.71	11.29	4.79	6.03	4.70	5.47	5.17	2.30
O	67.13	66.84	67.29	66.71	69.07	68.33	69.03	68.13	68.39	72.99
					Statistics					
ΣX	18.82	19.07	18.87	19.06	18.21	18.59	18.32	18.89	18.77	15.70
ΣY	13.00	12.91	12.92	12.88	13.36	13.06	13.19	12.93	12.97	14.81
ΣZ	18.18	18.02	18.21	18.06	18.43	18.35	18.49	18.18	18.26	19.49

*Calculated for charge balance.

QUANTITATIVE WDS RESULTS (NMNS)

Ions p.f.u. (50-Cation Normalization)

	V72-7	V73-1	V73-2	V73-3	V74-1$_r$	V74-2	V74-3	V74-4	V74-5	V74-6
Si^{4+}	27.64	18.07	17.95	17.85	17.65	17.63	17.64	17.79	17.67	17.85
Al^{3+}	13.85	7.82	7.71	7.93	7.14	6.94	7.05	6.91	6.85	6.84
Ti^{4+}	0.56	0.00	0.00	0.00	0.37	0.38	0.27	0.35	0.34	0.34
Mg^{2+}	1.52	2.82	2.92	2.91	4.64	4.76	4.78	4.82	4.82	4.87
Mn^{2+}	0.17	0.08	0.07	0.08	0.00	0.00	0.00	0.03	0.02	0.03
Fe^{2+}	2.74	2.28	2.17	2.21	0.48	0.51	0.52	0.50	0.50	0.50
Fe^{3+}	–	–	–	–	0.81	0.86	0.87	0.85	0.85	0.85
Cr^{3+}	0.00	–	–	–	–	–	–	–	–	–
Cu^{2+}	–	–	–	–	–	–	–	–	–	–
Zn^{2+}	0.00	0.00	0.00	0.00	0.00	0.00	0.00	0.00	0.00	0.00
Ca^{2+}	2.55	18.92	19.19	19.01	18.90	18.89	18.85	18.70	18.88	18.66
Na^{+}	0.69	0.00	0.00	0.00	0.00	0.00	0.00	0.00	0.00	0.00
K^{+}	0.27	0.00	0.00	0.00	0.00	0.00	0.00	0.00	0.00	0.00
La^{3+}	–	–	–	–	0.00	0.01	0.00	0.00	0.02	0.02
Ce^{3+}	0.02	0.00	0.00	0.00	0.02	0.02	0.03	0.03	0.03	0.04
Pr^{3+}	–	–	–	–	0.00	0.00	0.00	0.00	0.00	0.00
Nd^{3+}	–	–	–	–	0.00	0.00	0.00	0.00	0.00	0.00
Sm^{3+}	–	–	–	–	0.00	0.00	0.00	0.00	0.00	0.00
Eu^{3+}	–	–	–	–	0.00	0.00	0.00	0.00	0.00	0.00
Gd^{3+}	–	–	–	–	0.00	0.00	0.00	0.00	0.00	0.00
Pb^{2+}	–	–	–	–	–	–	–	–	–	–
Bi^{3+}	–	–	–	–	–	–	–	–	–	–
Th^{4+}	0.00	–	–	–	–	–	–	–	–	–
U^{4+}	0.00	–	–	–	–	–	–	–	–	–
B^{3+}	–	–	–	–	2.60	†2.43	†2.43	†2.43	2.56	†2.41
S^{6+}	0.00	0.00	0.00	0.00	0.00	0.00	0.00	0.00	0.07	0.00
F^{-}	0.00	3.35	3.19	3.02	0.77	0.00	0.00	0.00	0.78	0.00
Cl^{-}	0.00	0.14	0.18	0.16	0.00	0.00	0.00	0.00	0.00	0.00
OH^{-}*	-13.30	8.55	9.03	9.18	3.42	4.84	4.93	4.63	3.36	4.64
O	91.30	65.96	65.61	65.63	73.81	73.16	73.07	73.37	73.86	73.36
					Statistics					
ΣX	3.52	18.92	19.19	19.01	18.92	18.92	18.88	18.74	18.93	18.72
ΣY	18.84	13.01	12.86	13.14	13.43	13.45	13.48	13.47	13.40	13.43
ΣZ	27.64	18.07	17.95	17.85	17.65	17.63	17.64	17.79	17.67	17.85

*Calculated for charge balance. †Average value of 2.84 B_2O_3 used in calculations.

V74 includes 0.01 Be.

QUANTITATIVE WDS RESULTS (NMNS)

Ions p.f.u. (50-Cation Normalization)

	V74-7	V74-8	V74-9	V74-10	V74-11	V74-12	V74-13	V74-14	V74-15	V74-16
Si^{4+}	17.78	17.80	17.64	17.92	17.80	17.72	17.69	17.76	17.91	17.77
Al^{3+}	6.67	6.65	6.85	6.78	6.74	6.75	6.77	6.76	6.75	6.80
Ti^{4+}	0.35	0.33	0.32	0.33	0.33	0.35	0.32	0.33	0.33	0.33
Mg^{2+}	4.92	4.91	4.86	4.84	4.84	4.83	4.93	4.88	4.87	4.85
Mn^{2+}	0.00	0.03	0.00	0.00	0.00	0.00	0.00	0.00	0.00	0.00
Fe^{2+}	0.51	0.51	0.50	0.51	0.51	0.52	0.51	0.50	0.51	0.51
Fe^{3+}	0.86	0.87	0.84	0.85	0.86	0.87	0.87	0.84	0.87	0.85
Cr^{3+}	–	–	–	–	–	–	–	–	–	–
Cu^{2+}	–	–	–	–	–	–	–	–	–	–
Zn^{2+}	0.00	0.00	0.00	0.00	0.00	0.00	0.00	0.00	0.00	0.00
Ca^{2+}	18.86	18.82	18.91	18.71	18.85	18.89	18.85	18.85	18.70	18.82
Na^{+}	0.00	0.00	0.00	0.00	0.00	0.00	0.00	0.00	0.00	0.00
K^{+}	0.00	0.00	0.00	0.00	0.00	0.00	0.00	0.00	0.00	0.00
La^{3+}	0.02	0.02	0.03	0.02	0.02	0.02	0.03	0.03	0.03	0.02
Ce^{3+}	0.05	0.05	0.05	0.04	0.04	0.05	0.05	0.04	0.04	0.04
Pr^{3+}	0.00	0.00	0.00	0.00	0.00	0.00	0.00	0.00	0.00	0.00
Nd^{3+}	0.00	0.00	0.00	0.00	0.00	0.00	0.00	0.00	0.00	0.00
Sm^{3+}	0.00	0.00	0.00	0.00	0.00	0.00	0.00	0.00	0.00	0.00
Eu^{3+}	0.00	0.00	0.00	0.00	0.00	0.00	0.00	0.00	0.00	0.00
Gd^{3+}	0.00	0.00	0.00	0.00	0.00	0.00	0.00	0.00	0.00	0.00
Pb^{2+}	–	–	–	–	–	–	–	–	–	–
Bi^{3+}	–	–	–	–	–	–	–	–	–	–
Th^{4+}	–	–	–	–	–	–	–	–	–	–
U^{4+}	–	–	–	–	–	–	–	–	–	–
B^{3+}	†2.42	†2.42	†2.41	2.04	†2.41	†2.42	†2.42	†2.42	2.37	†2.43
S^{6+}	0.09	0.08	0.08	0.09	0.08	0.09	0.10	0.07	0.11	0.11
F^{-}	0.00	0.00	0.00	0.00	0.00	0.00	0.00	0.66	0.00	0.00
Cl^{-}	0.00	0.00	0.04	0.00	0.00	0.00	0.00	0.00	0.00	0.00
OH^{-}*	4.38	4.41	4.56	5.16	4.39	4.36	4.44	3.80	4.07	4.12
O	73.62	73.59	73.39	72.84	73.61	73.64	73.56	73.54	73.93	73.88
					Statistics					
ΣX	18.92	18.89	18.99	18.78	18.91	18.96	18.92	18.93	18.77	18.89
ΣY	13.30	13.31	13.37	13.30	13.29	13.32	13.39	13.31	13.32	13.34
ΣZ	17.78	17.80	17.64	17.92	17.80	17.72	17.69	17.76	17.91	17.77

*Calculated for charge balance. †Average value of 2.84 B_2O_3 used in calculations.
V74 includes 0.01 Be.

QUANTITATIVE WDS RESULTS (NMNS)

Ions p.f.u. (50-Cation Normalization)

	V74-17	V74-18	V74-19	V74-20	V74-21	V74-22	V74-23	V74-24	V74-25$_r$	V75-1
Si^{4+}	17.71	17.85	17.65	17.80	17.92	17.74	17.64	17.69	17.67	17.47
Al^{3+}	6.74	6.74	6.95	6.99	6.90	6.90	6.90	6.96	6.84	11.02
Ti^{4+}	0.31	0.30	0.27	0.30	0.20	0.37	0.46	0.37	0.42	0.02
Mg^{2+}	4.85	4.91	4.78	4.76	4.74	4.74	4.67	4.76	4.71	2.36
Mn^{2+}	0.00	0.00	0.00	0.00	0.00	0.00	0.04	0.00	0.02	0.00
Fe^{2+}	0.52	0.51	0.49	0.50	0.56	0.50	0.50	0.50	0.50	0.07
Fe^{3+}	0.87	0.87	0.84	0.85	0.95	0.85	0.85	0.84	0.85	0.19
Cr^{3+}	–	–	–	–	–	–	–	–	–	–
Cu^{2+}	–	–	–	–	–	–	–	–	–	–
Zn^{2+}	0.00	0.00	0.00	0.00	0.00	0.00	0.00	0.00	0.00	0.00
Ca^{2+}	18.92	18.74	18.96	18.77	18.68	18.86	18.93	18.87	18.96	18.88
Na^{+}	0.00	0.00	0.00	0.00	0.00	0.00	0.00	0.00	0.00	0.00
K^{+}	0.00	0.00	0.00	0.00	0.00	0.00	0.00	0.00	0.00	0.00
La^{3+}	0.03	0.02	0.02	0.00	0.02	0.00	0.00	0.00	0.00	–
Ce^{3+}	0.05	0.06	0.03	0.03	0.03	0.03	0.02	0.02	0.03	0.00
Pr^{3+}	0.00	0.00	0.00	0.00	0.00	0.00	0.00	0.00	0.00	–
Nd^{3+}	0.00	0.00	0.00	0.00	0.00	0.00	0.00	0.00	0.00	–
Sm^{3+}	0.00	0.00	0.00	0.00	0.00	0.00	0.00	0.00	0.00	–
Eu^{3+}	0.00	0.00	0.00	0.00	0.00	0.00	0.00	0.00	0.00	–
Gd^{3+}	0.00	0.00	0.00	0.00	0.00	0.00	0.00	0.00	0.00	–
Pb^{2+}	–	–	–	–	–	–	–	–	–	–
Bi^{3+}	–	–	–	–	–	–	–	–	–	–
Th^{4+}	–	–	–	–	–	–	–	–	–	–
U^{4+}	–	–	–	–	–	–	–	–	–	–
B^{3+}	†2.40	†2.42	†2.41	2.60	†2.41	†2.42	†2.42	†2.41	2.26	–
S^{6+}	0.11	0.11	0.05	0.00	0.00	0.00	0.04	0.00	0.00	0.00
F^{-}	0.00	0.76	0.00	0.00	0.00	0.00	0.00	0.00	0.61	0.00
Cl^{-}	0.00	0.00	0.00	0.00	0.00	0.00	0.00	0.00	0.00	0.00
OH^{-}*	4.40	3.33	4.77	4.12	4.62	4.72	4.52	4.82	4.72	9.82
O	73.60	73.90	73.23	73.88	73.38	73.28	73.48	73.18	72.67	68.18
					Statistics					
ΣX	19.00	18.81	19.01	18.80	18.73	18.89	18.95	18.89	18.99	18.88
ΣY	13.29	13.34	13.34	13.40	13.35	13.37	13.41	13.42	13.43	13.65
ΣZ	17.71	17.85	17.65	17.80	17.92	17.74	17.64	17.69	17.67	17.47

*Calculated for charge balance. †Average value of 2.84 B_2O_3 used in calculations.

V74 includes 0.01 Be.

QUANTITATIVE WDS RESULTS (NMNS)

Ions p.f.u. (50-Cation Normalization)

	V75-2	V75-3
Si^{4+}	17.47	17.87
Al^{3+}	10.09	10.05
Ti^{4+}	0.00	0.00
Mg^{2+}	2.68	2.57
Mn^{2+}	0.02	0.00
Fe^{2+}	0.09	0.07
Fe^{3+}	0.23	0.21
Cr^{3+}	–	–
Cu^{2+}	–	–
Zn^{2+}	0.00	0.00
Ca^{2+}	19.42	19.23
Na^{+}	0.00	0.00
K^{+}	0.00	0.00
La^{3+}	–	–
Ce^{3+}	0.00	0.00
Pr^{3+}	–	–
Nd^{3+}	–	–
Sm^{3+}	–	–
Eu^{3+}	–	–
Gd^{3+}	–	–
Pb^{2+}	–	–
Bi^{3+}	–	–
Th^{4+}	–	–
U^{4+}	–	–
B^{3+}	0.00	–
S^{6+}	0.00	0.00
F^{-}	0.00	0.00
Cl^{-}	0.00	0.00
OH^{-*}	10.75	10.01
O	67.25	67.99
ΣX	19.42	19.23
ΣY	13.11	12.90
ΣZ	17.47	17.87

*Calculated for charge balance.

Appendix F

DETAILS OF CHEMICAL METHODS

Table F.1: Sample dissolution for atomic absorption spectroscopy.

1. Weigh ≈0.2 g of dry, sieved powder into a teflon beaker.
2. Add enough distilled water to completely wet the powder.
3. Add ≈40.0 ml HF and reflux for ≈30 minutes, or until the HF fumes.
4. Add ≈4.0 ml $HClO_4$ and reflux overnight.
5. Remove cover and fume to near dryness.
6. Add ≈20 ml of distilled water and fume until nearly dry.
7. Wash the remaining liquid into a 25 ml volumetric and add 0.75 ml of 3% HCl.
8. Bring the volume up to 25 ml with distilled water after the solution has reached room temperature.

Table F.2: H_2O and CO_2 calculations.

$$H_2O\ (CO_2)\ \text{wt.\%} = \frac{\Delta\text{weight (g)} - \text{blank (g)}}{\text{sample weight (g)}} \times 100$$

e.g. for analysis SY-2_1:

$$H_2O = \frac{(86.0262\ \text{g} - 86.0194\ \text{g}) - 0.0022\ \text{g}}{1.0126\ \text{g}} \times 100 = 0.45\ \text{wt.\%}$$

Table F.3: Condensed procedure for ferrous iron determinations.

1. Weigh ≈0.2 g of dry, sieved powder into a teflon beaker.
2. Add ≈15 ml HCl and ≈4 ml HF and reflux for 10 minutes.
3. Wash the sample into a 500 ml Erlenmeyer flask containing ≈150 ml drowning solution (40 ml boric acid + 5 ml H_3PO_4 + 5 ml H_2SO_4 + 100 ml H_2O).
4. Add 2–5 drops of Na-DPS (diphenylaminesulphonate) indicator solution and titrate with 0.01N standardized potassium dichromate to the violet blue end-point.

Calculations

$$Fe^{2+}\ \text{wt.\%} = \frac{(V_s - V_b) \times Fe_{eq}}{\text{sample mass (mg)}} \times 100$$

$$FeO\ (\text{wt.\%}) = 1.287 \times \text{wt.\%}\ Fe^{2+}$$

where:

V_s = volume (ml) of potassium dichromate required by the sample solution.
V_b = volume (ml) of potassium dichromate required by the reagent blank solution.
Fe_{eq} = iron equivalent (mg/ml) of the potassium dichromate solution.

e.g. for analysis $V4_1$

$$Fe^{2+} = \frac{(7.25\ \text{ml} - 0.00\ \text{ml}) \times 0.5586\ \text{mg/ml}}{199.8\ \text{mg}} \times 100 = 2.03\ \text{wt.\%}$$

$$FeO = 1.287 \times 2.03 = 2.61\ \text{wt.\%}$$

Table F.4: Li and Be analyses (ppm and wt.% oxide).

Sample	Li	Be	Li_2O	BeO	Sample	Li	Be	Li_2O	BeO
V2	98	407	0.02	0.11					
V3	8	*	–	–	V36	*	*	–	–
$V4_1$	114	74	0.02	0.02					
$V4_2$	128	75	0.03	0.02	V43	*	*	–	–
$V4_3$	126	71	0.03	0.02					
$V4_4$	117	68	0.03	0.02	V44	13	21	–	–
$V4_5$	128	67	0.03	0.02	V46	*	35	–	0.01
$V4_6$	160	68	0.03	0.02					
$V4_7$	141	61	0.03	0.02	V56	66	13	0.01	–
V5	52	44	0.01	0.02	V58	*	*	–	–
V11	12	*	–	–	V59	*	*	–	–
V13	14	*	–	–	V60	*	*	–	–
V14	23	*	–	–	V61	7	*	–	–
V17	15	9	–	–	$V67_1$	30	207	0.01	0.06
V22	17	*	–	–	$V67_2$	27	204	0.01	0.06
V23	25	*	0.01	–	V70	15	6	–	–
V24	34	6	0.01	–					
V26	87	89	0.02	0.03	$V74_1$	*	108	–	0.03
V27	22	19	–	0.01	$V74_2$	24	98	0.01	0.03
V30	*	8	–	–	$V74_3$	7	98	–	0.03
V31	57	19	0.01	0.01					
V33	92	552	0.02	0.15	V75	*	*	–	–
V35	167	20	0.04	0.01					

*Below detection limit (≈5 ppm for Li and ≈2 ppm for Be.

Li standards were GSP–1 (30 ppm) and GH (45 ppm). Measured values were 46 and 30 ppm.
Be standards were GH (6 ppm) and SY2 (23 ppm). Measured values were 4 and 23 ppm.

Table X: Ferrous iron determinations (values in wt.%).

Sample	Fe^{2+}	Fe	Fe^{3+}	$\frac{Fe^{2+}}{Fe^{3+}}$	$\frac{Fe^{2+}}{Fe^{2+}+Fe^{3+}}$
V2	2.56	3.19	0.63	4.06	0.80
$V2_2$	2.63	3.19	0.56	4.70	0.82
V3	0.16	1.24	1.08	0.15	0.13
V4	2.03	4.42	2.39	0.85	0.46
$V4_2$	2.02	4.42	2.40	0.84	0.46
$V4_3$	2.03	4.42	2.39	0.85	0.46
$V4_4$	2.05	4.42	2.37	0.86	0.46
$V4_5$	2.10	4.42	2.32	0.91	0.48
$V4_6$	2.08	4.42	2.34	0.89	0.47
$V4_7$	2.05	4.42	2.37	0.86	0.46
$V4_8$	2.04	4.42	2.38	0.86	0.46
V5	2.23	3.15	0.92	2.42	0.71
$V5_2$	2.37	3.15	0.78	3.04	0.75
V13	1.06	2.34	1.28	0.83	0.45
V14	0.16	0.96	0.80	0.20	0.17
V17	0.57	2.21	1.64	0.35	0.26
$V17_2$	0.58	2.21	1.63	0.36	0.26
V22	0.25	1.82	1.57	0.16	0.14
V23	0.22	0.99	0.77	0.29	0.22
V24	0.50	0.74	0.24	2.08	0.68
V26	0.31	2.44	2.13	0.15	0.13
V33	2.43	2.70	0.27	9.00	0.90
$V33_2$	2.46	2.70	0.24	10.25	0.91
V36	0.31	2.48	2.17	0.14	0.13
V39	0.77	3.68	2.91	0.26	0.21
V43	0.30	3.89	3.59	0.08	0.08
V46	0.47	1.31	0.84	0.56	0.36
V56	2.94	5.58	2.64	1.11	0.53
$V56_2$	2.87	5.58	2.71	1.06	0.51
V58	0.04	0.72	0.68	0.06	0.06
$V58_2$	0.05	0.72	0.67	0.07	0.07

Table F.6: H_2O (measured and calculated) and CO_2 values.

Sample	H_2O (meas.)	H_2O (calc.)*	CO_2 (meas.)
V2	1.66	1.32	0.20
V3	4.29	3.00	0.09
$V3_2$	4.18	3.00	0.17
V4	1.56	1.53	0.13
V5	1.70	1.50	0.10
$V5_2$	1.70	1.64	0.11
V11	2.77	2.77	0.11
V17	2.79	2.75	0.12
$V17_2$	2.95	2.75	0.09
V22	2.87	2.70	0.14
V24	1.51	1.50	0.13
V26	5.37	1.75	0.23
V33	1.63	1.30	0.29
V43	2.47	2.92	0.18
V44	1.79	2.63	0.33
$V44_2$	1.88	2.63	0.26
V56	0.86	1.27	0.50
V58	2.96	2.89	0.14
V60	2.16	2.77	0.36
V61	1.41	2.00	0.38
V74	0.61	1.33	0.12
V75	3.57	3.12	0.15

Appendix G.1

UNCONSTRAINED CELL DIMENSIONS

Single-Crystal Diffractometer

ABBREVIATIONS USED IN APPENDIX G.1

(c): centre of grain
(r): rim of grain
(i): intermediate between core and rim
(b): blue
(g): green
(p): pink
(w): white

Subscripted numbers refer to different crystals.

UNCONSTRAINED CELL DIMENSIONS

Single-Crystal Diffractometer

Sample	a_1 (Å)	a_2 (Å)	c (Å)	α (°)	β (°)	γ (°)	V (Å^3)	Δa (Å)
V1	15.539(2)	15.543(2)	11.811(1)	89.96(1)	89.97(1)	90.01(1)	2852.6(5)	0.004
V2	15.516(2)	15.516(3)	11.780(1)	90.01(1)	90.00(1)	89.99(1)	2836.0(7)	0.000
V3	microcrystalline							
V4	15.557(1)	15.557(1)	11.791(1)	90.01(1)	90.03(1)	90.02(1)	2853.9(4)	0.000
V5	15.527(1)	15.528(1)	11.786(1)	90.00(1)	90.02(1)	90.00(1)	2841.5(4)	0.002
V6	15.645(2)	15.652(3)	11.828(2)	90.03(1)	90.02(1)	89.99(1)	2896.5(8)	0.007
V7	15.585(2)	15.593(2)	11.849(1)	90.04(1)	90.01(1)	89.99(1)	2879.4(6)	0.008
V8	15.538(2)	15.555(2)	11.821(1)	90.01(1)	90.02(1)	90.02(1)	2857.1(5)	0.018
$V8_g$	15.541(1)	15.550(2)	11.820(1)	90.01(1)	90.04(1)	90.02(1)	2856.4(5)	0.009
$V8_b$	15.501(2)	15.502(2)	11.760(1)	90.00(1)	90.00(1)	89.99(1)	2825.6(5)	0.001
V9	15.524(3)	15.535(3)	11.803(2)	90.04(1)	90.03(1)	89.98(2)	2846.6(8)	0.011
V10	15.536(2)	15.536(2)	11.815(1)	90.02(1)	89.98(1)	89.99(1)	2851.5(6)	0.000
$V11_1$	15.517(2)	15.530(3)	11.816(2)	89.97(1)	90.00(1)	90.01(1)	2847.3(8)	0.012
$V11_2$	15.506(3)	15.507(4)	11.812(2)	90.01(2)	90.01(1)	90.01(2)	2840(1)	0.001
$V11_3$	15.514(3)	15.532(3)	11.829(3)	89.98(2)	90.00(2)	90.00(2)	2850(1)	0.018
V12	15.534(1)	15.535(2)	11.815(1)	90.02(1)	90.01(1)	90.05(1)	2851.1(5)	0.000
$V13_c$	15.516(2)	15.521(1)	11.800(2)	90.00(1)	90.05(1)	89.97(1)	2841.9(7)	0.005
$V13_i$	15.518(2)	15.519(2)	11.810(1)	89.99(1)	90.05(9)	90.02(1)	2844.1(6)	0.001
$V13_r$	15.522(2)	15.548(2)	11.816(2)	89.96(1)	90.05(1)	90.07(1)	2851.6(7)	0.026
V14	15.516(1)	15.519(2)	11.802(1)	90.02(1)	90.02(1)	90.00(1)	2841.8(4)	0.003
V15	15.521(2)	15.539(2)	11.807(1)	90.02(1)	90.02(1)	90.00(1)	2847.5(5)	0.018
V16	15.531(3)	15.539(2)	11.814(2)	90.01(1)	90.01(1)	90.02(1)	2851.3(7)	0.008
V17	15.541(2)	15.545(3)	11.818(2)	90.02(1)	90.04(1)	90.00(1)	2855.1(7)	0.004
V18	15.524(2)	15.528(2)	11.814(1)	90.00(1)	90.01(1)	90.01(1)	2847.9(5)	0.003
V19	15.529(2)	15.531(2)	11.822(1)	90.02(1)	90.01(1)	89.99(1)	2851.3(6)	0.002
V20	15.509(3)	15.534(2)	11.816(1)	90.01(1)	90.01(1)	89.99(1)	2846.6(6)	0.024
V21	15.514(2)	15.545(2)	11.812(2)	90.01(1)	90.01(1)	89.97(1)	2848.7(6)	0.031
$V21_p$	15.683(2)	15.689(3)	11.751(2)	89.99(1)	90.03(1)	90.03(1)	2891.3(8)	0.006
$V21_w$	15.511(1)	15.513(1)	11.798(1)	89.98(1)	90.02(1)	90.00(1)	2838.9(4)	0.002
V22	15.537(1)	15.543(2)	11.818(1)	90.01(1)	90.01(1)	90.02(1)	2854.1(4)	0.006
$V23_r$	15.504(2)	15.524(1)	11.808(1)	90.00(1)	90.01(1)	90.01(1)	2842.1(5)	0.020
$V23_c$	15.515(2)	15.517(2)	11.799(2)	90.01(1)	90.02(1)	89.96(1)	2840.6(6)	0.002
V24	15.523(2)	15.529(2)	11.785(1)	90.05(1)	90.00(1)	90.00(1)	2840.8(6)	0.005
V25	15.559(1)	15.568(2)	11.822(1)	89.98(1)	90.01(1)	89.99(1)	2863.3(5)	0.009
V26	15.550(2)	15.553(3)	11.802(1)	90.00(1)	90.00(1)	89.99(1)	2854.3(7)	0.003
V27	15.543(2)	15.548(2)	11.797(2)	90.00(1)	90.02(1)	89.97(1)	2850.8(7)	0.005
V28	15.534(1)	15.540(1)	11.791(1)	90.02(1)	90.02(1)	89.96(1)	2846.1(4)	0.006

UNCONSTRAINED CELL DIMENSIONS

Single-Crystal Diffractometer

Sample	a_1 (Å)	a_2 (Å)	c (Å)	α (°)	β (°)	γ (°)	V (Å^3)	Δa (Å)
V29	15.535(1)	15.541(1)	11.792(1)	90.01(1)	90.01(1)	89.98(1)	2847.0(4)	0.006
V30	15.728(2)	15.732(2)	11.731(1)	90.01(1)	90.02(1)	89.99(1)	2902.6(5)	0.004
V31	15.541(2)	15.557(3)	11.807(2)	89.98(1)	90.01(1)	90.06(1)	2854.5(8)	0.015
V32	15.530(1)	15.532(1)	11.788(1)	90.00(1)	90.02(1)	89.97(1)	2843.5(5)	0.002
V33	15.503(3)	15.512(2)	11.763(2)	89.94(1)	90.02(1)	90.03(1)	2828.7(8)	0.009
V34	15.559(2)	15.564(2)	11.773(1)	90.01(1)	90.02(1)	89.96(1)	2850.7(5)	0.005
V35	15.523(1)	15.525(1)	11.778(1)	89.98(1)	90.00(1)	90.00(1)	2838.3(4)	0.002
V36	15.562(2)	15.564(1)	11.837(1)	89.97(1)	90.00(1)	90.01(1)	2867.1(6)	0.001
V37	15.534(2)	15.537(2)	11.819(1)	90.00(1)	89.99(1)	90.00(1)	2852.6(5)	0.003
V38	15.702(2)	15.711(3)	11.747(2)	89.99(1)	89.96(1)	89.97(1)	2897.8(8)	0.009
V39	15.564(1)	15.566(2)	11.839(2)	90.01(1)	90.03(1)	90.01(1)	2868.3(6)	0.001
V40	15.579(3)	15.584(3)	11.833(1)	89.99(1)	90.00(1)	89.99(2)	2872.8(9)	0.005
V41	15.543(1)	15.561(1)	11.827(1)	89.99(1)	90.03(1)	90.03(1)	2860.6(3)	0.018
V42	15.599(1)	15.604(2)	11.854(1)	90.00(1)	90.00(1)	89.99(1)	2885.5(5)	0.005
V43	15.585(2)	15.586(2)	11.831(1)	89.99(1)	89.98(1)	90.04(1)	2873.9(6)	0.001
$V44_1$	15.596(2)	15.600(2)	11.784(1)	90.02(1)	90.03(1)	89.97(1)	2866.8(6)	0.004
$V44_2$	15.594(2)	15.597(2)	11.766(1)	90.02(1)	89.98(1)	90.00(1)	2861.6(5)	0.003
V45	15.622(3)	15.641(3)	11.746(3)	89.99(2)	90.06(2)	90.01(2)	2869(1)	0.019
V46	15.622(3)	15.624(3)	11.780(3)	90.10(2)	90.05(2)	89.95(2)	2875(1)	0.002
V47	15.516(3)	15.526(4)	11.773(2)	90.01(2)	89.99(2)	90.01(2)	2836(1)	0.010
$V48_1$	15.518(2)	15.520(2)	11.786(1)	90.01(1)	89.99(1)	89.98(1)	2838.5(6)	0.003
$V48_2$	15.520(2)	15.522(1)	11.780(1)	89.99(1)	90.02(1)	90.00(1)	2837.7(4)	0.002
$V49_1$	15.499(3)	15.511(2)	11.763(2)	90.03(1)	90.01(2)	90.09(1)	2827.8(8)	0.012
$V49_2$	15.487(2)	15.488(2)	11.763(1)	89.97(1)	89.97(1)	89.98(1)	2821.6(6)	0.001
V50	15.590(3)	15.591(3)	11.780(3)	90.02(2)	90.01(2)	89.96(1)	2863(1)	0.002
V51	15.518(2)	15.521(2)	11.807(1)	89.97(1)	90.02(1)	90.02(1)	2843.8(5)	0.004

UNCONSTRAINED CELL DIMENSIONS

Single-Crystal Diffractometer

Sample	a_1 (Å)	a_2 (Å)	c (Å)	α (°)	β (°)	γ (°)	V (Å^3)	Δa (Å)
$V52_1$	15.665(6)	15.684(7)	11.762(8)	90.03(5)	90.09(4)	89.94(3)	2889(3)	0.019
$V52_2$	15.651(5)	15.672(4)	11.744(3)	90.01(2)	90.14(2)	89.95(2)	2880(1)	0.021
V53	15.787(7)	15.792(6)	11.993(6)	90.03(4)	90.06(4)	89.97(3)	2990(2)	0.005
V54	15.561(2)	15.566(2)	11.827(2)	90.03(1)	89.98(1)	90.00(1)	2864.9(6)	0.005
V55	15.533(2)	15.544(2)	11.788(1)	90.03(1)	89.97(1)	89.99(1)	2846.0(6)	0.011
V56	15.735(2)	15.742(2)	11.730(2)	90.00(1)	90.00(1)	90.00(1)	2905.6(6)	0.007
$V57_1$	15.563(1)	15.568(2)	11.833(2)	90.00(1)	90.00(1)	90.02(1)	2867.0(6)	0.006
$V57_2$	15.550(1)	15.552(1)	11.821(1)	89.98(1)	90.00(1)	90.00(1)	2858.5(4)	0.002
V58	microcrystalline							
V59	15.559(2)	15.562(2)	11.827(1)	89.99(1)	90.01(1)	90.00(1)	2863.6(6)	0.004
V60	15.582(2)	15.585(2)	11.821(1)	90.00(1)	89.99(1)	90.01(1)	2870.7(6)	0.003
V61	15.662(2)	15.666(1)	11.769(1)	89.98(1)	90.01(1)	89.99(1)	2887.7(5)	0.004
V62	15.569(1)	15.575(2)	11.813(1)	90.03(1)	90.02(1)	90.02(1)	2864.5(5)	0.006
V63	15.509(1)	15.516(2)	11.763(1)	90.00(1)	90.01(1)	89.98(1)	2830.6(5)	0.007
V64	15.523(2)	15.526(1)	11.765(1)	89.97(1)	90.01(1)	89.99(1)	2835.5(5)	0.004
V65	15.504(2)	15.516(1)	11.781(1)	89.97(1)	89.99(1)	89.99(1)	2834.0(6)	0.011
$V66_1$	15.539(2)	15.544(2)	11.787(2)	90.01(1)	90.00(1)	89.99(1)	2847.0(7)	0.004
$V66_2$	15.519(2)	15.520(2)	11.771(1)	90.01(1)	90.02(1)	90.02(1)	2835.0(5)	0.001
V67	15.518(3)	15.525(2)	11.791(2)	90.03(1)	90.02(1)	90.01(1)	2840.7(7)	0.007
V68	15.563(2)	15.565(2)	11.830(2)	90.01(1)	90.03(1)	90.00(1)	2865.7(6)	0.002
V69	15.555(3)	15.556(2)	11.811(2)	90.02(1)	90.01(1)	89.99(1)	2857.9(8)	0.000
V70	15.540(2)	15.544(1)	11.791(1)	90.00(1)	90.00(1)	90.00(1)	2848.1(5)	0.004
V71	15.547(2)	15.564(2)	11.832(1)	89.98(1)	90.03(1)	90.02(1)	2863.1(6)	0.017
V72	metamict							
V73	15.649(2)	15.653(2)	11.792(1)	90.01(1)	90.00(1)	90.00(1)	2888.5(6)	0.004
$V74_c$	15.743(2)	15.752(2)	11.704(1)	89.99(1)	90.00(1)	89.97(1)	2902.4(5)	0.009
V75	microcrystalline							
AVG	15.56(6)	15.57(6)	11.80(4)	90.00(2)	90.01(3)	90.00(3)	2860(24)	0.01

UNCONSTRAINED CELL DIMENSIONS

Single-Crystal Diffractometer

Sample	a_1 (Å)	a_2 (Å)	c (Å)	α (°)	β (°)	γ (°)	V (Å^3)	Δa (Å)
			Repeat Refinements (Same Crystal, Remounted)					
V4	15.557(1)	15.557(1)	11.791(1)	90.01(1)	90.03(1)	90.02(1)	2853.9(4)	0.000
$V4_{R2}$	15.558(2)	15.559(2)	11.786(1)	90.01(1)	89.99(1)	90.03(1)	2853.0(6)	0.001
$V4_{R3}$	15.554(2)	15.555(2)	11.789(2)	89.97(1)	90.00(1)	90.02(1)	2852.2(6)	0.000
$V4_{R4}$	15.547(1)	15.554(1)	11.785(1)	90.00(1)	90.02(1)	89.98(1)	2849.9(4)	0.007
$V4_{R5}$	15.553(2)	15.554(2)	11.786(1)	90.02(1)	90.00(1)	90.00(1)	2851.1(5)	0.002
AVG	15.554(4)	15.556(2)	11.787(2)	90.00(2)	90.01(2)	90.01(2)	2852(1)	0.002
			High-angle Reflections					
$V13_c$	15.521(3)	15.523(2)	11.807(2)	90.01(1)	89.99(1)	89.99(1)	2844.6(8)	0.002
$V13_i$	15.538(1)	15.547(3)	11.822(2)	89.98(2)	89.98(1)	89.98(1)	2855.8(8)	0.009
$V13_r$	15.523(3)	15.567(2)	11.825(2)	90.01(1)	90.01(2)	90.03(1)	2857.3(8)	0.044
$V74_c$	15.746(2)	15.751(3)	11.708(2)	89.97(2)	90.00(1)	90.00(1)	2903.7(8)	0.005

Appendix G.2

CONSTRAINED CELL DIMENSIONS

Single-Crystal Diffractometer

ABBREVIATIONS USED IN APPENDIX G.2

(c): centre of grain
(r): rim of grain
(i): intermediate between core and rim
(b): blue
(g): green
(p): pink
(w): white

Subscripted numbers refer to different crystals.

CONSTRAINED CELL DIMENSIONS

Single-Crystal Diffractometer

Sample	a (Å)	c (Å)	V (Å^3)	Sample	a (Å)	c (Å)	V (Å^3)
V1	15.540(1)	11.809(1)	2851.7(6)	V40	15.581(2)	11.833(1)	2872.8(8)
V2	15.516(2)	11.781(1)	2836.3(7)	V41	15.548(2)	11.826(2)	2858.7(7)
V3	microcrystalline						
V4	15.557(1)	11.791(1)	2853.7(5)	V42	15.602(1)	11.854(1)	2885.5(5)
V5	15.527(1)	11.786(1)	2841.5(4)				
V6	15.648(2)	11.827(2)	2895.9(8)	V43	15.585(1)	11.830(2)	2873.3(6)
V7	15.591(2)	11.851(2)	2880.8(7)				
V8	15.546(2)	11.822(2)	2857.3(7)	$V44_1$	15.600(2)	11.786(2)	2868.1(7)
$V8_g$	15.544(1)	11.820(1)	2856.1(6)	$V44_2$	15.597(1)	11.767(1)	2862.3(5)
$V8_b$	15.501(1)	11.760(1)	2825.7(5)	V45	15.634(3)	11.747(3)	2872(1)
V9	15.529(2)	11.803(2)	2846(1)	V46	15.624(3)	11.780(5)	2876(2)
V10	15.535(2)	11.815(1)	2851.2(6)				
$V11_1$	15.523(2)	11.816(3)	2847.2(9)	V47	15.519(2)	11.773(2)	2835(1)
$V11_2$	15.507(2)	11.813(2)	2840(1)				
$V11_3$	15.522(2)	11.829(3)	2850(1)	$V48_1$	15.518(1)	11.786(1)	2838.2(6)
V12	15.537(1)	11.815(2)	2852.2(6)	$V48_2$	15.522(1)	11.780(1)	2838.2(5)
$V13_c$	15.522(1)	11.802(2)	2843.3(7)	$V49_1$	15.508(2)	11.763(3)	2829(1)
$V13_i$	15.521(1)	11.813(1)	2845.7(6)	$V49_2$	15.490(2)	11.765(2)	2822.9(7)
$V13_r$	15.538(3)	11.819(3)	2853(1)				
V14	15.518(1)	11.803(1)	2842.1(4)	V50	15.592(2)	11.780(3)	2864(1)
V15	15.531(2)	11.807(1)	2848.0(7)				
V16	15.537(2)	11.815(2)	2852.2(7)	V51	15.520(2)	11.807(1)	2844.0(6)
V17	15.543(2)	11.820(2)	2855.6(8)				
V18	15.526(1)	11.814(1)	2847.9(5)	$V52_1$	15.670(5)	11.759(9)	2888(3)
V19	15.532(1)	11.823(1)	2852.1(6)	$V52_2$	15.656(4)	11.736(4)	2876(2)
V20	15.526(2)	11.815(1)	2848.0(8)	V53	15.792(5)	11.993(8)	2991(3)
V21	15.529(2)	11.813(3)	2848(1)	V54	15.564(1)	11.827(2)	2864.8(6)
$V21_p$	15.689(2)	11.751(2)	2892.3(8)	V55	15.541(2)	11.789(2)	2847.2(7)
$V21_w$	15.512(1)	11.798(1)	2838.7(4)	V56	15.738(1)	11.730(2)	2905.2(6)
V22	15.540(1)	11.818(1)	2853.9(4)	$V57_1$	15.564(1)	11.833(2)	2866.5(6)
$V23_r$	15.519(1)	11.808(2)	2843.9(7)	$V57_2$	15.551(1)	11.820(1)	2858.4(4)
$V23_c$	15.520(1)	11.801(2)	2842.4(6)	V58	microcrystalline		
V24	15.529(2)	11.787(1)	2842.4(7)	V59	15.560(1)	11.827(1)	2863.5(6)
V25	15.562(1)	11.821(1)	2862.6(5)	V60	15.584(1)	11.822(1)	2870.8(5)
V26	15.552(2)	11.802(1)	2854.5(7)	V61	15.664(1)	11.769(1)	2887.8(5)
V27	15.545(2)	11.797(2)	2850.9(8)	V62	15.569(1)	11.811(2)	2862.9(6)
V28	15.539(1)	11.792(2)	2847.2(6)	V63	15.510(1)	11.763(2)	2829.8(5)

CONSTRAINED CELL DIMENSIONS

Single-Crystal Diffractometer

Sample	a (Å)	c (Å)	V (Å^3)
V29	15.539(1)	11.793(1)	2847.5(5)
V30	15.730(1)	11.731(1)	2902.6(5)
V31	15.547(2)	11.806(3)	2853.6(9)
V32	15.530(1)	11.788(2)	2842.7(6)
V33	15.510(2)	11.766(2)	2830(1)
V34	15.564(1)	11.774(2)	2851.9(6)
V35	15.524(1)	11.777(1)	2838.1(4)
V36	15.565(1)	11.839(2)	2868.0(5)
V37	15.535(1)	11.819(1)	2852.5(5)
V38	15.708(2)	11.748(2)	2898.5(8)
V39	15.566(1)	11.841(2)	2869.1(5)
V64	15.524(1)	11.764(1)	2834.9(5)
V65	15.513(1)	11.779(2)	2834.5(6)
$V66_1$	15.541(1)	11.787(2)	2846.7(6)
$V66_2$	15.519(2)	11.771(1)	2834.7(6)
V67	15.524(2)	11.793(2)	2841.8(7)
V68	15.565(1)	11.831(2)	2866.5(5)
V69	15.556(2)	11.811(2)	2858.3(7)
V70	15.543(1)	11.791(1)	2848.4(5)
V71	15.555(2)	11.833(1)	2862.8(7)
V72	metamict		
V73	15.651(2)	11.792(1)	2888.3(6)
$V74_c$	15.750(1)	11.704(2)	2903.4(6)
V75	microcrystalline		
AVG	15.56(6)	11.80(4)	2860(24)

Repeat Refinements
(Same Crystal, Remounted)

V4	15.557(1)	11.791(1)	2853.7(5)
$V4_{R2}$	15.561(1)	11.787(2)	2854.0(6)
$V4_{R3}$	15.556(1)	11.790(2)	2853.0(6)
$V4_{R4}$	15.550(1)	11.785(1)	2849.5(4)
$V4_{R5}$	15.554(1)	11.786(1)	2851.3(5)
AVG	15.555(4)	11.788(3)	2852(2)

High-angle Reflections

$V13_c$	15.5236(8)	11.807(2)	2845.2(6)
$V13_i$	15.538(1)	11.821(3)	2853.9(7)
$V13_r$	15.552(2)	11.824(4)	2860(1)
$V74_c$	15.7474(9)	11.709(3)	2903.5(7)

Appendix H
PRECESSION PHOTOGRAPHS

N.B. All precession photos were taken with Ni-filtered Cu radiation (40 keV, 40 ma). Each photograph is actually one of a pair; in every case a second photo was taken at a different precession angle ($\bar{\mu}$) to isolate double diffraction (Renninger) effects (see section 7.1)

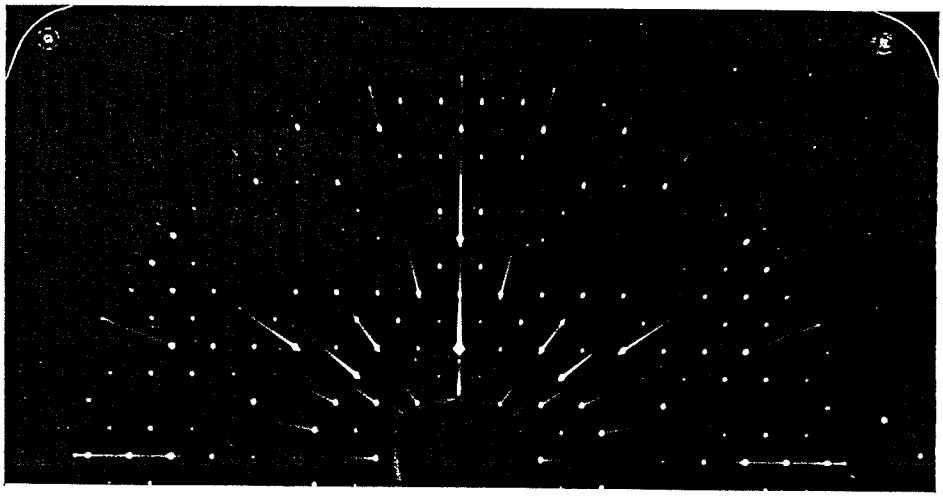

Figure H.1: $V74_c$ $h0l$ precession photograph (102.5 hrs.).

Figure H.2: $V74_c$ $h1l$ precession photograph (80.0 hrs.).

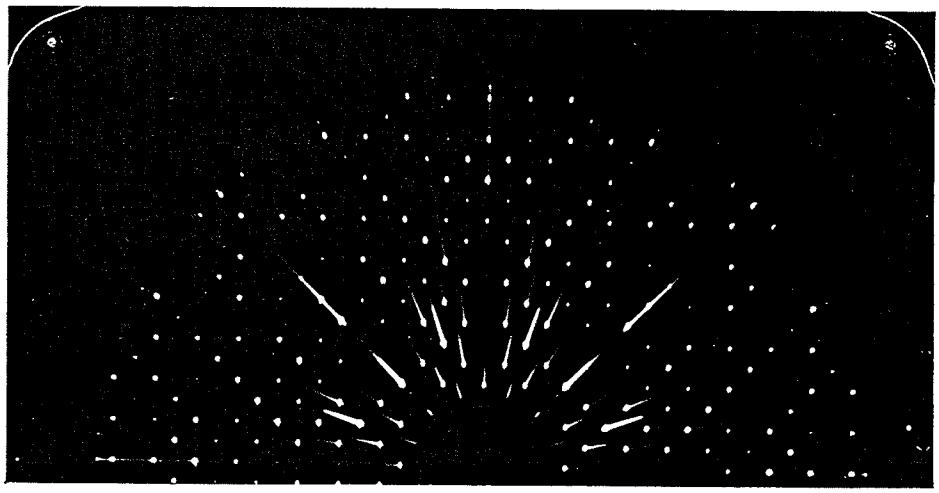

Figure H.3: $V74_c$ $hk0$ precession photograph (81 hrs.).

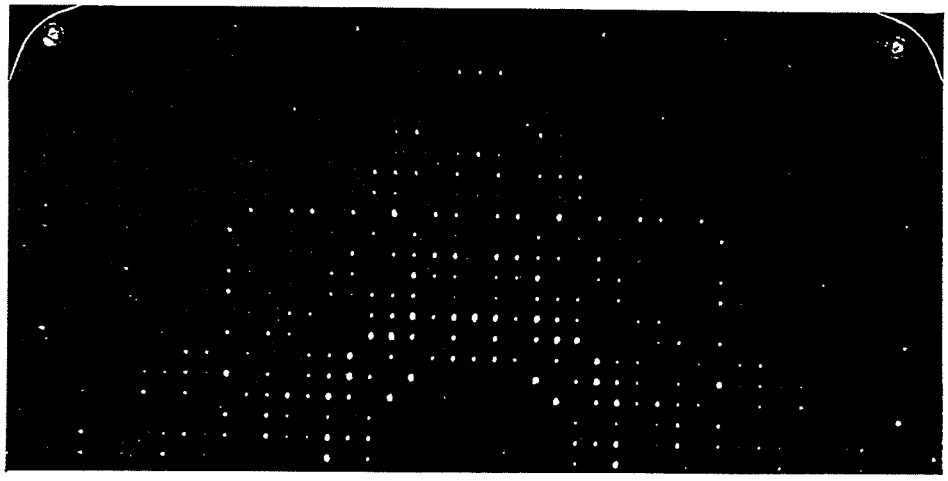

Figure H.4: $V74_c$ $hk1$ precession photograph (89.5 hrs.).

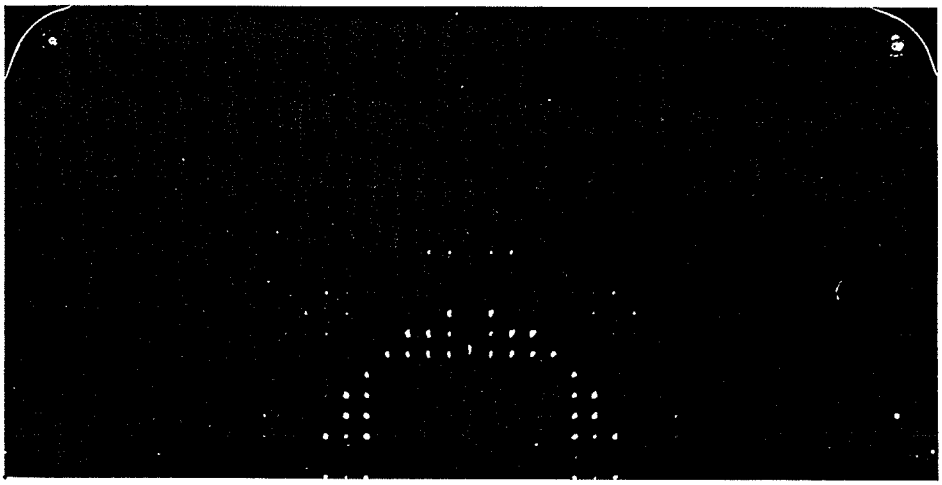

Figure H.5: $V74_c$ $hk3$ precession photograph (96 hrs.).

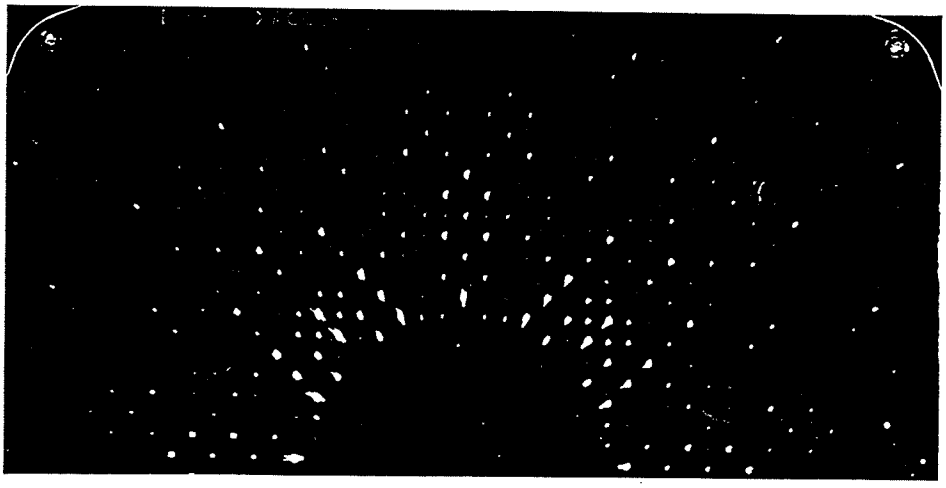

Figure H.6: $V74_c$ $hk4$ precession photograph (95 hrs.).

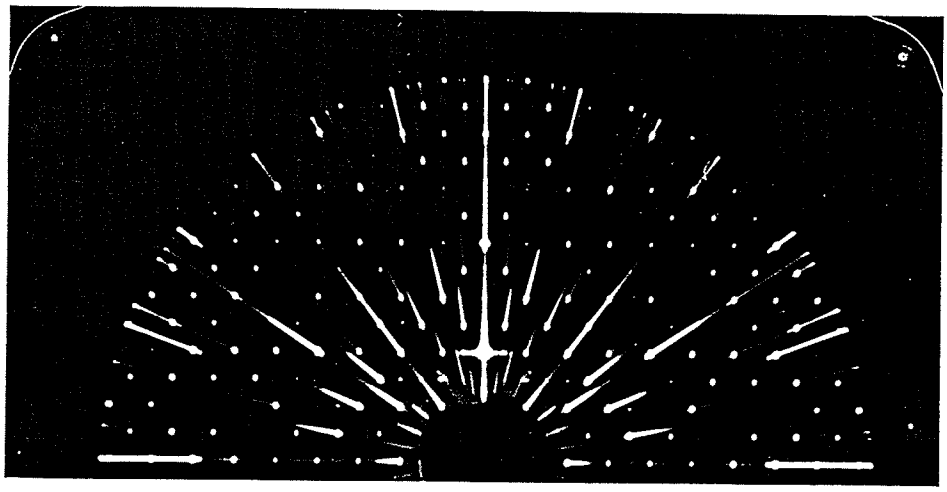

Figure H.7: $V13_c$ $h0l$ precession photograph (82 hrs.).

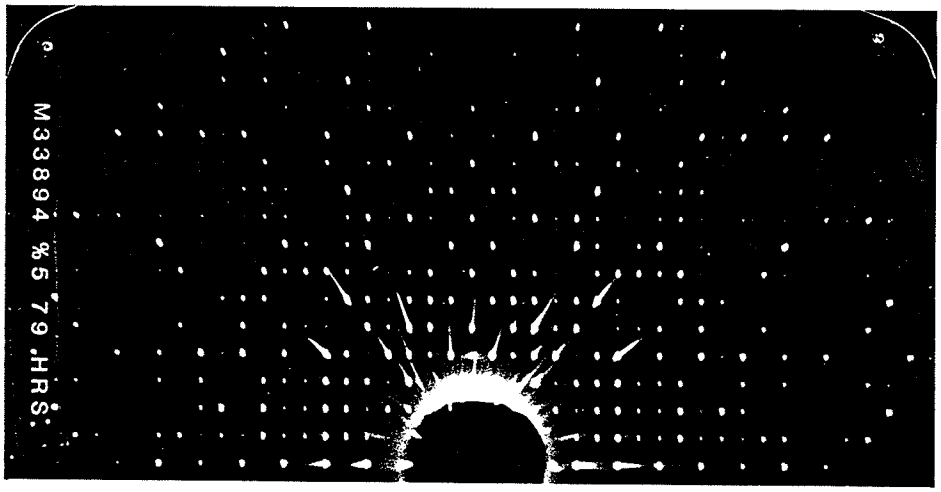

Figure H.8: $V13_c$ $h1l$ precession photograph (88 hrs.).

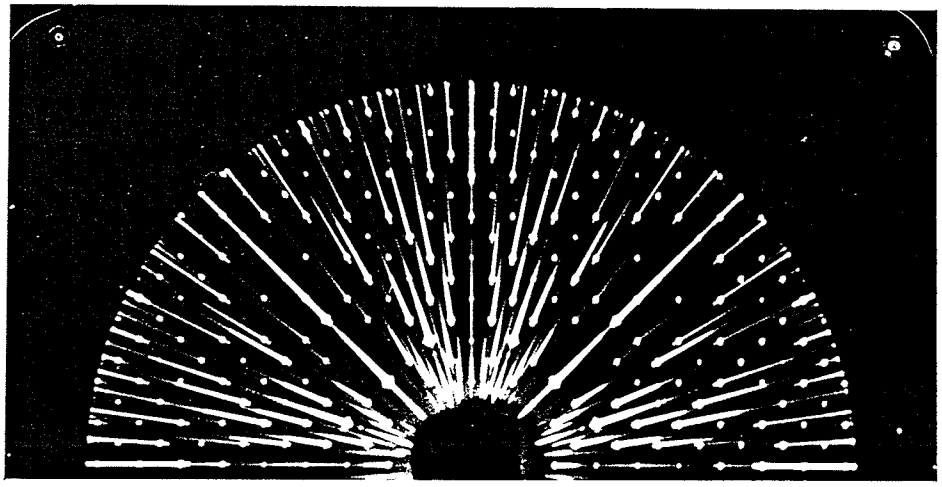

Figure H.9: $V13_c$ $hk0$ precession photograph (84 hrs.).

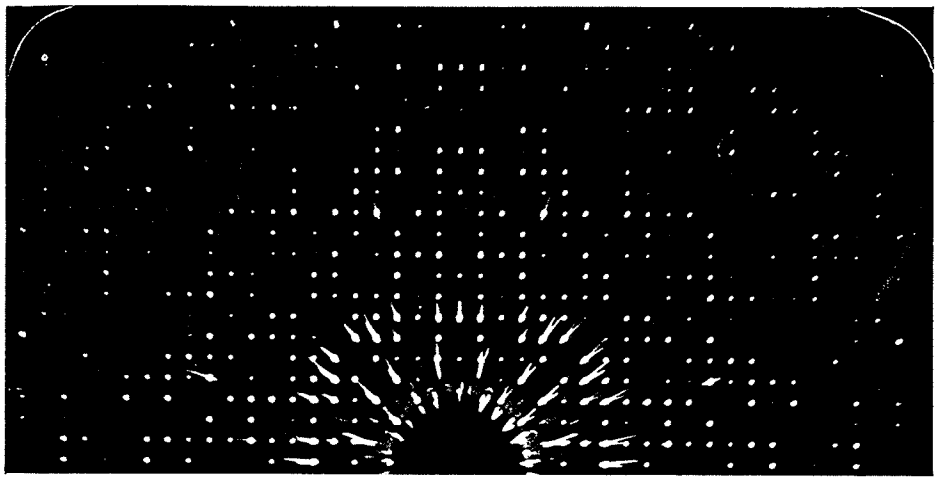

Figure H.10: $V13_c$ $hk1$ precession photograph (88 hrs.).

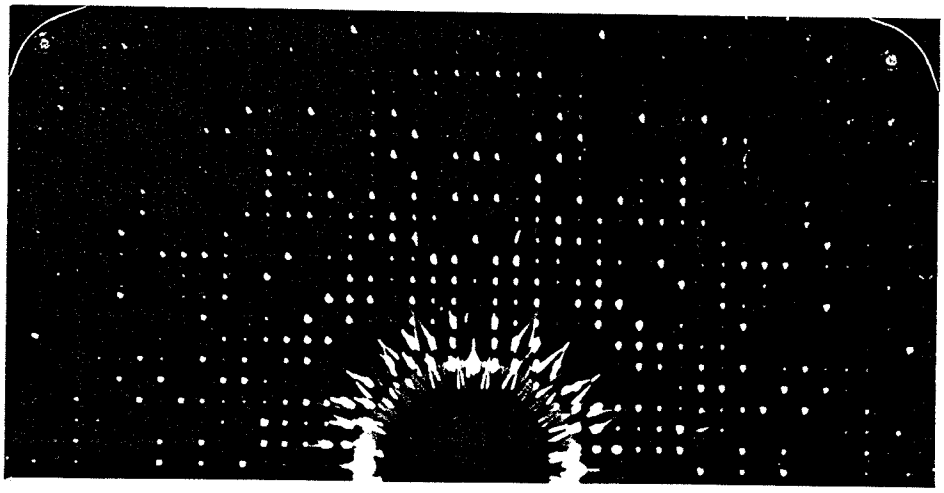

Figure H.11: $V13_c$ $hk3$ precession photograph (92 hrs.).

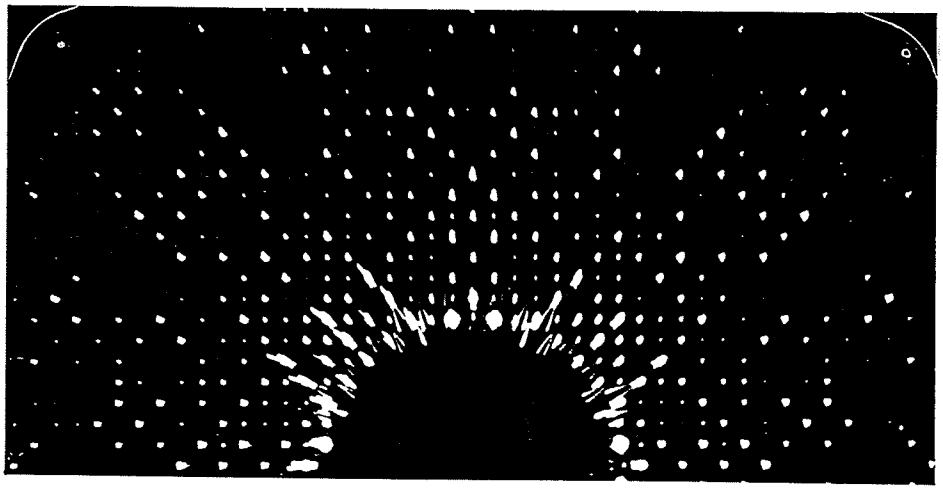

Figure H.12: $V13_c$ $hk4$ precession photograph (78 hrs.).

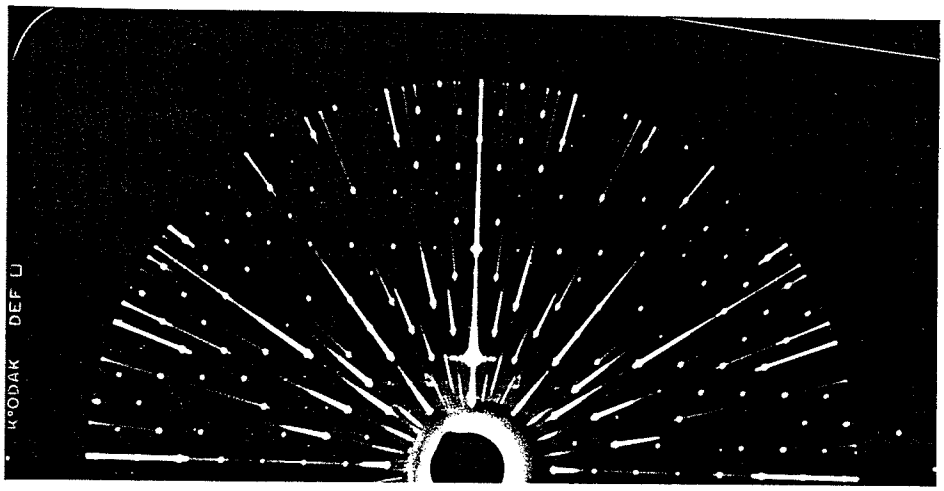

Figure H.13: V13$_i$ $h0l$ precession photograph (83 hrs.).

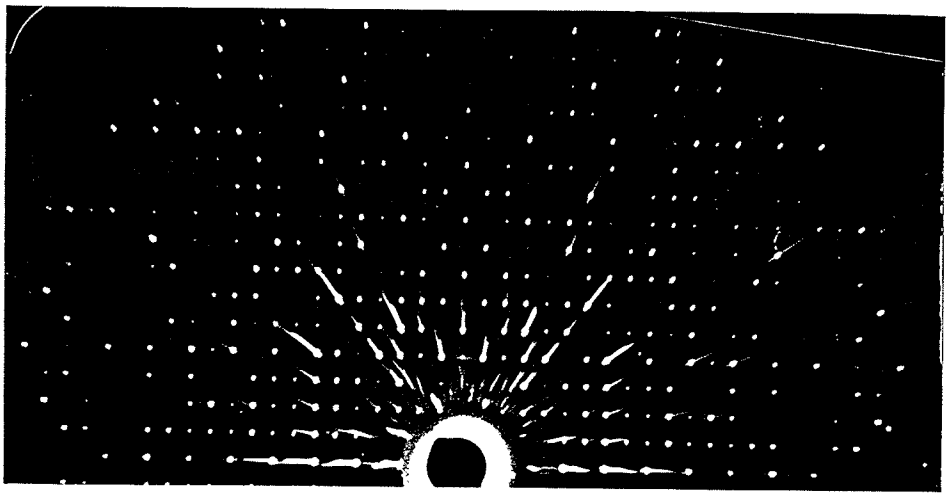

Figure H.14: V13$_i$ $h1l$ precession photograph (87 hrs.).

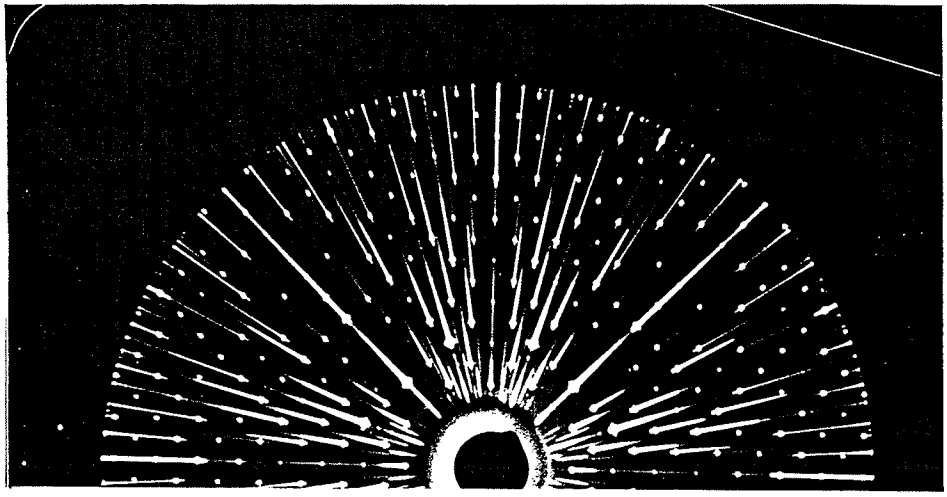

Figure H.15: V13$_i$ $hk0$ precession photograph (84 hrs.).

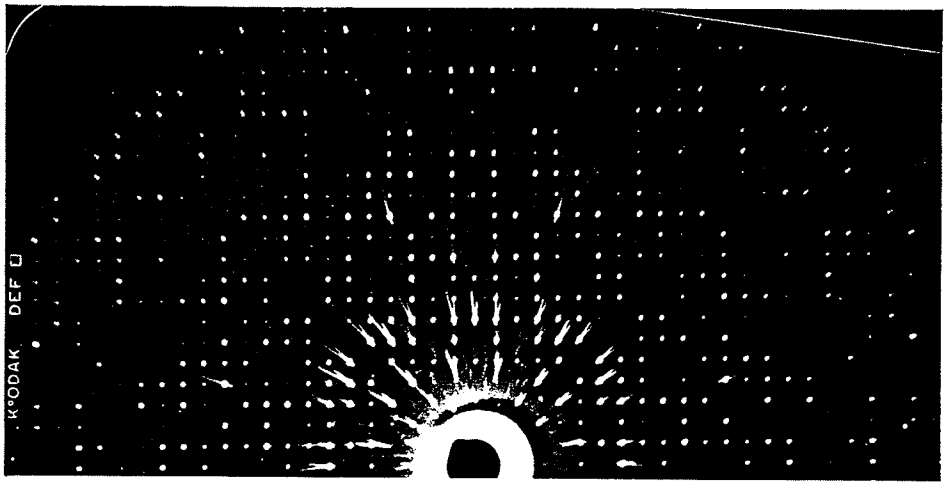

Figure H.16: V13$_i$ $hk1$ precession photograph (86.5 hrs.).

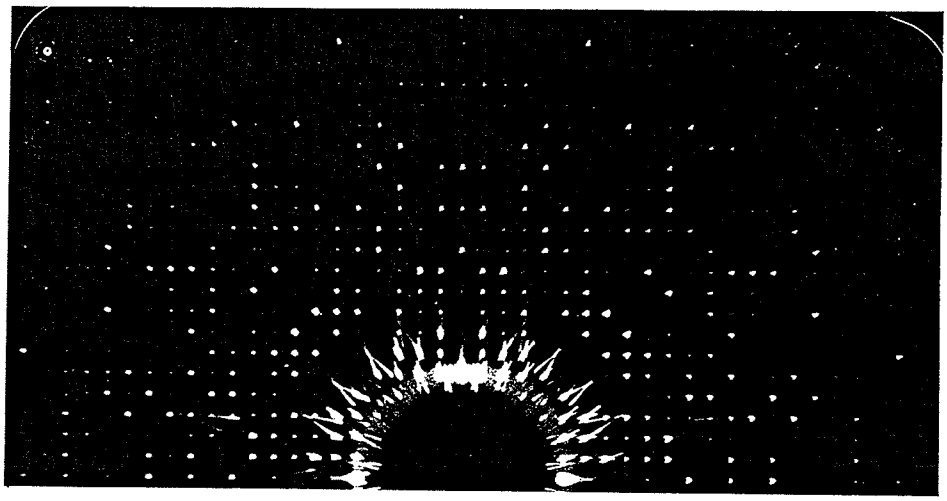

Figure H.17: V13$_i$ $hk3$ precession photograph (81.5 hrs.).

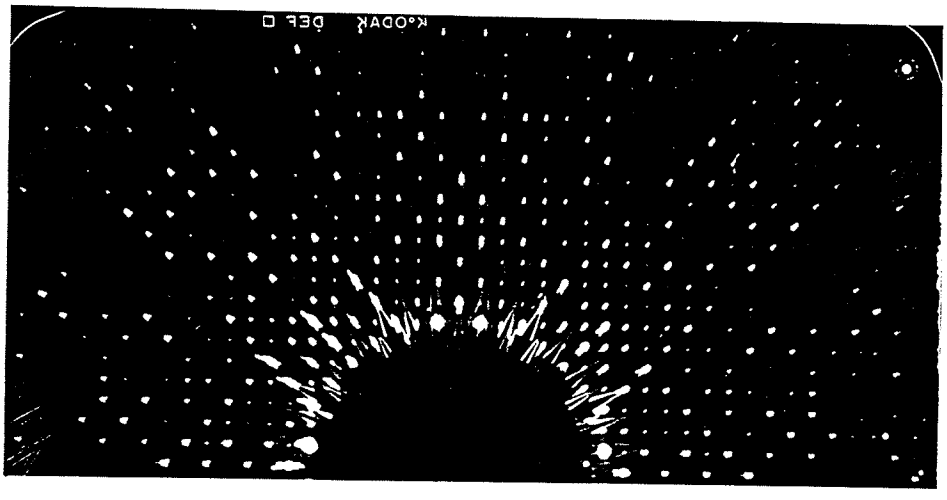

Figure H.18: V13$_i$ $hk4$ precession photograph (81.5 hrs.).

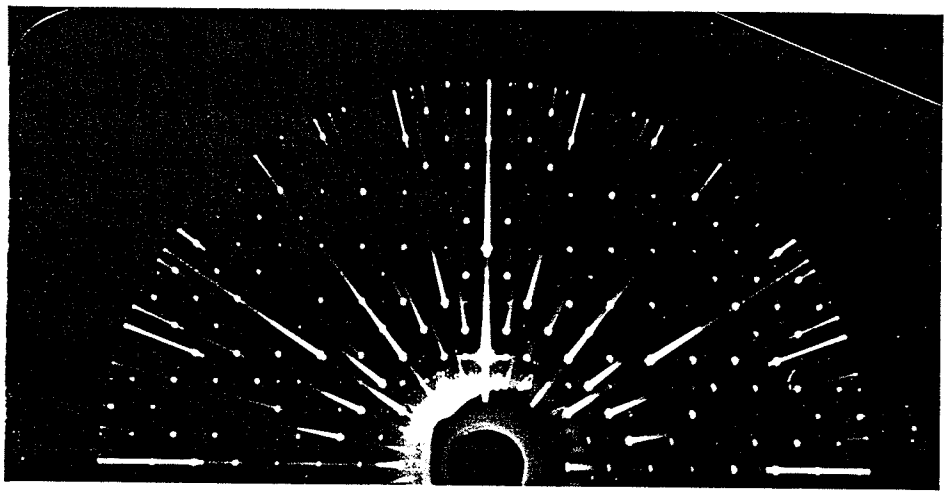

Figure H.19: $V13_r$ $h0l$ precession photograph (87 hrs.).

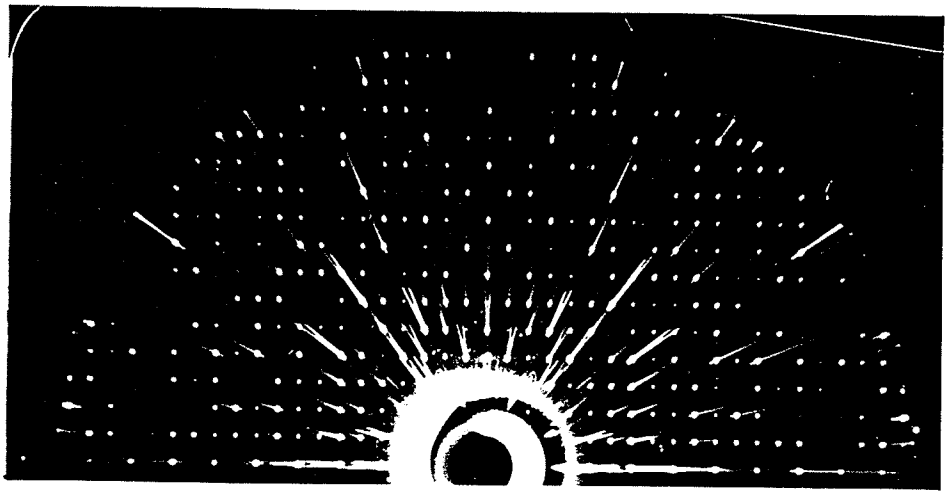

Figure H.20: $V13_r$ $h1l$ precession photograph (80.0 hrs.).

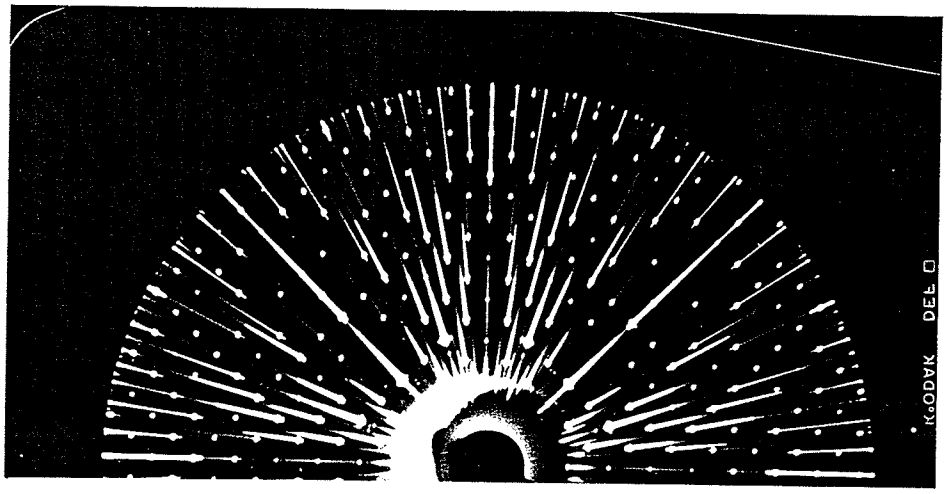

Figure H.21: V13$_r$ $hk0$ precession photograph (87 hrs.).

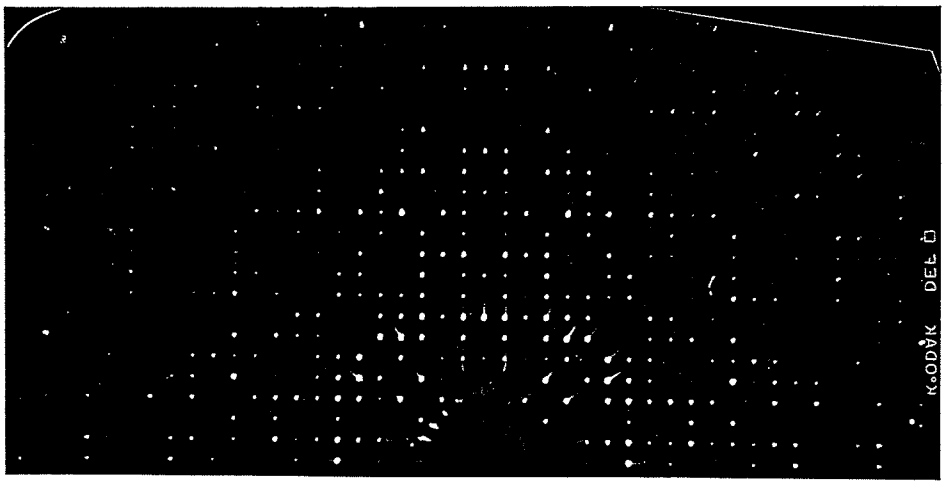

Figure H.22: V13$_r$ $hk1$ precession photograph (84.5 hrs.).

Figure H.23: $V13_r$ $hk3$ precession photograph (80.0 hrs.).

Figure H.24: $V13_r$ $hk4$ precession photograph (80.0 hrs.).

Appendix I

VIOLATING REFLECTIONS

Crystal Structure Refinements

ABBREVIATIONS USED IN APPENDIX I

(a'): reflection violates n glide $\perp c$

(b'): reflection violates n glide $\perp a$

(c'): reflection violates c glide $\perp$ [110]

All reflections with $3[\sigma|F|] > |F|$ were flagged as "unobserveds" in the data processing stage of the refinements. The following "observed" reflections violate $P4/nnc$ extinction criteria.

VIOLATING REFLECTIONS ($P4/nnc$)

$V74_c$ Wilui River, USSR

h	k	l	F	σF	$F/\sigma F$	a'	b'	c'	h	k	l	F	σF	$F/\sigma F$	a'	b'	c'
$\overline{17}$	0	$\overline{10}$	33.89	10.88	3.11		x		0	15	8	35.41	10.62	3.33		x	
$\overline{4}$	9	0	22.55	6.36	3.55	x			7	7	13	39.51	11.51	3.43			x

VIOLATING REFLECTIONS ($P4/nnc$)

V13$_c$ Jeffrey Mine, Richmond Co., PQ

h	k	l	F	σF	$F/\sigma F$	a'	b'	c'	h	k	l	F	σF	$F/\sigma F$	a'	b'	c'
$\overline{19}$	0	$\overline{2}$	136.32	12.70	10.73		x		$\overline{3}$	3	$\overline{3}$	17.20	5.40	3.19			x
$\overline{16}$	0	3	34.30	9.74	3.52		x		$\overline{2}$	2	$\overline{3}$	20.57	5.24	3.93			x
$\overline{14}$	0	$\overline{11}$	50.41	12.04	4.19		x		$\overline{2}$	2	3	22.55	5.16	4.37			x
$\overline{14}$	14	3	49.57	12.17	4.07			x	$\overline{1}$	0	$\overline{12}$	41.25	10.16	4.06		x	
$\overline{13}$	0	12	45.14	12.78	3.53		x		$\overline{1}$	0	$\overline{6}$	23.87	5.82	4.10		x	
$\overline{12}$	0	$\overline{13}$	45.67	12.37	3.69		x		$\overline{1}$	0	$\overline{4}$	37.26	5.45	6.84		x	
$\overline{11}$	0	$\overline{14}$	42.55	12.55	3.39		x		$\overline{1}$	0	4	29.03	5.59	5.19		x	
$\overline{11}$	0	$\overline{2}$	23.44	7.70	3.04		x		$\overline{1}$	0	6	26.58	5.88	4.52		x	
$\overline{11}$	0	14	36.84	12.19	3.02		x		$\overline{1}$	0	12	34.53	10.41	3.32		x	
$\overline{11}$	11	$\overline{3}$	38.38	10.52	3.65			x	$\overline{1}$	1	$\overline{3}$	16.62	4.92	3.38			x
$\overline{11}$	11	3	33.00	10.61	3.11			x	$\overline{1}$	1	5	15.92	5.20	3.06			x
$\overline{10}$	0	$\overline{7}$	27.43	8.75	3.13		x		$\overline{1}$	1	11	30.16	8.86	3.40			x
$\overline{10}$	0	$\overline{3}$	35.69	8.07	4.42		x		0	0	$\overline{11}$	47.01	9.98	4.71		x	x
$\overline{10}$	0	3	31.72	8.26	3.84		x		0	0	$\overline{7}$	27.33	6.11	4.47		x	x
$\overline{10}$	10	$\overline{3}$	41.74	9.82	4.25			x	0	0	7	21.96	6.41	3.43		x	x
$\overline{10}$	10	3	49.33	9.95	4.96			x	0	0	11	36.23	9.75	3.72		x	x
$\overline{10}$	10	5	28.45	9.38	3.03			x	0	1	$\overline{12}$	33.87	9.59	3.53		x	
$\overline{9}$	0	$\overline{8}$	31.39	8.66	3.62		x		0	1	$\overline{6}$	29.37	5.84	5.03		x	
$\overline{9}$	0	2	21.91	6.11	3.59		x		0	1	$\overline{4}$	33.85	5.46	6.20		x	
$\overline{9}$	0	14	48.30	12.13	3.98		x		0	1	4	26.86	5.43	4.95		x	
$\overline{7}$	0	$\overline{14}$	42.15	11.06	3.81		x		0	1	14	42.99	10.30	4.17		x	
$\overline{7}$	0	14	45.78	11.35	4.03		x		0	2	$\overline{3}$	20.63	5.07	4.07		x	
$\overline{7}$	7	$\overline{7}$	34.67	9.34	3.71			x	0	3	$\overline{2}$	17.15	5.04	3.40		x	
$\overline{7}$	7	$\overline{3}$	29.14	8.09	3.60			x	0	4	$\overline{15}$	39.17	11.75	3.33		x	
$\overline{7}$	7	3	47.59	8.02	5.93			x	0	4	$\overline{3}$	18.72	5.49	3.41		x	
$\overline{7}$	7	5	23.70	7.84	3.02			x	0	4	3	19.69	5.42	3.63		x	
$\overline{7}$	7	7	48.43	9.60	5.04			x	0	4	7	23.08	6.91	3.34		x	
$\overline{7}$	7	11	36.21	10.77	3.36			x	0	4	15	43.41	11.98	3.62		x	
$\overline{6}$	0	$\overline{13}$	32.19	10.21	3.15		x		0	5	$\overline{6}$	29.47	6.59	4.47		x	
$\overline{5}$	0	$\overline{6}$	25.58	6.51	3.93		x		0	6	3	26.20	5.77	4.54		x	
$\overline{5}$	5	$\overline{9}$	29.29	8.44	3.47			x	0	7	$\overline{6}$	22.54	7.36	3.06		x	
$\overline{4}$	0	$\overline{3}$	22.98	5.21	4.41		x		0	8	3	27.09	6.54	4.14		x	
$\overline{4}$	0	15	50.33	12.27	4.10		x		0	9	$\overline{10}$	28.76	9.57	3.01		x	
$\overline{4}$	4	$\overline{1}$	15.91	5.15	3.09			x	0	9	10	31.67	9.56	3.31		x	
$\overline{4}$	4	1	19.94	5.23	3.81			x	0	10	$\overline{7}$	31.82	9.28	3.43		x	
$\overline{3}$	0	6	18.38	5.89	3.12		x		0	10	$\overline{3}$	51.95	8.66	6.00		x	

VIOLATING REFLECTIONS ($P4/nnc$)

V13$_c$ Jeffrey Mine, Richmond Co., PQ

h	k	l	F	σF	$F/\sigma F$	a'	b'	c'	h	k	l	F	σF	$F/\sigma F$	a'	b'	c'
0	10	3	47.60	8.73	5.45		x		4	0	$\overline{15}$	38.80	11.54	3.36		x	
0	10	7	30.78	9.02	3.41		x		5	0	6	28.10	6.44	4.36		x	
0	10	11	40.38	10.03	4.03		x		6	6	$\overline{3}$	36.96	7.11	5.20			x
0	11	$\overline{10}$	29.45	9.72	3.03		x		6	6	15	42.93	13.11	3.27			x
0	11	$\overline{6}$	82.24	9.73	8.45		x		7	7	$\overline{7}$	33.46	9.87	3.39			x
0	11	8	47.30	9.32	5.08		x		7	7	3	40.44	8.44	4.79			x
0	14	$\overline{11}$	41.26	12.74	3.24		x		7	7	7	43.73	9.67	4.52			x
0	14	11	70.29	12.34	5.70		x		9	0	8	27.84	8.72	3.19		x	
0	21	2	37.22	12.01	3.10		x		9	0	10	33.88	9.37	3.62		x	
1	0	$\overline{14}$	39.51	10.76	3.67		x		10	0	$\overline{3}$	34.01	8.07	4.21		x	
1	0	$\overline{12}$	40.06	10.26	3.90		x		10	0	3	27.68	8.11	3.41		x	
1	0	$\overline{4}$	40.28	5.46	7.38		x		10	0	7	34.77	8.97	3.88		x	
1	0	4	33.42	5.42	6.17		x		10	0	11	30.65	10.15	3.02		x	
1	0	12	40.34	9.94	4.06		x		11	0	$\overline{2}$	72.52	8.41	8.62		x	
1	1	11	42.93	8.53	5.03			x	11	0	2	30.11	7.61	3.96		x	
2	0	$\overline{1}$	13.27	3.35	3.96		x		12	9	0	35.53	9.26	3.84	x		
2	0	3	19.98	4.96	4.03		x		13	0	12	42.27	12.13	3.48		x	
2	2	$\overline{3}$	19.97	5.41	3.69			x	14	0	$\overline{11}$	45.23	12.98	3.48		x	
2	2	3	23.02	5.28	4.36			x	14	0	11	43.36	12.77	3.40		x	
3	0	$\overline{8}$	25.60	7.29	3.51		x		17	0	$\overline{8}$	39.90	10.91	3.66		x	
3	0	$\overline{6}$	45.81	6.18	7.41		x		19	0	2	130.29	13.34	9.77		x	
3	0	6	50.66	6.27	8.08		x										

VIOLATING REFLECTIONS ($P4/nnc$)

V13; Jeffrey Mine, Richmond Co., PQ

h	k	l	F	σF	$F/\sigma F$	a'	b'	c'	h	k	l	F	σF	$F/\sigma F$	a'	b'	c'
$\overline{10}$	0	$\overline{3}$	24.00	7.02	3.42		x		0	9	$\overline{2}$	34.38	5.86	5.87		x	
$\overline{10}$	10	$\overline{5}$	22.92	7.38	3.11			x	0	10	$\overline{7}$	26.55	7.17	3.70		x	
$\overline{7}$	7	$\overline{11}$	26.76	8.46	3.16			x	2	0	$\overline{5}$	24.76	4.93	5.02		x	
$\overline{3}$	3	$\overline{7}$	25.31	5.66	4.47			x	2	2	3	16.63	4.80	3.46			x
$\overline{2}$	1	0	10.40	3.36	3.10	x			2	7	0	14.86	4.80	3.10	x		
$\overline{2}$	2	3	40.61	4.99	8.14			x	4	4	9	26.83	7.06	3.80			x
$\overline{1}$	0	$\overline{4}$	16.50	4.77	3.46		x		5	0	$\overline{6}$	24.19	5.70	4.24		x	
$\overline{1}$	0	4	14.59	4.85	3.01		x		5	0	8	19.35	6.21	3.12		x	
$\overline{1}$	1	$\overline{13}$	30.46	8.49	3.59			x	6	6	$\overline{15}$	34.74	10.19	3.41			x
0	0	$\overline{11}$	30.96	8.00	3.87		x	x	6	6	3	17.60	5.74	3.07			x
0	0	$\overline{5}$	26.59	5.08	5.23		x	x	7	0	10	57.92	8.29	6.99		x	
0	0	11	27.71	8.12	3.41		x	x	7	7	$\overline{7}$	23.56	7.62	3.09			x
0	1	$\overline{6}$	19.04	5.11	3.73		x		7	7	$\overline{3}$	26.14	6.48	4.03			x
0	4	$\overline{7}$	29.57	6.02	4.91		x		7	7	7	23.23	7.35	3.16			x
0	4	11	23.58	7.64	3.09		x		9	9	3	20.82	6.65	3.13			x
0	7	$\overline{2}$	50.79	5.39	9.42		x		12	13	0	27.83	7.55	3.69	x		
0	7	6	35.55	6.28	5.66		x										

VIOLATING REFLECTIONS ($P4/nnc$)

V13$_r$ Jeffrey Mine, Richmond Co., PQ

h	k	l	F	σF	$F/\sigma F$	a'	b'	c'	h	k	l	F	σF	$F/\sigma F$	a'	b'	c'
$\overline{18}$	0	3	29.29	9.04	3.24		x		$\overline{7}$	7	$\overline{3}$	43.59	7.24	6.02			x
$\overline{17}$	0	4	27.88	8.31	3.35		x		$\overline{7}$	7	3	47.78	7.19	6.65			x
$\overline{16}$	0	$\overline{5}$	25.05	7.83	3.20		x		$\overline{7}$	7	7	100.77	9.00	11.20			x
$\overline{14}$	0	$\overline{11}$	49.36	10.83	4.56		x		$\overline{7}$	7	11	75.58	9.85	7.67			x
$\overline{14}$	0	$\overline{7}$	35.11	8.19	4.29		x		$\overline{6}$	0	$\overline{3}$	34.40	4.78	7.20		x	
$\overline{14}$	0	11	70.37	10.89	6.46		x		$\overline{6}$	0	3	28.44	4.79	5.94		x	
$\overline{14}$	14	$\overline{3}$	31.48	10.23	3.08			x	$\overline{6}$	0	13	33.10	8.84	3.74		x	
$\overline{13}$	0	$\overline{12}$	31.38	10.43	3.01		x		$\overline{6}$	6	$\overline{15}$	53.64	10.83	4.95			x
$\overline{13}$	0	4	32.69	7.32	4.47		x		$\overline{6}$	6	$\overline{7}$	28.69	6.96	4.12			x
$\overline{13}$	0	6	28.93	7.57	3.82		x		$\overline{6}$	6	$\overline{3}$	49.00	6.20	7.90			x
$\overline{13}$	0	12	53.37	10.75	4.96		x		$\overline{6}$	6	3	39.56	6.53	6.06			x
$\overline{11}$	0	$\overline{8}$	21.90	6.95	3.15		x		$\overline{6}$	6	15	54.65	11.24	4.86			x
$\overline{11}$	0	$\overline{6}$	22.37	7.04	3.18		x		$\overline{5}$	0	$\overline{6}$	27.85	5.34	5.22		x	
$\overline{11}$	0	$\overline{2}$	44.90	6.93	6.48		x		$\overline{5}$	0	6	26.87	5.61	4.79		x	
$\overline{11}$	0	2	21.97	6.60	3.33		x		$\overline{5}$	0	8	24.86	6.94	3.58		x	
$\overline{11}$	0	6	39.45	7.46	5.29		x		$\overline{5}$	5	$\overline{3}$	20.02	5.04	3.97			x
$\overline{11}$	11	$\overline{3}$	45.25	9.66	4.68			x	$\overline{4}$	0	$\overline{11}$	29.11	7.63	3.82		x	
$\overline{11}$	11	3	51.06	9.69	5.27			x	$\overline{4}$	0	$\overline{7}$	19.31	5.75	3.36		x	
$\overline{10}$	0	$\overline{7}$	48.86	7.66	6.38		x		$\overline{4}$	0	$\overline{3}$	52.28	4.91	10.65		x	
$\overline{10}$	0	$\overline{3}$	76.88	7.62	10.09		x		$\overline{4}$	0	3	46.28	4.95	9.35		x	
$\overline{10}$	0	3	70.44	7.51	9.38		x		$\overline{4}$	0	7	27.31	6.17	4.43		x	
$\overline{10}$	0	7	31.27	8.21	3.81		x		$\overline{4}$	0	11	33.45	7.72	4.33		x	
$\overline{10}$	10	$\overline{3}$	47.93	8.72	5.50			x	$\overline{4}$	4	$\overline{1}$	19.39	4.69	4.13			x
$\overline{10}$	10	3	34.90	8.73	4.00			x	$\overline{4}$	4	1	22.62	4.90	4.62			x
$\overline{10}$	10	5	27.53	8.20	3.36			x	$\overline{3}$	0	4	14.34	4.30	3.33		x	
$\overline{9}$	0	$\overline{10}$	35.16	7.81	4.50		x		$\overline{3}$	3	$\overline{3}$	52.21	4.98	10.48			x
$\overline{9}$	0	$\overline{8}$	28.69	6.77	4.24		x		$\overline{3}$	3	3	54.90	5.09	10.79			x
$\overline{9}$	0	8	35.35	7.63	4.63		x		$\overline{3}$	3	7	25.89	5.98	4.33			x
$\overline{9}$	0	10	35.84	8.70	4.12		x		$\overline{2}$	0	$\overline{3}$	34.43	4.46	7.72		x	
$\overline{8}$	0	$\overline{3}$	41.75	5.71	7.31		x		$\overline{2}$	0	1	11.03	3.23	3.41		x	
$\overline{8}$	0	3	17.68	5.52	3.20		x		$\overline{2}$	0	3	28.33	4.93	5.75		x	
$\overline{8}$	8	$\overline{13}$	30.14	9.97	3.02			x	$\overline{2}$	0	5	16.30	4.65	3.51		x	
$\overline{8}$	8	1	27.33	7.21	3.79			x	$\overline{2}$	2	$\overline{3}$	51.02	4.80	10.63			x
$\overline{7}$	0	2	14.03	4.52	3.10		x		$\overline{2}$	2	3	51.27	5.21	9.84			x
$\overline{7}$	7	$\overline{11}$	46.67	9.50	4.91			x	$\overline{1}$	0	$\overline{16}$	48.29	10.63	4.54		x	
$\overline{7}$	7	$\overline{7}$	76.70	8.81	8.71			x	$\overline{1}$	0	$\overline{12}$	54.08	9.00	6.01		x	

VIOLATING REFLECTIONS ($P4/nnc$)

V13$_r$ Jeffrey Mine, Richmond Co., PQ

h	k	l	F	σF	$F/\sigma F$	a'	b'	c'	h	k	l	F	σF	$F/\sigma F$	a'	b'	c'
$\bar{1}$	0	$\bar{6}$	51.98	5.16	10.07		x		0	4	$\bar{7}$	37.25	6.14	6.07		x	
$\bar{1}$	0	$\bar{4}$	76.92	5.06	15.20		x		0	4	$\bar{5}$	18.79	4.82	3.90		x	
$\bar{1}$	0	2	26.87	3.73	7.20		x		0	4	$\bar{3}$	53.54	5.10	10.50		x	
$\bar{1}$	0	4	79.25	5.34	14.84		x		0	4	3	54.38	5.29	10.28		x	
$\bar{1}$	0	6	47.61	5.51	8.64		x		0	4	5	24.49	5.23	4.68		x	
$\bar{1}$	0	12	61.66	8.99	6.86		x		0	4	7	29.86	6.21	4.81		x	
$\bar{1}$	0	14	31.49	9.21	3.42		x		0	4	11	38.37	8.32	4.61		x	
$\bar{1}$	1	$\overline{13}$	30.17	8.56	3.52			x	0	5	$\bar{8}$	25.87	6.66	3.88		x	
$\bar{1}$	1	$\overline{11}$	27.08	7.56	3.58			x	0	5	$\bar{6}$	35.28	5.66	6.23		x	
$\bar{1}$	1	$\bar{5}$	19.20	4.54	4.23			x	0	5	$\bar{2}$	17.77	4.56	3.90		x	
$\bar{1}$	1	$\bar{3}$	20.26	4.50	4.50			x	0	5	6	27.56	5.97	4.62		x	
$\bar{1}$	1	3	31.41	4.87	6.45			x	0	6	$\overline{13}$	32.05	8.77	3.65		x	
$\bar{1}$	1	5	17.03	4.69	3.63			x	0	6	$\bar{3}$	27.58	5.02	5.49		x	
$\bar{1}$	1	7	16.92	5.27	3.21			x	0	6	3	29.62	5.48	5.41		x	
$\bar{1}$	2	0	13.08	3.17	4.13	x			0	6	5	16.82	5.48	3.07		x	
0	0	$\overline{13}$	41.37	11.21	3.69		x	x	0	7	$\overline{10}$	26.94	7.19	3.75		x	
0	0	$\overline{11}$	100.96	9.30	10.86		x	x	0	7	$\bar{4}$	21.69	5.31	4.08		x	
0	0	$\bar{7}$	25.33	5.32	4.76		x	x	0	7	$\bar{2}$	16.64	4.88	3.41		x	
0	0	$\bar{5}$	25.36	4.49	5.65		x	x	0	7	6	21.68	6.73	3.22		x	
0	0	3	22.12	4.54	4.87		x	x	0	8	$\bar{7}$	20.15	6.68	3.02		x	
0	0	5	14.34	4.58	3.13		x	x	0	8	$\bar{3}$	29.40	6.08	4.84		x	
0	0	7	26.48	5.68	4.66		x	x	0	8	$\bar{1}$	25.31	5.21	4.86		x	
0	0	11	109.75	9.59	11.44		x	x	0	8	3	30.11	6.03	4.99		x	
0	1	$\overline{16}$	41.65	10.69	3.90		x		0	9	$\overline{10}$	45.33	8.25	5.49		x	
0	1	$\overline{12}$	48.33	8.82	5.48		x		0	9	$\bar{8}$	33.03	7.62	4.33		x	
0	1	$\bar{6}$	35.12	5.06	6.94		x		0	9	8	31.99	8.20	3.90		x	
0	1	$\bar{4}$	83.42	5.04	16.55		x		0	9	10	34.93	8.50	4.11		x	
0	1	4	77.90	5.29	14.73		x		0	10	$\overline{11}$	39.72	8.95	4.44		x	
0	1	6	36.42	5.35	6.81		x		0	10	$\bar{7}$	48.76	8.73	5.59		x	
0	1	12	50.02	8.97	5.58		x		0	10	$\bar{3}$	81.23	8.07	10.07		x	
0	2	$\overline{13}$	23.62	7.85	3.01		x		0	10	3	78.53	8.30	9.46		x	
0	2	$\bar{3}$	37.15	4.73	7.85		x		0	10	7	59.95	8.84	6.78		x	
0	2	3	33.35	5.03	6.63		x		0	11	$\bar{6}$	37.56	7.90	4.75		x	
0	3	$\bar{6}$	17.10	4.80	3.56		x		0	11	$\bar{2}$	27.26	7.30	3.73		x	
0	3	2	19.25	4.90	3.93		x		0	11	2	70.86	8.16	8.68		x	
0	4	$\overline{15}$	39.59	10.30	3.84		x		0	11	6	47.91	8.71	5.50		x	

VIOLATING REFLECTIONS ($P4/nnc$)

V13$_r$ Jeffrey Mine, Richmond Co., PQ

h	k	l	F	σF	$F/\sigma F$	a'	b'	c'	h	k	l	F	σF	$F/\sigma F$	a'	b'	c'
0	12	$\overline{13}$	37.99	10.62	3.58		x		4	0	$\overline{7}$	35.55	6.03	5.90		x	
0	12	13	37.03	11.37	3.26		x		4	0	$\overline{3}$	45.00	5.03	8.95		x	
0	13	$\overline{12}$	47.03	11.18	4.21		x		4	0	3	54.91	5.10	10.77		x	
0	13	$\overline{4}$	30.81	7.63	4.04		x		4	0	7	37.13	6.31	5.88		x	
0	13	12	38.00	11.32	3.36		x		4	0	11	29.24	8.05	3.63		x	
0	14	$\overline{11}$	60.57	11.50	5.27		x		4	4	$\overline{9}$	23.92	7.16	3.34			x
0	4	11	41.59	11.74	3.54		x		5	0	$\overline{8}$	23.75	7.03	3.38		x	
0	15	4	36.75	9.25	3.97		x		5	0	$\overline{6}$	20.01	5.62	3.56		x	
0	17	8	37.35	10.33	3.62		x		5	0	6	27.68	5.79	4.78		x	
1	0	$\overline{16}$	61.98	10.75	5.77		x		5	0	8	25.94	6.90	3.76		x	
1	0	$\overline{14}$	33.84	9.09	3.72		x		5	4	0	32.10	4.62	6.95	x		
1	0	$\overline{12}$	52.42	8.75	5.99		x		6	0	$\overline{13}$	27.32	9.09	3.01		x	
1	0	$\overline{6}$	38.70	5.29	7.32		x		6	0	$\overline{3}$	29.81	4.95	6.02		x	
1	0	$\overline{4}$	75.67	5.17	14.64		x		6	0	3	36.90	5.28	6.99		x	
1	0	$\overline{2}$	30.05	3.75	8.01		x		6	6	$\overline{15}$	49.53	11.51	4.30			x
1	0	4	95.87	5.35	17.92		x		6	6	$\overline{7}$	33.42	7.27	4.60			x
1	0	6	36.77	5.49	6.70		x		6	6	$\overline{3}$	31.26	5.94	5.26			x
1	0	12	53.57	9.25	5.79		x		6	6	3	35.29	6.38	5.53			x
1	0	16	41.79	10.70	3.91		x		6	6	15	42.23	11.92	3.54			x
1	1	$\overline{13}$	31.72	8.58	3.70			x	7	0	$\overline{4}$	16.23	5.20	3.12		x	
1	1	$\overline{11}$	35.90	7.73	4.64			x	7	0	$\overline{2}$	16.17	5.00	3.23		x	
1	1	$\overline{5}$	19.06	4.50	4.24			x	7	0	6	19.75	6.37	3.10		x	
1	1	$\overline{3}$	19.33	4.57	4.23			x	7	0	10	28.98	7.83	3.70		x	
1	1	3	17.21	4.79	3.59			x	7	7	$\overline{11}$	45.84	9.57	4.79			x
1	1	5	15.43	4.66	3.31			x	7	7	$\overline{7}$	71.32	8.86	8.05			x
1	1	13	28.13	9.16	3.07			x	7	7	$\overline{3}$	51.15	7.22	7.08			x
1	1	15	30.78	9.97	3.09			x	7	7	3	54.41	7.73	7.04			x
2	0	$\overline{5}$	16.00	4.54	3.52		x		7	7	7	83.43	9.41	8.87			x
2	0	$\overline{3}$	30.66	4.88	6.28		x		7	7	11	37.36	9.84	3.80			x
2	0	3	31.84	4.88	6.52		x		8	0	$\overline{3}$	30.68	5.83	5.26		x	
2	2	$\overline{3}$	42.11	4.92	8.56			x	8	0	3	31.81	6.08	5.23		x	
2	2	3	51.32	5.05	10.16			x	8	8	1	27.99	6.92	4.04			x
3	0	4	18.80	4.54	4.14		x		9	0	$\overline{10}$	34.64	8.48	4.08		x	
3	3	$\overline{3}$	50.20	4.99	10.06			x	9	0	$\overline{8}$	27.90	7.64	3.65		x	
3	3	3	42.57	5.20	8.19			x	10	0	$\overline{7}$	53.77	8.44	6.37		x	
3	3	11	24.19	7.54	3.21			x	10	0	$\overline{5}$	23.16	6.91	3.35		x	

VIOLATING REFLECTIONS ($P4/nnc$)

V13$_r$ Jeffrey Mine, Richmond Co., PQ

h	k	l	F	σF	$F/\sigma F$	a'	b'	c'	h	k	l	F	σF	$F/\sigma F$	a'	b'	c'
10	0	$\bar{3}$	88.31	8.01	11.02		x		11	0	$\bar{2}$	28.02	7.46	3.76		x	
10	0	3	78.35	8.06	9.72		x		11	0	2	62.17	7.94	7.83		x	
10	0	7	45.45	8.41	5.40		x		11	11	3	49.19	9.63	5.11			x
10	0	11	30.47	8.85	3.44		x		14	0	$\bar{11}$	77.63	11.49	6.76		x	
10	10	$\bar{5}$	27.51	8.32	3.31			x	14	0	7	28.84	9.12	3.16		x	
10	10	$\bar{3}$	33.21	8.52	3.90			x	14	0	11	48.18	11.42	4.22		x	
10	10	3	31.23	9.29	3.36			x	16	0	$\bar{5}$	29.01	9.02	3.22		x	
11	0	$\bar{6}$	25.38	8.19	3.10		x		18	0	3	37.98	9.89	3.84		x	

Appendix J

ATOMIC PARAMETERS AND TEMPERATURE FACTORS

Table J.1: Atomic positions for $V74_c$ ($P4/nnc$).

Atom	x	y	z	$U^*_{equiv.}$
Si(1)	3/4	1/4	0	9.4(3)
Si(2)	0.82180(4)	0.4382(5)	0.87260(6)	13.1(2)
Si(3)	0.91589(4)	0.84997(4)	0.36489(6)	10.2(2)
Ca(1)	3/4	1/4	1/4	11.3(3)
Ca(2)	0.80929(3)	0.04540(3)	0.37984(4)	11.8(1)
Ca(3)	0.89871(3)	0.82055(3)	0.89718(5)	17.9(2)
C†	3/4	3/4	0.1429(2)	12.6(5)
B†	3/4	3/4	0.0563(2)	14.6(7)
AlFe	0.88858(4)	0.12017(4)	0.12807(6)	6.8(2)
A	0	0	0	8.9(3)
O(1)	0.7800(1)	0.1729(1)	0.0843(2)	12.7(5)
O(2)	0.8788(1)	0.1609(1)	0.2834(2)	15.3(5)
O(3)	0.9584(1)	0.2254(1)	0.0783(2)	15.2(5)
O(4)	0.9382(1)	0.1045(1)	0.4714(2)	12.9(5)
O(5)	0.8281(1)	0.0111(1)	0.1796(2)	13.7(5)
O(6)	0.8782(1)	0.7227(1)	0.0525(2)	17.0(5)
$O(7)_a$	0.0552(3)	0.1733(3)	0.3190(3)	16.7(6)
$O(7)_b$	0.0435(2)	0.1455(3)	0.3070(3)	16.7(6)
O(8)	0.9398(1)	0.9078(1)	0.0667(1)	11.9(5)
O(9)	0.8536(1)	0.8536(1)	1/4	14.4(5)
O(10)	3/4	3/4	0.8668(7)	22.5(17)
O(11)	0.1789(9)	0.2286(9)	0.297(1)	12.9(28)
OH	0.9982(1)	0.0577(1)	0.1469(2)	19.0(6)
Bo(1)	0.492(6)	0.0582(6)	1/4	15.1(12)
Bo(2)	1/4	1/4	1/4	9.7(14)

*$U_{equiv.}$=$U_{equiv.} \times 10^2$.

†Position half-occupied.

Table J.2: Anisotropic temperature factor coefficients: $V74_c$ ($P4/nnc$).

Atom	U_{11}^*	U_{22}	U_{33}	U_{23}	U_{13}	U_{12}
Si(1)	107(3)	107(3)	69(6)	0	0	0
Si(2)	122(3)	169(3)	102(3)	27(3)	-9(3)	11(3)
Si(3)	121(3)	89(3)	97(3)	6(2)	3(3)	13(2)
Ca(1)	155(5)	104(4)	81(4)	0	0	0
Ca(2)	112(2)	140(2)	103(2)	0(2)	-9(2)	16(2)
Ca(3)	134(2)	161(2)	241(3)	-31(2)	-41(2)	-2(2)
C	104(6)	104(6)	169(11)	0	0	0
B	77(8)	77(8)	282(17)	0	0	0
AlFe	71(4)	75(4)	58(3)	-4(3)	6(3)	4(2)
A	77(5)	73(4)	118(5)	-5(4)	2(4)	8(4)
O(1)	174(9)	110(8)	98(8)	6(7)	-9(7)	-1(7)
O(2)	187(9)	132(9)	138(9)	18(7)	-53(7)	-16(7)
O(3)	193(9)	154(9)	107(8)	14(7)	32(7)	58(7)
O(4)	161(9)	121(8)	104(9)	4(7)	-13(7)	10(7)
O(5)	147(9)	146(9)	118(9)	-27(7)	3(7)	54(7)
O(6)	209(10)	144(9)	155(9)	54(7)	32(8)	28(7)
$O(7)_a$	167(6)					
$O(7)_b$	167(6)					
O(8)	110(8)	110(8)	137(9)	-10(7)	22(6)	12(7)
O(9)	164(7)	164(7)	104(11)	23(7)	-23(7)	-4(10)
O(10)	225(17)					
O(11)	129(28)					
OH	142(9)	168(9)	259(11)	-73(8)	30(8)	-17(8)
Bo1	151(12)					
Bo2	97(14)					

*U_{ij}=$U_{ij} \times 10^3$.

Table J.3: Atomic positions for V13$_c$ ($P4/nnc$).

Atom	x	y	z	$U^*_{equiv.}$
Si(1)	3/4	1/4	0	6.0(2)
Si(2)	0.81911(4)	0.04110(4)	0.87099(5)	6.2(1)
Si(3)	0.91686(4)	0.84915(4)	0.36482(5)	7.2(1)
Ca(1)	3/4	1/4	1/4	7.7(2)
Ca(2)	0.81081	0.04379(3)	0.37990(4)	7.9(1)
Ca(3)	0.89868(3)	0.81877(3)	0.88698(4)	16.9(1)
C†	3/4	3/4	0.1493(2)	9.9(3)
B†	3/4	3/4	0.0358(1)	10.9(3)
AlFe	0.88797(4)	0.12089(4)	0.12640(5)	6.7(2)
A	0	0	0	7.2(2)
O(1)	0.7809(1)	0.17269(9)	0.0855(1)	8.2(4)
O(2)	0.8827(1)	0.1596(1)	0.2783(1)	8.9(4)
O(3)	0.9509(1)	0.2215(1)	0.0764(1)	8.4(4)
O(4)	0.9377(1)	0.1066(1)	0.4702(1)	8.4(4)
O(5)	0.82981(9)	0.0150(1)	0.1783(1)	9.9(4)
O(6)	0.8811(1)	0.7293(1)	0.0601(1)	13.2(4)
O(7)	0.0558(1)	0.1731(1)	0.3219(1)	11.5(4)
O(8)	0.9390(1)	0.90899(9)	0.0662(1)	8.8(4)
O(9)	0.8555(1)	0.8555(1)	1/4	0.2(4)
O(10)	3/4	3/4	0.8661(3)	15.1(7)
OH	0.9952(1)	0.0616(1)	0.1364(1)	9.5(4)

*$U_{equiv.}$=$U_{equiv.}$ × 10^2.

†Position half-occupied.

Table J.4: Anisotropic temperature factor coefficients: $V13_c$ ($P4/nnc$).

Atom	U_{11}^*	U_{22}	U_{33}	U_{23}	U_{13}	U_{12}
Si(1)	65(3)	65(3)	51(5)	0	0	0
Si(2)	57(2)	62(2)	66(2)	6(2)	1(2)	0(2)
Si(3)	100(3)	51(2)	64(2)	-1(2)	-6(2)	4(2)
Ca(1)	98(4)	71(4)	61(3)	0	0	0
Ca(2)	69(2)	91(2)	78(2)	5(1)	-5(1)	6(1)
Ca(3)	116(2)	138(2)	252(3)	-79(2)	-80(2)	45(2)
C	70(4)	70(4)	158(8)	0	0	0
B	62(5)	62(5)	202(8)	0	0	0
AlFe	66(3)	65(3)	72(3)	-2(2)	9(2)	0(2)
A	64(4)	61(4)	91(4)	7(3)	6(3)	9(3)
O(1)	105(7)	66(7)	75(7)	4(5)	-4(5)	7(6)
O(2)	80(7)	87(7)	99(7)	6(5)	-19(6)	-5(6)
O(3)	95(7)	76(7)	80(7)	-7(5)	-5(6)	-1(6)
O(4)	92(7)	68(7)	93(7)	9(5)	-13(5)	3(6)
O(5)	91(7)	122(7)	84(7)	-1(6)	8(6)	40(6)
O(6)	190(8)	88(7)	118(7)	29(6)	28(6)	31(6)
O(7)	73(7)	135(8)	137(7)	-17(6)	13(6)	10(6)
O(8)	72(7)	76(7)	117(7)	14(5)	27(5)	7(5)
O(9)	118(6)	118(6)	70(9)	14(6)	-14(6)	-23(8)
O(10)	111(9)	111(9)	231(17)	0	0	0
OH	86(7)	113(7)	88(7)	-21(5)	-1(6)	-10(6)

*U_{ij}=U_{ij} × 10^3.

Table J.5: Atomic positions for V13$_i$ ($P4/nnc$).

Atom	x	y	z	$U^*_{\text{equiv.}}$
Si(1)	3/4	1/4	0	6.2(3)
Si(2)	0.81921(4)	0.04091(4)	0.87113(6)	6.4(2)
Si(3)	0.91661(5)	0.84919(4)	0.36482(6)	7.6(2)
Ca(1)	3/4	1/4	1/4	7.9(2)
Ca(2)	0.81082(3)	0.04391(3)	0.37977(4)	8.1(1)
Ca(3)	0.89868(4)	0.81867(4)	0.88698(5)	16.5(2)
C†	3/4	3/4	0.1494(2)	10.3(4)
B†	3/4	3/4	0.0361(2)	12.4(4)
AlFe	0.88806(4)	0.12089(4)	0.1264(6)	6.9(2)
A	0	0	0	6.9(3)
O(1)	0.7805(1)	0.1726(1)	0.0854(2)	8.5(5)
O(2)	0.8828(1)	0.1597(1)	0.2788(1)	8.9(5)
O(3)	0.9512(1)	0.2217(1)	0.763(2)	8.1(5)
O(4)	0.9379(1)	0.1065(1)	0.4701(1)	8.7(5)
O(5)	0.8296(1)	0.0147(1)	0.1785(2)	10.4(5)
O(6)	0.8806(1)	0.7290(1)	0.0596(2)	14.0(5)
O(7)	0.0560(1)	0.1731(1)	0.3219(2)	11.8(5)
O(8)	0.9391(1)	0.9090(1)	0.0662(2)	8.9(5)
O(9)	0.8552(1)	0.8552(1)	3/4	10.4(5)
O(10)	3/4	3/4	0.8659(3)	16.2(9)
OH	0.9955(1)	0.0615(1)	0.1363(1)	9.9(5)

*$U_{\text{equiv.}}$=$U_{\text{equiv.}} \times 10^2$.

†Position half-occupied.

Table J.6: Anisotropic temperature factor coefficients: $V13_i$ ($P4/nnc$).

Atom	U_{11}^*	U_{22}	U_{33}	U_{23}	U_{13}	U_{12}
Si(1)	70(4)	70(4)	46(6)	0	0	0
Si(2)	61(3)	65(3)	66(3)	8(2)	2(3)	-1(2)
Si(3)	114(3)	54(3)	59(3)	-1(2)	-7(2)	5(2)
Ca(1)	107(4)	72(4)	58(4)	0	0	0
Ca(2)	72(2)	96(2)	75(2)	3(2)	-4(2)	7(2)
Ca(3)	118(2)	133(2)	242(3)	-73(2)	-78(2)	41(2)
C	76(5)	76(5)	159(10)	0	0	0
B	72(6)	72(6)	227(10)	0	0	0
AlFe	70(3)	69(3)	69(3)	-4(3)	15(3)	1(2)
A	62(4)	65(4)	81(4)	-3(4)	9(4)	9(4)
O(1)	114(8)	76(8)	65(8)	7(6)	-1(7)	4(7)
O(2)	85(8)	98(8)	85(8)	6(6)	-22(7)	-7(7)
O(3)	94(8)	82(8)	67(8)	-9(6)	-4(7)	5(7)
O(4)	97(9)	74(8)	90(8)	15(6)	-14(7)	3(7)
O(5)	95(9)	131(9)	86(8)	-5(7)	6(7)	35(7)
O(6)	208(10)	102(9)	111(9)	38(7)	28(8)	26(7)
O(7)	74(8)	149(9)	130(9)	-19(7)	9(7)	9(7)
O(8)	81(8)	83(8)	101(8)	13(6)	25(6)	8(7)
O(9)	127(7)	127(7)	58(11)	20(7)	-20(7)	-31(10)
O(10)	121(11)	121(11)	243(21)	0	0	0
OH	101(8)	123(8)	72(8)	-22(7)	2(7)	-7(7)

*U_{ij}=U_{ij} $\times$ 10^3.

Table J.7: Atomic positions for V13$_r$ ($P4/nnc$).

Atom	x	y	z	$U^*_{\text{equiv.}}$
Si(1)	3/4	1/4	0	6.5(3)
Si(2)	0.81929(6)	0.04076(6)	0.87112(7)	6.3(2)
Si	0.91648(6)	0.84920(6)	0.36477(7)	7.5(2)
Ca(1)	3/4	1/4	1/4	7.9(3)
Ca(2)	0.81080(4)	0.04407(4)	0.37966(5)	7.9(2)
Ca(3)	0.89862(5)	0.81833(5)	0.88725(7)	16.7(2)
C†	3/4	3/4	0.1494(2)	9.7(5)
B†	3/4	3/4	0.0347(2)	12.0(5)
AlFe	0.88782(6)	0.12101(6)	0.12637(7)	7.3(3)
A	0	0	0	6.6(3)
O(1)	0.7801(2)	0.1729(1)	0.0855(2)	8.5(6)
O(2)	0.8827(1)	0.1598(2)	0.29784(2)	9.2(6)
O(3)	0.9516(1)	0.2219(2)	0.0761(2)	7.3(6)
O(4)	0.9383(2)	0.1063(2)	0.4702(2)	8.9(6)
O(5)	0.8295(1)	0.0146(2)	0.1790(2)	10.5(6)
O(6)	0.8800(2)	0.7288(2)	0.0598(2)	13.9(7)
O(7)	0.0557(2)	0.1726(2)	0.3218(2)	11.1(7)
O(8)	0.9392(1)	0.9090(2)	0.0663(2)	8.4(6)
O(9)	0.8550(1)	0.8550(1)	1/4	10.3(6)
O(10)	3/4	3/4	0.8659(4)	16(1)
OH	0.9960(2)	0.0610(2)	0.1362(2)	9.7(6)

*$U_{\text{equiv.}}$=$U_{\text{equiv.}} \times 10^2$.

†Position half-occupied.

Table J.8: Anisotropic temperature factor coefficients: $V13_r$ ($P4/nnc$).

Atom	U_{11}^*	U_{22}	U_{33}	U_{23}	U_{13}	U_{12}
Si(1)	73(4)	73(4)	51(7)	0	0	0
Si(2)	60(4)	61(4)	67(4)	8(3)	1(3)	-3(3)
Si(3)	121(4)	44(4)	60(4)	0(3)	-6(3)	3(3)
Ca(1)	107(5)	73(5)	56(5)	0	0	0
Ca(2)	68(3)	95(3)	75(3)	6(2)	-5(2)	5(2)
Ca(3)	116(3)	132(3)	253(4)	-78(3)	-81(3)	38(3)
C	71(7)	71(7)	150(12)	0	0	0
B	73(7)	73(7)	216(12)	0	0	0
AlFe	71(5)	73(4)	76(4)	-1(3)	8(3)	-1(3)
A	53(6)	69(6)	75(5)	-1(5)	-1(5)	11(5)
O(1)	113(10)	75(10)	68(9)	-1(9)	-10(8)	9(9)
O(2)	78(10)	109(11)	89(11)	10(8)	-14(8)	-10(8)
O(3)	83(10)	76(10)	60(10)	-6(8)	0(8)	10(8)
O(4)	100(11)	85(11)	82(11)	17(9)	-6(8)	12(8)
O(5)	98(11)	133(11)	85(10)	-9(9)	3(9)	40(10)
O(6)	220(13)	96(12)	100(11)	27(9)	30(10)	30(9)
O(7)	67(11)	144(12)	123(11)	-24(9)	8(9)	1(9)
O(8)	78(10)	76(10)	98(11)	25(8)	31(8)	8(8)
O(9)	121(9)	121(9)	66(12)	19(10)	-19(10)	-30(12)
O(10)	124(14)	124(14)	243(28)	0	0	0
OH	98(11)	122(11)	70(10)	-28(8)	-X(9)	-4(9)

*U_{ij}=U_{ij} × 10^3.